RUTHENIUM POLYPYRIDYL COMPLEXES RELEVANT TO THE CATALYTIC PROCESSES IN ARTIFICIAL PHOTOSYNTHESIS

Nora Plana Roure

ISBN:
Dipòsit Legal: T.1222-2011

Nora Planas Roure

Ruthenium Polypyridyl Complexes Relevant to the Catalytic Processes in Artificial Photosynthesis

PhD Thesis

Supervised by Prof. Antoni Llobet Dalmases

Institut Català d'Investigació Química (ICIQ)

Tarragona, 2011

ICIQ
Institut Català d'Investigació Química

Universitat Rovira i Virgili

Antoni Llobet Dalmases, Group Leader at the Institute of Chemical Research of Catalonia (ICIQ) in Tarragona, and Full Professor of Chemistry in the Universitat Autonoma de Barcelona (UAB).

CERTIFIES, that the present research work entitled **"Ruthenium polypyridyl complexes relevant to the catalytic processes in artificial photosynthesis"** contains the work carried out by Nora Planas Roure under my supervision and constitutes the memory for the candidacy for the degree of Doctor of Philosophy in Chemistry.

Tarragona, May 2011

antoni

ICIQ
Institut Català d'Investigació Química

UNIVERSITAT ROVIRA I VIRGILI

"[...] Oui, mes amis, je crois que l'eau sera un jour employée comme combustible, que l'hydrogène et l'oxygène, qui la constituent, utilisés isolément ou simultanément, fourniront une source de chaleur et de lumière inépuisables et d'une intensité que la houille ne saurait avoir. [...]Je crois donc que lorsque les gisements de houille seront épuisés, on chauffera et on se chauffera avec de l'eau. L'eau est le charbon de l'avenir." (Cyrus Smith)

L'Île Mystérieuse, Jules Verne, 1874.

Als meus pares,

A en Toneti

ACKNOWLEDGEMENTS

Vull donar les gràcies al Prof. Antoni Llobet per haver-me donat la oportunitat de formar part del seu grup de recerca, per tot el que he après d'ell, per l'optimisme i il·lusió que transmet en parlar de química i, sobretot, per deixar sempre la porta del despatx oberta.

A en Xavi Sala li vull agrair l'empenta crucial que em va donar en els meus inicis en el món de la investigació i l'haver seguit escoltant i oferint consells en aquests darrers temps d'estrés i de nervis.

To all my present and past lab-mates I want to say: gràcies, gracias, grazzie, merci, danke, arigato, dziekuje, dhanyabaad, thank you for the companionship and the friendly atmosphere, both inside and outside the lab, which maked learning and working a nice experience. I am very happy for all of the friends I've made in the ICIQ both from my lab and from other groups, and all the good times we have shared.

A todos los miembros de "suport a la recerca" muchas gracias por el tiempo dedicado y la buena predisposición para ayudarme durante estos cuatro años.

I would like to thank Prof. Laura Gagliardi and Prof. Christopher Crammer for allowing me to perform my two short stays with them at the U of M. Thank you for introducing me to the world of computational chemistry and for making me feel like another member of your groups.

To all the Minnesota team: I'm very grateful for your kindness and all you have taught me. I would like to thank Zahid for his patience in introducing me to the research in theoretical chemistry. Very special thanks to Bess, Dongxia and Pere for all the "Typical American" experiences shared outside the office. Bess, thank you for all the sentences of this thesis that you have "repaired", gracies!.

A l'Anna, en Miquel, la Mariona, en Txepo i la Rocío els voldria agrair tots aquells vespres de jocs de taula i d' invents culinaris que ens han fet passar tant bones estones.

Als amics d' Argentona (i altres indrets del Maresme), Marçal, Sílvia, Abel, Víctor, Núria, Jordina, Elena, Carlos ... gràcies per ser-hi quan torno a casa, per les escapades a

la muntanya, els “ressopons” i les bones estones. Abel, moltes gràcies per cedir-me la foto de la portada.

De tot cor voldria agrair el suport incondicional de la meva familia, les croquetes de la mare, les trucades telefòniques i els ànims. També vull donar les gràcies pel suport d’en Toneti i de la seva familia. Toneti, gràcies per estar al meu costat i per fer que el camí sigui més planer.

Nora

The work performed in the present doctoral thesis has been possible thanks to the funding of:

- Institut Català d’Investigació Química (ICIQ).
- Grups de Recerca reconeguts de la Generalitat de Catalunya, SGR2009-69.
- Ministerio de Ciencia e Inovacion (MICINN) through Projects: CTQ2007-67918, CTQ2010-21497 .
- MICNN through Consolider Ingenio 2010 (CSD2006-0003) within the framework of “Diseño de Catalizadores para una Química Sostenible: Una Aproximación Integrada” (INTECAT).
- Comission of the European Union throgh project SOLAR-H2 (EU 212508).
- American Chemical Society through the Petroleun Research Fund, 48619-AC3.

Finally I would also like to thank MICINN for the pre-doctoral FPU grant.

GRAPHICAL ABSTRACTS

Chapter 1. General Introduction (pages 1-40)

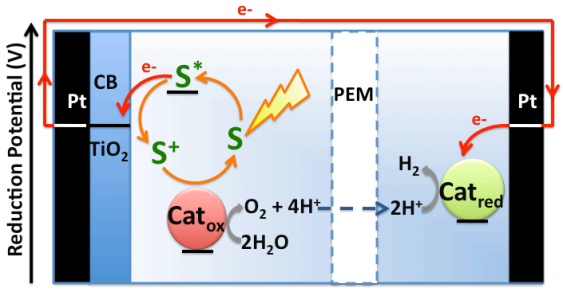

Photosynthesis is the biological process by which photons from the sun are captured and the energy is stored into the energy-rich carbon molecules needed to power life. Inspired by this process, artificial photosynthesis seeks to use water and sunlight to obtain H_2 as a carbon free fuel. Alternatively, CO_2 can be captured in the form of the so called "solar fuels" or other reduced products to be used for industrial applications. Thus, the paramount importance of understanding the principles governing photosynthesis and the steps occurring in the natural and artificial systems.

Chapter 2. Objectives (pages 41-44)

Chapter 3. Through Space Interactions in Dinuclear Ruthenium Polypyridyl Complexes (pages 45-100)

3.2. Through-Space Ligand Interactions in Enantiomeric Dinuclear Ru Complexes

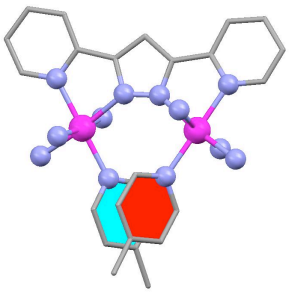

A family of dinuclear Ru complexes of general formula $[\{Ru(T)(L)\}_2(\mu\text{-bpp})]^{(n+1)+}$ (T=tridentate meridional ligand; bpp=tetradentate bridging ligand and L=monodentate ligand, n=1 or 2) have been prepared and thoroughly characterized. In solution these complexes display a global dynamic behavior in which the monodentate ligands undergo a synchronized twisting motion.

3.3. Substitution Reactions in Dinuclear Ru-HBpp Complexes: an Evaluation of Intrasupramolecular Effects

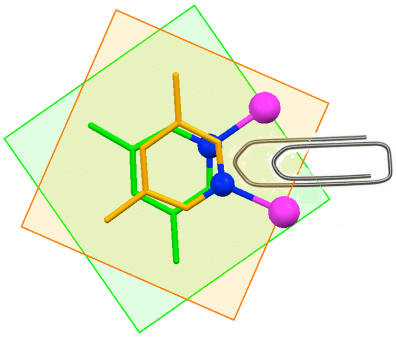

In the present paper we present a comprehensive work, including both experiment and theory via DFT, of intrasupramolecular effects between two pyridylic type of ligands bonded to Ru centers. The chosen dinuclear Ru complexes provide a scaffold that allows framing two pyridyl groups in a manner that has not been achieved previously and thus constitutes an excellent ground to explore the consequences of this particular effect.

Chapter 4. New Insights Into Ruthenium Polypyridyl Complexes as Water Oxidation Catalysts (pages 101-170)

4.2. The Bpp Catalyst Anchored on TiO_2 by Sulfonate Groups

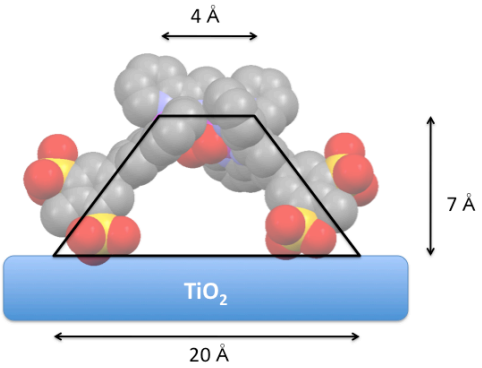

A new μ-acetato-bridged complex with general formula in,in-[{Ru^{II}(trpy)$_2$(μ-bpp)(μ-AcO)]$^{2-}$ (tpy* is 5-([2,2':6',2''-terpyridin]-4'-yl)-2-methylbenzene-1,3-disulfonate), was prepared and fully characterized. Major alterations are observed on the sulfonated compound when anchored onto TiO_2 covered ITO surface. The electrochemically generated Ru^{VI}–Ru^{IV} form of the complex is not capable of oxidizing water but oxidizes ethanol at pH = 1 (triflic acid).*

4.3. The Electronic Structure of Higher Oxidation States Derived from *cis*-$[Ru^{II}(bpy)_2(H_2O)_2]^{2+}$ and its Photoisomerization Mechanism

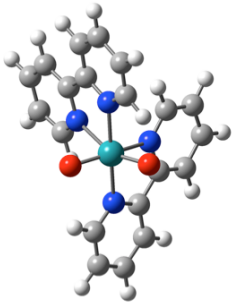

O—Ru—O = 124.5°

The attention is focused on the characterization of higher oxidation state species derived from water oxidation catalyst cis-$[Ru^{II}(bpy)_2(H_2O)_2]^{2+}$ (where bpy is the 2,2'-bypyridine bidentate ligand) by means of EPR and XAS spectroscopy together with DFT and CASPT2 calculations. We have further analyzed the cis- to trans- photoisomerization process suffered by his complex by means of DFT methodologies.

Chapter 5. Polypyridyl Ruthenium Catalysts for Hydrogenative CO_2 Reduction (pages 171-196)

5.2. CO_2 Reduction by Mononuclear Ruthenium Polypyridyl Complexes

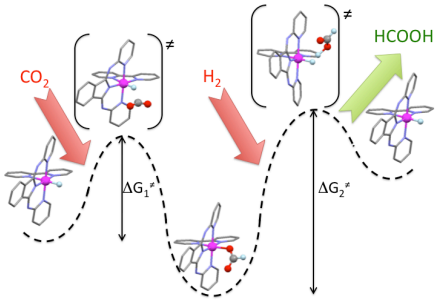

A family of new mononuclear ruthenium complexes with general formula [Ru(T)(bpy)(Cl)]^n (T = tridentate meridional ligand trpy or bid$^-$; bpy = bidentate ligand 2,2'-bipyridine or R_2-bpy, where R = H, COOEt or OEt; n = charge ranging from 0 to +1) have been synthesized and fully characterized. These complexes act as precatalysts for the hydrogenative reduction of CO_2 to formic acid. Further, their mechanistic pathways have been investigated by means of DFT.

Chapter 6. Summary and Conclusions (pages 197-201)

TABLE OF CONTENTS

GLOSSARY OF TERMS AND ABBREVIATIONS

ADP	Adenosine diphosphate
NHE	Normal Hydrogen Electrode
3-PGA	3-phosphoglycerate
ACN	Acetonitrile
ATP	adenosine triphosphate
Ep,a	Anodic peak
2D	Bidimensional
Ep,c	Cathodic peak
eq.	Chemicals equivalent
CASPT2	Complete Active Space Perturbation Theory
COSY	Correlation Spectroscopy
J	Coupling Constant
CV	Cyclic Voltammetry
Cp	Cyclopentadienyl
DFT	Density Functional Theory
DNA	Deoxyribonucleic acid
DCM	Dichloromethane
DPV	Differential Pulse Voltammetry
d	doublet
DNMR	Dynamic Nuclear Magnetic Ressonance
EPR	Electron paramagnetic resonance
ET	Electron Transfer

ET	Electron Transfer
Eq.	Equation
EET	Excitation Energy Transfer
EXAFS	Extended X-ray absorption fine structure
Epsylon	Extintion coefficient
FTO	Fluorine-doped Tin Oxide
FTIR	Fourier transform infrared spectroscopy
GC	Gas Chromatography
GT	Giga Tons
Triose-P	glyceraldehyde-3-phosphate
g	gram
$E_{1/2}$	Half potential
His	Histidine
h	hours
ITO	Indium Tin Oxide
IR	Infra Red
MS	Mass Spectroscopy
m/z	Mass-to-charge ratio
MALDI	Matrix assisted lased desorption/ionization
MHz	Megahertz
MLCT	Metal to Ligand Charge Transfer
mg	milligram
ml	millilitre
M	molar
MM	Molecular Mechanics

1D	Monodimensional
NADP+	nicotinamide adenine dinucleotide
NMR	Nuclear Magnetic ressonance
NOESY	Nuclear Overhouser Spectroscopy
ONIOM	own n-layered integrated molecular orbital and molecular mechanics method
Mu-O	Oxo bridge
OEC	Oxygen Evolving Center
ppm	Parts per million
PSI	Photosystem I
PSII	Photosystem II
PC	Plastocyanine
POM	Polyoxometalate
E	potential
PCET	Proton Coupled Electron Transfer
PEM	proton exchange membrane
py	pyridine
Ca.	quasi
NADPH	reduced form of NADP+
RuBP	ribulose-1,5-bisphosphate
RuBisCO	Ribulose-1,5-bisphosphate Carboxylase/Oxygenase
RT	Room Temperature
SCE	Saturated Calomel Electrode
s	singlet
SPS	Solvent Purification System
R2	Standart deviation

E^0	Standart potential
SSCE	Standart Saturated Calomel Electrode
$scCO_2$	Super Critical Carbon Dioxide
TBAH	Tetrea(n-butyl)ammonium hexafluorophosphate
TM	Transition Metal
t	triplet
TOF	Turn Over Frequency
TON	Turn Over Noumber
Yz	Tyrozine Z
UV-vis	Ultraviolet-visible spectroscopy
VT-NMR	Vatiable Temperature Nuclear Magnetic Ressonance
Vs.	versus
WOC	Water Oxidation Catalyst
λ	wavelength
XAS	X-ray absorption spectroscopy

SUPPLEMENTARY DIGITAL MATERIAL

The material listed below can be found in the attached CD:

- pdf file of the PhD dissertation.

- ".cif" files for each crystal structure presented within this thesis.

- PDF files of the Appendixes containing the Supporting Information of the different sections.

Chapter 1

General Introduction

Photosynthesis is the biological process by which photons from the sun are captured and the energy is stored into the energy-rich carbon molecules needed to power life. Inspired by this process, artificial photosynthesis seeks to use water and sunlight to obtain H_2 as a carbon free solar fuel. Alternatively, CO_2 can be captured in the form of carbon-based solar fuels or transformed into other reduced products having industrial applications. Thus, it is of paramount importance to understand the principles governing photosynthesis and the steps that occur in the natural and artificial systems.

TABLE OF CONTENTS

1.1. NATURAL PHOTOSYNTHESIS

Photosynthesis is carried out by a wide variety of organisms. Most of the advanced eukaryotic photosynthetic organisms have their photosynthetic mechanism isolated in organelles called chloroplasts (Figure 1). Light capture takes place on the tylakoid membranes and the light dependent reactions in their interior while reduction of CO_2 to carbohydrates occurs in the stroma. The adenosine triphosphate (ATP) and NADPH, the reduced form of nicotinamide adenine dinucleotide, produced in the light dependent reactions are used in the Calvin cycle to reduce CO_2 into carbohydrates.

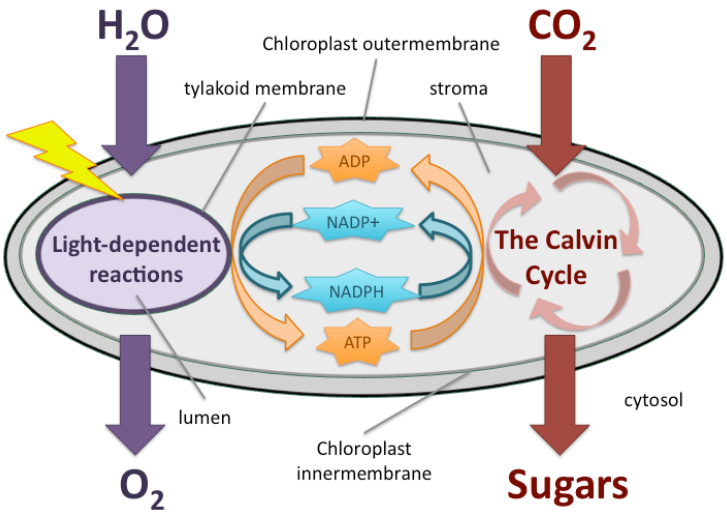

Figure 1. Representation of the overall photosynthetic processes occurring in chloroplasts. $NADP^+$ and NADPH, nicotinamide adenine dinucleotide phosphate and its reduced form; ADP, Adenosine diphosphate; ATP, Adenosine triphosphate.

Thus, the overall photosynthetic process can be divided in four stages;

a) Light absorption and energy delivery by the antenna systems.

b) Primary electron transfer to the reaction centers.

c) Energy stabilization by secondary processes.

d) Synthesis and export of stable products.

The three earlier stages which compose the so-called light dependent processes are carried out by pigment containing proteins that are integrally associated with the membrane of the tylakoids, the membrane-bound compartments present inside the chloroplasts. The latter stage can be referred to as the light independent or dark processes which are promoted by freely diffusible proteins in the stroma, the nonmembraneous aqueous interior of chloroplasts (Figure 1).

1.1.1. Light-dependent processes

Water oxidation and NADH production

In all oxygen evolving photosynthetic organisms (plants, algae and cyanobacteria) the primary light induced processes take place in multisubunit protein complexes called Photosystems I and II (PSI and PSII).[1, 2] The structure and functional organisation of both PSI[3, 4] and PSII[5] can in principle be simplified following the same basic steps. (see Equations 1-4)

$$[ANT][P_{RC}\text{-}A_1\text{-}A_2] + h\nu\ (\textit{Absortion}) \rightarrow [ANT^*][P_{RC}\text{-}A_1\text{-}A_2] \quad (1)$$

$$[ANT^*][P_{RC}\text{-}A_1\text{-}A_2]\ (\textit{EET}) \rightarrow \rightarrow \rightarrow [ANT][^*P_{RC}\text{-}A_1\text{-}A_2] \quad (2)$$

$$[ANT][^*P_{RC}\text{-}A_1\text{-}A_2]\ (\textit{ET}) \rightarrow [ANT][P_{RC}^{+\cdot}\text{-}A_1^{-\cdot}\text{-}A_2] \quad (3)$$

$$[ANT][P_{RC}^{+\cdot}\text{-}A_1^{-\cdot}\text{-}A_2]\ (\textit{Stabilization}) \rightarrow [ANT][P_{RC}^{+\cdot}\text{-}A_1\text{-}A_2^{-\cdot}] \quad (4)$$

Light absorption in photosynthesis involves a wide variety of pigments (chlorophyls, carotenoids and phycobilins), the vast majority of which are contained in a light harvesting antenna system (ANT) bound to the photosystem.[6-10] (Equation 1) The excitation energy is transferred from the light absorbing pigment of the antenna complex to the photosystem through a series of efficient consecutive excitation energy transfer (EET) processes. This electronic excited state energy is ultimately transferred to a photochemically active pigment (P_{RC}) (Equation 2). An electron transfer (ET) process occurs from P_{RC} to a primary acceptor cofactor (A_1) leading to the formation of the ion radical pair $P_{RC}^{+\cdot}\text{-}A_1^{-\cdot}$ (Equation 3). This charge separation is further stabilized

by a second electron transfer from $A_1^{\cdot-}$ to a second cofactor (A_2) as the physical distance between charges increases (Equation 4). Thus, ET is a key step in the overall transformation process of solar radiation into chemical energy.[11, 12] The resulting highly energetic $P_{RC}^{+\cdot}$ and $A_2^{\cdot-}$ are the oxidant and reductant species, respectively, that initially drive the downhill electron transfer reactions of photosynthesis.

PSI and PSII act as the solar energy power stations of the photosynthetic apparatus. These two reaction centers work in series, promoting a linear electron transport from H_2O to $NADP^+$ as represented in the so-called Z-scheme (Scheme 1).[2, 13, 14]

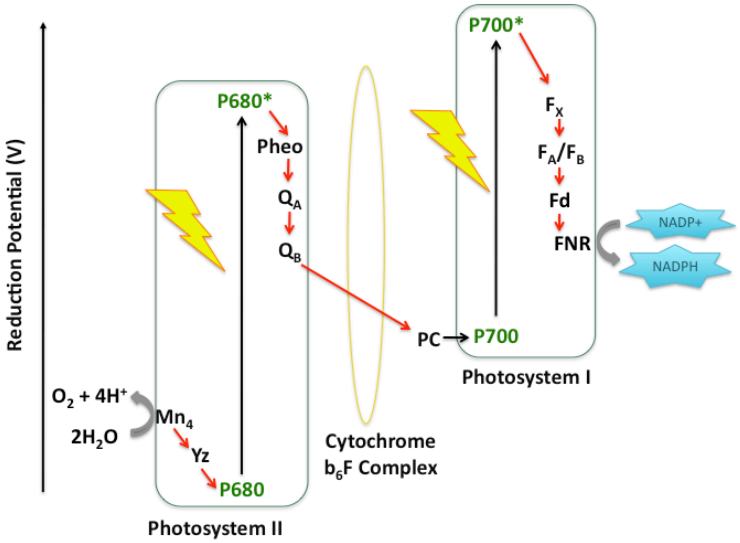

Scheme 1. The Z-scheme of photosynthesis. The direction of electron transfer is shown in red, the photoexcitations in black and the chemical reactions in grey.

Upon photon absorption by the PSII antenna complex the excited state is transferred to the photoactive pigment P680 (corresponding to P_{RC} in Equations 1-4) generating the excited state [ANT][$P680^+ \cdot Pheo^- \cdot Q_A$]. A first light induced charge separation and the subsequent stabilization process in PSII lead to the formation of the radical pair [ANT][$P680^+ \cdot PheoQ_A^- \cdot$] ([ANT][$P_{RC}^+ \cdot A_1A_2^- \cdot$] in Equation 4) where Pheo is pheophytin and Q_A a special noncovalently and permanently bound plastoquinone-9 molecule.

Thereafter, a fast Electron Transfer (ET) from Tyr161 (Yz) to $P680^{+\cdot}$ yields neutral P680. The tyrosine radical $Yz^{\cdot}$ then, oxidizes the tetra-manganese cluster (Mn_4).

The electron rich $Q_A^{-}\cdot$ transfers the electrons to the secondary quinone acceptor (Q_B). When a second photon is absorbed, Q_B becomes doubly reduced, takes up two protons and enters in the mobile lipophylic electron carrier system of plastoquinones encharged of the electronic connection between PSII and the cytochrome b_6f complex ($Cytb_6f$).

Plastocyanines (PC) act as electron donors for $P700^{+}\cdot$ in PSI. Light induced charge separation at PSI gives rise to the reduction of bound ferredoxin (FX, FA, FB) which then acts as electron donor for the soluble ferredoxin(Fd). Fd is used by ferredoxin-$NADP^+$ reductase (FNR) to reduce $NADP^+$ to NADPH.

The two photosystems are situated along the tylakoid membrane of chloroplasts as represented in Figure 2. This disposition has as direct consequence that the oxidative and reductive processes take place in different reaction compartments. While water is oxidized in the interior of the tylakoid (lumen), NADPH is produced in the chloroplast's stroma.

The proton uptake in the reductive reactions, combined with the proton release in the oxidative transformations, gives rise to a transmembrane pH gradient (ΔpH). This ΔpH is used by ATP-synthase for ATP synthesis, hence playing a crucial role as a proton pumping enzyme. [15-17]

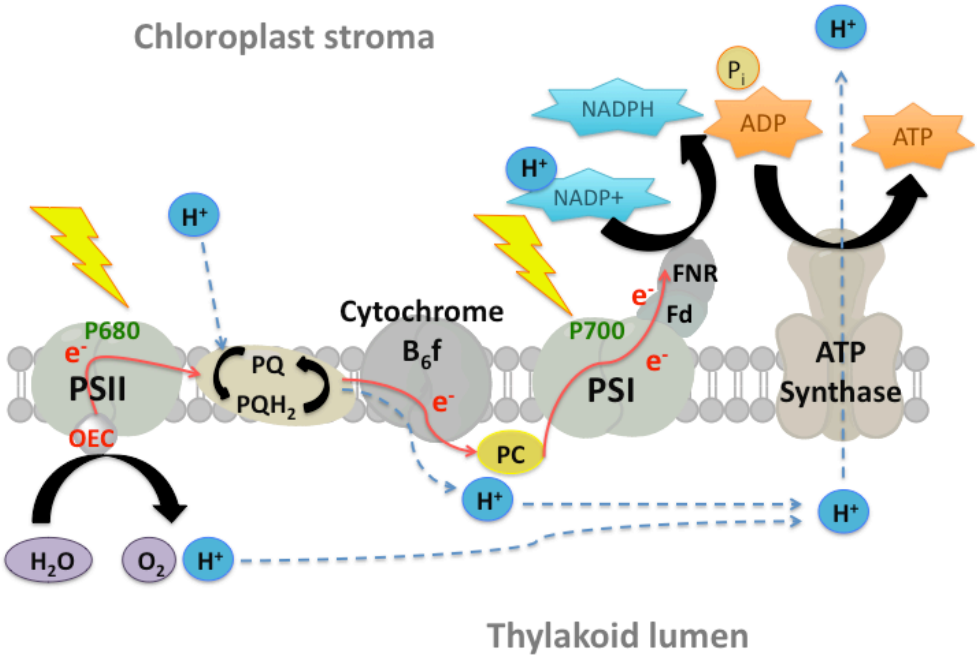

Figure 2. The structural model of the electron and proton transport chain in oxygen evolving organisms. Electron transfer through the tylakoid membrane is shown in red, black arrows indicate redox chemical process, and the light blue dashed arrows show proton transfer. OEC; oxygen evolving center; PSI and PSII, photosystem I and II respectively; P680, photoactive pigment of PSII; P700, photoactive pigment of PSI; PQ, plastoquinone; PQH_2, plastoquinol; PC , plastocyanin; Fd, soluble ferredoxin; FNR, ferredoxin-NADP reductase; NADPH, reduced form of nicotinamide adenine dinucleotide phosphate; ADP, Adenosine diphosphate; ATP, Adenosine triphosphate.

1.1.2. Water oxidation at PSII

The Oxygen Evolving Complex

The oxidative splitting of two water molecules into molecular dioxygen and four protons involves the intermediate storage of the four oxidising equivalents in a functional unit referred to as oxygen evolving complex (OEC). The OEC is composed of a tetra-manganese core with the general formula Mn_4O_xCa. The quaternary electron accumulation function of the oxidising site of PSII can be described as the S-state cycle, [18-22] namely the Kok cycle (Scheme 2).

PSII cycles through five redox states designated S_0 to S_4, that depend on the number of stored oxidising equivalents, where S_4 is the oxidation state capable of oxidising water.

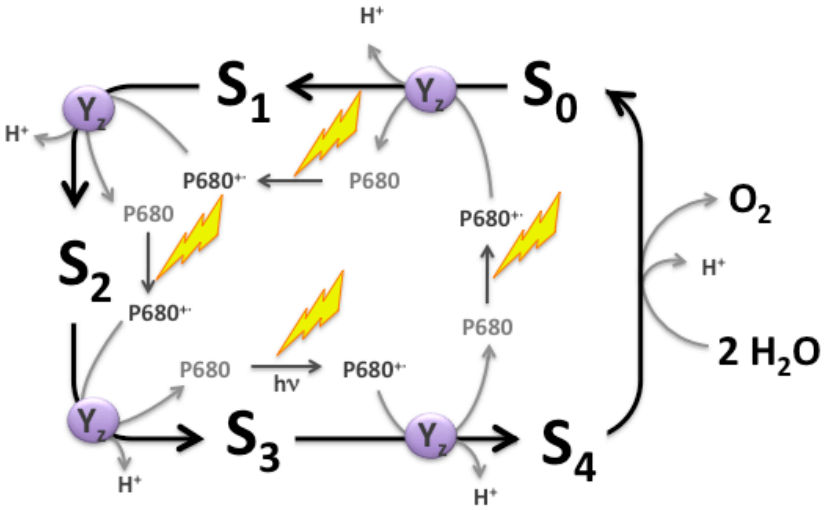

Scheme 2. The extended Kok cycle of oxidative water splitting. The oxidation states of the OEC are symbolized by S_i where i is the number of oxidizing redox equivalents above the lowest level S_0. Yz is the tyrosine161 residue and P680 is the photoactive pigment of PSII.

The stepwise oxidation of the OEC by $P680^{+\cdot}$ is mediated by the redox active tyrosine Y_Z. The oxidation of Y_Z by $P680^{+\cdot}$ is in turn coupled with the release of a proton

assisted by a hystidine residue (His190). Thus, proton coupled electron transfer (PCET) makes the process energetically favourable (Figure 3, right).

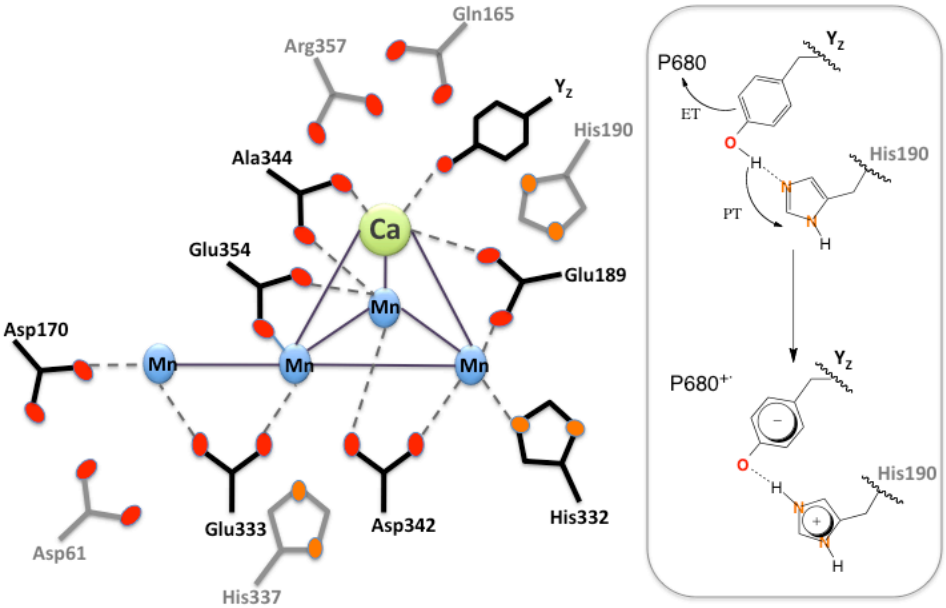

Figure 3. Left, Schematic representation of the structure and ligation of the Mn_4O_xCa cluster.[23] Right, PCET by Yz.

Information about the structure of the Mn_4O_xCa cluster and the nature and geometry of its coordination sphere have been gathered using different techniques including X-ray,[23-25] EXAFS[25, 26] and FTIR-spectroscopy.[27-30] Even though the number and nature of Mn-mono-μ-oxo-Mn and Mn-di-μ-oxo-Mn bonds present in the structure is still under discussion,[26, 31-33] all of the data supports the general formula Mn_4O_xCa and an active metal ligation role of bridging carboxylate moieties from vicinal aminoacid residues of PSII protein complex. (Figure 3, left). These residues act as a scaffold fixing the crucial distances between the metal centres and ligands (including the substrate water molecules) during the catalytic cycle.

1.1.3. Light-independent processes

The Calvin Cycle

The photosynthetic carbon reduction pentose phosphate pathway also referred to as the Calvin cycle is one of the four known pathways that can catalyse the net fixation of carbon dioxide in nature. The three other pathways are the reverse citric acid cycle (reverse Krebs cycle),[34] the reductive acetyl CoA pathway[35] and the 3-hydroxypropionate pathway.[36]

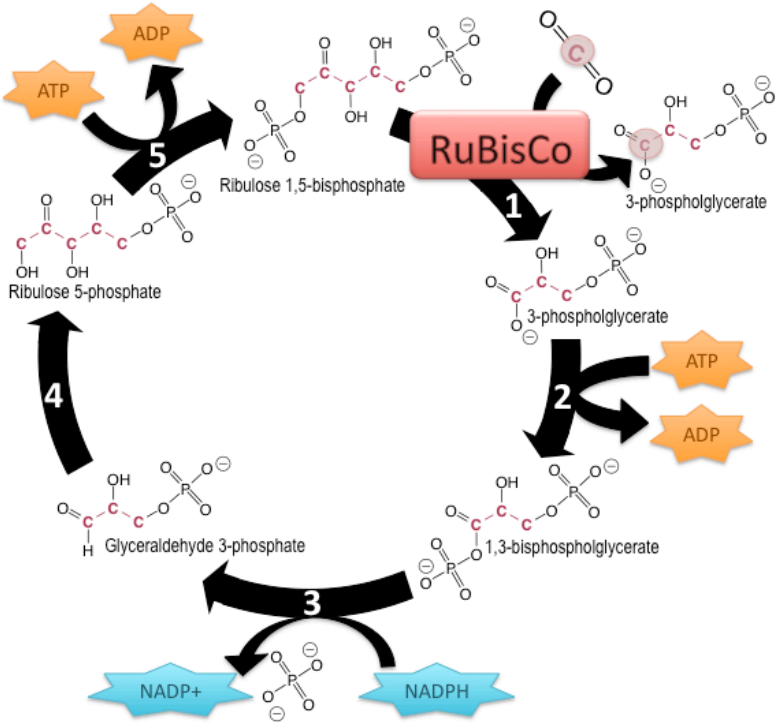

Figure 4. Simplified version of the porcesses defined by the Calvin Cycle.

The Calvin cycle is the primary CO_2 fixation pathway in higher plants. In the chloroplast's stroma ATP and NADPH, the products of the light induced reactions of photosynthesis, are spent to reduce CO_2 to carbon-sugar phosphates.[37] A simplified

version of this complex cycle, involving the participation of eleven different enzymes catalysing thirteen reactions, is represented in Figure 4.

The cycle is initiated by the enzyme Ribulose-1,5-bisphosphate Carboxylase/ Oxygenase (RuBisCO) catalysing the carboxylation of ribulose-1,5-bisphosphate (RuBP) which acts as CO_2 primary acceptor (step 1, Figure 4). The 3-phosphoglycerate (3-PGA) formed is then utilised to form triose phosphates (step 2, Figure 4), glyceraldehyde-3-phosphate (step3, Figure 4) and dihydroxyacetone-phosphate (step 4, Figure 4) via two reactions that consume ATP and NADPH. The regenerative phase of the cycle involves a series of reactions that convert triose phosphates into the CO_2 acceptor RuBP (step 5, Figure 4).

As result of the Calvin cycle, CO_2 molecules are incorporated into the carbon-sugar phosphate glyceraldehyde-3-phosphate (triose-P). Triose-P can be exported to the cytosol where it can be utilised to make soluble sugars, sugar alcohols, soluble oligosacarids or used directly for respiration and amino acid biosynthesis. Alternatively, it can be retained in the chloroplast either to make starch or regenerate the initial CO_2 acceptor RuBP.

The RuBisCO enzyme

RuBisCO is the most abundant enzyme on earth. It is a bifunctional enzyme which catalyses both the carboxylation and the oxygenation of RuBP. The oxygenation of RuBP leads to glycerate-3-pandone and one molecule of glycollate-2-P, the latter is used in photorespiration.

X-ray crystal structures of Rubisco from different organisms have been reported.[38-42] The holoenzyme form I of RuBisCO, present in the oxygenic photosynthetic organisms, is a hexadecamer complex made up of eight small subunits and eight large identical subunits arranged in four dimers. The active site that catalyses the initial CO_2 fixation step of the Calvin cycle is located at the interface between the monomers of each dimer.

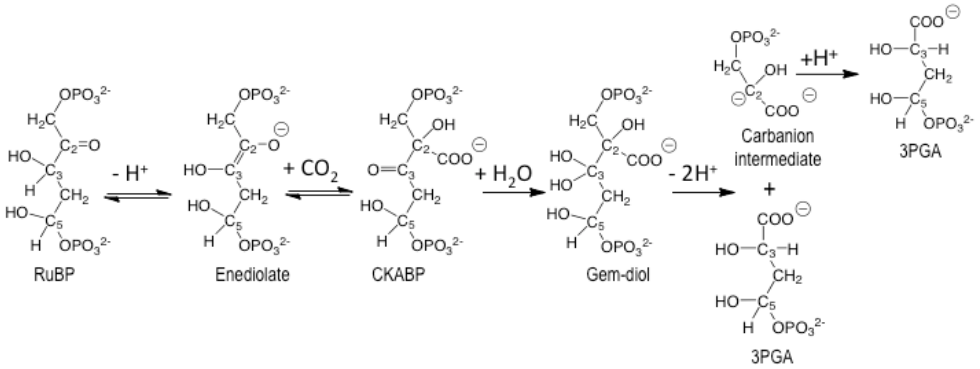

Scheme 3. Five reaction steps in the CO_2 fixation reaction catalyzed by RuBisco enzyme. Enolysation of RuBP assisted by the abstraction of the C_3 proton by KCX201, carboxylation, hydration, C_2-C_3 bond cleavage and stereospecific protonation of C_2 assisted by Lys175. All the aminoacid residues refer to spinach Rubisco.[38, 43]

The enzyme is activated by the capture of CO_2 by carbamylation of a crucial lysosyme residue, Lys201 in spinach's RuBisCO,[38, 43] yielding KCX201 (Figure 5, right) which then binds to a Mg^{2+} ion. The octahedral coordination shell of the metal is completed by Asp203, Glu204 and three more water molecules. Subsequently, a RuBP molecule binds to the Mg^{2+} displacing two of the aqua molecules (Figure 5, left). At this point, the enzyme suffers a conformation change resulting in the occlusion of the active site from the solvent. This "substrate trapped active site" catalyses the sequence of reactions depicted in Scheme 3.

Even though the general reaction steps by which RuBisCO captures CO_2 to react with RuBP are now understood, there are still many uncertainties in the roles played by some key amino acid residues proven to be critical in the process. [43-45]

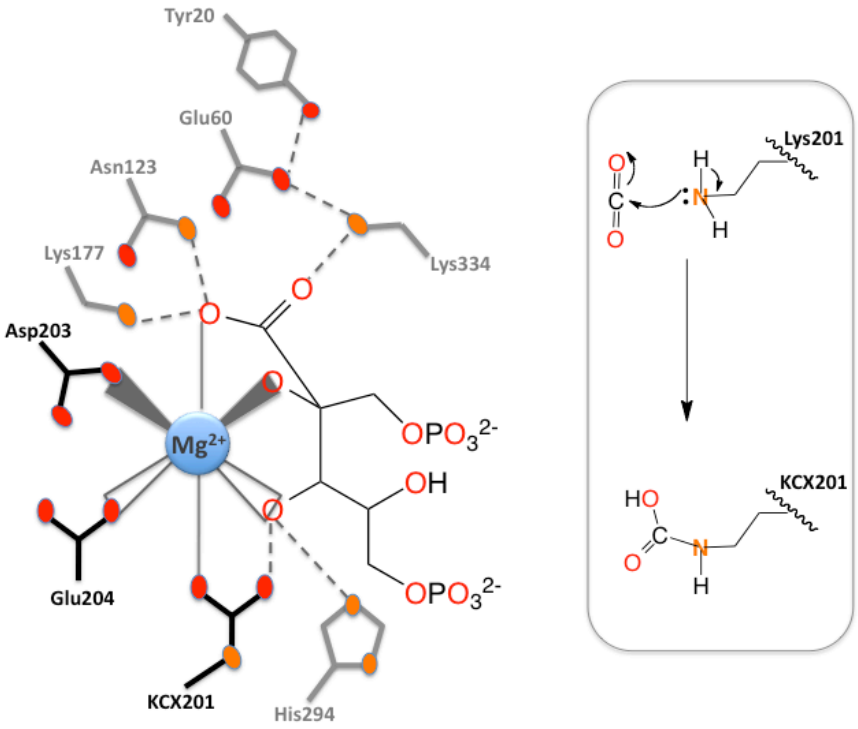

Figure 5. Right, the schematic representation of the structure and ligation of the active site of RuBisCO with Mg^{2+} and 2-carboxy-D-arabinitol-1,5-bisphosphate (2CABP) reaction-intermediate analog used as inhibitor for Rubisco's crystallization.[41, 46] In grey key amino acid residues proven to be involved in crucial hydrogen bonding interactions (dashed lines).Left, carbamylation of Lys201.

1.2. BIO-INSPIRED ARTIFICIAL PHOTOSYNTHESIS

The predicted escalation in energy demand in the near future,[47, 48] added to the increase of global consciousness about the impact of anthropogenic CO_2[49-52] in the planet's climate, has stimulated the search of energy sources other than the combustion of fossil fuels. Amongst all the known energy sources, solar power represents the most promising renewable energy source. Due to the diffuse and intermittent nature of solar radiation, a substantial use of solar energy will require energy storage in a dense and transportable media via chemical bond formation.

Arising from the combination of knowledge from the diverse fields of research contributing to the subject -chemistry, biochemistry, physics, materials science, chemical engineering, environmental studies- many different strategies have been employed to try to mimic nature's ability to photocatalytically convert water into O_2 and a reduced fuel material.[53-55] The key elements and basic processes present in the natural reaction centres must be functionally reproduced in all the artificial endeavours, therefore they must all have at least three indispensable components;

a) A photosensitive material (S in Figure 6) capable of absorbing and generating an electrochemical potential, thus acting as an antenna-reaction centre.

b) An electron donor moiety (D_{ox} in Figure 6) capable of oxidising water as electron source, mimicking the function of OEC in PSII.

c) An electron acceptor moiety (A_{red} in Figure 6) responsible for the final storage of the energy by reducing the election precursors to a fuel.

A first approach into artificial photosynthesis is the so called photo-driven water splitting process (I, Figure 6). Water is oxidised to dioxygen and the protons reduced to dihydrogen (Equations 5-7). The latter could be used as a carbon free solar fuel.

$$2H_2O \rightarrow O_2 + 2H_2 \qquad (\Delta G = 57\ kcal/mol,\ pH = 0) \qquad (5)$$

$$2H_2O(l) \rightarrow O_2(g) + 4H^+(aq) + 4e^- \qquad (E^o_{ox} = -1.23\ V,\ pH = 0\ vs\ NHE) \qquad (6)$$

$2H^+(aq) + 2e^- \rightarrow H_2(g)$ *(E^o_{red} = 0.00 V, pH = 0 vs NHE)* (7)

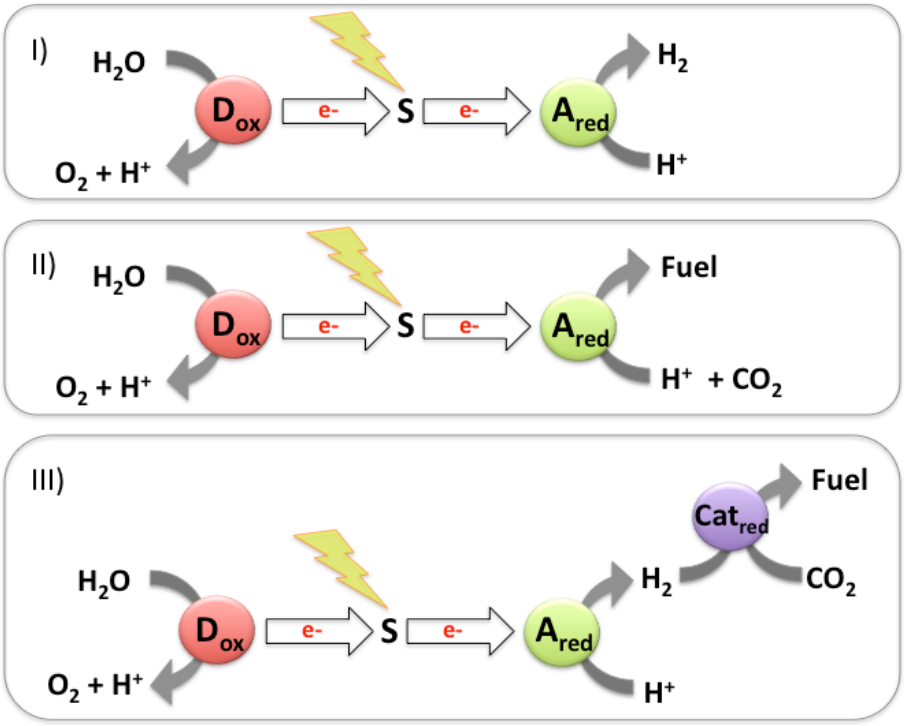

Figure 6. Different setups of the three main components of artificial photosynthesis. The function of artificial photosynthesis starts by photon absorption and activation of a photosensitizer molecule (S), followed by the concomitant electron transfer of the excited electron from an electron donor (D_{ox}) and electron capture by an electron acceptor (A_{red}). The former catalyzes the oxidation of water to dioxygen and the latter the reductive step for the production of H_2 (I) or a carbon based fuel (II) by CO_2 uptake. Alternatively, a second CO_2 reduction catalyst can be used to obtain a fuel by combining CO_2 and H_2 (III).

A second approach, which is at an even less scientifically evolved stage, is the photo-driven CO_2 reduction in water media. It could be carried out by substituting the hydrogen evolving moiety by a catalyst capable of electrocatalytically reduce CO_2 to a high value reduced species (II, Figure 6). Alternatively, the H_2 generated in the water

splitting setup could be employed, as it is in natural photosynthesis, by a third reactive component (Cat_{red}) to reduce CO_2 (III, Figure 6).

From a chemical point of view, the design of a viable and well-characterised photocatalytic artificial system can be tackled by a synthetic modular strategy. Photosensitive molecules as well as molecular catalysts, representing discrete modules, can be independently studied and optimised in view of their future assemble in a solar fuel cell. A device designed taking advantage of the vast current knowledge in the field of photovoltaics. Moreover, the basic physical principles and some of the components of dye sensitized solar cells can be applied to solar fuel cells.[56, 57] A schematic representation of the composition and function of a solar fuel cell is depicted in Figure 7.

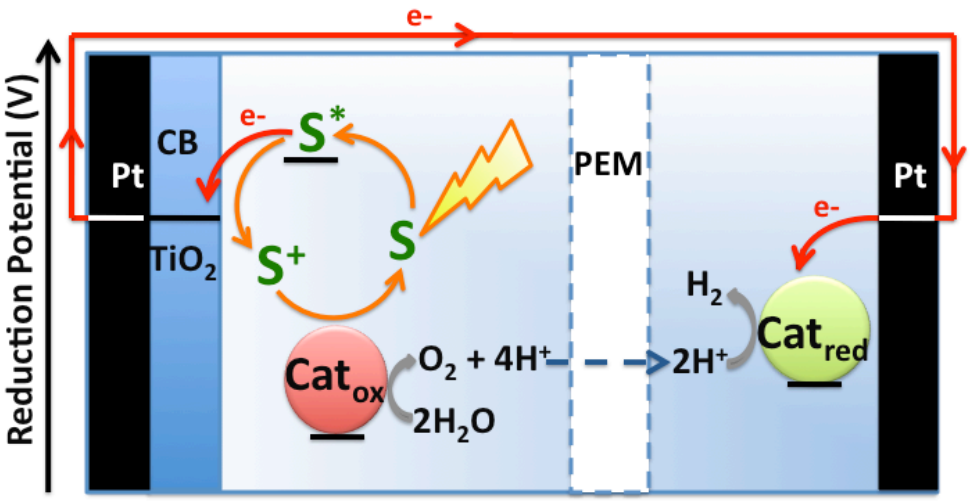

Figure 7. Schematic drawing of the water-splitting photochemical cell. In red the electron transefer in the cell, the orange arrows the excitation-quenching-regeneration process of the dye, light blue dashed arrow represent the proton transfer and in grey the chemical reactions are shown.

Light induced excited states of the chosen photoactive chromophore (S*) inject electrons to the semiconductor's (TiO_2) conduction band (CB). Following, the oxidised S^+ moiety is regenerated (S) by oxidising the water oxidation catalyst (Cat_{ox}). The electrons from TiO_2 are transferred through an electron conductive circuit to a

platinum cathode (Pt) and subsequently to the hydrogen production catalyst (Cat_{red}). Like in PSI andPSII, in a solar fuel cell the two electrochemical reactions, and consequently the generation of the two gases, occurs in different compartments. The pH difference in the two compartments is balanced through a proton exchange membrane (PEM).

While some progress has been made mimicking crucial steps of photosynthesis in artificial systems, researches have not yet developed sufficiently efficient and robust components to be incorporated into a working device for large scale solar fuel production. To date, the main focus of research in the area has been the design and synthesis of molecular photosensitizers and the reduction and oxidation catalysts. Current advances in these key molecular systems for artificial photosynthesis will be discussed in the following sections of this chapter.

1.2.1. Molecular photosensitizers

The light harvesting moiety is a crucial element in artificial photosynthetic devices. The properties required from a photosensitizer may vary from one device to another depending on the specific setup (Figure 8) and the nature of the other components in the device. However, there are some requirements that any photosensitizer must fulfil :

-Absorption bands with a high intensity in a wide range of the visible, near-IR and IR regions.

-Redox properties in the ground and excited states that ensure fast and efficient charge injection into the semiconductor's conduction band.

-Reversibility of the S^+/S redox pair.

As a result, the photosensitizers of choice are usually transition metal complexes with polypiridines, porphyrines or phtalocianines as ligands.[58, 59]

These primary photoactive chromophores, like natural pigments, don not absorb equally at all wavelengths. Inspired by the natural systems, sophisticated artificial

antenna complexes have also been investigated in order to increase the overall efficiency of solar radiation capture. Generally, these complex architectures combine several primary photosensitizers linked by covalent bonds and/or supramolecular interactions to a central site where all the excitation energy is delivered and the electrochemical potential is generated.[60-68]

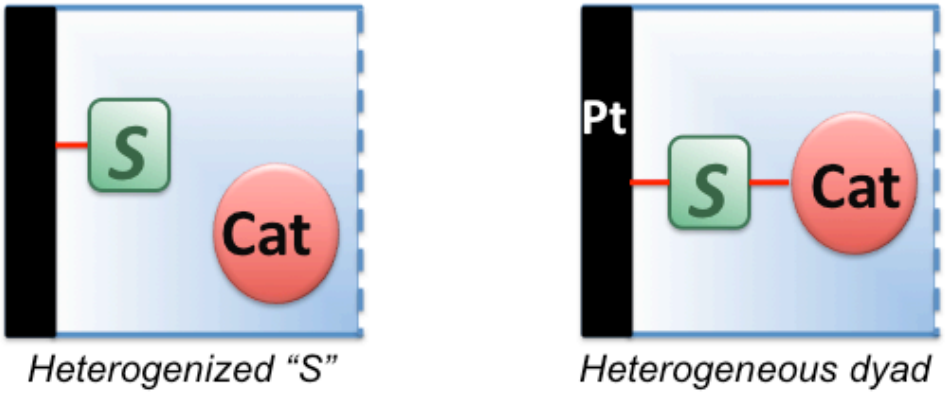

Figure 8. Representation of two of the most viable setups for one of the compartments of a solar fuel device. Pt, semiconducting electrode surface; S, photosensitizer moiety; Cat, oxidation/reduction catalyst.

1.2.2. Molecular catalysts for water reduction

Nature catalyses the two-electron redox proton-to-hydrogen conversion (Equation 7) and its reverse process by using a variety of enzymes referred as to hydrogenases[69, 70] which are responsible for physiological pH regulation. Hydrogenases can be classified in three categories based on their metal content; [NiFe], [FeFe] and metal-free. Even though there are some examples of Iron and Nickel-based catalysts that have been reported to mimic these natural enzymes,[71-73] within the framework of synthetic homogeneous catalysts for hydrogen production most catalysts involve precious metals as iridium, platinum and cobalt.[74-77]

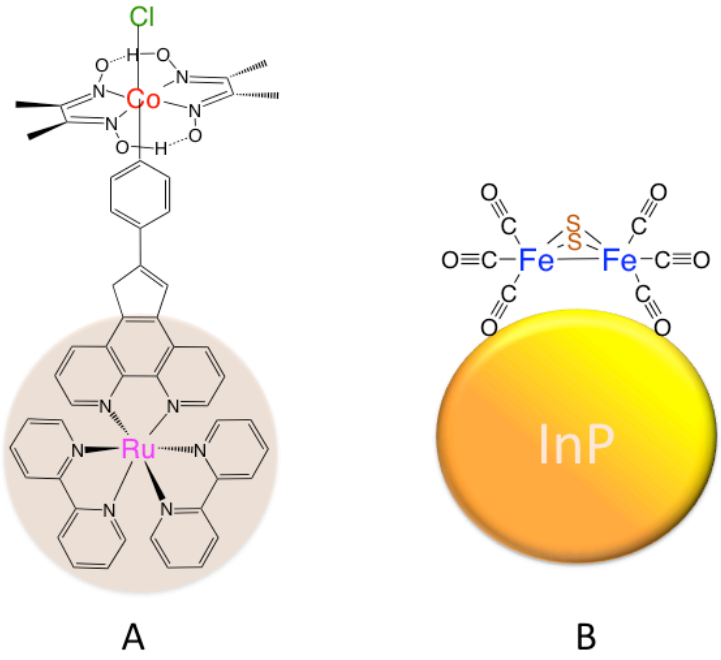

Figure 9. Some recent representatives of catalysts for hydrogen production from water. A, Ruthenium-Cobaloxyme photocatalysts[76] Fe-Fe catalyst adsorved onto InP nanocrystals (orange sphere) [73]

Some innovative examples, have accomplished the photo reduction of water using different strategies.[75, 78, 79] For example, Artero and coo-workers have reported two ruthenium-cobaloxyme photocatalysts for hydrogen production achieving up to 103 turn over numbers (A, Figure 9).[76] Going back to the Fe-Fe hydrogenase-mimicks, Naan et al. have developed a nanophotocathode, in which a gold electrode is covered with InP nanocrystals intercalated with adsorbed catalyst molecules (B, Figure 9).[73]

1.2.3. Molecular catalysts for water oxidation

Water oxidation is the half reaction in artificial photosynthesis responsible for the electron and proton supply for the production of dihydrogen or other reduced materials. The molecular complexity of this reaction, that involves a four-electron oxidation coupled with proton transfer and O–O bond formation, is the origin of the large activation barriers generally associated with it.

Although there are many reported examples of attempts of both structural and functional analogy to the OEC with synthetic manganese compounds,[80-86] to date non of them has been successful to reproduce its function or spectroscopic properties. However, molecularly well characterised synthetic complexes mainly based on Ru and Ir, but also on Co and Fe, have proven to catalytically oxidise water to dioxygen in homogeneous phase.

Polypyridyl aqua Transition Metal complexes

The Ru-H_2O/Ru=O system discovered by Thomas J. Meyer's group more than thirty years ago[87] constitutes the base for the activity of most of the Ru water oxidation catalysts. As we have seen for the PSII, ruthenium aqua polypyridyl complexes take advantage of PCET processes to, by concomitantly losing protons and electrons, reach high oxidation states within a narrow potential range (Scheme 4). Moreover, by PCET high energy oxidation intermediates such as radical species are avoided.

$$Ru^{II}\text{-}OH_2 \underset{+1H^+ +1e^-}{\overset{-1H^+ -1e^-}{\rightleftharpoons}} Ru^{III}\text{-}OH \underset{+1H^+ +1e^-}{\overset{-1H^+ -1e^-}{\rightleftharpoons}} Ru^{IV}=O$$

Scheme 4. Proton coupled electron transfer processes in ruthenium aqua complexes.

If $2e^-$ and $2H^+$ can be obtained from the Ru-H_2O/Ru=O system, the design of complexes containing two Ru-aqua groups seems a rational approach to fulfill the $4e^-$ and $4H^+$ required for the oxidation of water to O_2.

Invoking the natural strategy of cooperation between metal centers, in the early 1980's Meyer et al. reported the first homogeneous water oxidation ruthenium catalyst now known as "the blue dimer" (**A**, Figure 10) which, in the presence of excess of Ce^{IV} gave 13.2 turnover cycles.[88] Significant progress has been made since then in the development of polynuclear ruthenium complexes bearing polypyridyl ligands for catalytic water oxidation.[89-91] For instance, in 2004 Llobet et al. replaced the oxo bridge by the more robust and rigid polypyridyl dinucleating ligand *Hbpp* (3,5-bis(2-pyridyl pyrazole)) in complex *in,in*-$[\{Ru^{II}(trpy)(H_2O)I\}_2(\mu\text{-bpp})]^{3+}$ (**B**, Figure 10). Using Ce^{IV} as chemical oxidant this complex generates dioxygen very rapidly giving TON close to 200, under optimized conditions.

Following a similar strategy, Thummel et al. synthesized a octadentated ligand which acts as hexadentated in $[\{Ru^{II}(pic)(\mu\text{-Cl})\}_2(\mu\text{-binapyr})]^{3+}$ (**C**, Figure 10). This catalyst gave significant TON (538) when more than 9000 equivalents of Ce^{IV} were employed as external oxidant.[89]

Another important ruthenium dinuclear catalyst is the $[\{Ru^{II}(tBu_2Quinone)(OH)\}_2(\mu\text{-btpyan})]^{2+}$ reported by Tanaka et. al. (**D**, Figure 10). The redox active ligands ($tBu_2Quinone$) are thought to act as an electron pool in the catalytic process. When adsorbed onto an ITO electrode at pH = 4, this catalyst was reported to undergo 6730 TONs upon the application of 1.7 V vs Ag/AgCl.[92, 93]

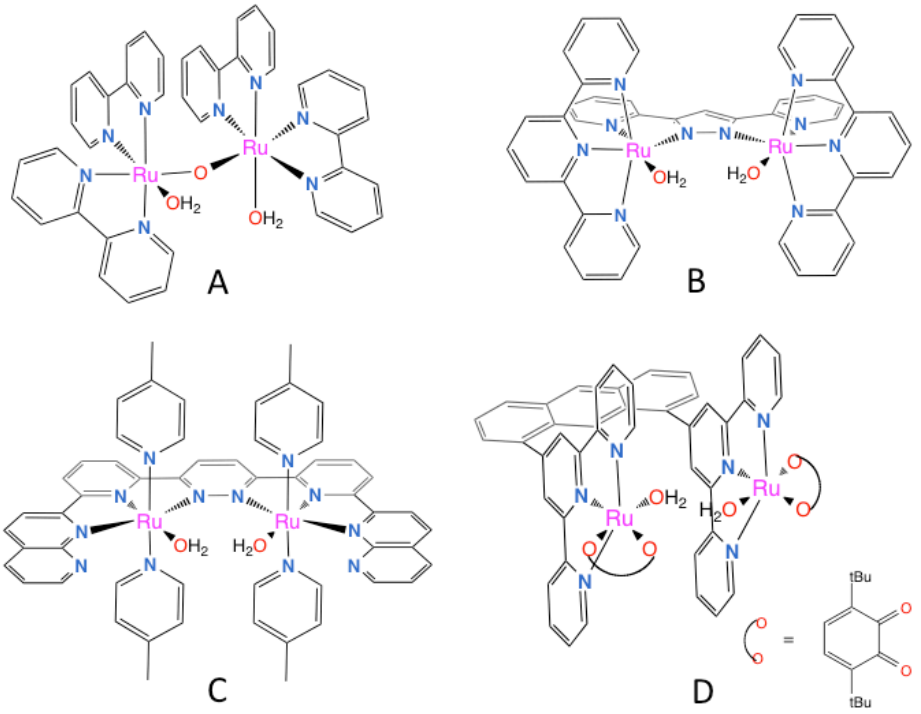

Figure 10. Representative dinuclear ruthenium water oxidation catalysts.[88, 92, 94, 95]

Many mechanistic studies have been carried out for these dinuclear catalysts.[96-101] Even though multiple different proposals have been made over the years, for the different catalysts and by different authors, only few have reported experimental data that sustains them. Summarising these studies, the intra-, inter- or bi-molecular O-O formation may be considered as the most plausible pathways for this complex reaction (Scheme 5).

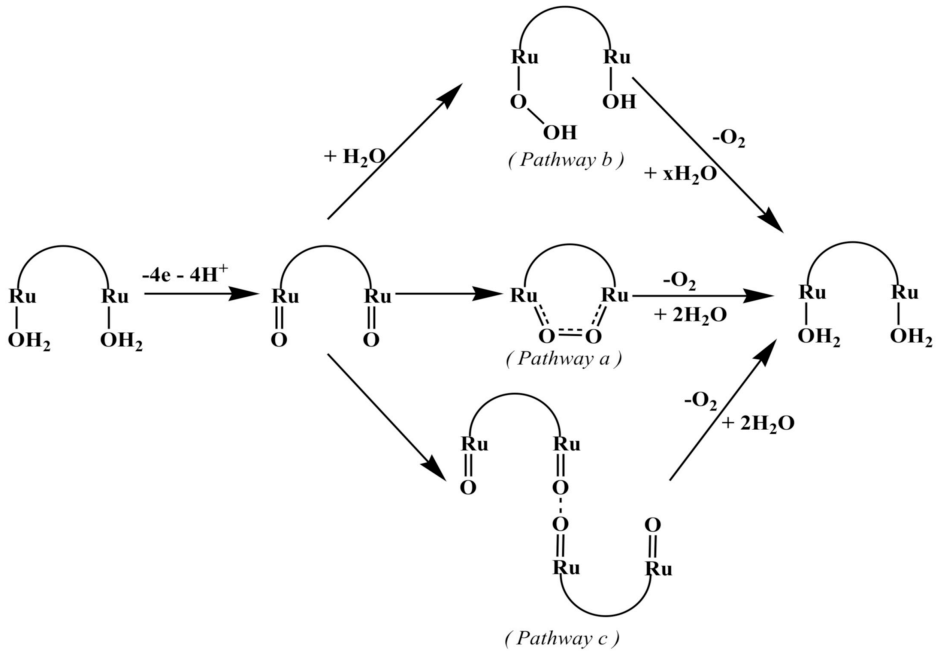

Scheme 5. Proposed water oxidation pathways for dinuclear ruthenium catalysts. Pathway a, Intramolecular O-O coupling followed by reductive elimination of the neighbouring ruthenyl oxoatoms;[98-100, 102, 103] Pathway b, Nucleophilic attack by solvent water to a ruthenyl oxo atom assisted through hydrogen boding by the second metal center; [100] [99]Pathway c, bimolecular O-O coupling involving two catalyst ions [98, 100]

Complementing the previously mentioned dinuclear catalysts, a series of ruthenium-monoaquo complexes bearing multidentate polypyridyl ligands have been found to work as mononuclear homogeneous catalysts for water oxidation undergoing hundreds of TON's[99, 104-106] and even in one case exceeding 1100 TONs with complex [Ru(trpy)(pynap)(Cl)](PF_6) (**E**, Figure 11) (*trpy* is 4,4'-terpyridine; *pynap*, 2-(pyrodyl-2'-yl)-1,8-naphthyridine).[107] These catalysts provide a different catalytic scenario in which the intramolecular O-O bond formation is not possible. The studies reported to date, point in the direction of a mechanism involving nucleophilic attack by solvent water forming peroxidic intermediate species (Pathway B, Scheme 5).[108, 109]

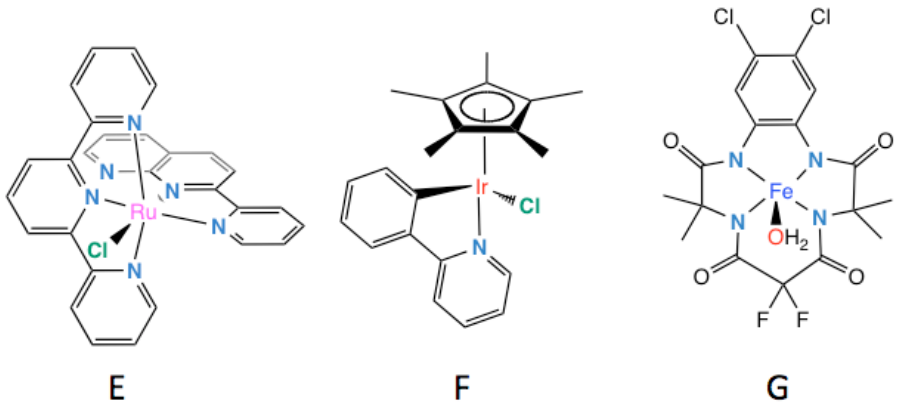

Figure 11. Representative mononuclear precursor compounds of water oxidation catalysts. E, [Ru (trpy)(pynap)(Cl)](PF6)[107]; F, [IrCp*Cl(ppy)][110]; G, Fe complex coordinated with a tetraamido macrocyclic ligand[111]

Even though the activity of these catalysts has mostly been tested using a sacrificial chemical oxidant as Ce^{IV} (Scheme 6), there are some cases in which mono- or dinuclear ruthenium-polypyridyl catalysts have been anchored/absorbed on heterogeneous surfaces,[112-115] enhancing thereby their stability and, potentially, their productivity. One step further, there are a few cases which have proven undergo photo-induced water oxidation catalysis in the presence of a photosensitizer moiety. [116-118]

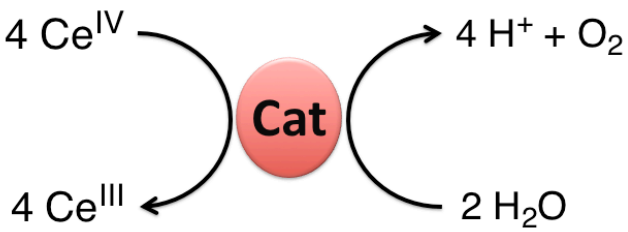

Scheme 6. Chemical oxidation by Ce^{IV} as sacrificial oxidant

In 2008 Bernhard and co-workers[119] reported the first iridium water oxidation catalysts. Oxygen evolution by *cis*–$[Ir^{III}(ppy)_2(H_2O)_2]^+$ (*ppy* = 2-phenyl pyridine anion and functionalized derivatives) catalysts, was confirmed by GC and quantified by a

pressure transducer, reporting spectacular TONs in the order of 2500. This singular catalyst evidenced the potential applicability of transition metals other than Ru and Mn in this important oxidation process. More Ir-based catalysts have been reported since then with really promising performances.[119-122] For example Crabtree and coworkers achieved 1500 TNs and TOFs of 0.9, with complex $[Ir^{III}(Cp^*)(ppy)(Cl)]$ as catalyst precursor (**F**, Figure 10).[110]

A unique example with iron, the Fe complex coordinated with a tetra-amido macrocyclic ligand depicted as **G** in Figure 10, has recently been reported by Bernhard and Collins to achieve moderate TON but TOFs amongst the highest reported in the literature (up to 1.3 s^{-1}) for this oxidative process.[111]

Transition Metal oxo clusters with Polyoxometalate ligands

Polyoxometalates (POMs) are placed at the borderline between molecules and extended solids. Some POMs are capable to act as inorganic ligands through encapsulation of metal clusters. Following this approach, Shannon et al. reported in 2004 the first Ru-POM water oxidation catalyst containing $[Ru^{III}_2Zn_2(H_2O)_2(ZnW_9O_{34})_2]^{14-}$ which worked electrocatalytically giving quite low efficiencies and TONs.[123]

A very important breakthrough in the field was the POM complex $Cs_{10}[Ru_4(\mu\text{-}O)_4(\mu\text{-}OH)_2(H_2O)_4(\gamma\text{-}SiW_{10}O_{36})_2]$ (**H**, Figure 11) published independently and nearly simultaneously by the groups of Bonchio[124] and Hill[125]. This catalyst was reported to achieve 450 cycles of dioxygen formation (TONs) at considerably high rates reaching, under optimised conditions, 0.13 TON/s^{-1}.[126] More recently, a Cobalt based POM has also been published as water oxidation catalyst.[127] The interest of these complexes lies in two aspects; the totally inorganic core that prevents the intermolecular catalyst-with-catalyst deactivation pathways previously observed with polypyridine containing catalysts, and the impossibility of intramolecular O-O bond formation due to the large distance between M-OH moieties in their structure. Based on kinetic studies on compound **H** and supported by DFT, water nucleophilic attack has been proposed as the most plausible pathway.[126, 128]

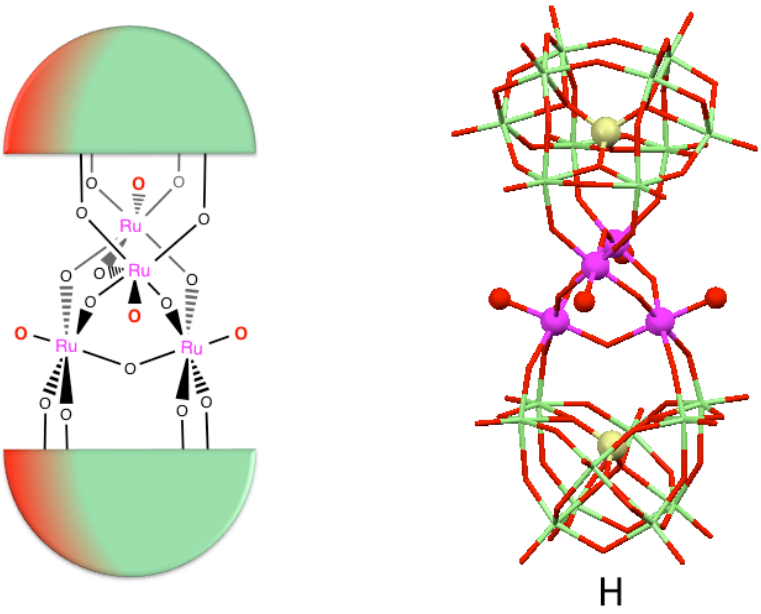

Figure 11. Right, X-ray of the cation $[Ru_4(\mu\text{-}O)_4(\mu\text{-}OH)_2(H_2O)_4(\gamma\text{-}SiW_{10}O_{36})_2]^{10+}$.[124] Left, schematic representation of the tetra-ruthenium core and in green the inorganic ligands.

Electrochemical water oxidation was successfully achieved when the Ru_4-POM catalytic system **H** was immobilised on carbon nanotubes deposited on an ITO covered electrode.[129]Additionally, photoinduced oxygen evolution with this POM system was reported in homogeneous phase, activated by a tetraruthenium photosensitizer molecule.[130]

1.2.4. Electrocatalytic CO_2 reduction

Reduction of CO_2 is a difficult task because of its high stability as the most oxidised carbon compound. High reduction potential is required for electrochemical activation of CO_2 (-1.9 V vs NHE/-2.14 vs SSCE) giving unstable $CO_2^{\bullet-}$. Additionally, rapid reduction involves an over-potential of 0.1-0.6 V. These difficulties can be overcome by the use of PCET in the reduction of CO_2. As was the case in water oxidation, from a

thermodynamic point of view, the more reduced the product obtained, the PCET multi-electron reductions become more favourable as can be seen in equations 8 to 13.

$CO_2 + e^- \rightarrow CO_2^{\cdot-}$ (E^o_{red} = -1.90 at pH7) (8)

$CO_2 + 2H^+ + 2e^- \rightarrow HCOOH$ (E^o_{red}=-0.61 at pH7) (9)

$CO_2 + 2H^+ + 2e^- \rightarrow CO + H_2O$ (E^o_{red}=-0.53 at pH7) (10)

$CO_2 + 4H^+ + 4e^- \rightarrow HCHO + H_2O$ (E^o_{red}= -0.48 at pH7) (11)

$CO_2 + 6H^+ + 6e^- \rightarrow CH_3OH + H_2O$ (E^o_{red}= -0.38 at pH7) (12)

$CO_2 + 8H^+ + 8e^- \rightarrow CH_4 + 2H_2O$ (E^o_{red}= -0.24 at pH7) (13)

Many different metals, such as Hg, Pb and Co amongst others, have been used as electrodes for the reduction of CO_2 in organic solvents and in water.[131, 132] The most common products are formic acid, oxalate and carbon monoxide. Although examples of reduction of CO_2 into methanol and methane have been reported, in these cases data on the mechanism of the process is lacking.

Metal complexes are good candidates to be used as catalysts in the transformation reactions of CO_2. Three main types of transition metal compounds have been studied so far as homogeneous catalysts for electrocatalytic CO_2 reduction:

I) Metal complexes with macrocyclic ligands were the first electrocatalysts reported for this reductive process. The Ni, Co and Fe catalysts produced almost exclusively CO.[133-137]

II) Polypyridyl metal complexes having Re, Ru, Os Co,Fe, Ni, Cu, Pd and Rh as metal centers produce mainly CO and HCOO.[138-146]

III) Phosphine complexes of Rh, Pd and Ni yield CO in acidic acetonitrile and DMF as solvents.[147-153] Also found in this category, Fe and Co complexes containing polyphosphine ligands and weakly coordinated solvent molecules of general formula $[M(Phosphine)_n(CH_3CN)_x]^m$ lead mainly to HCOOH.[154]

In most cases, the production of formate by electrocatalytic CO_2 reduction promoted by transition metal complexes is thought to occur as represented in Scheme 6.

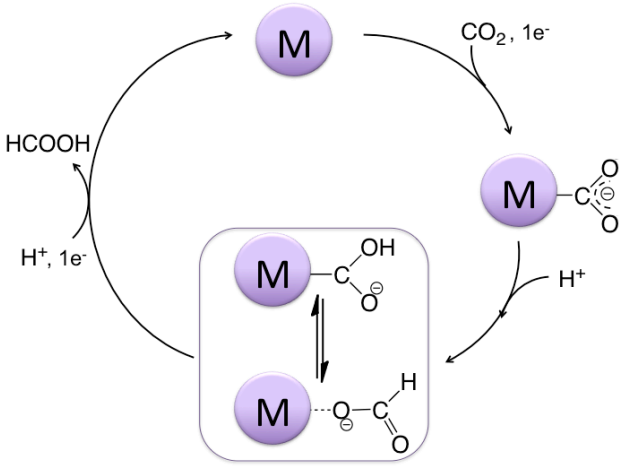

Scheme 7. General mechanism of electocatalytic CO_2 reduction to formic acid. A first coordination of CO_2 to the metal center followed by a sequence of ET, PT, and PCET steps.

Some of these catalysts have also been tested supported on polymer films in pure water solutions or in mixtures of organic solvents with water.[155, 156]

1.2.5. Catalysts for hydrogenative CO_2 reduction

Heterolytic activation of dihydrogen by transition metal complexes has widely been used in catalytic hydrogenation of polar bonds. The heterolysis process typically proceeds in the manner that H^+ is stripped from the M-H_2 moiety with the assistance of an external base or internal ancillary ligand, leaving H^- on the metal centre (Scheme 7).[157]

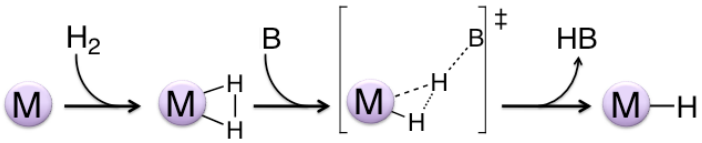

Scheme 8. General mechanism for the heterolytic cleavage of dihydrogen to yield a metal hydride.

Transition metal hydrides have been of high interest for many years because they often play an important role as intermediates in catalytic redox processes such as CO_2 reduction.[158-160] Thus, hydrogenative CO_2 reduction by TM catalysts represents a promising option for the use of carbon dioxide as building block for the synthesis of useful chemicals.

Even though, there have been many reports in the literature describing this process by homogeneous TM-catalysts mainly yielding CO, formic acid and its derivatives,[161-165] the hydrogenative reduction of CO_2 with a catalytic system to be used at large scale is still an unsolved challenge. The major reasons for the difficulty of these reactions are that they are thermodynamically unfavorable, they involve many electron processes and the reaction with at least two gas molecules.

The first step in this reductive process is the insertion of CO_2 in a metal hydride to form formate anion. There are potentially two ways by which this reaction can proceed:

1) The formation of a mono-dentate formato complex, which in some cases is in equilibrium with the bi-dentate formato complex (I, Scheme 9).

2) Generation of a hydrocarbonyl metal complex (II, Scheme 9).

To date, the one that predominates is the first case due to the general instability of the metallocarboxylic acid complex.

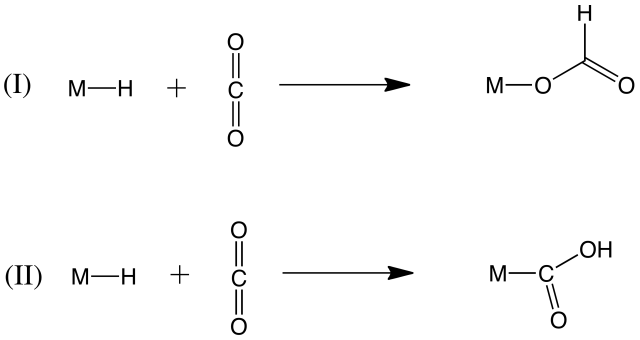

Scheme 9. Two main pathways for CO_2 insertion into a metal hydride.

Rhodium, Ruthenium and to a lesser extent Iridium are the TM more commonly used in catalysts for the conversion of CO_2 to formic acid, formic acid esters and formamides.

Amongst Rh^I catalysts, those with general formula [Rh(H)(diphosphine)] are the most active.[163, 166-169] For example, in the case of the [Rh(H)(hfacac)(dpcb)] (hfacac= hexafluoroacetylacetonate) (**A**, Figure 12) catalyst containing the *dpcb* ($Cy_2P(CH_2)_4PCy_2$,) bulky ligand hydrogenations proceed efficiently at r.t. with relatively low pressures (41 bar) in DMSO (with NEt_3) yielding HCOOH (TON 3005, TOF 1335 h^{-1}). [170]

In the case of ruthenium, Cp^- and phosphine-containing complexes have been extensively studied.[161, 171-175] In the latter case, the use of $scCO_2$ as solvent increases significantly their performance,[172, 176] achieving up to 28 500 TONs and 95 000 h-1 TOF with [Ru(Cl)(OAc)(PMe_3)$_4$] (**B**, Figure 12).[174]

More recently, Ir based catalysts have been introduced in this field,[177-179] achieving in the case of the [Ir^{III}(PNP)] (**C**, Figure 12) (PNP, 2,6-bis((diisopropylphosphino)methyl) pyridine) catalyst reported by Nozaki and co-workers the remarkable TON of 3500 000 and TOF 150 000h^{-1} in aqueous KOH generating potassium formate.[180]

[$NiCl_2$(dcpe)] (**D**, Figure 12) (*dcpe*=$Cy_2P(CH_2)_2PCy_2$) is the most active complex for hydrogenative CO_2 reduction of the other TM catalysts (Ni, Fe, Mo, Pd),[181] but still its performance results in TONs and TOFs really far from the obtained with Rh, Ru and Ir containing catalysts.[161]

In most of the above mentioned catalytic systems an amine acts as promoting agent for the process. The positive effect of the presence of an amine in the media is attributed to the conversion of the formed acid into ammonium formate. The thermodynamics of the process are improved as a consequence of the formation of the weaker acid HNR_3^+, having a K_a four to five orders of magnitude smaller than formic acid. The amine is also thought to play, in some cases, an important role in the heterolytic cleavage of the coordinate hydrogen molecule that yields the hydride species. Therefore, ligands bearing pendant amines were found to improve the catalytic activity of the catalysts.[171, 182]

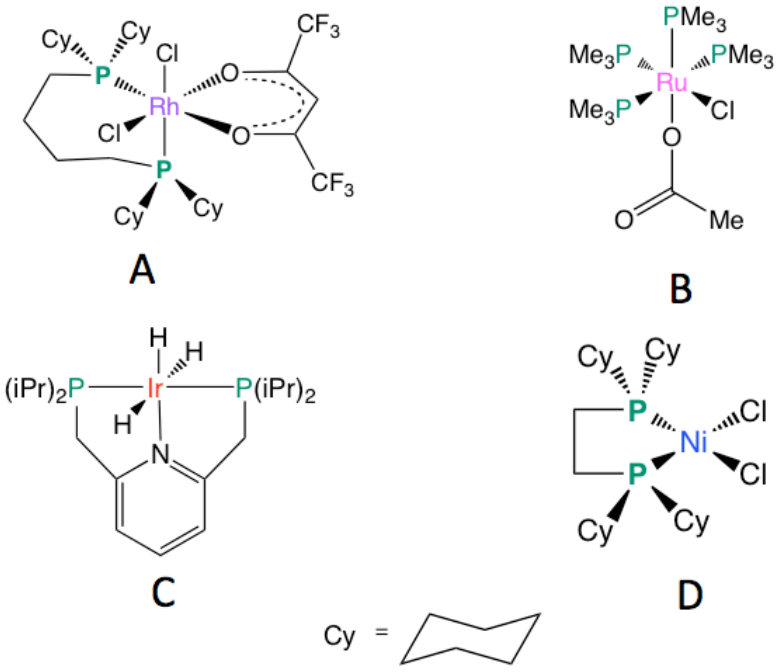

Figure 12. Some significant representatives of the different types of molecular hydrogenative CO_2 reduction catalysts. A, $[Ru(Cl)_2(OAc)(PMe_3)_4]$.[176] B, Rh(hfacac)(dpcb).[165]C, $[Ir^{III}(PNP)(H)_3]$.[180]D, $[NiCl_2(dcpe)]$[181]

The differences in the coordination chemistry of the diverse metal centres and the variable number of labile positions on the structure of the catalysts have given rise to the proposal of very diverse mechanisms but, in most cases, there is a lack of substantial experimental data supporting them.

1.3. REFERENCES

[1] J. Barber, *Q. Rev. Biophys.* **2003**, *36*, 71-89.
[2] R. Hill and F. Bendall, *Nature (London, U. K.)* **1960**, *186*, 136-137.
[3] P. E. Jensen, R. Bassi, E. J. Boekema, J. P. Dekker, S. Jansson, D. Leister, C. Robinson and H. V. Scheller, *Biochim. Biophys. Acta, Bioenerg.* **2007**, *1767*, 335-352.
[4] T. Renger and E. Schlodder, *Adv. Photosynth. Respir.* **2006**, *24*, 595-610.
[5] G. Renger and T. Renger, *Photosynth. Res.* **2008**, *98*, 53-80.
[6] J. P. Thornber and J. P. Markwell, *Trends Biochem. Sci. (Pers. Ed.)* **1981**, *6*, 122-125.
[7] K. Nakayama, M. Mimuro, Y. Nishimura, I. Yamazaki and M. Okada, *Biochim. Biophys. Acta, Bioenerg.* **1994**, *1188*, 117-124.
[8] H. Scheer, *Adv. Photosynth. Respir.* **2003**, *13*, 29-81.
[9] G. C. Papageorgiou, *Adv. Photosynth. Respir.* **2004**, *19*, 43-63.
[10] T. Zhang, W.-j. Wu, B.-r. Hu, Y.-h. Man and Z.-m. Liu, *Adv. Nat. Sci. 3*, 291-298.
[11] P. D. Harvey, C. Stern, C. P. Gros and R. Guilard, *J. Inorg. Biochem.* **2008**, *102*, 395-405.
[12] K. Redding and A. van der Est, *Adv. Photosynth. Respir.* **2006**, *24*, 413-437.
[13] D. A. Walker, *Trends Plant Sci.* **2002**, *7*, 183-185.
[14] R. Hill, *Essays Biochem.* **1965**, *1*, 121-151.
[15] R. P. Hangarter and N. E. Good, *Photosynth. Res.* **1988**, *19*, 237-250.
[16] T. Bizouarn, Y. de Kouchkovsky and F. Haraux, *Biochemistry* **1991**, *30*, 6847-6853.
[17] C. von Ballmoos and P. Dimroth, *Biochemistry* **2007**, *46*, 11800-11809.
[18] B. Kok, B. Forbush and M. McGloin, *Photochem. Photobiol.* **1970**, *11*, 457-475.
[19] G. Renger and Govindjee, *Photosynth. Res.* **1985**, *6*, 33-55.
[20] G. Renger, *Biochim. Biophys. Acta, Bioenerg.* **2001**, *1503*, 210-228.
[21] M. Haumann, P. Liebisch, C. Muller, M. Barra, M. Grabolle and H. Dau, *Science* **2005**, *310*, 1019-1021.
[22] L. Iuzzolino, J. Dittmer, W. Doerner, W. Meyer-Klaucke and H. Dau, *Biochemistry* **1998**, *37*, 17112-17119.
[23] K. N. Ferreira, T. M. Iverson, K. Maghlaoui, J. Barber and S. Iwata, *Science (Washington, DC, U. S.)* **2004**, *303*, 1831-1838.
[24] B. Loll, J. Kern, W. Saenger, A. Zouni and J. Biesiadka, *Nature (London, U. K.)* **2005**, *438*, 1040-1044.
[25] J. Yano, J. Kern, K. Sauer, M. J. Latimer, Y. Pushkar, J. Biesiadka, B. Loll, W. Saenger, J. Messinger, A. Zouni and V. K. Yachandra, *Science (Washington, DC, U. S.)* **2006**, *314*, 821-825.
[26] J. Barber, *Inorg. Chem. (Washington, DC, U. S.)* **2008**, *47*, 1700-1710.
[27] R. J. Service, W. Hillier and R. J. Debus, *Biochemistry 49*, 6655-6669.
[28] H. Suzuki, M. Sugiura and T. Noguchi, *Biochemistry* **2008**, *47*, 11024-11030.
[29] M. Iizasa, H. Suzuki and T. Noguchi, *Biochemistry* **2010**, *49*, 3074-3082.
[30] R. J. Service, W. Hillier and R. J. Debus, *Biochemistry* **2010**, *49*, 6655-6669.
[31] J. Yano and V. K. Yachandra, *Inorg. Chem. (Washington, DC, U. S.)* **2008**, *47*, 1711-1726.
[32] K. Kawakami, Y. Umena, N. Kamiya and J.-R. Shen, *Proc. Natl. Acad. Sci. U. S. A.* **2009**, *106*, 8567-8572.
[33] P. E. M. Siegbahn, *Acc. Chem. Res.* **2009**, *42*, 1871-1880.
[34] B. B. Buchanan and D. I. Arnon, *Photosynth. Res.* **1990**, *24*, 47-53.
[35] R. Schauder, B. Eikmanns, R. K. Thauer, F. Widdel and G. Fuchs, *Arch. Microbiol.* **1986**, *145*, 162-172.
[36] G. Strauss and G. Fuchs, *Eur. J. Biochem.* **1993**, *215*, 633-643.

[37] C. A. Raines, *Photosynth. Res.* **2003**, *75*, 1-10.
[38] C. I. Braenden, G. Schneider, Y. Lindqvist, I. Andersson, S. Knight and G. H. Lorimer, *Philos. Trans. R. Soc. London, B* **1986**, *313*, 359-365.
[39] M. S. Chapman, W. W. Smith, S. W. Suh, D. Cascio, A. Howard, R. Hamlin, N. H. Xuong and D. Eisenberg, *Philos Trans R Soc Lond B Biol Sci* **1986**, *313*, 367-378.
[40] S. Knight, I. Andersson and C. I. Braenden, *Science (Washington, D. C., 1883-)* **1989**, *244*, 702-705.
[41] I. Andersson, *J Mol Biol* **1996**, *259*, 160-174.
[42] S. Hansen, E. Hough and K. Andersen, *Acta Crystallogr., Sect. D: Biol. Crystallogr.* **1999**, *D55*, 310-313.
[43] C. Li, M. E. Salvucci and A. R. Portis, Jr., *J. Biol. Chem.* **2005**, *280*, 24864-24869.
[44] F. J. van de Loo and M. E. Salvucci, *Biochemistry* **1998**, *37*, 4621-4625.
[45] A. R. Portis, Jr. and M. A. J. Parry, *Photosynth. Res.* **2007**, *94*, 121-143.
[46] G. H. Lorimer, S. Gutteridge and G. S. Reddy, *J. Biol. Chem.* **1989**, *264*, 9873-9879.
[47] N. S. Lewis and D. G. Nocera, *Proc. Natl. Acad. Sci. U. S. A.* **2006**, *103*, 15729-15735.
[48] N. Armaroli and V. Balzani, *Angew. Chem., Int. Ed.* **2007**, *46*, 52-66.
[49] J. G. Canadell, C. Le Quere, M. R. Raupach, C. B. Field, E. T. Buitenhuis, P. Ciais, T. J. Conway, N. P. Gillett, R. A. Houghton and G. Marland, *Proc. Natl. Acad. Sci. U. S. A.* **2007**, *104*, 18866-18870, S18866/18861-S18866/18865.
[50] S. Rahmstorf, A. Cazenave, J. A. Church, J. E. Hansen, R. F. Keeling, D. E. Parker and R. C. J. Somerville, *Science (Washington, DC, U. S.)* **2007**, *316*, 709.
[51] M. R. Raupach, G. Marland, P. Ciais, C. Le Quere, J. G. Canadell, G. Klepper and C. B. Filed, *Proc. Natl. Acad. Sci. U. S. A.* **2007**, *104*, 10288-10293.
[52] T. R. Karl and K. E. Trenberth, *Science (Washington, DC, U. S.)* **2003**, *302*, 1719-1723.
[53] A. J. Bard and M. A. Fox, *Acc. Chem. Res.* **1995**, *28*, 141-145.
[54] D. Carrieri, D. Kolling, G. Ananyev and G. C. Dismukes, *Ind. Biotechnol.* **2006**, *2*, 133-137.
[55] L. B. Brentner, J. Peccia and J. B. Zimmerman, *Environ. Sci. Technol.* **2010**, *44*, 2243-2254.
[56] M. Gratzel, *Nature (London, U. K.)* **2001**, *414*, 338-344.
[57] M. Gratzel, *Inorg Chem* **2005**, *44*, 6841-6851.
[58] K. Kalyanasundaram and M. Gratzel, *Coord. Chem. Rev.* **1998**, *177*, 347-414.
[59] C. Klein, K. Nazeeruddin Md, D. Di Censo, P. Liska and M. Gratzel, *Inorg Chem* **2004**, *43*, 4216-4226.
[60] D. Gust, T. A. Moore and A. L. Moore, *Acc. Chem. Res.* **2009**, *42*, 1890-1898.
[61] J. Savolainen, R. Fanciulli, N. Dijkhuizen, A. L. Moore, J. Hauer, T. Buckup, M. Motzkus and J. L. Herek, *Springer Ser. Chem. Phys.* **2009**, *92*, 454-456.
[62] B. A. Gregg and U. Resch, *J. Photochem. Photobiol., A* **1995**, *87*, 157-162.
[63] B. Branchi, G. Bergamini, L. Fiandro, P. Ceroni, F. Voegtle and F.-G. Klaerner, *Chem. Commun. (Cambridge, U. K.)* **2010**, *46*, 3571-3573.
[64] M. R. Wasielewski, *Acc. Chem. Res.* **2009**, *42*, 1910-1921.
[65] S. Schlundt, G. Kuzmanich, F. Spaenig, G. d. M. Rojas, C. Kovacs, M. A. Garcia-Garibay, D. M. Guldi and A. Hirsch, *Chem.--Eur. J.* **2009**, *15*, 12223-12233, S12223/12221-S12223/12226.
[66] C. V. Kumar and M. R. Duff, *J. Am. Chem. Soc.* **2009**, *131*, 16024-16026.
[67] N. Aratani, D. Kim and A. Osuka, *Acc. Chem. Res.* **2009**, *42*, 1922-1934.
[68] N. Solladie, R. Rein and M. Walther, *J. Porphyrins Phthalocyanines* **2007**, *11*, 375-382.
[69] W. Lubitz, E. Reijerse and M. van Gastel, *Chem. Rev. (Washington, DC, U. S.)* **2007**, *107*, 4331-4365.
[70] A. Silakov, E. J. Reijerse, S. P. J. Albracht, E. C. Hatchikian and W. Lubitz, *J. Am. Chem. Soc.* **2007**, *129*, 11447-11458.
[71] C. Tard, X. Liu, S. K. Ibrahim, M. Bruschi, L. De Gioia, S. C. Davies, X. Yang, L.-S. Wang, G. Sawers and C. J. Pickett, *Nature (London, U. K.)* **2005**, *433*, 610-613.

[72] L. Schwartz, J. Ekstrom, R. Lomoth and S. Ott, *Chem Commun (Camb)* **2006**, 4206-4208.
[73] T. Nann, S. K. Ibrahim, P.-M. Woi, S. Xu, J. Ziegler and C. J. Pickett, *Angew. Chem., Int. Ed.* **2010**, *49*, 1574-1577.
[74] Y. Oudart, V. Artero, J. Pecaut and M. Fontecave, *Inorg Chem* **2006**, *45*, 4334-4336.
[75] K. Sakai and H. Ozawa, *Coord. Chem. Rev.* **2007**, *251*, 2753-2766.
[76] A. Fihri, V. Artero, M. Razavet, C. Baffert, W. Leibl and M. Fontecave, *Angew. Chem., Int. Ed.* **2008**, *47*, 564-567.
[77] M. S. Lowry, J. I. Goldsmith, J. D. Slinker, R. Rohl, R. A. Pascal, Jr., G. G. Malliaras and S. Bernhard, *Chem. Mater.* **2005**, *17*, 5712-5719.
[78] H. Ozawa, M. Haga and K. Sakai, *J. Am. Chem. Soc.* **2006**, *128*, 4926-4927.
[79] N. Sutin, C. Creutz and E. Fujita, *Comments Inorg. Chem.* **1997**, *19*, 67-92.
[80] J. Limburg, J. S. Vrettos, L. M. Liable-Sands, A. L. Rheingold, R. H. Crabtree and G. W. Brudvig, *Science (Washington, D. C.)* **1999**, *283*, 1524-1527.
[81] R. Tagore, H. Crabtree Robert and W. Brudvig Gary, *Inorg Chem* **2008**, *47*, 1815-1823.
[82] M. Yagi, K. V. Wolf, P. J. Baesjou, S. L. Bernasek and G. C. Dismukes, *Angew. Chem., Int. Ed.* **2001**, *40*, 2925-2928.
[83] W. F. Ruettinger, C. Campana and G. C. Dismukes, *J. Am. Chem. Soc.* **1997**, *119*, 6670-6671.
[84] H. H. Thorp, J. E. Sarneski, R. J. Kulawiec, G. W. Brudvig, R. H. Crabtree and G. C. Papaefthymiou, *Inorg. Chem.* **1991**, *30*, 1153-1155.
[85] G. W. Brudvig and R. H. Crabtree, *Prog. Inorg. Chem.* **1989**, *37*, 99-142.
[86] W. F. Ruettinger and G. C. Dismukes, *Inorg. Chem.* **2000**, *39*, 4186.
[87] T. J. Meyer and M. H. V. Huynh, *Inorg. Chem.* **2003**, *42*, 8140-8160.
[88] S. W. Gersten, G. J. Samuels and T. J. Meyer, *J. Am. Chem. Soc.* **1982**, *104*, 4029-4030.
[89] I. Romero, M. Rodriguez, C. Sens, J. Mola, M. R. Kollipara, L. Francas, E. Mas-Marza, L. Escriche and A. Llobet, *Inorg. Chem. (Washington, DC, U. S.)* **2008**, *47*, 1824-1834.
[90] X. Sala, I. Romero, M. Rodriguez, L. Escriche and A. Llobet, *Angew. Chem., Int. Ed.* **2009**, *48*, 2842-2852.
[91] J. J. Concepcion, J. W. Jurss, M. K. Brennaman, P. G. Hoertz, A. O. T. Patrocinio, N. Y. Murakami Iha, J. L. Templeton and T. J. Meyer, *Acc. Chem. Res.* **2009**, *42*, 1954-1965.
[92] T. Wada, K. Tsuge and K. Tanaka, *Inorg. Chem.* **2001**, *40*, 329-337.
[93] J. T. Muckerman, D. E. Polyansky, T. Wada, K. Tanaka and E. Fujita, *Inorg. Chem. (Washington, DC, U. S.)* **2008**, *47*, 1787-1802.
[94] C. Sens, I. Romero, M. Rodriguez, A. Llobet, T. Parella and J. Benet-Buchholz, *J. Am. Chem. Soc.* **2004**, *126*, 7798-7799.
[95] Z. Deng, H.-W. Tseng, R. Zong, D. Wang and R. Thummel, *Inorg. Chem. (Washington, DC, U. S.)* **2008**, *47*, 1835-1848.
[96] S. Romain, L. Vigara and A. Llobet, *Acc. Chem. Res.* **2009**, *42*, 1944-1953.
[97] F. Liu, J. J. Concepcion, J. W. Jurss, T. Cardolaccia, J. L. Templeton and T. J. Meyer, *Inorg. Chem. (Washington, DC, U. S.)* **2008**, *47*, 1727-1752.
[98] R. A. Binstead, C. W. Chronister, J. Ni, C. M. Hartshorn and T. J. Meyer, *J. Am. Chem. Soc.* **2000**, *122*, 8464-8473.
[99] M. Z. Ertem, T. K. Todorova, A. Llobet, L. Gagliardi and C. J. Cramer, *Abstracts of Papers, 239th ACS National Meeting, San Francisco, CA, United States, March 21-25, 2010* COMP-176.
[100] H. Yamada, W. F. Siems, T. Koike and J. K. Hurst, *J. Am. Chem. Soc.* **2004**, *126*, 9786-9795.
[101] N. Planas, S. Romain, S. Roeser, X. Sala, F. Bozoglian and A. Llobet, *Abstract of Papers, 238th ACS National Meeting, Washington, DC, United States, August 16-20, 2009* **2009**, CATL-030.
[102] S. Romain, F. Bozoglian, X. Sala and A. Llobet, *J. Am. Chem. Soc.* **2009**, *131*, 2768-2769.
[103] F. Bozoglian, S. Romain, M. Z. Ertem, T. K. Todorova, C. Sens, J. Mola, M. Rodriguez, I. Romero, J. Benet-Buchholz, X. Fontrodona, C. J. Cramer, L. Gagliardi and A. Llobet, *J. Am. Chem. Soc.* **2009**, *131*, 15176-15187.

[104] R. Zong and R. P. Thummel, *J. Am. Chem. Soc.* **2005**, *127*, 12802-12803.
[105] J. J. Concepcion, J. W. Jurss, J. L. Templeton and T. J. Meyer, *J. Am. Chem. Soc.* **2008**, *130*, 16462-16463.
[106] X. Sala, Z. Ertem Mehmed, L. Vigara, K. Todorova Tanya, W. Chen, C. Rocha Reginaldo, F. Aquilante, J. Cramer Christopher, L. Gagliardi and A. Llobet, *Angew Chem Int Ed Engl* **2010**, *49*, 7745-7747.
[107] H.-W. Tseng, R. Zong, J. T. Muckerman and R. Thummel, *Inorg. Chem. (Washington, DC, U. S.)* **2008**, *47*, 11763-11773.
[108] J. J. Concepcion, M.-K. Tsai, J. T. Muckerman and T. J. Meyer, *J. Am. Chem. Soc.* **2010**, *132*, 1545-1557.
[109] X. Sala, M. Z. Ertem, L. Vigara, T. K. Todorova, W. Chen, R. C. Rocha, F. Aquilante, C. J. Cramer, L. Gagliardi and A. Llobet, *Angew. Chem., Int. Ed.* **2010**, *49*, 7745-7747, S7745/7741-S7745/7727.
[110] J. D. Blakemore, N. D. Schley, D. Balcells, J. F. Hull, G. W. Olack, C. D. Incarvito, O. Eisenstein, G. W. Brudvig and R. H. Crabtree, *J. Am. Chem. Soc.* **2010**, *132*, 16017-16029.
[111] W. C. Ellis, N. D. McDaniel, S. Bernhard and T. J. Collins, *J. Am. Chem. Soc.* **2010**, *132*, 10990-10991.
[112] J. W. Jurss, J. C. Concepcion, M. R. Norris, J. L. Templeton and T. J. Meyer, *Inorg. Chem. (Washington, DC, U. S.)* **2010**, *49*, 3980-3982.
[113] L. Francas, X. Sala, J. Benet-Buchholz, L. Escriche and A. Llobet, *ChemSusChem* **2009**, *2*, 321-329.
[114] J. Mola, E. Mas-Marza, X. Sala, I. Romero, M. Rodriguez, C. Vinas, T. Parella and A. Llobet, *Angew. Chem., Int. Ed.* **2008**, *47*, 5830-5832.
[115] J. J. Concepcion, J. W. Jurss, P. G. Hoertz and T. J. Meyer, *Angew. Chem., Int. Ed.* **2009**, *48*, 9473-9476, S9473/9471-S9473/9411.
[116] Y. Xu, L. Duan, L. Tong, B. Aakermark and L. Sun, *Chem. Commun. (Cambridge, U. K.)* **2010**, *46*, 6506-6508.
[117] H. Yamazaki, A. Shouji, M. Kajita and M. Yagi, *Coord. Chem. Rev.* **2010**, *254*, 2483-2491.
[118] L. Duan, Y. Xu, M. Gorlov, L. Tong, S. Andersson and L. Sun, *Chem.--Eur. J.* **2010**, *16*, 4659-4668, S4659/4651-S4659/4656.
[119] N. D. McDaniel, F. J. Coughlin, L. L. Tinker and S. Bernhard, *J. Am. Chem. Soc.* **2008**, *130*, 210-217.
[120] S. Metz and S. Bernhard, *Chem. Commun. (Cambridge, U. K.)* **2010**, *46*, 7551-7553.
[121] J. F. Hull, D. Balcells, J. D. Blakemore, C. D. Incarvito, O. Eisenstein, G. W. Brudvig and R. H. Crabtree, *J. Am. Chem. Soc.* **2009**, *131*, 8730-8731.
[122] R. Lalrempuia, N. D. McDaniel, H. Mueller-Bunz, S. Bernhard and M. Albrecht, *Angew. Chem., Int. Ed.* **2010**, *49*, 9765-9768.
[123] A. R. Howells, A. Sankarraj and C. Shannon, *J. Am. Chem. Soc.* **2004**, *126*, 12258-12259.
[124] A. Sartorel, M. Carraro, G. Scorrano, R. De Zorzi, S. Geremia, N. D. McDaniel, S. Bernhard and M. Bonchio, *J. Am. Chem. Soc.* **2008**, *130*, 5006-5007.
[125] V. Geletii Yurii, B. Botar, P. Kogerler, A. Hillesheim Daniel, G. Musaev Djamaladdin and L. Hill Craig, *Angew Chem Int Ed Engl* **2008**, *47*, 3896-3899.
[126] A. Sartorel, P. Miro, E. Salvadori, S. Romain, M. Carraro, G. Scorrano, M. Di Valentin, A. Llobet, C. Bo and M. Bonchio, *J. Am. Chem. Soc.* **2009**, *131*, 16051-16053.
[127] Q. Yin, J. M. Tan, C. Besson, Y. V. Geletii, D. G. Musaev, A. E. Kuznetsov, Z. Luo, K. I. Hardcastle and C. L. Hill, *Science (Washington, DC, U. S.)* **2010**, *328*, 342-345.
[128] A. E. Kuznetsov, Y. V. Geletii, C. L. Hill, K. Morokuma and D. G. Musaev, *J. Am. Chem. Soc.* **2009**, *131*, 6844-6854.

[129] F. M. Toma, A. Sartorel, M. Iurlo, M. Carraro, P. Parisse, C. Maccato, S. Rapino, B. R. Gonzalez, H. Amenitsch, T. Da Ros, L. Casalis, A. Goldoni, M. Marcaccio, G. Scorrano, G. Scoles, F. Paolucci, M. Prato and M. Bonchio, *Nat. Chem.* **2010**, *2*, 826-831.
[130] F. Puntoriero, G. La Ganga, A. Sartorel, M. Carraro, G. Scorrano, M. Bonchio and S. Campagna, *Chem. Commun. (Cambridge, U. K.)* **2010**, *46*, 4725-4727.
[131] M. Gattrell, N. Gupta and A. Co, *J. Electroanal. Chem.* **2006**, *594*, 1-19.
[132] A. Gennaro, A. A. Isse, M.-G. Severin, E. Vianello, I. Bhugun and J.-M. Saveant, *J. Chem. Soc., Faraday Trans.* **1996**, *92*, 3963-3968.
[133] J. P. Collin, A. Jouaiti and J. P. Sauvage, *Inorg. Chem.* **1988**, *27*, 1986-1990.
[134] M. Hammouche, D. Lexa, J. M. Saveant and M. Momenteau, *J. Electroanal. Chem. Interfacial Electrochem.* **1988**, *249*, 347-351.
[135] M. Hammouche, D. Lexa, M. Momenteau and J. M. Saveant, *J. Am. Chem. Soc.* **1991**, *113*, 8455-8466.
[136] I. Bhugun, D. Lexa and J.-M. Saveant, *J. Am. Chem. Soc.* **1996**, *118*, 1769-1776.
[137] J. Grodkowski, P. Neta, E. Fujita, A. Mahammed, L. Simkhovich and Z. Gross, *J. Phys. Chem. A* **2002**, *106*, 4772-4778.
[138] H. Ishida, K. Fujiki, T. Ohba, K. Ohkubo, K. Tanaka, T. Terada and T. Tanaka, *J. Chem. Soc., Dalton Trans.* **1990**, 2155-2160.
[139] H. Nagao, T. Mizukawa and K. Tanaka, *Chem. Lett.* **1993**, 955-958.
[140] H. Nakajima, Y. Kushi, H. Nagao and K. Tanaka, *Organometallics* **1995**, *14*, 5093-5098.
[141] T. Mizukawa, K. Tsuge, H. Nakajima and K. Tanaka, *Angew. Chem., Int. Ed.* **1999**, *38*, 362-363.
[142] C. M. Bolinger, B. P. Sullivan, D. Conrad, J. A. Gilbert, N. Story and T. J. Meyer, *J. Chem. Soc., Chem. Commun.* **1985**, 796-797.
[143] C. M. Bolinger, N. Story, B. P. Sullivan and T. J. Meyer, *Inorg. Chem.* **1988**, *27*, 4582-4587.
[144] M. R. M. Bruce, E. Megehee, B. P. Sullivan, H. H. Thorp, T. R. O'Toole, A. Downard, J. R. Pugh and T. J. Meyer, *Inorg. Chem.* **1992**, *31*, 4864-4873.
[145] D. Ooyama, T. Tomon, K. Tsuge and K. Tanaka, *J. Organomet. Chem.* **2001**, *619*, 299-304.
[146] P. Christensen, A. Hamnett, A. V. G. Muir and J. A. Timney, *J. Chem. Soc., Dalton Trans.* **1992**, 1455-1463.
[147] S. Slater and J. H. Wagenknecht, *J. Am. Chem. Soc.* **1984**, *106*, 5367-5368.
[148] D. L. DuBois, A. Miedaner and R. C. Haltiwanger, *J. Am. Chem. Soc.* **1991**, *113*, 8753-8764.
[149] P. R. Bernatis, A. Miedaner, R. C. Haltiwanger and D. L. DuBois, *Organometallics* **1994**, *13*, 4835-4843.
[150] A. M. Herring, B. D. Steffey, A. Miedaner, S. A. Wander and D. L. DuBois, *Inorg. Chem.* **1995**, *34*, 1100-1109.
[151] B. D. Steffey, C. J. Curtis and D. L. DuBois, *Organometallics* **1995**, *14*, 4937-4943.
[152] A. Miedaner, B. C. Noll and D. L. DuBois, *Organometallics* **1997**, *16*, 5779-5791.
[153] J. W. Raebiger, J. W. Turner, B. C. Noll, C. J. Curtis, A. Miedaner, B. Cox and D. L. DuBois, *Organometallics* **2006**, *25*, 3345-3351.
[154] C. Arana, S. Yan, M. Keshavarz-K, K. T. Potts and H. D. Abruna, *Inorg. Chem.* **1992**, *31*, 3680-3682.
[155] T. Yoshida, K. Tsutsumida, S. Teratani, K. Yasufuku and M. Kaneko, *J. Chem. Soc., Chem. Commun.* **1993**, 631-633.
[156] S. Chardon-Noblat, A. Deronzier, F. Hartl, J. Van Slageren and T. Mahabiersing, *Eur. J. Inorg. Chem.* **2001**, 613-617.
[157] G. J. Kubas, *Adv. Inorg. Chem.* **2004**, *56*, 127-177.
[158] J. R. Pugh, M. R. M. Bruce, B. P. Sullivan and T. J. Meyer, *Inorg. Chem.* **1991**, *30*, 86-91.
[159] Y. Musashi and S. Sakaki, *J. Chem. Soc., Dalton Trans.* **1998**, 577-583.
[160] R. H. Crabtree, *Mod. Coord. Chem.* **2002**, 31-44.
[161] P. G. Jessop, F. Joo and C.-C. Tai, *Coord. Chem. Rev.* **2004**, *248*, 2425-2442.

[162] C. Federsel, R. Jackstell and M. Beller, *Angew. Chem., Int. Ed.* **2010**, *49*, 6254-6257.
[163] P. G. Jessop, *Handb. Homogeneous Hydrogenation* **2007**, *1*, 489-511.
[164] Y. Himeda, *Eur. J. Inorg. Chem.* **2007**, 3927-3941.
[165] W. Leitner, *Angew. Chem., Int. Ed. Engl.* **1995**, *34*, 2207-2221.
[166] F. Hutschka, A. Dedieu, M. Eichberger, R. Fornika and W. Leitner, *J. Am. Chem. Soc.* **1997**, *119*, 4432-4443.
[167] E. Graf and W. Leitner, *J. Chem. Soc., Chem. Commun.* **1992**, 623-624.
[168] K. Angermund, W. Baumann, E. Dinjus, R. Fornika, H. Goerls, M. Kessler, C. Krueger, W. Leitner and F. Lutz, *Chem.--Eur. J.* **1997**, *3*, 755-764.
[169] F. Gassner and W. Leitner, *J. Chem. Soc., Chem. Commun.* **1993**, 1465-1466.
[170] R. Fornika, H. Goerls, B. Seemann and W. Leitner, *J. Chem. Soc., Chem. Commun.* **1995**, 1479-1481.
[171] C. P. Lau, S. M. Ng, G. Jia and Z. Lin, *Coord. Chem. Rev.* **2007**, *251*, 2223-2237.
[172] P. G. Jessop, T. Ikarlya and R. Noyori, *Nature (London)* **1994**, *368*, 231-233.
[173] P. G. Jessop, Y. Hsiao, T. Ikariya and R. Noyori, *J. Am. Chem. Soc.* **1996**, *118*, 344-355.
[174] P. Munshi, A. D. Main, J. C. Linehan, C.-C. Tai and P. G. Jessop, *J. Am. Chem. Soc.* **2002**, *124*, 7963-7971.
[175] A. Urakawa, F. Jutz, G. Laurenczy and A. Baiker, *Chem.--Eur. J.* **2007**, *13*, 3886-3899.
[176] P. G. Jessop, *J. Supercrit. Fluids* **2006**, *38*, 211-231.
[177] Y. Himeda, N. Onozawa-Komatsuzaki, H. Sugihara and K. Kasuga, *Organometallics* **2007**, *26*, 702-712.
[178] S. Sanz, M. Benitez and E. Peris, *Organometallics* **2010**, *29*, 275-277.
[179] S. Sanz, A. Azua and E. Peris, *Dalton Trans.* **2010**, *39*, 6339-6343.
[180] R. Tanaka, M. Yamashita and K. Nozaki, *J. Am. Chem. Soc.* **2009**, *131*, 14168-14169.
[181] C.-C. Tai, T. Chang, B. Roller and P. G. Jessop, *Inorg. Chem.* **2003**, *42*, 7340-7341.
[182] H. S. Chu, C. P. Lau, K. Y. Wong and W. T. Wong, *Organometallics* **1998**, *17*, 2768-2777.

Chapter 2

Objectives

Science evolves as an accumulation of little steps. Accordingly, all of the previous knowledge and concepts discussed in Chapter 1 have contributed to choose the starting goals of this thesis. The following points are the initial ideas from which this work was originally designed. On occasions, the course of research deviated us from the planned direction. Fortunately, all the unexpected discoveries one encounters on the way are what make research so challenging and at the same time so fascinating.

OBJECTIVES

The aim of this work focuses on three main topics:

(a) The synthesis and study of the electrochemical and spectroscopic properties of new ruthenium polypyridyl complexes where the interactions occur at a supramolecular level.

(b) The study of the application of ruthenium polypyridyl complexes as catalysts precursors in highly important reactions like water oxidation and CO_2 reduction.

(c) The computational study of selected phenomena regarding these ruthenium polypyridyl complexes.

Therefore, the first objective of this work was to synthesise and study dinuclear ruthenium complexes containing the *bpp*- ligand combined with different monodentate and tridentate meridional ligands in order to gain a deeper insight into the processes occurring at the molecular level.

Regarding water oxidation, the second objective included the synthesis and characterisation of a new dinuclear ruthenium water oxidation catalyst to be anchored onto TiO_2 semiconductor films to test its potential as a water oxidation electrocatalyst. Additionally, a combined experimental and computational study of the nature of the species related to the previously reported $[Ru^{II}(bpy)_2(H_2O)_2]^{2+}$ water oxidation catalyst was proposed to get deeper comprehension of the system.

Finally, we were also interested in employing the rich chemistry of ruthenium polypyridyl complexes towards the discovery of new ruthenium CO_2 reduction catalysts. Our approach was to screen different catalysts supplemented with theoretical calculations.

Chapter 3

Through Space Interactions in Dinuclear Ruthenium Polypyridyl Complexes

The present chapter deals with a study of the intra-supramolecular interactions for Ru dinuclear complexes with general formula in,in-[(Ru(T)(L)]$_2$(μ-bpp)]$^{n+}$. With L being different monodentate bulky ligands and T the 2,2':2',6'-terpydidine (trpy) neutral meridional ligand or the bis-pyridyl–indazolate (bid$^-$) anionic tridentate meridional ligand. The effects of the nature of the meridional and monodentated ligands on the structure, electrochemical and spectroscopic properties are studied. A deep analysis of the kinetics of the dynamic process by the line-shape analysis Dynamic ^{1}H-NMR technique and a UV-vis spectroscopy study of the kinetics of monodentated ligand exchange are reported. Both studies are supported by theoretical calculations.

TABLE OF CONTENTS

3.1. INTRODUCTION

Over the last three decades, the rich coordination chemistry of ruthenium has been actively studied.[1-4] The relative ease with which mixed-ligand complexes can be prepared by controllable stepwise methods, the kinetic stability of this metal in diverse oxidation states and the often reversible nature of the redox couples, make ruthenium complexes particularly appealing targets of investigation.

In particular, ruthenium complexes coordinated to different polypyridyl ligands have received growing attention for their unique spectroscopic, photophysical, photochemical and electrochemical properties.[5, 6] Additionally, the popularity of these compounds arises from the ease with which these properties can be tuned through the use of different ligands and/or functionalizations. Thus, enabling a rational design of ruthenium complexes with the desired qualities.

3.1.1. Polynuclear ruthenium polypyridyl complexes

Ruthenium (II) polypyridyl complexes are particularly useful building blocks to design and synthesize photoactive and redox active multicomponent (supramolecular) systems. Whereas the coordination chemistry of mononuclear ruthenium complexes has been well established and their photophysical, photochemical and redox properties have been thoroughly studied, much less data is available regarding their polynuclear counterparts.

Attention on ruthenium polypyridyl coordination polymers, grids and rods has increased over the last decade.[7-10] The capacity to perform photoinduced energy migration and charge separation processes makes them good candidates to be used in molecular scale electronic devices.[7, 11-15] Therefore, many coordinatively saturated and rugged dinuclear ruthenium polypyridyl complexes have been reported for the fundamental study of the electron transfer process that occur in these complex systems.[7, 16, 17]

Otherwise, the presence of chemically, photochemically or thermally labile ligands in the dinuclear complex's structure, opens the possibility to generate vacant positions. These empty coordination sites can interact with substrates promoting chemical transformations in which one or the two metal centers are involved. This feature has been exploited in numerous catalytic processes.[18-28] Furthermore, applications in medicine and pharmacy have been found for these compounds thanks to their selective double interaction with biomolecules such as DNA.[29-37]

All the above-mentioned rationale makes the understanding of the supramolecular chemistry of these dinuclear compounds highly important.

3.1.2. Supramolecular interactions in dinuclear ruthenium polypyridyl complexes

The presence of the second metal center in a dinuclear ruthenium polypyridyl complex adds complexity to both the synthetic reactions and the understanding of the physical properties of the resulting compound. The bridging ligand is the key component in dinuclear polypyridyl complexes since the interactions between the metal centers, and thereby the properties of the complex, are critically dependent on the nature of the bridge. For example, when there is a strong electronic coupling between the metal centers, through the bridging ligand, the possibility of mixed valence species appears.[38-42]

Whereas most of the research on these compounds is focused on examining the effects of the nature of the bridging ligand on the photo-physical and electrochemical properties of these complexes, much less information can be found regarding their supra/intra molecular interactions.

When the two metal centers are in close proximity, the coordination chemistry of one metal center may be affected by the ligands coordinated to the other, by electronic and/or steric effects. This is the case of the dinuclear ruthenium complexes containing the 3,5-bis(2-pyridyl) pyrazole dinucleating ligand (*Hbpp*) (Figure 1).[43-46]

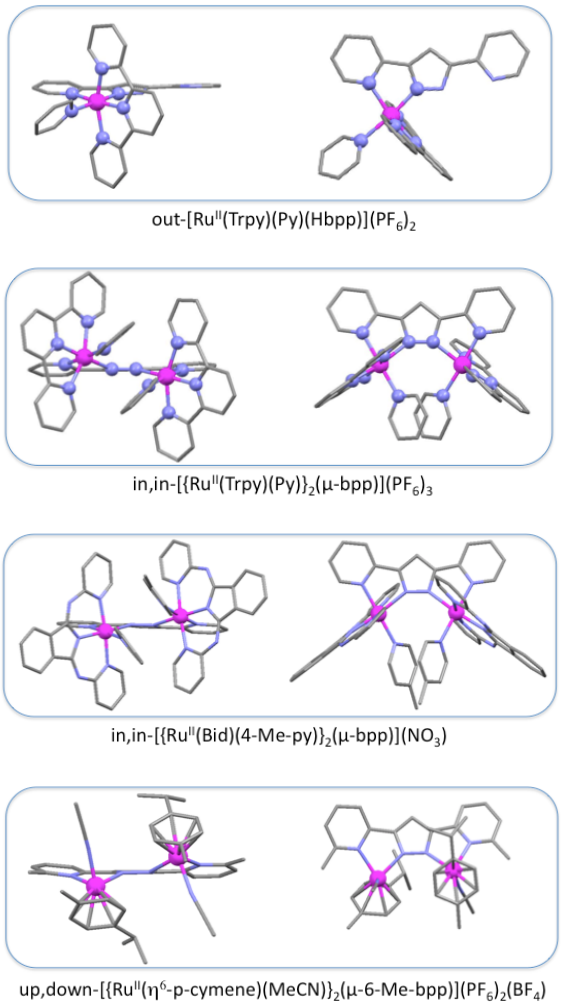

Figure 1. Front (left) and top (right) views of representative complexes containing the 3,5-bis(2-pyridyl pyrazole) (bpp) dinucleating ligand. *trpy,* 2,2':2',6'-terpydidine; *bid*$^-$*,* bis-pyridyl–indazolate;6-Me-bpp, 3,5-bis(6-methylpyrid-2-yl) pyrazole; *py*, pyridine: 4-Me-py, 4-methylpyridine.[47-49]

A close look to the X-ray crystal structure of *out*-[Ru^{II}(py)(bpp)](PF$_6$)$_2$ reveals a slightly distorted octahedral geometry, mainly due to the bite angle of the *trpy* ligand, in which the ruthenium atom is situated in the plane of the *bpp*$^-$ ligand (First, Figure 1).[47] The presence of a second metal center in the structure of *in,in*-[{Ru^{II}(trpy)(py)}$_2$

(μ-bpp)](PF$_6$)$_3$ not only forces the "*in,in*" disposition of the monodentated ligands (pyridines) but, as can be seen in Figure 1 the ruthenium centers force each other to be placed above and below the *bpp*$^-$ plane.

All the diruthenium complexes containing the dinucleating *bpp*$^-$ ligand, have been isolated as a mixture of two enantiomeric isomers with C_2 symmetry (see Figure 1). Both enantiomers are usually present in the unit cell of the corresponding X-ray crystal structures.[43, 48] The "*in,in*" type complexes which contain a N_3-meridional ligand on each Ru center, present a fast interconversion between the two isomers in solution. At RT, as a consequence of this dynamic behavior, these compounds present a NMR spectra corresponding to an apparent C_{2V} average geometry (Figure 2).

It is important to remark that a closely related "bis-aquo" complex *in,in*-[(Ru^{II}(trpy)(OH$_2$)]$_2$(μ-bpp)]$^{3+}$ has been reported to be active as water oxidation catalyst (see Chapter 4).[43, 50-52] Furthermore, both complexes *in,in*-[{Ru^{II}(trpy)}$_2$(μ-bpp)(μ-Cl)]$^{2+}$ and *in,in*-[{Ru^{II}(bid)}$_2$(μ-bpp)(μ-AcO)]^0 have proven to act as catalyst precursors for the reduction of CO_2.[53, 54]

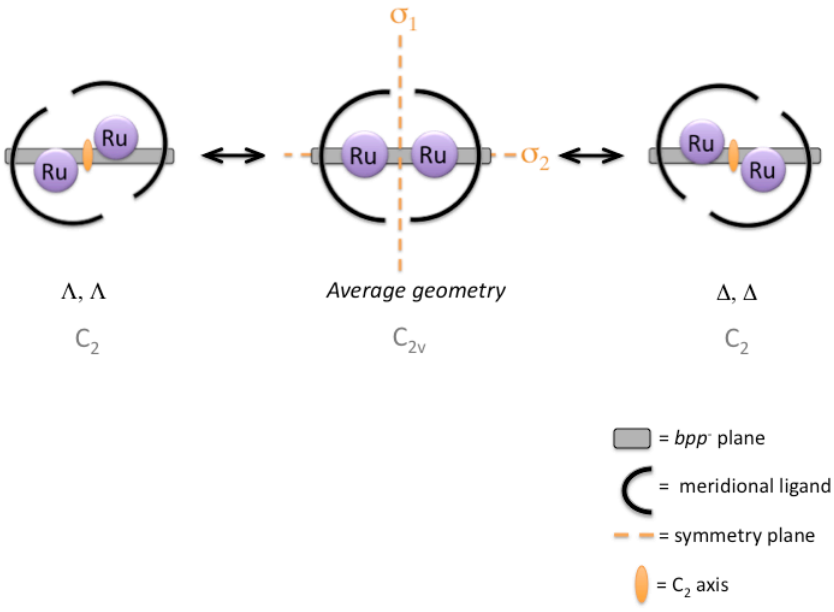

Figure 2. Representation of the isomerization equilibrium occurring in solution.

3.1.3. Dynamic NMR

Dynamic molecules are those which undergo reorganization such that atoms interchange relative positions. Therefore, these species present more than one low energy configuration, and rather low energetic barriers or intermediate species so that a structural reorganization process takes place at temperatures close to RT.

When the reorganization of a molecule leads to symmetrically equivalent configurations, from a chemical point of view, the molecule is considered *fluxional*. Alternatively, when the reorganization originates chemically distinguishable molecules, we refer to the dynamic process as *isomerism*.

The archetypal of dynamic species is $Fe(CO)_5$ which at room temperature, as is also the case for many d^8 pentacoordinated species, presents a "Berry pseudo-rotation mechanism". This type of mechanism causes fluxionality by the exchange of two axial ligands for two of the equatorial ones through a low energy square planar intermediate, as shown in Figure 3.[55]

Since all spectroscopic methods involving UV visible or IR radiation are in general much faster than the molecular vibrations or interconversions, the IR spectrum of $Fe(CO)_5$ presents two signals corresponding to the vibrations of axial and equatorial CO ligands. NMR spectroscopy though, has an interaction period usually comparable to the kinetics of this kind of processes enabling their study.

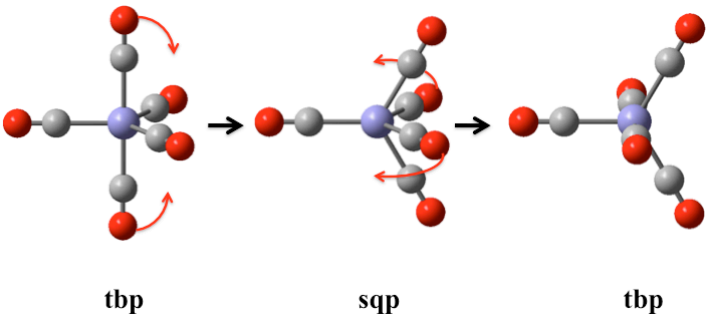

Figure 3. Images of the $Fe(CO)_5$ species intervening in the Berry mechanism, trigonal bipyramid (tbp) and square planar intermediate (sqp).[55]

At room temperature, the pseudorotation process is very fast in the NMR timescale. Instead of two different carbon signals for the resonance of the carbonyl-carbon atoms, an average signal is observed in the ^{13}C-NMR spectra of $Fe(CO)_5$. By changing the ligands (i.e. with more sterically demanding functional groups) or by lowering the temperature, the reaction can be slowed down. Then, the signals can be detected separately, since the NMR timescale is faster than the rate of the pseudo-rotation. Thereby, dynamic nuclear magnetic resonance (DNMR) is a powerful tool for the study of the kinetics of chemical exchange.

The exchange process is manifested in NMR by changes in the shape of the NMR signal; broadening, coalescence and re-sharpening (Figure 5). The most classical of the DNMR techniques is the line-shape analysis (more properly called total band-shape analysis). Line-shape analysis profits from the fact that the line shapes of the NMR signals of nuclei involved in an exchange processes contain information on the rate constants for processes occurring with lifetimes comparable to the reciprocal of the frequency difference between the exchanging sites.[56]

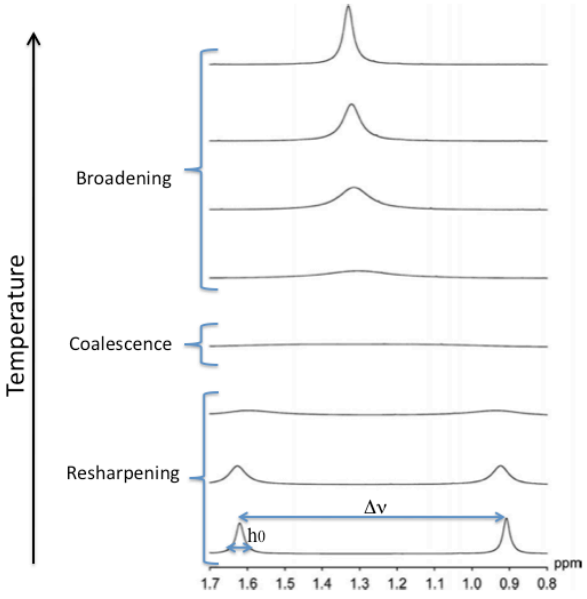

Figure 5. Example of the evolution of a resonance peak involved in a dynamic process as the temperature is varied.[57]

This technique is specially well suited to characterize kinetic processes consisting on an equally populated two-site system involving two nuclei not coupled to each other, with a chemical shift difference ($\Delta\nu_0$) much greater than the line with (h_0), both in the absence of exchange, and undergoing the exchange with a rate constant smaller than the intrinsic transverse relaxation time.[56]

Very illustrative is the example of the dynamic behavior of *cis*-$[Ru^{II}(bpy)_2(4\text{-picoline})_2]^{2+}$ reported by Reedijk[46] (Figure 6) in which the L's (4-picoline ligands) can flip around their Ru-N axis, either fast or slow on the NMR timescale, depending on the temperature.

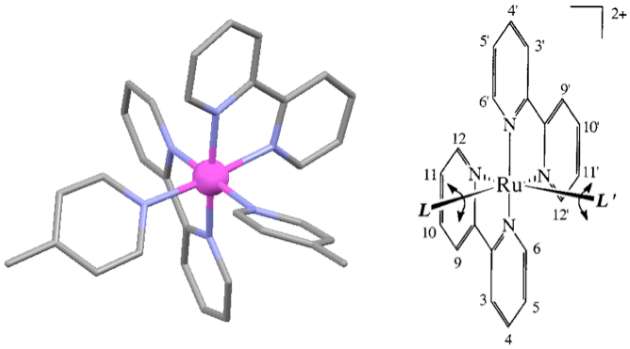

Figure 6. Structural (left) and schematic (right) representation of *cis*-$[Ru^{II}(bpy)_2(L)]^{2+}$ system, L = 4-methyl-pyridine.[46]

At room temperature the two *ortho* protons (and the two *metha* protons) resonate at the same frequency indicating that the picolines (L) rotate fast on the ^{1}H-NMR time scale. Upon lowering the temperature all *bpy* signals show a slight down-field shift but remain sharply defined. In contrast the two 4-picoline's doublets start broadening until disappearance, this temperature is called coalescence. By continuing to Lower the temperature the absent protons re-resolve split up in two doublets. At this point the four aromatic 4-picoline protons resonate at different frequencies indicating a slow flip of the monodentated ligands with regard to the NMR timescale (Figure 7).

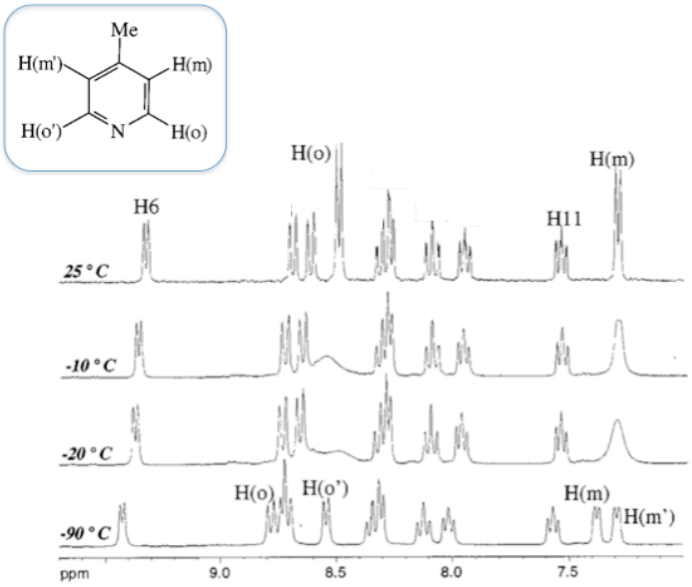

Figure 7. Proton numbering scheme of 4-methylpyridine (4-picoline) and the aromatic region of the ^{1}H-NMR spectra of *cis*-$[Ru(bpy)_2(L)_2]^{2+}$ in acetone at various temperatures.[46]

3.1.4. References

[1] J. C. Toledo, B. dos Santos Lima Neto and D. W. Franco, *Coord. Chem. Rev.* **2005**, *249*, 419-431.
[2] T.-A. Koizumi, T. Tomon and K. Tanaka, *J. Organomet. Chem.* **2005**, *690*, 4272-4279.
[3] J. Halpern, *Pure Appl. Chem.* **1987**, *59*, 173-180.
[4] J. Maurer, M. Linseis, B. Sarkar, B. Schwederski, M. Niemeyer, W. Kaim, S. Zalis, C. Anson, M. Zabel and F. Winter Rainer, *J Am Chem Soc* **2008**, *130*, 259-268.
[5] J.-C. Chambron, J.-P. Collin, J.-O. Dalbavie, C. O. Dietrich-Buchecker, V. Heitz, F. Odobel, N. Solladie and J.-P. Sauvage, *Coord. Chem. Rev.* **1998**, *178-180*, 1299-1312.
[6] A. Dovletoglou, S. A. Adeyemi and T. J. Meyer, *Inorg. Chem.* **1996**, *35*, 4120-4127.
[7] F. Puntoriero, S. Campagna, A.-M. Stadler and J.-M. Lehn, *Coord. Chem. Rev.* **2008**, *252*, 2480-2492.
[8] A. Credi, V. Balzani, S. Campagna, G. S. Hanan, C. R. Arana and J.-M. Lehn, *Chem. Phys. Lett.* **1995**, *243*, 102-107.
[9] D. M. Bassani, J.-m. Lehn, S. Serroni, F. Puntoriero and S. Campagna, *Chem.--Eur. J.* **2003**, *9*, 5936-5946.
[10] A.-M. Stadler, F. Puntoriero, F. Nastasi, S. Campagna and J.-M. Lehn, *Chemistry* **2010**, *16*, 5645-5660.
[11] T.-Y. Dong, M.-c. Lin, M. Y.-N. Chiang and J.-Y. Wu, *Organometallics* **2004**, *23*, 3921-3930.
[12] C. N. Fleming, M. K. Brennaman, J. M. Papanikolas and T. J. Meyer, *Dalton Trans.* **2009**, 3903-3910.

[13] S. Serroni, S. Campagna, F. Puntoriero, C. Di Pietro, N. D. McClenaghan and F. Loiseau, *Chem. Soc. Rev.* **2001**, *30*, 367-375.
[14] S. Serroni, S. Campagna, F. Puntoriero, F. Loiseau, V. Ricevuto, R. Passalacqua and M. Galletta, *C. R. Chim.* **2003**, *6*, 883-893.
[15] R. Kikkeri, I. Garcia-Rubio and P. H. Seeberger, *Chem. Commun. (Cambridge, U. K.)* **2009**, 235-237.
[16] R. H. Laye, S. M. Couchman and M. D. Ward, *Inorg. Chem.* **2001**, *40*, 4089-4092.
[17] R. Mosurkal, Y.-G. Kim, J. Kumar, L. Li, J. Walker and L. A. Samuelson, *J. Macromol. Sci., Pure Appl. Chem.* **2003**, *A40*, 1317-1325.
[18] D. P. Klein, A. Ellern and R. J. Angelici, *Organometallics* **2004**, *23*, 5662-5670.
[19] Y. Takai, R. Kitaura, E. Nakatani, T. Onishi and H. Kurosawa, *Organometallics* **2005**, *24*, 4729-4733.
[20] R. Ramaraj, A. Kira and M. Kaneko, *J. Chem. Soc., Faraday Trans. 1* **1986**, *82*, 3515-3524.
[21] F. P. Rotzinger, S. Munavalli, P. Comte, J. K. Hurst, M. Graetzel, F. J. Pern and A. J. Frank, *J. Am. Chem. Soc.* **1987**, *109*, 6619-6626.
[22] J. Jenck, P. Kalck, E. Pinelli, M. Siani and A. Thorez, *J. Chem. Soc., Chem. Commun.* **1988**, 1428-1430.
[23] H. Matsuzaka, Y. Mizobe, M. Nishio and M. Hidai, *J. Chem. Soc., Chem. Commun.* **1991**, 1011-1012.
[24] A. Beguin, H. C. Boettcher, G. Suess-Fink and B. Walther, *J. Chem. Soc., Dalton Trans.* **1992**, 2133-2134.
[25] H. P. Hughes and J. G. Vos, *Inorg. Chem.* **1995**, *34*, 4001-4003.
[26] M. M. Ali, H. Sato, T. Mizukawa, K. Tsuge, M.-a. Haga and K. Tanaka, *Chem. Commun. (Cambridge)* **1998**, 249-250.
[27] Y.-Y. Tang, R.-X. Li, X.-J. Li, N.-B. Wong, K.-C. Tin, Z.-Y. Zhang and T. C. W. Mak, *Chin. J. Chem.* **2004**, *22*, 738-742.
[28] D. Sellmann, S. Y. Shaban, A. Roesler and F. W. Heinemann, *Inorg. Chim. Acta* **2005**, *358*, 1798-1806.
[29] B. T. Patterson, J. G. Collins, F. M. Foley and F. R. Keene, *J. Chem. Soc., Dalton Trans.* **2002**, 4343-4350.
[30] J. Aldrich-Wright, C. Brodie, E. C. Glazer, N. W. Luedtke, L. Elson-Schwab and Y. Tor, *Chem. Commun. (Cambridge, U. K.)* **2004**, 1018-1019.
[31] T. K. Janaratne and F. M. MacDonnell, *Abstracts, 60th Southwest Regional Meeting of the American Chemical Society, Fort Worth, TX, United States, September 29-October 4* **2004**, SEPT04-037.
[32] J. A. Smith, J. G. Collins, B. T. Patterson and F. R. Keene, *Dalton Trans.* **2004**, 1277-1283.
[33] P. U. Maheswari, V. Rajendiran, M. Palaniandavar, R. Parthasarathi and V. Subramanian, *Bull. Chem. Soc. Jpn.* **2005**, *78*, 835-844.
[34] V. Gonzalez, T. Wilson, I. Kurihara, A. Imai, J. A. Thomas and J. Otsuki, *Chem. Commun. (Cambridge, U. K.)* **2008**, 1868-1870.
[35] J. Andersson, M. Li and P. Lincoln, *Chem.--Eur. J.* **2010**, *16*, 11037-11046, S11037/11031-S11037/11032.
[36] J. A. Thomas and G. Battaglia in *Dinuclear ruthenium complexes for staining cellular DNA*, *Vol.* (University of Sheffield, UK). Application: WO
WO, **2010**, p. 58pp.
[37] T. Wilson, M. P. Williamson and J. A. Thomas, *Org. Biomol. Chem.* **2010**, *8*, 2617-2621.
[38] R. Lomoth, A. Magnuson, Y. Xu and L. Sun, *J. Phys. Chem. A* **2003**, *107*, 4373-4380.
[39] W. Kaim and B. Sarkar, *Coord. Chem. Rev.* **2007**, *251*, 584-594.
[40] L.-B. Gao, J. Kan, Y. Fan, L.-Y. Zhang, S.-H. Liu and Z.-N. Chen, *Inorg. Chem. (Washington, DC, U. S.)* **2007**, *46*, 5651-5664.
[41] M. Fabre and J. Bonvoisin, *J. Am. Chem. Soc.* **2007**, *129*, 1434-1444.

[42] J. W. Slater, D. M. D'Alessandro, F. R. Keene and P. J. Steel, *Dalton Trans.* **2006**, 1954-1962.
[43] C. Sens, I. Romero, M. Rodriguez, A. Llobet, T. Parella and J. Benet-Buchholz, *J. Am. Chem. Soc.* **2004**, *126*, 7798-7799.
[44] J. Mola, E. Mas-Marza, X. Sala, I. Romero, M. Rodriguez, C. Vinas, T. Parella and A. Llobet, *Angew. Chem., Int. Ed.* **2008**, *47*, 5830-5832.
[45] L. Francas, X. Sala, J. Benet-Buchholz, L. Escriche and A. Llobet, *ChemSusChem* **2009**, *2*, 321-329.
[46] A. H. Velders, C. Massera, F. Ugozzoli, M. Biagini-Cingi, A. M. Manotti-Lanfredi, J. G. Haasnoot and J. Reedijk, *Eur. J. Inorg. Chem.* **2002**, 193-198.
[47] C. Sens in *New mono- and dinuclear ruthenium complexes containing the 3,5-bis(2-pyridyl)pyrazole ligand. Synthesis, characterization and applications*, *Vol. PhD Thesis* UdG, Girona, **2005**.
[48] N. Planas, G. J. Christian, E. Mas-Marza, X. Sala, X. Fontrodona, F. Maseras and A. Llobet, *Chem.--Eur. J.* **2010**, *16*, 7965-7968, S7965/7961-S7965/7965.
[49] V. J. Catalano and T. J. Craig, *Polyhedron* **2000**, *19*, 475-485.
[50] F. Bozoglian, S. Romain, M. Z. Ertem, T. K. Todorova, C. Sens, J. Mola, M. Rodriguez, I. Romero, J. Benet-Buchholz, X. Fontrodona, C. J. Cramer, L. Gagliardi and A. Llobet, *J. Am. Chem. Soc.* **2009**, *131*, 15176-15187.
[51] S. Romain, F. Bozoglian, X. Sala and A. Llobet, *J. Am. Chem. Soc.* **2009**, *131*, 2768-2769.
[52] S. Romain, L. Vigara and A. Llobet, *Acc. Chem. Res.* **2009**, *42*, 1944-1953.
[53] N. P. Takashi Ono in *Work in progress*, *Vol.* **2011**.
[54] T. Ono, N. Planas and A. Llobet in *Work in progress*, *Vol.* **2011**.
[55] M. E. Cass, K. K. Hiib and H. S. Rzepa, *J. Chem. Educ.* **2006**, *83*, 336.
[56] H. Friebolin, *Basic One- and Two- Dimensional NMR Spectroscopy. 4th Completely Revised and Expanded Edition*, **2004**, p. 286 pp (approx).
[57] H.-C. Chang, K. Mochizuki and S. Kitagawa, *J. Mol. Struct.* **2008**, *890*, 303-308.

3.2. THROUGH SPACE LIGAND INTERACTIONS IN ENANTIOMERIC DINUCLEAR Ru COMPLEXES

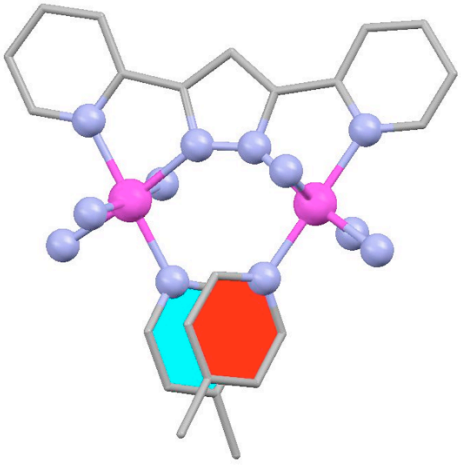

A family of dinuclear Ru complexes of general formula $[\{Ru(T)(L)\}_2(\mu\text{-bpp})]^{(n+1)+}$ *(T = tridentate meridional ligand;* bpp^- *= tetradentate bridging ligand and L = monodentate ligand, n = 1 or 2) have been prepared and thoroughly characterized. In solution these complexes display a global dynamic behavior in which the monodentate ligands undergo a synchronized twisting motion.*

Through Space Ligand Interactions in Enantiomeric Dinuclear Ru Complexes†

Chem. Eur. J. 2010, 16, 7965 – 7968

Nora Planas,[a] Gemma J. Christian,[a] Elena Mas-Marzá,[a] Xavier Sala,[a] Xavier Fontrodona,[b] Feliu Maseras,*[a, c] and Antoni Llobet*[a, c]

[a] *Institute of Chemical Research of Catalonia (ICIQ), Av. Països Catalans 16, E-43007 Tarragona, Spain. Fax: 34 977 902 228; Tel: 34 977 902 200; E-mail: fmaseras@iciq.es, allobet@iciq.es*

[b] *Serveis Tècnics, Universitat de Girona Campus de Montilivi, 17071 Girona (Spain)*

[c] *Departament de Química, Universitat Autònoma de Barcelona, Cerdanyola del Vallès, E-08193 Barcelona, Spain.*

Keywords: N ligands, NMR spectroscopy, ruthenium, structure elucidation

3.2.1. Abstract

A family of dinuclear Ru-complexes containing monodentate ligands displays dynamics based on supramolecular through space interactions. The electronic and steric nature of the monodentate ligands allow a fine tuning of the kinetic parameters of this dynamic behavior that can be monitored by VT-NMR.

3.2.2. Introduction

Water oxidation to molecular dioxygen is a key reaction that needs to be fully understood in order to be able to design new energy conversion schemes based on water and sunshine.[1] Furthermore, from a biological point of view it is an important reaction that takes place at the OEC-PSII. However even though it is under thorough scrutiny[2] its mechanisms are not fully understood. Hence the need to have low molecular weight functional models. While at the moment there are few well defined

complexes that have been shown to be capable of oxidizing water to molecular dioxygen even fewer of them have been studied from a mechanistic perspective.[3] Water nucleophilic attack to a high valent Ru=O group and intramolecular O-O bond formation are the two metal based mechanisms that have been observed so far based on experimental and theoretical grounds. While the synthetic demands for a catalyst capable of carrying out a nucleophilic water attack mechanism are relatively simple, for an intramolecular mechanism the catalysts are based on dinuclear complexes whose structures are extraordinarily sophisticated. Thus it is imperative to understand all the relevant aspects of such a mechanism to be able to design efficient and rugged water oxidation catalysts. In this particular field, the two key challenging factors that need to be addressed are first the degree of electronic coupling between the two metal centers through the bridging ligand and secondly the degree and nature of the through space interactions between the active groups that provides the right conditions so that an O-O bond can be formed. The present paper sheds light into the latter factor setting up the basis for further ligand/complex design.

3.2.3. Results and Discussion

We report here the synthesis and thorough characterization of a family of Ru-*Hbpp* related dinuclear Ru complexes of general formula $[\{Ru(T)\}_2(\mu\text{-bpp})(\mu\text{-MeCOO})]^{n+}$ (T: *trpy* or *bid*-, see Figure 1) and $[\{Ru(T)(L)\}_2(\mu\text{-bpp})\}^{(n+1)+}$ (L = MeCN or substituted pyridines; see Table 1 for complex label assignment).

This family of complexes constitute an ideal basis to understand and quantify ligand through space interactions. Figure 2 shows the cationic moiety the complex Δ,Δ-**3**,[4] containing 4-picoline ligands.

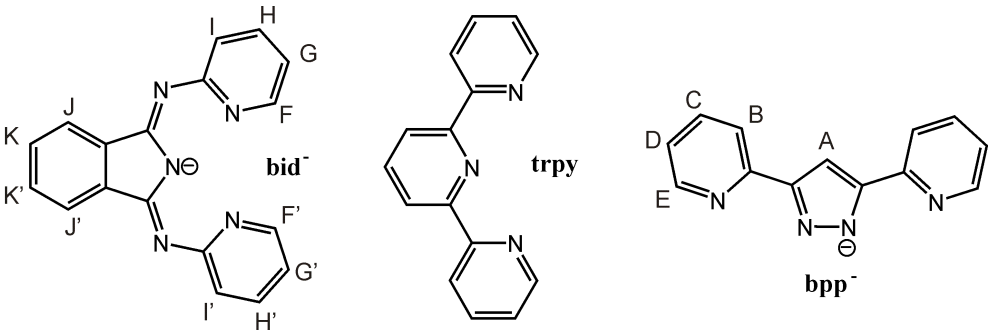

Figure 1. Drawing of the ligands and labeling used for the ^{1}H-NMR assignment.

These molecules posses C_2 symmetry with the C_2 axis running through the pyrazolate group, bisecting the N-N bond and through to the opposite C atom of the pyrazolate ring. As it can be observed in the Figure 2 left, each metal center present a distorted octahedral geometry, due to both the bite angle of the chelating ligands and to the need to accommodate the encumbering monodentate ligands.

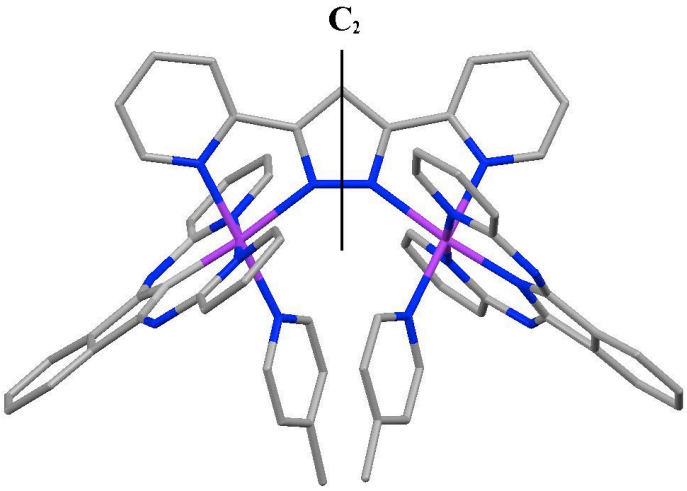

Figure 2. X-ray crystal structure for the cationic part of Δ,Δ−**3**. The C_2 axis is shown with a broken line. The *bpp*$^-$ ligand is placed in the plane of the paper whereas the meridional *bid*$^-$ ligands are nearly perpendicular to mentioned plane. Color codes: Ru, pink: N, blue; C, gray. H atoms have been omitted for clarity purposes.

The distortion can be described as an inverse synchronized rotation of the pyridyl *Hbpp* groups (the angle between these two pyridyls is 17.5º) via an imaginary axis that would go through the C-C bonds connecting the pyridyl and pyrazolate groups of the *bpp*$^-$ ligand, from an ideal octahedral geometry. This distortion provokes the displacement of the metal center above and below the equatorial plane in which the *bpp*$^-$ ligand would normally lie.

It is also interesting to observe that the rings of the monodentate picoline ligands lie nearly parallel to one another (angle between best planes is 3.2º) and with the distance between the centroids of the pyridine rings of 3.43 Å suggesting significant π –π interactions.

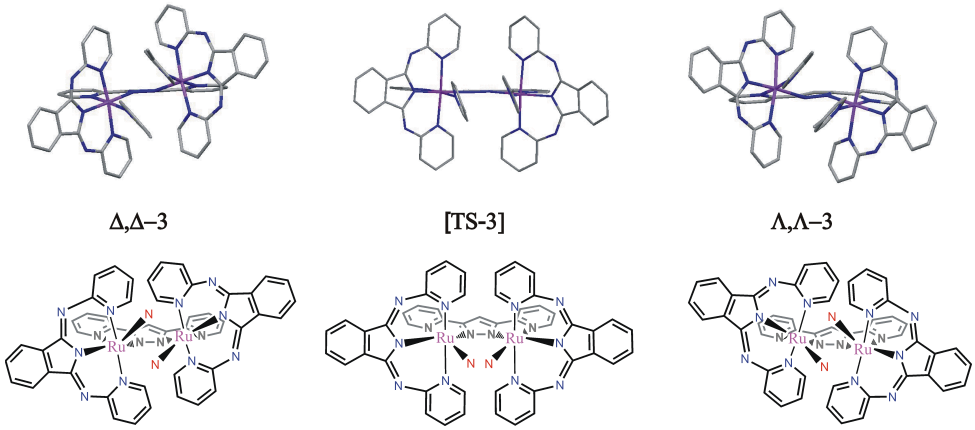

Figure 3. Top, stick models for the cationic parts of **3**. Left, X-ray crystal structure of **Δ,Δ–3**. Center, Computed transition state structure of [**TS-3**]*. Right, computed structure of **Λ,Λ–3**. In all cases the *bpp*$^-$ ligand is placed perpendicular to the plane of the paper. Bottom, ChemDraw drawings of the top structures. The monodentate 4-picoline ligand is not drawn for clarity purposes and is represented by the red Ns.

In solution at room temperature the two enantiomers shown in Figure 3 rapidly interconvert between each other. As a consequence the resonances observed in the NMR at RT can be interpreted as if the molecule possessed C_{2v} symmetry for the case of **1**. For the case of the other complexes with N-containing monodentate ligands some of the resonances at RT are so wide that they are nearly not observed. Variable Temperature (VT) NMR (298-218 K) makes it possible to monitor the speed of this equilibrium as shown in Figure 3 for the pair of enantiomers **Δ,Δ-4** and **Λ,Λ-4**, and

thus the activation energy can be extracted for this isomeric interconversion process. No evidence in the NMR is observed for Ru-N bond breaking under these conditions indicating that the interconversion involves ligand-rotation type of processes only, besides the correspondingly coupled vibrations, translations and solvent interactions.

Table 1. Experimental and calculated free energies in kcal mol^{-1} at 298 K, for the transition states of the isomeric interconversion reaction of complexes **1-9**, with general formula $[\{Ru(T)\}_2(\mu\text{-bpp})(\mu\text{-MeCOO})]^{n+}$ (T: *trpy* or *bid*-) and $[\{Ru(T)(L)\}_2(\mu\text{-bpp})]^{(n+1)+}$ (L = H_2O, MeCN or substituted pyridines).

T	L	Complex	ΔG^o, Exp. (Solv.)[a]	ΔG^o, Calc. (Solv.) [a]
bid$^-$	MeCOO [b]	**1**	< 3.4 (D)	
	Py	**2**	7.2 (D)	7.76 (D)
	4-Me-py	**3**	8.5 (D)	9.29 (D)
	3,5-$(Me)_2$-py	**4**	9.4 (D)	9.53 (D)
	4-CF_3-py	**5**	9.5 (D)	9.06 (D)
	MeCN	**6**	10.4 (D)	14.3 (D)
trpy	MeCOO [b]	**7**	< 4.2 (A)	
	H_2O	**8**	< 4.2 (A)	
	Py	**9**	8.6 (A)	

[a]Solvents used are abbreviated as D for dichloromethane and A for acetone. [b] MeCOO- act as bidentate bridging ligand between the two Ru metals and thus occupy the coordination positions of the two L ligands

DFT/MM calculations[5] have been used to study the reaction pathway for the interconversion process. The enantiomers are found to be connected via the transition state shown in Figure 3 (center) which has an approximately planar *bpp*$^-$ backbone with the metal centers also lying in the plane defined by the ligand. The picoline ligands remain parallel to one another (angle between planes is 3.8º) and approximately perpendicular to the equatorial plane. However, unlike the enantiomers they are almost eclipsed, forcing the methyl substituents closer together. It is likely for

this reason that the distance between the centroids of the picoline rings is larger compared to the two enantiomers, at 3.71 Å. However, while this it increases the strain in the rest of the molecule, resulting in longer Ru-N(*bpp*$^-$) bond lengths, and a more open N(pyrazol-*bpp*$^-$)-Ru-N(picoline) bond angle.

Δ,Δ−4 → [**TS-4**]* → **Λ,Λ−4** (1)

The transition vector is associated both with flexing of the backbone *bpp*$^-$ ligand and with the rotation of the Ru-N(picoline) bonds with respect to each other. Clockwise rotation of the axes defined by the Ru-N(picoline) bonds and corresponding flexing of the *bpp*$^-$ ligand generates the Δ,Δ isomer, while anticlockwise rotation generates the Λ,Λ isomer.

While in this case both movements have an important contribution to the transition vector, it is likely that for related ligand systems with more rigid meridional ligands the transition vector may have a larger contribution from the rotation of the Ru-N axes than from backbone ligand movement.

Table 1 presents the experimental[7] and DFT calculated activation barriers obtained for the family of complexes **1-9**. In general the calculated activation barriers slightly overestimate the experimental values but reproduce the experimental trends. From the table the activation barriers are found to vary depending on the class of monodentate ligand, with higher activation barriers observed for the nitrile ligand, which is known to have stronger π-backbonding interactions,[6] than for the pyridylic type of ligands (compare complexes **2** and **6** in Table 1). In comparison, the lowest activation barriers were found for the O-donor type ligands (compare **1**, **7**, **8** with **2**). The activation barriers were also found to be dependent on the meridional ligand where lower activation barriers were found for the more flexible *bid*$^-$ ligand than for the *trpy* ligand. Finally, within the family of pyridylic ligands, the activation barriers increase with steric bulk, from L = *py*, picoline to lutidine.

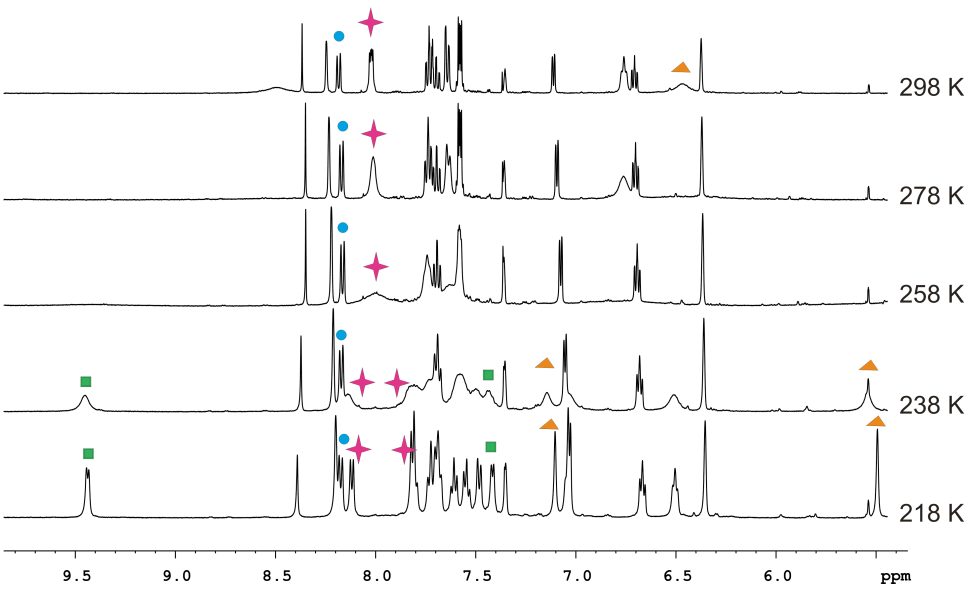

Figure 4. VT ^{1}H-NMR for **4** in CD_2Cl_2. The assignment of the resonances is keyed in Figure 1. The colored symbols indicate the splitting observed upon reducing the temperature: green squares are for H_F and $H_{F'}$, blue spheres for H_E; pink stars for H_J and $H_{J'}$; and orange triangles for H_L (ortho protons of the 3,5-lutidine ligand).

The trends in activation barriers can be rationalized by considering the nature of the transition state where the Ru-N(picoline), or more generally Ru-N(L), axes are approximately eclipsed. For the pyridylic type ligands, the substituents of the pyridine ring are forced closer together, leading to increasing activation barriers as the number of substituents increases. The increasing steric strain can be seen in the distance between the centroids of the pyridylic rings, which increases from 3.69 Å, to 3.71 Å to 3.78 Å, for pyridine, picoline and lutidine, respectively. The differences in activation energies between types of ligand donors can also be attributed to through space interactions and the rearrangement required to reach the transition state. This is most significant for the MeCN ligand, where the rearrangement required to reach the transition state is greatest, and consequently gives the highest barrier. The O-type donor ligands however, either bridge the metal centres, $MeCOO^{-}$, or have little steric bulk, H_2O, so the rearrangement required and steric strain in the transition state is not as significant, resulting in much lower activation barriers

This family of complexes, therefore, provides a basis to understand the electronic and steric factors that influence the interconversion process and thus the dynamics involved in Equation 1. These are shown to be chiefly governed by the monodentate ligands where the degree of through space interactions (an intra-supramolecular effect) dictates the interconversion barriers. Furthermore the design of the complex is fundamental. In particular the bridging *bpp*$^-$ ligand, which acts as backbone for the two metal centers, places them at the correct distance and relative orientation to allow this dynamic behavior. At longer distances the through space interactions would be too weak and the metal centers would acquire an ideal type of octahedral geometry and no dynamic effects would be observed. In contrast if the two monodentate ligands were placed too close the barriers would be so high that at RT the isomeric interconversion would not occur. Thus the present family of complexes display the delicate electronic and steric balance needed for these intra-supramolecular interactions to take place. In turn, this understanding is of paramount importance in order to design water oxidation catalysts, especially for the particular case where the oxygen-oxygen bond formation takes place in an intramolecular manner. Thus in the case where the monodentate ligand is an aqua ligand the access to higher oxidation states provides Ru=O groups properly oriented and with the right through space interaction that, once generated, are ready to couple to one another and thus provide a viable scenario for the elusive intramolecular mechanism.

3.2.4. Conclusions

We have prepared and thoroughly characterized a family of dinuclear Ru-complexes where the through space interaction can be fine tuned by steric and electronic effects. In particular we have shown that the *bpp*$^-$ pyrazolate bridge acts as an spectator ligand but provides the right topology so that the monodentate ligands bonded to them can adequately interact in a supramolecular manner. We have also put forward the important implication this control has for the future design of water oxidation catalysts. Finally, this work constitutes an unprecedented example where the dynamic behavior between two ligands bonded to two different metals is established and understood.[8]

3.2.5. Acknowledgements

Support from SOLAR-H2 (EU 212508), ACS (PRF 46819-AC3), MEC (CTQ2007-67918 and CTQ2008-06866-CO2-02) and from the Consolider Ingenio 2010 (CSD2006-0003) are gratefully acknowledged.

The theoretical calculations reported in this work were carried out by Gemma J. Christian as a post-Doc in Dr. Maseras' group.

3.2.6. References

[1] See for instance; X. Sala, M. Rodriguez, I. Romero, L. Escriche, A. Llobet, *Angew. Chem. Int. Ed.* **2009**, *48*, 2842.

[2](a) J. Yano, J. Kern, K. Sauer, M. J. Latimer, Y. Pushkar, J. Biesiadka, B. Loll, W. Saenger, J. Messinger, A. Zouni, V. K. Yachandra, *Science,* **2006**, *314*, 821. (b) M. Haumann, P. Liebisch, C. Müller, M. Barra, M. Grabolle, H. Dau, *Science*, **2005**, *310*, 1019.

[3] (a) J. J. Concepcion, J. W. Jurss, J. L. Templeton, T.J. Meyer, *J. Am. Chem. Soc.,***2008**, *130*, 16462. (b) S. Romain, F. Bozoglian, X. Sala, A. Llobet, *J. Am. Chem. Soc.,* **2009**, *131*, 2768. (c) F. Liu, J.J. Concepcion, J. W. Jurss, T. Cardolaccia, J.L. Templeton, T.J. Meyer, *Inorg. Chem.*, **2008**, *47*, 1727. (d) J. J. Concepcion, J. W. Jurss, J. L. Templeton, T. J. Meyer, *Proc. Nat. Acad. Sci.*, **2008**, *105*, 17635. (e) F. Bozoglian, S. Romain, M. Z. Ertem, T. K. Todorova, C. Sens, J. Mola, M, Rodríguez, I. Romero, J. Benet-Buchholz, X. Fontrodona, C. J. Cramer, L. Gagliardi, A. Llobet, *J. Am. Chem. Soc.,* **2009**, *131*, 15176-15187. (f) S. Romain, L. Vigara, A. Llobet, A., *Acc. Chem. Res.,* **2009**, *42*, 1944.

[4] For these complexes the helicity and the connectivity are exactly the same for both enantiomers and, the chirality arises from the different orientations of the monodentate ligand, either above or below the equatorial plane defined by the *bpp*- ligand. Therefore the assignment has been carried out in an arbitrary manner.

[5] ONIOM (B3LYP:UFF) calculations with solvent and free energy corrections. See Supporting Information for computational details

[6] C. Sens, M. Rodríguez, I. Romero, A. Llobet, T. Parella, J. Benet-Buchholz, *Inorg. Chem.,* **2003**, *42*, 8385.

[7] H. Friebolin, in Basic One- and Two- Dimensional NMR Spectroscopy, 4th Ed., WILEY-VCH, Weinheim, 2004, pp. 158-370.

[8]G. R. Owen, J. Stahl, F. Hampel, J.A. Gladysz, *Chem. Eur. J.,* **2008**, *14*, 73

3.3. SUBSTITUTION REACTIONS IN DINUCLEAR Ru-Hbpp COMPLEXES: AN EVALUATION OF INTRASUPRAMOLECULAR EFFECTS

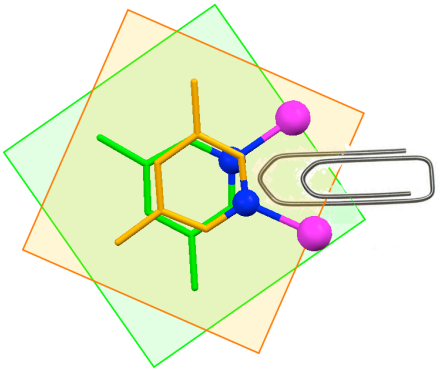

In the present paper we present a comprehensive work, including both experiment and theory via DFT, of intrasupramolecular effects between two pyridylic type of ligands bonded to Ru centers. The chosen dinuclear Ru complexes provide a scaffold that allows framing two pyridyl groups in a manner that has not been achieved previously and thus constitutes an excellent ground to explore the consequences of this particular effect.

Substitution Reactions in Dinuclear Ru-HBpp Complexes: and Evaluation of Intrasupramolecular Effects†

Submitted to Inorg. Chem. 2011

Nora Planas,[a] Gemma Christian, [a] Elena Mas-Marzá, [a] Mohan R. Kollipara,[b] Jordi Benet-Buchholz, [a] Feliu Maseras *[a,b] and Antoni Llobet *[a,b]

[a] *Institute of Chemical Research of Catalonia (ICIQ), Av. Països Catalans 16, E-43007 Tarragona, Spain. Fax: 34 977 902 228; Tel: 34 977 902 200; E-mail: fmaseras@iciq.es*, *allobet@iciq.es*

[b] *Departament de Química, Universitat Autònoma de Barcelona, Cerdanyola del Vallès, E-08193 Barcelona, Spain.*

†Electronic Supplementary Information (ESI) available: Detalied experimental procedures, full spectroscopic and electrochemical characterizations and all catalytic fittings.

Keywords: Ruthenium complexes, Substitution reactions, DFT calculations, Supramolecular chemistry

3.3.1. Abstract

The synthesis of new dinuclear complexes of general formula *in,in*-[{Ru^{II}(T)(L)}$_2$(μ-bpp)]$^{n+}$ has been carried out and the complexes isolated in the solid state where *bpp*$^-$ is the bis(2-pyridyl)-3,5-pyrazolate anionic ligand, T is the 2,2':2',6'-terpyridine neutral meridional ligand (*trpy*) or bis-pyridyl–indazolate (*bid*$^-$) anionic tridentate meridional ligand and L is a monodentate ligand. For T = *trpy* complexes: **3a^{3+}**, L = MeCN; 3b^{3+}, L = pyridine (py); **3c^{3+}**, L = 3,5-lutidine (3,5-Me_2-py). For T = *bid*$^-$: **3a'$^+$**, L = MeCN; **3b'$^+$**, L = pyridine (py); **3c'$^+$**, L = 3,5-lutidine (3,5-Me_2-py). The complexes have been characterized in the solid state by X-ray crystallography and in solution by spectroscopic methods including ^{1}H-NMR and UV-vis spectroscopy. Their redox properties have also been investigated by means of CV and DPV and show the existence of two one electron waves assigned to the formation of the II,III and III,III

species. For the specific case of $\mathbf{3b^{3+}}$, the two oxidation waves are associated with the two equations: $\mathbf{3b^{4+}}$ + 1e- → $\mathbf{3b^{3+}}$ ($E_{1/2}$ = 1.05 V) and $\mathbf{3b^{5+}}$ + 1e- → $\mathbf{3b^{4+}}$, ($E_{1/2}$ = 1.34 V) both potentials measured vs. SSCE. Pyridyl complexes $\mathbf{3b^{3+}}$, $\mathbf{3b'^{+}}$ and $\mathbf{3c^{3+}}$ undergo two consecutive substitution reactions of their monodentate ligands by MeCN. The substitution kinetics have been monitored by ^{1}H-NMR and UV-vis spectroscopy and follow pseudo first order behaviour. For the case of $\mathbf{3b^{3+}}$ the first rate constant k_1 = 1.72 ± 0.04x10^{-3} s^{-1} whereas for the second substitution the k obtained is k_2 = 1.0 ± 0.4x10^{-4} s^{-1} both measured at 313 K. Their energies of activation at 298 K are 95.8 and 104.2 kJ/mol respectively. DFT calculations have also been carried for the consecutive reactions of $\mathbf{3b^{3+}}$ leading to $\mathbf{3a^{3+}}$ giving insight, at a molecular level, regarding the nature of the intermediates. Furthermore the energetics obtained by DFT calculations of the two consecutive substitution reactions agree with the experimental values obtained. The kinetic properties of the two consecutive substitution reactions point out that the slower nature of the first with regard to second one is due to an intrasupramolecular π–π interaction between the monodentate ligands.

3.3.2. Introduction

Ru complexes are of interest for a variety of applications including bioinorganic chemistry, photochemistry and photophysics, and catalysis.[1] In all these cases, the kinetic and thermodynamic stability of the ligands is of paramount importance so that the complex can be used for the desired applications. For the particular case of catalysis, Ru complexes are generally designed with at least one labile Ru-L bond so that it can suffer easy substitution reactions by a particular substrate and thus enter a potential catalytic cycle for its subsequent transformation.[2] In some cases such as hydrogenation[3] or hydroformilation[4] reactions the substitution process constitutes the rate determining step and thus it is important to understand at a molecular level the factors that govern these processes. In the field of complexes interacting with DNA mainly two types of interactions can take place, π-π stacking between the nucleobases and the aromatic rings of the ligands or direct coordination of the Ru metal to a potential coordination site of the DNA. For the latter a sufficiently labile Ru-L bond is needed and thus manifests again the importance of substitution reactions.[5]

In water oxidation catalysis, a recent example involving the $[Ru(Cl)(trpy)(bpy)]^{2+}$ (*bpy* represents 2,2'-bpyridine and also its 4,4'-substituted analogues) family of catalysts highlights the importance of understanding the substitution process. While an inert Ru-Cl bond leads the authors to propose a mechanism involving coordination expansion[6] with the metal center possessing seven coordination, in the case of a labile Ru-Cl bond would implicate aqua substitution forming a $Ru\text{-}OH_2$ bond and maintaining the pseudo octahedral coordination over all the intermediate species of the catalytic cycle. [7] For the labile case the relative Ru-Cl substitution rates with regard to the rates of formation of the catalytic species $Ru\text{-}OH_2$ will dictate the feasibility or not of the whole process.

Within the same topic equilibrium reactions involving solvent coordination such as MeCN in different oxidation states of the metal center as well as exchange reactions are also key to understanding the catalytic cycle, [8]

$$Ru\text{-}OH_2 + MeCN \rightleftharpoons Ru\text{-}MeCN + H_2O \qquad (1)$$

$$Ru\text{-}OH_2 + H_2O^* \rightleftharpoons Ru\text{-}H_2O^* + H_2O \qquad (2)$$

For the particular case of *in,in*-RuHbpp complexes (*in, in*-$[\{Ru(T)(L)\}_2(\mu\text{-bpp})]^{n+}$), L = acetonitrile, pyridine or 3,5-dimethylpyridine; T= terpyridine or *bid-*; a drawing of the polydentate ligands is depicted in Scheme 1) a further intra-supramolecular interaction has to be taken into consideration. This phenomenon is related to the through space interaction between the monodentate ligands[9] and constitutes a specific case of the stereochemistry of ligand bridged dinuclear coordination complexes. It is exemplified in the equation (3) for complex $\mathbf{3b^{3+}}$ where the interconversion of the two isomers in solution takes place very fast at room temperature

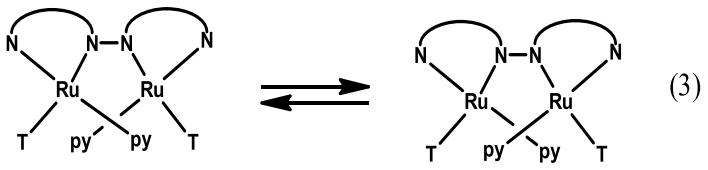

(3)

Δ, Δ-*in, in*-$[Ru_2(py)_2]$ Λ, Λ-*in, in*-$[Ru_2(py)_2]$

The axial coordination of the *trpy* ligands are not shown for clarity purposes and the formula at the bottom excludes the *trpy* and *bpp*$^-$ ligands. The two isomers differ from one another in the relative position of the pyridyl ligands, whether they are situated above or below the equatorial plane. If temperature is maintained at RT or below, the equilibrium occurs without breaking any Ru-N bonds, as has been clearly demonstrated by NMR spectroscopy.[9]

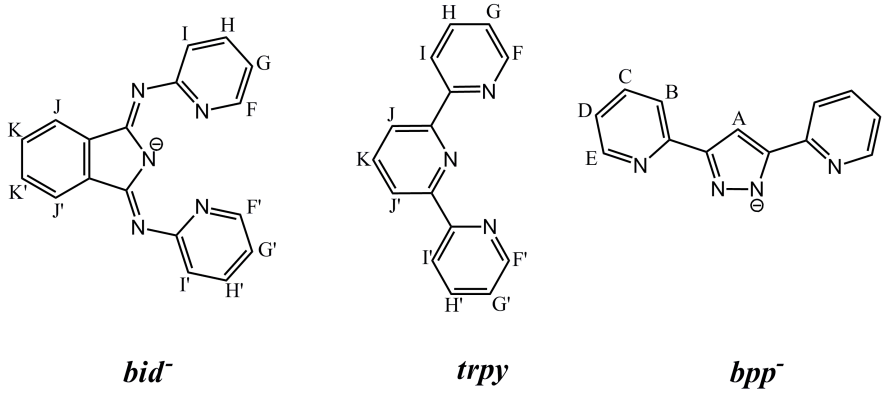

Scheme 1. Ligands used in this work and including their abbreviations and NMR labeling scheme.

In the present work we wish to report on the behavior of the *in,in*-RuHbpp complexes when exposed to temperatures above RT and describe the intimate details of the labile Ru-N bond scission. For this purpose we have completed the synthesis of a large family of Ru-Hbpp complexes with general formula $[\{Ru(T)(L)\}_2(\mu\text{-bpp})]^{n+}$ (L = acetonitrile, pyridine and 3,5-dimethylpyridine; T= *trpy* or *bid*$^-$) and have carried out a complementary DFT work.

3.3.3. Experimental Section

Materials

All reagents used in present work were obtained from Aldrich Chemical Co. or Alfa Aesar and were used without further purification. Synthesis grade organic solvents were obtained from SDS and were routinely degassed with argon. Methanol was

destilled over MgI, ethanol was dried with 3.5 Å molecular sieve and acetonitrile, dichloromethane (DCM), hexane and diethyl ether were used from the SPS. High purity deionized water was obtained by passing distilled water through a nanopure Mili-Q water purification system.

The 3,5-bis(2-pyridyl)pirazole (Hbpp) ligand,[10] $[Ru^{III}Cl_3(Hbid)]$,[11] $[\{Ru(trpy)\}_2(\mu\text{-}bpp)(\mu\text{-}AcO)](PF_6)_3$, **$2(PF_6)_3$,** [12] $[\{Ru(bid)(MeCN)\}_2(\mu\text{-}bpp)](NO_3)$, **$3a'(NO_3)$,** $[\{Ru(bid)(py)\}_2(\mu\text{-}bpp)](Cl)$, **3b'(Cl),** and $[\{Ru(trpy)(py)\}_2(\mu\text{-}bpp)](PF_6)_3$, **$3b(PF_6)_3$**, were prepared as described in the literature.[9] All synthetic manipulations were routinely performed under argon atmosphere using Schlenck and vacuum line techniques.

***in,in*-[{Ru^{II}(bid)(Cl)}(μ-bpp){Ru^{II}(bid)(MeOH)}], 1'.** A solution of 0.290 g (0.5 mmol) of $RuCl_3Bid$ and 0.20 mL (1.5 mmol) of triethylamine in MeOH (10 mL) was stirred at room temperature, under argon atmosphere and in the absence of light, for 30 min. Then, 0.056 g (0.25 mmol) of Hbpp, 0.014 g (0.25 mmol) of NaOMe and 0.424 g (10 mmol) of LiCl were added to the initial mixture in 10 mL of methanol. The resulting solution was heated at reflux for 2 h in the presence of a 200 W tungsten lamp, cooled to room temperature and filtered off in a Schlenck frit. The dark green solid obtained was washed with diethyl ether and dried under vacuum. Yield: 80% (0.220 g). Anal. Calc. for $C_{50}H_{41}ClN_{14}ORu_2$: C, 55.02; H, 3.79; N, 17.96. Found: C, 54.80; H, 3.49; N, 17.57. ^{1}H-RMN (400 MHz, d_2-DCM, 298 K, ppm): δ, 1.89 (d, J_{LO}= 4.58 Hz, 3H, H_O), 6.02(t, $J_{F\text{-}G}$=$J_{G\text{-}H}$= 6.84 Hz, 2H ,H_G), 6.15 (td, $J_{f\text{-}g}$=$J_{g\text{-}h}$= 6.33, $J_{g\text{-}i}$=1.9 Hz, 2H, H_g), 6.53 (td, $J_{C\text{-}D}$=$J_{E\text{-}D}$=5.91, $J_{B\text{-}D}$=1.27 Hz, 1H, H_D), 6.58 (t, $J_{c\text{-}d}$ =$J_{d\text{-}e}$ =5.91 Hz,1H, H_d), 6.91 (q, $J_{L\text{-}O}$ = 4.58 Hz, 1H, H_L), 7.05 (dd, $J_{D\text{-}E}$ = 5.91, $J_{C\text{-}E}$ = 1.47 Hz, 1H, H_E), 7.22 (dd, 1H, $J_{d\text{-}e}$ = 5.91, $J_{c\text{-}e}$ = 1.47 Hz, H_e), 7.38 (td, $J_{C\text{-}D}$ = 5.91, $J_{C\text{-}E}$ = 1.47 Hz, 1H, H_C), 7.42 (dd, $J_{c\text{-}b}$ = 8.26, $J_{c\text{-}d}$ = 5.91 Hz, 1H, H_c), 7.45 (dd, $J_{H\text{-}I}$ = 6.84, $J_{G\text{-}I}$ = 1.90 Hz, 2H, H_I), 7.51 (td, 2H, J_{gh} = J_{hi} = 6.33, J_{hi} = 1.58 Hz, Hi), 7.54 (td, $J_{G\text{-}H}$ = $J_{H\text{-}I}$ = 6.84, $J_{F\text{-}H}$ = 1.62 Hz, 2H, H_H), 7.58 (dd, $J_{J\text{-}K}$ = 5.51, $J_{J\text{-}K}$ = 3.13 Hz, 2H, H_J), 7.60 (dd, J_{hi} = 6.33, J_{ig} = 1.9 Hz, 2H, H_i), 7.65 (dd, $J_{k\text{-}j}$ = 5.51, $J_{j\text{-}i'}$ = 3.13 Hz, 2H, H_j), 7.74 (dd, $J_{B\text{-}C}$ = 8.26, $J_{B\text{-}D}$ = 1.27, 1H, H_B), 7.76 (d, $J_{b\text{-}c}$ = 8.26, $J_{b\text{-}d}$ = 1.27, 1H, H_b), 7.80 (s, 1H, H_A), 8.15 (dd, $J_{J\text{-}K}$ = 5.51, $J_{K\text{-}K'}$ = 3.13 Hz, 2H, H_K), 8.20 (d, $J_{F\text{-}G}$ = 6.84, $J_{F\text{-}H}$ = 1.62 Hz, 2H, H_F), 8.22 (dd, J_{kj} = 5.51, $J_{k\text{-}k'}$ = 3.13 Hz, 2H, H_k), 8.30 (dd, $J_{f\text{-}g}$ = 6.33, $J_{f\text{-}h}$ = 1.58 Hz, 2H, H_f). UV-vis (CH_2Cl_2) [λ_{max}, nm (ε, $M^{-1}cm^{-1}$)]: 271 (34332), 279 (33628),

303 (31124), 368 (27104), 424 (10491), 609 (3516). $E_{1/2}$ (CH_2Cl_2, V vs SSCE): 0.204, 0.611.

***in,in*-[{Ru^{II}(bid)(MeCN)}$_2$(μ-bpp)}(PF_6) (3a'(PF_6)).** ^{1}H-RMN (500 MHz, CD_3CN 240 K, ppm): δ, 1.00 (s, 6H, H_O), 5.66 (t, J_{FG} = 6.36, J_{GH} = 1.14 Hz, 2H ,H_G), 6.67 (dd, $J_{F'G'}$ = 7.50, $J_{F'H'}$ = 1.56 Hz, 2H, $H_{F'}$), 6.79 (td, $J_{F'G'}$ = $J_{G'H'}$ = 7.50, $J_{G'I'}$ = 1.79 Hz, 2H, $H_{G'}$), 6.82 (t, J_{CD} = J_{DE} = 5.92 Hz, 2H, H_D), 7.35 (d, J_{DE} = 5.92 Hz, 2H, H_E), 7.49 (m, J_{GH} = J_{HI} = 6.36, J_{FH} = 1.22 Hz, 4H, H_I, H_I), 7.56 (dd, J_{HG} = 6.36, J_{GI} = 1.70 Hz, 2H, H_G), 7.63 (d, J_{BC} = 7.00, J_{CD} = 5.92 Hz, 2H, H_C), 7.68 (dd, J_{JK} = 7.50, $J_{JJ'}$ = 1.79 Hz, 4H, $H_{J'}$, H_J), 7.71 (dd, J_{JK} = 4.08, $J_{JK'}$ = 2.92 Hz, 4H, H_J, $H_{J'}$), 7.75 (d, $J_{H'I'}$ = $J_{G'H'}$ = 7.50, $J_{H'F'}$ = 1.56 Hz, 2H, $H_{H'}$), 7.96 (d, J_{BC} = 7.00 Hz, 2H, H_B), 8.09 (s, 1H, H_A), 8.15 (dt, J_{JK} = $J_{J'K'}$ = 4.08, $J_{KK'}$ = 2.92 Hz, 4H, H_K, $H_{K'}$), 9.41 (dd, J_{FG} = 6.36, J_{FH} = 1.22 Hz, 2H, H_F). ^{13}C-RMN (500MHz, CD_3CN, 240 K, ppm): δ, 158.9 (C_F), 153.4 ($C_{F'}$), 150.0 (C_E),137.0 (C_C),135.6 (C_H), 135.6 ($C_{H'}$), 130.2 (C_J), 130.2 ($C_{J'}$), 128.4 ($C_{I'}$), 128.0 (C_D), 127.1 (C_I), 120.8 (C_B), 120.8 (C_K), 120.8 ($C_{K'}$), 117.9($C_{G'}$), 115.6 (C_G), 106.0 (C_A), 30.4 (C_O). UV-vis (CH_2Cl_2) [λ_{max}, nm (ε, $M^{-1}cm^{-1}$)]: 265 (42331), 284 (41836), 229 (39517), 341 (36757), 352 (38303), 382 (22132), 414 (13346), 503 (4005), 540 (5290), 598 (4062). $E_{1/2}$(CH_2Cl_2, V vs SSCE): 0.739, 0.954.

***in,in*-[{Ru^{II}(trpy)(MeCN)}$_2$(μ-bpp)](PF$_6$)$_3$, 3a(PF$_6$)$_3$.** A 100 mg (0.08 mmol) sample of complex [{Ru(trpy)}$_2$(μ-bpp)(μ-AcO)](PF$_6$)$_3$ (0.08 mmol) were dissolved in 50 mL of MeCN/water (3/1), following 2 mL of a pH = 1 water solution (triflic acid) were added. The mixture was heated at reflux for 6 hours. Upon cooling to room temperature, the unreacted starting material was filtered and 1 mL of a saturated aqueous solution of KPF_6 was added to the solution. After partial evaporation of the solvent in a rotary evaporator a brown solid precipitated. Recrystallization from acetonitrile/ether yielded dark brown small crystals. Yield: 70% (0.079 g). Anal. Calc. for $C_{47}H_{37}F_{18}N_{12}P_3Ru_2$: C, 40.12; H, 2.65; N, 11.95. Found: C, 40.37; H, 2.22; N, 11.75. ^{1}H-RMN (400 MHz, Acetone-d_6, 298 K, ppm): δ, 1.43 (s, 6H, H_O), 7.02 (t, J_{CD} = J_{ED} = 7.74 Hz, 2H, H_D) 7.46 (d, J_{DE} = 7.74 Hz, 2H, H_E), 7.56 (t, J_{GH} = J_{FG} = 8.08 Hz, 2H, H_G), 7.89 (t, J_{BC} = J_{CD} = 7.74 Hz, 2H, H_C), 8.15 (t, J_{HI} = J_{HG} = 8.08 Hz, 2H, H_H), 8.20 (d, J_{BC} = 7.74 Hz, 2H, H_B), 8.39 (t, J_{JK} = 8.33 Hz, 2H, H_K), 8.47 (s, 1H, H_A), 8.68 (d, J_{HI} = 8.08 Hz, 4H, H_I), 8.80 (d, J_{JK} = 8.33 Hz, 4H, H_J). ^{1}H-RMN (400 MHz, MeCN-d_6, 298 K, ppm): δ 1.12 (s, 6H, H_O), 6.90 (t,

J_{CD} = J_{ED} = 7.74 Hz, 2H, H_D), 7.17 (d, J_{DE} = 7.74 Hz, 2H, H_E), 7.37 (t, J_{GH} = J_{FG} = 8.08 Hz, 2H, H_G), 7.78 (t, J_{BC} = J_{CD} = 7.74 Hz, 2H, H_C), 8.0.2 (t, J_{HI} = J_{HG} = 8.08 Hz, 2H, H_H), 8.17 (s, 1H, H_A), 8.27 (t, J_{JK} = 8.33 Hz, 2H, H_K), 8.43 (d, J_{HI} = 8.08 Hz, 4H, H_I), 8.85 (d, J_{JK} = 8.33 Hz, 4H, H_J). UV-vis (CH_2Cl_2) [λ_{max}, nm (ε, $M^{-1}cm^{-1}$)]: 272 (59626), 311 (70425), 359 (26803), 444 (13238), 476 (11874), 541 (3154). $E_{1/2}$ (CH_2Cl_2, V vs SSCE): 1.084, 1.392. MALDI(+)- MS: (MeOH): 558.6 $[M\text{-}PF_6\text{-}PF_6]^{2+}$**.**

***in,in*-[{Ru^{II}(trpy)(py)}(μ-bpp){Ru^{II}(trpy)(MeCN)}](PF$_6$)$_3$·CH$_2$Cl$_2$, 4(PF$_6$)$_3$·CH$_2$Cl$_2$.** A 50 mg (0.035 mmol) sample of complex **3b(PF$_6$)$_3$** were dissolved in 25 mL of MeCN. The mixture was heated at 70 ºC for 3 h and quickly cooled with an ice bath. After fast complete evaporation of the solvent with a rotary evaporator the brown product was redissolved in 5 mL of acetone and 1mL of a saturated aqueous solution of KPF_6 was added followed by the addition of 5 more mL of water. After partial evaporation of the acetone in a rotary evaporator a brown solid precipitated. The dark brown solid was filtered and rinsed with diethylether. Recrystallization from acetone/ether yielded dark brown small crystals. Yield: 78 % (0.039 g). Anal. Calc. for $C_{50}H_{39}F_{18}N_{12}P_3Ru_2$: C, 41.88; H, 2.97; N, 11.59. Found: C, 41.07; H, 2.72; N, 11.63. ^{1}H-RMN (400 MHz, CD_3CN, 298 K, ppm): δ, 1.27 (s, 3H, H_O), 6.70 (t, J_{ML} = J_{MN} = 6.96 Hz, 2H, H_M), 7.03 (t, J_{DE} = J_{DC} = 7.23 Hz, 1H, H_D), 7.04 (t, J_{de} = J_{dc} = 7.23 Hz, 1H, H_d) 7.35 (d, J_{ed} = 7.23 Hz, 1H, H_e), 7.43 (t, J_{GF} = J_{GH} = 6.80 Hz, 2H, H_G), 7.44 (t, J_{NM} = $J_{NM'}$ = 6.96 Hz, 1H, H_N). 7.52 (d, J_{ED} = 6.96 Hz, 1H, H_E), 7.73 (t, J_{gf} = J_{gh} = 6.82 Hz, 2H, H_g), 7.89 (t, J_{cd} = J_{cb} = 7.23 Hz, 1H, H_c) 7.96 (t, J_{CD} = J_{CB} = 7.23 Hz, 1H, H_C), 8.11 (t, J_{HI} = J_{HG} = 6.80 Hz, 2H, H_H) 8.20 (t, J_{hi} = J_{hg} = 6.80 Hz, 2H, H_h), 8.24 (d, J_{bc} = 7.23 Hz, 1H, H_b), 8.26 (d, J_{BC} = 8.30 Hz, 1H, H_B), 7.30 (t, J_{kj} = 8.10 Hz, 1H, H_k), 8.33 (t, J_{KI} = 8.10 Hz, 1H, H_K), 8.37 (d, J_{fg} = 8.10 Hz, 2H, H_f), 8.46 (d, J_{ML} = 6.96 Hz, 2H, H_L), 8.60 (d, J_{FG} = 6.82 Hz, 2H, H_F), 8.60 (s, 1H, H_A), 8.68 (d, J_{IH} = 6.80 Hz, 2H, H_I), 8.70 (d, J_{ih} = 6.80 Hz, 2H, H_i), 8.75 (d, J_{jk} = 8.10 Hz, 2H, H_j), 8.84 (d, J_{JK} = 8.10 Hz, 2H, H_K).UV-vis (MeCN) [λ_{max}, nm (ε, $M^{-1}cm^{-1}$)]: 271 (55806), 312 (66667), 356 (24028), 440 (9127),469 (11727), 495 (8533), 574 (1856). $E_{1/2}$ (CH_2Cl_2, V vs SSCE): 1.086, 1.340. MALDI(+)- MS: (MeOH):1301.4 $[M\text{-}PF_6]^+$**.**

***in,in*-[{Ru^{II}(trpy)(lut)}$_2$(μ-bpp)](ClO$_4$)$_3$·CHCl$_3$, 3c(ClO$_4$)$_3$·CHCl$_3$.** A 50 mg sample of complex [{Ru(trpy)}$_2$(μ-bpp)(μ-AcO)](PF$_6$)$_3$ (0.035 mmol) were dissolved in 40mL of acetone/water (3:1), following 2 mL of a pH = 1 water solution (triflic acid) were

added. After the addition of 0.15 mL of 3,5-dimethyl-pyridine (4 mmol), the mixture was heated under reflux for 6 hours. Upon cooling to room temperature, the unreacted starting material was filtered and 1mL of a saturated aqueous solution of KPF_6 was added to the solution. After evaporation of the acetone in a rotary evaporator a brown-black solid was obtained which was recrystallized from chloroform/ether yielding dark brown small crystals. Yield: 90% (0.048 g). Anal. Calc. for $C_{58}H_{50}Cl_6N_{12}O_{12}Ru_2$: C, 45.77; H, 3.30; N, 11.04. Found: C, 45.65; H, 3.03; N, 10.90. ^{1}H-RMN (400MHz, Acetone-d_6, 188 K, ppm): δ, 1.24 (s, 6H, $H_{O'}$), 1.53 (s, 6H, H_O), 6.48 (s, 2H, H_L), 7.00 (t, $J_{ED} = J_{CD}$ = 5.94 Hz, 2H, H_D), 7.03 (s, 2H, $H_{L'}$), 7.41(d, J_{ED} = 5.94 Hz, 2H, H_E), 7.91 (t, $J_{F'G'} = J_{H'G'}$= 4.90 Hz, 2H, $H_{G'}$), 7.93 (t, $J_{FG} = J_{HG}$= 5.26 Hz, 2H, H_G), 7.95 (t, $J_{BC} = J_{CD}$ = 5.94 Hz, 2H, H_C), 7.97 (s, 2H, H_N), 8.16 (t, $J_{H'I'} = J_{H'G'}$ = 4.90 Hz, 2H, $H_{H'}$), 8.28 (t, $J_{KJ} = J_{KJ'}$ = 8.35 Hz, 2H, H_K), 8.33 (t, $J_{HI} = J_{HG}$ = 5.26 Hz, 2H, H_H), 8.38 (d, J_{BC} = 5.94 Hz, 2H, H_B), 8.46 (d, $J_{H'I'}$ = 4.90 Hz, 2H, $H_{I'}$), 8.54 (d, $J_{J'K}$ = 8.35 Hz, 2H, $H_{J'}$), 8.66 (d, $J_{F'G'}$ = 4.90 Hz, 2H, $H_{F'}$), 8.94 (d, J_{HI} = 5.26 Hz, 2H, H_I), 8.95 (s, 1H, H_A), 8.97 (d, J_{JK} = 8.35 Hz, 2H, H_J), 9.21 (d, J_{FG} = 5.26 Hz, 2H, H_F). UV-vis (CH_2Cl_2) [λ_{max}, nm (ε, $M^{-1}cm^{-1}$)]: 275 (54000), 317(62450), 361 (25704), 470 (9412), 502 (10059), 566 (2439), 660 (1009). $E_{1/2}$(CH_2Cl_2, V vs SSCE): 1.064, 1.332. MALDI(+)-MS: (DCM): 1198.2 $[M\text{-}CHCl_3\text{-}ClO_4\text{-}LUT]^+$, 663 $[M\text{-}CHCl_3\text{-}ClO_4\text{+}Na]^{2+}$.

Equipment and measurements

All electrochemical experiments were performed in a PAR 263A EG&G potentiostat or in a IJ-Cambria IH-660 potentiostat, using a three electrode cell. Glassy carbon electrodes (3 mm diameter) from BAS were used as working electrode, platinum wire as auxiliary and SSCE as the reference electrode. Cyclic voltammograms (CV) were recorded at 100 mV/s scan rate under nitrogen atmosphere. The complexes were dissolved in previously degassed dichloromethane containing the necessary amount of (n-Bu_4N)(PF_6), used as supporting electrolyte, to yield a 0.1 M ionic strength solution. All $E_{1/2}$ values reported in this work were estimated from cyclic voltammetry as the average of the oxidative and reductive peak potentials ($E_{p,a}$+$E_{p,c}$)/2 or from Differential Pulse Voltammetry (DPV; pulse amplitudes of 0.05 V, pulse widths of 0.05 s, sampling width of 0.02 s and a pulse period of 0.1 seconds). Unless explicitly mentioned the concentration of the complexes were approximately 1 mM. The NMR spectroscopy at

room temperature was performed on a 400 MHz Bruker avance II and at low temperatures with a Bruker avance 500 MHz. Samples were run in CD_2Cl_2, d_6-acetone or d_3-acetonitrile. The ESI and MALDI mass spectroscopy experiments were performed on a Waters Micromass LCT Premier equipment and a Bruker Daltonics Autoflex equipped with a nitrogen laser (337 nm), respectively. UV-Vis spectroscopy was performed on a CARY 50 Bio (VARIAN) UV-vis spectrophotometer with 1 cm quartz cells.

UV-vis Kinetic studies on the ligand-substitution processes were performed at various concentrations of dinuclear complex and always using Acetonitrile as solvent. In a typical experiment, a solution of starting complex at concentrations varying from 5 μM to 350 μM were prepared at 0 ºC and introduced to the quartz cells which where preheated at the desired temperature, typically a full spectra was recorded every 10 minutes. In all cases, the temperature was maintained at ± 0.1 ºC with a Huber CC3-905 VPCw cryostat. First and second rate constants where calculated by a global fitting method or single wavelength fitting using Specfit.[13] The data was reproduced by two first order consecutive reactions (A→B→C). In all cases rate constants were measured between 10.0 ºC and 68.0 ºC.

X-Ray structure determination

All measured crystals were prepared under inert conditions immersed in perfluoropolyether as protecting oil for manipulation. The measured crystals were mounted using a nylon loop directly from the crystallization solution to the diffractometer cooled at -120 ºC. Measurements were made on a Bruker-Nonius diffractometer equipped with an APPEX 2 4K CCD area detector, a FR591 rotating anode with MoK_α radiation, Montel mirrors as monochromator and a Kryoflex low temperature device (T = -173 °C). Full-sphere data collection was used with ω and φ scans. Programs used: data collection Apex2 v. 1.0-22;[14] data reduction, Saint + Version 6.22; [15] absorption correction, SADABS V. 2.10; [16] structure solution and refinement, SHELXTL Version 6.14. [17]

Crystals for complex $\mathbf{3c}^{3+}$ were grown from MeCN at 4 °C. Data was obtained from two twin crystals and the absorption correction was carried out with TWINABS.[18] Suitable crystals for complex $\mathbf{4}^{3+}$ and complex $\mathbf{3b}^{3+}$ were grown by slow diffusion of diethylether into an acetone solution of the complex**.** Crystals for $\mathbf{3a'}^{+}$ were grown by slow diffusion of diethyether into an acetonitrile solution.

Computational methods

Calculations on the reaction mechanism were carried out with the Gaussian 03 suite of programs,[19] using the ONIOM method[20,21] at the ONIOM(B3LYP:HF)//ONIOM (B3LYP:UFF) level of theory.[12-24] The SDD basis set and ECP was used to describe Ru [25] while 6-31G(d)[26,27] was used for all remaining atoms. The ONIOM partitioning is shown in the Figure S4.1 in the Supp. Inf. H atoms were used to cap the bonds which cross the partition between the high and low levels. Since the substitution reactions occur at different metal centers there is a discontinuity in the reaction profile because the metal centre involved in the substitution reaction must be modeled with DFT. That means that *in,in*-[{Ru^{II}(trpy)(py)}(μ-bpp){Ru^{II}(trpy)(MeCN)}]$^{3+}$ can be described by two ONIOM partitions depending on which reaction is of interest. However the relative energies of the two processes can be compared without problems.

Minima were confirmed through frequency calculations. Both potential and free energies are reported. There is currently significant discussion about how to better estimate entropy corrections for dissociation reactions in solution,[28] with some authors suggesting that the entropy corrections should be halved.[29] Therefore the true free energy of dissociation lies between the predicted potential and free energy values. Since the free energy correction is very similar for the two substitution reactions in this study we can assume that the errors are similar for both and that a comparison of the two reactions is still very useful.

Solvent effects for the model system were calculated using the PCM model[30] with UAHF radii, through single point HF calculations on the ONIOM optimized geometries. Calculations were carried out using the experimental solvent, acetonitrile.

An additional set of calculations on the pyridine-pyridine and lutidine-lutidine interactions were carried out using the ORCA 2.7 package.[31] Apart from the B3LYP functional,[18,19] these calculations were also carried out with dispersion-corrected density functional theory (DFT-D), as implemented in ORCA, which uses a semi-empirical correction proposed by Grimme[32] to account for Van der Waals forces. The TZVP basis set[33] was used for this additional set of calculations.

3.3.4. Results and discussion

Synthesis and structure

The synthetic strategy followed for the preparation of the complexes described here is depicted in Scheme 2. Addition of the octahedral Ru complex $TRu^{III}Cl_3$ to the tetraaza dinucleating *Hbpp* ligand in the presence of NEt_3 generates the corresponding dinuclear Ru complexes $\mathbf{1^{2+}}$ and **1'** with C_2 and C_S symmetry respectively. Whereas for $\mathbf{1^{2+}}$ the monodenate Cl ligand acts as a bridging ligand for **1'** the Cl simply acts as a non-bridging monodentate ligand to one of the Ru centers while the second centre is coordinated by a MeOH. For easy follow up of the complex nomenclature in this paper all complexes containing the anionic bid^- ligand are denoted with a prime whereas the ones with *trpy* are not.

Subsequent reaction of $\mathbf{1^{2+}}$ or **1'** with acetate anion generate the corresponding $\mathbf{2^{2+}}$ and **2'** complexes with C_2 symmetry that contain two bridging ligands, the original bpp^- and the acetato that acts now as a bidentate bridging the two Ru metal centers. These acetato bridge complexes are excellent starting materials since they are easy to handle crystalline materials that are obtained with relatively reasonable good yields. In addition the lability of the acetato bridge allows to easily obtain the family of $\mathbf{3^{3+}}$ and $\mathbf{3'^{+}}$ complexes containing the corresponding monodentate ligands.

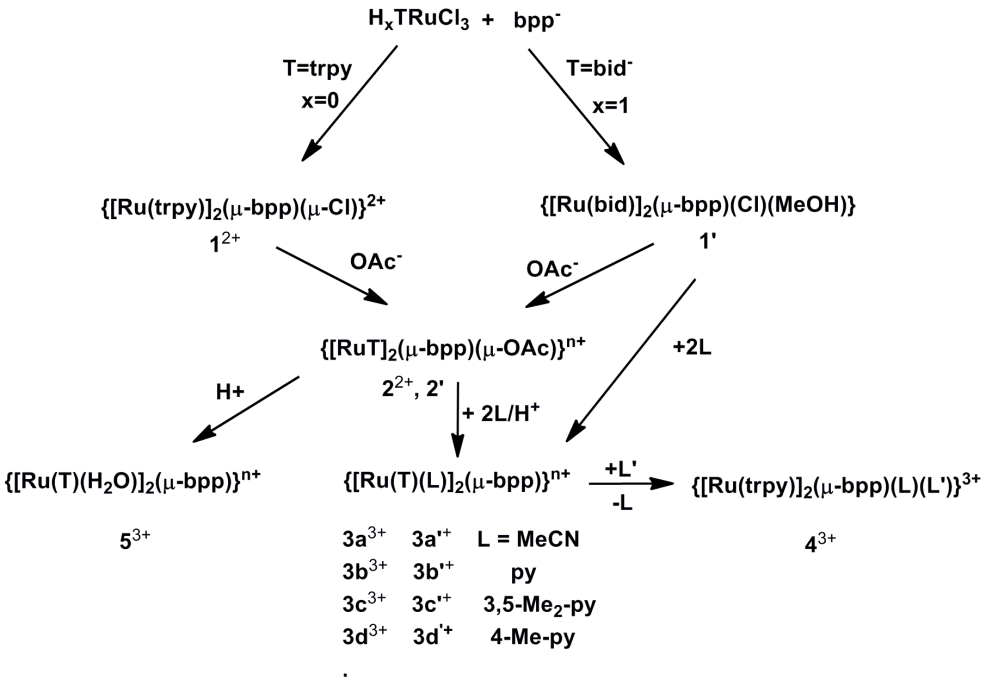

Scheme 2. Synthetic strategy. Complexes containing the prime refer to the ones that contain the *bid*$^-$ ligand whereas those that do not have the prime contain the *trpy* ligand.

Complex $\mathbf{4^{3+}}$, containing mixed monodenate ligands can be obtained by careful control of the reaction time using the bis-pyridyl complex $\mathbf{3b^{3+}}$ or $\mathbf{3b'^{+}}$ as starting material, using acetonitrile as solvent.

Spectroscopic Properties

X-ray crystal structures have been obtained for complexes $\mathbf{3a'^{+}}$, $\mathbf{3b^{3+}}$, $\mathbf{3d^{3+}}$ and $\mathbf{4^{3+}}$, their most relevant crystallographic parameters are reported in Table 1 and 2 whereas their molecular plots are shown in Figure 1. All their Ru-N bond distances and angles are within the typical values for octahedral d^6 Ru(II)N_6 type of cations.[34]

Table 1. X-ray crystallographic parameters for complexes $\mathbf{3b^{3+}}$, $\mathbf{3a'^{+}}$, $\mathbf{3c^{3+}}$ and $\mathbf{4^{3+}}$.

	3a'(NO_3)	**3b(PF_6)$_3$**	**3c(ClO_4)$_3$**	**4(PF_6)$_3$**
Emp. Form.	$C_{55}H_{42}N_{18}O_3Ru_2$	$C_{62}H_{61}F_{18}N_{12}O_4P_3Ru_2$	$C_{61}H_{56}Cl_3N_{14}O_{12}Ru_2$	$C_{56}H_{54}F_{18}N_{12}O_2P_3Ru_2$
Mr	1205.21	1674.70	1493.69	1576.47
Cryst. Syst.	monoclinic	triclinic	triclinic	monoclinic
Space group	P 21/n	P -1	P-1	P2(1)/n
a (Å)	15.5976(7)	14.5367(6))	13.2188(3)	13.2129(4)
b (Å)	14.0158(7)	15.9696(6	15.9950(5	19.9774(5)
c (Å)	23.0456(11)	17.9748(7)	16.5739(5)	23.3886(6)
α (deg)	90.00	92.694(2)	73.258(1)	90
β (deg)	98.178(2)	110.779(2)	74.330(1)	93.961(2)
γ (deg)	90.00	113.366(2)	69.045(1)	90
V(Å^3)	4986.83	3494.7(3)	3078.64(15)	6158.9(3)
Z	4	2	2	4
ρcalc (g · cm-3)	1.605	1.592	1.611	1.700
μ (mm-1)	0.673	0.604	0.697	0.680
GOF on F2	1.128	1.024	1.009	1.032
R1	0.0593	0.0621	0.0566	0.0562
WR2	0.1496	0.2077	0.1324	0.1577

The Ru centres possess an octahedrally distorted coordination geometry as a consequence of the steric encumbrance provoked by the mutual interaction of the monodentate ligands, that force them to accommodate above and below an ideal equatorial plane respectively. As a result of this all complexes posses C_2 symmetry and their optical image counterpart can also be found in each unit cell. At room temperature in solution the two enantiomers indicated in Equation 3 interconvert very fast. In order to quantify the degree of distortion of the octahedral geometry around the Ru centres two parameters have been measured and are reported in Table

2: a) the RuNNRu dihedral angle, where the Ns belong to the N atoms of the pyrazolate group of the *bpp*$^-$ ligand and b) the py-py' (*bpp*$^-$) angle, that is the angle between the best planes described by the pyridyl groups of the *bpp*$^-$ ligand. As it can be observed in the Table 2 the RuNNRu angle ranges from 44º to 53º for all complexes except for **3c**$^{3+}$ containing the lutidine ligand that is only 26º. For the py-py' (*bpp*$^-$) case the angles range from 17º till 24º with the lutidine one having the lowest value. These two parameters clearly indicate that in the lutidine complex the degree of distortion is lower than in any of the other complexes described here.

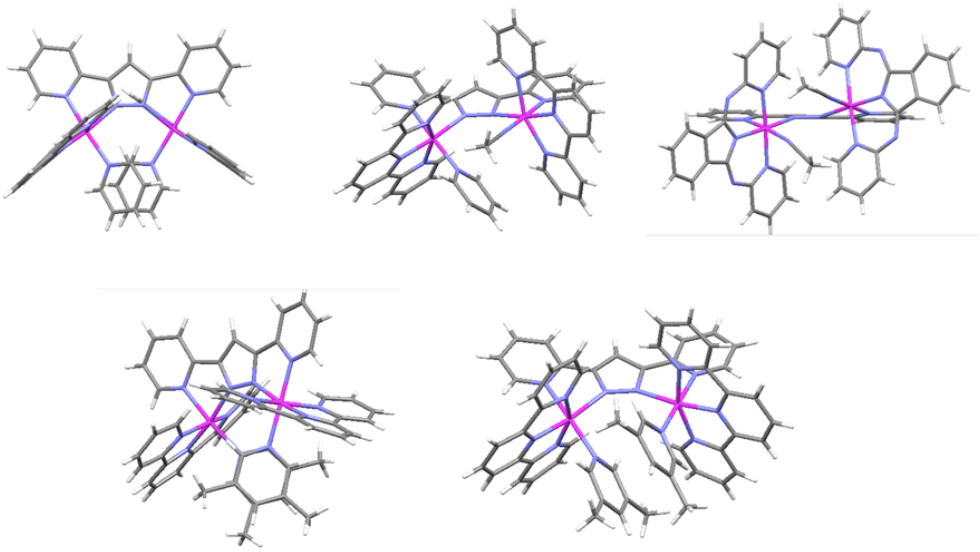

Figure 1. Caped stick diagram for the molecular structure of the cationic part of complexes **3b**$^{3+}$ (top left), **4**$^{3+}$ (top center), **3a'**$^{+}$ (top right) and **3c**$^{3+}$ (bottom; two orientations shown) obtained from X-ray diffraction analysis. Color code: Ru, pink; N, blue; C, gray; H, white.

Another interesting structural feature of the present complexes is the nearly parallel disposition of the aromatic rings of the monodentade ligands containing pyridyllic groups, as can also be seen in Table 2.

This indicates a certain degree of π-π interaction between the mentioned aromatic rings. Whereas for complexes **3b**$^{3+}$ the aromatic rings are slightly rotated with regard

to one another for the **3c**$^{3+}$ complexes the aromatic rings are situated in an eclipsed manner as can be observed in Figure 1, bottom right.

Table 2. Selected metric parameter (distances in Å and angles in deg) for the complexes described in this paper together with related complexes for comparison purposes.

Complex	RuNNRu[a]	py-py' (bpp-)[b]	py-py' (L)[c]	dc[d]
3b^{3+}	45.7	22.3	6.5	3.48
3c^{3+}	26.8	15.9	2.3	3.34
4^{3+}	44.7	20.4	- -	3.52
3a^{3+} [e]	53.2	25.9	- -	3.27e
3d'$^{+}$ [e]	44.3	17.5	0.8	3.52e
3a'$^{+}$	44.5	17.6	- -	3.28

[a] Dihedral angle that involves the two N belonging to the pyrazolate bridged group of the bpp- ligand and two metal centers. [b]Angle between the pyridyl groups of the *bpp*$^{-}$ anionic ligand. [c]Angle between the best planes that run through the pyridylic monodentate ligands. [d]Distance between the centroids of the two monodentate pyridyl rings. The C atom of the nitrile group is used in the case of complexes containing MeCN monodentate ligands. [e]For complexes **3a**$^{3+}$ and **3d'**$^{+}$ see reference 9.

All this particularities associated with the lutidine complex point out the existence of a certain degree of attractive interaction between rings that will be further discussed later aromatic region for **3a**$^{3+}$, **3b**$^{3+}$ and **4**$^{3+}$ is plotted in Figure 2 whereas the rest of 1D and 2D NMR for this and all the other complexes described in this work are presented as Supp. Inf. An interesting feature of these complexes that is reflected in NMR spectroscopy at low temperatures is the relative rotation of the *trpy* ligands needed to accommodate the monodentate ligands. This produces an upfield shift of the external pyridyl of *trpy*, the H_F proton, whereas the opposite external $H_{F'}$ proton suffers a downfield shift[9] (see Scheme 1). Finally it is also worth mentioning here that the Me group of the monodentate MeCN ligand in the mixed ligand complex **4**, has a

0.17 ppm shift with regard to the bis-MeCN, **2a**, due to the interaction of the Me group with the aromatic ring current of the pyridyl ligand.

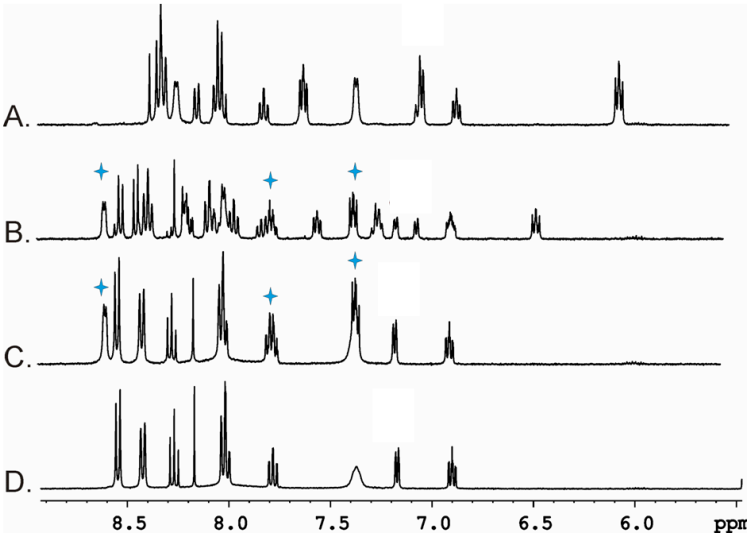

Figure 2. ^{1}H-NMR spectra. (A) $\mathbf{3b}^{3+}$ $6\cdot10^{-3}$M in d_3-MeCN taken after 10 minutes at RT. (B) $\mathbf{4}^{3+}$ formed by dissolving $\mathbf{3b}^{3+}$ in d_3-MeCN after 7 h at 70 °C. The stars indicate free pyridine resonances. (C) $\mathbf{3a}^{3+}$ formed by dissolving $\mathbf{3b}^{3+}$ in d_3-MeCN after 15 h at 70 °C. (D) $\mathbf{3b}^{3+}$ in d_3-MeCN obtained from an authentic sample. The assignment of all resonances can be found in the experimental section.

The family of complexes described in the present work contain strongly bonded polydentate ligands that coordinate the Ru(II) centers and benefit from the chelating effect for extra stability. In sharp contrast their respective monodentate ligands exchange with coordinating solvents, if they are treated at sufficiently high temperatures. As an example the following equations show the substitution reactions that operate when $\mathbf{3b}^{3+}$ is heated in d_3-MeCN (the *trpy* and *bpp*$^-$ ligands are not displayed).

$$\underset{\mathbf{3b}^{3+}}{\textit{in,in}\text{-}[Ru_2(py)_2]^{3+}} + MeCN \rightarrow \underset{\mathbf{4}^{3+}}{\textit{in,in}\text{-}[Ru_2(py)(MeCN)]^{3+}} + py \qquad (4)$$

$$\underset{\mathbf{4}^{3+}}{\textit{in,in}\text{-}[Ru_2[(py)(MeCN)]^{3+}} + MeCN \rightarrow \underset{\mathbf{3a}^{3+}}{\textit{in,in}\text{-}[Ru_2(MeCN)_2]^{3+}} + py \qquad (5)$$

The substitution process can be nicely followed by NMR spectroscopy as shown in Figure 2, and it is interesting to realize here that the substitution process proceeds very cleanly from $\mathbf{3b}^{3+}$ to $\mathbf{4}^{3+}$ to $\mathbf{3a}^{3+}$ without the presence of any other product at the end of the reaction except for free pyridine. In other words the *in,in* configuration is maintained in the two substitution reactions and no isomerization to the potential *in,out* or *out,out* isomers occur (See Scheme 3).

UV-vis spectroscopy has been recorded both in a non coordinating solvent such as DCM and in MeCN as a coordinating solvent at room temperature. Figure 3 shows the spectra for complexes $\mathbf{3a}^{3+}$, $\mathbf{3b}^{3+}$, $\mathbf{4}^{3+}$ and $\mathbf{3b'}^{+}$, and for the rest of the complexes their spectra is presented in the Supp. Inf.

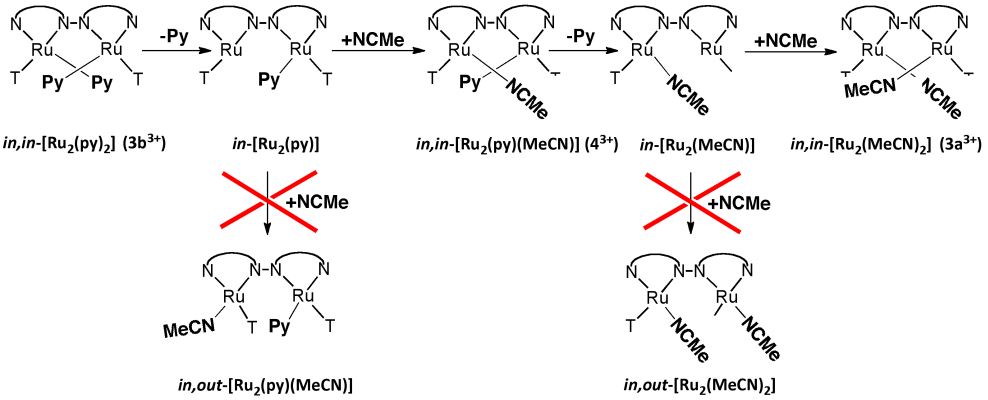

Scheme 3. Proposed reaction mechanism. The arcs connecting the four N atoms represent the *bpp*- ligand whereas the *trpy* or *bid*- ligand are represented by T. The axial coordination of T ligands is not shown for clarity purposes. In the formulas below the structures the *trpy* and *bpp*- ligands are not written.

Table 3 contains the most prominent UV-vis spectroscopic features together with their redox potentials. As expected for Ru(II)N_6 type of complexes with polypyridylic ligands [35] they present π-π ligand based allowed transitions below 300 nm and MLCT and dd bands above 300 nm. Two MLCT bands that appear in the range of 400-550 nm are particularly interesting since they shift to the blue when comparing the pyridine complex $\mathbf{3b}^{3+}$ with the MeCN complex $\mathbf{3a}^{3+}$.

Table 3. UV-vis spectroscopic features and redox properties for complexes $\mathbf{3}^{3+}$, $\mathbf{3'}^{+}$and $\mathbf{4}^{3+}$ recorded in DCM.

Complex	UV-vis λmax, nm (ε, $M^{-1}cm^{-1}$)	$E_{1/2}$ [a] (V) III,II →II,II	$E_{1/2}$ [a] (V) III,III →III,II	$\Delta E_{1/2}$ (mV)
$\mathbf{3b}^{3+}$	464 (12867) 498 (11730)	1.05	1.34	290
$\mathbf{4}^{3+}$	440 (9127) 469 (11727) 495 (8533)	1.09	1.34	250
$\mathbf{3a}^{3+}$	444 (13238) 476 (11874)	1.08	1.40	320
$\mathbf{3c}^{3+}$	470 (9412) 502 (10059)	1.04	1.29	250
$\mathbf{3b'}^{+}$	524 (2129) 574 (2760) 646 (2157) 717 (1850)	0.72	0.98	260
$\mathbf{3a'}^{+}$	503 (4005) 540 (5290) 598 (4062) 660 (2265)	0.74	0.95	210
$\mathbf{3d'}^{+}$	530 (2939) 576 (3794) 650 (2984) 723 (1586)	0.70	0.95	250

[a] $E_{1/2}$ obtained from DPV (pulse amplitudes of 0.05 V, pulse widths of 0.05 s, sampling width of 0.02 s and a pulse period of 0.1 seconds) reported vs. SSCE.

The latter is known to produce a stronger backbonding interaction with Ru, that in turn destabilizes dπ(Ru) orbitals and as consequences the two MLCT shift to higher energy, this is graphically shown in Figure 3 top. For the case of the *bid*$^{-}$ complexes the anionic character of the ligand produces a destabilization of the dπ(Ru) orbitals that as a consequence produce a red shift of the MLCT bands, nicely shown for complexes $\mathbf{3a}^{3+}$ and $\mathbf{3a'}^{+}$ in Figure 3 bottom. Finally for complexes containing the *bid*$^{-}$ ligand a larger amount of π-π* bands are observed which are associated with the *bid*$^{-}$ ligand (see Supp. Inf. for a UV-vis of the free ligands).

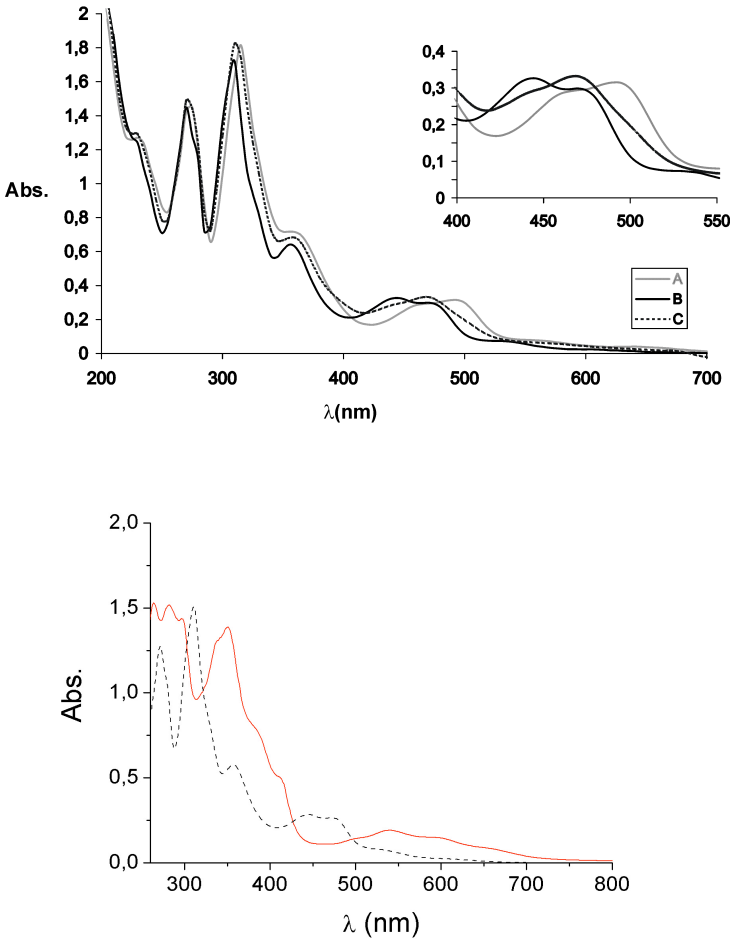

Figure 3. UV-vis spectra in CH_2Cl_2 for 36 µM solutions of complexes: Top, **3b**$^{3+}$ (gray line, A), **3a**$^{3+}$ (black solid line, B) and **4**$^{3+}$ (dotted line, C). The inset show en enlargement in the 400-550 nm region. Bottom, **3a**$^{3+}$ (dotted line) and **3a'**$^{+}$ (solid line).

The energy shifts of the MLCT bands observed in the UV-vis are in agreement with the electrochemistry displayed by these complexes which is described below.

Redox properties have been investigated by means of CV and DPV in CH_2Cl_2 and their clyclic and differential plulse voltammograms are presented in the Supp. Inf., whereas their formal redox potentials are shown in the experimental section and in Table 3.

All the complexes studied in the present work display two redox processes, that are due to two consecutive 1e- removals. Equations 6 and 7 exemplify the case for **3b**$^{3+}$ (*trpy* and *bpp*- ligands not shown),

in,in-[$Ru^{III}Ru^{II}(py)_2$]$^{4+}$ + 1e- → *in,in*-[$Ru^{II}_2(py)_2$]$^{3+}$ $E_{1/2}$=1.05 (6)
3b^{4+} **3b**$^{3+}$

in,in-[$Ru^{III}_2(py)_2$]$^{5+}$ + 1e- → *in,in*-[$Ru^{III}Ru^{II}(py)_2$]$^{4+}$ $E_{1/2}$=1.34 (7)
3b^{5+} **3b**$^{4+}$

A first glance at Table 3 shows that in general complexes containing the MeCN ligand have slightly higher redox potentials compared to the ones containing the pyridyl ligand, as a consequence of the stronger π-acceptor character of the former with regard to the latter. On the other hand the replacement of *trpy* by the *bid*$^-$ ligand produce a decrease of redox potentials by about 330 to 450 mV due to anionic character of the latter. It is also interesting to realize that the difference between the III,III/III,II – III,II/II,II oscillates between 210 and 320 mV and thus indicates a significant variation of the degree of coupling between the Ru metal centers.

Substitution reactions kinetics

Thermal substitution kinetics of **3b**$^{3+}$, **3b'**$^{+}$ and **3c**$^{3+}$ to their corresponding MeCN derivatives **3a**$^{3+}$, **3a'**$^{+}$ have been thoroughly studied at different temperatures and concentrations by ^{1}H-NMR and UV-Vis repetitive scans, using SPECFIT to fit the data and extract kinetic and thermodynamic parameters. For specific cases kinetics were also followed by ^{1}H-NMR spectroscopy and both methods gave fully consistent results. Furthermore as mentioned earlier NMR spectroscopy clearly showed that no other reactions besides the nitrile substitution processes takes place under the conditions studied here. In all cases the data could be fitted with a simple model involving two consecutive reactions with second order rate constants as indicated in Equations 4 and 5 for the **3b**$^{3+}$ case.

The first substitution reaction follows the rate law "$v = k'_1[\mathbf{3b}^{3+}][MeCN]$" whereas the second one follows "$v = k'_2[\mathbf{4}^{3+}][MeCN]$". All the studied reactions were carried out in

neat MeCN as solvent and thus pseudo-first order rate constants were obtained for the two processes with rates laws: "$v = k_1[\mathbf{3b}^{3+}]$" (with $k_1 = k_1'[MeCN]$) and "$v = k_2[\mathbf{4}^{3+}]$" (with $k_2 = k_2'[MeCN]$).

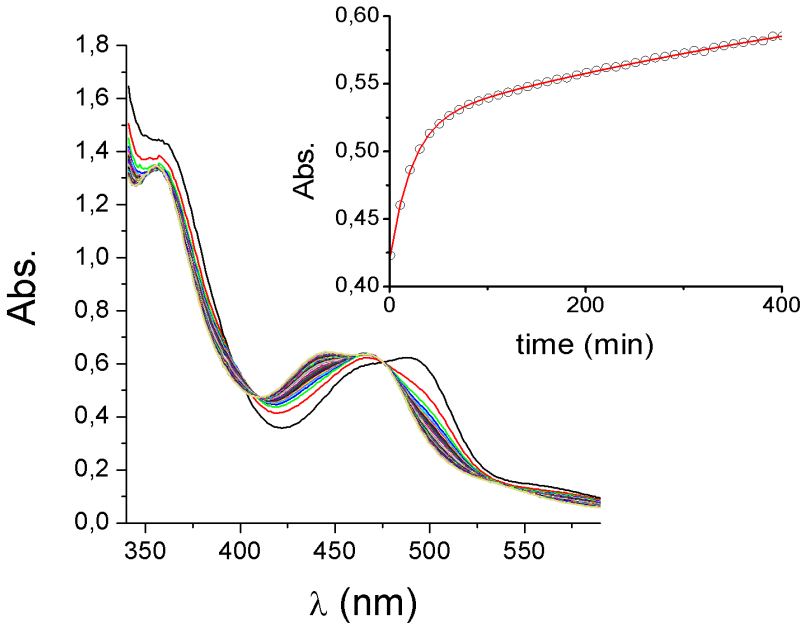

Figure 4. Kinetic profile for the reaction of $\mathbf{3c}^{3+}$ (61·μM) in MeCN at 66.3 °C monitored by UV-vis spectroscopy. Inset, plot of the 438 nm absorbance vs. time (black circles) together with fit (solid line). See text for details.

Figure 4 shows the spectral changes every 10 minutes that occur when 6.1 x 10^{-5} M solution of complex $\mathbf{3c}^{3+}$ in MeCN at 66.3 °C, whereas a plot of absorbance vs. time at λmax = 438 nm is shown in the inset. Mathematical treatment of the data gives k_1 = 9.0 x10-3 s^{-1} and a k_2 = 4.2 x10^{-3} s^{-1} and shows that the first process is much faster than the second one.

Table 4. Rate constants calculated at 40.0 and at 20.0 °C, together with their corresponding activation parameters, for the two substitution reactions.

Complex	k	k x10^3 (313 K)	k x10^3 (293 K)	ΔH^b	$\Delta S^{\neq}$ x10$^{3\,c}$	$\Delta G^{\neq\,b}$ (298K)
3b'$^{+}$	k_1	119 ± 2	9.6 ± 0.3	93.7	29.3	84.9
	k_2	0.9 ± 0.2	0.04 ± 0.03	133.5	117.1	98.7
3b^{3+}	k_1	1.72 ± 0.04	$2{\cdot}10^{-2}$ [a]	110.0	46.0	95.8
	k_2	0.10 ± 0.04	$4{\cdot}10^{-4}$ [a]	129.3	83.7	104.2
3c^{3+}	k_1	0.18 ± 0.02	$4{\cdot}10^{-3}$ [a]	108.4	29.3	99.6
	k_2	0.09 ± 0.03	$2{\cdot}10^{-3}$ [a]	106.3	16.7	101.7

[a]Calculated values from Eyring equation. [b] In kJ ·mol-1. [c] In J ·mol^{-1}·K^{-1}

Evaluation of rate constants at different temperatures allowed us to calculate enthalpies and entropies of activation for the two consecutive processes from their corresponding Eyring plots. Rate constants at 20 and 40 °C and activation parameters for the three complexes are reported in Table 3 whereas the Eyring plots are presented as Supp. Inf.

A first glance at the Table shows that in general the first substitution reaction, k_1, is faster than the second one k_2, for the three systems studied here. In particular at 40 °C for **3b'$^{+}$** k_1 is more than two orders of magnitude higher than k_2 whereas for **3b^{3+}** they differ a little more than one order of magnitude. Finally for **3c^{3+}** k_1 is about two times larger than k_2. A second trend that can be deduced from Table 3 is that the complex that contains the anionic *bid*$^-$ ligand, **3b'$^{+}$** has much larger rate constants than the ones containing the *trpy* ligand. In particular k_1 at 293 K for **3b'$^{+}$** is more than two orders of magnitude higher than for **3b^{3+}**, this phenomenon is clearly linked to the stronger sigma donation capacity of *bid*$^-$, as shown also by UV-vis spectroscopy and electrochemistry, *vide supra*. [36]

DFT Calculations on the Substitution Mechanism

Geometric optimization of complexes $\mathbf{3b^{3+}}$, $\mathbf{4^{3+}}$ and $\mathbf{3a^{3+}}$ was carried out following the ONIOM methodology described in the Experimental Section of the Supp. Inf.. Calculated structures are shown in the Supp Inf. and selected structural parameters displayed in Table S4.1 in the Supp. Inf. Comparison with experimental values obtained by X-ray diffraction analysis show an excellent agreement. The substitution reactions indicated in Equations 4 and 5 were also explored by ONIOM calculations. For this purpose the reaction was divided in two steps as follows:

First substitution,

$$\underset{\mathbf{3b^{3+}}}{\textit{in,in}\text{-}[Ru_2(py)_2]^{3+}} \rightarrow \textit{in}\text{-}[Ru_2(py)]^{3+} + py \qquad (4a)$$

$$\textit{in}\text{-}[Ru_2(py)]^{3+} + MeCN \rightarrow \underset{\mathbf{4^{3+}}}{\textit{in,in}\text{-}[Ru_2(py)(MeCN)]^{3+}} \qquad (4b)$$

Second Substitution,

$$\underset{\mathbf{4^{3+}}}{\textit{in,in}\text{-}[Ru_2(py)(MeCN)]^{3+}} \rightarrow \textit{in}\text{-}[Ru_2(MeCN)]^{3+} + py \qquad (5a)$$

$$\textit{in}\text{-}[Ru_2(MeCN)]^{3+} + MeCN \rightarrow \underset{\mathbf{3a^{3+}}}{\textit{in,in}\text{-}[Ru_2(MeCN)_2]^{3+}} \qquad (5b)$$

This dissociative mechanism, where the pyridine dissociates fully before the acetonitrile comes in was found to provide good agreement with experiment, while we could not locate the corresponding transition states to the alternative associative mechanism, which would require 7-coordination.

On dissociation of pyridine the structures of the intermediates, *in*-$[Ru_2(py)]^{3+}$ and *in*-$[Ru_2(MeCN)]^{3+}$, are found to relax to geometries with approximately planar backbone ligands and with the terpyridine ligands in the out position. This geometry favours the formation of *in,in* complexes. The coordination at the metal centre is closer to octahedral, with one vacant coordination site at the second metal centre. Some

rearrangement is necessary in the dissociation and coordination of ligands but this appears to be compensated for by the coordination energy. The dissociation of pyridine was found to occur with a smooth increase in energy with no transition state.

As shown in Figure 6, substitution reactions 4 and 5 are calculated to be exothermic by 24 kJ mol^{-1} and 18 kJ mol^{-1}, respectively.

The potential formation of the in,out isomer, as indicated in the following equation,

$$\textit{in}\text{-}[Ru_2(py)]^{3+} + MeCN \rightarrow \textit{in,out}\text{-}[Ru_2(py)(MeCN)]^{3+} \quad (8)$$
$$\textit{in,out}\textbf{-4}^{\mathbf{3+}}$$

is calculated to be less favorable than formation of *in,in*-$[Ru_2(py)(MeCN)]^{3+}$ by 24 kJ mol^{-1}, which along with the geometry of the dissociated complex explains why it has not observed experimentally.

The calculated activation barriers depend quite heavily on the free energy corrections, which are very large for the dissociation step, decreasing the dissociation energy from 59 kJ mol^{-1} to -6 kJ mol^{-1}. However entropy corrections are usually overestimated in solution and the true value is likely to be somewhere between the two. This is discussed in the theoretical section, and explains why the potential energies overestimate the experimentally calculated values. Despite the challenges, the differences between the reactions still give valuable insight into the reaction, especially since the free energy correction is similar for the two cases.

The experimental $\Delta H^{\neq}$ in Table 4 range between 92-134 kJ/mol in agreement with the breaking of a Ru-N bond as has been previously reported in the literature for related complexes.[37] All the experimental and kinetic data obtained is in agreement with the mechanism proposed in Scheme 3. That is upon heating the complex a Ru-N bond from the pyridine monodentate ligand is broken with the formation of a 5 coordinated intermediate that quickly reacts with a solvent molecule to generate a the mixed monodentate complex ($\mathbf{4}^{\mathbf{3+}}$ for the case of $\mathbf{3b}^{\mathbf{3+}}$). At this point two isomers could be obtained the *in,in*-$\mathbf{4}^{\mathbf{3+}}$ or the *in,out*-$\mathbf{4}^{\mathbf{3+}}$, however only the former is generated since it is much more thermodynamically stable as has been put forward by DFT calculations. The stronger Ru^{II}-N bond formation by the MeCN ligand given its higher π-

backbonding character, with regard to the pyridine ligand, together with the intrasuparmolecular effects are the thermodynamic driving force for the two consecutive substitution reactions.

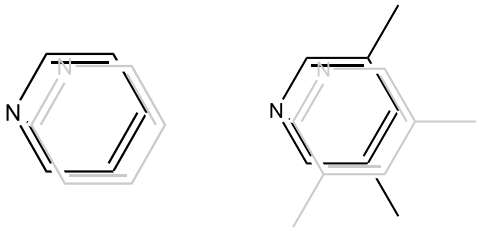

Figure 5. Parallel arrangement of two pyridine rings, left, and two lutidine rings, right, in the structures of **3b**$^{3+}$ and **3c**$^{3+}$. The rings are rotated 60^{o} with regard to one another

The differences in the overall exothermicity of the substitution reactions can be explained through a reduction in steric crowding on replacement of pyridine with acetonitrile. This is especially evident when looking at the calculated energy of dissociation. Dissociation of the pyridine ligand in reaction 4a is calculated to be approximately 40 kJ mol^{-1} less endothermic than in reaction 5a (the corresponding experimental value is 19 kJ·mol^{-1}). Since each substitution reaction is chemically identical for the metal centre at which the reaction occurs, the difference must be primarily due to the changes in steric crowding between the metal centers. This is clearly more important for the first substitution since even from inspection it is possible to see that the intermediate *in,in*-[Ru_2(py)(MeCN)]$^{3+}$ is less sterically crowded than the reactant *in,in*-[$Ru_2(py)_2$]$^{3+}$.

The reduction in steric strain through the reaction is reflected in the changes in bond lengths and angles. There is a consistent decrease in Ru-N bond lengths from *in,in*-[$Ru_2(py)_2$]$^{3+}$, *in,in*-[Ru_2(MeCN)(py)]$^{3+}$ to *in,in*-[$Ru_2(MeCN)_2$]$^{3+}$. The Ru-Ru and L-L distances also decrease. Ru-N and Ru-Ru distances are smaller for the intermediate five coordinate complexes with only one ligand L, *in*-[Ru_2(py)]$^{3+}$ and *in*-[Ru_2(MeCN)]$^{3+}$. All of these results are consistent with a decrease in unfavorable steric interactions when pyridine is removed. It also suggests that the interaction between the pyridine groups in the *in,in*-[$Ru_2(py)_2$]$^{3+}$ complex is repulsive and thus it is destabilized with regard to *in,in*-[$Ru_2(MeCN)_2$]$^{3+}$.

Finally, the $\Delta G^{\neq}$ of activation at 298 K for all the systems are in the range 85.0-101.7 kJ/mol. However for **3b'**$^{+}$ and **3b**$^{3+}$ the difference between the first and second process is 13.8 and 8.4 kJ/mol respectively whereas for **3c** (L = 3,5-lutidine) is only 2.1 kJ/mol. This is a key observation since as mentioned earlier the net process that occurs in the two consecutive reactions are exactly the same, that is the breaking of a Ru-N (pyridine) bond and the formation of a Ru-N(acetonitrile) bond. Therefore the energetic differences must be due to boundary effects. The through-space interaction between the ligands involved was confirmed through an additional set of single-point calculations on the ligands frozen at the geometry they have in the optimized ruthenium dimers, as shown in Figure 5. The interaction is repulsive at the B3LYP level (23 kJ/mol for pyridine, 28 kJ/mol for lutidine), but attractive when dispersion corrections are included at the B3LYP-D level (-7 kJ/mol for pyridine, -18 kJ/mol for lutidine). The importance of dispersion corrections is not surprising, and adds to the growing number of examples showing their importance.[37] The result is however relevant to the topic under discussion because it shows an attraction which is 11 kJ/mol larger for lutidine than for pyridine.

For the case of **3b**$^{3+}$ and **3b'**$^{+}$ the comparison between the barriers for the two steps show that the pyridine-pyridine interaction broken in the first substitution is slightly less favored than the pyridine-acetonitrile interaction broken in the second substitution. As a consequence the first process is more favored than the second 3.2 and 2.0 kJ/mol for **3b'**$^{+}$ and **3b**$^{3+}$ respectively. On the contrary, for the lutidine case, **3c**$^{3+}$, the barriers are much more similar, with a difference of 2.1 kJ/mol. This means that the lutidine-lutidine interaction is less disfavored with respect to lutidine-acetonitrile. And as a consequence, that lutidine-lutidine is more favorable than pyridine-pyridine. This is in sharp contrast with the intuitive notion that the more substituted aryl ring would end up having the larger steric repulsions. This is actually the case for the isomerization process shown in Equation 3 where the interconversion of the two isomers is highly dependent on steric effects that occur at the transition state, since in this particular case there is no bond breaking or forming. [9]

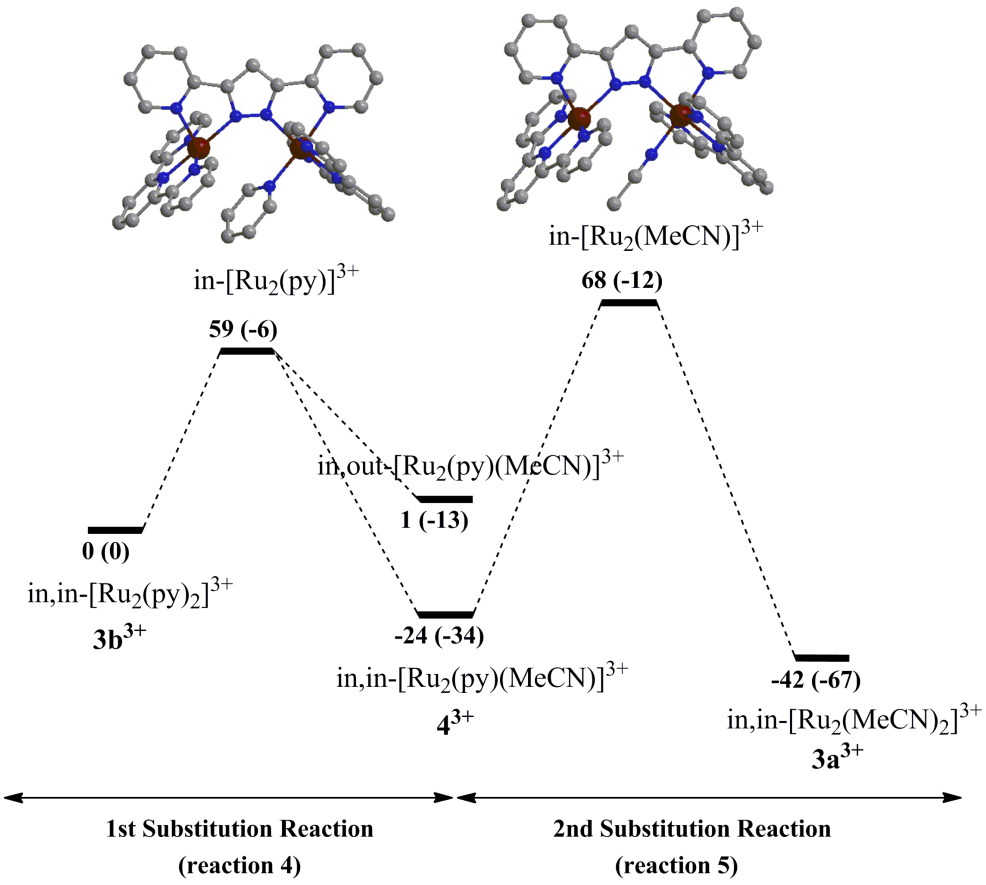

Figure 6. DFT/MM Computed potential energy profile (free energy) in kJ/mol for the first and second substitution reactions.

The stronger attractive interaction between the monodentate ligands in the lutidine case, **3c^{3+}**, is very likely associated to the special spatial arrangement of the monodentate ligands provoked by the bridging *bbp*$^{-}$ ligand in combination with the auxiliary *trpy* ligands. As mentioned earlier in the structural section, for the case of the pyridine and pyridine substituted ligands the aromatic rings are situated in a nearly parallel manner. As shown schematically in Figure 5, they are in a nearly eclipsed conformation, which is rotated 60º with regard to an imaginary axis that would be perpendicular to the mentioned aromatic ring. This particular arrangement is provoked by the auxiliary and bridging ligand scaffold, but it has the consequence of

reducing the eventual steric repulsion between the methyl substituents, and favoring attractive interactions, which are likely of C-H π or π−π nature.

3.3.5. Conclusions

We have prepared and thoroughly characterized a family of dinuclear complexes of general formula *in,in*-[{Ru^{II}(T)(L)}$_2$(μ-bpp)]$^{n+}$ briged by the *bpp*$^-$ ligand and containing two additional meridional ligands the neutral *trpy* or the anionic *bid*$^-$. The final octahedral coordination is occupied by monodentate ligands such as pyridine, substituted pyridines and MeCN. We have also investigated the substitution kinetics of the monodentate ligands that in turn have allowed us to understand the intrasupramolecular effect that exists between the monodenate ligands. In the case of lutidine the precise disposition of the monodentate ligands show the existence of an attractive interaction between the ligands. The present work constitutes an example of how dinculear complexes with the right ligand design can permit a precise control of supraintramolecular interactions that can be both, attractive or repulsive depending on the ligands used.

3.3.6. Acknowledgements

Support from SOLAR-H2 (EU 212508), MEC (CTQ2007-67918 and CTQ2008-06866-CO2-02) and from the Consolider Ingenio 2010 (CSD2006-0003) are gratefully acknowledged. NP is grateful for a MICINN doctoral grant.

The theoretical calculations reported in this work were carried out by Gemma J. Christian as a post-Doc in Dr. Maseras' group. .

3.3.7. References

[1] V. Balzani, G. Bergamini, P. Ceroni, *Coord. Chem. Rev.*, **2008**, *252*, 2456-2469; M. Hang, V Huynh , T. J. Meyer, *Chem. Rev.*, **2007**, *107*, 5004-5064; N. A. P. Kane-Maguire, J. F. Wheeler, *Coord. Chem. Rev.*, **2001**, *211*, 145-162; X. Sala, I. Romero, M. Rodriguez, L. Escriche, A. Llobet, *Angew. Chem. Int. Ed.*, **2009**, *48*, 2842-2852; I. Romero, M. Rodríguez, C. Sens, J. Mola, M. Rao Kollipara, L. Francàs, E. Mas-Marza, L. Escriche, A. Llobet, *Inorg. Chem.*, **2008**, *47*, 1824-1834.

[2] R. Ziessel, V. Grosshenny, M. Hissler, C. Stroh, *Inorg. Chem.*, **2004**, *43*, 4262-4271; S. Roche, C. Haslam, S. L. Heath, J. A. Thomas, *Chem. Commun.*, **1998**, *16*, 1681-1682; K. J. Tony, *React. Kinet. Catal. Lett.*, **1997**, *60*, 145-155; K. Kohichi, *Organometallics*, **1997**, *16*, 2233-2336; C. Sens, M. Rodríguez.; I. Romero, A. Llobet, T. Parella, B. P. Sullivan, J. Benet-Buchholz, *Inorg. Chem.*, **2003**, *42*, 2040-2048; A. M. Khenkin, L. J. W. Shimon, R. Neumann, *Inorg. Chem.* **2003**, *42*, 3331-3339; L. Gonsalvi, I. W. C. E. Arends, R. A. Sheldon, *Chem. Commun.*, **2002**, *3*, 202-203; M. H. V. Huynh, L. M. Witham, J. M. Lasker, M. Wetzler, B. Mort, D. L. Jameson, P. S. White, K. J. Takeuchi, *J. Am. Chem. Soc.*, **2003**, *125*, 308-309; D. P. Riley, R. F. Shumate, *J. Am. Chem. Soc.*, **1984**, *106*, 3179-3184.

[3] M. M. T. Khan, R. Mohiuddin, S. Vancheesan, B. Swamy, I*nd. J. Chem., Sect. A: Inorg. Bioinorg., Phys., Theor. Anal. Chem,*. **1981**, *20*, 56; J. P. Genet, *Acc. Chem. Res.*, **2003**, *36*, 908-918; I. Serrano, A. Llobet, M. Rodríguez, I. Romero, J. Benet-Buchholz, T. Parella, J. Campelo, D. Luna, J. Marinas, *Inorg. Chem.*, **2006**, *45*, 6, 2644-2651.

[4] K. Takahashi, M. Yamashita, T. Ichihara, K. Nakano, K. Nozaki, *Angew. Chem. Intl. Ed.*, **2010**, *49*, 4488-4490; J. Zakzeski, H. Lee, Y. L. Leung, A. T. Bell, *Applied Catalysis*, **2010**, *374*, 201-212; G. Fachinetti, T. Funaioli, F. Marchetti, *Chem. Commun.*, **2005**, *23*, 2912-2914.

[5] S. O. Kelly, J.K. Barton, *Science*, **1999**, *238*, 375; D. B.Hall, R. E. Holmlin, J. K. Barton, *Nature*, **1996**, *384*, 731; C. J. Burrows, J. G. Muller, *Chem. Rev.,* **1998**, *98*, 1109; S.C. Weatherly, I.V. Yang, H. H. Thorp, *J. Am. Chem. Soc.*, **2001**, *123*, 1236; A. Arbuse, M. Font, M. A. Martinez, X. Fontrodona, M. J. Prieto, V. Moreno, X. Sala, A. Llobet, *Inorg. Chem.*, **2009**, *48*, 11098-11107.

[6] H. Tseng, R. Zong, J. T. Muckerman, R. Thummel, *Inorg. Chem.*, **2008**, *47*, 11763–11773.

[7] D. J. Wasylenko, C. Ganesamoorthy, B. D. Koivisto, M. A. Henderson, C. P. Berlinguette, *Inorg. Chem.*, **2010**, *49*, 2202–2209.

[8] H. Yamada, T. Koike, J. K. Hurst, J. Am. Chem. Soc., 2001, 123, 12775–12780; M. J.Collins, K. Ray, L. Que, Inorg. Chem., 2006, 45, 8009.

[9] N. Planas, G. J. Christian, E. Mas-Marzá, X. Sala, X. Fontrodona, F. Maseras, A. Llobet, Chem. Eur. J., 2010, 16, 7965-7968.

[10] [a) J. Casabo, J. Pons, K. S. Siddiqi, F. Teixidor, E. Molins, C. J. Miravitlles, *Dalton Trans.* **1989**, 1401-3. b) R. Levine, J. K. Sneed, *J. Am. Chem. Soc.* **1951**, *73*, 5614-16.

[11] a) R. R. Gagne, W. A. Marritt, D. N. Marks, W. O. Siegl, *Inorg. Chem.* **1981**, *20*, 3260-7. b) D. N. Marks, W. O. Siegl, R. R. Gagne, *Inorg. Chem.* **1982**, *21*, 3140-7.

[12] C. Sens, I. Romero, M. Rodriguez, A. Llobet, T. Parella, J. Benet-Buchholz, *J. Am. Chem. Soc.,* **2004**, *126*, 7798-7799.

[13] Specfit is a trademark of Spectrum Software Associates.

[14] Data collection with APEX II v2009.1-02. Bruker (2007). Bruker AXS Inc., Madison, Wisconsin, USA.

[15] Data reduction with Bruker SAINT V7.60A. Bruker (2007). Bruker AXS Inc., Madison, Wisconsin, USA.

[16] SADABS: V2008/1 Bruker (2001). Bruker AXS Inc., Madison, Wisconsin, USA.

[17] SHELXTL V6.14, Structure solution and refinement.G. M. Sheldrick, Acta Cryst. 2008, A64, 112-122.

[18] TWINABS Version 2008/4 Bruker AXS. R. H. Blessing, Acta Cryst. 1995, A51 33-38.

[19] Gaussian 03, M. J. Frisch, G. W. Trucks, H. B. Schlegel, G. E. Scuseria, M. A. Robb, J. R. Cheeseman, J. J. A. Montgomery, K. N. K. T. Vreven, J. C. Burant, J. M. Millam, S. S. Iyengar, J. Tomasi, V. Barone, B. Mennucci, M. Cossi, G. Scalmani, N. Rega, G. A. Petersson, H. Nakatsuji, M. Hada, M. Ehara, K. Toyota, R. Fukuda, J. Hasegawa, M. Ishida, T. Nakajima, Y. Honda, O. Kitao, H. Nakai, M. Klene, X. Li, J.E. Knox, H. P. Hratchian, J. B. Cross, V. Bakken, C. Adamo, J. Jaramillo, R. Gomperts, R. E. Stratmann, O. Yazyev, A. J. Austin, R. Cammi, C. Pomelli, J. W. Ochterski, P. Y. Ayala, K. Morokuma, G. A. Voth, P. Salvador, J. J. Dannenberg, V. G. Zakrzewski, S. Dapprich, A. D. Daniels, M. C. Strain, O. Farkas, D. K. Malick, A. D. Rabuck, K. Raghavachari, J. B. Foresman, J. V. Ortiz, Q. Cui, A. G. Baboul, S. Clifford, J. Cioslowski, B. B. Stefanov, G. Liu, A. Liashenko, P. Piskorz, I. Komaromi, R. L. Martin, D. J. Fox, T. Keith, M. A. Al-Laham, C. Y. Peng, A. Nanayakkara, M. Challacombe, P. M. W. Gill, B. Johnson, W. Chen, M. W. Wong, C. Gonzalez, J. A. Pople, Gaussian, Inc.: Wallingford CT, 2004.

[20] S. Dapprich, I. Komaromi, K. S. Byun, K. Morokuma, M. J. Frisch, *J. Mol. Struc-Theochem*., **1999**, *461-462*, 1-21.

[21] M. Svensson, S. Humbel, R. D. J. Froese, T. Matsubara, S. Sieber, K. J. Morokuma, *Phys. Chem.* **1996**, *100*, 19357-19363.

[22] A. D. Becke, *J. Chem. Phys.* **1993**, *98*, 5648.

[23] C. T. Lee, W. T. Yang, R. G. Parr, *Phys. Rev. B,* **1988**, *37*, 785-789.

[24] A. K. Rappe, C. J. Casewit, K.S. Colwell, W. A. Goddard, W. M. Skiff, *J. Am. Chem. Soc.,* **1992**, *114*, 10024-10035.

[25] D. Andrae, U. Häußermann, M. Dolg, H. Stoll, H. Preuß, *Theor. Chim. Acta,* **1990**, *77*, 123-141.

[26] W. J. Hehre, R. Ditchfield, J. A. Pople, *J. Chem. Phys.* **1972**, *56*, 2257-2261

[27] M. F. Michelle, J. P. William, J. H. Warren, J. S. Binkley, S. G. Mark, J. D.Douglas, A. P. John, *J. Chem. Phys.* **1982**, *77*, 3654-3665.

[28] J. N. Harvey, *Faraday Discuss.* **2010**, *145*, 487-505.

[29] J. K.-C. Lau, D. V. Deubel, *J. Chem. Theory Comput.* **2006**, *2*, 103-106.

[30] S. Miertus, E. Scrocco, J. Tomasi, *J. Chem. Phys.* **1981**, *55*, 117-129.

[31] F. Neese, ORCA - an ab initio, Density Functional and Semiempirical Program Package, 2.7, 2009 ed., Universität Bonn, Bonn, Germany.

[32] a) S. J. Grimme, *Comput. Chem.* **2004**, *25*, 1463-1473; b) S. J. Grimme, *Comput. Chem.* **2006**, *27*, 1787-1799.

[33] a) A. Schafer, H. Horn, R. Ahlrichs, *J. Chem. Phys.* **1992**, *97*, 2571-2577; b) A. Schafer, C. Huber, R. Ahlrichs, *J. Chem. Phys.* **1994**, *100*, 5829-5835.

[34] F. Laurent, E. Plantalech, B. Donnadieu, A. Jimenez, F. Hernandez, M. Martinez-Ripoll, M. Biner, A. Llobet, *Polyhedron,* **1999**, *18*, 3321-3331; I. Romero, M. Rodriguez, A. Llobet, M. N. Collomb-Dunand-Sauthier, A. Deronzier, T. Parella, H. Soteckli-Evans, *J. Chem. Soc. Dalton Trans*., **2000**, 1689-1694; X. Sala, E. Plantalech, A. Poater, M. Rodriguez, I. Romero, M. Sola, A. Llobet, S. Jansat, M. Gomez, H. Stoeckli-Evans, J. Benet-Buchholz, *Chem. Eur. J.*, **2006**, *12*, 2798-2807; C. Sens, M. Rodríguez, I. Romero, A. Llobet, T. Parella, J. Benet-Buchholz. *Inorg. Chem.*, **2003**, *42*, 8385-8394; E. Masllorens, M. Rodríguez, I. Romero, A. Roglans, T. Parella, J. Benet-Buchholz, M. Poyatos, A. Llobet. *J. Am. Chem. Soc.*, **2006**, *128*, 16, 5306-5307.

[35] P. E. Anderson, G. B. Deacon, K. H. Haarmann, F. R. Keene, T. J. Meyer, D. A. Reitsma, B. W. Skelton, G. F. Strouse, N. C. Thomas, T. A. Treadway, T. A. White, *Inorg. Chem.*, **1995**, *34*, 6145–6157; K. R. Barqawi, A. Llobet, T. J. Meyer, *J. Am. Chem. Soc.*, **1988**, *110*, 7751-7759.

[36] J. Mola, C. Dinoi, X. Sala, M. Rodríguez, I. Romero, T. Parella, X. Fontrodona, A. Llobet, *Dalton Trans*, **2011**, submitted.
[37] J. N. Harvey, *Faraday Discuss.*, **2010**, *145*, 487-505.

Chapter 4

New Insights Into Ruthenium Polypyridyl Complexes as Water Oxidation Catalysts

During the last decade there has been a significant development in the field of homogeneous catalytic water oxidation. Although different metal centers, such as Ru, Mn, Ir, Fe and Co, have been utilized as catalysts, to date ruthenium polypyridyl catalysts remain the most intensively studied. The high control achieved for the coordination and synthetic chemistry of these molecular complexes offer the prospect of specific tailoring of the structure and composition of suchs catalysts. Herein we report the synthesis, characterization and electrocatalytic experiments performed with a new catalyst derivative of the bpp system in which the terpyridine ligands have been functionalized with a sulphonate group to be anchored onto TiO_2 covered FTO films. Additionally the study of the relative stability of the different oxidation states and the photoisomerization process at oxidation state II of the water oxidation catalyst cis-$[Ru^{II}(bpy)_2(H_2O)_2]^{2+}$ has been studied by DFT theoretical calculations.

TABLE OF CONTENTS

4.1. INTRODUCTION

Ruthenium complexes exhibit a large amount of applications in very diverse fields of chemistry in part as result of nice correlations between their properties and the nature of the ligands bound to the central metal. In the majority of cases, the most stable oxidation state of Ru complexes is II or III, but Ru compounds can display a wide range of oxidation states, from formal oxidation state -II in $[Ru(CO)_4]^{2-}$ to VIII in RuO_4. Therefore, ruthenium complexes are redox-active compounds and their application as redox reagents in different chemical transformations has been widely studied.[1, 2] Thus, it should come as no surprise that ruthenium complexes have played a leading role in the field of catalytic homogeneous water oxidation.

The presence of N and O donor atoms on ruthenium polypyridyl complexes allow the stabilization of high oxidation states, which make this complexes especially suitable to be used in oxidative processes such as water oxidation. These catalytic systems take advantage of the favorable energetics provided by proton-coupled electron transfer and cycle through the so called Ru-aqua/Ru-oxo chemistry. In some cases high efficiencies and rates of oxygen evolution have been reached with these catalysts.[3, 4] However, their performances remain far below from that of the naturally occurring water oxidizing complex. The OEC of PSII is known to reach TOF of ca. 1000 s^{-1} and TON of more than 1 million.[5]

The main challenges in the field are still the understanding the reaction mechanisms of the known active catalysts and finding an efficient and rugged catalyst. A deep knowledge of all the processes occurring in the active catalytic systems, and the factors governing and influencing them, should set the basis for future development and rational design of water oxidation catalysts.

4.1.1. The 3,5-Bis(2-pyridyl)pyrazole (Hbpp) system

Since the first molecularly well characterized homogeneous water oxidation catalyst *cis,cis*-$[\{Ru^{III}(trpy)(H_2O)\}_2(\mu\text{-}O)]^{4+}$ (I, Figure 1), the binuclear ruthenium "Blue dimmer", was reported in 1982 Meyer's group many derivatives have been synthesized

and a large number of studies regarding their structure, redox properties and catalytic mechanism have been reported.[6-12] Even though, to date no consensus has been met yet regarding the catalytic pathway,[13-18] it can be extracted from these studies that the two most important deactivation pathways of this catalytic system are the following:

- The so called anation process. The coordination of anions compete with water for the first coordination sphere of the ruthenium centres. In some cases, as with triflate, the anion can block the labile sites in a chelating manner (Scheme 1, I).

- The cleavage of the μ-O bridge that holds together the two ruthenium centres. In the lower oxidation states, such as II,II, this complex undergoes reductive cleavage of the Ru-o-Ru bond within the cyclic voltammetry time scale, leading to the corresponding mononuclear complexes (Scheme 1, II).[19]

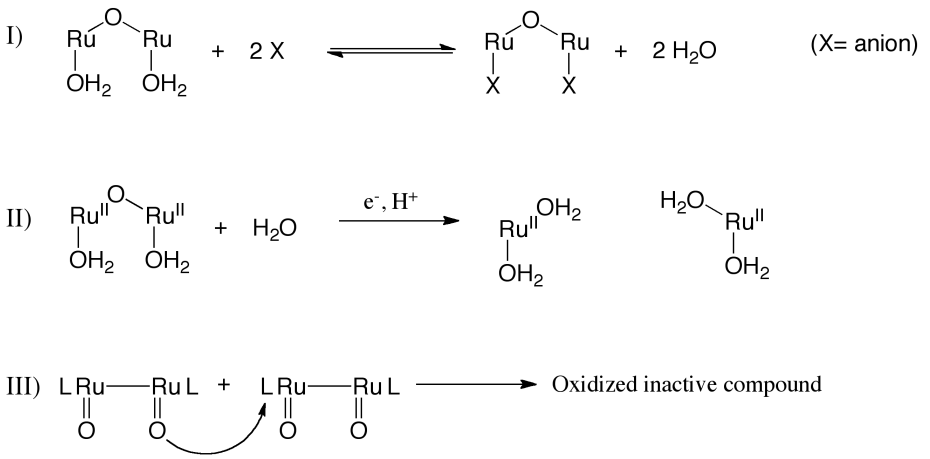

Scheme 1. Proposed deactivation pathways for binuclear ruthenium polypyridyl complexes. Anation process (I). Reductive cleavage (II). Bimolecular catalyst-to-catalyst oxidative deactivation (III).

Another of the most studied catalyst from a mechanistic standpoint is the *in,in*-[{Ru^{II}(trpy)(H_2O)}$_2$(μ-bpp)]$^{3+}$ (Right, Figure 1) reported by Llobet's group in 2004.[20]

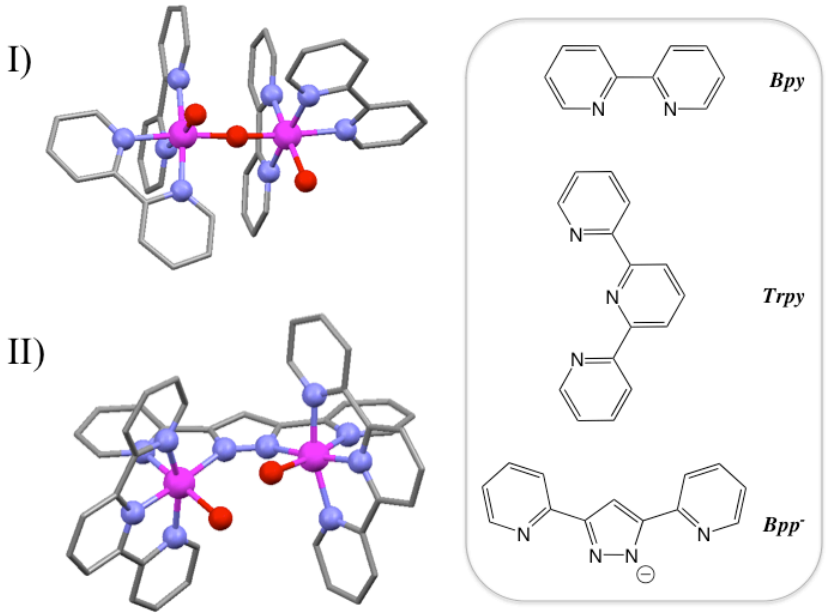

Figure 1. Structures of the two mechanistically more studied complexes for homogeneous water oxidation. I) *cis,cis*-[{Ru^{III}(trpy)(H_2O)}$_2$(μ-O)]$^{4+}$ form the X-ray crystal[21] and II) *in,in*-[{Ru^{II}(trpy)(H_2O)}$_2$(μ-bpp)]$^{3+}$ from calculated coordinates.[22] Left, drawing of the polypyridylic ligands *trpy*, *bpy* and *bpp*$^-$.

In the absence of the *oxo* bridge the reductive cleavage deactivation pathway is excluded, as well as the potential cis-trans isomerization of the bisoxo group that is known to happen in *cis*-[Ru^{II}(bpy)$_2$(H_2O)$_2$]$^{2+}$.[23] Additionally, the competing anation process was reduced due to a lower the overall positive charge of the active species.

The introduction of the more rugged dinucleating multidentate polypyridyl ligand *bpp*$^-$ to replace the *oxo* bridge not only attempted to overcome the previously mentioned handicaps of the blue dimmer, but also sought to force a rigid face to face relative disposition of the two aqua ligands. The disposition of the two ruthenium centers is close enough to ensure significant through space interactions between the aqua ligands, but still far enough so that a μ-O bridge is not favored.

A thorough UV-vis kinetic analysis combined with ^{18}O labeling experiments and theory have been really useful to reveal the mechanism of the latter catalyst which is depicted in Figure 2.[22, 24]

The process starts with four consecutive ET processes, all first order with respect to both the catalyst and Ce^{IV}. The rate of these ET processes decreases as the oxidation increases, being the fourth the slowest ET step. Unlike with the blue dimmer, no O_2 evolution was observed until the IV,IV state was reached.

After reaching IV,IV oxidation state an intermediate was observed prior to oxygen evolution. The last two steps are much slower than the ET processes and are first order in catalyst concentration, excluding a bimolecular O-O bond formation pathway.

The O^{18} labeling studies of the first catalytic cycle were consistent with an intramolecular O-O bond formation as the only mechanism operating in the system. Thus, the solvent water nucleophilic attack pathway was excluded.

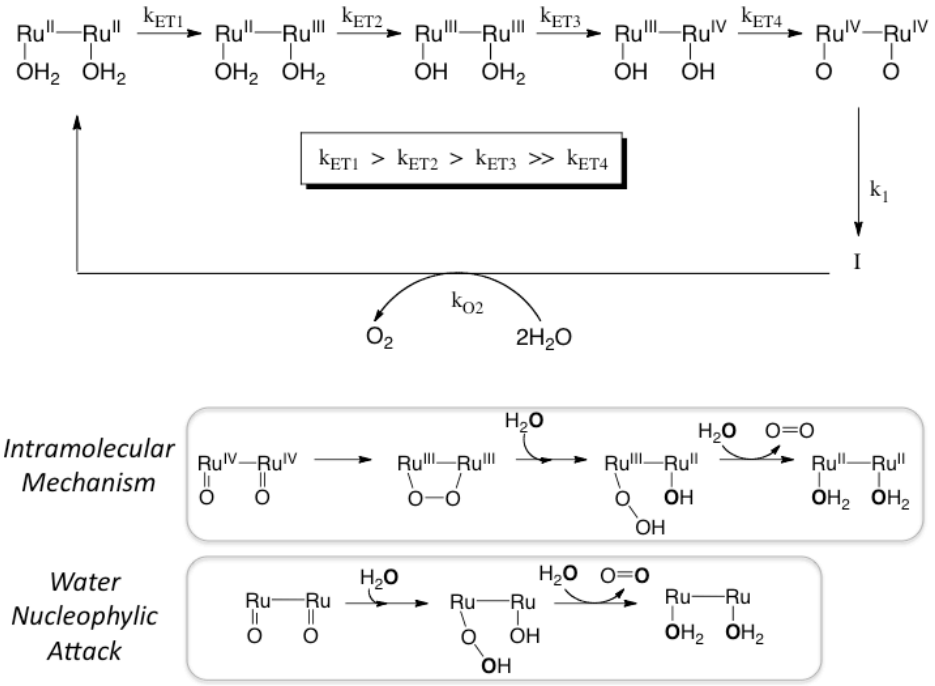

Figure 2. Mechanism of water oxidation for *in,in*-[{Ru^{II}(trpy)(H_2O)}$_2$(μ-bpp)]$^{3+}$. Squared, the two considered oxygen evolution pathways.

Combined DFT and CASSCF/CASPT2 theoretical calculations were run to study the last two steps of the catalytic cycle. The results suggested an initial formation of a μ-(1,2)-peroxo bridged structure, in oxidation state III,III, that evolves to a terminal hydroperoxo which, in turn, releases oxygen regenerating the initial active species. The slowness in the last steps was attributed to a mismatch between spin states for the oxyl coupling.

The deactivation pathways for this catalyst were also evaluated in these studies. The participation of an anation process was evidenced by the dependence of the kinetic profile on the nature of the catalyst's precursor anion used.

The demonstrated high oxidative power of the catalyst, added to the fact that CO_2 evolution has been detected when slight changes on the catalyst 's structure were introduced, lead the authors to propose an additional bimolecular catalyst-to-catalyst oxidative deactivation pathway (Scheme 1, III).

Two derivatives of the *in,in*-[{Ru^{II}(trpy)(H_2O)}$_2$(μ-bpp)]$^{3+}$, functionalized in different positions with different functionalities, to be anchored on solid surfaces of semiconductor materials have been reported. In both cases still Ce^{IV} was used as sacrificial oxidant.

In the first case the *trpy* ligands were functionalized with pyrol units and the resulting catalyst was electropolymerized onto carbon and FTO electrodes. Upon addition of a dilution agent copolymerized with the catalyst a substantial increase of the number of TONs was observed, from 18 with the homogeneous unmodified catalyst to 250.[25] This increase in performance was attributed to the reduction of the catalyst-to-catalyst deactivation pathway. In a second attempt, a catalyst with the *bpp*$^-$ functionalized with a carboxylate was synthesized and anchored onto TiO_2 powder, unfortunately the initial oxygen evolution was followed by CO_2 release which led to the deanchoring of the catalyst.[26]

Even though these two systems were not fully satisfactory they represent a proof of principle and set the basis for the development of a solid-state modular devices. These sort of systems should potentially present better performances if the Ce^{IV} previously used as an indiscriminate chemical oxidant is replaced by a more clean oxidative

source such as the one resulting by applying the proper potential on a conducting solid support.

4.1.2. The *cis*-$[Ru(bpy)_2(H_2O)_2]^{2+}$ mononuclear water oxidation catalyst

Inspired by the natural system, initial efforts in the field of water oxidation were focused on multinuclear approaches. More recently a series of ruthenium polypyridyl aquo complexes have also been found to be active as mononuclear homogeneous catalysts for water oxidation without catalyst dimerization (see Chapter 1).[27, 28]

Long before these revolutionary mononuclear catalysts appeared, Meyer's group reported the detection of oxygen after chemical oxidation of the *cis*-$[Ru^{II}(bpy)_2(H_2O)_2]^{2+}$ complex, a precursor of the blue dimmer. The authors attributed the oxygen evolution to the formation of RuO_2 as active catalyst, which appeared as a black solid in the reaction vessel.[12, 29]

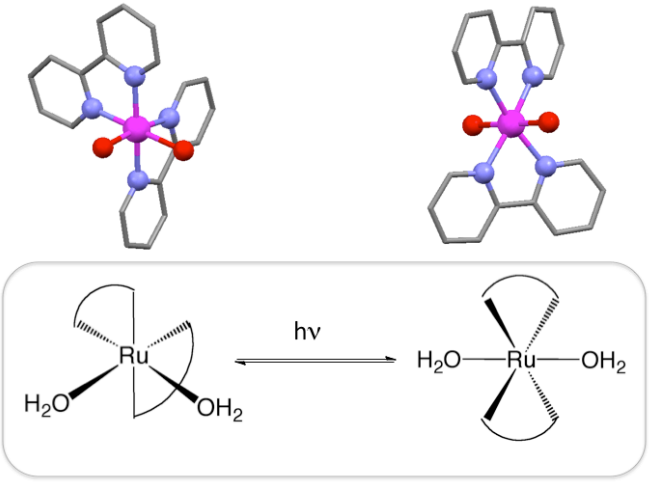

Figure 3. Bottom, schematic representation of the *cis/trans* photo isomerization process observed by $[Ru^{II}(bpy)_2(H_2O)_2]^{2+}$. Top, X-ray structures of the *cis*-$[Ru^{II}(bpy)_2(H_2O)_2]^{2+}$[30] and *trans*-$[Ru^{II}(bpy)_2(H_2O)_2]^{2+}$[31] cations.

More than twenty years later, this catalytic system has been "revisited" and its performance studied with the state-of-the-art technologies in the field.[32] It was not only novel the demonstration that the *cis*-$[Ru^{II}(bpy)_2(H_2O)_2]^{2+}$ species was the real catalyst, but it was the first example of full prove of water oxidation by water nucleophilic attack as sole mechanism.

Since the original article by Meyer's group was focused on the *cis/trans* photoisomerization, observed in oxidation states II and III of this ruthenium compound, the new study compared the performances of *cis*- and *trans*-$[Ru^{II}(bpy)_2(H_2O)_2]^{2+}$ isomers of with that of the RuO_2.

The marked divergence between the O_2-evolution profiles of the different catalysts evidenced that in all cases the mechanisms, and therefore the active species, were different.

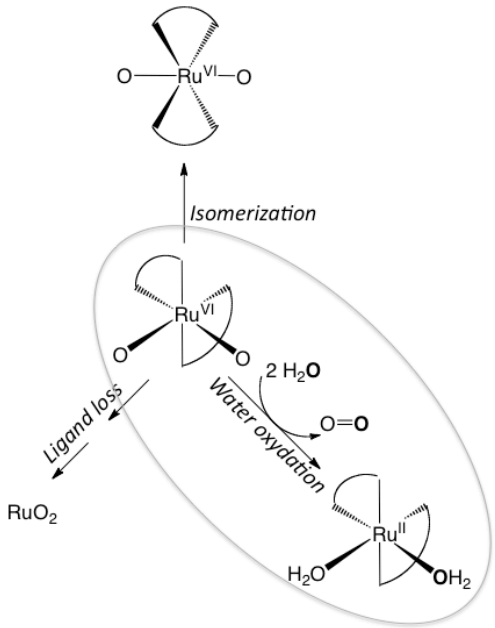

Scheme 2. Considered reaction pathways for the oxidized complex *cis*-$[Ru^{VI}(bpy)_2(O)_2]^{2+}$

As the initial electron transfer steps in this type of catalysts are usually much faster than the chemical reactions that follow, the much slower performance of the *trans*

isomer revealed that the *cis/trans* isomerization in the higher oxidation states did not occur, under the working conditions.

Additionally water labeling experiments of the first catalytic cycle unambiguously demonstrated that the mechanism operating in the *cis*-$[Ru^{II}(bpy)_2(H_2O)_2]^{2+}$ is the water nucleophilic attack. This results were in good agreement with the energetic barriers calculated at DFT and CASPT2 levels of theory for the nucleophilic attack compared to those of an intramolecular O-O bond formation pathway.

Even though the mechanism of this catalytic system has been clearly elucidated, the reasons for its poor performance are not yet fully understood.

4.1.3. References

[1] V. Dragutan, I. Dragutan, L. Delaude and A. Demonceau, *Coord. Chem. Rev.* **2007**, *251*, 765-794.
[2] K. Sumi and H. Kumobayashi, *Top. Organomet. Chem.* **2004**, *6*, 63-95.
[3] Y. Xu, L. Duan, L. Tong, B. Aakermark and L. Sun, *Chem. Commun. (Cambridge, U. K.)* **2010**, *46*, 6506-6508.
[4] Y. Xu, A. Fischer, L. Duan, L. Tong, E. Gabrielsson, B. Aakermark and L. Sun, *Angew. Chem., Int. Ed.* **2010**, *49*, 8934-8937, S8934/8931-S8934/8915.
[5] G. Ananyev and G. C. Dismukes, *Photosynth. Res.* **2005**, *84*, 355-365.
[6] F. Liu, T. Cardolaccia, B. J. Hornstein, J. R. Schoonover and T. J. Meyer, *J. Am. Chem. Soc.* **2007**, *129*, 2446-2447.
[7] H. H. Petach and C. M. Elliott, *J. Electrochem. Soc.* **1992**, *139*, 2217-2221.
[8] Y.-K. Lai and K.-Y. Wong, *J. Electroanal. Chem.* **1995**, *380*, 193-200.
[9] F. P. Rotzinger, S. Munavalli, P. Comte, J. K. Hurst, M. Graetzel, F. J. Pern and A. J. Frank, *J. Am. Chem. Soc.* **1987**, *109*, 6619-6626.
[10] M. K. Nazeeruddin, F. P. Rotzinger, P. Comte and M. Gratzel, *J. Chem. Soc., Chem. Commun.* **1988**, 872-874.
[11] J. A. Gilbert, D. Geselowitz and T. J. Meyer, *J. Am. Chem. Soc.* **1986**, *108*, 1493-1501.
[12] J. C. Dobson and T. J. Meyer, *Inorg. Chem.* **1988**, *27*, 3283-3291.
[13] H. Yamada, W. F. Siems, T. Koike and J. K. Hurst, *J. Am. Chem. Soc.* **2004**, *126*, 9786-9795.
[14] J. L. Cape, W. F. Siems and J. K. Hurst, *Inorg. Chem. (Washington, DC, U. S.)* **2009**, *48*, 8729-8735.
[15] X. Yang and M.-H. Baik, *J. Am. Chem. Soc.* **2004**, *126*, 13222-13223.
[16] H. Yamada, T. Koike and J. K. Hurst, *J. Am. Chem. Soc.* **2001**, *123*, 12775-12780.
[17] E. L. Lebeau, S. A. Adeyemi and T. J. Meyer, *Inorg. Chem.* **1998**, *37*, 6476-6484.
[18] J. J. Concepcion, J. W. Jurss, J. L. Templeton and T. J. Meyer, *Proc. Natl. Acad. Sci. U. S. A.* **2008**, *105*, 17632-17635.
[19] A. Llobet, M. E. Curry, H. T. Evans and T. J. Meyer, *Inorg. Chem.* **1989**, *28*, 3131-3137.
[20] C. Sens, I. Romero, M. Rodriguez, A. Llobet, T. Parella and J. Benet-Buchholz, *J. Am. Chem. Soc.* **2004**, *126*, 7798-7799.

[21] J. A. Gilbert, D. S. Eggleston, W. R. Murphy, Jr., D. A. Geselowitz, S. W. Gersten, D. J. Hodgson and T. J. Meyer, *J. Am. Chem. Soc.* **1985**, *107*, 3855-3864.
[22] F. Bozoglian, S. Romain, M. Z. Ertem, T. K. Todorova, C. Sens, J. Mola, M. Rodriguez, I. Romero, J. Benet-Buchholz, X. Fontrodona, C. J. Cramer, L. Gagliardi and A. Llobet, *J. Am. Chem. Soc.* **2009**, *131*, 15176-15187.
[23] B. P. Sullivan, J. M. Calvert and T. J. Meyer, *Inorg. Chem.* **1980**, *19*, 1404-1407.
[24] S. Romain, F. Bozoglian, X. Sala and A. Llobet, *J. Am. Chem. Soc.* **2009**, *131*, 2768-2769.
[25] J. Mola, E. Mas-Marza, X. Sala, I. Romero, M. Rodriguez, C. Vinas, T. Parella and A. Llobet, *Angew. Chem., Int. Ed.* **2008**, *47*, 5830-5832.
[26] L. Francas, X. Sala, J. Benet-Buchholz, L. Escriche and A. Llobet, *ChemSusChem* **2009**, *2*, 321-329.
[27] H.-W. Tseng, R. Zong, J. T. Muckerman and R. Thummel, *Inorg. Chem. (Washington, DC, U. S.)* **2008**, *47*, 11763-11773.
[28] J. J. Concepcion, J. W. Jurss, J. L. Templeton and T. J. Meyer, *J. Am. Chem. Soc.* **2008**, *130*, 16462-16463.
[29] J. P. Collin and J. P. Sauvage, *Inorg. Chem.* **1986**, *25*, 135-141.
[30] M. Gama Sauaia, E. Tfouni, R. Helena de Almeida Santos, M. T. Do Prado Gambardella, M. P. F. M. Del Lama, L. Fernando Guimaraes and R. Santana da Silva, *Inorg. Chem. Commun.* **2003**, *6*, 864-868.
[31] H. Jude, P. S. White, D. M. Dattelbaum and R. C. Rocha, *Acta Crystallogr., Sect. E: Struct. Rep. Online* **2008**, *E64*, m1388-m1389, m1388/1381-m1388/1388.
[32] X. Sala, Z. Ertem Mehmed, L. Vigara, K. Todorova Tanya, W. Chen, C. Rocha Reginaldo, F. Aquilante, J. Cramer Christopher, L. Gagliardi and A. Llobet, *Angew Chem Int Ed Engl* **2010**, *49*, 7745-7747.

4.2. THE Bpp CATALYST ANCHORED ON TiO_2 BY SULFONATE GROUPS

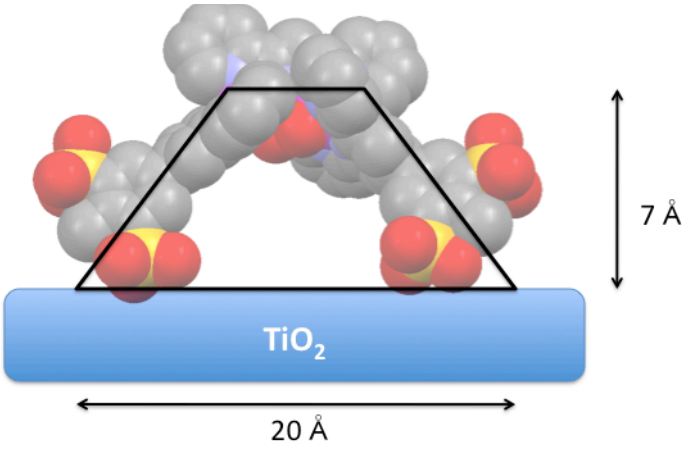

A new μ-acetato-bridged complex with general formula in,in-[{Ru^{II}(trpy)}$_2$ (μ-bpp)(μ-AcO)]$^{2-}$ (tpy* is 5-([2,2':6',2''-terpyridin]-4'-yl)-2-methylbenzene-1,3-disulfonate), was prepared and fully characterized. Major alterations are observed on the sulfonated compound when anchored onto TiO_2 covered FTO surface. The electrochemically generated Ru^{IV}–Ru^{IV} form of the complex is not capable of oxidizing water but oxidizes ethanol at pH = 1 (triflic acid).*

The Bpp Catalyst Anchored on TiO_2 by Sulfonate Groups†

To be Submitted

Nora Planas,[a] Stephan Roeser,[a] Jordi Benet-Buchholz [a] and Antoni Llobet *[a,b]

[a] *Institute of Chemical Research of Catalonia (ICIQ), Av. Països Catalans 16, E-43007 Tarragona, Spain. Fax: 34 977 902 228; Tel: 34 977 902 200; E-mail: fmaseras@iciq.es, allobet@iciq.es*

[b] *Departament de Química, Universitat Autònoma de Barcelona, Cerdanyola del Vallès, E-08193 Barcelona, Spain.*

†Electronic Supplementary Information (ESI) available: Full spectroscopic and electrochemical characterisations and all catalytic measurements.

Keywords: Ruthenium, supported catalysts, water splitting, redox chemistry, organic-inorganic hybrid materials

4.2.1. Abstract

An organic ligand based on 4'-(p-tolyl)-2,2':6',2''-terpyridine functionalized with two sulphonate groups (*trpy**) was prepared and characterised. The ligand was then used to synthesise a series of ruthenium compounds with formulas $[Ru^{III}(Cl)_3$ (*trpy**)] (**1***), $[Ru^{II}(trpy^*)_2]^{2-}$ (**2***) and *in,in*-$[\{Ru^{II}(trpy^*)\}_2(\mu\text{-bpp})(L\text{-}L)]^{n-}$ (L-L= μ-AcO and n = 2 in **3***; L-L = $(H_2O)_2$ and n = 1 in **4***). The complexes were characterised in solution by 1D and 2D ^{1}H-NMR spectroscopy, UV/Vis spectroscopy and electrochemical techniques. The dinuclear complex **4*** was anchored on anatase disperse nanoparticles and the reactivity of this new material as water oxidation catalyst was tested using Ce^{IV} as chemical oxidant. The little formation of dioxygen was accompanied by carbon dioxide release. In a different approach, complex **4*** was anchored on anatase coated FTO film. Upon heterogenization, the electrochemical properties of compound **4*** were significantly modified which had direct implication in its deactivation as water oxidation catalyst.

4.2.2. Introduction

Inspired by the photosynthetic natural processes, scientists envision the design of a device capable of using water and sunlight to obtain the so called solar fuels as an alternative energy source to the fossil fuels that drive today's global economy.

To achieve artificial photosynthesis, a set of reactions should be coupled to a light harvesting device/molecular assembly in such a way that the overall process is driven by sunlight. Additionally, it would be desirable that the two half reactions involved in the process took place in physically different compartments so that the oxygen released and the reduced fuel material could be stored separately. Thus, any device design should have at least four basic components: A a sun light harvesting moiety, a water oxidation catalyst, a reduction catalyst and a proton selective membrane that ensures the balance of the proton gradient between the reaction compartments.

One strategy towards the design of a device for artificial photosynthesis is a modular approach in which the components that will be assembled in the final operational device are designed and studied separately. Subsequently, gradual coupling of the device's subunits should allow a full control of all the features intervening in the process. This would ultimately lead to an accurate understanding of the resulting performance and, consequently, open the possibility of a rational design and improvement.

Significant steps have been done towards the understanding and the design of oxidation and reduction catalysts in homogeneous phase.[1-4] Even though it is widely accepted that a rugged device will most likely involve immobilised materials on conducting surfaces, very little is known regarding the impact of the immobilisation of such catalysts on their properties and performances.[5-7]

Here we report the synthesis and characterisation of complex *in,in*-[{Ru^{II}(trpy*)(H_2O)}$_2$(μ-bpp)]$^{2-}$ (**4***) as new water oxidation catalyst. Its terpyridine ligands contain sulfonate groups (*trpy**, Scheme 1) to enable its anchoring onto the surface of TiO_2. Its structural, spectroscopic and electrochemical properties, both in solution and anchored onto TiO_2, have been studied and compared with the previously reported

non-sulfonated water oxidation catalyst *in,in*-[{Ru^{II}(trpy)(H_2O)}$_2$(μ-bpp)]$^{3+}$ (**4**) (the ligands are drawn in Scheme 1).[8, 9]

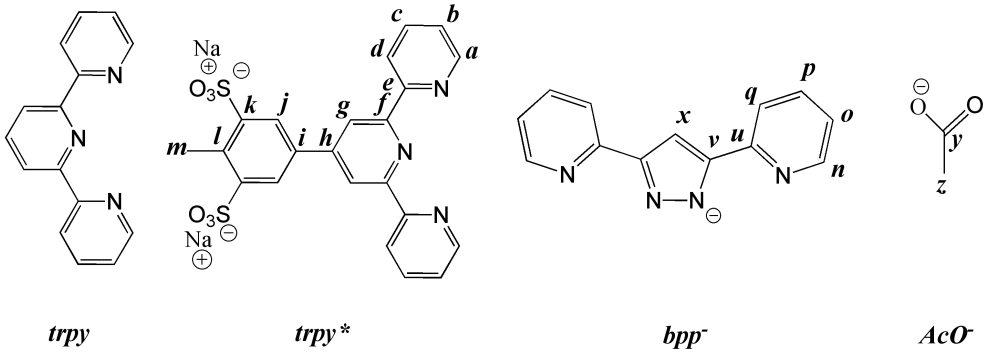

Scheme 1. Ligands used in this work and including their abbreviations and NMR labeling scheme.

Finally, the performance of **4*-TiO_2** as heterogeneized water oxidation catalyst using Ce^{IV} as sacrificial chemical oxidant and its applicability as electrocatalyst supported onto TiO_2 coated FTO films have been tested.

4.2.3. Experimental Section

Materials

All reagents used in the present work were obtained from Aldrich Chemical Co. or Alfa Aesar and were used without further purification. Synthesis grade organic solvents were obtained from SDS and were routinely degassed with argon. Methanol was distilled over MgI, ethanol was dried with 3.5 Å molecular sieve and diethyl ether was used from the SPS. High purity deionized water was obtained by passing distilled water through a nanopure Mili-Q water purification system. The titanium oxide powder was supplied by Aldrich and described as nanopowder TiO_2-Anatase (particle size < 25 nm). TiO_2 paste for film coating was purchased from Solaronix SA (average particle size 13 nm).

Preparations

The 3,5-bis(2-pyridyl)pirazole (Hbpp) ligand,[10, 11] $[Ru^{III}Cl_3(trpy)]$ (**2**),[12] $\{[Ru(trpy)]_2(\mu\text{-bpp})(\mu\text{-AcO})\}(PF_6)_3$ (**3(PF$_6$)$_3$**)[8] were prepared as described in the literature. All synthetic manipulations were routinely performed under argon atmosphere using Schlenck and vacuum line techniques.

Synthesis of 5-([2,2':6',2''-terpyridin]-4'-yl)-2-methylbenzene-1,3-disulfonate (***trpy****). To 4 mL of oleum (20 % free SO_3) in a 10 mL shlenck flask, 500 mg (1.55 mmol) of 4'-p-Tolyl-2,2':4',2''-terpyridine were added in small portions. The flask was connected to a glass-condensator (previously purged with argon and connected to an argon filled balloon) and the solution was then refluxed at 200 ºC for 3 h. After cooling to room temperature, the solution was poured onto a 250 mL flask containing 150 mL of aqueous NaOH solution (1g NaOH in 150 mL H_2O) resulting in a suspension with pH = 0.5-1. Then, the light brownish solid was filtrated and dried over vacuum. Once dry, the powder was dissolved in 100 mL of MeOH and NEt_3 was added until complete solubilization of the solid. After reducing the volume to 50 mL, the addition of 50mL of diethyl ether resulted in the precipitation of the deprotonated product as a white powder which was filtrated and dried over vacuum. Yield: 90%. Anal. Calc. for $C_{22}H_{15}N_3Na_2O_6S_2 \cdot 2H_2O$: C, 46.89; H, 3.40; N, 7.46; S, 11.38. Found: C, 47.72; H, 3.52; N, 7.50; S, 10.03. ^{1}H-RMN (400 MHz, MeOH-d_4, 298 K, ppm): δ, 8.80 (s, 2H); 8.78 (d, 2H); 8.75 (s, 2H); 8.72 (d, 2H); 8.09 (dt, 2H); 7.56 (ddd, 2H); 3.23 (s, 3H). ^{13}C-RMN (400MHz, MeOH-d_4, 298 K, ppm): δ 156.3; 155.8; 149.1; 149.0; 146.3; 137.5; 137.2; 134.4; 127.4; 124.3; 121.6; 118.3; 16.3. UV-vis (H_2O) [λ_{max}, nm (ε, $M^{-1}cm^{-1}$)]: 222 (35308), 252(28233), 278 (34167), 314 (8651). MALDI(-)- MS: (MeOH): 504 [M-Na]-, 240.5 $[M-2Na]^{2-}$

Synthesis of [Ru(Cl)$_3$(trpy*)]·MeOH (**1***). 0.230 g of $RuCl_3 \cdot xH_2O$ (1.1 mmol) and 0.468 g of LiCl (11 mmol) were dissolved in 30 mL of absolute ethanol and heated to 75 ºC. Then, 0.485 mg of *trpy** (0.92 mmol) dissolved in 170 mL of absolute ethanol were added drop wise during 3 h. Following, the reaction solution was kept at 75 ºC for one more hour. After cooling to room temperature, 287 mg of a red precipitate was filtered off ([Ru (*trpy**)]Na_2 (**3***)). The volume of the mother liquor solution was reduced to 15 mL in a rotatory evaporator and more of the red precipitate was filtered

off. Then, 50 mL of diethyl ether were added slowly to the filtrated EtOH solution from which a dark brown solid precipitated. The solid was then filtrated and was redissolved in dry methanol, reprecipitated with dry diethyl ether and filtrated. After rinsing several times with diethyl ether. 0.187 g (0.25 mmol) of the highly hydroscopic solid were obtained. Yield: 30 %. Anal. Calc. for $C_{23}H_{19}Cl_3N_3Na_2O_7RuS_2$: C, 36.02; H, 2.50; N, 5.48; S, 8.36. Found: C, 35.69; H, 3.0; N, 5.80; S, 8.52. MALDI(-)- MS: (MeOH): 333 $[M\text{-}2Na\text{-}Cl]^{2-}$, 344 $[M\text{-}2Na]^{2-}$.

Synthesis of $[Ru^{II}(trpy^*)_2]Na_2$ (**2***). 50 mg of $RuCl_3 \cdot xH_2O$ and 0.250 g of *trpy** were dissolved in 80 mL of a mixture 2:1 (absolute ethanol:water) and heated to 95 ºC overnight. After cooling to room temperature an undesired grey precipitate was filtered off and the mother liquid solution was evaporated to dryness. The resulting orange solid was redissolved in 30 mL of methanol containing 10 drops of water. Consecutively, diethyl ether was added until complete precipitation. The orange product was filtered and dried over vacuum for several hours. Yield: 56 %. Anal. Calc. for $C_{44}H_{46}N_6Na_2O_{20}RuS_4$: C, 42.14; H, 3.70; N, 6.70; S, 10.23. Found: C, 41.79; H, 4.02; N, 7.04; S, 9.89. ^{1}H-RMN (400 MHz, MeOH-d_4, 298 K, ppm): δ, 9.020 (s, 4H, H_g); 8.715 (s, 4H, H_j); 8.57 (d, 4H, H_a, J_{ab} = 8.04 Hz); 7.86 (t, 4H, H_c, $J_{dc} = J_{cb}$ = 8.04 Hz); 7.38 (d, 4H, H_d, J_{dc} = 8.04 Hz); 7.09 (t, 4H, H_b, $J_{ba} = J_{cb}$ = 8.04 Hz); 2.998 (s, 6H, H_m). UV-vis (H_2O) [λ_{max}, nm (ε, $M^{-1}cm^{-1}$)]: 286 (58200), 310 (60676), 492 (26029). $E_{1/2}$(H_2O pH = 7, V vs SSCE): 1.043. MALDI(-)- MS: (MeOH): 532 $[M\text{-}2Na]^{2-}$.

Synthesis of $[\{Ru^{II}(trpy^*)\}_2(\mu\text{-bpp})(\mu\text{-}O_2CMe)](Na)_2$·Acetone (**3***). 25 mg of Hbpp ligand and 0.16 mL of NEt_3 were dissolved in 40 mL of freshly distilled methanol (solution A) in a 250 mL round bottom flask endowed with a stirring magnet and a condenser. In another flask, 156 mg of *trpy** and 0.125 g of LiCl were dissolved in 160 mL of methanol (solution B). After heating solution A to 50 ºC, the reagents in solution B were added drop-wise with a syringe pump over 3 h. Then the reaction mixture was heated to 100 ºC for one hour. After cooling to room temperature, the solution was irradiated overnight with a 200 W tungsten lamp. The brown solution was kept for one hour in the fridge (4 ºC) and a little undesired product (**2***) was filtrated. After evaporating to dryness and redissolving in 25 mL of methanol, 25 mL of diethyl ether were added resulting in the precipitation of a brown solid which was filtrated and dried under vacuum for several hours. The brown solid was purified by reverse phase

flash chromatography (using ISCO CombiFlash® system and RedySep® 13 g C-18 as stationary phase) eluting with an initial mixture of 15/85 of methanol/acetate buffer (pH = 4.64). The methanol content in the solvent mixture was progressively increased to a solvent ratio of 80/20. The last purple fraction was the desired product. Anal. Calc. for $C_{62}H_{49}N_{10}Na_2O_{15}Ru_2S_4$ C, 48.03; H, 3.19; N, 9.03; S, 8.27. Found: C, 47.37; H, 3.29; N, 8.69; S, 8.00. ^{1}H-RMN (400 MHz, MeOH-d_4, 298 K, ppm): δ, 9.05 (s, 4H, H_g); 8.83 (s, 4H, H_j); 8.78 (d, 4H, H_a, J_{ab} = 7.26 Hz); 8.46 (s, 1H, H_x); 8.35 (d, 4H, H_d, J_{dc}= 7.26 Hz); 8.20 (d, 2H, H_q, J_{qp} = 7.87 Hz); 8.04 (t, 4H, Hb, J_{ab} = J_{bc} = 7.26 Hz), 7.73 (t, 2H, H_p, J_{qp} = J_{po} = 7.87 Hz), 7.46 (t, 4H, H_c, J_{cd} = J_{bc} = 7.26 Hz), 7.32 (d, 2H, H_n, J_{no} = 7.87 Hz), 6.86 (t, 2H, H_o, J_{no} = J_{op} = 7.87 Hz), 1.98 (s, 6H, H_m), 0.57 (s, 3H, Hz). UV-vis (H_2O) [λ_{max}, nm (ε, $M^{-1}cm^{-1}$)]: 316 (57440), 364 (28410), 496 (15310), 526 (14860). $E_{1/2}$(H_2O pH = 7, V vs SSCE): 0.449, 0.815. ESI(-)- MS: (MeOH): 723 $[M-2Na]^{2-}$.

Anchoring on anatase disperse nanoparticles. Anatase TiO_2 was calcinated at 450 ^oC before use. The TiO_2 powder (250-500 mg) was added to a 6mL acidic aqueous solution of **4*** (1-2 μmol of **3*** in MiliQ water solution with HNO_3, pH=2). After 12 hours, the solution was completely colourless and was centrifuged and the nitric acid solution was discarded. 6 mL of triflic acid solution (pH = 1) was added to the powder, the resulting suspension was stirred for 2 hours and then centrifuged. This process was repeated three times. The final powder was introduced into the reaction vessel with 4 mL of fresh acid solution (pH = 1, triflic acid) and then degassed.

Cleaning procedure for FTO slides. The slides were put in a beaker filled with Mili-Q water and a detergent solution (Hellmanex) using an ultrasonic bath for 10 minutes and rinsed with Mili-Q water. After filling the beaker with plane Mili-Q water the slides were put in the ultrasonic bath for 10 more minutes and rinsed with ethanol. A third 10-minute sonication period was carried out with pure EtOH followed by rinsing with clean EtOH. Finally the slides were dried with lens cleaning paper and kept 10 minutes at 100 ^oC in the stove and 30 min at 495 ^oC in the Muffle furnace.

Film coating. To obtain a crystalline mesoporous film of uniform thickness, we used Scotch tape in both sides (longitudinal) as a framer and a glass rood to spread a little amount of the viscous TiO_2 paste onto a 75 x 25 x 1 mm^3 glass covered with FTO

(Doctor Blade technique). After removal of the tape the films were dried 10 min in the stove at 100 ºC to reduce surface irregularities.

Film sintering and calcination. The films were put in a Pyrex Petri disk and introduced in the muffle furnace for the following temperature ramps: 25 ºC → 325 ºC (20 min), 325 ºC (5min), 325 ºC → 375 ºC (5min), 375 ºC (5min), 375 ºC → 450 ºC (5min), 450 ºC (15min), 450 ºC → 500 ºC (5 min), 500 ºC (15 min). Then it was let to cool with the muffle off and closed for 10 min. Finally, it was let to cool to room temperature outside the muffle for about 30 min.

After cutting the resulting films transversally to obtain 8 smaller films (5 x 25 x 1 mm^3) they were stored in a dry atmosphere individually wrapped with wax paper. When these films were used more than 48 hours after the calcination process a second calcination was carried out for 30 minutes at 450 ºC.

Sensitization (Anchoring). The films were soaked in 5 mL of a 0.05 mM solution of complex **3*** in acidic aqueous solution (MiliQ water solution with HNO_3, pH = 2) for 36 hours. After rinsing with miliQ water, the films where soaked in a pH = 1 solution of triflic acid overnight.

Instrumentation and measurements

The NMR spectroscopy at room temperature was performed on a 400 MHz Bruker Avance II. Samples were run in MeOD or D_2O. The ESI and MALDI mass spectroscopy experiments were performed on a Waters Micromass LCT Premier equipment and a Bruker Daltonics Autoflex equipped with a nitrogen laser (337 nm), respectively. UV-Vis spectroscopy was performed on a CARY 50 Bio (VARIAN) UV-vis spectrophotometer with 1 cm quartz cells.

All electrochemical experiments, except from those directly related to the bulk electrolysis experiments, were performed in a PAR 263A EG&G potentiostat or in a IJ-Cambria IH-660 potentiostat, using a three electrode cell. Glassy carbon electrodes (3 mm diameter) from BAS were used as working electrode, platinum wire as auxiliary and SSCE as the reference electrode. Cyclic Voltammograms (CV) were recorded at 100

mV/s scan rate under argon atmosphere. The complexes were dissolved in previously degassed water at the desired pH with a minimum 0.1 M ionic strength. All $E_{1/2}$ values reported in this work were estimated from cyclic voltammetry as the average of the oxidative and reductive peak potentials $(E_{p,a}+E_{p,c})/2$ or from Differential Pulse Voltammetry (DPV; pulse amplitudes of 0.05 V, pulse widths of 0.05 s, sampling width of 0.02 s and a pulse period of 0.1 seconds). Unless explicitly mentioned the concentration of the complexes were approximately 0.3 mM.

Online manometric measurements were carried out on a Testo-521 differential pressure manometer with an operating range of 1–100 hPa and accuracy within 0.5% of the measurement, coupled to thermostated reaction vessels for dynamic monitoring of the headspace pressure above each reaction. The secondary ports of the manometers were connected to thermostatically controlled reaction vessels that contained the same solvents and headspace volumes as the sample vials. Online monitoring of the gas evolution was performed on a Pfeiffer Ominstar GSD 301C mass spectrometer. Typically, 16.04 mL degassed vials containing a suspension of the supported catalysts in 0.1 M triflic acid (1.5 mL) were connected to the apparatus capillary tubing. Subsequently, the previously degassed solution of Ce^{IV} (0.5 mL) at pH = 1 (triflic acid, 100 equivalents) was introduced using a Hamilton gas-tight syringe and the reaction was dynamically monitored. A response ratio of 1:2 was observed when injecting equal concentrations of O_2 and CO_2, respectively, and thus was used for the calculation of their relative concentrations.

Electrocatalytic experiments were performed always using pH = 1 solution with prepared with triflic acid in Mili-Q water. All bulk electrolysis for electrocatalysis and CV of anchored compounds were performed in two compartement/three electrode cell using a Bio-Logic potentiostat/galvanostat and EC-Lab software. Sensitized **4*-TiO_2-FTO** films connected to a tin wire were used as working electrode, platinum grid as auxiliary and SSCE as the reference electrode. The O_2 concentration of the head space of the compartment containing the working electrode was monitored with a Clark's fast-response oxygen micro-electrode needle sensor (OX-N, 40 mm needle length, 1.1 mm diameter, 90% response time <10 s) commercialized by Unisense A/S.

X-Ray structure determination

The measured crystals were prepared under inert conditions immersed in perfluoropolyether as protecting oil for manipulation. The measured crystals were mounted using a nylon loop directly from the crystallisation solution to the diffractometer cooled at -120 °C. Measurements were made on a Bruker-Nonius diffractometer equipped with an APPEX 2 4K CCD area detector, a FR591 rotating anode with MoK_α radiation, Montel mirrors as monochromator and a Kryoflex low temperature device (T = -173 °C). Full-sphere data collection was used with ω and φ scans. Programs used: data collection Apex2 v. 1.0-22;[13] data reduction, Saint + Version 6.22;[14] absorption correction, SADABS V. 2.10;[15] structure solution and refinement, SHELXTL Version 6.14.[16]

Crystals for complex **2*** were grown from water at RT by slow diffusion of methanol and ethanol. The asymmetric unit is made up by one molecule of the complex linked to two sodium atoms and water/methanol/ethanol molecules which are partially disordered. The sodium atoms are linked to water, methanol and ethanol. The the latter are disordered and located at the same positions. The water and methanol molecules not linked to the sodium atoms are also partially disordered. In total the asymmetric unit contains 4.8 molecules of water, 1.9 molecules of methanol and 0.64 molecules of ethanol. In the main molecule the atoms N3, C11, C12, C13, C14 and C15 are disordered in two positions (ratio 49:51). The alert A obtained doing checkcif is due to the disorder of the solvent molecules linked to the sodium atoms.

Crystals for the *trpy** ligand were grown from water by slow diffusion of methanol. The asymmetric unit is contains one complex formed by one molecule of *trpy** ligand, two sodium atoms, two methanol molecules and one water molecule. The measured crystal contained probably an additional second crystal which affected the quality of the data. Of 64227 reflections 3693 were rejected, they should be systematically absent and were observed with weak intensity. The presence of this second crystal probably explains the unusually large value of the second parameter in the weighting line for refinement and the relatively high R1 value.

DFT geometry optimization

The molecular geometry of **4*** was fully optimized in the gas phase at the M06-L level of density functional theory (DFT)[17] using the Stuttgart ECP28MWB contracted pseudopotential basis set [8s7p6d2f | 6s5p3d2f][18, 19] on Ru and the MIDI![20] basis set on all other atoms. Full geometry optimization was performed without imposing any symmetry constraint.

4.2.4. Results and discussion

Synthesis of Ligands and Complexes

The synthetic strategy followed for the preparation of the complexes described herein is depicted in Scheme 2. Treatment of commercial 4'-(p-tolyl)-2,2':6',2''-terpyridine with oleum yielded the 5-([2,2':6',2''-terpyridin]-4'-yl)-2-methylbenzene-1,3-disulfonate (*trpy**) ligand. Drop-by-drop-addition of a highly diluted ethanol solution of *trpy** on a concentrated ethanol solution of ruthenium trichloride (saturated with LiCl) allowed the isolation of complex $[Ru^{III}(Cl)_3$ (trpy*)] (**1***). Reaction of **1*** with an additional *trpy** ligand affords the anionic compound $[Ru^{II}(trpy^*)_2]^{2-}$ (**2***).

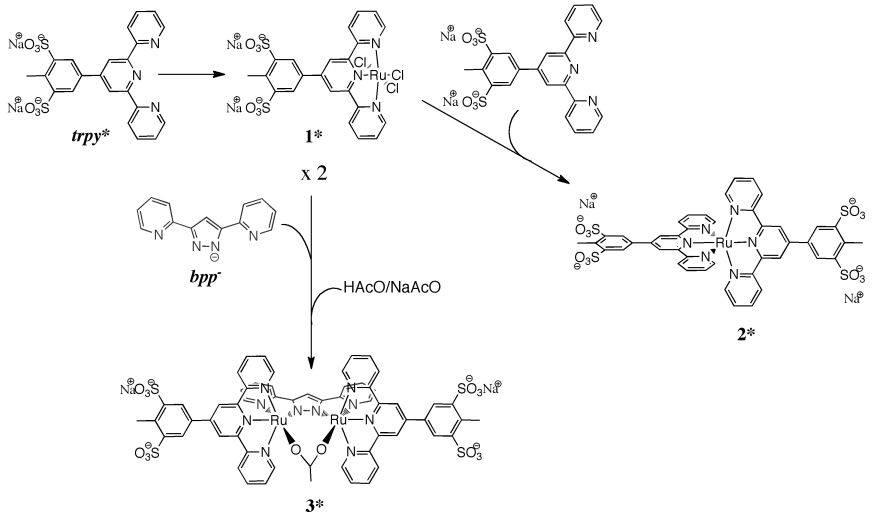

Scheme 2. Synthetic strategy. Complexes containing the star refer to the ones that contain the sulfonated terpyridine ligand (*trpy**) whereas those that do not have the star contain the *trpy* ligand.

Dropwise addition of the octahedral Ru complex **1*** to a reflux solution of the deprotonated dinucleating *bpp*$^-$ ligand in the presence of NEt_3, followed by light irradiation, generates a mixture of dinuclear and mononuclear (**2***) Ru complexes. Reverse phase (C18) chromatography eluting with methanol and a sodium acetate/ acetic acid buffer solution (pH = 4), allowed the direct isolation of complex *in,in*-[{Ru^{II}(*trpy**)}$_2$(μ-*bpp*)(μ-AcO)]$^{2-}$ (**3***). The acetato bridged complex **3*** is an excellent precatalyst since it is an easy to handle crystalline material obtained with relatively reasonable good yield. In addition, the lability of the acetato bridge in acidic media allows the clean obtention of the bisaquo derivative *in,in*-[{Ru^{II}(*trpy**)(H_2O)}$_2$(μ-*bpp*)]$^-$ (**4***) (Equation 1) as can be followed by UV-vis and cyclic voltammetry, *vide infra*.

in,in-[{Ru^{II}(*trpy**)}$_2$(μ-*bpp*)(μ-AcO)]$^{2-}$ + 2H_2O →

3* *in,in*-[{Ru^{II}(*trpy**)(H_2O)}$_2$(μ-*bpp*)]$^-$ + AcO^- (1)
4*

For easy follow up of the nomenclature, in this work all complexes containing the sulfonated *trpy** ligand will be denoted with a star (**1*-4***) whereas the analogous complexes perviously reported[8, 9] which contain the *trpy* meridional ligand will not (compounds **1**- **4** respectively).

Anchoring on Anatase TiO_2 Surfaces

Compound **4*** was anchored both onto the surface of anatase disperse nanoparticles (**4*-TiO_2-disperse**) and onto a mesoporous anatase film deposited on a conductive FTO covered glass slide (**4*-TiO_2-FTO**).

In both cases compound **3*** was first dissolved in a pH = 2 aqueous solution (HNO_3) which in short time leaded to the complete hydrolization of the acetato bridge affording compound **4***. Then, either the disperse nanoparticles or the TiO_2 covered FTO films, were soaked in the solution and the resulting pH was readjusted to 2 if required.

The **4*-TiO_2** materials were rinsed several times with water and then soaked in a pH = 1 trifilc acid soltution for 12 h. No compound desorption was observed in any case

when the final acidic solution was analysed by UV-vis spectroscopy and electrochemical techniques.

The sensitization process of the FTO-TiO_2 films was followed by consecutive registering of the UV-vis spectra of the acidic solution over time (Figure 1). Concluding that, under our working conditions, 48h were required for maximum sensitization.

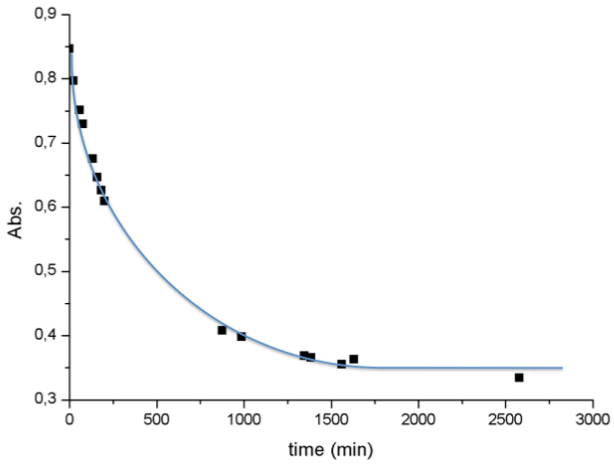

Figure 1. Kinetics of the adsorption of compound **4*** on TiO_2 covered FTO film following the absorbance changes of the sensitization solution over time, at 500 nm.

Upon anchoring **4*** onto anatase disperse nanoparticles, the acidic solution became completely colourless in 2 h. UV-vis spectroscopy of the solution before and after the sensitization process point to complete anchoring of the compound.

Characterization and Spectroscopic Properties

The structural, spectroscopic and electrochemical properties of the new family of compounds **1*-4*** have been studied with the standard spectroscopical and electrochemical techniques, including ^{1}H-NMR for diamagnetic species **2*** and **3***. Figure 2 shows the ^{1}H-NMR spectra for complex **3*.**

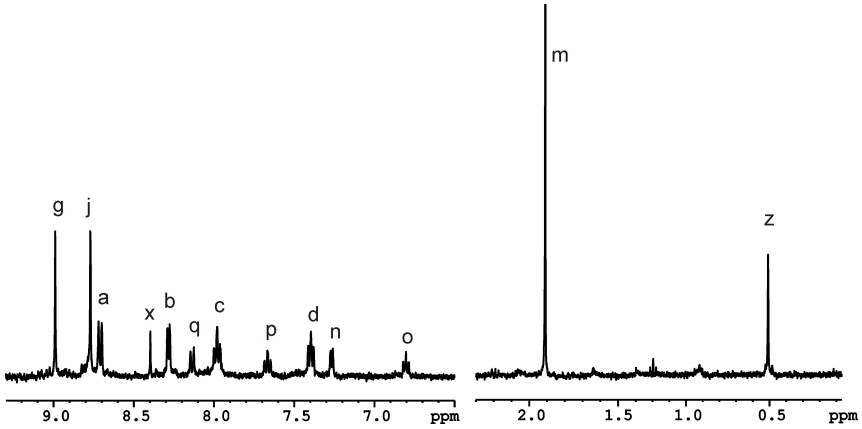

Figure 2. ^{1}H-NMR spectra in MeOD of complex **3*** and resonance assignation corresponding to the labeling in Scheme 1.

For the *trpy** ligand and complex **2***, solid state structural characterisation was achieved by X-ray diffraction analysis. Capped stick views of the structures of the respective anions are shown in Figure 3 and their most relevant crystallographic parameters are listed in Table 1.

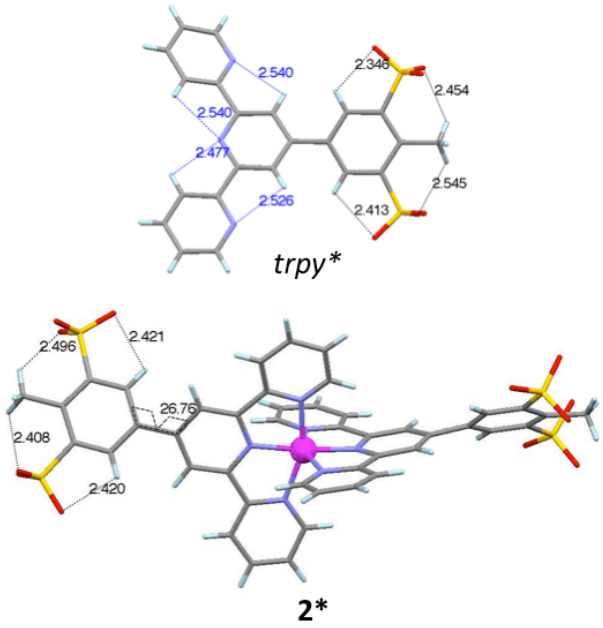

Figure 3. Caped stick diagram for the molecular structure of the anionic part of complex **2*** (top) and ligand *trpy** (bottom). Selected metric parameters related to H interactions are included.

All the Ru-N bond distances and angles of compound **2*** (see Sup. Inf.) are within the typical values obtained for related Ru(II)N_6 complexes.[11, 21] The pyridyl rings of the *trpy** ligand are strongly twisted by both, crystal packing forces and the strong interactions of the sulfonate functionalities with sodium cations. As can be seen in Figure 1 the sulfonate groups interact by hydrogen bonding with the hydrogens of the methyl group and the hydrogens contained in the tolyl ring. In the case of the *trpy** ligand, the absence of the metal centre permits rotation of the pyridyl rings that allow additional hydrogen bond formation between the N of one pyridyl ring with the aromatic hydrogen of the neighbour ring (blue in Figure 2).

Table 1. X-ray crystallographic parameters for complex **2*** and *trpy** ligand.

	2*(Na)$_2$	*trpy**
Emp. Form.	$C_{47.08}H_{50.60}N_6Na_2O_{19.94}RuS_4$	$C_{24}H_{25}N_3Na_2O_9S_2$
Mr	129.483	60.957
Cryst. Syst.	Triclinic	Orthorhombic
Space group	P -1	Pbca
a (Å)	12.4171(9)	7.9409(7)
b (Å)	14.9612(11)	0.7087(17)
c (Å)	15.1369(11)	33.068(3)
α (deg)	66.340(2)	90.00 °
β (deg)	88.735(2)	90.00 °
γ (deg)	84.479(2)	90.00 °
V(Å^3)	2563.3(3)	5437.9(8)
Z	2	8
ρcalc (Mg·m^{-3})	1.678	1.489
μ (mm-1)	0,573	0,285
GOF on F2	1,060	1,333
R1	0,0346	0,0893
WR2	0,0876	0,1778

The structure of **4*** was computed at the M06L DFT level of theory, in the gas phase. The resulting structure was employed to estimate the dimensions of the cavity

originated by anchoring the complex onto the TiO_2 surface. As can be seen in Figure 4 the size of the hole of the cavity would be of around 100 $Å^2$ which should allow enough room for water molecules to flow through it (note that the Van der Waals diameter of water is 2.82 Å).

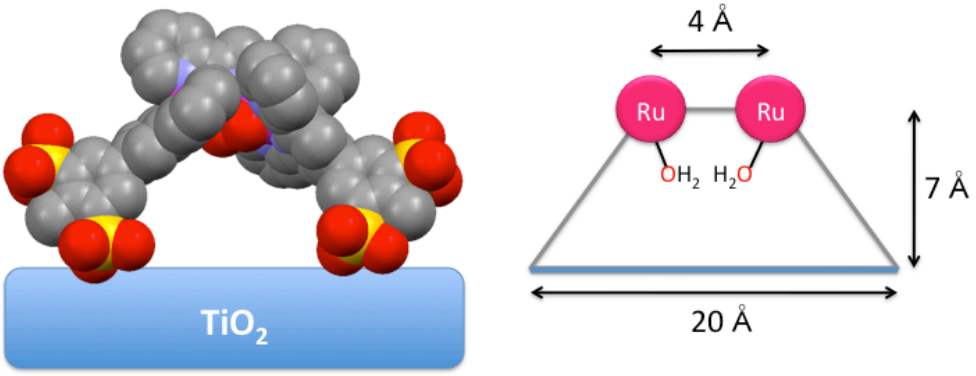

Figure 4. Left, structure of **4*** optimized at the M06L DFT level of theory, H are not shown. Right, schematic representation of compound **4*** anchored on TiO_2 with the most relevant approximate distances.

The normalised UV-vis spectra of the *trpy* and *trpy** ligands as well as the ones for complexes **2**, **2***, **3** and **3*** all measured in methanol as solvent are presented in Figure 5. As expected for Ru(II)N type of complexes with polypyridylic ligands[11, 21] they present π-π ligand based allowed transitions below 300 nm and MLCT and d-d bands above 300 nm. The MLCT bands that appear in the range of 400-600 nm in the spectra of the ruthenium complexes represented in Figure 2 are particularly interesting. For the case of the *trpy** complexes the anionic character of the ligand produces a destabilisation of the dπ(Ru) orbitals that as a consequence produces a red shift of the MLCT bands, as is nicely shown for complexes **2*** and **3*** when compared with **2** and **3** in Figure 5. Additionally, in the complexes containing the *trpy** ligand a larger number of π-π* bands are observed which are associated with the additional tolyl group in the *trpy** ligand. Finally, an increase in the extinction coefficient (ε) is observed in the *trpy**-based compounds.

When the visible region of the UV-vis spectra of compound **4*** and **4*-TiO_2-FTO** in water at pH = 1 (triflic acid) are overlaid, the two characteristic d-d bands are almost

equal. Just a very slight red shift is observed for the adsorbed compound (Figure 6), as it has been previously observed for other TiO_2 adsorbed compounds reported in the literature.[22] When considering the possibility of the coordination of O atoms of TiO_2 to the Ru metal centers a significant red shift on the resulting spectra would be expected as is the case for compound **3*** containing the electron rich anionic AcO^- chelating ligand.

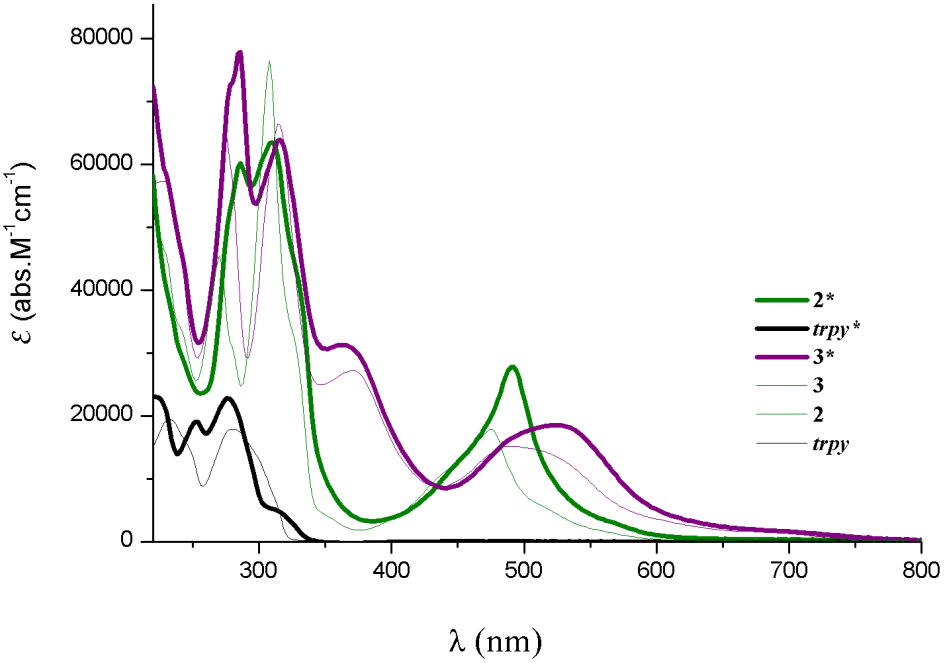

Figure 5. UV-vis spectra in Methanol for 0.3 mM solutions of compound. For easy follow up the spectra of the sulfonated compounds are presented with thicker lines. Black, *trpy* and *trpy** liagnds; Green, **2** and **2***; Purple, **3** and **3***.

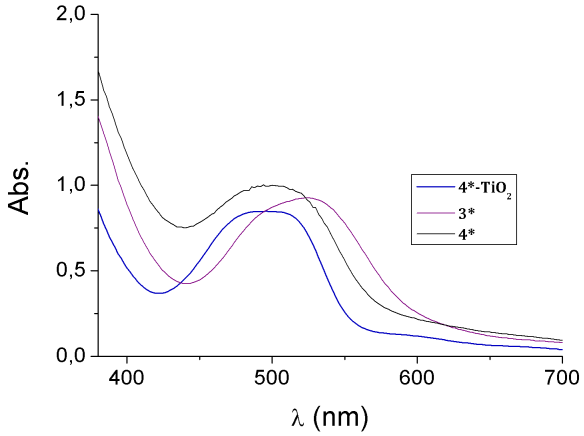

Figure 6. In blue, UV-vis spectra of compound **4*** adsorbed on TiO_2 covered glass slide without FTO. In black, the spectra of **4*** in a pH =1 solution (triflic acid). In purple, compound 3* in MeOH.

Table 2 presents the most prominent UV-vis spectroscopic features together with their redox potentials for compounds **1*-4*** and **1-4**. The previously described energy shifts of the MLCT bands observed in the UV-vis are in good agreement with the electrochemistry displayed by these complexes as is described below.

Table 2. UV-vis spectroscopic features and redox properties for *trpy, trpy**, **1-4**, **1*-4*** and **4*-TiO2-FTO**.

Complex	UV-vis, λmax, nm (ε, $M^{-1}cm^{-1}$) π-π*	UV-vis, λmax, nm (ε, $M^{-1}cm^{-1}$) MLCT, d-d	$E_{1/2}$ [a] (V) (II,III/II,II)	$E_{1/2}$ [a] (V) (III,III/II,III)	$E_{1/2}$ [a] (V) (III,IV/III,III)	$E_{1/2}$ [a] (V) (IV,IV/IV,III)
trpy[b]	282 (17843) 232 (19585)	---	---	---	---	---
1[b,d]	---	---	0.13	---	---	---
2[b,e]	307 (764987) 270 (45445)	474 (17820)	1.046	---	---	---
3[b,f]	314 (66402) 274 (66169) 230 (57231)	521 (13797) 490 (15160) 372 (27210)	0.77	1.1	---	---
4[c]	314 (57661) 270 (56559)	490 (11021) 471 (11882) 354 (20322)	0.59	0.65	0.88	1.1
trpy*[b]	278 (22724) 252 (19057) 225 (22626)	---	---	---	---	---
1*[b,d]	---		0.11	---	---	---
2*[b,e]	310 (63480) 286 (60225)	492 (27773)	1.043	---	---	---
3*[b, g]	316 (63881) 286 (77939)	530 (18377) 490 (16396) 364 (31275)	0.65	0.95	---	---
4*[c]	315 (57937) 284 (78015)	513 (16513) 480 (16906) 360 (25879)	0.55	0.64	0.87	1.08
4*-TiO_2[d]	---	517 486	0.56	0.61	0.81	0.92

[a] $E_{1/2}$ obtained from DPV (pulse amplitudes of 0.05 V, pulse widths of 0.05 s, sampling width of 0.02 s and a pulse period of 0.1 seconds) reported vs. SSCE. [b] UV-vis spectra recorded in Methanol.[c] UV-vis spectra and CV recorded in water pH = 1, triflic acid. [c] CV recorded in water pH = 1, triflic acid, UV-vis spectra of the film. [d] CV in EtOH with LiCl. [e] CV recorded in water pH = 7 with phosphate buffer. [f]CV in Acetone with TBAH. [g]CV in Methanol and LiCl.

The redox properties of all the reported compounds have been investigated by means of CV. The solvents employed where the ones that permitted to dissolve both the *trpy** containing compounds and their analogous with *trpy*. Their cyclic voltammograms are presented in the Supp. Inf., whereas their formal redox potentials are shown in the experimental section and in Table 2.

A first glance at Table 2 shows that the replacement of *trpy* by the *trpy** ligand produces a decrease of redox potentials by about 20 to 120 mV due to the presence of the $-SO_3^-$ groups.

All the mononuclear complexes studied in the present work display one redox process. The dinuclear complexes **3** and **3*** containing the acetato bridges present two consecutive 1e- oxidations (seen in Figure 7 for CV of complex **3***) that correspond to Equations 3-4 (ligands are not shown).

$$[Ru^{II}Ru^{III}] + 1e^- \rightarrow [Ru^{II}Ru^{II}] \quad (3)$$

$$[Ru^{III}Ru^{III}] + 1e^- \rightarrow [Ru^{II}Ru^{III}] \quad (4)$$

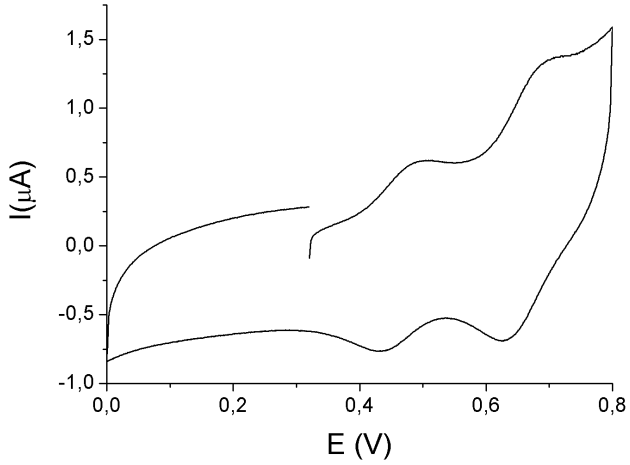

Figure 7. Cyclic voltammogram of **3*** in a MeOH solution with LiCl (1mM).

The cyclic voltammogram of the aquo compound **4*** in pH=1 triflic acid solution is presented in Figure 8. The cyclic voltammogram of compound **4*** differs very little from that of the widely studied *bpp*-aquo system **4**, both registered in the same conditions.[23] Despite of the slight shift towards lower potentials, the four waves observed for **4*** could be tentatively assigned by analogy to the processes proposed for compound **4** as depicted in Equations 5-8.

$$[H_2O\text{-}Ru^{II}Ru^{III}\text{-}OH_2] + 1e^- \rightarrow [H_2O\text{-}Ru^{II}Ru^{II}\text{-}OH_2] \quad (5)$$

$$[H_2O\text{-}Ru^{III}Ru^{III}\text{-}OH] + 1e^- + 1H^+ \rightarrow [H_2O\text{-}Ru^{II}Ru^{II}\text{-}OH_2] \quad (6)$$

$$[HO\text{-}Ru^{IV}Ru^{III}\text{-}OH] + 1e^- + 1H^+ \rightarrow [H_2O\text{-}Ru^{III}Ru^{III}\text{-}OH] \quad (7)$$

$$[O\text{-}Ru^{IV}Ru^{IV}\text{-}O] + 1e^- + 2H^+ \rightarrow [HO\text{-}Ru^{IV}Ru^{III}\text{-}OH] \quad (8)$$

Additionally, it is really important to note the presence of the beginning of an electrocatalytic wave starting around 1.3 V vs SSCE. Which in system **4** already appeared at 1.2 V.

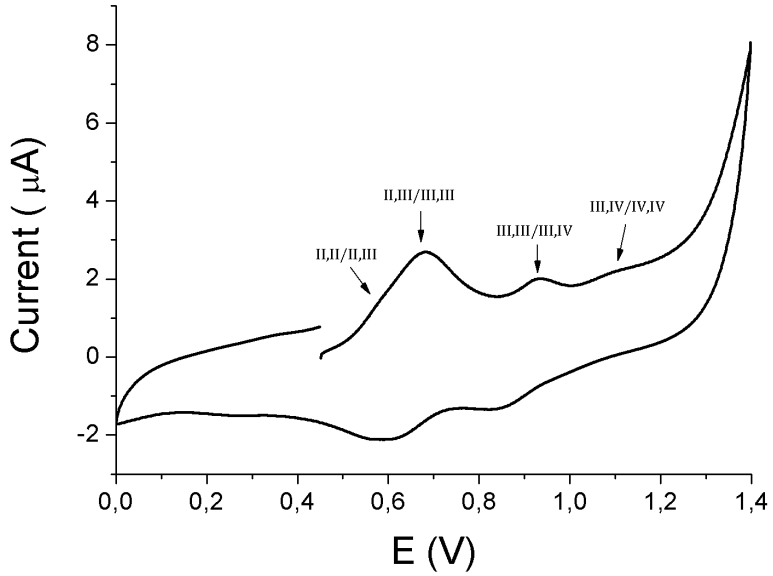

Figure 8. Cyclic voltammogram in pH = 1 for compound **4*** using SSCE as reference electrode.

The cyclic voltammetry of **4*-TiO$_2$-FTO** presents oxidation waves shifted to lower potentials with respect to those of **4***. Interestingly, the little or no shift observed for the first one electron process (II,III/II,II; Equation 5), becomes evident in the second (III,III/II,III; Equation 6; 30 mV shift) and third (III,IV/III,III; Equation 7; 60 mV shift) processes involving 1 electron and 1 proton each. The shift in potentials is drastically magnified in the fourth oxidative process (IV,IV/III,IV; Equation 7; 270 mV shift), this last step involves a 1 electron and 2 protons. Additionally, the electrocatalytic wave observed for compound **4*** in solution, was not observed for **4*-TiO$_2$-FTO** when CV was performed scanning up to 1.4 V (vs SSCE), see Figure 9.

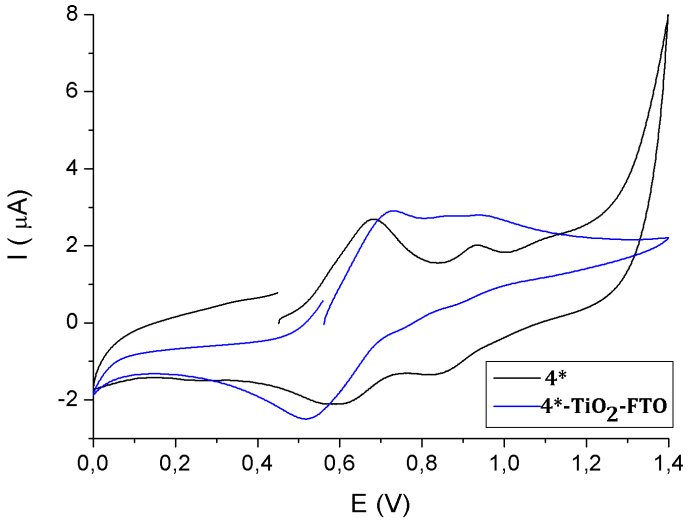

Figure 9. Cyclic voltammogram of **4*-TiO$_2$-FTO** (I= 10^{-1} mA) composite material (blue) and the corresponding voltammogram of **4*** (black), both in a pH = 1 solution (triflic acid).

Chemical water oxidation

The addition of Ce^{IV} (100 equivalents) in a 0.1 M triflic acid suspension of the **4*-TiO$_2$-disperse** composite material immediately released gas as was monitored by online manometry. The composition of the generated gas was analysed by online mass spectrometry which revealed the evolution of a significant amount of CO_2. Different ratios of TiO_2: **3*** (acetato starting material) were tested and their performances

analysed by the combination of the two online techniques. The resulting data is summarised in Table 3.

Interestingly, the solid state dilution of the anchored material resulted in both smaller turn over numbers (TONs) and a higher O_2/CO_2 ratio. This data suggest that the CO_2 measured may come from the oxidation of the ligands of one catalyst molecule by another catalyst molecule.

Table 3. Results of the catalytic experiments with compound **3*** hydrolized (**4***) and anchored on anatase powder. All experiments were performed in a pH = 1 solution (triflic acid) and 100 eq. of Ce^{IV} were added.

mg of 3*	µmols of 3* (and 4* in pH=1)	mg anatase	TON of gas	ratio O_2/CO_2
2	1.29	250	2.2	6/1
1	0.65	250	1.8	9/1
0,5	0.32	500	1.0	20/1

The absence of characteristic absorption bands of **4*** type of products in the UV-vis spectra and non detectable waves in the CV of the final solution (added to the brownish colour of the final anatase powder) suggest that at least most of the ruthenium is retained in the TiO_2 nanoparticles at the end of the experiment.

Electrocatalytic experiments

As has been mentioned earlier, even though compound **4*** in solution presents an electrocatalytic wave, in the case of **4*-TiO_2-FTO** one must scan up to 1.5 V (vs. SSCE) to observe what seems to be the beginning of an electrocatalytic process. Therefore, a 1.6 V potential was chosen to undergo bulk electrolysis with the **4*-TiO_2-FTO** electrodes.

In Figure 10 a schematic representation of the experiment's setup is shown, complemented by pictures of the real components. The experiment was carried out in a two compartment teflon cell (A and C indicate the two compartments)divided by a

nafion membrane (B). After six hours, the current that circulated throughout the system was equivalent to 14 mols of electrons per mol of anchored **4***. Online O_2 measurement of the headspace of the compartment containing the **4*-TiO$_2$-FTO** electrode with a clack electrode prove (1 in Figure 8), revealed that no oxygen was released.

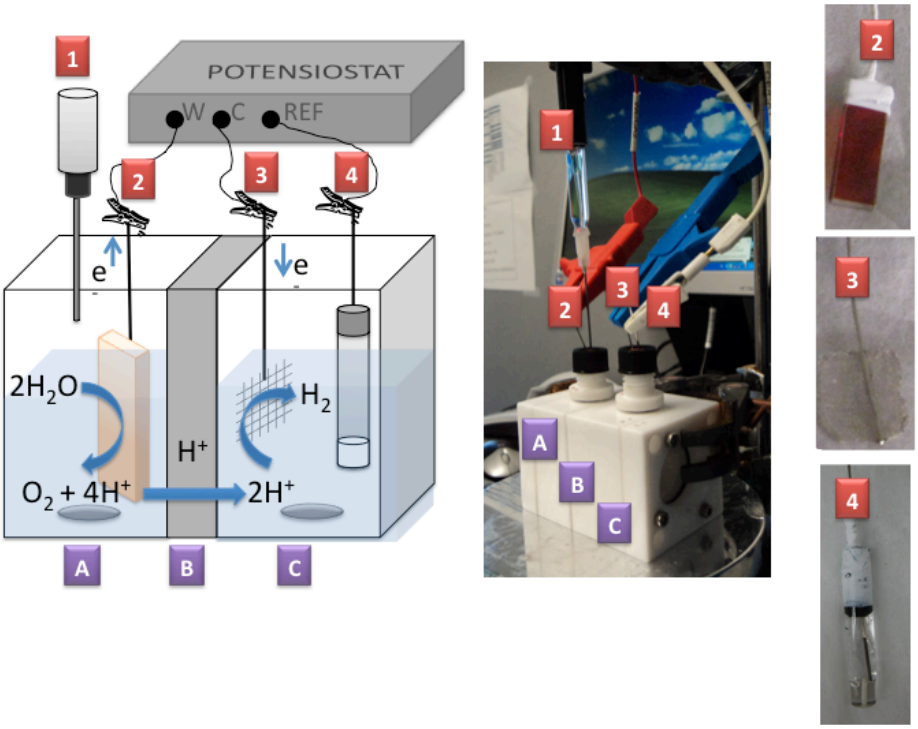

Figure 10. Left, Schematic drawing of the experimental setup for the bulk electrolysis experiment. Right, pictures of the real setup and basic components. A, Anodic compartment; B, nafion proton permeable membrane; C, cathodic compartment;1, clark electrode as oxygen sensor; 2, **4*-TiO$_2$-FTO** film as working electrode; 3, platinum net as counter electrode; 4, SSCE reference electrode.

As can be seen in Figure 11, UV-vis analysis of the acidic solution in the anodic compartment of the cell at the end of the experiment presented absorption spectra corresponding to a species closely related to **4*** as can be deduced by comparison of UV-vis spectra.

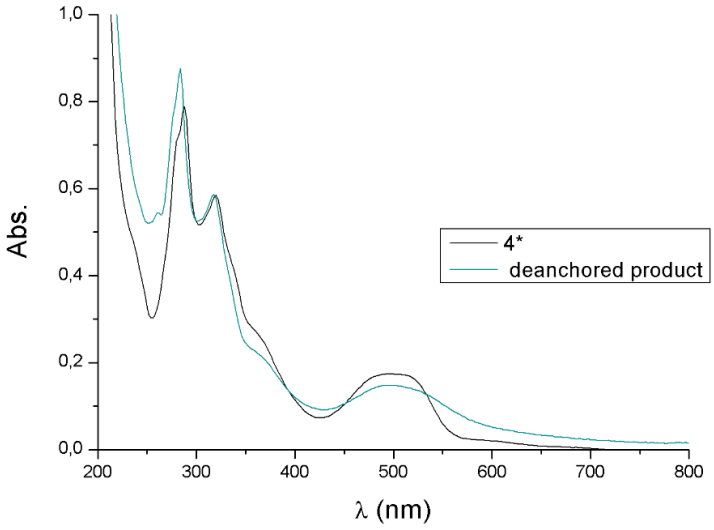

Figure 11. UV-vis spectra of **4*** in solution (black) and overlaid the spectra of the pH = 1 (triflic acid) solution present in the compartment of the **4*-TiO_2-FTO** electrode, at the end of the electrolytic experiment (cyan).

Accordingly, cyclic voltammograms of the electrode **4*-TiO_2-FTO** after the electrolysis (Figure 12) reveal an important decrease of dinuclear ruthenium compound anchored on the electrode's surface. Additionally, new redox active species were detected. All this data indicates that a major part of the current was employed in undesired processes such as catalyst's deanchoring, catalyst decomposition reactions yielding new products and energy dissipation in the form of heat.

The fact that all the attempts to undergo water oxidation with **4*-TiO_2-FTO** failed should be attributed to the significant down shift of the potentials of **4*-TiO_2-FTO** wich result in a redox potential for the IV,IV/III,IV process (0.92 V vs SSCE) too low to promote water oxidation. This potential lies 10 mV below the thermodynamic redox potential of water oxidation at pH = 1 (0.93 V vs SSCE).

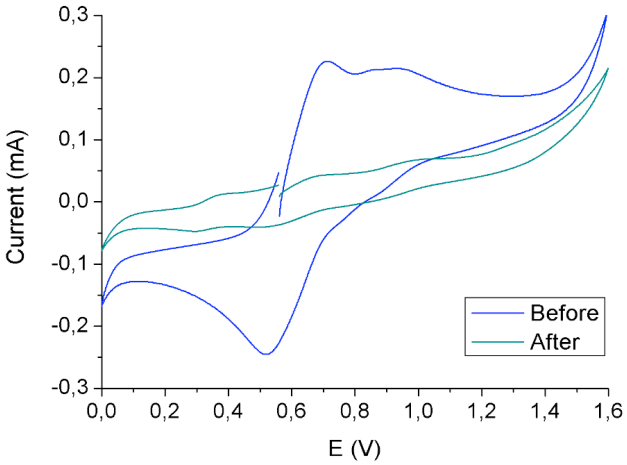

Figure 12. Cyclic voltammograms of **4*-TiO$_2$-FTO** composite material before the electrocatalytic experiment (blue) and after (cyan), in a fresh pH = 1 solution (triflic acid).

Electrochemical experiments preformed in aqueous solution at pH = 1 with added ethanol were performed. The cyclic voltammograms of **4*-TiO$_2$-FTO**, after successive additions of ethanol as substrate, showed the existence of a slow oxidative electrocatalytic process (see Figure 13). This can be observed by the increase of intensity of the electrochemical wave assigned as III,IV/IV,IV in the cyclic voltammetry of the anchored compound.

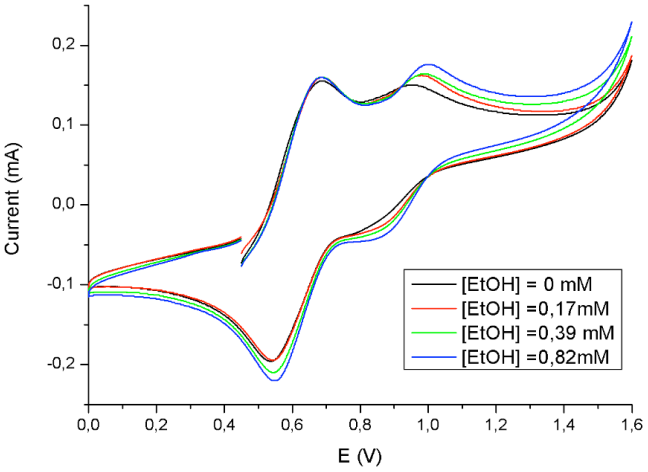

Figure 13. Cyclic voltammograms in different concentrations of Ethanol of **4*-TiO$_2$-FTO** composite material in a pH = 1 solution (triflic acid).

In hypothesising about the origin of the down shift in the redox potentials resulting from the anchoring of compound **4***, three additional actors should be considered: a) the aqueous phase composition, including potentially coordinating anions b) the semiconductor surface and c) the nature of the cavity formed upon anchoring.

As has been previously reported for other water oxidation catalysts in homogeneous phase, the anions present in solution could participate in an anation process.[24-26] Likewise, the coordination of O atoms from TiO_2 to the Ru centres would yield a compound with lower potentials and blocked active sites. Both cases should be discarded based on the observed capacity of the compound to oxidize ethanol. Additionally, the spectroscopic and electrochemical properties of the resulting compound, in both cases, would be expected to be closer to those of **3*** than those of **4***, and it is not the case (see, Figure 6 and Table 2).

Alternatively, since we are dealing with a thermodynamic rather than kinetic phenomena, a hydrophobic nature of the resulting cavity would explain the properties observed. As has been previously described, the down shift of the redox potentials is greater when the number of protons lost in the process is higher. Hence, a hydrophobic nature of the cavity thermodynamically favouring the redox processes by ejecting H_3O^+ could be a plausible explanation of the observed redox properties.

4.2.5. Conclusions

With respect of a modular approach for the elaboration of a device for artificial photosynthesis, accurate understanding of the limitations and implications of the heterogenization of water oxidation catalysts onto semiconductor surfaces such as TiO_2 is needed. To this end, we have prepared and thoroughly characterised the dinuclear complex *in,in*-$[\{Ru^{II}(trpy^*)\}_2(\mu\text{-bpp})(\mu\text{-AcO})]^{2-}$ (**3***) as water oxidation catalyst precursor. In acidic media, the acetato bridging ligand is hydrolysed yielding the "bisaquo" derivative *in,in*-$[\{Ru^{II}(trpy^*)(H_2O)\}_2(\mu\text{-bpp})]^-$ (**4***). The presence of $-SO_3^-$ groups on complex **4*** has a minimal impact on the electrochemical and spectroscopical properties of the compound in solution, as has been demonstrated by comparison with the non-sulfonated catalyst **4.** Upon anchoring **4*** onto a TiO_2

covered FTO electrode the electrochemical properties of the higher oxidation states of **4*** are dramatically modified, to the extent that it is no longer active as water oxidation catalyst. Water oxidation with Ce^{IV} as sacrificial oxidant by **4*** anchored onto anatase disperse nanoparticles has also been tested. The significant amount of CO_2 evolved can be indicative of an important catalyst to catalyst oxidative deactivation pathway.

The present work constitutes an example of how the heterogeneization of a catalyst can result in a material with drastically changed properties. This work shows that catalyst heterogeneization is not a straightforward matter. Thus, more research is urgently needed to understand the additional requirements that a water oxidation catalyst should fulfil to be employed supported onto conductive surfaces.

4.2.6. Acknowledgements

Support from SOLAR-H2 (EU 212508), American Chemical Society through the Petroleum Research Fund (48619-AC3), MICINN (CTQ2010-21497) and from the Consolider Ingenio 2010 (CSD2006-0003) are gratefully acknowledged. NP is grateful for a MICINN doctoral grant.

*The synthesis, characterization and crystalization of the **trpy*** ligand reported in this work was carried out by Stephan Roeser as part of his PhD in Dr. Llobet's group.*

4.2.7. References

[1] H. Yamazaki, A. Shouji, M. Kajita and M. Yagi, *Coord. Chem. Rev.* **2010**, *254*, 2483-2491.
[2] D. J. Wasylenko, C. Ganesamoorthy, B. D. Koivisto, M. A. Henderson and C. P. Berlinguette, *Inorg. Chem. (Washington, DC, U. S.)* **2010**, *49*, 2202-2209.
[3] J. J. Concepcion, M.-K. Tsai, J. T. Muckerman and T. J. Meyer, *J. Am. Chem. Soc.* **2010**, *132*, 1545-1557.
[4] M. Yagi, A. Syouji, S. Yamada, M. Komi, H. Yamazaki and S. Tajima, *Photochem. Photobiol. Sci.* **2009**, *8*, 139-147.

[5] F. M. Toma, A. Sartorel, M. Iurlo, M. Carraro, P. Parisse, C. Maccato, S. Rapino, B. R. Gonzalez, H. Amenitsch, T. Da Ros, L. Casalis, A. Goldoni, M. Marcaccio, G. Scorrano, G. Scoles, F. Paolucci, M. Prato and M. Bonchio, *Nat. Chem.* **2010**, *2*, 826-831.

[6] J. W. Jurss, J. C. Concepcion, M. R. Norris, J. L. Templeton and T. J. Meyer, *Inorg. Chem. (Washington, DC, U. S.)* **2010**, *49*, 3980-3982.

[7] Z. Chen, J. J. Concepcion, J. F. Hull, P. G. Hoertz and T. J. Meyer, *Dalton Trans.* **2010**, *39*, 6950-6952.

[8] C. Sens, I. Romero, M. Rodriguez, A. Llobet, T. Parella and J. Benet-Buchholz, *J. Am. Chem. Soc.* **2004**, *126*, 7798-7799.

[9] F. Bozoglian, S. Romain, M. Z. Ertem, T. K. Todorova, C. Sens, J. Mola, M. Rodriguez, I. Romero, J. Benet-Buchholz, X. Fontrodona, C. J. Cramer, L. Gagliardi and A. Llobet, *J. Am. Chem. Soc.* **2009**, *131*, 15176-15187.

[10] J. Casabo, J. Pons, K. S. Siddiqi, F. Teixidor, E. Molins and C. Miravitlles, *J. Chem. Soc., Dalton Trans.* **1989**, 1401-1403.

[11] R. Levine and J. K. Sneed, *J. Am. Chem. Soc.* **1951**, *73*, 5614-5616.

[12] B. P. Sullivan, J. M. Calvert and T. J. Meyer, *Inorg. Chem.* **1980**, *19*, 1404-1407.

[13] in *Data collection with APEX II v2009.1-02. Bruker (2007), Bruker AXS Inc., Bruker AXS Inc. Madison, Wisconsin, USA*, *Vol.*

[14] in *Data reduction with Bruker SAINT V7.60A. Bruker (2007). Bruker AXS Inc., Madison, Wisconsin, USA.*, *Vol.*

[15] in *SADABS: V2008/1 Bruker (2001). Bruker AXS Inc., Madison, Wisconsin, USA.*, *Vol.*

[16] in *SHELXTL V6.14, Structure solution and refinement.G. M. Sheldrick, Acta Cryst. 2008, A64, 112-122.*, *Vol.*

[17] Y. Zhao and D. G. Truhlar, *J. Chem. Phys.* **2006**, *125*, 194101/194101-194101/194118.

[18] D. Andrae, U. Haeussermann, M. Dolg, H. Stoll and H. Preuss, *Theor. Chim. Acta* **1990**, *77*, 123-141.

[19] M. Dolg, U. Wedig, H. Stoll and H. Preuss, *J. Chem. Phys.* **1987**, *86*, 866-872.

[20] R. E. Easton, D. J. Giesen, A. Welch, C. J. Cramer and D. G. Truhlar, *Theor. Chim. Acta* **1996**, *93*, 281-301.

[21] F. Laurent, E. Plantalech, B. Donnadieu, A. Jimenez, F. Hernandez, M. Martinez-Ripoll, M. Biner and A. Llobet, *Polyhedron* **1999**, *18*, 3321-3331.

[22] P. Wang, R. Humphry-Baker, J. E. Moser, S. M. Zakeeruddin and M. Graetzel, *Chem. Mater.* **2004**, *16*, 3246-3251.

[23] S. Romain, F. Bozoglian, X. Sala and A. Llobet, *J. Am. Chem. Soc.* **2009**, *131*, 2768-2769.

[24] F. Liu, J. J. Concepcion, J. W. Jurss, T. Cardolaccia, J. L. Templeton and T. J. Meyer, *Inorg. Chem. (Washington, DC, U. S.)* **2008**, *47*, 1727-1752.

[25] J. J. Concepcion, J. W. Jurss, J. L. Templeton and T. J. Meyer, *Proc. Natl. Acad. Sci. U. S. A.* **2008**, *105*, 17632-17635.

[26] X. Ottenwaelder, D. J. Rudd, M. C. Corbett, K. O. Hodgson, B. Hedman and T. D. P. Stack, *J. Am. Chem. Soc.* **2006**, *128*, 9268-9269.

4.3. THE ELECTRONIC STRUCTURE OF HIGHER OXIDATION STATES DERIVED FROM *cis*-$[Ru^{II}(BPY)_2(H_2O)_2]^{2+}$ AND ITS PHOTOISOMERIZATION MECHANISM

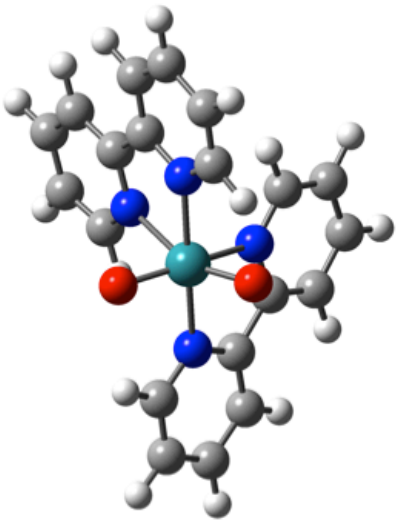

The attention is focused on the characterization of higher oxidation state species derived from water oxidation catalyst cis-$[Ru^{II}(bpy)_2(H_2O)_2]^{2+}$ (where bpy is the 2,2'-bypyridine bidentate ligand) by means of EPR and XAS spectroscopy together with DFT and CASPT2 calculations. We have further analyzed the cis- to trans-photoisomerization process suffered by this complex by means of DFT methodologies.

The Electronic Structure of Higher Oxidation States Derived from *cis*-$[Ru^{II}(bpy)_2(H_2O)_2]^{2+}$ and its Photoisomerization Mechanism

To be Submitted

Nora Planas,[a] Laura Vigara,[a] Clyde Cady,[b] Ping Huang,[b] Leif Hammarstrom,[b] Stenbjorn Styring,[b] Nils Leidel,[c] Holger Dau,[c] Michael Haumann,[c] Pere Miró,[d] Laura Gagliardi,[d] Christopher Cramer[d] and Antoni Llobet[a,e,]

[a] *Institute of Chemical Research of Catalonia (ICIQ), Av. Països Catalans 16, E-43007 Tarragona, Spain.*

[b] *Department of Photochemistry and Molecular Science, Ångström Laboratory, Box 523, Uppsala University, SE-751 20 Uppsala, Sweden.*

[c] *Department of Physics, Free University Berlin, D-14195 Berlin, Germany.*

[d] *Department of Chemistry and Supercomputing Institute University of Minnesota, 207 Pleasant St. SE, Minneapolis, MN 55455-0431 (USA)*

[e] *Departament de Química, Universitat Autònoma de Barcelona, Cerdanyola del Vallès, E-08193 Barcelona, Spain.*

†Electronic Supplementary Information (ESI) available: Experimental section,characterizations and coordinates of computed structures.

Keywords: Ruthenium Complexes, Electronic Structure, Higher Oxidation States, Photoisomerization, DFT calculations.

4.3.1. Abstract

The electronic structure of *cis*-$[Ru^{II}(bpy)_2(H_2O)_2]^{2+}$ (*cis*-$Ru^{II}(H_2O)_2^{2+}$) and its higher oxidation states species, generated upon addition of the corresponding equivalents of

Ce^{IV}, have been studied by means of UV-vis, EPR, XAS and DFT and CASSCF/CASPT2 calculations. EPR spectroscopy together with DFT show that in all cases lower spin configurations are favoured and thus oxidation state IV is a singlet, EPR silent at low temperature. For oxidation state V, DFT predicts a doublet as the ground state configuration with a quintet lying 12.7 kcal/mol above. This is in very good agreement with EPR spectroscopy where a signal with S = ½ is found. XAS spectroscopy of higher oxidation state species together with DFT further allow to understand the electronic structure of these complexes and in particular show the decrease of Ru-O bond distances as oxidation state increases. Further, the photochemical isomerization, *cis*-$[Ru^{II}(bpy)(H_2O)_2]^{2+}$ → *trans*-$[Ru^{II}(bpy)(H_2O)_2]^{2+}$, has been fully characterized by DFT methodologies and show that the process involves the decoordination of one aqua ligand leading to a coordinatively unsaturated complex that isomerizes and recoordinates the aqua ligand, to finally yield the *trans* isomer.

4.3.2. Introduction

Molecular Ru complexes are of interest in a wide variety of fields including photophysics, photochemistry,[1, 2] bioninorganics [3] and catalysis.[4] In the latter field, redox catalysis plays one of the major roles where invariably the Ru-O group is involved. Within redox catalysis the oxidation of water to dioxygen is one of the most important reactions to study because of its implication in both new sustainable energy conversion schemes and environmental issues.[5] Recently, an important number of Ru complexes capable of oxidizing water to molecular oxygen have been reported in the literature.[6-8] All these complexes share a common feature, the active species that trigger the reactions that evolve dioxygen are constituted by a Ru-O group where the metal center is formally in a high oxidation state.

While the electronic structure of the lower oxidation states such as Ru^{II}-O or Ru^{III}-O are accurately understood, information regarding the higher oxidation states in their Ru^{IV}-O, Ru^{V}-O and Ru^{VI}-O counterparts are very scarce.[9] Paradoxically, the latter ones are of paramount importance since they are responsible for their performance as catalysts. The difficulty of characterizing higher oxidation states is due to the intrinsic

high reactivity of these species. In addition there are relatively few complexes where these high oxidation states can be reached and thus constitutes an additional handicap for comparative purposes. The precise characterization of higher oxidation states is of importance because it will render information regarding the degree of oxidation of the oxygen atom in the Ru-O group and also regarding the extent of covalency of the Ru-O bond.

The difficulty to characterize the electronic structure of the high oxidation states of Ru-O is in contrast with the relatively large amount of information available regarding first row transition homologues such as Cr, Mn or Fe.[10]

In the present study we have focused our attention on the characterization of higher oxidation state species derived from water oxidation catalyst[11] *cis*-$[Ru^{II}(bpy)_2(H_2O)_2]^{2+}$ (where *bpy* is the 2,2'-bypyridine bidentate ligand), (*cis*-$Ru^{II}(H_2O)_2$), by means of UV-vis, Electron Paramagnetic Resonance (EPR) and X-ray absorption spectroscopy (XAS) together with Density Funtional Teory (DFT) and Multiconfigurational Complete Active Space (CASSCF) calculations followed by second-order Perturbation Theory (CASPT2) calculations. We have further analyzed the *cis*- to *trans*- photoisomerization process suffered by *cis*-$Ru^{II}(H_2O)_2$ by means of Time-Dependent DFT (TD-DFT) methodologies.

4.3.3. Experimental Section

Materials. All reagents used in the present work were obtained from Aldrich Chemical Co with the highest purity commercially available and were used as received. High purity de-ionized water was obtained by passing distilled water through a nano-pure Mili-Q water purification system. Complex *cis*-$[Ru(bpy)_2CO_3]$ was prepared following literature procedures.[12]

Instrumentation and Measurements.

UV-vis Spectroscopy. Redox spectrophotometric titrations were performed by sequential addition of a 3×10^{-3} M $(NH_4)_2[Ce(NO_3)_6]$ (Ce^{IV}) in 0.1M CF_3SO_3H aqueous

solution at pH = 1.0 to a 0.1×10^{-3} M solution of *cis*-$Ru^{II}(H_2O)_2$ in the same media. The spectra were recorded at 25 °C in a 1.0 cm path length quartz cell on a VARIAN CARY 50-Bio.

Electron Paramagnetic Resonance. EPR spectra were recorded on a Bruker ELEXYS-E500 spectrometer equipped with a supers-EPR049 microwave bridge and an SHQ4122 rectangular resonator. Low temperature was reached by using an oxford 900 liquid helium cryostat and an ITC-503 temperature controller. EPR parameters: microwave frequency: 9.27 GHz; Modulation frequency: 100 kHz; modulation amplitude 10 G; temperature 6 K; microwave power 2.0 mW. UV-vis spectroscopy measurements were carried out with a CARY 50-Bio (VARIAN) or TIDAS using 1 cm quartz cells. EPR simulation was performed using Bruker XSophe-Xepr View software suit (v.1.1.4). Spin Hamiltonian;

$$\hat{H} = \mu_B \hat{B} \cdot g \cdot \hat{S} + \hat{S} \cdot A \cdot \hat{I}$$

was used for analysis, where spin-nuclear hyperfine coupling was introduced in addition to the Zeeman term. The g- and A- tensors were calculated using matrix diagonalization method. The simulated spectrum was obtained after iterative optimization. Samples were prepared in the same manner as for the UV-vis, transferred to an EPR tube and immediately frozen in liquid nitrogen.

X-ray Absorption Spectroscopy (XAS). XAS at the ruthenium K-edge was performed at the SuperXAS beamline at Swiss Light Source (SLS at Paul Scherrer Institute, Villigen, Switzerland) with the storage ring operated in top-up mode. Kα-fluorescence-detected XAS spectra were measured with an energy-resolving 13-element Ge-detector (Canberra, shielded by a 25 μm thick Mo-foil against scattered incident X-rays) on samples held in Teflon holders in a liquid-helium cryostat (Oxford) at 20 K, using excitation by X-rays from a double-crystal (Si311) monochromator (scan range 21.95-22.75 keV). Harmonics rejection was achieved by a platinum-covered toroidal mirror in grazing incidence mode. The beam was shaped by slits to a spot size on the sample of about 4x0.5 mm^2. Energy calibration of each scan was done using the peak at 22.117 keV in the first derivative of absorption spectra of a Ru–metal powder sample measured in parallel to the complexes. About 5-8 spectra of powder samples and 12-18 spectra of solution samples (one scan of ~20 min duration per sample spot)

were averaged, normalized, and EXAFS spectra were derived as described previously [13] EXAFS simulations were carried out using the software SimX[13] and phase functions calculated with FEFF8.[14] The absence of X-ray induced photoreduction of ruthenium in solution and powder samples was verified by measurements of XAS spectra on a single sample spot, which were identical after 1-3 scans. Samples were prepared in the same manner as in the UV-vis spectroscopy, transferred into Teflon buckets and immediately frozen in liquid nitrogen.

Computational details

Density Funtional Theory (DFT) Calculations. All molecular geometries were fully optimized with at the M06-L level of density functional theory (DFT)[15] using the Stuttgart ECP28MWB contracted pseudopotential basis set [8s7p6d2f | 6s5p3d2f] on Ru[16] and the 6-31G(d) basis set[17] on all other atoms. Full geometry optimizations were performed without imposing any symmetry constraint. Initial structures were taken from experiment, when available. Integral evaluation made use of the grid defined as "ultrafine" in the Gaussian series of programs. In addition, an automatically generated density-fitting basis set was used within the resolution of the identity approximation for the evaluation of Coulomb integrals. The nature of all stationary points was verified by analytic computation of vibrational frequencies, which were also used for the computation of molecular partition functions and 298 K thermal contributions to free energies, invoking the usual rigid rotator, harmonic oscillator, ideal-gas approximation. For singlet state DFT calculations, restricted self-consistent field solutions were obtained first, and then checked for restricted-to-unrestricted instabilities. When such instabilities were found, the Kohn-Sham (KS) wave functions were reoptimized with an unrestricted formalism. Spin purification involved the elimination of triplet-state spin contamination from broken-spin-symmetry KS determinants. Thus, the singlet energy is computed as:[18]

$$E_{Singlet} = \frac{2E_{(S_z)=0} - \langle S^2 \rangle E_{(S_z)=1}}{2 - \langle S^2 \rangle}$$

in which the triplet energy is computed for the single-determinantal high-spin configuration $S_z \sim 1$ (at the UDFT level) and $< S_2 >$ is the expectation value of the total spin operator applied to the KS determinant for the unrestricted broken-symmetry calculation.

For species *cis*-$Ru^{II}(OH_2)_2$, *trans*-$Ru^{II}(OH_2)_2$ and all intermediate species present in the isomerization process (all in oxidation state II) additional calculations in a continuum water solvent were performed. Free energies of aqueous solvation were computed at the SMD/M06-L[19] level based on the gas-phase geometries. A 1 M standard state was used for all species in aqueous solution except for water itself, for which a 55.5 M standard state was employed. Time-dependent DFT (TD-DFT) also at the same level of theory was employed to study the first excited singlet states of the compounds intervening in the isomerization process, including gas-phase geometry optimization. Thus, for all molecules but water, the free energy in solution is computed as the 1 atm gas-phase free energy, plus a 1 atm to 1 M concentration standard-state change of RT ln (24.5) or 8 kJ/mol, plus the 1 M to 1 M SMD solvation free energy. In the case of water, the 1 atm gas-phase free energy is adjusted by the sum of a 1 atm to 55.56 M concentration standard-state change of 17.9 kJ/mol and the experimental 1 M to 1 M solvation free energy, -26.4 kJ/mol.[20] For S_1 spin states gas phase thermal contributions were taken from the corresponding S_0 species.

Multiconfigurational Calculations. Multiconfigurational complete active space (CASSCF) calculations followed by second-order perturbation theory (CASPT2)[21] were performed at the DFT optimized geometries of *cis*-$[Ru^{VI}(bpy)_2(O)_2]^{2+}$ and *trans*-$[Ru^{VI}(bpy)_2(O)_2]^{2+}$ for both the S_0 and T_1 spin states. Scalar relativistic effects were included by use of the Douglas-Kroll-Hess Hamiltonian to second order[22] and the relativistic all-electron ANO-RCC basis sets[23] with triple-z quality (ANO- RCC-VTZP) with the [7s6p4d2f1g] contraction for Ru. The double-z quality (ANO- RCC-VDZP) with the following contractions: [3s2p1d] for O, C and N. The ANO-RCC-MB basis set was employed for H with a contraction of [1s]. Several active spaces were tested. For CASSCF/CASPT2 calculations, the chosen active space was fourteen electrons in eleven orbitals, corresponding to linear combinations of the 4d orbitals of Ru^{VI} (2 electrons) and the valence orbitals of both O atoms (12 electrons). Two virtual orbitals of the 13 orbitals that would be generated from all possible metal d and oxygen valence orbitals

had occupation numbers so near to zero that they were eliminated from the active space in production runs. All systems were found to be essentially single-configurational.

DFT computations were performed for compounds *cis*-$[Ru^{II}(bpy)_2(OH_2)_2]^{2+}$, *trans*-$[Ru^{II}(bpy)_2(OH_2)_2]^{2+}$ and their higher oxdation states with MN-GFM, [24] a locally modified version of Gaussian 03.[25] For all the species present in the photoisomerization process, the electronic structure program suite Gaussian 09[26] was used for all DFT and TD-DFT calculations. CASSCF/CASPT2 calculations were performed with the MOLCAS 7.5 program package.[27]

4.3.4. Results and discussion

The mononuclear complexes *cis*-$Ru^{II}(H_2O)_2$ and *trans*-$Ru^{II}(H_2O)_2$ were described by T. J. Meyer et al. and reported in 1988.[28] The complexes were thoroughly characterized by UV-vis spectroscopy and by Electrochemical techniques. The variation of the different redox potentials with pH, Pourbaix diagram, was also registered and allows to have a full thermodynamic characterization of the two complexes, including their degree of protonation at a given oxidation state and pH.

We have recently shown that the complex *cis*-$Ru^{II}(H_2O)_2$ acts as a water oxidation catalyst at pH = 1.0 in a triflic acid solution upon the addition of a strong oxidant such as Ce^{IV}.[11] It is therefore at this pH that we have carried out all the experiments described in the present work.

For *cis*-$Ru^{II}(H_2O)_2$ at pH = 1.0 a series of consecutive PCET steps take place when it is oxidized that are displayed in the following scheme,

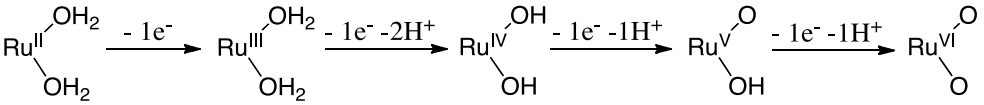

and therefore the present report will be mainly devoted to the electronic characterization of these species by means of UV-vis, EPR, XAS and by theoretical models such as DFT, CASPT2 and CASSCF.

Geometry and electronic structure of higher oxidation states. Calculations were performed with density functional theory (DFT) for the *cis*- and *trans*- isomers in formal oxidation states II to VI. In all cases, singlet and triplet electronic states were considered for species with an even number of electrons and doublet and quartet electronic states for species with an odd number of electrons. Additionally, single point calculations with multiconfigurational methods (CASSCF/CASPT2) were carried for the highest oxidation state (VI) at the optimized DFT structures. The computed relative energies are listed in Table 1 together with the abbreviated notation that will be further used in this work.

Table 1. Electronic states for the *trans* and *cis* isomers in the various oxidation states. $\Delta G_{trans\text{-}cis}$ includes the zero-point energy correction except for the CASSCF/CASPT2 values, which are only electronic energy differences.

Ox. State	Species	Abbreviations	Ground State (symmetry)	Lowest excited state (kcal·mol^{-1})	$\Delta G_{trans\text{-}cis}$ (kcal/mol)
II	*cis*-[Ru (bpy)$_2$(H$_2$O)$_2$]$^{2+}$	*cis*-Ru^{II}(OH$_2$)$_2$	S$_0$ (^{1}A)	----	15,59
	trans-[Ru (bpy)$_2$(H$_2$O)$_2$]$^{2+}$	*trans*-Ru^{II}(OH$_2$)$_2$	S$_0$ (^{1}A)	----	
III	*cis*-[Ru(bpy)$_2$(H$_2$O)$_2$]$^{3+}$	*cis*-Ru^{III}(OH$_2$)$_2$	D$_0$ (^{2}A)	Q$_1$ (^{4}A) 27.21	13,26
	trans-[Ru(bpy)$_2$(H$_2$O)$_2$]$^{3+}$	*trans*-Ru^{III}(OH$_2$)$_2$	D$_0$ (^{2}A)	Q$_1$ (^{4}A) 11.36	
IV	*cis*-[Ru(bpy)$_2$(OH)$_2$]$^{2+}$	*cis*-Ru^{IV}(OH)$_2$	S$_0$ (^{1}A)	T$_1$ (^{3}A) 2.83	9,24
	trans-[Ru(bpy)$_2$(OH$_2$)(O)]$^{2+}$	*trans*–Ru^{IV}(OH$_2$)(O)	T$_0$ (^{3}A)	S$_1$ (^{1}A) 14.31	
V	*cis*-[Ru(bpy)$_2$(OH)(O)]$^{2+}$	*cis*-Ru^{V}(OH)(O)	D$_0$ (^{2}A)	Q$_1$ (^{4}A) 12.74	13,82
	trans-[Ru(bpy)$_2$(OH)(O)]$^{2+}$	*trans*-Ru^{V}(OH)(O)	D$_0$ (^{2}A)	Q$_1$ (^{4}A) 24.36	
VI	*cis*-[Ru(bpy)$_2$(O)$_2$]$^{2+}$	*cis* –Ru^{VI}(O)$_2$	S$_0$ (^{1}A)	T$_1$ (^{3}A) 3.81 7.78/2.95 [a]	8.80
	trans-[Ru(bpy)$_2$(O)$_2$]$^{2+}$	*trans* –Ru^{VI}(O)$_2$	S$_0$ (u) (^{1}A)	T$_1$ (^{3}A) 34.73 43.49/39.60 [a]	6.71/4.77 [a]

[a] CASSCF/CASPT2 electronic energy differences.

As expected from experimental data, in oxidation state II the *cis* isomer is found to be thermodynamically the most stable isomer. This feature is maintained for all oxidation states in which the *cis* isomer is more stable than the *trans* isomer by at least 8 kcal·mol^{-1}. The general trend manifests a decrease of relative stability of the *cis* isomer as the oxidation state increases. In all cases the lowest spin state is the most stable, except for the *trans* species in oxidation state IV as will be further discussed below.

Selected bond distances and angles of the ground state optimized structures for the *cis* and *trans* isomers at the different oxidation states as well as the corresponding data from the available X-ray structures are presented in Table 2.

Table 2. Selected bond distances (Å) and angles (o) for *cis*- and *trans*-[Ru^{II}(bpy)$_2$(H$_2$O)$_2$]$^{2+}$ and their corresponding higher oxidation state species calculated by means of DFT. In bold, data corresponding to the X-Ray crystal structure of *cis*-[29] and *trans*-[Ru^{II}(bpy)$_2$(H$_2$O)$_2$]$^{2+}$.[30] See Supp. Inf. for atom labeling.

Ox. state	isomer	S	Ru-O1	Ru-O2	O-Ru-O	N1-N2-N3-N4[a]	Ru-N1	Ru-N2	Ru-N3	Ru-N4
II	*cis*-Ru^{II}(OH$_2$)$_2$	S_0	2.226	2.226	82.9	91.5	2.024	2.075	2.075	2.024
II	***cis*-Ru^{II}(OH$_2$)$_2$**	--	**2.151**	**2.147**	**86.7**	**92.1**	**2.005**	**2.070**	**2.053**	**2.001**
III	*cis*-Ru^{III}(OH$_2$)$_2$	D_0	2.176	2.201	83.5	87.5	2.027	2.095	2.094	2.031
IV	*cis*-Ru^{IV}(OH)$_2$	S_0	1.869	1.869	110.8	76.8	2.121	2.093	2.093	2.121
V	*cis*-Ru^{V}(OH)(O)	D_0	1.696	1.881	111.2	79.2	2.138	2.086	2.123	2.204
VI	*cis* -Ru^{VI}(O)$_2$	S_0	1.688	1.688	124.5	75.0	2.218	2.115	2.114	2.218
II	*trans*-Ru^{II}(OH$_2$)$_2$	S_0	2.165	2.166	176.4	154.9	2.129	2.083	2.131	2.082
II	***trans*-Ru^{II}(OH$_2$)$_2$**	--	**2.105**	**2.105**	**180.0**	**180.0**	**2.074**	**2.074**	**2.073**	**2.074**
III	*trans*-Ru^{III}(OH$_2$)$_2$	D_0	2.081	2.081	175.0	154.5	2.123	2.110	2.122	2.110
III	***trans*-Ru^{III}(OH$_2$)$_2$**	--	**2.008**	**2.006**	**178.4**	**156.5**	**2.099**	**2.090**	**2.099**	**2.090**
IV	*trans*-Ru^{IV}(H$_2$O)(O)	T_0	1.738	2.305	178.3	153.1	2.120	2.124	2.116	2.133
V	*trans*-Ru^{V}(OH)(O)	D_0	1.922	1.715	177.8	154.1	2.127	2.126	2.148	2.125
VI	*trans*-Ru^{VI}(O)$_2$	S_0	1.713	1.713	180.0	155.9	2.151	2.151	2.151	2.151

[a]Dihedral angle between the N atoms of the two bipyridines passing through the Ru atom.

In general the Ru-O bond distances for the *trans* species are significantly shorter than in the corresponding *cis* isomers. Additionally, a significant decrease in the Ru-O bond is observed as the oxidation state increases, indicating an increase in Ru-O bond order. This trend is consistent with the experimental distances extracted form the X-ray structures (Table 2).

In oxidation state II the triplet state decoordinates a water molecule in both the *cis* and *trans* complexes, which is the responsible of the photoisomerization experienced by this species (*see below*).

In formal oxidation state IV, the structures of the two possible species $Ru^{IV}(OH)_2$ vs $Ru^{IV}(OH_2)(O)$ have been optimized for both the *cis* and *trans* isomers (see Supp. Inf.). Whereas for the *cis* isomer $Ru^{IV}(OH)_2$ is more stable than $Ru^{IV}(OH_2)(O)$ (by 0.6 kcal/mol) differently from what was predicted by T. J. Meyer,[28] for the *trans* isomer the "aqua-oxo" species is more stable (by 1.4 kcal/mol). Moreover, for the *trans*-$Ru^{IV}(OH_2)(O)$ species the ground state is a T_0 (^3A) state, unlike in all other cases, where the ground state is always the lowest spin state. Additionally, the *cis*-$Ru^{IV}(OH)_2$ present longer distances for the Ru-N bonds in which the N coordination site of the *bpy* ligands are trans to the O atoms than those observed in the Ru-N bonds in which the N is trans to the N atom of the other *bpy* ligand.

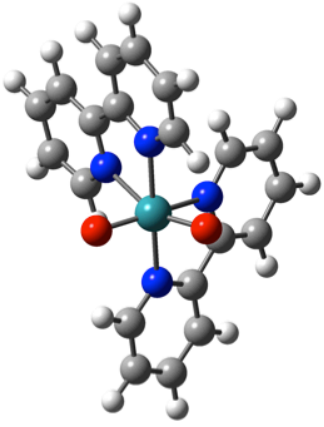

Figure 1. DFT calculated structure for *cis*-$[Ru^{VI}(bpy)_2(O)_2]^{2+}$. Color codes: Ru, green; N, blue, O, red; C, gray; H, white.

Finally, as can be seen in Table 2, as the oxidation state increases in the *cis* isomer, the O-Ru-O angle also increases (from 83º in oxidation state II to 124º in oxidation state VI) which could be the origin of the previously demonstrated very unfavourable intramolecular O-O bond formation for the *cis*-$[Ru^{VI}(bpy)_2(O)_2]^{2+}$ active species of this water oxidation catalytic system, which's DFT-optimized structure is shown in Figure 1.

UV-vis and EPR spectroscopy. The UV-vis spectra of complexes *cis*-$Ru^{II}(H_2O)_2$, *cis*-$Ru^{III}(H_2O)_2$, *cis*-$Ru^{IV}(OH)_2$ and *cis*-$Ru^{V}(O)(OH)$ are reported in Figure 2. All the species were generated in situ by adding the corresponding amount of Ce^{IV} in the absence of light, to avoid the *cis* → *trans* isomerization reaction. For *cis*-$Ru^{II}(H_2O)_2$, the spectra presents mainly two regions below 300 nm where *bpy* based π-π* transitions are observed and above 300 nm where MLCT and d-d bands occurs. At the oxidation state II the *cis* isomer presents mainly two MLCT bands centered at 350 and 490 nm respectively and a shoulder at 575 nm that can be assigned to a d-d band. At oxidation state III the spectra changes radically, the largest MLCT at 490 basically disappears and two low intensity bands are observed at 350 and 550 nm. For oxidations states IV and V are characteristic because of the absence of MLCT and d-d bands.

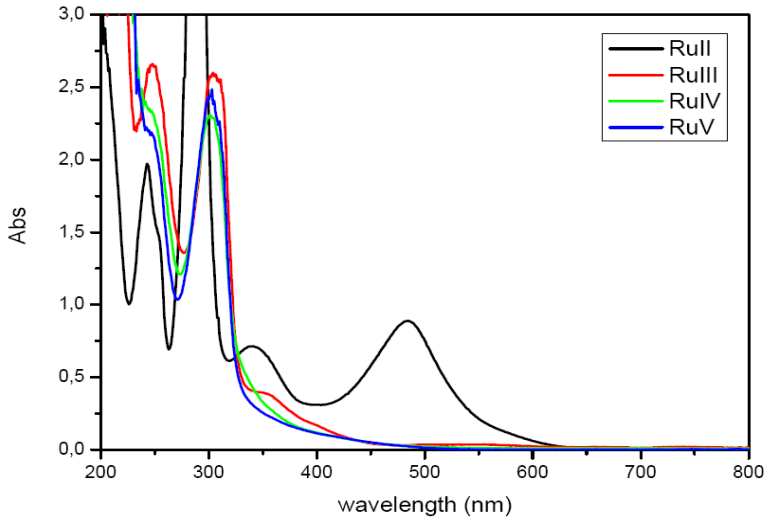

Figure 2. UV-vis spectra for *cis*-$[Ru^{II}(bpy)_2(H_2O)_2]^{2+}$ (0.1×10^{-3} M) at pH = 1.0 trilfic acid aqueous solution and its corresponding higher oxidation state species.

The EPR spectra of complexes *cis*-$Ru^{III}(H_2O)_2$, *trans*-$Ru^{III}(H_2O)_2$ and *cis*-$Ru^{V}(O)(OH)$ are depicted in Figure 3. The complexes *cis*-$Ru^{II}(H_2O)_2$ and *cis*-$Ru^{IV}(OH)_2$ were EPR silent, indicating that the Ru center in both complexes is in the low spin configuration, resulting in a diamagnetic ground state in both complexes. This is in good agreement with the DFT calculated result (*vide supra*).

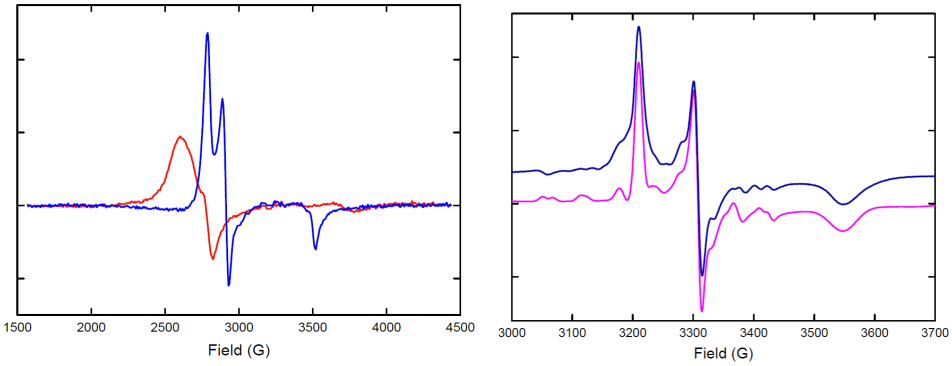

Figure 3. Left, EPR spectra of complexes *cis*-$Ru^{III}(H_2O)_2$ (red) and *trans*-$Ru^{III}(H_2O)_2$ (blue). Right, The experimental (dark blue) and the simulated (pink) EPR spectra of the complex *cis*-$Ru^{V}(O)(OH)$. Simulation parameters: g_x = 2.065, g_y = 2.004, g_z = 1.868, and A_x = 54.3, A_y = 40.2 and A_z = 39.3×10^{-4} cm^{-1}. EPR recording conditions see experimental section.

The EPR spectra of complexes *cis*-$Ru^{III}(H_2O)_2$ and *trans*-$Ru^{III}(H_2O)_2$ (Figure 3 left, red and blue respectively) show spectral features characteristic for a spin S=1/2 in a rhombic symmetry, indicating that also in this oxidation state low spin is the more stable configuration, as DFT suggested. The anisotropic g-values, arbitrarily denoted as g_1, g_2 and g_3, for the *cis*-$Ru^{III}(H_2O)_2$ complex are 2.55, 2.40 and 1.75 respectively; and for the *trans*-$Ru^{III}(H_2O)_2$ are 2.38, 2.27 and 1.88 respectively. It is observed that the anisotropy (measured by the largest Δg) in the *cis*-conformation is 0.8 which is significantly larger than Δg = 0.5 measured in the trans-conformation. Moreover, the line-width in the EPR spectrum of the *cis*-$Ru^{III}(H_2O)_2$ complex (Figure 3, left, red) is much broader than that of the *trans*-$Ru^{III}(H_2O)_2$ (Figure 3, left, blue). The larger spin anisotropy and the broad line-width in the *cis*-form are attributed to the larger ligand conformational strain, probably is related to the O-Ru-O bond strain.

Oxidation of the *cis*-$Ru^{III}(H_2O)_2$ complex by two equivalents Ce^{IV} resulted in the formation the *cis*-$Ru^{V}(O)(OH)$ complex. The recorded EPR spectrum for the *cis*-$Ru^{V}(O)$

(OH) complex is shown in Figure 3 (right, blue). In this complex, the Ru^{V} center is a d^3 ion, both low spin (S = 1/2) and high spin (S = 3/2) configurations are possible.

To assert the ground spin state of this complex, EPR simulations assuming either an S = 3/2 or S = 1/2 ground state have been performed using spin Hamiltonian $\hat{H} = \mu_B \hat{B} \cdot g \cdot \hat{S} + \hat{S} \cdot A \cdot \hat{I}$.

Whereas no success in simulation when S=3/2 was taken, a relatively good agreement between the simulated and the experimental spectra (Figure 3, right; pink and blue spectrum respectively) was achieved when S = 1/2 was taken as the ground spin state. The calculated EPR spectrum is obtained by using a set of anisotropic EPR parameters with $g_x = 2.065$, $g_y = 2.004$, $g_z = 1.868$, and $A_x = 54.3$, $A_y = 40.2$ and $A_z = 39.3 \times 10^{-4}$ cm^{-1}. It is quite unexpected for a d^3 ion with an S = 1/2 as the ground spin state. On the other hand, it is in good agreement with DFT calculation, which suggests that the low spin (doublet) state is more stable by 14 kcal/mol than the high spin (quartet) state.

Despite the extensive data available in the literature on EPR of Ru^{III} complexes, examples with Ru^{V} are very scarce.[31] The g values for *cis*-$Ru^{V}(O)(OH)$ are closer to those of $[Ru^{V}O(O_2COEt_2)_2](nPr_4N)$ ($g_x = 2.076$, $g_y = 1.977$, $g_z = 1.910$)[32] than those of *cis*-$Ru^{III}(H_2O)_2$ and other Ru^{III} species found in the literature[33] which further sustains the oxidation state V of *cis*-$Ru^{V}(O)(OH)$.

XAS spectroscopy. XAS measurements were carried out to derive experimental information on the electronic structure of Ru-O type complexes in their higher oxidation states. For this purpose, the complexes *cis*-$Ru^{IV}(OH)_2$ and *cis*-$Ru^{V}(O)(OH)$ (1 mM) were prepared in aqueous solution containing 0.1 M triflic acid by adding two and three equivalents of Ce^{IV}, respectively.

A in Figure 4 shows the X-ray absorption near edge structure (XANES) spectra obtained for *cis*-$Ru^{IV}(OH)_2$ and *cis*-$Ru^{V}(OH)(O)$ complexes together with their first derivatives and isolated pre-edge features due to 1s → 4d electronic transitions in the insets. B in Figure 4 presents a graph of the Ru K-edge energies (at 50 % level of spectra) versus the ruthenium oxidation state for our complexes and representative literature data and the respective pre-edge peak areas in the inset. The edge shapes of *cis*-$Ru^{IV}(OH)_2$ and *cis*-$Ru^{V}(OH)(O)$ complexes were rather similar, indicating that only

minor structural changes in the first ruthenium coordination sphere occurred upon the oxidation.

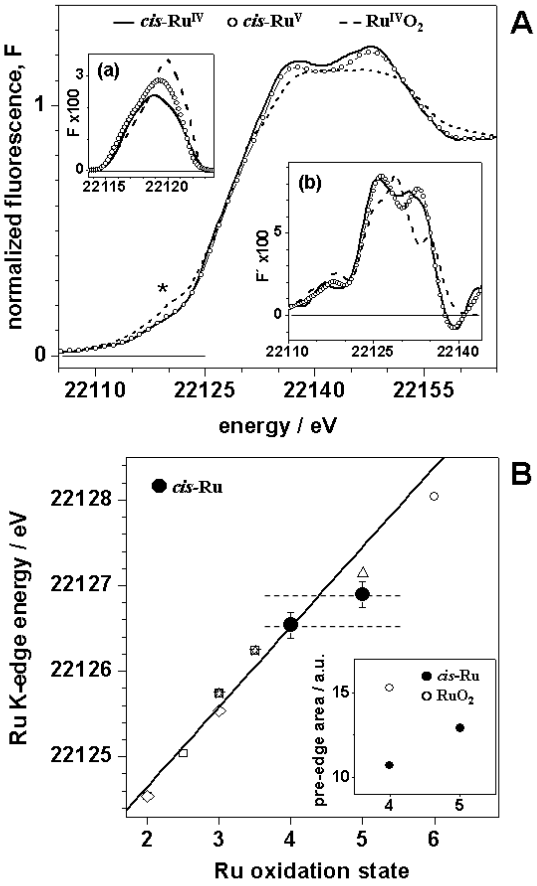

Figure 4. (A) Ruthenium K-edge spectra of *cis*-Ru complexes. The spectrum of $Ru^{IV}O_2$ is shown for comparison. *Pre-edge feature due to 1s → 4d electronic transitions. Inset (a): Extracted pre-edge peak features of spectra. Inset (b): First derivatives of K-edge spectra. (B) K-edge energies of *cis*-Ru complexes and literature data versus metal oxidation state. K-edge energies correspond to values at 50 % levels of edge rise. Literature values (open symbols) were derived from K-edge spectra of complexes in refs. [34] and normalized to the value for *cis*-$Ru^{IV}(OH)_2$. The regression line is for ruthenium II, III, and IV complexes and has a slope of 1.04 eV per Ru oxidation state. Dashed lines mark the energy difference for *cis*-$Ru^{IV}(OH)_2$ and *cis*-$Ru^{V}(OH)(O)$. Inset: pre-edge peak areas of cis-Ru (solid circles) and RuO_2 (open circle) derived from spectra in (A).

Literature complexes showed that when Ru is oxidized from II to IV the K-edge energies increases rather linearly and by close to 1.0 eV on each metal-centered oxidation step (Figure 4, B). This notion takes into account the limited accuracy of the edge energy determination, which is on the order of ± 0.15 eV, and edge shape changes due to the various Ru coordinations in the complexes, which slightly affect the apparent edge energy.[35] Smaller edge shifts were observed for higher Ru oxidation levels. A smaller edge energy increase was expected for an enhancement in covalent character of the ruthenium-ligand bonds and in the particular case of the Ru-O bond, for partial oxidation of the oxygen atom. As an example, in the case of Ru-oxo formally in oxidation state V, two resonance forms can be formulated.

$$Ru^{V}=O \leftrightarrow Ru^{IV}\text{-}O\cdot \qquad (2)$$

The K-edge energy for the complex *cis*-$Ru^{IV}(OH)_2$ was close to that typical for the Ru^{IV} level, i.e. as exemplified by RuO_2. However, for *cis*-$Ru^{V}(OH)(O)$ the edge energy increased by only ~0.35 eV with respect to *cis*-$Ru^{IV}(OH)_2$ (Figure 4, B). This was suggestive of the resonance phenomenon explained above (2), meaning that the larger fraction of about 65 % of the *cis*-$Ru^{V}(OH)(O)$ complex in solution rather showed a Ru^{IV}-O· motif and only the remainder a Ru^{V}=O bond. However, the pre-edge peak area (Figure 4, B) considerably increased from *cis*-$Ru^{IV}(OH)_2$ to *cis*-$Ru^{V}(OH)(O)$, but was smaller than for RuO_2, indicating a significantly higher double bond character of the ruthenium-oxygen bond in *cis*-$Ru^{V}(OH)(O)$. This was in agreement with the DFT analysis, which suggested for the *cis*-$Ru^{IV}(OH)_2$ a HO-Ru^{IV}-OH and for *cis*-$Ru^{V}(OH)(O)$ a O =Ru^{V}-OH configuration.

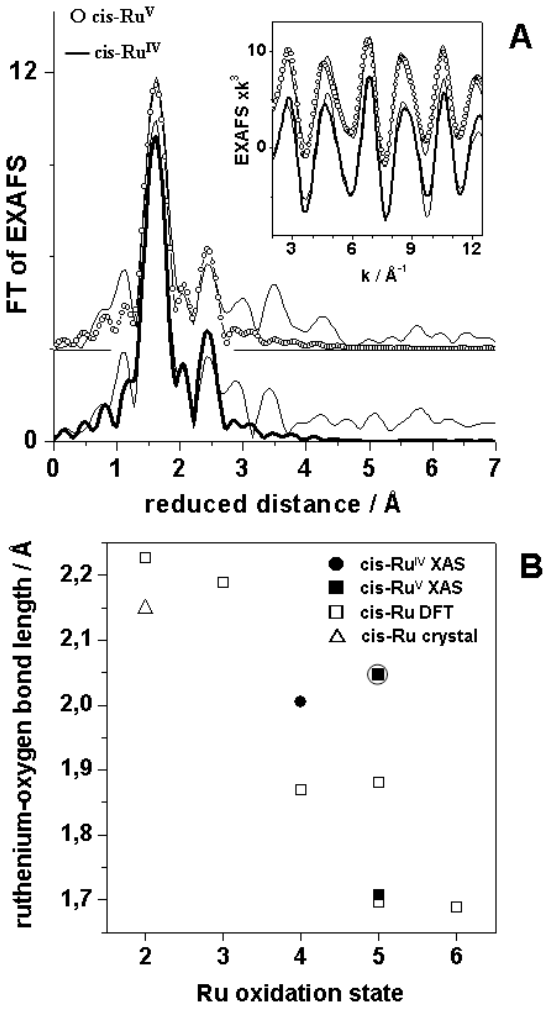

Figure 5. (A) Fourier-transforms (FTs) of EXAFS spectra of *cis*-Ru complexes. FTs were calculated for k-values of 2-12.5 $Å^{-1}$ and using cos^2 windows extending over 10 % at both k-range ends. Inset: Fourier-filtered EXAFS data corresponding to backtransforms of FT spectra in a range of 1-3 Å of reduced distance. Solid lines and open circles, simulations with parameters in Table 3 (fits a and d); thin black lines, experimental spectra. FT and k-space spectra were vertically displaced for comparison. (B) Ruthenium-oxygen bond lengths versus the ruthenium oxidation state from XAS, DFT, and crystallography. The circle marks the distance from XAS attributed to a Ru-OH bond in the *cis*-Ru^V(OH)(O) sample (Table 3).

EXAFS analysis was carried out for the *cis*-$Ru^{IV}(OH)_2$ and *cis*-$Ru^{V}(OH)(O)$ complexes (Figure 2, A) to derive precise bond lengths in the solution samples. The EXAFS spectra were well described by the inclusion of first-sphere ruthenium-oxygen and nitrogen and second-sphere ruthenium-carbon distances in the simulations. Inclusion of longer interatomic distances did not alter the results for the first sphere (not shown). The determined bond lengths are reported in Table 3. With increasing metal oxidation state and increasing deprotonation of bound oxygen species a shortening of ruthenium-oxygen bonds was observed, as expected.

Table 3. Ruthenium-ligand distances in *cis*-Ru complexes from EXAFS analysis.

		N [per Ru] / *R* [Å] / $2\sigma^2$ x10^3 [$Å^{-1}$]				
	fit	Ru=O	Ru-O	Ru-N	Ru-C	R_F [%]
cis-$Ru^{IV}(OH)_2$	a	-	2 / 2.005 / 2	4 / 2.073 / 2	8 / 2.963 / 8	21.1
	b	0.11* / 1.698 / 2	1.89* / 2.005 / 2	4 / 2.072 / 2	8 / 2.963 / 8	20.1
cis-$Ru^{V}(OH)(O)$	c	-	2 / 2.002 / 2	4 / 2.095 / 2	8 / 2.968 / 11	26.3
	d	0.36* / 1.710 / 2	1.64* / 2.046 / 2	4 / 2.074 / 6	8 / 2.972 / 10	22.2

N, coordination number; R, metal-ligand distance; $2\sigma^2$, Debye-Waller parameter; RF, error sum calculated over reduced distances of Fourier-transforms of 1-3 Å. Coordination numbers were fixed at their chemical values in the simulations except for (*), values coupled to yield a sum of 1 (*cis*-$Ru^{IV}(OH)_2$ or *cis*-$Ru^{V}(OH)(O)$) in the simulations. $2\sigma^2$ of the Ru-oxygen bonds was fixed in the simulations.

In the *cis*-$Ru^{IV}(OH)_2$ sample, short ruthenium-oxygen distances of ~1.7 Å due to a Ru=O bond were barely detectable and both Ru-O bonds therefore were of similar lengths. For *cis*-$Ru^{V}(OH)(O)$ a similar ratio of about 35 % and 65 % of Ru^{V}=O and Ru^{IV}-O· forms as concluded from the XANES data was observed. For the *cis*-$Ru^{IV}(OH)_2$ and *cis*-$Ru^{V}(OH)(O)$ complexes, bond lengths for Ru-OH (~1.9 Å) and Ru=O (~1.7 Å) motifs were in good agreement with respective values from the DFT calculations (Figure 5, B). The ruthenium-oxyl distance tentatively attributed in the EXAFS simulations appeared to be by about 0.3-0.4 Å longer for a *cis*-Ru^{IV}-O· species compared to *cis*-Ru^{V}=O (Figure 5, B).

DFT Analysis of the *cis/trans* Isomerization Process. In the presence of light the *cis*-$[Ru^{II}(H_2O)_2]^{2+}$ complex isomerizes to the corresponding *trans*, as shown in the following equation for the complex in oxidation state II.

cis-$[Ru^{II}(H_2O)_2]^{2+} \rightarrow$ *trans*-$[Ru^{II}(H_2O)_2]^{2+}$ (3)

It is also known that isomerization takes place at oxidation state III but no information is available for the corresponding species with oxidation states IV, V and VI. As has been previously discussed a spectroscopic study and a DFT analysis have been carried out aimed at understanding the electronic structure of *cis*-$Ru(H_2O)_2$ and the corresponding species in higher oxidation states together with their *trans* analogues. Further, a detailed study of the photoisomerization process for oxidation state II has been carried out at the time-dependent density functional (TD-DFT) level of theory. We propose a mechanism in which upon light irradiation of the "cis-bisaquo" complex *cis*-$[Ru^{II}(bpy)_2(H_2O)_2]^{2+}$ a photodissociation step leads to an aquo ligand loss and a species we will call "cis-mono-aquo", referring to the relative disposition of the remaining aquo ligand with the vacant coordination position. Following, this species undergoes ligand reorganization to a "trans-monoaquo" species and, finally, the recoordination of an aquo ligand yields the "trans-bisaquo" complex *trans*-$[Ru^{II}(bpy)_2(H_2O)_2]^{2+}$ as represented in Top of Figure 6. The relative energies of all species for different spin states are summarized in Table 4 and the relative energies of the species involved in the process are reported in Figure 6.

Table 4. Free energy in kcal/mol for the different species intervening in the photoisomerization process from the *cis*-$Ru^{II}(OH_2)$ to the *trans*-$Ru^{II}(OH_2)$ isomers. Energies of the Ru^{II} species which geometry has been optimized are accompanied by the energies for the other spin states considered for the study of vertical excitations computed retaining the geometry. All energies are reported with respect to *cis*-$Ru^{II}(H_2O)_2$-S_0 (**C**-S_0 in Figure 6) as 0 energy reference species.

Species of the Optimized Geometry (Corresponding notation in Figure 6)	spin state	G (kcal·mol^{-1})
cis-$Ru^{II}(H_2O)_2$-S_0 (**C**-S_0)	S_0	0.00
	S_1	44.58
	T_1	39.41
cis-$Ru^{II}(H_2O)_2$-S_1 (**C**-S_1)	S_1	40.83
	S_0	5.82
cis-$Ru^{II}(H_2O)$-S_0 (**c**-S_0)	S_0	9.29
	S_1	53.46
cis-$Ru^{II}(H_2O)$-T_1 (**c**-T_1)	T_1	24.18
TS-$Ru^{II}(H_2O)$-T_1 (**TS**-T_1)	T_1	28.46
trans-Ru^{II} (H_2O)-T_1 (**t**-T_1)	T_1	21.84
trans-$Ru^{II}(H_2O)$-S_0 (**t**-S_0)	S_0	25.46
	S_1	32.88
trans-$Ru^{II}(H_2O)_2$-S_0 (**T**-S_0)	S_0	12.27
	S_1	50.65
trans-$Ru^{II}(H_2O)_2$-S_1 (**T**-S_1)	S_1	47.25
	S_0	19.64

When optimizing T_1 geometries for the "*cis*-bisaquo" complex, as described earlier, one aquo ligand is decoordinated leading to a "mono-aquo" species and a free water molecule. This indicates that the *cis/trans* photochemical isomerization of $[Ru^{II}(bpy)_2(H_2O)_2]^{2+}$ compound is likely to start by intersystem crossing form the S_1 photoexcited state (**C**-S_1 in Figure 6) to the T_1 spin state (**C**-T_1 in Figure 6) of the *cis*-$Ru^{II}(H_2O)_2$ bisaquo compound. Upon relaxation, this *cis*-$Ru^{II}(H_2O)_2$-T_1 bisaquo species suffers decoordination of an aquo ligand leading to the *cis*-$Ru^{II}(H_2O)$-T_1 mono-aquo species (**c**-T_1 in Figure 6) and a free water molecule. The optimization of isolated "mono-aquo"

intermediate species in the gas phase retains the octahedral coordination typical of Ru d6 complexes with one coordination site remaining vacant. Therefore it is important to consider both, the *cis*- and *trans*-$Ru^{II}(H_2O)$ monoaquo intermediates.

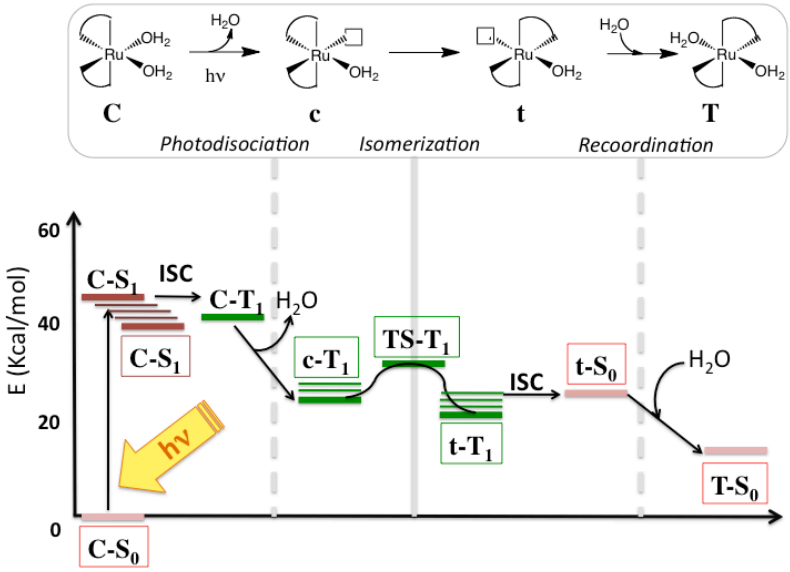

Figure 6. Energy diagram (TD DFT) of the isomerization process. For each set of structures in a vertical stack, a box indicates the singlet state for which the geometry was optimized, and the second singlet-state energy is for a single-point calculation at that same geometry. Triplet state energies for mono-aquo species are shown for separately optimized structures. In the central structures, a vacant coordination site is indicated to forward right in the line structures.

The isomerization step, which involves the reorganization of the bpy ligands around the metal center, would then occur from the *cis*-$Ru^{II}(H_2O)$-T_1 (**c**-T_1 in Figure 6) to the *trans*-$Ru^{II}(H_2O)$-T_0 mono-aqua species (**t**-T_0 in Figure 6), in the triplet state. We have localized and optimized the transition state of this isomerization presenting a ΔG barrier over 4 kcal·mol^{-1}. This transition state is closer, both energetically and by geometry, to the *cis*-$Ru^{II}(H_2O)$-T_1 species.

Finally, since the *trans*-$Ru^{II}(H_2O)$ species has as ground state triplet really close in energy to the corresponding S_1 spin state(**t**-S_1 in Figure 6), the next step should be a second intersystem crossing, after which point coordination of water would complete the mechanism yielding the *trans*-$Ru^{II}(H_2O)_2$-S_0 (**T**-S_0 in Figure 6).

4.3.5. Conclusions

The electronic structure of *cis*-$[Ru^{II}(bpy)_2(H_2O)_2]^{2+}$ and their higher oxidation states species have been studied by means of UV-vis, EPR, XAS and DFT calculations. EPR spectroscopy together with DFT show that in all cases lower spin configurations are favored and thus oxidation state (IV) is a singlet, EPR silent at low temperature. For oxidation state V, DFT calculations propose a doublet in very good agreement with EPR that can be nicely simulated as S=1/2. XAS spectroscopy of higher oxidation state species together with DFT allowed to understand the electronic structure of these complexes and in particular the decrease of Ru-O bond distances as oxidation state increases together with an enhancement of the double bond character of the O-Ru-O unit. Finally, the photochemical isomerization of the *cis* → *trans* complex at oxidation state II has been fully characterized by DFT methodologies and show that the process involves the decoordiantion of one aqua ligand leading to a coordinatively unsaturated complex that isomerizes and recoordinates the aqua ligand, to finally yield the trans isomer.

4.3.6. Acknowledgements

Support form SOLAR-H2 (EU 212508), MICINN (CTQ2010-21497 and Consolider Ingenio CSD2006-0003) and from Generalitat de Catalunya (CIRIT/2009 SGR 69) are gratefully acknowledged. NP is grateful for a MICINN doctoral grant. M.H. thanks the Deutsche Forschungsgemeinschaft for a Heisenberg-Fellowship and for funding (grant Ha3265/3-1). We thank Dr. Maarten Nachtegaal at SuperXAS beamline of SLS for excellent technical support.

The synthesis and UV-vis spectroscopy was carried out by Laura Vigara as a post-doc in Prof. Llobet's Group, EPR characterization was carried out by Ping Huan and Clyde Cady in Prof. Leif Hammarstrom and Prof. Stenbjorn Styring groups, EXAFS measurements were carried out by Nils Leidel and Michael Haumann.

4.3.7. References

[1] (a) Lappin, A. G.; Marusak, R. A. *Coord. Chem. Rev.* **1991**, *109*, 125-180. (b) Griffith. W. P. *Chem. Soc. Rev.* **1992**, *21*, 179-185. (c) Wing-Sze Hui, J.; Wong, W-T. *Coord. Chem. Rev.* **1998**, *172*, 389-436. (d) Clarke, M. J. *Coord. Chem. Rev.* **2002**, *232*, 69-93. (e) Meyer, T. J.; Huynh, M. H. V. *Inorg. Chem.* **2003**, *42*, 8140-8169.

[2] (a) Balzani, V.; Juris, A. *Coord. Chem. Rev.* **2001**, *211*, 97-115. (b) Coudret, C.; Balzani, V.; Barigelletti, F.; De Cola, L.; Fannigni, L. *Chem. Rev.* **1994**, *94*, 993–1019. (c) Meyer, T. J. *Acc. Chem. Res.* **1989**, *22*, 163.

[3] (a) Kelley, S. O.; Barton, J.K. *Science* **1999**, 238, 375. (b) Hall, D. B.; Holmlin, R. E.; Barton, J. K. *Nature* **1996**, 384, 731. (c) Burrows, C.J.; Muller, J.G. *Chem. Rev.* **1998**, 98, 1109. (d) Weatherly, S.C.; Yang, I.V.; Thorp, H.H. *J. Am. Chem. Soc.* **2001**, 123, 1236.

[4] (a) Murahashi, S. I.; Takaya, H.; Naota, T. *Pure Appl. Chem.* **2002**, *74*, 19-24. (b) Naota, T.; Takaya, H.; Murahashi, S.-I. *Chem. Rev.* **1998**, *98*, 2599-2660. (c) Rodríguez, M.; Romero, I.; Llobet, A.; Deronzier, A.; Biner, M.; Parella, T.; Stoeckli-Evans, H. *Inorg. Chem.* **2001**, *40*, 4150-4156. (d) Jauregui-Haza, U. J.; Dessoudeix, M.; Kalck, Ph.; Wilhelm, A. M.; Delmas, H. *Catal. Today* **2001**, *66*, 297-302.

[5] Benniston, A. C.; Harriman, A. *Materials Today*, **2008**, *11*, 26-34.

[6] (a) Sala, X.; Rodriguez, M.; Romero, I.; Escriche, L.; Llobet, A. *Angew. Chem. Int. Ed.* **2009**, *48*, 2842. (b) Romain, S.; Vigara, L.; Llobet, A. *Acc. Chem. Res.* **2009**, *42*, 1944-1953. (c) Sartorel, A.; Miró, A.; Salvadori, E.; Romain, S.; Carraro, M.; Scorrano, G.; Di Valentin, M.; Llobet, A.; Bo, C.; Bonchio, M. *J. Am. Chem. Soc.* **2009**, *131*, 1651-1653. (d) A. Sartorel, M. Carraro, G. Scorrano, R. De Zorzi, S.Geremia, N. D. McDaniel, S. Bernhard, M. Bonchio, *J. Am.Chem. Soc.* **2008**, *130*, 5006. (e) Puntoriero, F.; La Ganga, G.; Sartorel, A.;Carraro, M.; Scorrano, G.; Bonchio, M.; Campagna, S. *Chem. Commun.* **2010**, *46*, 4725-4727. (f) Geletii, Y. V.; Botar, B.; Koegler, P.; Hillesheim, D. A.; Musaev, D. G.; Hill, C. L., *Angew. Chem. Int. Ed.* **2008**, *47*, 3896–3899. (g) Geletii, Y. V.; Huang, Z.; Hou, Y.; Musaev, D. G.; Lian, T.; Hill, C. L., *J. Am. Chem. Soc.*, **2009**, *131*, 7522-7523.

[7] (a) Gilbert, J. A.; Eggleston, D. S.; Murphy, W. R.; Geselowitz, D. A.; Gersten, S. W.; Hodgson, D. J.; Meyer, T. J., *J. Am. Chem. Soc.* **1985**, *107*, 3855–3864. (b) Concepcion, J.¸ Jurss, J. W. ; Templeton, J. L.; Meyer, T. J.*, J. Am. Chem. Soc.* **2008**, *130*, 16462-16463. (c) Zhang, G.; Zong, R., Tseng, H. W.; Thummel, R. P., *Inorg. Chem.* **2008**, *47*, 990-998.

[8] (a) Alstrum-Acevedo, J. H.; Brennaman, M. K.; Meyer, T. J. *Inorg. Chem.*, **2005**, *44*, 6802-6827. (b) Magnuson, A.; Anderlund, M.; Johansson, O.; Lindblad, P.; Lomoth, R.; Polivka, T.; Ott, S.; Stensjo, K.; Styring, S.; Sundstrom, V.; Hammarstrom, L. *Acc. Chem. Res.* **2009**, *42*, 1899-1909. (c) Concepcion, J. J.; Jurss, J. W.; Brennaman, M. K.; Hoertz, P. G.; Patrocinio, A. O. T.; Iha, N. Y. M.; Templeton, J. L.; Meyer, T. J. *Acc. Chem. Res.* **2009**, *42*, 1954-1965. (d) Youngblood, W. J.; Lee, S. H.-A.; Maeda, K.; Mallouk, T. E. *Acc. Chem. Res.* **2009**, *42*, 1966-1973.

[9] (a) Bozoglian, F.; Romain, S.; Ertem, M. Z.; Todorova, T. K.; Sens, C.; Mola, J.; Rodríguez, M.; Romero, I.; Benet-Buchholz, J.; Fontrodona, X.; Cramer, C. J.; Gagliardi, L.; Llobet, A. *J. Am. Chem. Soc.* **2009**, *131*, 15176-15187 (b) Sartorel, A.; Miró, A.; Salvadori, E.; Romain, S.; Carraro, M.; Scorrano, G.; Di Valentin, M.; Llobet, A.; Bo, C.; Bonchio, M. *J. Am. Chem. Soc.* **2009**, *131*, 1651-1653.

[10] R. L. Carlin, *Magnetochemistry*, Springer-Verlag Berlin Heidelberg, **1986**, p. 328 pp.

[11] Sala, X.; Ertem, M. Z.; Vigara, L.; Todorova, T. K.; Chen, W.; Rocha, R. C.; Cramer, C. J.; Gagliardi, L.; Llobet, A. *Angew. Chem. Int. Ed.* **2010**, *49*, 7745-7747.

[12] Johnson, E.C.; Sullivan, B.P.; Salmon, D.J.; Adeyemi, S.A.; Meyer, T.J. *Inorg. Chem.* **1978**, *17*, 2211-2215.

[13] Dau, H.; Liebisch, P.; Haumann, M.; *Anal. and Bioanal. Chem.* **2003**, *376*, 562-583.
[14] Zabinsky, S. I., Rehr, J. J., Ankudinov, A. L., Albers, R. C., and Eller, M. J., *Phy. Rev. B* **1995***, 52*, 2995-3009.
[15] Zhao, Y.; Truhlar, D. G. *J. Chem. Phys.* **2006**, *125*, 194101.
[16] Dolg, M.; Wedig, U.; Stoll, H.; Preuss, H. *J. Chem. Phys.* **1987**, *86*, 866.
[17] Hehre, W. J.; Radom, L.; Schleyer, P. V. R.; Pople, J. A. Ab Initio Molecular Orbital Theory, Wiley, New York, **1986**.
[18] (a) Ziegler, T. ; Rauk, A.; E. J. Baerends, *Theor. Chim. Acta* **1977**, *43*, 261. (b) Noodleman, L.; Norman, J. G. *J. Chem. Phys.* **1979**, *70*, 4903; (c) Yamaguchi, K.; Jensen, F.; Dorigo, A.; Houk, K. N. *Chem. Phys. Lett.* **1988**, *149*, 537. (d) Noodleman, L; Case, D. A. *Adv. Inorg. Chem.* **1992**, *38*, 423. (e) Lim, M. H.; Worthington, S. E.; Dulles, F. J.; Cramer C. J. Chemical Applications of Density Functional Theory, Vol. 629 (Eds.: B. B. Laird, R. B. Ross, T. Ziegler), ACS, Washington, **1996**, p. 402. (f) Isobe, H.; Takano, Y.; Kitagawa, Y.; Kawaka- mi, T.; Yamanaka, S.; Yamaguchi, K.; Houk, K. N. *Mol. Phys.* **2002**, *100*,717.
[19] Marenich, A. V.; Cramer, C. J.; Truhlar, D. G. *J. Phys. Chem. B*, **2009**, *113*, 6378.
[20] (a) Ben-Naim, A. Statistical Thermodynamics for Chemists and Biochemists; Plenum: New York, **1992**; (b) Kelly, C. P.; Cramer, C. J.; Truhlar, D. G. *J. Phys. Chem. A* **2006**, *110*, 2493-2499; (c) Kelly, C. P.; Cramer, C. J.; Truhlar, D. G. *J. Phys. Chem. B* **2006**, *110*, 16066-16081; (d) Bryantsev, V. S.; Diallo, M. S.; Goddard, W. A. *J. Phys. Chem. B* **2008**, *112*, 9709-9719.
[21] Orellana, W.; da Silva, A. J. R.; Fazzio, A. *Phys. Rev. Lett.* **2001**, *87*, 155901.
[22] Hess, B. A. *Phys. Rev. A* **1986**, *33*, 3742.
[23] Roos, B. O.; Lindh, R.; Malmqvist, P.-.; Veryazov, V.; Wid-Mark, P.-O., *J. Phys. Chem. A* **2005**, *109*, 6575.
[24] Zhao, Y.; Truhlar, D. G. *MN-GFM version 4.1*; University of Minnesota: Minneapolis, **2008**.
[25] Frisch et al., *Gaussian 03, Revision D.01*; Gaussian, Inc.: Wallingford, CT, **2004**.
[26] Frisch et al., *Gaussian 09, Revision A.02*; Gaussian, Inc.: Wallingford, CT, **2010**.
[27] Aquilante, F.; De Vico, L.; Ferre, N.; Ghigo, G.; Malmqvist, P. A.; Neogrady, P.; Pedersen, T. B.; Pitonak, M.; Reiher, M.; Roos, B. O.; Serrano-Andres, L.; Urban, M.; Veryazov, V.; Lindh, R. "Software News and Update MOLCAS 7: The Next Generation" *J. Comp. Chem.* **2010**, *31*, 224-247.
[28] Dobson, J. C.; Meyer, T. J. *Inorg. Chem.* **1988**, *27*, 3283-3291.
[29] Gama Sauaia, M; Founi, E; de Almeida Santos, H; Do Prado Gambardelia, M. T. ; Del Lama, M. P. F. M.; Fernando Guimeraes, L; Santana da Silva, R. *Inorg. Chem. Commun.* **2003***, 6,* 864-868.
[30] (a) Jude, H; White, P. S.; Dattelbaum, D. M.; Rocha, R. C. *Acta Crystallogr., Sect. E Struct. Ep. Online* **2008***, E64*. (b) Dobson, J. C.; Meyer, T. J. *Inorg. Chem.* **1988**, *27*, 3283-3291.
[31] (a) Dengel, A. C.; Griffith, W. P. *Inorg. Chem.* **1991**, *30*, 869-871. (b) Kuan, S. L. et al *Organomet.* **2006**, *25*, 6134-6141. (c) Dengel, A. C.; Griffith, W. P.; O'Mahoney, C. A.; Williams, D. J. *J. Chem. Soc. Chem. Commun.* **1989**, *22*, 1720.
[32] Dengel, A. C.; Griffith, W. P. *Inorg. Chem.* **1991**, *30*, 869-871
[33] (a)Raja, N.; Ramesh, R.; *Spectrochim Acta A Mol Biomol Spectrosc.* **2010**, 713-8. (b)Taqui Khan, M. M., Srinivas, D; Kureshy, R. I.; Khan, N. H. *Polyhedron*, **1991**, *22*,2559-2565 (c) Prabhakaran, R.; Krishnan, V.; Geetha, A.; Bertagnolli, H.; Natarajan,K. *Inorg. Chim. Acta* **2006**, *4*, 1114-1120
[34] (a) Okamoto, K.; Miyawaki, J.; Nagai, K.; Matsumura, D.; Nojima, A.; Yokoyama, T.; Kondoh, H.; Ohta, T., *Inorg. Chem.* **2003**, *42*, 8682-8689. (b) Valli, M.; Miyata, S.; Wakita, H.; Yamaguchi, T.; Kikuchi, A.; Umakoshi, K.; Imamura, T.; Sasaki, Y., *Inorg. Chem.* **1997**, *36*, 4622-4626. (c) Sikora, M.; Oates, C. J.; Szczerba, W.; Kapusta, C.; Zukrowski, J.; Zajac, D.; Borowiec, A.; Ruiz-Bustos, R.; Battle, P. D.; Rosseinsky, M. J., *Alloy. Compd.* **2007**, *442*, 265-267. (d) Artero, V.; Proust, A.; Herson, P.; Villain, F.; Moulin, C. C. D.; Gouzerh, P., *J. Am. Chem. Soc.* **2003**, *125*, 11156-11157. (e) Lahootun, V.; Besson, C.; Villanneau, R.; Villain, F.; Chamoreau, L. M.;

Boubekeur, K.; Blanchard, S.; Thouvenot, R.; Proust, A., *J. Am. Chem. Soc.* **2007**, *129*, 7127-7135.

[35] (a) Dau, H.; Liebisch, P.; Haumann, M., *Physica Scripta* **2005**, *T115*, 844-846. (b) Haumann, M.; Muller, C.; Liebisch, P.; Iuzzolino, L.; Dittmer, J.; Grabolle, M.; Neisius, T.; Meyer-Klaucke, W.; Dau, H.; *Biochemistry-Us* **2005**, *44*, 1894-1908. (c) Havelius, K. G.; Reschke, S.; Horn, S.; Doring, A.; Niks, D.; Hille, R.; Schulzke, C.; Leimkuhler, S.; Haumann, M., *Inorg Chem* 2011, *50*, 741-748.

Chapter 5

Polypyridyl Ruthenium Catalysts for Hydrogenative CO_2 Reduction

Hydrogenation of CO_2 is one of the important and attractive subjects of research in recent transition metal, catalytic and organometallic chemistry. Most of the catalysts reported to date are Rh, Ru and Ir complexes containing phosphine ligands. In a different approach, the present chapter reports a series of N_5-Ru-Cl polypyridyl complexes as catalyst precursors for the hydrogenative reduction of CO_2. Experimental evidence of their good performance in the production of formic acid is accompanied by a thorough theoretical study of the proposed mechanism. Additionally, initial results of the performance of the analogous dinuclear ruthenium complexes bearing the bpp- dinucleating ligand as catalysts for the reductive process are included.

TABLE OF CONTENTS

5.1. INTRODUCTION

The most important industrial processes in which carbon dioxide is used as a reagent are the synthesis of carboxylic acids,[1] inorganic carbonates, urea and methanol.[2, 3]

The overall CO_2 fixed by industry annually adds up only to 0.5% of the total anthropogenic CO_2 emissions, which is about 24 GT of CO_2/year.[4] Thus, the utilization of CO_2 as carbon source for the synthesis of liquid fuels or fuel precursors results a convenient alternative to the quite little efficient and strongly endothermic (indirectly CO_2 emitting) current processes used to obtain C_1 reduced molecules like methanol and formic acid.

The catalytic hydrogenative reduction of CO_2 to form formic acid[1-5] and its derivatives [1, 6, 7] have gained specific attention. In particular, the high activity of some transition metal catalysts, as Rh, Ru and Ir, offers the possibility of utilizing CO_2 as a C_1 chemical feedstock.

5.1.1. Ruthenium phosphine catalysts

The homogeneous catalytic production of formic acid by hydrogenative reduction of CO_2 represents the primary step in CO_2 fixation. This catalytic reaction was initially achieved in 1970's with only modest activity.[1, 8, 9] The field reblossomed at the beginning of the 1990's, many Rh-phosphine-based catalysts achieving higher efficiencies were reported and complemented by important theoretical mechanistic studies.[2, 3, 10-13]

The employment of new Ru^{II} phosphine catalysts to promote the reductive process represented a real break through in the field. Especially due to the investigations by Jessop, Ikariya and Noyori whose catalysts achieved extremely high turnover numbers when $scCO_2$ was used as both reactant and solvent.[4-6] Musashi and Sakaki elaborated a theoretical mechanistic study with *ab initio* calculations on the model catalyst *cis*-[$Ru(H)_2(PH_3)_4$] in the gas phase. The mechanism they proposed is depicted in Figure 1.[14]

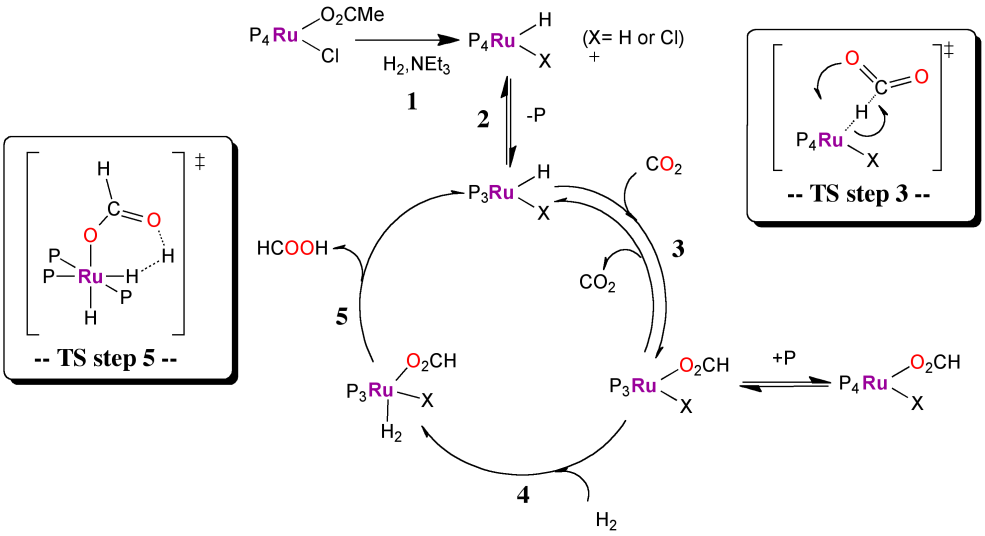

Figure 1. Mechanism for the hydrogenative reduction of CO_2 by $[Ru(P)_4(H)_2]$ catalysts, being P trimethyl-phosphine or PH_3. Squared, the theoretically studied transition states. Hydride species generation (1), entrance to the catalytic cycle by phosphine ligand dissociation (2), CO_2 insertion (3), hydrogen insertion (4), hydride regeneration by intramolecular hydrogen cleavage and formic acid release (5).[14]

Even though very detailed reaction steps were reported, discrepancies between the mechanism and experimental data observations existed. Theoretic results sustained that the rate determining step was the CO_2 insertion into the Ru-H bond, which was contradicted by the experimental evidence of a high dependence of the reaction rate on the partial pressure of H_2. This inconsistency was later overcomed by Sakaki and co-workers in a study of the full structure of the catalyst *cis*-$[Ru(H)_2(PMe_3)_4]$. They followed the same mechanism but, accounting for solvation effects, they demonstrated that the rate determining step was the regeneration of the Ru-hydrido species, through what the authors claimed to be a new type of sigma-bond methathesis.[15]

Big efforts have also been put in the elucidation of the mechanism of the more rigid catalyst $[Ru(dmpe)H_2]$ containing the diphosphine chelating ligand *dmpe* ($Me_2PCH_2CH_2PMe_2$) by combined experimental and theoretical techniques.[16, 17] The authors described for the *cis* species a very similar mechanism as the one previously reported for *cis*-$[Ru(H)_2(PMe_3)_4]$ (Figure 1). Though, the *trans* isomer was proposed to

be more active presenting overall smaller energy barriers in the mechanism described in Figure 2.[16]

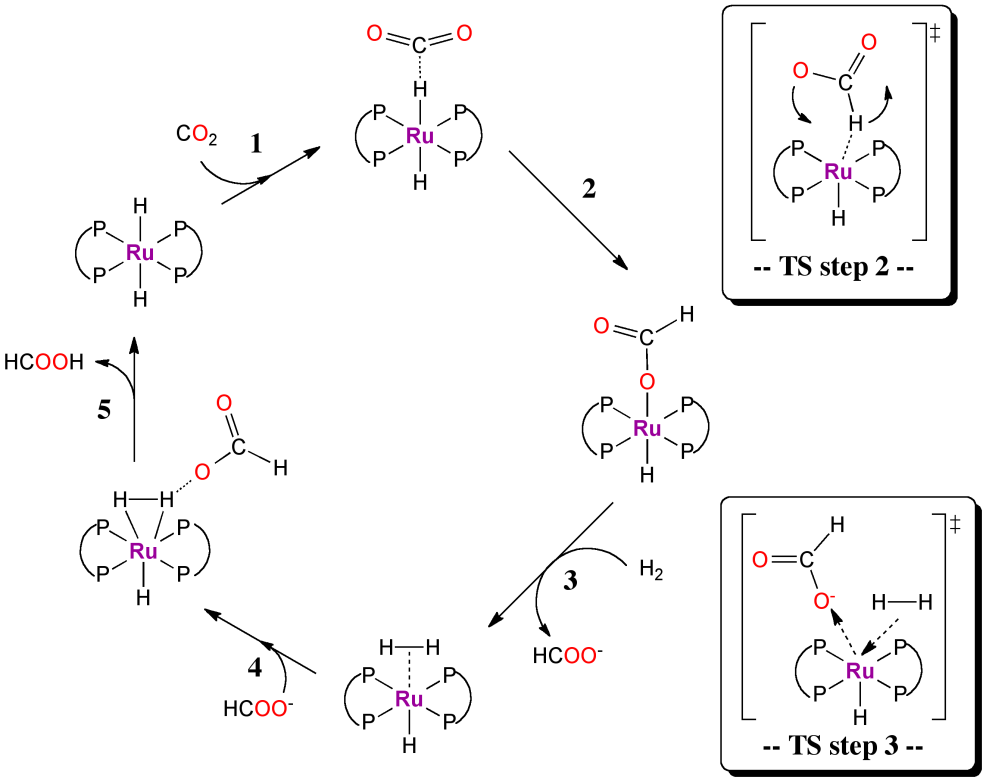

Figure 2. Mechanism for the hydrogenative reduction of CO_2 by $Ru(P\text{-}P)_2H_2$ catalysts, P-P being the dmpe ligand ($CH_3PCH_2CH_2PCH_3$). Squared, the theoretically studied transition states. CO_2 interaction with the Ru-H species (1), isomerization of the formato complex (2), formate release by H_2 insertion (3), stabilization of the Ru-H_2 species by formate anion (4), and hydride regeneration by heterolytic cleavage of H-H bond assisted by formate (5).[16, 17]

5.1.2. Ruthenium polypydridyl catalysts

In the fields of electrochemical and photochemical reduction of CO_2, non-phosphine-based ruthenium complexes containing polypyridyl ligands play an important role as electrocatalysts and photocatalysts respectively.[18-22] In contrast, there are very few cases in which ruthenium polypyridyl catalysts are reported to be capable to transform ing CO_2 by a hidrogenative reduction process. Himeda and co-workers

presented a new family of Ir^{III}, Rh^{III} and Ru^{II} half sandwich mono hydride species containing bpy/phenantroline and Cp/C_6Me_6 ligands, or their functionalized derivatives.[23-25] These catalysts achieved in some cases high TON and TOF for the catalytic homogeneous hydrogenation of CO_2 to formic acid in water and with KOH as a base. For example, the iridium catalyst $[Cp^*Ir(phen)H]^+$ presented performances amongst the highest reported to date.[26, 27]

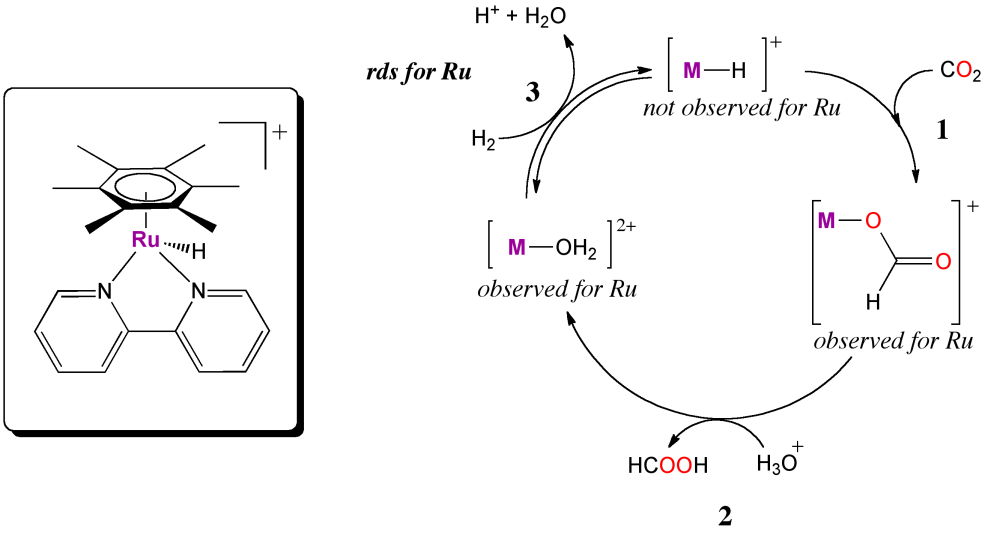

Figure 3. Left, drawing of the M-H ruthenium catalyst structure. Right, mechanism for the reduction of CO_2 to HCOOH by half sandwich Ru and Ir hydride complexes. CO_2 insertion to the M-H bond (1), formic acid release (2) and hydride species regeneration (3).[23]

Fukuzumi and coworkers tested $[Ru(C_6Me_6)(bpy)(H)]^+$ and $[Ir(Cp^*)(bpy)(H)]^+$ in acidic media with no added base. Both were proposed to proceed through the mechanism shown in Figure 3. Interestingly, experimental data point to differences in the nature of the rate determining step. The slow kinetics of the CO_2 insertion process of the Iridium catalyst enabled the isolation in the solid state of the M-hydride complex which was characterized by MS and ^{1}HNMR. In the case of Ruthenium, the analogous species was not observed. The detection of the respective ruthenium *formato* and *aquo* complexes, added to the strong dependence of the TOF on H_2 partial

pressure, lead the authors to propose the hydride regeneration to be the rate determining step.[23]

5.1.3. State-of-the-art in hydrogenative CO_2 reduction

Present research in the field is mainly focused of rhodium, ruthenium and a few iridium catalysts, most of them containing phosphine ligands, in different organic solvents,[24, 25, 28-30] water, super critical CO_2 ($scCO_2$)[31] and even ionic liquids.[32, 33] Both in homogeneous phase and in heterogeneous phase. [7, 32, 34]

The performance of some representative examples of the catalysts for the hydrogenation of CO_2 reported to date, is summarized in Table 1.

Table 1. Significative catalytic systems, their catalytic conditions and their performances in the hydrogenation of CO_2 to formic acid.

	catalyst precursor	**solvent**	**Add-itives**	**pH_2/ pCO_2 (bar)**	**T (ºC)**	**t (h)**	**TON**
1	$[IrH_3(PNP)]$[43]	H_2O	KOH	30/30	120	48	4E+06
2	$[C_6Me_6$ Ir(4,4'-$(OH)_2$-(phen)Cl]Cl[26]	H_2O	KOH	20/20	60	20	5500
3	[Cp*Ir(phen)Cl]Cl[26]	H_2O	KOH	30/30	120	48	2E+05
4	$[RhCl(tppts)_3]$[10]	H_2O	$NHMe_2$	20/20	RT	12	3439
5	$[RhCl(PPh_3)_3]$[42]	MeOH	PPh_3, NEt_3	20/40	25	20	2700
6	[(dcpb)Rh(acac)][39]	DMSO	NEt_3	20/20	RT	0,2	263
7	$[(C_6Me_6)Ru(4,4'-(OH)_2$-bpy)Cl][26]	H_2O	KOH	20/20	60	20	4400
8	$[(C_6Me_6)Ru(bpy)Cl]$[26]	H_2O	KOH	20/20	60	20	68
9	$[Ru(Cl_2$-bpy$)_2(H_2O)_2]^{2+}$[41]	EtOH	NEt_3	30/30	150	8	5000
11	$[RuH_2(PPh_3)_4]$[40]	C_6H_6	Na_2CO_3	25/25	100	4	169
12	$[RuH_2(PMe_3)_4]$ [17]	$scCO_2$	CH_3OH	80/120	50	0,5	2000
13	$[RuCl(OAc)(PMe_3)_4]$ [35]	$scCO_2$	NEt_3, TFE	70/120	50	0,3	28500

As can be seen the catalyst that has the best performances so far is the $Ir^{III}(H)_3$ catalyst reported by Nozaki (Entry 1, Table 1) which's mechanism remains unknown. Continuing with iridium, comparison of the entries 2 and 3 indicate the importance of the auxiliary ligand's electronic effects on the catalyst performance (upon ligand functionalization, the relative little increase of the total gas pressure results in an increase of 400 times of the TONs).

Interestingly, even though their overall performances are not extremely high, the Rh based catalysts (Entries 4-6, Table 1) are capable to work at very mild temperatures.

The ruthenium catalysts can be generally classified in two groups; those which will lead to Ru-H species and those who will potentially lead to $Ru(H)_2$ species by substitution of their labile ligands.

In the first case, the Ru-H catalysts derived from the compounds in entries 7 and 8 exemplify again the importance of the electronic effects of the ligands on the catalyst's performance.

The second case, complexes leading to $Ru(H)_2$ active species (Entries 9-13, Table 1) are the ones which have been most deeply studied, as already mentioned in section 5.1.3.

The high positive effect of using $scCO_2$ as both reactant and solvent can be seen in entries 11 and 12 where the same catalyst is employed in benzene and in $scCO_2$ respectively.

A trustful assignment of the rate determining step of these systems and understanding of some of the experimental results is still lacking. The positive effect on the catalytic performance of some bases, such as amines (Entries 4-6,9-10 and 13, Table 1), and protic solvents, like water and alcohols (Entries 12 and 13, Table 1), in the reaction media has drawn special attention.[35-38] Even though, the exact role of them is not fully understood and may change from one catalytic system to the other, it is well established that, at the very last, the base acts to thermodynamically stabilize the formic acid product.[13, 36]

5.1.4. References

[1] Y. Inoue, H. Izumida, Y. Sasaki and H. Hashimoto, *Chem. Lett.* **1976**, 863-864.
[2] E. Graf and W. Leitner, *J. Chem. Soc., Chem. Commun.* **1992**, 623-624.
[3] J. C. Tsai and K. M. Nicholas, *J. Am. Chem. Soc.* **1992**, *114*, 5117-5124.
[4] P. G. Jessop, T. Ikarlya and R. Noyori, *Nature (London)* **1994**, *368*, 231-233.
[5] P. G. Jessop, Y. Hsiao, T. Ikariya and R. Noyori, *J. Am. Chem. Soc.* **1996**, *118*, 344-355.
[6] P. G. Jessop, Y. Hsiao, T. Ikariya and R. Noyori, *J. Am. Chem. Soc.* **1994**, *116*, 8851-8852.
[7] O. Krocher, R. A. Koppel and A. Baiker, *Chimia* **1997**, *51*, 48-51.
[8] M. Shiotsuka, Y. Inui, Y. Sekioka, Y. Yamamoto and S. Onaka, *J. Organomet. Chem.* **2007**, *692*, 2441-2447.
[9] Y. Sasaki, Y. Inoue and H. Hashimoto, *J. Chem. Soc., Chem. Commun.* **1976**, 605-606.
[10] F. Gassner and W. Leitner, *J. Chem. Soc., Chem. Commun.* **1993**, 1465-1466.
[11] Y. Musashi and S. Sakaki, *J. Am. Chem. Soc.* **2002**, *124*, 7588-7603.
[12] F. Hutschka, A. Dedieu, M. Eichberger, R. Fornika and W. Leitner, *J. Am. Chem. Soc.* **1997**, *119*, 4432-4443.
[13] F. Hutschka and A. Dedieu, *J. Chem. Soc., Dalton Trans.* **1997**, 1899-1902.
[14] Y. Musashi and S. Sakaki, *J. Am. Chem. Soc.* **2000**, *122*, 3867-3877.
[15] Y. Ohnishi, T. Matsunaga, Y. Nakao, H. Sato and S. Sakaki, *J. Am. Chem. Soc.* **2005**, *127*, 4021-4032.
[16] A. Urakawa, M. Iannuzzi, J. Hutter and A. Baiker, *Chem.--Eur. J.* **2007**, *13*, 6828-6840.
[17] A. Urakawa, F. Jutz, G. Laurenczy and A. Baiker, *Chem.--Eur. J.* **2007**, *13*, 3886-3899.
[18] K. Tanaka and D. Ooyama, *Coord. Chem. Rev.* **2002**, *226*, 211-218.
[19] S. Chardon-Noblat, A. Deronzier, R. Ziessel and D. Zsoldos, *Inorg. Chem.* **1997**, *36*, 5384-5389.
[20] H. Takeda and O. Ishitani, *Coord. Chem. Rev.* **2010**, *254*, 346-354.
[21] S. Sato, T. Morikawa, S. Saeki, T. Kajino and T. Motohiro, *Angew. Chem., Int. Ed.* **2010**, *49*, 5101-5105, S5101/5101-S5101/5111.
[22] M. D. Doherty, D. C. Grills, J. T. Muckerman, D. E. Polyansky and E. Fujita, *Coord. Chem. Rev.* **2010**, *254*, 2472-2482.
[23] S. Ogo, R. Kabe, H. Hayashi, R. Harada and S. Fukuzumi, *Dalton Trans.* **2006**, 4657-4663.
[24] Y. Himeda, N. Onozawa-Komatsuzaki, H. Sugihara and K. Kasuga, *J. Photochem. Photobiol., A* **2006**, *182*, 306-309.
[25] Y. Himeda, *Eur. J. Inorg. Chem.* **2007**, 3927-3941.
[26] Y. Himeda, N. Onozawa-Komatsuzaki, H. Sugihara and K. Kasuga, *Organometallics* **2007**, *26*, 702-712.
[27] C. Federsel, R. Jackstell and M. Beller, *Angew. Chem., Int. Ed.* **2010**, *49*, 6254-6257.
[28] D. Preti, S. Squarcialupi and G. Fachinetti, *Angew. Chem., Int. Ed.* **2010**, *49*, 2581-2584, S2581/2581-S2581/2588.
[29] Y. Himeda, N. Onozawa-Komatsuzaki, H. Sugihara and K. Kasuga, *J. Am. Chem. Soc.* **2005**, *127*, 13118-13119.
[30] M. S. G. Ahlquist, *J. Mol. Catal. A: Chem.* **2010**, *324*, 3-8.
[31] T. Hirose, S. Shigaki, M. Hirose and A. Fushimi, *J. Fluorine Chem.* **2010**, *131*, 915-921.
[32] Z. Zhang, Y. Xie, W. Li, S. Hu, J. Song, T. Jiang and B. Han, *Angew. Chem., Int. Ed.* **2008**, *47*, 1127-1129.
[33] Z. Zhang, S. Hu, J. Song, W. Li, G. Yang and B. Han, *ChemSusChem* **2009**, *2*, 234-238.
[34] A. Baiker, *Appl. Organomet. Chem.* **2000**, *14*, 751-762.
[35] P. Munshi, A. D. Main, J. C. Linehan, C.-C. Tai and P. G. Jessop, *J. Am. Chem. Soc.* **2002**, *124*, 7963-7971.
[36] H. S. Chu, C. P. Lau, K. Y. Wong and W. T. Wong, *Organometallics* **1998**, *17*, 2768-2777.

[37] S. M. Ng, C. Yin, C. H. Yeung, T. C. Chan and C. P. Lau, *Eur. J. Inorg. Chem.* **2004**, 1788-1793.
[38] C. Yin, Z. Xu, S.-Y. Yang, S. M. Ng, K. Y. Wong, Z. Lin and C. P. Lau, *Organometallics* **2001**, *20*, 1216-1222.
[39] K. Angermund, W. Baumann, E. Dinjus, R. Fornika, H. Goerls, M. Kessler, C. Krueger, W. Leitner and F. Lutz, *Chem.--Eur. J.* **1997**, *3*, 755-764.
[40] P. G. Jessop, F. Joo and C.-C. Tai, *Coord. Chem. Rev.* **2004**, *248*, 2425-2442.
[41] C. P. Lau and Y. Z. Chen, *J. Mol. Catal. A: Chem.* **1995**, *101*, 33-36.
[42] N. N. Ezhova, N. V. Kolesnichenko, A. V. Bulygin, E. V. Slivinskii and S. Han, *Russ. Chem. Bull.* **2002**, *51*, 2165-2169.
[43] R. Tanaka, M. Yamashita and K. Nozaki, *J. Am. Chem. Soc.* **2009**, *131*, 14168-14169.
[44] C. Sens, I. Romero, M. Rodriguez, A. Llobet, T. Parella and J. Benet-Buchholz, *J. Am. Chem. Soc.* **2004**, *126*, 7798-7799.

5.2. CO_2 REDUCTION BY MONONUCLEAR RUTHENIUM POLYPYRIDYL COMPLEXES

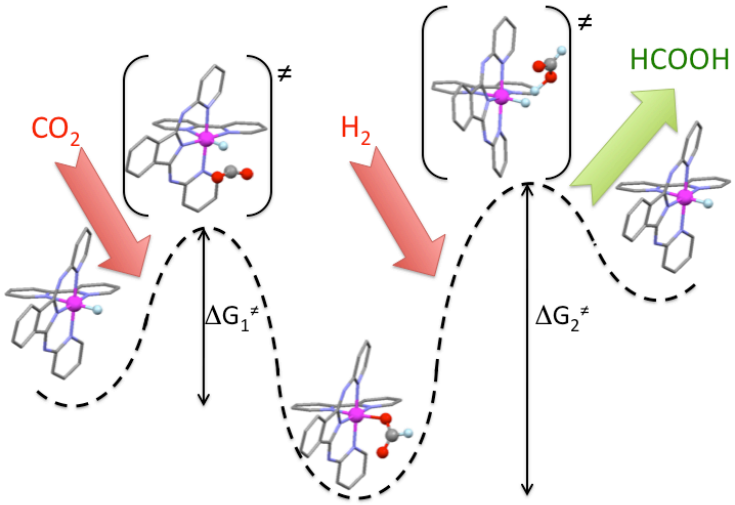

A family of new mononuclear ruthenium complexes with general formula [Ru(T)(bpy)(Cl)]^n (T: tridentate meridional ligand trpy or the anionic bid-; bpy: bidentate ligand 4,4'-R_2-2,2'-bipyridine, where R = H, COOEt or OEt; n: charge ranging from 0 to +1, see Figure 1) have been synthesised and fully characterized. These complexes act as precatalysts for the hydrogenative reduction of CO_2 to formic acid. Further, their mechanistic pathways have been investigated by means of DFT.

CO_2 Reduction by Mononuclear Ruthenium Polypyridyl Complexes†

To be Submitted

Nora Planas,[a] Takashi Ono,[a] Lydia Vaquer,[a] Pere Miró,[b] Laura Gagliardi,[b] Christopher Cramer,[b] and Antoni Llobet*[a, c]

[a] *Institute of Chemical Research of Catalonia (ICIQ), Av. Països Catalans 16, E-43007 Tarragona, Spain. Fax: 34 977 902 228; Tel: 34 977 902 200; E-mail: fmaseras@iciq.es, allobet@iciq.es*

[b] *Department of Chemistry and Supercomputing Institute University of Minnesota, 207 Pleasant St. SE, Minneapolis, MN 55455-0431 (USA)*

[c] *Departament de Química, Universitat Autònoma de Barcelona, Cerdanyola del Vallès, E-08193 Barcelona, Spain.*

†Electronic Supplementary Information (ESI) available: Experimental section, full spectroscopic and electrochemical characterizations , catalytic measurements and coordinates of computed structures.

Keywords: Carbon dioxide hydrogenation, Ruthenium polypyridyl

5.2.1. Abstract

A family of new mononuclear ruthenium complexes with general formula [Ru(T)(bpy)(Cl)]^n (T: tridentate meridional ligand *trpy* or the anionic *bid*-; *bpy*: bidentate ligand 4,4'-R_2-2,2'-bipyridine, where R = H, COOEt or OEt; n: charge ranging from 0 to +1, see Figure 1) have been prepared, isolated and characterized. Further, they have been experimentally tested as precatalysts for the hydrogenative reduction of CO_2 in 2,2,2-Trifluoroethanol (TFE) as solvent in the presence of NEt_3. Significant amounts of formic acid were produced by some of these catalysts which's kinetics of formation was followed by ^{1}H-NMR. The potential mechanisms and intermediate species for these catalytic systems have been investigated by means of DFT to get deeper insight in the process. Furthermore, the effect of the electron donor and electron withdrawing

groups on the catalyst's performance has been studied both experimentally and theoretically.

5.2.2. Introduction

The use of carbon dioxide (CO_2) as a raw material for Chemicals synthesis is gaining growing attention, driven by environmental, legal and social factors. Atmospheric Carbon dioxide is the most abundant greenhouse gas and the scientific community now agrees that the increase of its concentration in the atmosphere in the last decades is mainly due to human activity. [1-3] Although up to now the use of CO_2 in chemical synthesis contributes very little in the decrease of CO_2 concentration in the atmosphere, there are several other factors that render CO_2 an interesting chemical feedstock; High abundance, low toxicity, low cost and low critical temperature.

Hydrogenative reduction promoted by transition metal catalysts represents a viable way to obtain reduced C1 products from CO_2 such as formic acid, formaldehyde and methanol. These transformations require multiple proton coupled electron transfer processes as shown in equations 1-3. The need of concerted many PCET adds complexity to the already the intricate catalytic process involving the reaction of two gases (CO_2 and H_2).

$$CO_2 + 2H^+ + 2e^- \rightarrow HCOOH \qquad (E^o_{red} = -0.61 \text{ at pH7 vs NHE}) \qquad (1)$$

$$CO_2 + 4H^+ + 4e^- \rightarrow HCHO + H_2O \qquad (E^o_{red} = -0.48 \text{ at pH7 vs NHE}) \qquad (2)$$

$$CO_2 + 6H^+ + 6e^- \rightarrow CH_3OH + H_2O \qquad (E^o_{red} = -0.38 \text{ at pH7 vs NHE}) \qquad (3)$$

Rhodium and, to a lesser extent, ruthenium complexes bearing phosphine ligands have been reported to catalytically reduce CO_2 obtaining as main products formaldehyde and formic acid (and their derivatives).[4-6] Furthermore it has also been shown that the efficiency of these complexes as catalysts is strongly dependent of the electronic nature of the auxiliary ligands.[7]

The production of formic acid is thought to be the first required step for the reduction of CO_2 to the more reduced C1 products. Hence, the paramount importance of understanding the catalytic mechanism and the factors governing it.

The present work presents a new family of catalysts for the hydrogenative reduction of CO_2 to formic acid. Combined experimental and theoretical studies allowed to shed light into the ligand effects on the catalytic performance and sets the basis for further ligand/catalyst design.

5.2.3. Results and discussion

A family of new mononuclear ruthenium complexes with general formula [Ru(T)(bpy)(Cl)]^n (T: tridentate meridional ligand *trpy* or the anionic *bid*-; *bpy*: bidentate ligand 4,4'-R_2-2,2'-bipyridine, where R = H, COOEt or OEt; n: charge ranging from 0 to +1, see Figure 1) have been synthesised. This family of complexes constitute an ideal basis to understand how the electronic tuning, by ligand modification, affects the activity of ruthenium catalysts for hydrogenative CO_2 reduction.

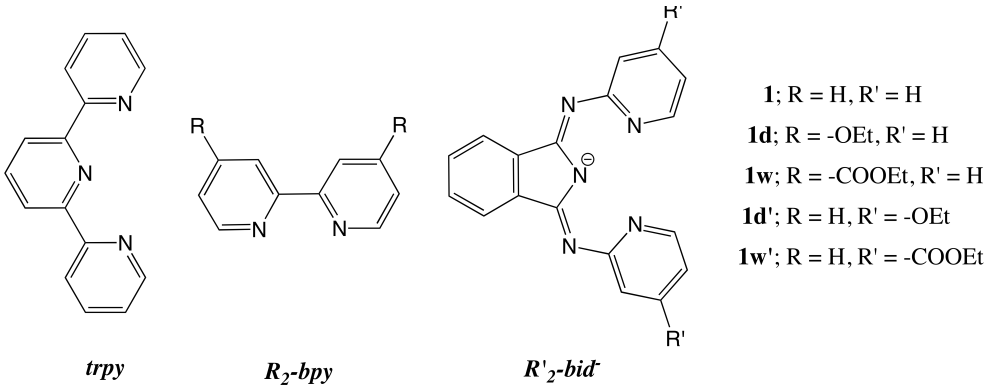

Figure 1. Polidentate ligands and their functionalizations.

For T = *bid* complex **1** (R = H, R'= H) was newly synthesized and complex **2** with T = *trpy* was obtained as previously reported.[8] The catalyst's precursors **1** and **2** are shown in Figure 2.

In the case of **1,** two derivatives were obtained by introduction of electron donor (R= -OEt) and electron withdrawing (R= -COOEt) functionalities on the 4,4'-R_2-*bpy* ligands in compounds **1d** and **1w** respectively (See Figure 1). These functionalizations were chosen as they do not involve overall charge modification of the catalytic species.

All the *bid*$^-$ containing compounds were synthesized following the same "one pot" procedure. An ethanol solution with the mixture of [$RuCl_3$(bid)] with the bidentate ligand 4,4'-R_2-*bpy* was put at reflux for one hour. Then, the addition of an excess of NEt_3 and LiCl was followed by four more hours of reflux. Cooling the solution yield the desired product as a crystalline powder.

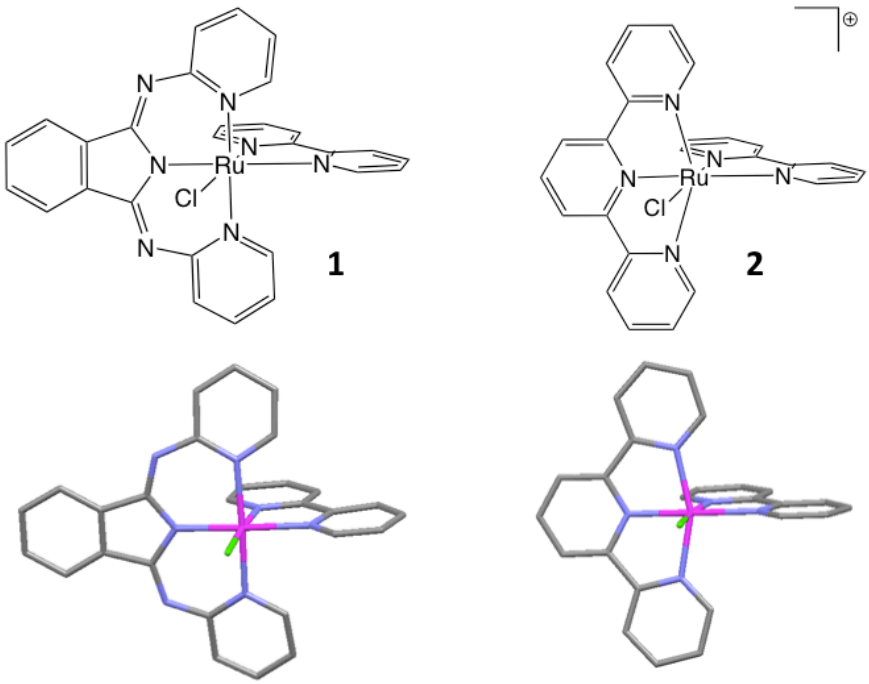

Figure 2. Top, drawing of the mononuclar **1** and **2** precatalysts. Bottom, capped stick X-ray structure of complex **1** and capped stick calculated structure of **2**. Ru, pink; N, blue; Cl, green; C, grey; H are not shown for clarity.

Complex **1** was characterized by X-ray monocrystal diffraction analysis and its crystal structure is shown in Figure 2 (bottom). As it can be observed, the metal centre presents a slightly distorted octahedral geometry. The distortion is more significative

in complex **2** due to the marked difference in the bite angle of the tridentate chelating ligands. All these Ru-Cl complexes were tested as catalyst precursors in the hydrogenative reduction of CO_2 obtaining formic acid as the sole detected product.

Catalytic experiments

All experiments were carried out in a HEL multireactor connected to second 100 mL high pressure reactor (as is schematically presented in Figure 3). The latter served as an external "lung" reducing the overall gas pressure variations during the reaction.

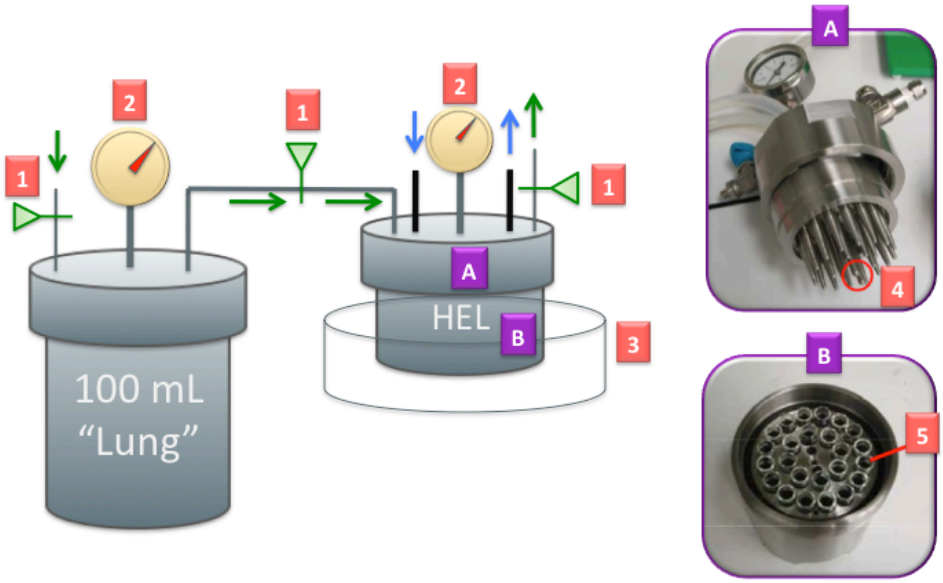

Figure 3. Experimental setup for the catalytic experiments.Valves (1), manometer (2), oil bath (3), cold fingers (4), reaction vessels (5), HEL reactor's lid (A) and HEL reactor bottom (B). Gas flow, green arrows; cooling system, blue arrows.

In a typical catalytic run, 0.9 mL of a 0.3 mM catalyst's solution of a mixture of 2,2,2-trifluoroethanol and triethylamine (8:1) was introduced in each reaction vessel of a HEL multireactor. Once loaded with samples and connected to an additional 100 mL "Lung" reactor, the system was purged with 5 bars of nitrogen three times and charged with the CO_2/H_2 mixture (45 bars of CO_2:H_2 in a 1:1 ratio). After cooling the

reflux "cold fingers" to 5 °C, the reactor was introduced to a preheated oil bath at 100 °C and stirred at 500 rpm. At the desired time, the reaction was stopped by removing the reactor from the bath and subsequently introducing it in an ice bath for 10 minutes without stirring. The samples were analyzed by ^{1}H-NMR, taking 0.2 mL of the reaction solution and mixing them with 0.25 ml of D_2O containing DMF as internal standard (120 µL in 10 mL). Three replicates were performed for each measurement.

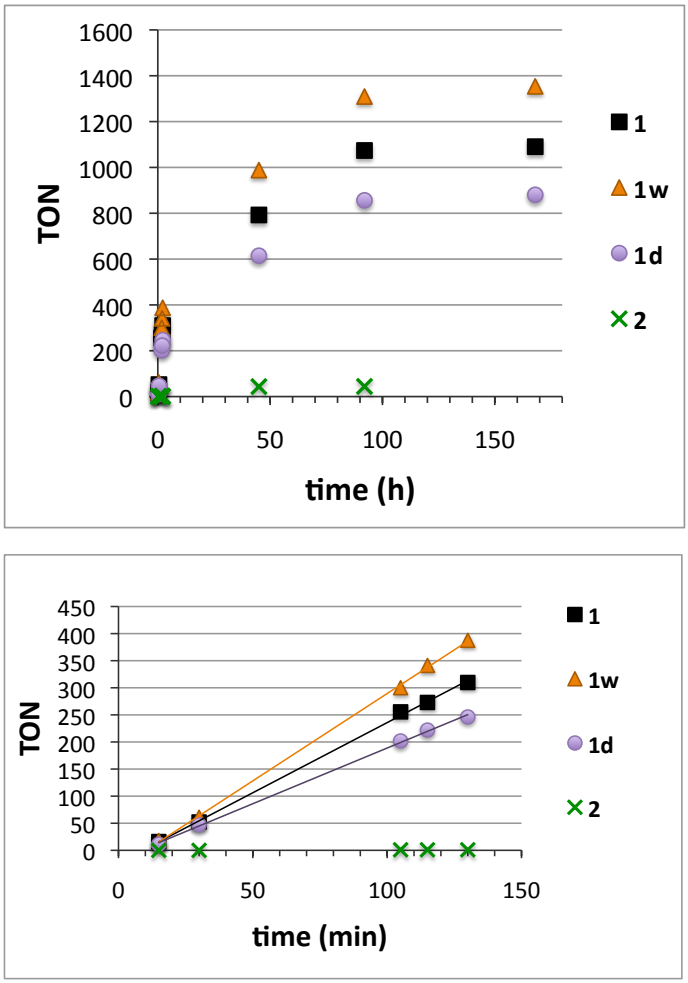

Figure 4. Top, catalytic profile. Bottom, initial HCOOH formation.

In Figure 4 the formic acid produced in TONs over the initial 130 minutes are represented. As can be seen in Table 1, the initial rates for catalysts **1**, **1d** and **1w** are significantly higher than those of **2**. Which is in good agreement with the poor performances previously reported with the latter catalyst precursor in other catalytic conditions[9-11] and the demonstrated high stability of the corresponding hydride active species, which was even crystalized from an aqueous solution.[12]

The performance of the most active catalysts (**1**, **1d** and **1w**) was studied for a longer period. As can be seen in Figure 4 after 7 days (168 h) all three catalysts were deactivated. The maximum TON of 1400 was reached with **1w**, whereas the presence of an electron donor group in **1d** slows down the process and decreases the overall performance. In the case of the slower catalyst **2** its performance remains far below those of **1**, **1d** and **1w** after long periods.

Table 1. Catalytic performances.

catalyst precursor	TOF_0 [b] (h^{-1})	TON_f [a]
1	155,3	1090
1d	120,3	880
1w	193,4	1354
2	0,5	44

[a] TON of HCOOH detected after 7 days for all catalysts except for **2** (92 h). [b] Initial Turn Over Frequencies, considering the first 130 minutes.

DFT Calculations on the catalytic mechanism

DFT calculations have been undertaken to study the reaction pathway for the catalytic process and to understand the origin of the different performances between catalysts. Based on bibliography,[5, 13, 14] the catalytic conditions and observations, the mechanism proposed consists on the four general steps depicted in Figure 5.

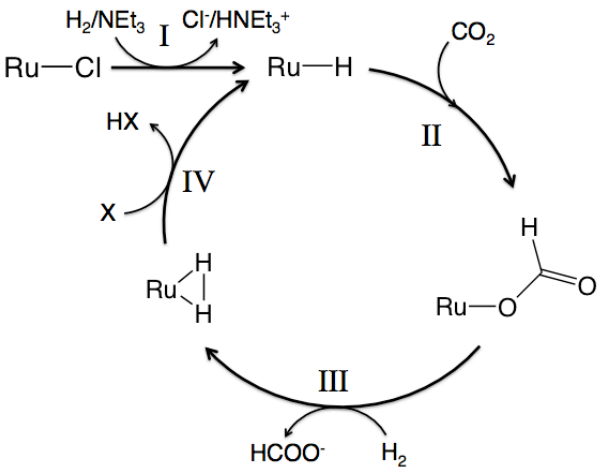

Figure 5. Catalytic cycle under study. A first step from Ru-Cl to form the ruthenium hydride (I), which is the active species, followed by the three consecutive steps that constitute the catalytic cycle. CO_2 insertion into the metal hydride (II), substitution of the formato ligand by dihydrogen (III) and regeneration of the hydride by heterolytic cleavage (IV).

Geometry optimisations of the Ru-Cl complexes **1**, **1w**, **1d** and **2** as well as the corresponding reaction intermediates and transition states involved in the catalytic cycle, have been carried out at the M06L-DFT level of theory following the methodology described in the Experimental Section of the Supp. Inf.. The Ethyl groups of the -OEt and -COOEt functionalizations, as well as the ones of the NEt_3 base, have been substituted by methyl groups for computational simplification.

In addition to all the catalytic systems experimentally studied, two additional catalytic systems based on derivatives of **1** functionalized with -OMe (complex **1d'**) and -COOMe (complex **1w'**) on the 4 and 4' position of the pyridyl rings of the *bid*$^-$ ligand have been considered (see Figure 1).

Coordinates for all the calculated structures and selected structural parameters (displayed in Tables S2-S8) are contained in the Supp. Inf.. Comparison with experimental values obtained for structures from X-ray diffraction analysis show an excellent agreement.

The catalytic steps I to IV (Figure 5) were divided as follows (the tridentated meridional ligand T and the bidentated *bpy* ligands are not shown for clarity):

Entrance to the cycle,

$[Ru\text{-}Cl] + H_2 \rightarrow [Ru\text{-}H] + HCl$ (I)

CO_2 insertion,

$[Ru\text{-}H] + CO_2 \rightarrow [Ru\text{-}H\text{--}CO_2]^{\neq}$ (IIa)

$[Ru\text{-}H\text{--}CO_2]^{\neq} \rightarrow [Ru\text{-}H\text{-}CO_2]$ (IIb)

$[Ru\text{-}H\text{-}CO_2] \rightarrow [Ru\text{-}O\text{-}CHO]$ (IIc)

Substitution,

$[Ru\text{-}O\text{-}CHO] \rightarrow [Ru\text{---}O\text{-}CHO]^{\neq}$ (IIIa)

$[Ru\text{---}O\text{-}CHO]^{\neq} \rightarrow [Ru] + HCOO^-$ (IIIb)

$[Ru] + H_2 \rightarrow [Ru\text{-}H_2]$ (IIIc)

Heterolytic cleavage,

$[Ru\text{-}H_2] + X \rightarrow [Ru\text{-}H\text{--}H\text{--}X]^{\neq}$ (IVa-x)

$[Ru\text{-}H\text{--}H\text{--}X]^{\neq} \rightarrow [Ru\text{-}H] + HX$ (IVb-x)

(x=O for $X=HCOO^-$ or x=N for $X=NMe_3$)

The optimised structures and the energetic profile of the computed species intervening in the catalytic cycle for systems **1, 1w** and **1d** are shown in Figure 6. Two energetic barriers have to be considered $\Delta G^{o\neq}_1$ and $\Delta G^{o\neq}_2$. First, the CO_2 insertion in the Ru-H bond yields the corresponding Ru-OCOH species. Second, the Ru-hydride regeneration from the "formato" intermediate which represents the rate determining process for these catalytic systems. More precisely, the substitution of the "formato" ligand by dihydrogen is followed by the heterolytic cleavage of the H-H bond assisted by the formato anion (Equations III and IVa-x where X is $HCOO^-$) regenerating the hydride active species.

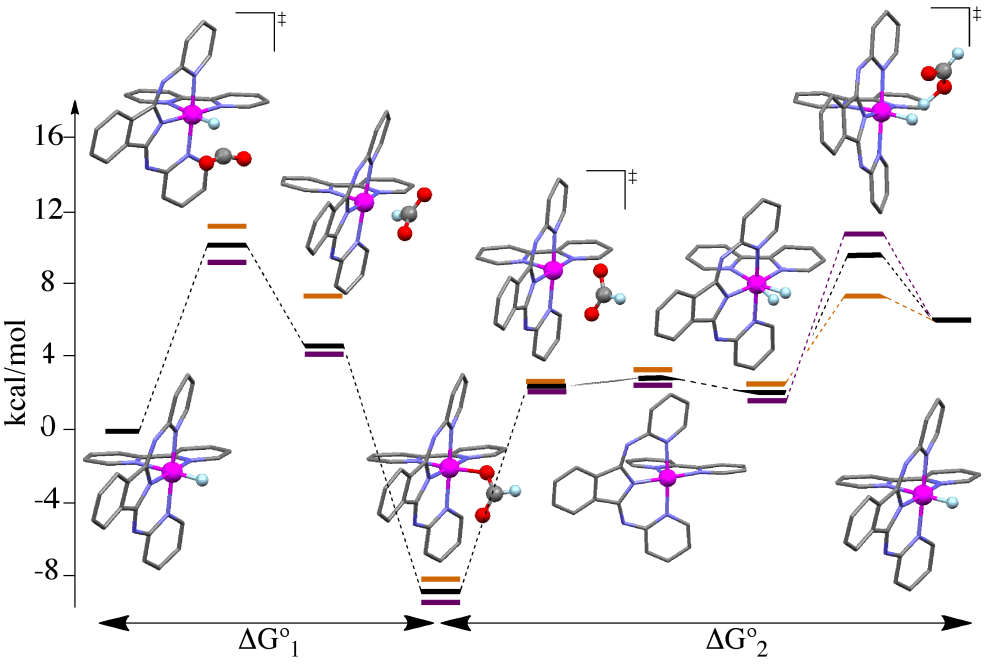

Figure 6. DFT computed potential energy profile (free energy) in kcal/mol for the cycle of the catalytic systems based on **1** (black lines)**, 1d** (purple lines) and **1w** (orange lines). For comparison purposes all energies of Ru-H species have been set as 0.

For the last step (IV), the role of the amine has also been considered. The amine could directly intervene as X in the transition state in equations IVa-x and IVb-x. In all cases, the energies for IVa-N where greater than the corresponding to IVa-O. Alternatively, the calculations indicate that the amine acts as thermodynamic driving force stabilising the final product by 4.85 kcal/mol as exemplified in the following equation:

$$[\text{Ru-H--H--OCHO}]^{\neq} + \text{NMe}_3 \rightarrow [\text{Ru-H}] + [\text{HCOO}][\text{HNMe}_3] \qquad \text{(IVb-ON)}$$

The free energies of steps I-IV for all the catalytic systems under study are summarized in Table 3.

Table 2. Gibbs Free energies at the M06L DFT level of theory of the different steps in the catalytic cycle, kcal ·mol^{-1}, for catalytic systems based on **1**, **1d**, **1d'**,**1w**,**1w'** and **2**.

catalyst precursor	1w	1	1d	2	1w'	1d'
I	27.53	27.48	26.80	24.30	26.82	29,25
II	-8.78	-9.39	-9.60	-9.78	-7.70	-11.66
IIa	*11.12*	*10.19*	*9.00*	*12.23*	*10.93*	*7.3*
IIb	*-4.32*	*-5.91*	-4.93	*-1.07*	*-4.79*	*-6.33*
IIc	*-15.58*	*-13.67*	*-13.68*	*-20.94*	*-13.83*	*-12.63*
III	12.00	11.03	10.45	22.62	13.23	10.60
IIIa	*11.47*	*11.75*	---	---	*11.28*	---
IIIb	*1.27*	*0.28*	---	---	*0.76*	---
IIIc	*-0.74*	*-1.00*	*-0.72*	*-1.05*	*1.19*	*0.24*
IV-O	3.04	4.62	5.41	-4.70	0.72	7.31
IVa O	*4.57*	*7.97*	*9.55*	*2.53*	*5.90*	*8.84*
IVb O	*-1.53*	*-3.35*	*-4.14*	*-7.23*	*-5.18*	*-1.52*
IV-ON	-1.81	-0.23	0.57	-9.54	-4.13	2.47
IV-N	1,80	3.38	3.48	-5.94	-1.14	3,43
IVa N	*8.44*	*8.78*	*9.88*	*7.42*	*6.06*	*9.42*
IVb N	*6.64*	*-5.40*	*-5.71*	*-13.36*	*-6.58*	*-3.35*
$\Delta G^{\neq}_1$	11.12	10.19	9.00	12.23	10.24	7.3
$\Delta G^{\neq}_2$	16.56	19.00	22.00	25.16	19,13	19.43

As a general trend, the catalysts containing ligands with more electron donor nature yield more reactive hydride species, with less energy demanding barriers for step IIa. As would be expected, these catalysts also favour the formato ligand substitution by dihydrogen (corresponding to step III). Accordingly, the catalytic systems with electron acceptor ligands favour the heterolytic cleavage assisted by the formato anion in IVa-O.

The electronic differences of the systems derived from **1, 1d, 1d', 1w** and **1w'** gain in significance in the last step (IV). The presence of electron-withdrawing groups on **1w** and **1w'** induce considerably large energy stabilization of the transition state for the heterolytic cleavage step IVa-O (ca. 3.5 kcal/mol lower in **1w** with respect to **1**). Accordingly, the presence of electron donor groups in **1d** and **1d'** result in more energetically demanding transition states (**1d** has an energetic barrier 1 kcal/mol higher than that of **1**). These differences have a direct impact on the rate determining

step ($\Delta G^{o\neq}_2$ = III + IVa-O). These results are in good agreement with the experimental data previously discussed.

The presence of the substituents on **1d** and **1w** have a stronger effect on $\Delta G^{o\neq}_2$ than in **1d'** and **1w'**. In the latter cases, the influence of the substituents on the R_2-*bpy* ligands on step III is fully contrarested in step IVa-O, resulting in $\Delta G^{\neq}_2$ values almost equal to those of **1**.

Significant differences can be observed between systems **1** and **2** in Table 2. Summarizing, the presence of less electron rich ligands in catalyst **2** makes the corresponding Ru-H hydride species less reactive with CO_2. Therefore, **2** presents the higher energetic barriers for IIa ($\Delta G^{\neq}_1$ = 12.23). This result is consistent with the previously reported high stability of the hydride species.[9-11] Moreover, the substitution of the formato ligand by neutral dihydrogen to afford the Ru-H_2 species (step III) requires 12.59 kcal/mol more for the catalytic system of **2** than for **1**. System **2** presents the less energy demanding barrier for step IVa-O (only 2.53 kcal/mol). Despite of its highly favored dihydrogen heterolytic cleavage, the computed rds ($\Delta G^{\neq}_2$ = III + IVa-O) for the catalytic system **2** is substantially more energetically demanding than that of **1**. Thus, a drastically slower performance of this catalyst would be expected, as it is observed experimentally.

Few thorough theoretical studies can be found in the literature regarding Ru catalysts for hydrogenative reduction of CO_2.[13-18] Most of the catalysts previously studied contain phosphine ligands and present distinct geometries and/or different number of labile ligands (active sites) than the ones reported herein. Since the species to intervene in the respective catalytic cycles are $Ru(H)_2$, no direct comparison of the catalytic activation barriers is possible.

5.2.4. Conclusions

We have prepared and thoroughly characterised a family of mononuclear complexes of general formula $[Ru(T)(bpy)(Cl)]^n$ (T: tridentate meridional ligand *trpy* or *bid*$^-$; *bpy*: bidentated ligand 4,4'-R_2-2,2'-bipyridine , where R = H, COOEt or OEt; n = charge ranging from 0 to +1). The ligands of these non-phosphine-containing ruthenium

polypyridyl compounds have been sequentially modified maintaining the essential structure. The electronic properties of the catalyst have been tuned in a controlled manner by the addition of functional groups. The resulted complexes have proven to be active as catalyst's precursors for the hydrogenative reduction of CO_2 yielding formic acid. Their catalytic mechanism has been studied by DFT and has allowed to understand the relationship between the ligands that constitute the catalysts and their performance. In the case of **1** the functionalization of the polypyridyl ligands have a direct influence on the velocity of the catalytic process. The present work constitutes an example of how phosphine-free mononuclear ruthenium complexes with the right ligand design can successfully catalyse the hydrogenative reduction of CO_2 . Moreover, it proves that theory can be used to understand the catalyst's performance and can allow to envision the design of future active catalysts.

5.2.5. Acknowledgements

Support from ACS (PRF 46819-AC3), MEC ((CTQ2010-21497) and from the Consolider Ingenio 2010 (CSD2006-0003) are gratefully acknowledged. NP is grateful for a MICINN doctoral grant.

The synthesis, characterization and crystalization of the precatalysts reported in this work was carried out by Lydia Vaquer and Takashi Ono as part of their PhD in Dr. Llobet's group.

5.2.6. References

[1] M. R. Raupach, G. Marland, P. Ciais, C. Le Quere, J. G. Canadell, G. Klepper and C. B. Filed, *Proc. Natl. Acad. Sci. U. S. A.* **2007**, *104*, 10288-10293.

[2] J. G. Canadell, C. Le Quere, M. R. Raupach, C. B. Field, E. T. Buitenhuis, P. Ciais, T. J. Conway, N. P. Gillett, R. A. Houghton and G. Marland, *Proc. Natl. Acad. Sci. U. S. A.* **2007**, *104*, 18866-18870, S18866/18861-S18866/18865.

[3] T. R. Karl and K. E. Trenberth, *Science (Washington, DC, U. S.)* **2003**, *302*, 1719-1723.

[4] P. G. Jessop, *Handb. Homogeneous Hydrogenation* **2007**, *1*, 489-511.

[5] P. G. Jessop, F. Joo and C.-C. Tai, *Coord. Chem. Rev.* **2004**, *248*, 2425-2442.

[6] C. Federsel, R. Jackstell and M. Beller, *Angew. Chem., Int. Ed.* **2010**, *49*, 6254-6257.

[7] Y. Himeda, N. Onozawa-Komatsuzaki, H. Sugihara and K. Kasuga, *Organometallics* **2007**, *26*, 702-712.
[8] S. C. Rasmussen, S. E. Ronco, D. A. Mlsna, M. A. Billadeau, W. T. Pennington, J. W. Kolis and J. D. Petersen, *Inorg. Chem.* **1995**, *34*, 821-829.
[9] C. Creutz, M. H. Chou, H. Hou and J. T. Muckerman, *Inorg. Chem. (Washington, DC, U. S.)* **2010**, *49*, 9809-9822.
[10] C. Creutz and M. H. Chou, *J. Am. Chem. Soc.* **2007**, *129*, 10108-10109.
[11] C. Creutz and M. H. Chou, *J. Am. Chem. Soc.* **2009**, *131*, 2794-2795.
[12] H. Konno, A. Kobayashi, K. Sakamoto, F. Fagalde, N. E. Katz, H. Saitoh and O. Ishitani, *Inorg. Chim. Acta* **2000**, *299*, 155-163.
[13] A. Urakawa, M. Iannuzzi, J. Hutter and A. Baiker, *Chem.--Eur. J.* **2007**, *13*, 6828-6840.
[14] A. Urakawa, F. Jutz, G. Laurenczy and A. Baiker, *Chem.--Eur. J.* **2007**, *13*, 3886-3899.
[15] M. S. G. Ahlquist, *J. Mol. Catal. A: Chem.* **2010**, *324*, 3-8.
[16] Y. Musashi and S. Sakaki, *J. Am. Chem. Soc.* **2000**, *122*, 3867-3877.
[17] Y. Musashi and S. Sakaki, *J. Am. Chem. Soc.* **2002**, *124*, 7588-7603.
[18] Y. Ohnishi, T. Matsunaga, Y. Nakao, H. Sato and S. Sakaki, *J. Am. Chem. Soc.* **2005**, *127*, 4021-4032.
[19] C. Sens, I. Romero, M. Rodriguez, A. Llobet, T. Parella and J. Benet-Buchholz, *J. Am. Chem. Soc.* **2004**, *126*, 7798-7799.

Chapter 6

Summary and Conclusions

Specific points for each project developed along this thesis as well as general conclusions are presented in this chapter.

SUMMARY AND CONCLUSIONS

Chapter 3

- A new family of dinuclear Ru(II) complexes containing the tetra-dentate dinucleating ligand *bpp*$^-$, of general formula *in,in*-[{Ru^{II}(T)(L)}$_2$(μ-bpp)]$^{(n+1)+}$ (T= *trpy* or *bid* tridentated meridional ligands; *bpp*=tetradentate bridging ligand and L=MeCN or pyridine type monodentated ligands, n=1 or 3), have been prepared and structurally, spectroscopically and electrochemically characterized.

- These dinuclear molecules present a dynamic process, based on a synchronised twisting motion, due to the steric hindrance between the monodentated ligands bound to the metal centres that force a distortion of the preferred octahedral coordination geometry. The rates of these dynamic processes have been investigated by VT-^{1}H-NMR and QM/MM calculations.

- The velocity of the process is chiefly governed by the monodentated ligands . The combination of the Ru-N bond strength (N being the binding site of the monodentated ligands) added to the relative steric constrain of the monodentated ligands dictates the interconversion energetic barriers. To a lesser extent, the nature of the meridional ligand also influences the process. The compounds containing the more flexible *bid*$^-$ ligand being energetically less demanding than those containing the rigid *trpy*.

- The through space interactions described above have direct influence on the ligand exchange processes of these complexes. That has been demonstrated by UV-vis kinetic studies following the ligand exchange process of the monodentated pyridine type of ligands by acetonitrile.

- Both, the QM/MM calculated activation barriers and experimental ligand dissociation kinetics for compound *in,in*-[{Ru^{II}(trpy)(3,5-Me_2-pyr)}$_2$(μ-bpp)]$^{3+}$ agree with an attractive π-π stacking interaction between the two lutidine ligands. This supramolecular attractive interaction is responsible for the higher ligand substitution barrier encountered for this compound with regard to its

analogous compound $[\{Ru^{II}(trpy)(pyr)\}_2(\mu\text{-}bpp)]^{3+}$ containing the less sterically demanding pyridine as monodentated ligand.

Chapter 4

- The new tridentated meridional ligand 5-([2,2':6',2''-terpyridin]-4'-yl)-2-methylbenzene-1,3-disulfonate (*trpy**) containing two sulfonate functionalities has been prepared. This new ligand has been used in the synthesis of the following ruthenium complexes: $[Ru^{III}(Cl)_3(trpy^*)]$, $[Ru^{ii}(trpy^*)_2]Na_2$ and *in,in*-$[\{Ru^{II}(trpy^*)\}_2(\mu\text{-}O_2CMe)(\mu\text{-}bpp)](Na)_2$.

- The presence of the negatively charged sulfonate functionalities on the ruthenium complexes originates a negative shift of the redox potentials.

- In the case of the *in,in*-$[\{Ru^{II}(trpy^*)\}_2(\mu\text{-}O_2CMe)(\mu\text{-}bpp)](Na)_2$ dinuclear compound CV in pH=1 reveals a need of higher applied voltage for water oxidation (100 mV higher than those of $[\{Ru^{II}(trpy)(H_2O)\}_2(\mu\text{-}bpp)]^{3+}$) in homogeneous phase. Anchoring this compound on anatase surfaces, results on further down shift of the redox potentials to the extent that the oxidation state IV,IV is no longer active for water oxidation. However, this oxidation state is able to catalyse the oxidation of organic substrates such as EtOH.

- The electronic structure of the *cis*-$[Ru^{II}(Bpy)_2(H_2O)_2]^{2+}$ water oxidation catalyst and its *trans* isomer in their different oxidation states have been studied by theoretical calculations at the DFT and CASPT2 levels of theory. The computational results are in concordance with the experimental data acquired by EPR and XAS spectroscopies.

- The mechanism of the *cis/ trans* isomerization process experimented for this system has been elucidated by DFT /TDDFT techniques. Photo irradiation of the singlet ground state of the *cis* isomer leads, through intersystem crossing, to a triplet state which is responsible for the *aquo* ligand decoordination and consecutive isomerization.

Chapter 5

- A new family of mononuclear ruthenium polypyridyl complexes with general formula [Ru(T)(B)(Cl)] (T = meridional tridentate ligand, B = bidentate ligand) have been tested as catalyst precursors in the hydrogenative reduction of CO_2 to formic acid. Their most plausible mechanism has been investigated at the M06L DFT level of theory.

- The catalytic performances of these complexes are directly related to the ligands bound to the metal centre. Two crucial steps govern the overall rate of the catalytic process. First, the substitution of the anionic formato ligand, which is favoured in complexes with electron donor ligands. Secondly, the heterolytic cleavage of the H-H bond of the Ru-H_2 species, which is favoured by electron acceptor ligands. In the design of an active catalyst a compromise should be reached when considering the electronic nature of the ligands.

APENDIX A

EXPERIMENTAL SUPPORTING INFORMATION FOR:

Through Space Ligand Interactions in Enantiomeric Dinuclear Ru Complexes

Nora Planas, Gemma J. Christian, Elena Mas-Marza, Xavier Sala, Xavier Fontrodona, Feliu Maseras and Antoni Llobet

[a] Institute of Chemical Research of Catalonia (ICIQ), Av. Països Catalans 16, E-43007 Tarragona, Spain.

[b] Serveis Tècnics, Universitat de Girona, Campus de Montilivi, E-17071 Girona, Spain.

[c] Departament de Química, Universitat Autònoma de Barcelona, Cerdanyola del Vallès, E-08193 Barcelona, Spain.

The supporting information section also includes "cif" magnetic files of the crystal structures of complex 3.

I. Synthesis and characterization

I-I Materials

All reagents used in present work were obtained from Aldrich Chemical Co. or Alfa Aesar and were used without further purification. Reagent grade organic solvents were obtained from SDS and were routinely degassed with Argon. Methanol was destilled over MgI and DCM, hexane and diethyl ether were used from the SPS. High purity deionized water was obtained by passing distilled water through a nanopure Mili-Q water purification system.

I-II Preparations

The 3,5-bis(2-pyridyl)pirazole[S1] (Hbpp) and 1,3-Bis(2-pyridylimino)isoindoline[S2] (Hbid) ligands, the starting complex $[Ru^{III}Cl_3(Hbid)]$[S3] and complex $[Ru^{II}_2(\mu\text{–}O_2CMe)(trpy)_2(bpp)](PF_6)_2$, **7**, and $[Ru^{II}_2(trpy)_2(bpp)(H_2O)_2](PF_6)_2$, **8**,[S4] were prepared as described in the literature. All synthetic manipulations were routinely performed under argon atmosphere using Schlenck and vacuum line techniques. All NMR resonances were assigned using the labelling scheme shown in figure S1.

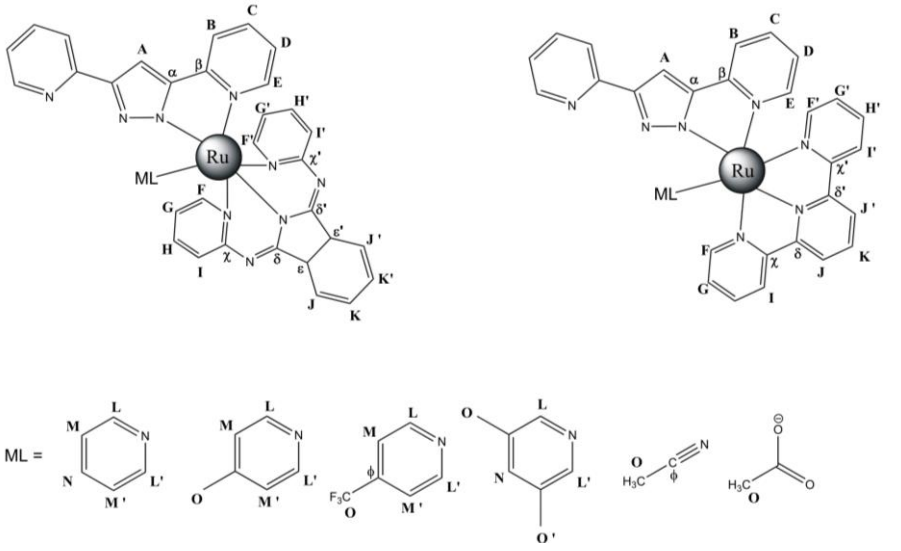

Figure S1.

{[Ru(bid)]$_2$(μ-bpp)(μ-MeCOO)}·CHCl$_3$ (1). A solution of 66 mg of $RuCl_3(Hbid)$[i] (0.11 mmols) and 45 mL of NEt_3 (0.33 mmols) in MeOH (5 mL) was stirred for 30 min at RT under argon atmosphere in the absence of light. A 12.7 mg sample of Hbpp (0.054mmols) with 32 mg of NaOMe (0.059 mmols) and 96 mg of LiCl (2.26 mmols) were added to the initial mixture in 5 mL of MeOH. The resulting solution was heated at reflux for 2 h in the presence of a 200 W tungsten lamp. When cooled to room temperature and filtered off, 50 mg of a dark green solid was obtained. This solid dissolved in dichloromethane (5 mL) was added to a solution of 0.411 g of anhydrous sodium acetate in methanol (100 mL) and the resulting solution was heated at reflux for 2 h. Upon cooling to room temperature, the unreacted starting material was filtered and the methanol solution evaporated to dryness. The green product obtained was then dissolved in dichloromethane and the insoluble sodium acetate was filtered. The dichloromethane solution was evaporated to dryness and the light green solid attained was washed with hexane and dried under vacuum. Yield: 52% (0.035 g). Anal. Calc. for $C_{52}H_{41}Cl_3N_{14}O_2Ru_2$: C, 51.94; H, 3.44; N, 16.31. Found: C, 52.12; H, 3.23; N, 16.18. ^{1}H-RMN (400 MHz, DCM-d, 298K, ppm): δ, 0.55(s, 3H, H_O), 6.09 (t, J_{FG}=J_{GH}= 6.18 Hz, 4H, H_H), 6.52(t, J_{CD}=J_{DE}=7.77 Hz, 2H, H_D), 7.19(d, J_{DE}=7.77 Hz, 2H, H_E), 7.45 (t, J_{BC}=J_{CD}= 7.77 Hz, 2H, H_C), 7.45(t, J_{GH}=J_{HI}=6.18 Hz, 4H, H_H), 7.52(d, J_{HI}=6.18 Hz, 4H, H_I), 7.62(dd, J_{JK}= 5.34, $J_{JK'}$= 3.06 Hz ,4H, H_K), 7.88(d, J_{BC}= 7.77 Hz, 2H, H_B), 7.96 (s, 1H, H_A), 8.04 (d, J_{FG}= 6.18 Hz , 4H, H_F), 8.17(dd, J_{JK}= 5.34, $J_{JK'}$= 3.06 Hz, 4H, H_J). MALDI(+)-MS (MeOH): 1079 M+

{[Ru(bid)(py)]$_2$(μ-bpp)}(Cl)·CHCl$_3$ (2). This complex was prepared in the same manner as 1, except that the dark green solid was mixed in 100 mL of chloroform containing 0.40 mL of pyridine. The resulting solution was heated at reflux during 4 h. After cooling to room temperature the solvent volume was reduced to 10 ml. Then, 40 mL of diethyl ether were added slowly and the resulting solution was kept in the fridge for 3 hours. The dark green precipitate obtained was filtered, washed

with more diethyl ether and dried under vacuum. Yield: 68% (0.048 g). Anal. Calc. for $C_{60}H_{48}Cl_4N_{17}Ru_2$: C, 53.90; H, 3.62; N, 16.76. Found: C, 53.83; H, 3.84; N, 16.80. ^{1}H-RMN (500 MHz, DCM-d, 298K, ppm): δ, 5.74(t, J_{ML}=J_{MN}= 6.79 Hz, 4H, H_M), 6.68 (t, J_{CD}=J_{ED}= 5.85 Hz, 4H, H_D), 6.69(t, J_{GH}=J_{FG}= 6.01 Hz, 2H, H_G), 6.81(t, J_{MN}= 6.79 Hz, 2H, H_N), 6.85(d, J_{ML}= 6.79 Hz, 4H, H_L), 7.07(d, J_{ED}= 5.85 Hz, 2H, H_E), 7.55 (dd, J_{JK}= 5.29, $J_{JK'}$= 3.15 Hz, 4H, 4H, H_K), 7.61 (d, 4H, J_{HI}= 8.02 Hz, H_I), 7.68(t, J_{CD}=J_{EC}= 5.85 Hz, 2H, H_C), 7.70(dd, , J_{HI}= 8.02 Hz, J_{GH}= 6.01 Hz, 4H, H_H), 8.00(dd, J_{JK}= 5.29, $J_{K'J}$= 3.15 Hz, 4H, H_J), 8.21(d, J_{BC}= 8.0 Hz, 2H, H_B), 8.37(d, J_{FG}= 6.01 Hz, 4H, H_F), 8.45(s, 1H, H_A). MALDI(+)-MS (DCM): 1020 [M-Cl-2Pyridine]+, 1055 [M -2Pyridine]+, 1099 [M - NO_3-Pyridine]+

{[Ru(bid)(4-Me-py)]$_2$(μ-bpp)}(NO_3)·$CHCl_3$ (3) This complex was prepared following the same procedure as for **2**, except that that picoline instead of pyridine was used as monodentate ligand and that before reducing the volume of chloroform of 0.010 g of $NaNO_3$ were added to the solution. Recrystallization from Dichloromethane/Ether yield black small crystals suitable for X-ray spectroscopy. Yield: 77% (0.060 g). Anal. Calc. for $C_{62}H_{52}Cl_4N_{16}Ru_2$: C, 54.55; H, 3.84; N, 16.42. Found: C, 54.20; H, 4.06; N, 16.45. ^{1}H-RMN (500MHz, DCM-d, 298K, ppm): δ, 1.74(s, 6H ,H_O), 5.56(d, J_{ML}=6.16 Hz, 4H, H_M), 6.66(d, J_{LM}=6.16 Hz, 4H,H_L), 6.67(t, J_{CD}=J_{CD}= 8.35 Hz, 2H,H_D), 6.67(t, J_{FG}=J_{GH}= 8.42 Hz, 4H, H_D), 7.00(d, J_{DE}= 8.42 Hz, 2H, H_E), 7.56(dd, J_{JK}=5.43, $J_{JK'}$= 2.95 Hz, 4H, Hh), 7.63 (d, J_{HI}= 8.42 Hz, 4H, H_I), 7.66 (t, J_{BC}=J_{CD} = 8.35 Hz, 2H, H_C), 7.71(t, 4H, J_{HG}=J_{HI}= 8.42 Hz, H_H), 8.01(dd, J_{JK}=5.43, $J_{JK'}$= 2.95 Hz 4H, H_J), 8.26(d, J_{BC}= 8.35 Hz, 2H, H_B), 8.42(d, J_{FG}= 8.42 Hz, 4H, H_F), 8.61(s, 1H, H_A). MALDI(+)-MS (DCM): 1020 [M-NO_3-2Picoline]+

{[Ru(bid)(3,5-(Me)$_2$-py)]$_2$(μ-bpp)}(NO_3)·$2CH_2Cl_2$ (4) This complex was prepared in the same manner as **3**, except that lutidine instead of picoline was used as monodentate ligand and dichloromethane instead of chloroform was used as

solvent. Yield: 64% (0.050g). Anal. Calc. for $C_{65}H_{59}Cl_4N_{17}O_3Ru_2$: C, 53.10; H, 4.04; N, 16.20. Found: C, 53.39; H, 3.98; N, 15.99. ^{1}H-RMN (500 MHz, DCM-d, 208K, ppm): δ, 0.78(s, 6H, H_O), 1.15(s, 6H, $H_{O'}$), 5.43 (s, 2H, H_V), 6.31(s, 2H, H_M), 6.46(t, J_{GH}=J_{FG}=5.63 Hz, 2H, H_G), 6.62(t, J_{CD}=J_{ED}=6.26 Hz, 2H, H_D), 6.98(d, J_{DE}=6.26 Hz, 2H, H_E), 7.00(t, $J_{F'G'}$=$J_{G'H'}$=5.82 H, 2H, $H_{G'}$), 7.04(s, 2H, $H_{L'}$), 7.37 (d, $J_{F'G'}$= 5.82 Hz, 2H, $H_{F'}$), 7.43 (d, $J_{H'I'}$=8.26 H, 2H, $H_{I'}$), 7.50(t, $J_{KK'}$=$J_{J'K'}$'=8.26 Hz, 2H, $H_{K'}$), 7.57(t, J_{KJ}=$J_{JK'}$= 8.26 Hz, 2H, $H_{K'}$), 7.66(t, J_{BC}=J_{CD}= 6.26 Hz, 2H, H_C), 7.68(t, J_{HI}=J_{GH}= 5.63 Hz, 2H,H_H), 7.77(d, J_{HI}= 5.63 Hz, 2H, H_I), 7.78 (d, $J_{J'K'}$=8.26 Hz , 2H, $H_{J'}$), 7,80 (dd, $J_{H'I'}$=8.26, $J_{G'H'}$=5.82 Hz, 2H, $H_{H'}$), 8.07 (d, J_{JK}= 8.26 Hz, 2H, H_J), 8.13(d, J_{BC}= 6.26 Hz, 2H, H_B), 8.36(s, 1H, H_A), 9.39(d, J_{FG}=5.63 Hz, 2H, H_F). MALDI(+)-MS (DCM): 1020 [M-NO_3-2Lutidine]+

{[Ru(bid)(4-CF_3-py)]$_2$(μ-bpp)}(NO_3) (5) This compound was prepared in a similar manner of **2-4**. The dark green solid was mixed in 20 mL of dichloromethane with 0.54 mL of 4-trifluoromethyl pyridine and stirred at room temperature during 30 min. Then the reacting mixture was heated to reflux during 3 h. Upon cooling to room temperature, 0.007g of $AgNO_3$ were added and the white precipitate formed (AgCl) was filtered. The mother liquor solution was reduced to 8 mL and SPS dry hexane was added dropwise until the first precipitate appeared. After 4 h at 4 ºC the dark green solid obtained was filtered, washed with diethyl ether and dried under vacuum. Yield: 68 % (0.050g). ^{1}H-RMN (500 MHz, DCM-d, 298K, ppm): δ, 5.89(d, J_{ML}=6.60 Hz, 4H, H_M), 6.74(t, J_{GH}= 8.57 Hz, 4H, H_G), 6.75 (t, J_{CD}=J_{DE}= 7.97 Hz 2H, H_D), 7.11(d, J_{ED}= 7.97 Hz 2H, H_E), 7.20(d, J_{ML}=6.60 Hz , 4H, H_L), 7.59(dd, J_{JK}= 5.85, $J_{JK'}$= 3.04 Hz, 4H, H_H), 7.65 (d, J_{HI}=8.57 Hz , 4H, H_I), 7.73(t, J_{CD}= J_{BC}=7.97 Hz, 2H, H_C), 7.75(t, J_{GH}=J_{HI}=8.57 Hz, 4H, H_H), 8.03(dd, J_{JK}= 5.85, $J_{JK'}$= 3.04 Hz, 4H, H_J), 8.26(d, J_{BC}=7.97 Hz , 2H, H_B), 8.46(s, 1H, H_A). MALDI(+)-MS (DCM): 1020 [M-NO_3-2CF_3-pyridine]+

{[Ru(bid)(Me-CN)]$_2$(μ-bpp)}(NO$_3$)·CH$_2$Cl$_2$ (6). For the synthesis of this complex differently from 1-5 the dark green solid was dissolved 0.054 g in 50 mL of acetonitrile and heated at reflux for 4 h. The resulting solution was cooled to room temperature and the volume reduced to 20 mL in the rotary evaporator. Then, 1 mL of a 5M acetonitrile solution of $NaNO_3$ was added. Diethyl ether was then introduced dropwise until the first precipitate appeared and the solution was left at 4ºC overnight. The dark purple solid obtained was filtered, washed with diethyl ether and dried under vacuum. Yield: 70% (0.052 g). Anal. Calc. for $C_{54}H_{45}Cl_2N_{17}O_3Ru_2$: C, 51.76; H, 3.62; N, 19.10. Found: C, 52.00; H, 3.21; N, 19.10. ^{1}H-RMN (500MHz, DCM-d_2 230 K, ppm): δ, 1.01 (s, 6H, H_O), 5.66(td, J_{FG}= 6.36, J_{HI}= 1.14 Hz, 2H ,H_G), 6.67(dd, $J_{F'G'}$= 7.50, $J_{H'F'}$= 1.56 Hz , 2H, HF'), 6.79(td, $J_{F'L'}$ =$J_{G'H'}$=7.50, $J_{G'I'}$= 1.79 Hz, 2H, $H_{G'}$), 6.82(t, J_{CD}=J_{DE}=5.92 Hz, 2H, H_D), 7.35(d, J_{DE}=5.92 Hz, 2H, H_E), 7.49(td, J_{GH}= J_{HI} =6.36, J_{FH}= 1.22 Hz, 2H, H_H), 7.56 (dd, J_{IH} =6.36, J_{GI}= 1.70 Hz, 2H, H_I), 7.66(dd, J_{BC}=7.00, J_{CD}= 5.92 Hz, 2H, H_C), 7.68(dd, $J_{H'I'}$= 7.50, $J_{G'I'}$= 1.79 Hz, 2H, $H_{I'}$), 7.70 (dd, J_{JK}= 4.08, J_{JK}'= 2.92 Hz, 4H, H_J, $H_{J'}$), 7.75 (d, $J_{H'I'}$=$J_{G'H'}$=7.50, $J_{F'H'}$= 1.56 Hz, 2H, $H_{H'}$), 7.96(d, J_{BC}=7.00 Hz, 2H, H_B), 8.00(s, 1H, H_A), 8.15(dt, J_{JK}= 4.08, $J_{KK'}$=$J_{JK'}$= 2.92 Hz 2H, H_K, $H_{K'}$), 9.41(dd, J_{FG}= 6.36 , J_{FH}= 1.22 Hz ,2H, H_F). MALDI(+)-MS (MeOH):1020 [M-Cl-2CH3CN]+

{[Ru(trpy)(py)]$_2$(μ–bpp)}(PF$_6$)$_3$·CH$_2$Cl$_2$ (9) 100 mg of complex [Ru^{II}_2(μ–O_2CMe)(trpy)$_2$(bpp)](PF$_6$)$_2$ were dissolved in 40mL of acetone/water (3:1) and then 2 mL of a pH=1 water solution (triflic acid) were added. After the addition of 0.15 mL of pyridine, the mixture was heated under reflux for 6 h. Upon cooling to room temperature, the unreacted starting material was filtered and 1mL of a saturated aqueous solution of KPF_6 was added to the solution. After evaporation of the Acetone in a rotary evaporator a brown-black solid was obtained which was recrystallized from Dichloromethane/Ether yielding small black crystals. Yield: 65% (g). Anal. Calc. for $C_{54}H_{43}Cl_2F_{18}N_{12}P_3Ru_2$: C, 41.36; H, 2.76; N, 10.72. Found: C, 41.51; H, 2.46; N, 10.77. ^{1}H-RMN (400MHz, Acetone-d_6, 298 K, ppm):

δ, 6.28 (t, J_{ML}=J_{MN}=5.45 Hz, 4H, H_M), 6.98 (t, J_{DE}=J_{CD}= 7.77 Hz, 2H, H_D), 7.19 (t, J_{MN}=5.45 Hz, 2H, H_N), 7.36 (d, J_{DE}= 7.77 Hz, 2H, H_E), 7.72 (d, J_{LM}= 5.45 Hz, 4H, H_L), 7.78 (t, J_{FG}=J_{GH}= 7.85 Hz, H_G), 7.90 (t, J_{BC}=J_{CD} = 7.77 Hz, 2H, H_C), 8.16 (t, J_{GH}=J_{HI}=7.85 Hz, 4H, H_H), 8.19 (t, J_{JK}= 8.17 Hz, 2H, H_K), 8.32 (d, J_{BC}= 7.77 Hz, 2H, H_B), 8.59 (d, J_{HI}=7.85 Hz, 4H, H_I), 8.63 (d, J_{JK}= 8.17 Hz, 4H, H_J), 8.67 (d, J_{FG}= 7.85 Hz, 4H, H_F), 8.71(s, 1H, H_A). ^{13}C-RMN (400MHz, Acetone-d_6, 298 K, ppm): δ, 160.46 (C_F), 159.46 (C_L), 156.65 (C_N), 155.77 (C_M), 154.77 (C_α), 152.65 (C_δ), 150.96 (C_χ), 139.53 (C_E), 138.60 (C_K), 137.91 (C_I), 136.54 (C_D), 129.98 (C_J), 125.77 (C_B), 125.75 (C_G), 124.81 (C_β), 124.52 (C_H), 121.61 (C_C), 103.84 (C_A). MALDI(+)- MS: (MeOH):1339.2[M-PF_6]+

I-III Crystal structure determination. –

Crystals of C61 H47 N16 Ru2, N O3, were grown from acetone, and used for low temperature (100(2) K) X-ray structure determination. The measurement was carried out on a *BRUKER SMART APEX CCD* diffractometer using graphite-monochromated Mo *K*α radiation (λ = 0.71073 Å) from an x-Ray Tube. The measurements were made in the range 1.89 to 28.62° for θ. Full-sphere data collection was carried out with ω and φ scans. A total of 50710 reflections were collected of which 8314 [R(int) = 0.0929] were unique. Programs used: data collection, Smart[1]; data reduction, Saint+[2]; absorption correction, SADABS[3]. Structure solution and refinement was done using SHELXTL[4] Version 6.14 (Bruker AXS 2000-2003).

The structure was solved by direct methods and refined by full-matrix least-squares methods on F^2. The non-hydrogen atoms were refined anisotropically. The H-atoms were placed in geometrically optimized positions and forced to ride on the atom to which they are attached. Spurious electron density peaks non attributable to any solvent molecule were removed using the SQUEEZE option in PLATON[5].

Final R indices [I>2sigma(I)] R1 = 0.0440, wR2 = 0.1190

R indices (all data) R1 = 0.0509, wR2 = 0.1214

1. Bruker Advanced X-ray Solutions. SMART: Version 5.631, 1997-2002.
2. Bruker Advanced X-ray Solutions. SAINT +, Version 6.36A, 2001.
3. G. M. Sheldrick, *Empirical Absorption Correction Program*, Universität Göttingen, 1996 Bruker Advanced X-ray Solutions. SADABS Version 2.10, 2001.
4. G. M. Sheldrick, *Program for Crystal Structure Refinement*, Universität Göttingen, 1997 Bruker Advanced X-ray Solutions. SHELXTL Version 6.14, 2000-2003.
5. Spek, A. L. (2005). PLATON, A Multipurpose Crystallographic Tool, Utrecht University, Utrecht, The Netherlands

Figure S2. 1D and 2D NMR spectra (500 MHz, CD2Cl2) for complex 1 (a) ^{1}H-NMR(298K), (b) COSY(298K), (c) NOESY(298K) and (d) Variable Temperature ^{1}H-NMR

(a)

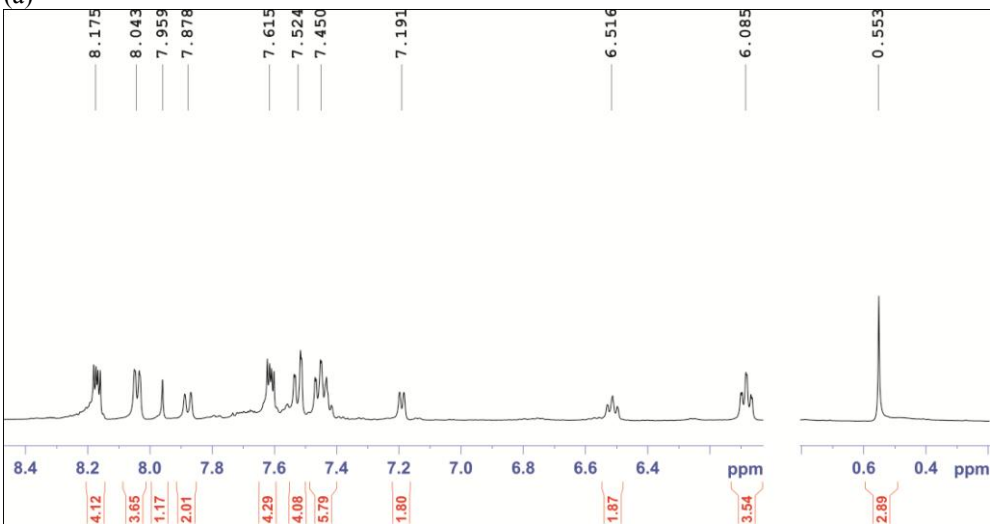

(b)

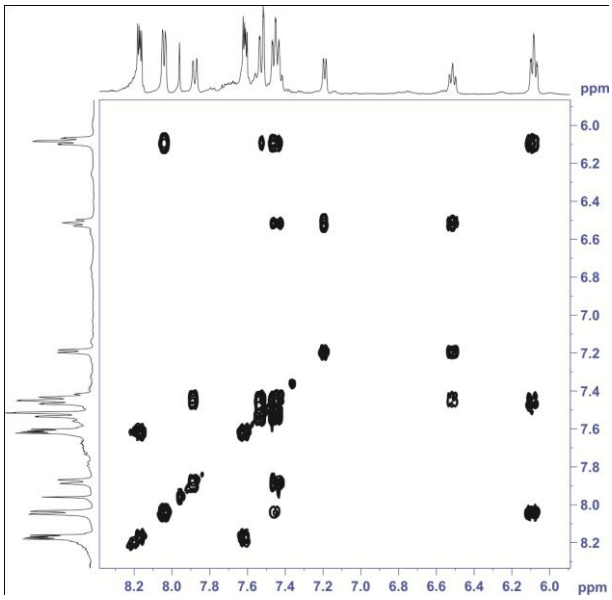

(c)

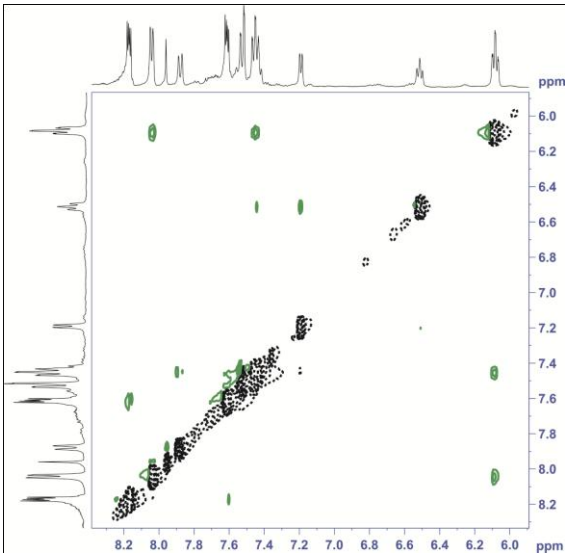
ppm
6.0
6.2
6.4
6.6
6.8
7.0
7.2
7.4
7.6
7.8
8.0
8.2
8.2 8.0 7.8 7.6 7.4 7.2 7.0 6.8 6.6 6.4 6.2 6.0 ppm

(d)

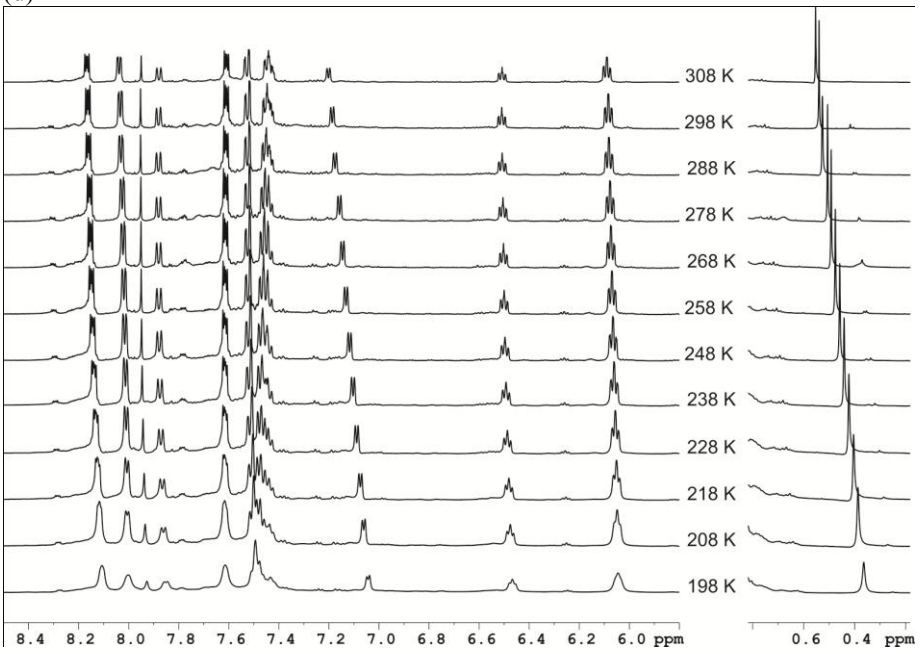
308 K
298 K
288 K
278 K
268 K
258 K
248 K
238 K
228 K
218 K
208 K
198 K
8.4 8.2 8.0 7.8 7.6 7.4 7.2 7.0 6.8 6.6 6.4 6.2 6.0 ppm
0.6 0.4 ppm

Figure S3. 1D and 2D NMR spectra (500 MHz, CD2Cl2) for complex 2 (a) 1H-NMR (298 K), (b) COSY (298 K), (c) NOESY (298 K) and (d) Variable Temperature 1H-NMR

(a)

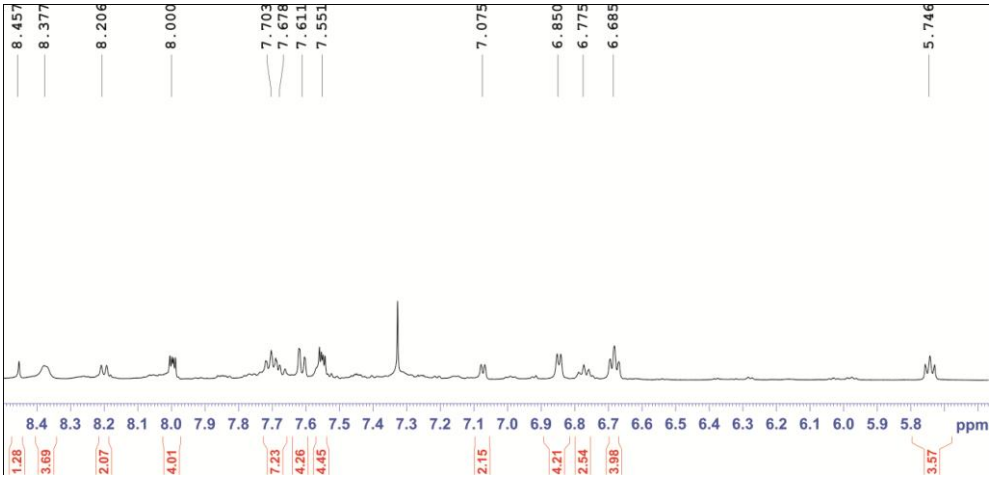

(b)

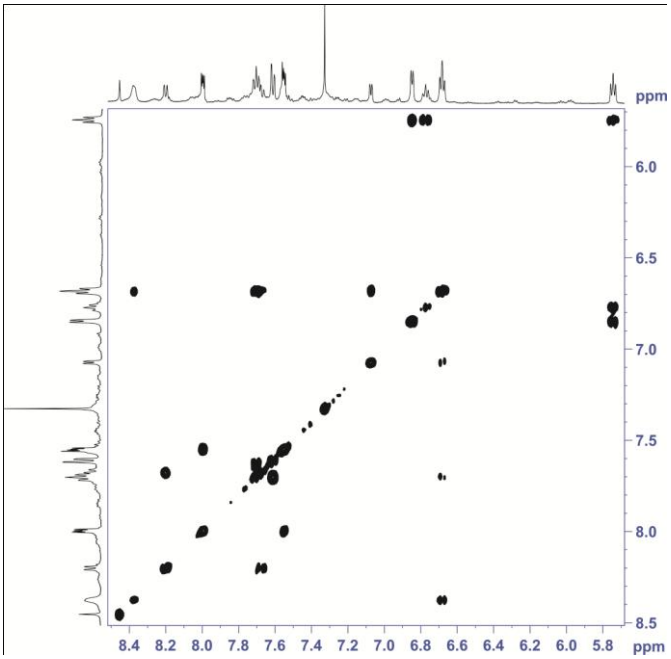

(c)

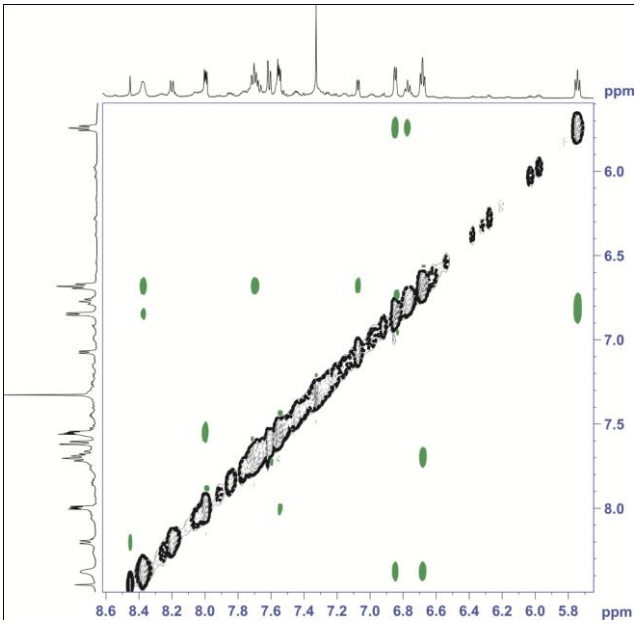
ppm
6.0
6.5
7.0
7.5
8.0
8.6 8.4 8.2 8.0 7.8 7.6 7.4 7.2 7.0 6.8 6.6 6.4 6.2 6.0 5.8
ppm

(d)

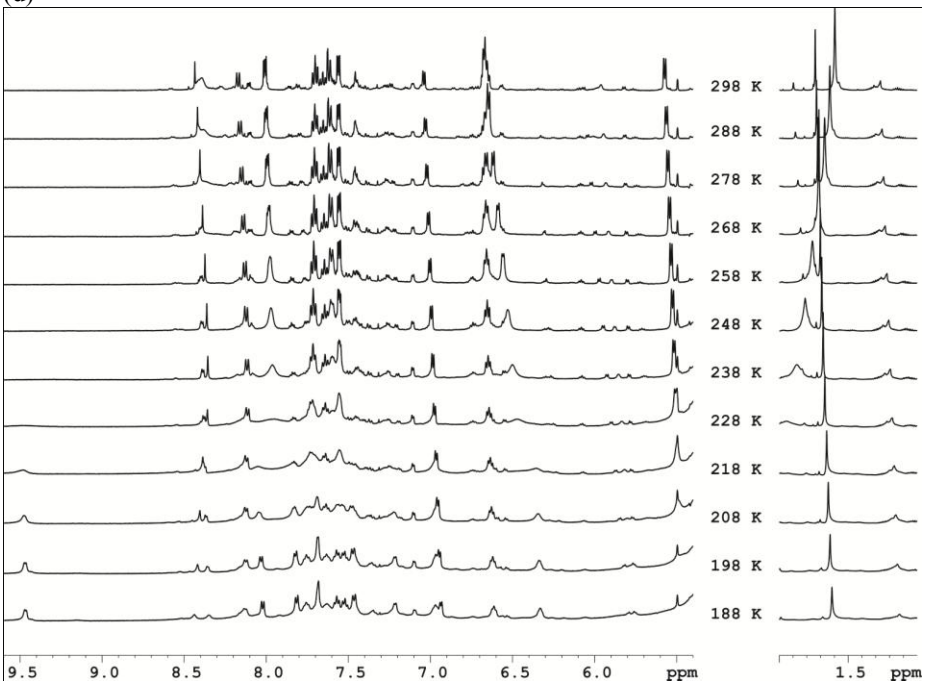
298 K
288 K
278 K
268 K
258 K
248 K
238 K
228 K
218 K
208 K
198 K
188 K
9.5 9.0 8.5 8.0 7.5 7.0 6.5 6.0 ppm
1.5 ppm

Figure S4. 1D and 2D NMR spectra (500 MHz, CD2Cl2) for complex 3 (a) 1H-NMR (298 K), (b) COSY (298 K), (c) NOESY (298 K) and (d) Variable Temperature 1HNMR

(a)

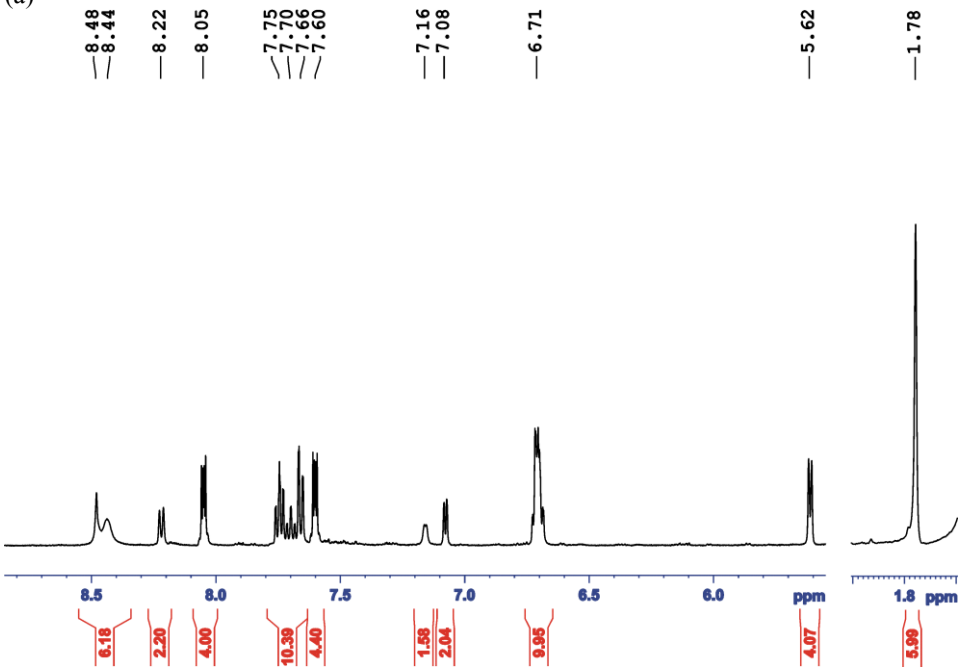

(b)

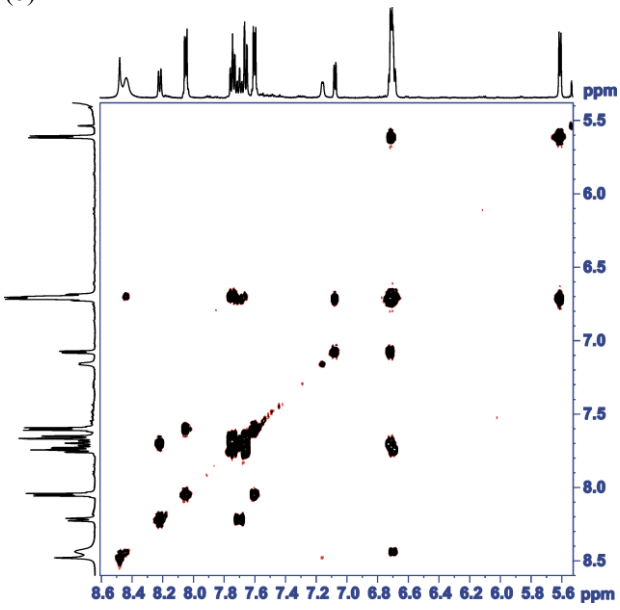

(c)

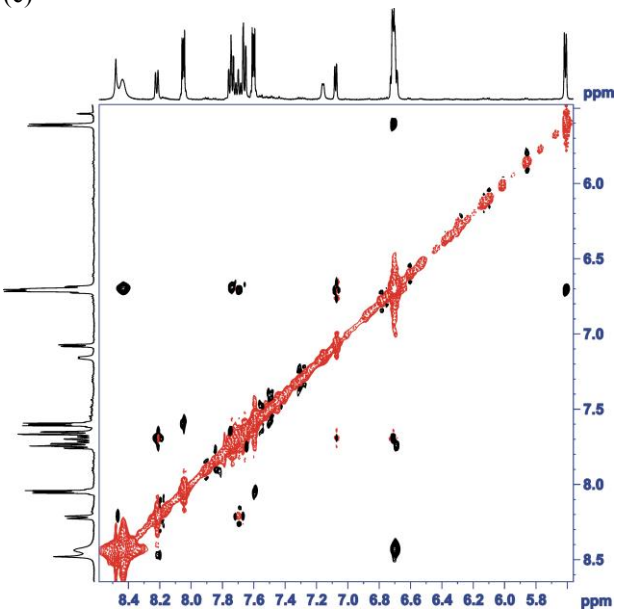
ppm
6.0
6.5
7.0
7.5
8.0
8.5
8.4 8.2 8.0 7.8 7.6 7.4 7.2 7.0 6.8 6.6 6.4 6.2 6.0 5.8
ppm

(d)

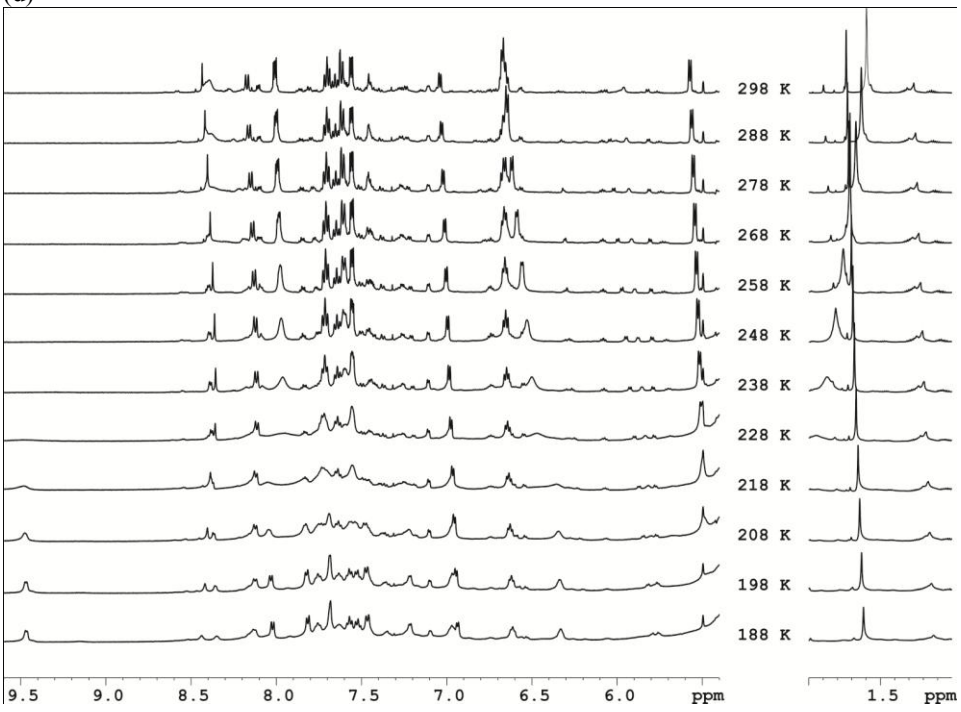
298 K
288 K
278 K
268 K
258 K
248 K
238 K
228 K
218 K
208 K
198 K
188 K
9.5 9.0 8.5 8.0 7.5 7.0 6.5 6.0 ppm
1.5 ppm

Figure S5. 1D and 2D NMR spectra (500 MHz, CD2Cl2) for complex 4 (a) 1H-NMR (208 K), (b) COSY(208 K), (c) NOESY(208 K) and (d) Variable Temperature 1HNMR

(a)

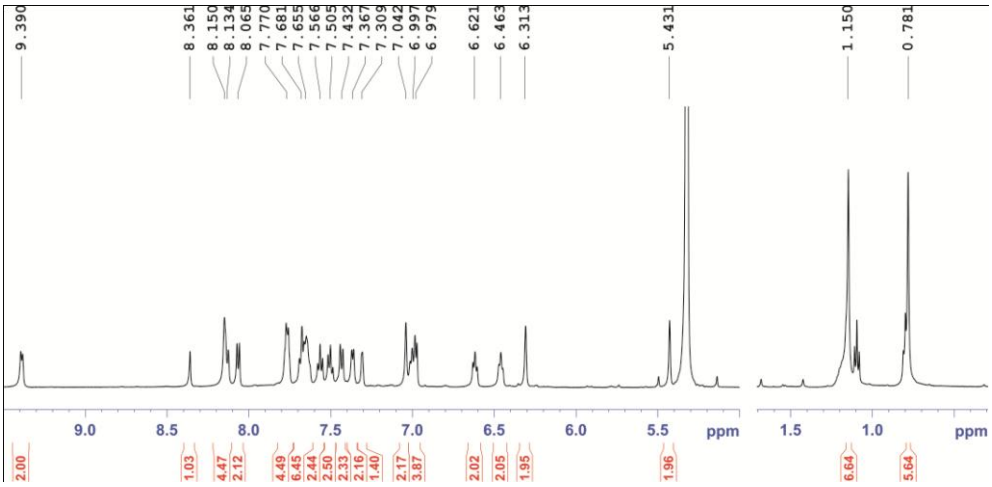

(b)

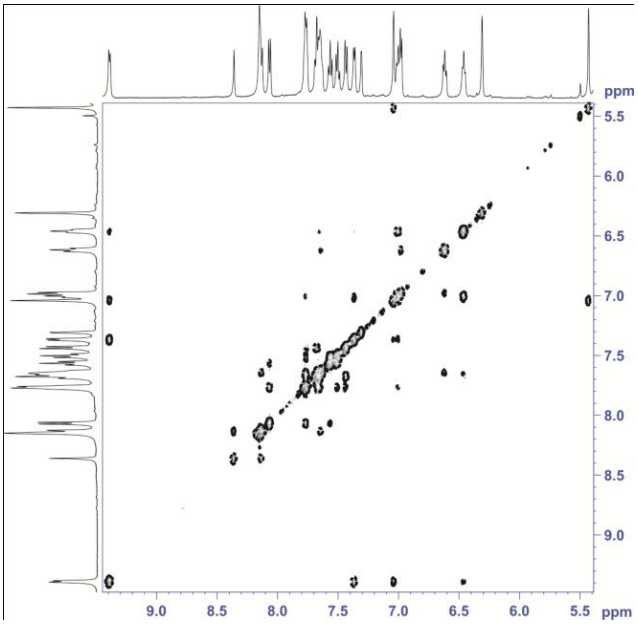

(c)

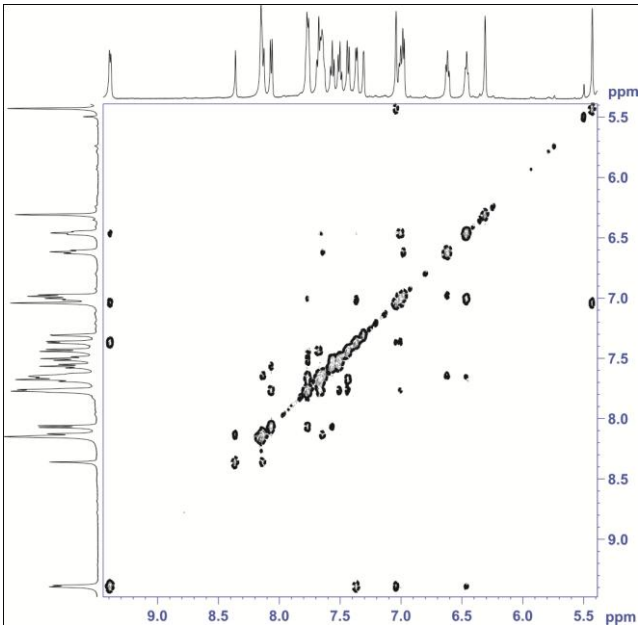
ppm
5.5
6.0
6.5
7.0
7.5
8.0
8.5
9.0
9.0
8.5
8.0
7.5
7.0
6.5
6.0
5.5
ppm

(d)

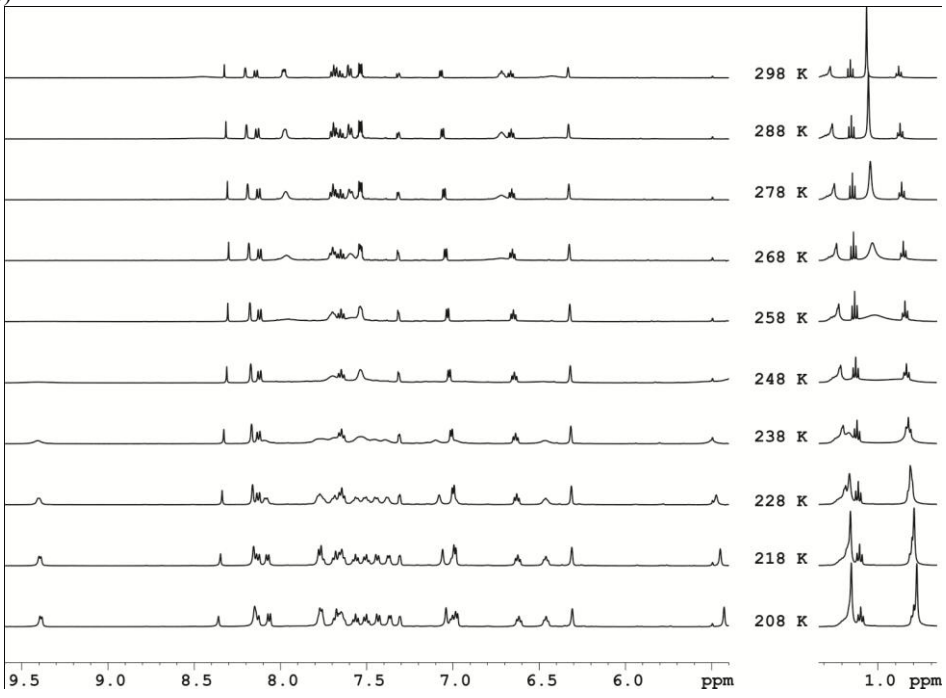
298 K
288 K
278 K
268 K
258 K
248 K
238 K
228 K
218 K
208 K
9.5
9.0
8.5
8.0
7.5
7.0
6.5
6.0
ppm
1.0 ppm

Figure S6. 1D and 2D NMR spectra (500 MHz, CD_2Cl_2, under Ar atmosphere) for complex 5 (a) 1H-NMR (298K), (b) COSY(298K), (c) NOESY(298K) and (d) Variable Temperature 1H-NMR. The 1H-NMR spectra shows 2-4% of a decomposition product that we have not been able to eliminate, due to the fact that 5 is very sensitive to oxidation and ligand decomposition. However the presence of this impurity doesn't interfere with the NMR dynamic characterization of 5.

(a)

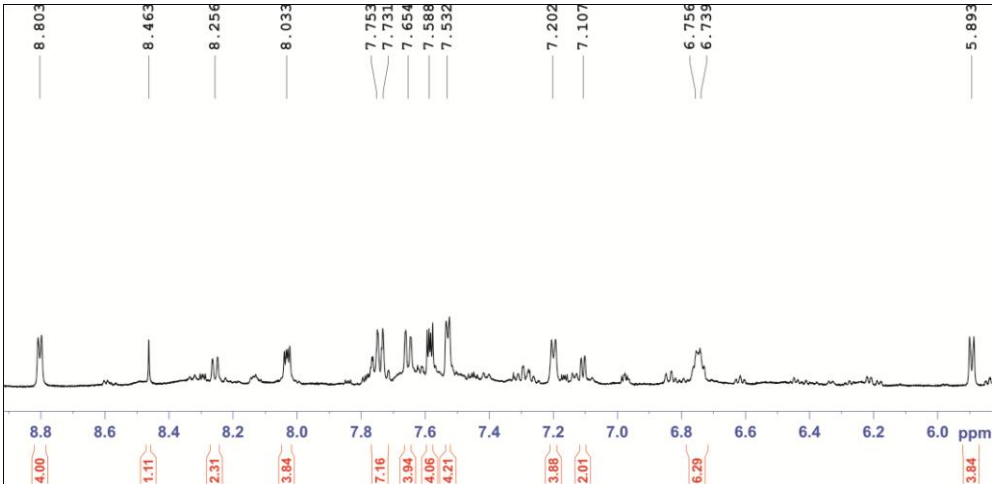

(b)

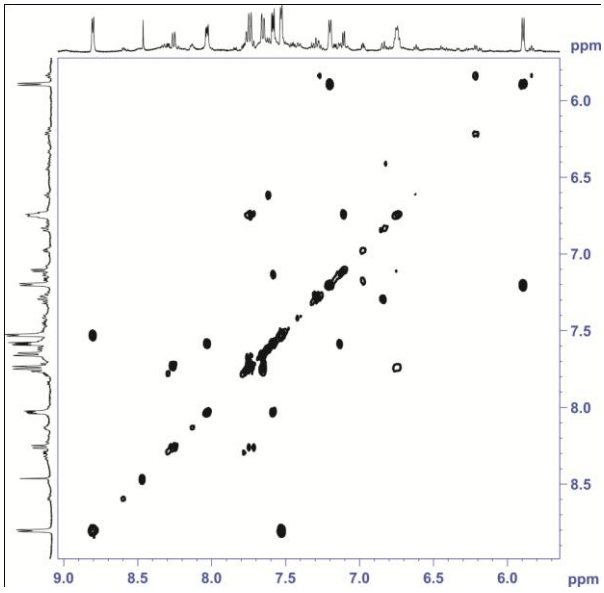

(c)

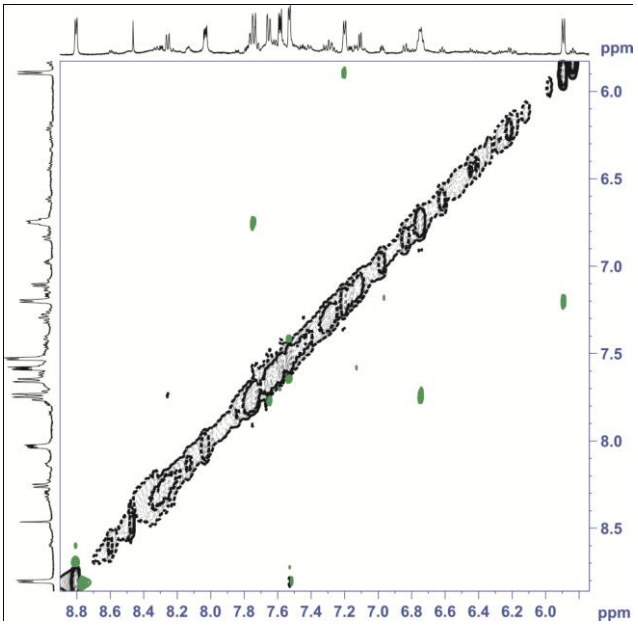
ppm
6.0
6.5
7.0
7.5
8.0
8.5
8.8 8.6 8.4 8.2 8.0 7.8 7.6 7.4 7.2 7.0 6.8 6.6 6.4 6.2 6.0
ppm

(d)

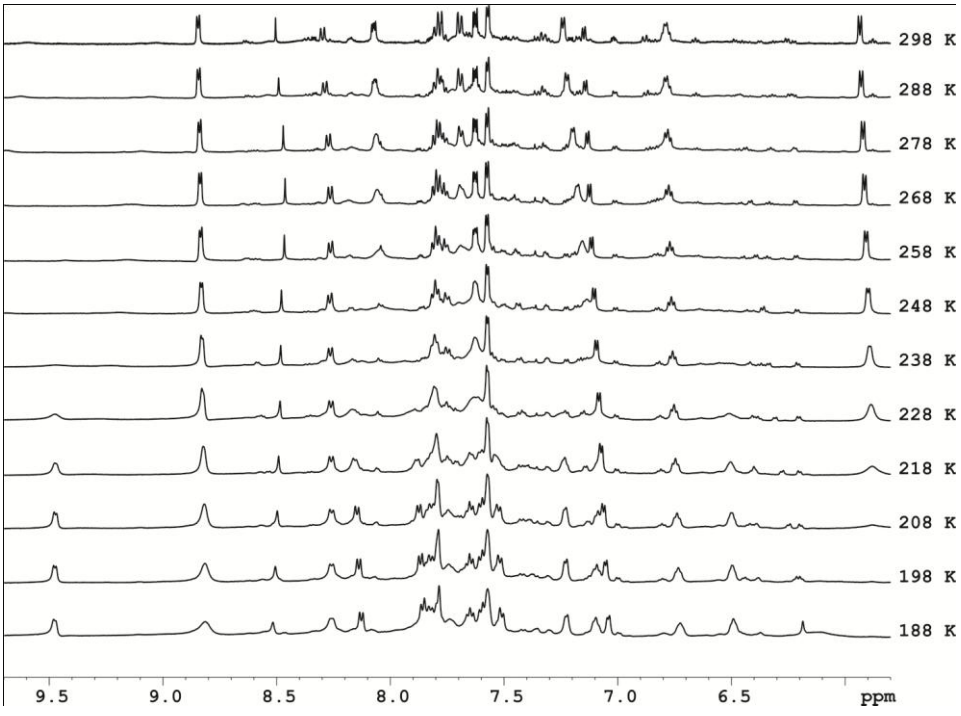
298 K
288 K
278 K
268 K
258 K
248 K
238 K
228 K
218 K
208 K
198 K
188 K
9.5 9.0 8.5 8.0 7.5 7.0 6.5
ppm

Figure S7. 1D and 2D NMR spectra (500 MHz, CD2Cl2) for complex 6 (a) 1H-NMR (230 K), (b) COSY(230 K), (c) NOESY(230 K), (d) 1H-13C correlation (230 K) and (e) Variable Temperature 1H-NMR.

(a)

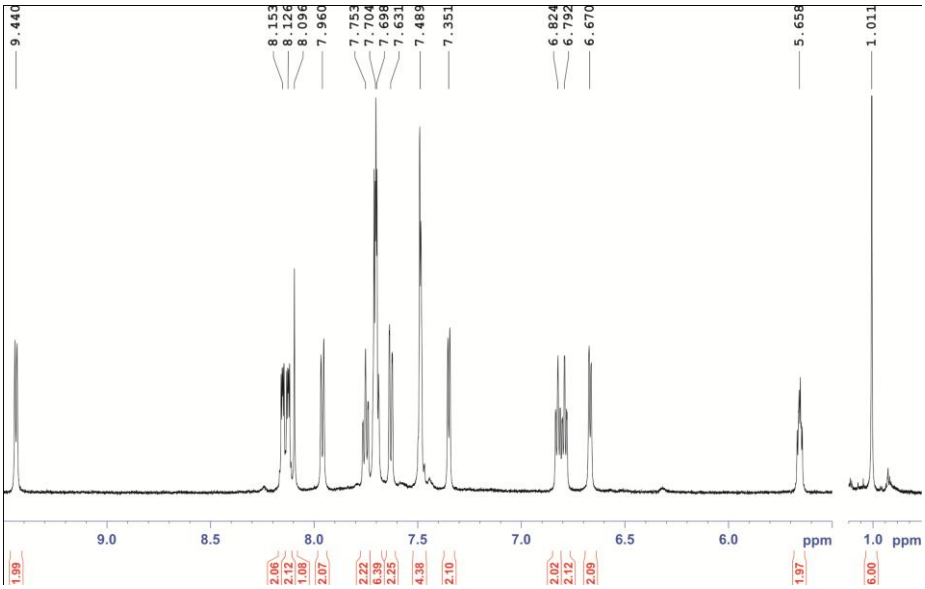

(b)

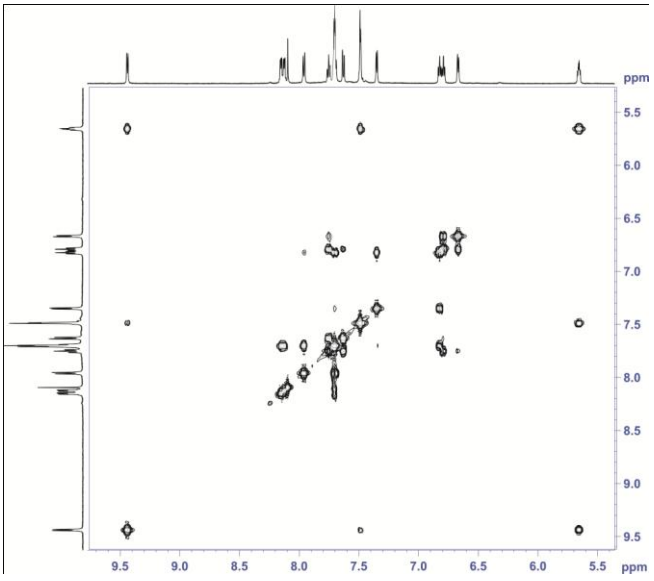

(c)

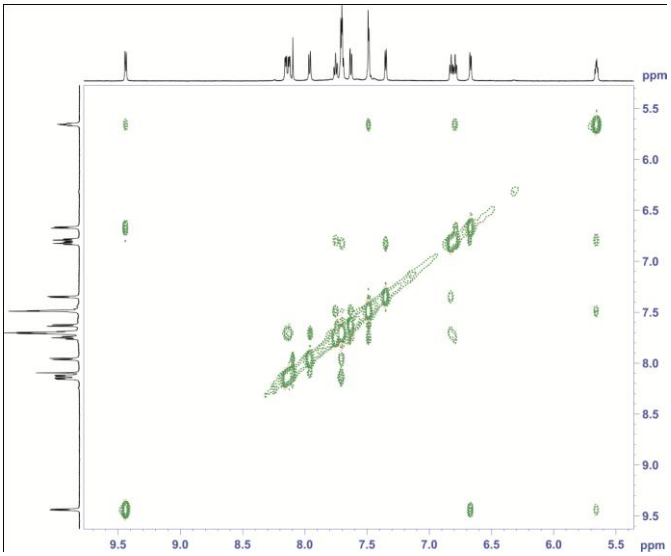
ppm
5.5
6.0
6.5
7.0
7.5
8.0
8.5
9.0
9.5
9.5
9.0
8.5
8.0
7.5
7.0
6.5
6.0
5.5
ppm

(d)

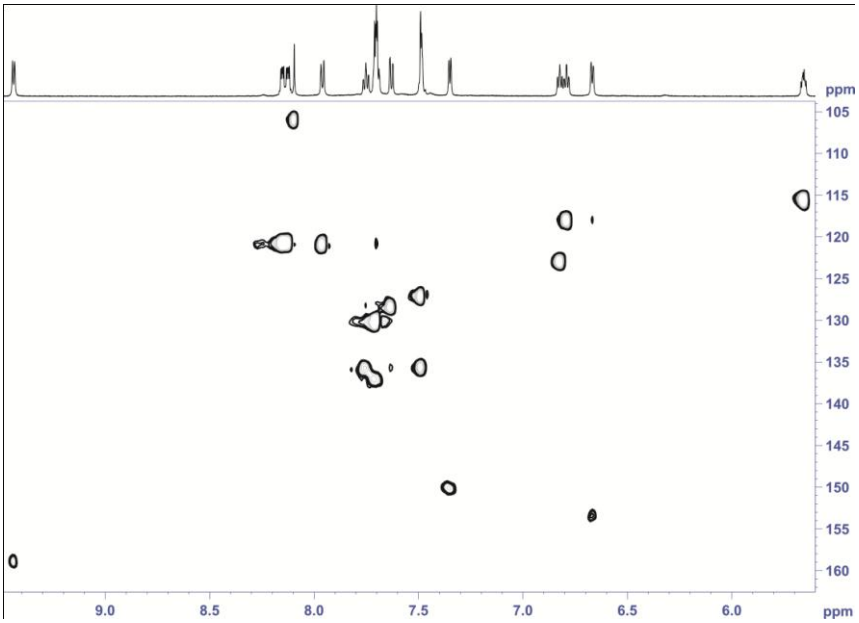
ppm
105
110
115
120
125
130
135
140
145
150
155
160
9.0
8.5
8.0
7.5
7.0
6.5
6.0
ppm

(e)

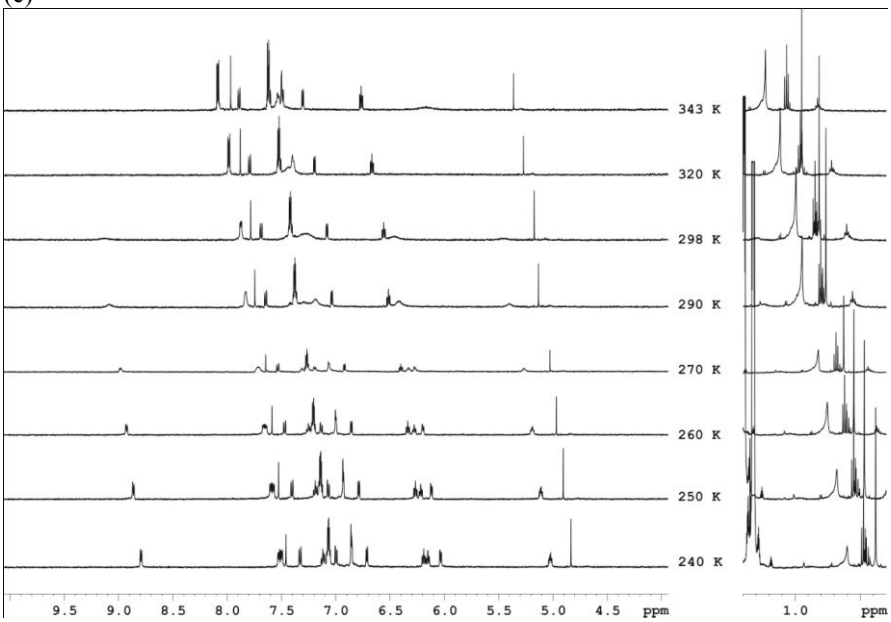

Figure S8. 1D NMR spectra (500 MHz, Acetone-d_6) for complex 7 (a) 1H-NMR (298K), (b) Variable Temperature 1H-NMR

(a)

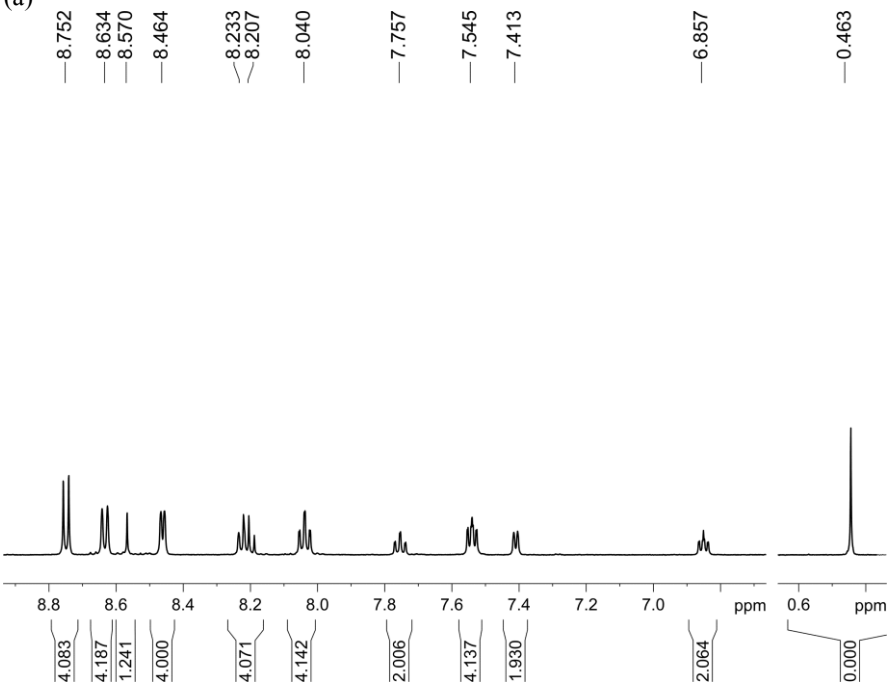

(b)

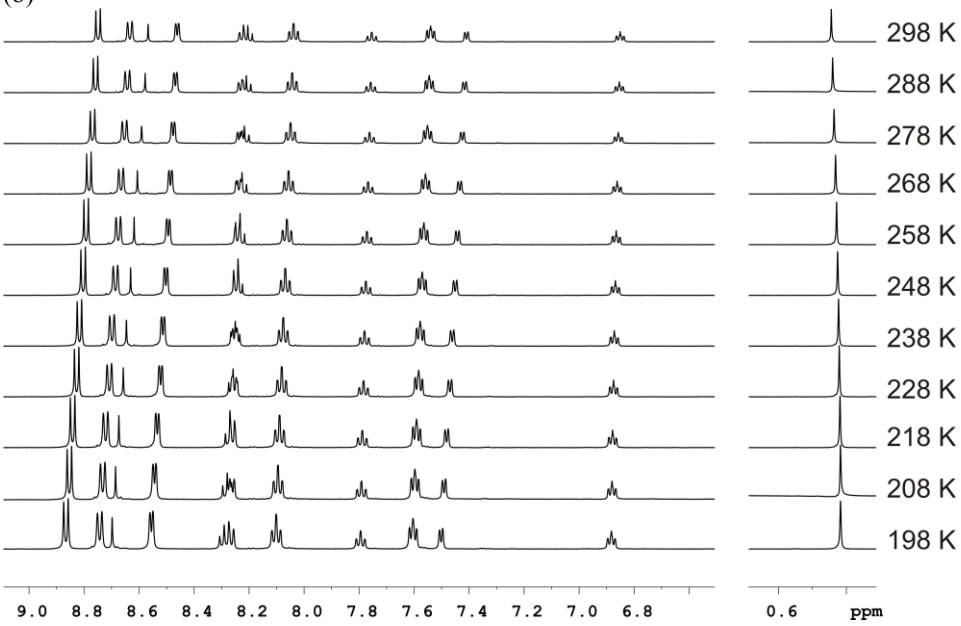

Figure S9. 1D spectra (500 MHz, Acetone-d_6 / D_2O1M CF_3SO_3D (5/1, v/v)) for complex 8 (a) 1H-NMR (298K), (b) Variable Temperature 1H-NMR

(a)

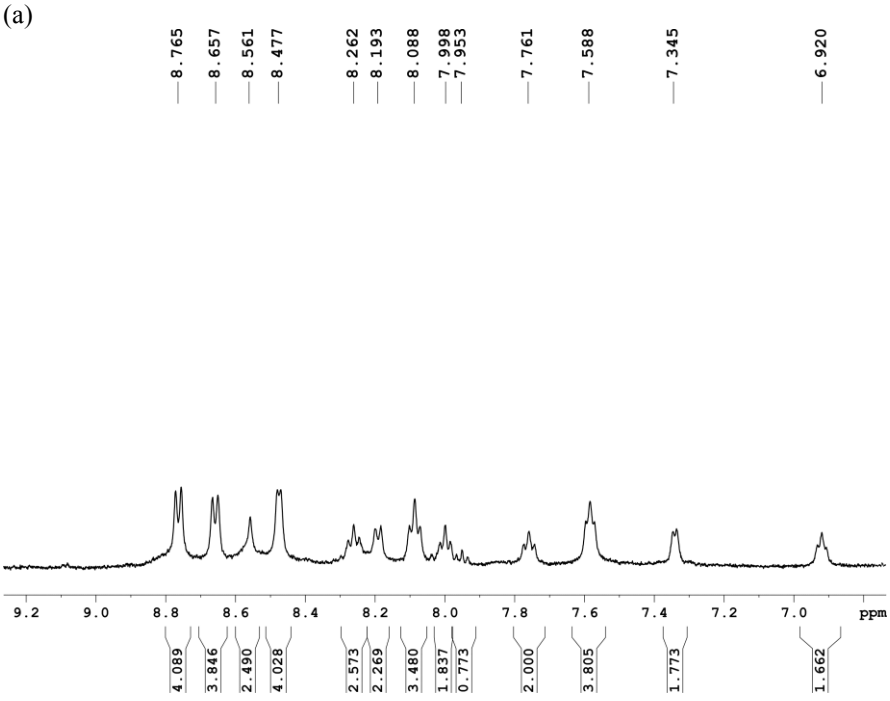

(b)

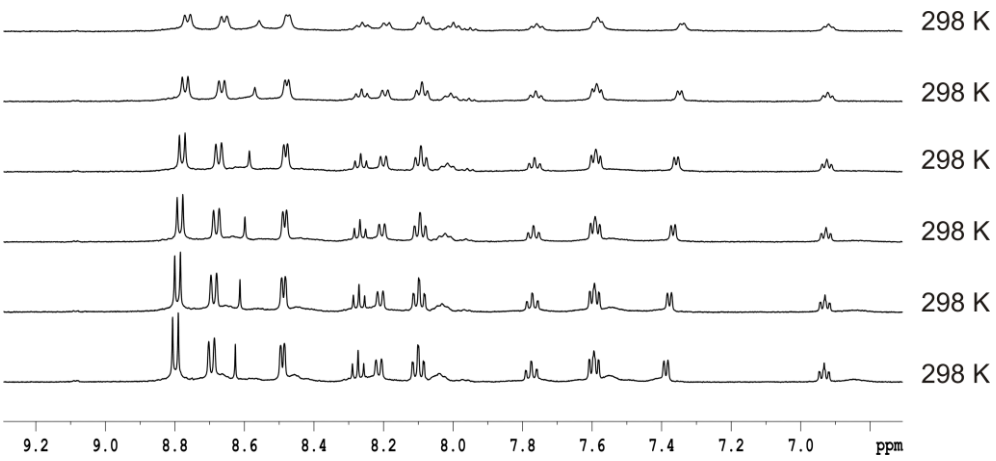

Figure S10. 1D and 2D NMR spectra (500 MHz, Acetone-d_6) for complex 9 (a) 1H-NMR (298K), (b) COSY(298K), (c) NOESY (298K) (d), Variable Temperature 1H-NMR (e) ^{13}C-NMR, (f) HMBC and (g) HSQC.

(a)

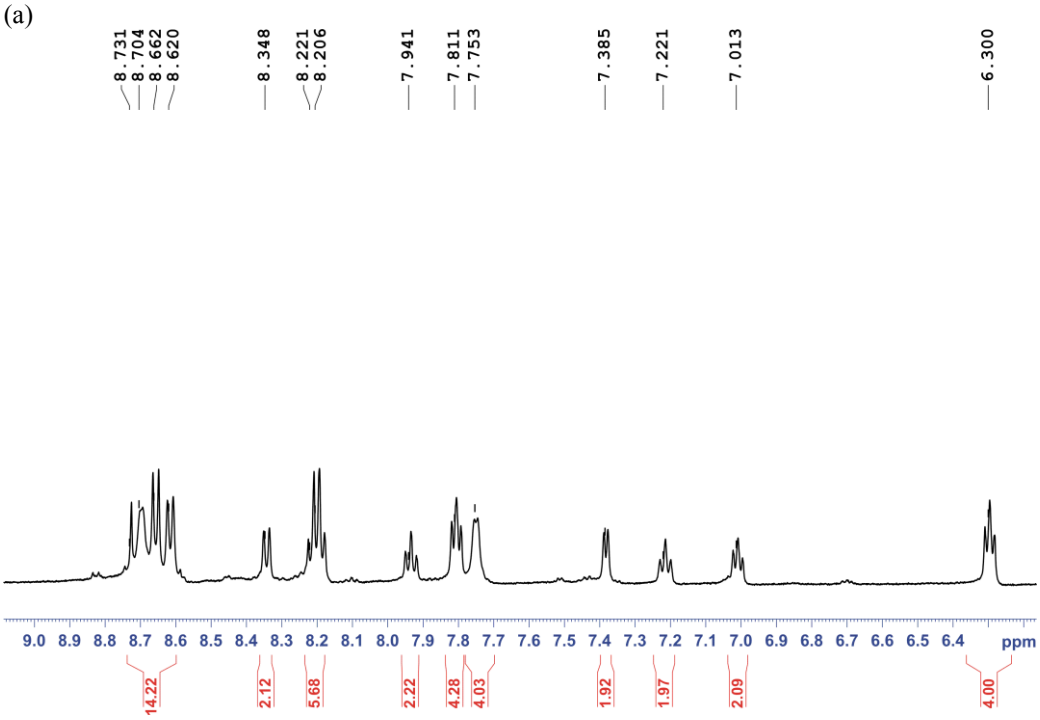

(b)

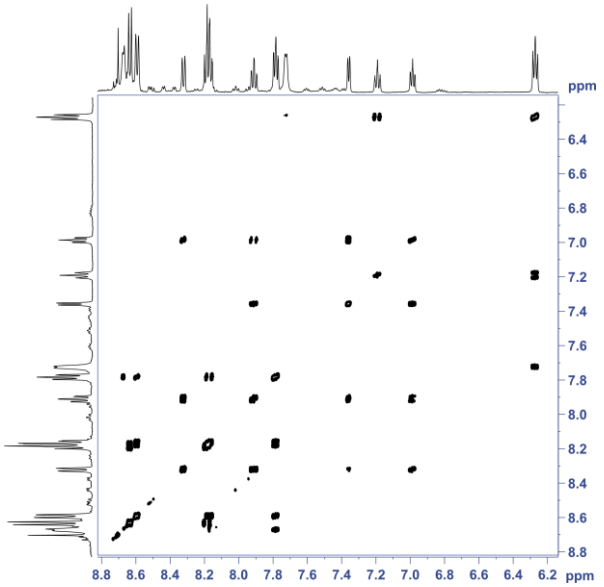
ppm
6.4
6.6
6.8
7.0
7.2
7.4
7.6
7.8
8.0
8.2
8.4
8.6
8.8
8.8 8.6 8.4 8.2 8.0 7.8 7.6 7.4 7.2 7.0 6.8 6.6 6.4 6.2 ppm

(c)

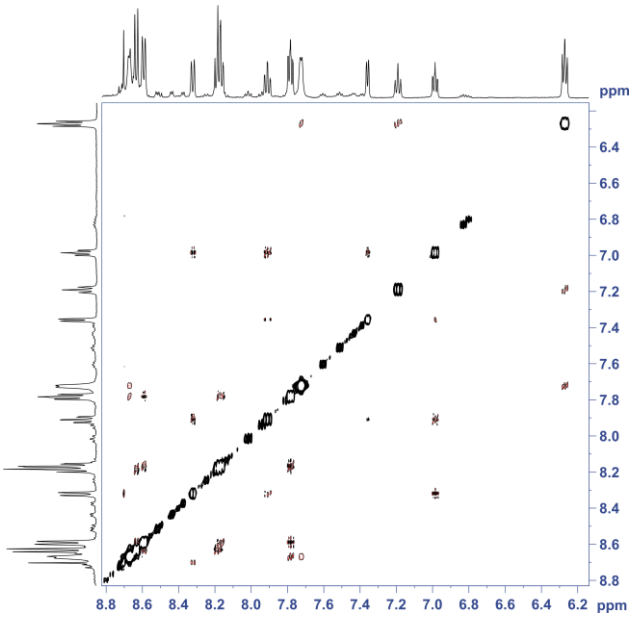
ppm
6.4
6.6
6.8
7.0
7.2
7.4
7.6
7.8
8.0
8.2
8.4
8.6
8.8
8.8 8.6 8.4 8.2 8.0 7.8 7.6 7.4 7.2 7.0 6.8 6.6 6.4 6.2 ppm

(d)

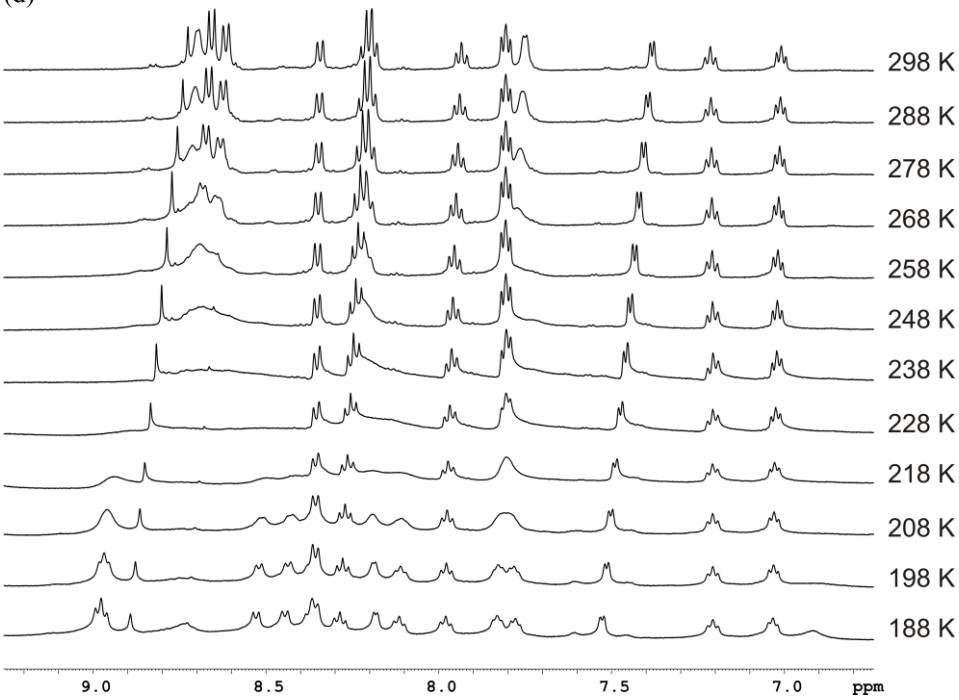
298 K
288 K
278 K
268 K
258 K
248 K
238 K
228 K
218 K
208 K
198 K
188 K
9.0
8.5
8.0
7.5
7.0
ppm

(e)

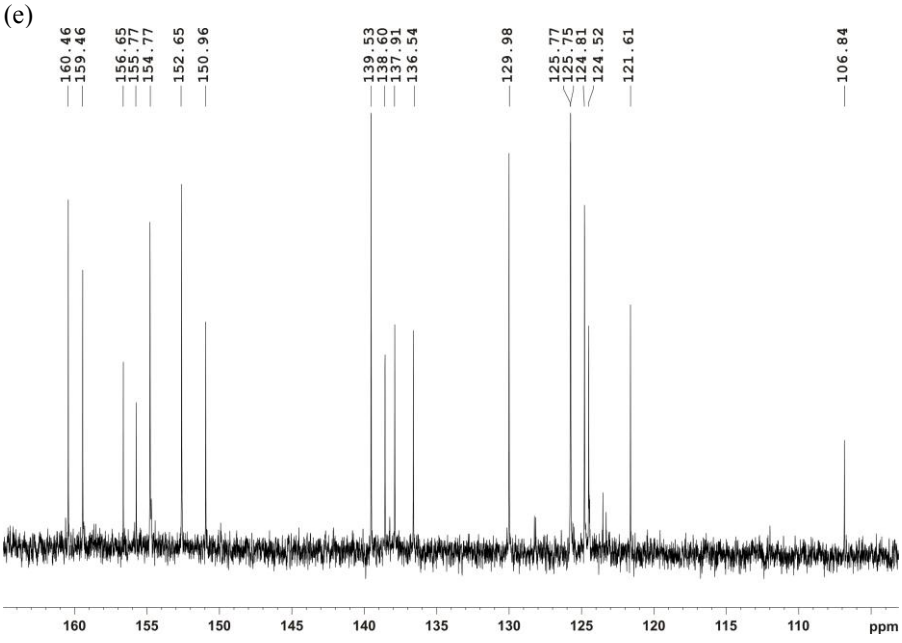
160.46
159.46
156.65
155.77
154.77
152.65
150.96
139.53
138.60
137.91
136.54
129.98
125.77
125.75
124.81
124.52
121.61
106.84
160
155
150
145
140
135
130
125
120
115
110
ppm

(f)

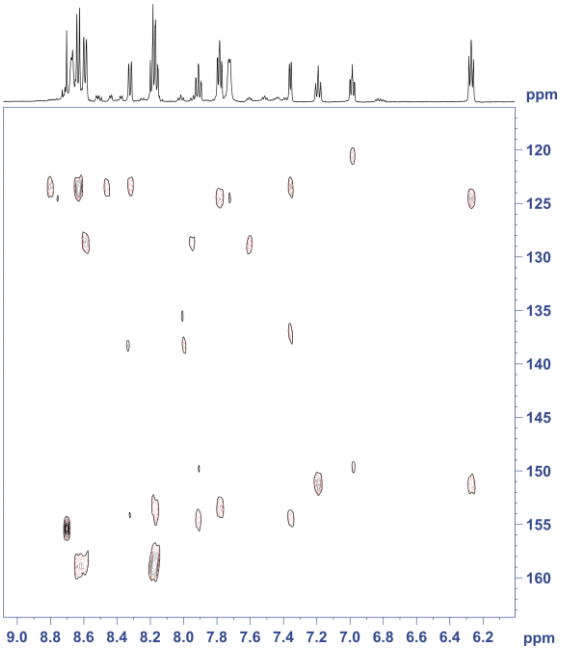
ppm
120
125
130
135
140
145
150
155
160
9.0 8.8 8.6 8.4 8.2 8.0 7.8 7.6 7.4 7.2 7.0 6.8 6.6 6.4 6.2
ppm

(g)

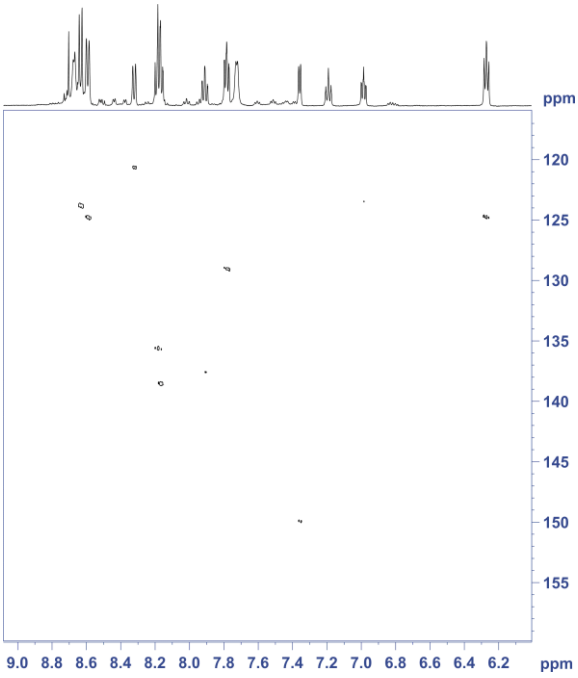
ppm
120
125
130
135
140
145
150
155
9.0 8.8 8.6 8.4 8.2 8.0 7.8 7.6 7.4 7.2 7.0 6.8 6.6 6.4 6.2
ppm

II. Activation energy calculated from VT ^{1}H-NMR

II.I. Slow dynamic regime (complexes 2-6 and 9)

For systems undergoing an exchange process at slow rate, below and up to coalescence, the relationship between the observed separation of the two peaks ($\delta\nu_T$) at a given temperature (T) and the rate constant can be calculated with the following equation[S5]:

$$k_s = \frac{\pi}{\sqrt{2}} \times \left(\delta\upsilon_0{}^2 - \delta\upsilon_T^2 \right)^{1/2} \qquad \text{(S1)}$$

$\delta\nu_0$ is the separation of the two exchanging peaks in the absence of exchange.

The evolution of the ^{1}H-NMR resonances of H_A and $H_{A'}$ upon temperature decrease (from 298 to 188 K) allowed to calculate rate constants at different temperatures for complexes 2-6 and 9. By representation of the respective Eyring plots (Figures S11-S16) the activation energies of the process was calculated as summarized in table S3.

Table S3.

Complex	a	b	R2	ΔG298K
2	-5692	30,7	0,987	7,2
3	-3749	22,0	0,998	8,5
4	-4611	23,4	0,994	9,4
5	-1966	14,3	0,976	9,5
6	-1231	11,2	0,999	10,4
9	-3377	20,6	0,996	8,6

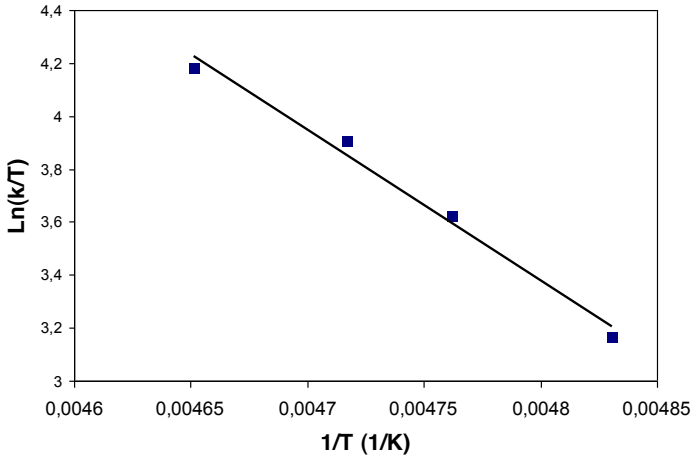

Figure S11. Eyring plot for complex 2

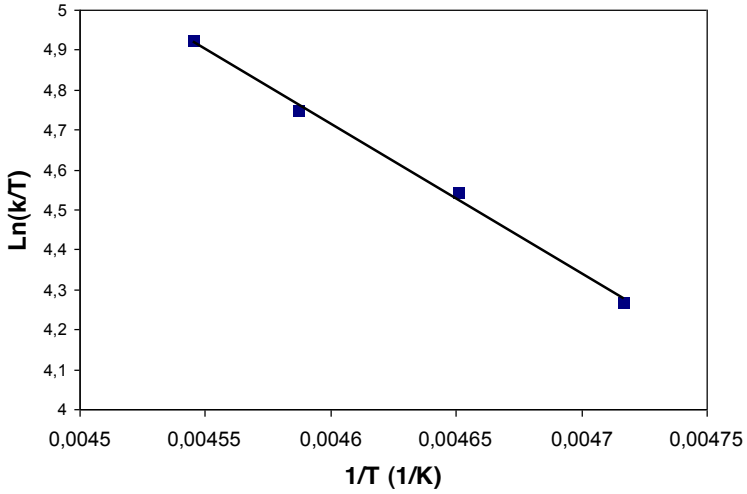

Figure S12. Eyring plot for complex 3

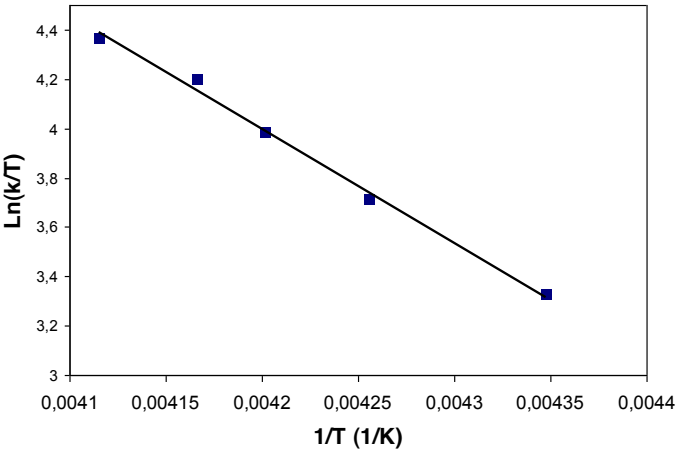

Figure S13. Eyring plot for complex 4

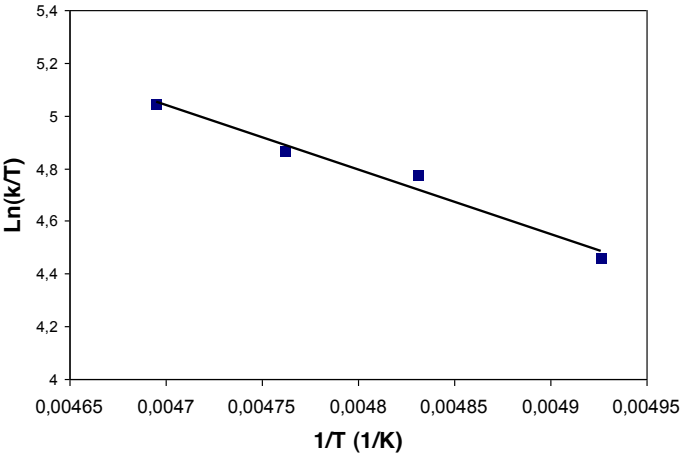

Figure S14. Eyring plot for complex 5

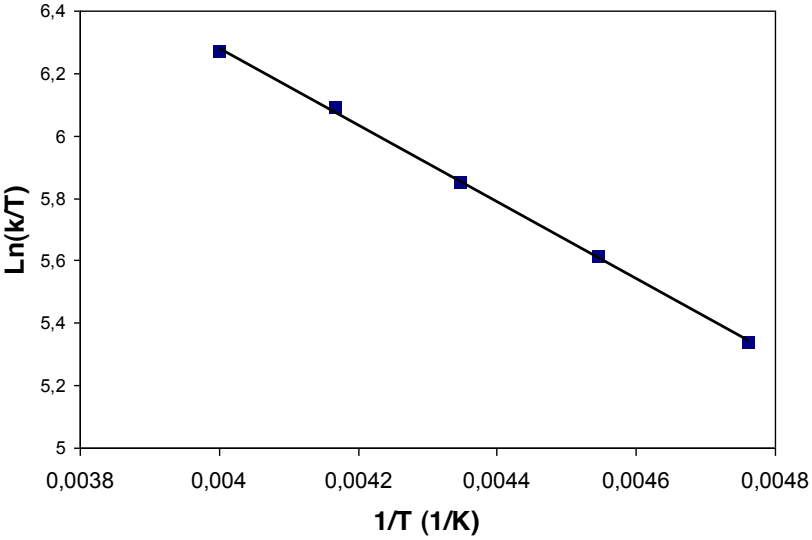

Figure S15. Eyring plot for complex 6

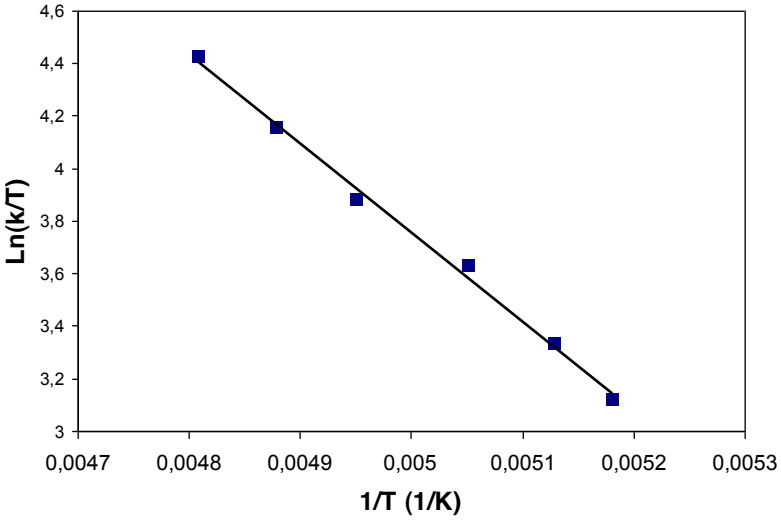

Figure S16. Eyring plot for complex 9

III. Fast dynamic regime (complexes 1,7 and 8)

In the case of systems with a fast exchange process (at least 10-15 degrees over coalescence) the rate constant at a given temperature can be obtained from the line width at half height (h_T) with the following equation.[S5]

$$k_f = \frac{\pi}{2} \times \frac{(\delta\upsilon_0)^2}{(h_T - h_\infty)} \qquad \text{(S2)}$$

h_∞ is the width at half height due to spin-spin relaxation (usually taken to be equal to the half width of the signal at the fast-exchange limit) .

Estimation of the maximum activation energy for complex 7. From 298K to 248K the peak with at half height (h_T) remain the same when we follow the HNMR resonances corresponding to the protons of the complex species affected by the dynamic process as the doublet at 8.45 ppm (see Figure S8b) which corresponds to H_F (Figure S1). Below 248 K to 218 K the peak widens by lowering the temperature. If we follow h_T of a resonance corresponding to a proton not affected by the process such as the singlet at 8.58 ppm corresponding to H_A (Figure S1) we observe the same behaviour. Which means that, below 248K, the product is precipitating causing the general loss of spectra resolution. All the values for h_T of the two mentioned protons are listed in Table S4.

From the experimental data summarized in table S4 we can assume that- since a change of h_T induced by the dynamic process is not observed- the widening due to the dynamic process should be in the range, if not smaller, of the experimental error (± 0.0001 Hz). Therefore, if we apply equation S2 introducing the ± 0.0001 Hz as ($h_T - h_\infty$) and the value of $\delta\upsilon_0$ for $\{[Ru(trpy)(py)]_2(\mu\text{-bpp})\}^{+3}$ (Table S5) we obtain an estimation of the rate constant at 298 K. Equations S3 and S4 also allows to estimate the maximum value for the activation energy of the process (See table S6).

$$k = x \frac{k_B T}{h} e^{-\Delta G^{\ddagger}/RT} \quad \text{(S3)}$$

k_B= Boltzman constant= 3.2995 x 10^{-24}calK^{-1}

x= transmission coefficient (usually assumed to be 1)

h= Planck constant= 1.5836 x 10^{-34} cal s

$$\Delta G^{\neq}_{298K} \leq (\ln(k_B/h) - \ln(k_T/T)) \cdot RT \quad \text{(S4)}$$

Table S4.

T(K)	h_T of H_F (Hz)	h_T of H_A (Hz)
298	2.9344	1.1004
288	2.9345	1.1005
278	2.9345	1.1004
268	2.9344	1.1004
258	2.9344	1.1005
248	2.9344	1.1004
238	3.1178	1.2838
228	3.3012	1.3652
218	3.4846	1.4672

Estimation of the maximum activation energy for complex 1. When studying the low temperature HNMR of complex 1 we saw the same tendency described for complex 7 (see Figure S2b). Therefore, the same procedure was carried out to obtain a maximum activation energy using the value of $\delta\upsilon_0$ obtained for $\{[Ru(bid)(py)]_2(\mu\text{-bpp})\}^+$ (tables S5 and S6)

Table S5.

T(K)	h_T of H_F (Hz)	h_T of H_A (Hz)
308	2.3431	1.5630
298	2.3431	1.5630
288	2.3431	1.5629
278	2.3432	1.5631
268	2.3433	1.5630
258	2.3486	1.5630
248	2.3916	1.5883
238	2.4259	1.6382
228	2.4879	1.6910
218	2.5317	1.7371

Table S6.

Complex	$\delta\upsilon_0$ (Hz)	$k_{298K}(s^{-1})$	$\Delta G^{\neq}_{298K}$ *(Kcal/mol)*
1	575,6	$5.14\cdot10^9$	≤ 3.4
7	1095,6	$1.88\cdot10^{10}$	≤ 4.2

Activation energy for complex 8. When studying the low temperature ^{1}H-NMR of complex 8 we saw the inverse tendency of the described for complex 7; that is all resonances widen as the temperature is decreased (see Figure S9b). This can be due to the presence of a fast Ru-OH_2 proton exchange process with the solvent and thus prevents to calculate the energy as done in the previous case. Since we have proved

that the nature of the bond and the steric hindrance are the major factors governing the dynamic process, we can assume that the activation energy for complex 8 should be at least lower than that of 7.

IV. REFERENCES:

S1. a) Casabo, J.; Pons, J.; Siddiqi, K. S.; Teixidor, F.; Molins, E.; Miravitlles, C. *J. Chem. Soc., Dalton Trans.* 1989, 1401-3. b) Gonzalez-Duarte, P.; Leiva, A.; March, R.; Pons, J.; Clegg, W.; Solans, X.; Alvarez-Larena, A.; Piniella, J. F. *Polyhedron* 1998, *17*, 1591-1600. c) Levine, R.; Sneed, J. K. *J. Am. Chem. Soc.* 1951, *73*, 5614-16. d) Pons, J.; Lopez, X.; Benet, E.; Casabo, J.; Teixidor, F.; Sanchez, F. J. *Polyhedron* 1990, *9*, 2839-45.
S2. Siegl, W. O. *J. Organomet. Chem.* 1976, *107*, C27-C30.
S3. Marks, D. N.; Siegl, W. O.; Gagne, R. R. *Inorg. Chem.* 1982, *21*, 3140-7.
S4. Sens, C.; Romero, I.; Rodriguez, M.; Llobet, A.; Parella, T.; Benet-Buchholz, J. *J. Am. Chem. Soc.* 2004, *126*, 7798-7799.
S5. H.Friebolin, in *Basic One- and Two-DimensionalNMR Spectroscopy*, *4th Ed.* WILEY-VCH, Weinheim, 2004, pp. 158-370.

COMPUTATIONAL SUPPORTING INFORMATION FOR

Through Space Ligand Interactions in Enantiomeric Dinuclear Ru Complexes

Nora Planas, Gemma J. Christian, Elena Mas-Marza, Xavier Sala, Xavier Fontrodona, Feliu Maseras and Antoni Llobet

[a] Institute of Chemical Research of Catalonia (ICIQ), Av. Països Catalans 16, E-43007 Tarragona, Spain.

[b] Serveis Tècnics, Universitat de Girona, Campus de Montilivi, E-17071 Girona, Spain.

[c] Departament de Química, Universitat Autònoma de Barcelona, Cerdanyola del Vallès, E-08193 Barcelona, Spain.

V. Computational details

Density functional theory calculations were performed with the Gaussian 03 suite of programs,[1] using the ONIOM method[2, 3] at the ONIOM(B3LYP:UFF) level of theory.[4-6] The SDD basis set and ECP was used to describe Ru[7] while 6-31G(d)[8, 9] was used for all remaining atoms. The ONIOM partitioning is shown in Figure 1. H atoms were used to cap the bonds which cross the partition between the high and low levels. This partition was chosen as part of a more general study of the system which includes Ru-L dissociation processes. Minima were confirmed through frequency calculations. Reported energies include free energy corrections.

Solvent effects for the model system were calculated using the PCM model[10] with UAHF radii, through single point HF calculations on the ONIOM optimized geometries. Calculations were carried out using the experimental solvent, DCM.

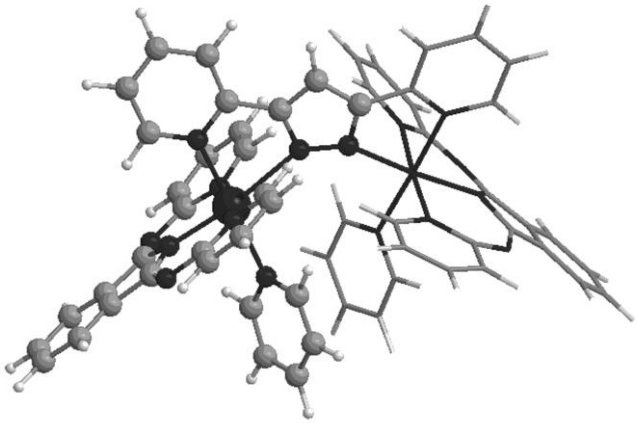

Figure 1 *ONIOM partitioning for $[Ru_2(bpp)(BID)_2(py)_2]^{+3}$. The DFT region is shown using the ball and stick representation and ow evel by wire frame.*

References

[1] Gaussian 03, Revision C.02, M. J. Frisch, G. W. Trucks, H. B. Schlegel, G. E. Scuseria, M. A. Robb, J. R. Cheeseman, J. A. Montgomery, Jr., T. Vreven, K. N. Kudin, J. C. Burant, J. M. Millam, S. S. Iyengar, J. Tomasi, V. Barone, B. Mennucci, M. Cossi, G. Scalmani, N. Rega, G. A. Petersson, H. Nakatsuji, M.

Hada, M. Ehara, K. Toyota, R. Fukuda, J. Hasegawa, M. Ishida, T. Nakajima, Y. Honda, O. Kitao, H. Nakai, M. Klene, X. Li, J. E. Knox, H. P. Hratchian, J. B. Cross, C. Adamo, J. Jaramillo, R. Gomperts, R. E. Stratmann, O. Yazyev, A. J. Austin, R. Cammi, C. Pomelli, J. W. Ochterski, P. Y. Ayala, K. Morokuma, G. A. Voth, P. Salvador, J. J. Dannenberg, V. G. Zakrzewski, S. Dapprich, A. D. Daniels, M. C. Strain, O. Farkas, D. K. Malick, A. D. Rabuck, K. Raghavachari, J. B. Foresman, J. V. Ortiz, Q. Cui, A. G. Baboul, S. Clifford, J. Cioslowski, B. B. Stefanov, G. Liu, A. Liashenko, P. Piskorz, I. Komaromi, R. L. Martin, D. J. Fox, T. Keith, M. A. Al-Laham, C. Y. Peng, A. Nanayakkara, M. Challacombe, P. M. W. Gill, B. Johnson, W. Chen, M. W. Wong, C. Gonzalez, and J. A. Pople, Gaussian, Inc., Wallingford CT, 2004.

[2] S. Dapprich, I. Komaromi, K. S. Byun, K. Morokuma, M. J. Frisch, *J Mol Struc-Theochem* 1999, *461-462*, 1.

[3] M. Svensson, S. Humbel, R. D. J. Froese, T. Matsubara, S. Sieber, K. Morokuma, *J. Phys. Chem.* 1996, *100*, 19357.

[4] A. D. Becke, *J. Chem. Phys.* 1993, *98*, 5648.

[5] C. T. Lee, W. T. Yang, R. G. Parr, *Phys. Rev. B* 1988, *37*, 785.

[6] A. K. Rappe, C. J. Casewit, K. S. Colwell, W. A. Goddard, W. M. Skiff, *J. Am. Chem. Soc.* 1992, *114*, 10024.

[7] D. Andrae, U. Häußermann, M. Dolg, H. Stoll, H. Preuß, *Theor. Chim. Acta* 1990, *77*, 123.

[8] W. J. Hehre, R. Ditchfield, J. A. Pople, *J. Chem. Phys.* 1972, *56*, 2257.

[9] M. F. Michelle, J. P. William, J. H. Warren, J. S. Binkley, S. G. Mark, J. D. Douglas, A. P. John, *J. Chem. Phys.* 1982, *77*, 3654.

[10] S. Miertus, E. Scrocco, J. Tomasi, *Chem. Phys.* 1981, *55*, 117.

VI. Coordinates for optimised structures

Complex 2: L = Pyridine

Enantiomer

1 1

C	2.107321	-1.086657	4.882442
C	-0.650452	-3.92503	0.741522
C	1.247767	-0.136729	4.316206
C	3.104853	-1.607615	4.086540
C	-0.427510	-2.893904	1.651040
C	-1.324916	-3.658443	-0.448405
C	-2.789448	0.784879	4.925378
C	-3.548723	-0.173537	4.269799
C	1.407437	0.187313	2.982155
C	-5.843023	-2.301777	0.621593
C	-2.067656	1.703289	4.181340
C	3.250875	-1.204871	2.735083
C	-0.906284	-1.614754	1.362900

C	-3.573579	-0.219185	2.869286
C	-1.777638	-2.362008	-0.703867
C	6.044941	-1.981472	0.397339
N	2.341082	-0.356914	2.157015
C	2.033645	-3.871409	-1.133017
C	-4.860152	-1.325003	1.070858
C	2.189624	-2.698980	-0.399290
N	-1.569659	-1.361443	0.200535
C	4.809449	-1.386828	0.941446
C	-2.087557	1.626067	2.789985
N	-2.801076	0.658657	2.131840
C	-5.957695	-2.169779	-0.743091
C	6.193406	-1.483120	-0.899041
C	1.437100	-3.814320	-2.390808
N	-4.394626	-0.561578	-0.026377
N	1.808016	-1.485564	-0.856590
C	-5.020507	-1.134072	-1.161664
N	4.282097	-0.517647	0.004613
Ru	-2.605510	0.501649	-0.024708
Ru	2.448279	0.337447	0.120721
C	1.014205	-2.571619	-2.860734
C	4.375748	2.352411	1.359395
C	1.224628	-1.444833	-2.074623
C	4.796804	3.570414	1.880216
N	3.112467	2.135340	0.942253
C	5.048210	-0.585246	-1.142237
N	0.412025	1.588576	0.415148
C	-3.587889	-0.163108	-2.935652
N	-0.868088	1.752144	-0.032625
C	2.211860	3.146725	1.042243
C	3.877859	4.615198	1.981347
N	-2.546013	0.350946	-2.187056
C	-3.549868	-0.092597	-4.335294
C	0.840704	2.870478	0.597850
C	2.570939	4.396707	1.557914
N	-3.550789	2.374035	-0.247429
C	-1.229056	3.063028	-0.113990
C	-4.891671	2.567051	-0.360744
C	3.866215	0.848318	-2.634420
N	2.800510	1.194002	-1.840048
C	-0.153349	3.827821	0.274822
C	-2.660484	3.402704	-0.282654
C	-1.465522	0.884355	-2.834447
C	-2.460356	0.477206	-4.978841
C	-5.388196	3.864874	-0.510430
C	-1.402154	0.956022	-4.224541
C	1.969832	2.154225	-2.328463
C	4.010980	1.406238	-3.931937
C	-3.120740	4.716765	-0.421262

C	-4.495896	4.942435	-0.539621
C	3.125356	2.344632	-4.413953
C	2.078326	2.744461	-3.573076
H	5.052740	1.514327	1.251704
H	5.826920	3.688939	2.198412
H	4.170650	5.578598	2.386346
H	1.826810	5.180981	1.639645
H	-0.079394	4.902928	0.320691
H	-2.430811	5.550615	-0.439817
H	-4.870461	5.951621	-0.651699
H	-6.453148	4.034908	-0.601095
H	-5.572578	1.729149	-0.334484
H	1.177107	2.464629	-1.669362
H	1.354964	3.495409	-3.872129
H	3.245365	2.768672	-5.406226
H	4.861759	1.064613	-4.509140
H	3.834692	-2.314898	4.462045
H	2.006084	-1.389631	5.920090
H	0.462818	0.339521	4.893001
H	0.748577	0.903369	2.515133
H	-1.508588	2.350937	2.264810
H	-1.482977	2.467311	4.677655
H	-2.776457	0.826856	6.006822
H	-4.141453	-0.870197	4.850071
H	-4.356065	-0.510956	-4.925610
H	-2.426220	0.523866	-6.059653
H	-0.534803	1.383939	-4.710875
H	-0.628558	1.257021	-2.292639
H	0.953524	-0.464010	-2.435291
H	2.636880	-2.723730	0.584796
H	0.538371	-2.462573	-3.829687
H	2.372024	-4.810614	-0.708531
H	1.300154	-4.712321	-2.985139
H	-0.798790	-0.841729	2.097998
H	-2.329338	-2.176243	-1.608898
H	0.092049	-3.086233	2.580917
H	-1.502880	-4.450204	-1.164383
H	-0.294215	-4.924650	0.953484
N	4.359304	-1.716917	2.115955
N	4.867683	-0.015573	-2.294702
C	6.960757	-2.873690	0.942772
C	7.264214	-1.856478	-1.702612
H	6.834947	-3.256618	1.950378
H	7.368702	-1.465581	-2.709515
C	8.043634	-3.253985	0.141089
C	8.193040	-2.753067	-1.160982
H	8.781653	-3.948611	0.531768
H	9.044292	-3.068160	-1.757556
N	-4.655924	-0.943635	-2.384814

N	-4.472855	-1.176870	2.293531
C	-6.791813	-3.001818	-1.488831
C	-6.571582	-3.257899	1.327679
C	-7.544374	-3.970268	-0.800503
C	-7.435782	-4.096801	0.601583
H	-6.856912	-2.908240	-2.565033
H	-8.205467	-4.627469	-1.350221
H	-8.015732	-4.848978	1.120268
H	-6.472318	-3.355946	2.400867

Transition State

1 1

C	2.537216	0.091433	4.950982
C	-0.851888	-3.914365	0.008342
C	1.404821	0.431356	4.198982
C	3.686157	-0.255121	4.273731
C	-0.613077	-3.069156	1.089265
C	-1.485183	-3.416092	-1.127957
C	-2.892582	0.084608	5.055911
C	-3.593216	-0.826368	4.278729
C	1.489285	0.406393	2.819670
C	-5.815418	-2.558468	0.399316
C	-2.230366	1.133475	4.439496
C	3.723226	-0.269050	2.856932
C	-1.049063	-1.744644	1.030919
C	-3.631336	-0.682505	2.885479
C	-1.921829	-2.089872	-1.141468
C	6.575283	-1.142331	0.611010
N	2.608290	0.064366	2.128089
C	2.758983	-4.200179	0.567803
C	-4.934069	-1.555196	0.977892
C	2.653943	-2.825167	0.751509
N	-1.732730	-1.284387	-0.056421
C	5.238618	-0.717030	1.069465
C	-2.238929	1.228534	3.048741
N	-2.911286	0.321873	2.270785
C	-5.982475	-2.238408	-0.924025
C	6.578825	-1.036230	-0.783881
C	2.415028	-4.750007	-0.665186
N	-4.597201	-0.567611	0.013643
N	2.221599	-1.979149	-0.210368
C	-5.181730	-1.050259	-1.187571
N	4.485836	-0.382058	-0.038713
Ru	-2.833278	0.547533	0.115867
Ru	2.565275	0.160614	-0.001237
C	1.944938	-3.890954	-1.657285
C	4.364118	2.595050	0.109895
C	1.854217	-2.529267	-1.389777

C	4.795389	3.912784	0.070737
N	3.063162	2.225114	0.098313
C	5.243046	-0.550580	-1.180314
N	0.211643	1.603349	0.109777
C	-3.936900	0.331944	-2.822442
N	-1.126354	1.794212	0.271420
C	2.125590	3.208996	0.071627
C	3.840397	4.924024	0.006315
N	-2.914736	0.838609	-2.040593
C	-4.033387	0.678596	-4.177146
C	0.693221	2.877472	0.135450
C	2.501558	4.560876	0.010006
N	-3.810898	2.404083	0.316777
C	-1.487362	3.100412	0.335432
C	-5.156725	2.585916	0.352746
C	3.715543	0.100356	-2.886554
N	2.601149	0.309061	-2.116630
C	-0.341756	3.849164	0.269716
C	-2.929403	3.439693	0.391912
C	-2.021821	1.707660	-2.615189
C	-3.129112	1.565120	-4.739595
C	-5.669323	3.880901	0.471736
C	-2.118327	2.087328	-3.953022
C	1.442939	0.623638	-2.754530
C	3.652451	0.273711	-4.293111
C	-3.404880	4.749854	0.507423
C	-4.786761	4.965173	0.548535
C	2.470014	0.607609	-4.916374
C	1.324583	0.772688	-4.122934
H	5.078588	1.786917	0.146547
H	5.858421	4.127371	0.083104
H	4.127665	5.969610	-0.041660
H	1.740909	5.328704	-0.037815
H	-0.254462	4.921446	0.321130
H	-2.722380	5.587901	0.566373
H	-5.174153	5.971657	0.639212
H	-6.738771	4.043938	0.502079
H	-5.826778	1.740703	0.288387
H	0.592754	0.732485	-2.096238
H	0.363497	1.003423	-4.564704
H	2.423607	0.726015	-5.994633
H	4.570376	0.108411	-4.844551
H	4.599830	-0.531430	4.786324
H	2.511297	0.100175	6.036347
H	0.476946	0.712817	4.678991
H	0.642028	0.678385	2.206349
H	-1.699308	2.046488	2.619951
H	-1.700150	1.866471	5.033977
H	-2.880904	-0.010888	6.133977

H	-4.141065	-1.626681	4.761161
H	-4.816522	0.256141	-4.795078
H	-3.209712	1.842298	-5.782769
H	-1.407923	2.786900	-4.374929
H	-1.224369	2.148544	-2.060973
H	1.486300	-1.847871	-2.143988
H	2.926758	-2.377103	1.695989
H	1.642065	-4.261527	-2.630907
H	3.116595	-4.818227	1.384484
H	2.500197	-5.817202	-0.844809
H	-0.889306	-1.108262	1.885042
H	-2.454962	-1.732472	-2.003607
H	-0.104351	-3.438599	1.970177
H	-1.659365	-4.057914	-1.981714
H	-0.527166	-4.946068	0.042245
N	4.924592	-0.660978	2.329095
N	4.931502	-0.315955	-2.419747
C	7.697540	-1.572677	1.308857
C	7.704468	-1.357262	-1.533172
H	7.686179	-1.647966	2.391412
H	7.697743	-1.269472	-2.614784
C	8.834536	-1.901700	0.560874
C	8.837986	-1.795563	-0.837842
H	9.730394	-2.243974	1.070777
H	9.736412	-2.057471	-1.389159
N	-4.870271	-0.654800	-2.374303
N	-4.480153	-1.598916	2.185667
C	-6.729333	-3.045354	-1.782049
C	-6.398109	-3.696023	0.956943
C	-7.339666	-4.192720	-1.244485
C	-7.175543	-4.516217	0.119926
H	-6.833310	-2.799688	-2.830883
H	-7.930877	-4.836261	-1.882815
H	-7.643054	-5.405444	0.522225
H	-6.252652	-3.944410	2.000183

Complex 3: L = 4-Me-py

Enantiomer

1 1

C	2.010828	-0.400114	4.986825
C	-0.632547	-3.655662	1.255478
C	1.192966	0.521678	4.321337
C	2.998801	-1.027690	4.258388
C	-0.423377	-2.504516	2.019245
C	-1.302498	-3.545584	0.031622

C	-2.832546	1.521476	4.786367
C	-3.579158	0.482488	4.250251
C	1.375278	0.707547	2.963801
C	-5.811225	-2.124305	0.889913
C	-2.113218	2.346649	3.938301
C	3.174724	-0.758491	2.877748
C	-0.906951	-1.278825	1.560335
C	-3.593951	0.263444	2.866052
C	-1.758526	-2.295933	-0.394215
C	6.006363	-1.775272	0.682596
N	2.294868	0.051716	2.207226
C	2.000803	-3.797214	-0.758342
C	-4.857870	-1.072225	1.213835
C	2.172556	-2.569483	-0.130915
N	-1.564313	-1.184695	0.372285
C	4.761427	-1.128563	1.139389
C	-2.123386	2.097430	2.567127
N	-2.824511	1.049597	2.029294
C	-5.908819	-2.180050	-0.480219
C	6.183784	-1.406369	-0.652803
C	1.366042	-3.875117	-2.003141
N	-4.396091	-0.446357	0.029837
N	1.780151	-1.397496	-0.678346
C	-4.990637	-1.186491	-1.023500
N	4.256905	-0.354688	0.110845
Ru	-2.613907	0.626634	-0.091085
Ru	2.426149	0.513628	0.106176
C	0.943733	-2.660897	-2.557461
C	4.334235	2.659444	1.138812
C	1.173709	-1.469865	-1.882941
C	4.746743	3.930630	1.520926
N	3.078153	2.393387	0.728141
C	5.044905	-0.538206	-1.007868
N	0.392031	1.779344	0.235725
C	-3.553113	-0.438352	-2.899216
N	-0.884433	1.878768	-0.239482
C	2.176008	3.408373	0.695551
C	3.826972	4.978984	1.483070
N	-2.540320	0.214524	-2.221651
C	-3.503575	-0.559583	-4.295067
C	0.810999	3.076770	0.270032
C	2.527055	4.710676	1.066575
N	-3.569514	2.450218	-0.547825
C	-1.253259	3.168649	-0.478388
C	-4.910366	2.616990	-0.696237
C	3.884511	0.719879	-2.666420
N	2.803575	1.142139	-1.932512
C	-0.186096	3.982032	-0.172950
C	-2.685755	3.474362	-0.698395

C	-1.489760	0.723110	-2.936686
C	-2.437733	-0.029550	-5.007401
C	-5.414356	3.883411	-1.005240
C	-1.416915	0.608071	-4.323406
C	1.969862	2.028650	-2.539628
C	4.045357	1.130275	-4.016193
C	-3.153779	4.758461	-0.997902
C	-4.529294	4.957009	-1.155087
C	3.157395	1.996555	-4.614987
C	2.091421	2.474819	-3.841576
H	5.012318	1.815021	1.142529
H	5.771220	4.087135	1.840959
H	4.113641	5.983562	1.777229
H	1.781959	5.497945	1.043867
H	-0.119970	5.055709	-0.252720
H	-2.469499	5.589599	-1.110275
H	-4.909766	5.942367	-1.390936
H	-6.479475	4.032640	-1.125679
H	-5.585239	1.782291	-0.576179
H	1.164404	2.400943	-1.930499
H	1.364268	3.176924	-4.235227
H	3.289356	2.307053	-5.646987
H	4.908761	0.735748	-4.538266
H	3.701846	-1.716917	4.710744
H	1.887782	-0.599001	6.047048
H	0.421158	1.079898	4.839472
H	0.741966	1.393508	2.421848
H	-1.546436	2.756932	1.960907
H	-1.537888	3.171317	4.339345
H	-2.826996	1.697093	5.854347
H	-4.169223	-0.142959	4.909062
H	-4.284907	-1.090284	-4.825516
H	-2.395672	-0.128696	-6.084386
H	-0.571478	1.016933	-4.862038
H	-0.683437	1.223175	-2.455438
H	0.897539	-0.526351	-2.329281
H	2.644694	-2.514842	0.840493
H	0.446471	-2.631755	-3.522459
H	2.358462	-4.694216	-0.262047
H	-0.809742	-0.414790	2.187102
H	-2.301167	-2.233488	-1.320774
H	0.087528	-2.558198	2.972892
H	-1.481311	-4.417827	-0.584382
N	4.284672	-1.343840	2.330141
N	4.885739	-0.092406	-2.216793
C	6.908477	-2.609943	1.332141
C	7.270361	-1.856965	-1.392899
H	6.760321	-2.892451	2.369438
H	7.396968	-1.566416	-2.430767

C	8.007543	-3.066840	0.595077
C	8.185740	-2.696104	-0.746357
H	8.735658	-3.719640	1.067872
H	9.048991	-3.067892	-1.290789
N	-4.606868	-1.163344	-2.254902
N	-4.476239	-0.769964	2.409346
C	-6.708086	-3.129030	-1.116683
C	-6.522364	-2.998928	1.710338
C	-7.444191	-4.017948	-0.312947
C	-7.352708	-3.952328	1.094470
H	-6.758621	-3.183310	-2.196362
H	-8.078420	-4.762182	-0.776642
H	-7.918767	-4.645223	1.703256
H	-6.434751	-2.950355	2.787916
C	1.120308	-5.193413	-2.686322
C	-0.141110	-4.982420	1.752229
H	-0.644493	-5.230569	2.710120
H	-0.349769	-5.792698	1.021551
H	0.955045	-4.935555	1.922212
H	0.189267	-5.645416	-2.319998
H	1.927646	-5.904219	-2.485084
H	1.024055	-5.073887	-3.769436

Transition State

1 1

C	2.497746	-0.704988	-4.925730
C	-0.937956	3.813294	0.299983
C	1.341979	-0.894999	-4.153764
C	3.667518	-0.378570	-4.275654
C	-1.588475	3.396409	-0.864365
C	-0.612058	2.861773	1.272848
C	-3.233616	-1.370708	-4.834627
C	-4.112188	-0.503162	-4.205881
C	1.438537	-0.774864	-2.780855
C	-5.954874	2.245713	-0.753145
C	-2.224184	-1.961060	-4.095947
C	3.707756	-0.239579	-2.864370
C	-1.965903	2.059708	-1.001062
C	-3.991083	-0.243159	-2.833928
C	-1.011083	1.534904	1.097014
C	6.543246	0.838351	-0.698718
N	2.583373	-0.469927	-2.115800
C	1.872028	3.669758	-1.599420
C	-5.192325	1.053113	-1.098020
C	1.727059	2.319241	-1.308771
N	-1.724748	1.162135	-0.003264
C	5.212059	0.362556	-1.121579
C	-2.101104	-1.665223	-2.739108

N	-2.966662	-0.813539	-2.100436
C	-5.749862	2.490641	0.580713
C	6.522823	0.912612	0.697475
C	2.483397	4.528409	-0.678537
N	-4.596332	0.490699	0.062749
N	2.163532	1.755694	-0.161144
C	-4.886148	1.434021	1.085451
N	4.440466	0.164269	0.005861
Ru	-2.852161	-0.661096	0.067978
Ru	2.515731	-0.381168	0.007016
C	2.862154	3.955608	0.541318
C	4.307130	-2.824095	0.103963
C	2.694493	2.594961	0.757053
C	4.725764	-4.145657	0.055262
N	3.010484	-2.442550	0.061990
C	5.180606	0.477270	1.128955
N	0.179704	-1.777755	0.036008
C	-3.579814	0.417577	2.916695
N	-1.167919	-1.949817	0.122465
C	2.064204	-3.415347	-0.010248
C	3.762577	-5.146028	-0.049859
N	-2.901032	-0.570225	2.232673
C	-3.525238	0.471345	4.315718
C	0.636076	-3.062314	0.011474
C	2.427387	-4.770085	-0.079343
N	-3.863054	-2.508840	0.159246
C	-1.553814	-3.249882	0.112167
C	-5.211870	-2.666893	0.197250
C	3.646660	-0.007209	2.889764
N	2.544712	-0.343537	2.142925
C	-0.420317	-4.017702	0.052656
C	-3.001897	-3.564082	0.154050
C	-2.261651	-1.551664	2.944220
C	-2.857431	-0.515504	5.026489
C	-5.749081	-3.956767	0.235774
C	-2.243841	-1.549203	4.338021
C	1.431663	-0.732779	2.818582
C	3.597348	-0.046213	4.305598
C	-3.502300	-4.869597	0.189747
C	-4.887693	-5.060524	0.231473
C	2.452076	-0.433622	4.965936
C	1.337345	-0.790601	4.196433
H	5.026931	-2.022357	0.173382
H	5.785720	-4.372173	0.093374
H	4.041110	-6.193694	-0.103527
H	1.660891	-5.529819	-0.156368
H	-0.354571	-5.092757	0.050794
H	-2.836192	-5.722753	0.186916
H	-5.294186	-6.063142	0.260211

H	-6.821236	-4.100790	0.266765
H	-5.865640	-1.806645	0.196076
H	0.597872	-1.015710	2.192236
H	0.415979	-1.110924	4.663613
H	2.416614	-0.464348	6.050630
H	4.501018	0.239247	4.830692
H	4.593580	-0.195918	-4.807635
H	2.469106	-0.799410	-6.006980
H	0.389770	-1.124055	-4.614728
H	0.579430	-0.902935	-2.139123
H	-1.310165	-2.160240	-2.221987
H	-1.538798	-2.652663	-4.568990
H	-3.334882	-1.583023	-5.891139
H	-4.895819	-0.029656	-4.784956
H	-4.039438	1.258659	4.853386
H	-2.835601	-0.490766	6.108329
H	-1.741182	-2.340604	4.879225
H	-1.758437	-2.360596	2.458216
H	3.009111	2.149553	1.689937
H	1.263121	1.655010	-2.025540
H	3.308012	4.560361	1.325260
H	1.509415	4.044477	-2.551757
H	-2.517191	1.769380	-1.876511
H	-0.819426	0.826571	1.885056
H	-1.838529	4.107829	-1.641737
H	-0.095337	3.148811	2.180146
N	4.917070	0.163880	-2.370780
N	4.851443	0.402203	2.383427
C	7.677716	1.176473	-1.427034
C	7.636206	1.327184	1.418857
H	7.683902	1.113047	-2.510360
H	7.611378	1.377627	2.502637
C	8.802605	1.598630	-0.708234
C	8.782117	1.673018	0.692529
H	9.707816	1.872545	-1.242410
H	9.671791	2.003250	1.220922
N	-4.409258	1.398810	2.284830
N	-4.902473	0.727338	-2.311245
C	-6.284261	3.614498	1.209856
C	-6.692553	3.120008	-1.551095
C	-7.052775	4.500997	0.434567
C	-7.255251	4.255290	-0.940834
H	-6.108346	3.803412	2.260842
H	-7.483149	5.381733	0.893058
H	-7.838427	4.949713	-1.531439
H	-6.824576	2.934366	-2.609072
C	2.725130	5.983801	-0.978133
C	-0.638669	5.267752	0.508951
H	2.514612	6.610339	-0.105100

H	2.108151	6.331791	-1.811395
H	3.775452	6.148490	-1.250266
H	-0.019481	5.429547	1.416891
H	-1.591007	5.826581	0.623176
H	-0.095928	5.673371	-0.368522

Complex 4: L = 3,5-$(Me)_2$-py

Enantiomer

1 1

C	2.350009	0.240345	5.021133
C	-0.803440	-3.622379	1.327647
C	1.414800	0.997019	4.303411
C	3.300205	-0.455382	4.305261
C	-0.479761	-2.473623	2.053489
C	-1.493512	-3.512865	0.118830
C	-2.672808	1.612009	4.806044
C	-3.415991	0.554915	4.300147
C	1.468322	0.977837	2.922474
C	-5.761457	-2.050918	1.010884
C	-2.006365	2.453238	3.930083
C	3.340126	-0.398675	2.888835
C	-0.874309	-1.223261	1.555670
C	-3.478677	0.333744	2.917829
C	-1.853047	-2.240050	-0.341928
C	5.983636	-1.730265	0.626655
N	2.376999	0.280923	2.188285
C	1.960449	-3.768281	-0.452185
C	-4.795541	-1.002474	1.308191
C	2.126089	-2.484132	0.068235
N	-1.561497	-1.122936	0.384099
C	4.798387	-0.988749	1.098601
C	-2.059074	2.198612	2.560901
N	-2.753347	1.131976	2.054057
C	-5.923071	-2.083721	-0.354723
C	6.079082	-1.500625	-0.747764
C	1.341422	-3.883555	-1.700825
N	-4.386058	-0.361662	0.113328
N	1.743746	-1.363056	-0.579652
C	-5.029195	-1.082592	-0.924889
N	4.250621	-0.297471	0.034443
Ru	-2.602227	0.697814	-0.065187
Ru	2.424803	0.586616	0.050027
C	0.885611	-2.746514	-2.370989
C	4.395258	2.769313	0.867902
C	1.129312	-1.511077	-1.769755

C	4.826015	4.052668	1.183478
N	3.118649	2.490512	0.537373
C	4.954117	-0.617136	-1.109423
N	0.417078	1.859933	0.165554
C	-3.636822	-0.348454	-2.841476
N	-0.874304	1.947724	-0.272260
C	2.215594	3.503960	0.515341
C	3.903255	5.098964	1.162501
N	-2.584364	0.265858	-2.189767
C	-3.624026	-0.470489	-4.237945
C	0.835233	3.158627	0.156778
C	2.583414	4.817829	0.824496
N	-3.566692	2.519664	-0.512973
C	-1.249713	3.232679	-0.528175
C	-4.911477	2.688524	-0.619889
C	3.756727	0.568527	-2.791996
N	2.736155	1.088081	-2.034477
C	-0.175363	4.052779	-0.273795
C	-2.686645	3.538247	-0.709498
C	-1.521850	0.716116	-2.924661
C	-2.551032	0.012108	-4.973767
C	-5.422390	3.951084	-0.933140
C	-1.484949	0.598565	-4.312526
C	1.925818	1.991034	-2.648632
C	3.871901	0.895101	-4.168795
C	-3.160978	4.818759	-1.015197
C	-4.540228	5.019136	-1.130403
C	3.006228	1.781046	-4.771853
C	2.009734	2.362470	-3.976895
H	5.072515	1.924207	0.863600
H	5.866263	4.220080	1.441062
H	4.203661	6.112502	1.408284
H	1.837550	5.604607	0.814162
H	-0.112802	5.124378	-0.379534
H	-2.478827	5.645953	-1.163644
H	-4.925719	6.001607	-1.370123
H	-6.490544	4.101470	-1.020829
H	-5.584736	1.858638	-0.464047
H	1.169532	2.437626	-2.025710
H	1.306131	3.086158	-4.374230
H	3.104565	2.029598	-5.824212
H	4.685513	0.424698	-4.707758
H	4.071379	-1.044122	4.787385
H	2.334423	0.208155	6.106237
H	0.649742	1.580867	4.802530
H	0.749138	1.537449	2.344996
H	-1.522384	2.869226	1.928342
H	-1.438453	3.293894	4.307767
H	-2.632152	1.790990	5.872694

H	-3.969502	-0.080075	4.981117
H	-4.436514	-0.971453	-4.750095
H	-2.535985	-0.090622	-6.051098
H	-0.630759	0.961748	-4.869474
H	-0.678922	1.167175	-2.455600
H	0.856348	-0.596427	-2.275642
H	2.591528	-2.343485	1.034787
H	1.198380	-4.866456	-2.144569
H	-0.694275	-0.338794	2.138386
H	-2.421786	-2.155022	-1.250439
H	-0.523975	-4.599055	1.705272
N	4.405689	-1.056870	2.335912
N	4.736800	-0.268894	-2.341415
C	6.899864	-2.534545	1.294530
C	7.094608	-2.065715	-1.509994
H	6.817017	-2.706570	2.362880
H	7.159266	-1.881069	-2.577415
C	7.926353	-3.108122	0.534681
C	8.022158	-2.877420	-0.846016
H	8.662458	-3.742143	1.020522
H	8.830809	-3.336717	-1.407253
N	-4.686451	-1.055215	-2.169029
N	-4.368497	-0.707395	2.490942
C	-6.744162	-3.028532	-0.969122
C	-6.429135	-2.943316	1.848316
C	-7.437607	-3.934813	-0.147124
C	-7.281974	-3.891374	1.255484
H	-6.842138	-3.067392	-2.046196
H	-8.087583	-4.676062	-0.593458
H	-7.815169	-4.597995	1.877999
H	-6.290861	-2.913037	2.921236
C	0.138136	-2.825442	-3.679014
H	-0.939216	-2.945879	-3.506005
H	0.275995	-1.918371	-4.275843
H	0.469886	-3.679311	-4.277350
C	2.431379	-4.977258	0.316671
H	1.630936	-5.719325	0.412091
H	3.270647	-5.465737	-0.192535
H	2.763115	-4.706070	1.323030
C	-1.884523	-4.748118	-0.637484
H	-0.983212	-5.353824	-0.864423
H	-2.578653	-5.355922	-0.020032
H	-2.390341	-4.497160	-1.594110
C	0.238987	-2.598343	3.363008
H	1.247698	-3.030941	3.195861
H	0.350760	-1.613965	3.859404
H	-0.334439	-3.263404	4.042330

Transition State

1 1

C	-2.590863	-1.084368	4.846704
C	0.914237	3.712351	0.350919
C	-1.405273	-1.179138	4.105096
C	-3.751696	-0.758174	4.179004
C	0.733568	2.809696	1.404141
C	1.473936	3.273105	-0.854147
C	2.983899	-0.615647	5.067430
C	3.671509	0.348707	4.345184
C	-1.455841	-0.961914	2.741199
C	5.768418	2.413544	0.561789
C	2.319334	-1.624332	4.389718
C	-3.749759	-0.524362	2.780906
C	1.122284	1.477789	1.226769
C	3.694385	0.298561	2.945163
C	1.873012	1.936709	-0.968476
C	-6.564374	0.587893	0.590812
N	-2.588829	-0.649112	2.058663
C	-2.879231	3.757720	1.245111
C	4.941471	1.335722	1.083041
C	-2.687622	2.376774	1.176326
N	1.733901	1.073927	0.076982
C	-5.225889	0.146335	1.029891
C	2.317214	-1.629457	2.995554
N	2.976982	-0.669480	2.272165
C	5.907957	2.203303	-0.785631
C	-6.502974	0.752319	-0.797714
C	-2.583344	4.504567	0.103263
N	4.612038	0.410418	0.055118
N	-2.211682	1.734870	0.089106
C	5.145990	1.007686	-1.118892
N	-4.411985	0.066358	-0.081458
Ru	2.870372	-0.745687	0.106641
Ru	-2.482944	-0.432873	-0.055655
C	-2.088429	3.873772	-1.040684
C	-4.248587	-2.871561	-0.465544
C	-1.900403	2.491553	-0.984987
C	-4.650970	-4.178593	-0.698675
N	-2.960544	-2.495540	-0.294660
C	-5.128105	0.407973	-1.209764
N	-0.143041	-1.846865	-0.036381
C	3.917256	-0.296286	-2.827378
N	1.186592	-2.025879	0.200634
C	-2.010920	-3.465802	-0.344750
C	-3.679106	-5.172986	-0.772308
N	2.927818	-0.892488	-2.067238
C	3.999370	-0.540337	-4.205281
C	-0.597271	-3.125350	-0.135141

C	-2.353843	-4.804577	-0.592812
N	3.882992	-2.592141	0.174702
C	1.571949	-3.328659	0.173228
C	5.232028	-2.751573	0.182160
C	-3.506153	0.113859	-2.929712
N	-2.426929	-0.227892	-2.157542
C	0.447749	-4.088231	-0.014934
C	3.020167	-3.645421	0.200588
C	2.056417	-1.751190	-2.689060
C	3.113252	-1.412782	-4.816452
C	5.768107	-4.042097	0.214856
C	2.136075	-2.025639	-4.053322
C	-1.229698	-0.394416	-2.779233
C	-3.366409	0.223374	-4.337253
C	3.519255	-4.951628	0.226824
C	4.905088	-5.144536	0.236386
C	-2.144464	0.039791	-4.947398
C	-1.036628	-0.263457	-4.140953
H	-4.978803	-2.079504	-0.410834
H	-5.705855	-4.397114	-0.824055
H	-3.943068	-6.208036	-0.964727
H	-1.576992	-5.555368	-0.652609
H	0.378959	-5.162376	-0.057363
H	2.851816	-5.803639	0.241668
H	5.310668	-6.147672	0.259210
H	6.840481	-4.187683	0.221051
H	5.886393	-1.891949	0.161004
H	-0.411223	-0.619852	-2.109843
H	-0.047473	-0.386769	-4.564936
H	-2.040140	0.139523	-6.023542
H	-4.258738	0.479622	-4.895999
H	-4.701986	-0.651753	4.688544
H	-2.594793	-1.255278	5.918906
H	-0.462450	-1.419867	4.579046
H	-0.566010	-1.041682	2.133116
H	1.776299	-2.420119	2.519853
H	1.797557	-2.396818	4.939935
H	2.981693	-0.590696	6.149490
H	4.215917	1.121750	4.873758
H	4.755072	-0.046115	-4.803829
H	3.180253	-1.607155	-5.879106
H	1.434597	-2.709216	-4.514643
H	1.282684	-2.256163	-2.158242
H	-1.497641	1.969183	-1.841507
H	-2.925386	1.758023	2.029599
H	-2.738168	5.581554	0.103785
H	1.000822	0.787472	2.045250
H	2.353048	1.614991	-1.874917
H	0.631593	4.751175	0.471879

N	-4.959717	-0.135359	2.270610
N	-4.754518	0.410221	-2.455215
C	-7.737144	0.824803	1.297885
C	-7.612285	1.159028	-1.529502
H	-7.775631	0.691456	2.374230
H	-7.555455	1.280275	-2.606444
C	-8.858232	1.238418	0.567942
C	-8.796662	1.403123	-0.823658
H	-9.792418	1.434272	1.086303
H	-9.684115	1.724158	-1.361367
N	4.821024	0.691119	-2.325290
N	4.508235	1.281758	2.297766
C	6.588557	3.108514	-1.599702
C	6.313727	3.533455	1.188801
C	7.162537	4.239823	-0.992697
C	7.026541	4.450940	0.396521
H	6.667857	2.949792	-2.667277
H	7.702183	4.958115	-1.595990
H	7.463870	5.329370	0.852845
H	6.186523	3.696759	2.251044
C	-1.793508	4.644182	-2.303158
H	-2.718251	5.038484	-2.741122
H	-1.139010	5.499953	-2.105894
H	-1.314239	4.013266	-3.057154
C	-3.394787	4.401580	2.507943
H	-2.662002	5.106884	2.917186
H	-4.315914	4.963814	2.317386
H	-3.609343	3.655782	3.278813
C	1.718758	4.222338	-1.988703
H	1.189151	3.864395	-2.896017
H	1.362301	5.246096	-1.748041
H	2.807372	4.271105	-2.203016
C	0.216294	3.263934	2.737358
H	-0.105079	4.326576	2.708362
H	-0.646867	2.638786	3.045015
H	1.017493	3.157077	3.498545

Complex 5: L = 4-CF_3-py

Enantiomer

1 1

C	1.837633	-0.339863	-5.028271
C	-0.576911	3.151560	-1.584812
C	1.047780	-1.238526	-4.300312
C	2.835805	0.332396	-4.355136
C	-0.431692	1.928888	-2.248602

C	-1.220697	3.166572	-0.338664
C	-3.024561	-2.230408	-4.614743
C	-3.739574	-1.137423	-4.148290
C	1.262055	-1.354524	-2.939524
C	-5.796684	1.824815	-0.983276
C	-2.293794	-2.992961	-3.719742
C	3.048243	0.129972	-2.968669
C	-0.944206	0.765597	-1.674380
C	-3.712095	-0.802580	-2.787566
C	-1.707099	1.974261	0.203624
C	5.958318	1.208113	-0.909842
N	2.189868	-0.650382	-2.238381
C	1.994511	3.369497	0.556854
C	-4.898071	0.705893	-1.228575
C	2.166118	2.113368	-0.017899
N	-1.572186	0.795337	-0.467891
C	4.687547	0.566525	-1.296077
C	-2.263334	-2.630317	-2.374392
N	-2.934550	-1.529966	-1.906643
C	-5.838350	2.024594	0.374983
C	6.176697	0.891633	0.433153
C	1.345774	3.470277	1.784056
N	-4.418857	0.178428	-0.002983
N	1.758188	0.970608	0.575178
C	-4.941676	1.051527	0.985895
N	4.203946	-0.151250	-0.217079
Ru	-2.664753	-0.938555	0.168588
Ru	2.357416	-0.982059	-0.116247
C	0.899994	2.299600	2.397891
C	4.192849	-3.235063	-1.049836
C	1.135569	1.085725	1.769349
C	4.569187	-4.540497	-1.344529
N	2.954503	-2.912888	-0.627066
C	5.033638	0.065243	0.865580
N	0.302628	-2.197332	-0.121850
C	-3.475741	0.433959	2.887430
N	-0.966673	-2.224172	0.381423
C	2.032512	-3.901637	-0.494646
C	3.630198	-5.562380	-1.201817
N	-2.534084	-0.362194	2.261666
C	-3.378509	0.697773	4.261000
C	0.685445	-3.505227	-0.067577
C	2.347220	-5.235560	-0.773926
N	-3.659292	-2.690862	0.789914
C	-1.366443	-3.482912	0.719557
C	-4.999653	-2.804096	0.984801
C	3.892142	-1.071763	2.623448
N	2.771470	-1.492314	1.950587
C	-0.327789	-4.346874	0.457014

C	-2.801508	-3.727946	0.994508
C	-1.531685	-0.909543	3.018102
C	-2.347652	0.149737	5.009122
C	-5.531409	-4.027757	1.401034
C	-1.414880	-0.658747	4.383799
C	1.920313	-2.300811	2.637880
C	4.084340	-1.412639	3.988490
C	-3.298164	-4.970938	1.401666
C	-4.674058	-5.114323	1.608309
C	3.182258	-2.202568	4.666440
C	2.067978	-2.674257	3.959714
H	4.885947	-2.407256	-1.136762
H	5.580799	-4.743585	-1.678927
H	3.889049	-6.592407	-1.425265
H	1.587657	-6.002522	-0.672001
H	-0.290110	-5.413495	0.613453
H	-2.635379	-5.812077	1.559354
H	-5.076315	-6.067052	1.927390
H	-6.596626	-4.134425	1.559722
H	-5.652641	-1.959640	0.819635
H	1.078747	-2.670337	2.078249
H	1.324509	-3.316479	4.419518
H	3.337777	-2.458451	5.710035
H	4.980478	-1.025560	4.458311
H	3.521301	1.004366	-4.857580
H	1.686931	-0.193326	-6.093387
H	0.271290	-1.830337	-4.772249
H	0.644860	-2.015850	-2.350105
H	-1.677743	-3.246439	-1.733207
H	-1.741034	-3.857300	-4.065177
H	-3.050874	-2.494521	-5.664034
H	-4.336185	-0.557592	-4.842036
H	-4.100049	1.344313	4.745677
H	-2.270365	0.355687	6.068888
H	-0.604666	-1.097253	4.952513
H	-0.798250	-1.550378	2.591109
H	0.846774	0.158014	2.238136
H	2.643862	2.014781	-0.982840
H	0.378526	2.324138	3.348184
H	2.347480	4.252357	0.037258
H	-0.892563	-0.151123	-2.226887
H	-2.220996	2.011064	1.146744
H	0.051505	1.878945	-3.216778
H	-1.358102	4.088422	0.211423
N	4.173244	0.737974	-2.478412
N	4.903524	-0.319167	2.098627
C	6.852231	1.995652	-1.626116
C	7.297542	1.350862	1.114627
H	6.672371	2.237571	-2.668632

H	7.456165	1.102756	2.159056
C	7.985733	2.460274	-0.948353
C	8.204906	2.142729	0.400597
H	8.708402	3.077793	-1.473801
H	9.093865	2.519517	0.898050
N	-4.510811	1.142459	2.197944
N	-4.554772	0.289143	-2.400506
C	-6.571060	3.069650	0.936916
C	-6.499402	2.644476	-1.865580
C	-7.299065	3.905457	0.071245
C	-7.264283	3.693039	-1.324110
H	-6.577028	3.236058	2.006256
H	-7.882462	4.721727	0.476822
H	-7.822593	4.346296	-1.981899
H	-6.453990	2.483356	-2.934780
C	1.140820	4.807921	2.455815
C	-0.054683	4.411546	-2.226817
F	1.191103	5.816975	1.568038
F	2.090656	5.026086	3.385322
F	-0.054425	4.851718	3.076557
F	-0.740991	4.642948	-3.404735
F	-0.211741	5.509605	-1.398705
F	1.290476	4.263930	-2.513037

Transition State

1 1

C	-2.176168	-1.219090	4.996177
C	0.763815	3.439200	0.455362
C	-1.058479	-1.499635	4.200224
C	-3.348457	-0.867604	4.363990
C	0.521791	2.420269	1.387667
C	1.427188	3.115813	-0.734015
C	3.079983	-0.908854	4.969853
C	3.639635	0.162781	4.289146
C	-1.175586	-1.402105	2.826339
C	5.615544	2.508287	0.607431
C	2.553504	-1.968777	4.249812
C	-3.422084	-0.791756	2.950835
C	1.006295	1.132894	1.144934
C	3.674194	0.167041	2.888496
C	1.888241	1.814778	-0.938071
C	-6.391547	-0.000557	0.834800
N	-2.316134	-1.046830	2.177868
C	-3.049239	3.238736	0.646057
C	4.860200	1.359197	1.082373
C	-2.723038	1.904258	0.848720
N	1.727583	0.860145	0.021294

C	-5.016451	-0.359315	1.230324
C	2.544095	-1.915332	2.856930
N	3.075730	-0.851654	2.175810
C	5.824948	2.329768	-0.735822
C	-6.438006	-0.053102	-0.561621
C	-2.752628	3.826774	-0.582155
N	4.644574	0.427946	0.029866
N	-2.128201	1.134752	-0.091642
C	5.170595	1.084740	-1.115738
N	-4.281040	-0.604634	0.086686
Ru	3.001331	-0.865493	0.010028
Ru	-2.320547	-1.023942	0.036671
C	-2.059317	3.073108	-1.526442
C	-3.951653	-3.581116	0.101787
C	-1.761386	1.745753	-1.239334
C	-4.275339	-4.927754	0.018794
N	-2.687044	-3.107951	0.041557
C	-5.089826	-0.437329	-1.020489
N	0.067846	-2.227091	-0.018486
C	4.058262	-0.243431	-2.886494
N	1.427672	-2.289149	0.035320
C	-1.676009	-4.006858	-0.084289
C	-3.246171	-5.852250	-0.142467
N	3.099270	-0.929597	-2.163879
C	4.182593	-0.440665	-4.268573
C	-0.280707	-3.544167	-0.079982
C	-1.941679	-5.380972	-0.190157
N	4.160324	-2.626172	0.019360
C	1.918049	-3.552216	-0.025963
C	5.517905	-2.674292	0.035180
C	-3.590160	-0.910802	-2.806901
N	-2.432688	-1.068253	-2.090178
C	0.850302	-4.409218	-0.091771
C	3.387830	-3.747598	-0.014836
C	2.309651	-1.837042	-2.823843
C	3.378938	-1.362572	-4.919558
C	6.158954	-3.916301	0.019394
C	2.440489	-2.071621	-4.191928
C	-1.286703	-1.276571	-2.790033
C	-3.577920	-1.030467	-4.220484
C	3.993549	-5.008083	-0.033291
C	5.390395	-5.086099	-0.015350
C	-2.405511	-1.262250	-4.905362
C	-1.218413	-1.373026	-4.166452
H	-4.723433	-2.834750	0.215327
H	-5.314893	-5.231803	0.074391
H	-3.451057	-6.914911	-0.224701
H	-1.123989	-6.079595	-0.309817
H	0.871865	-5.485548	-0.129441

H	3.399284	-5.912372	-0.059360
H	5.877657	-6.052382	-0.028459
H	7.239626	-3.972942	0.032209
H	6.099149	-1.763731	0.058146
H	-0.403252	-1.345956	-2.173535
H	-0.264573	-1.524344	-4.655105
H	-2.399277	-1.341891	-5.988114
H	-4.528776	-0.909105	-4.725505
H	-4.256999	-0.642934	4.909728
H	-2.122431	-1.280799	6.078749
H	-0.117226	-1.792519	4.644806
H	-0.337702	-1.622213	2.180875
H	2.109457	-2.748367	2.346340
H	2.138103	-2.824629	4.766369
H	3.076254	-0.927889	6.052022
H	4.089001	0.973273	4.849973
H	4.911762	0.123093	-4.837882
H	3.484651	-1.526838	-5.984166
H	1.817892	-2.809013	-4.682206
H	1.578594	-2.424995	-2.316300
H	-1.237712	1.137807	-1.964161
H	-2.964484	1.421719	1.784530
H	-1.763686	3.499544	-2.477743
H	-3.545432	3.797021	1.432015
H	0.879376	0.379151	1.903510
H	2.444889	1.602867	-1.832199
H	0.012109	2.623800	2.320611
H	1.629204	3.875189	-1.479212
N	-4.656691	-0.436927	2.475882
N	-4.811213	-0.597512	-2.278558
C	-7.511925	0.332989	1.586784
C	-7.606423	0.227036	-1.260315
H	-7.466693	0.367559	2.670490
H	-7.632397	0.182589	-2.344232
C	-8.692159	0.620032	0.890541
C	-8.738675	0.567710	-0.510625
H	-9.588303	0.887246	1.442940
H	-9.669981	0.795623	-1.020849
N	4.888920	0.782665	-2.336936
N	4.401983	1.241217	2.283752
C	6.464001	3.298043	-1.510116
C	6.047612	3.656569	1.270257
C	6.923780	4.460678	-0.866088
C	6.717250	4.638785	0.519049
H	6.597528	3.162798	-2.575520
H	7.429183	5.227950	-1.437921
H	7.066841	5.540975	1.003788
H	5.867320	3.792349	2.328684
C	-3.225172	5.230759	-0.883597

C	0.410671	4.874721	0.749345
F	-2.570417	5.760930	-1.932282
F	-3.050201	6.039376	0.178357
F	-4.540094	5.225434	-1.177965
F	-0.131529	5.471593	-0.373352
F	1.558930	5.557900	1.104082
F	-0.503216	4.968778	1.784663

Complex 6: L = MeCN

Enantiomer

1 1

C	-1.768489	4.784835	-1.277407
C	-0.834395	4.104832	-0.485267
C	-2.921680	4.118657	-1.634097
C	3.155960	4.658023	1.601204
C	4.044424	4.089123	0.701382
C	-1.112871	2.802874	-0.116522
C	6.280884	0.657223	-1.787031
C	2.124195	3.888800	2.110077
C	-3.160776	2.783417	-1.219919
C	3.883777	2.757916	0.291572
C	-6.138707	0.649924	-1.895653
N	-2.230381	2.117437	-0.466294
C	5.045055	1.123306	-1.169595
N	1.271469	0.779846	-1.472597
C	-4.830012	1.091784	-1.374878
C	1.981953	2.567698	1.689667
N	2.827685	2.004544	0.769531
C	6.117599	-0.676411	-2.079879
C	-6.316229	-0.669053	-1.471016
N	4.080161	0.086471	-1.169110
N	-1.823061	-0.631527	-1.617710
C	4.769735	-1.049923	-1.671508
N	-4.283157	0.066620	-0.627807
Ru	2.411274	-0.011154	0.075409
Ru	-2.425552	0.084546	0.186657
C	-4.319726	1.157218	2.349241
C	-4.734160	1.493623	3.633757
N	-3.075075	0.720705	2.077388
C	-5.114813	-1.029734	-0.692595
N	-0.484697	0.214738	1.421510
C	3.036165	-2.765294	-1.263520
N	0.791772	-0.251096	1.429024
C	-2.185767	0.616744	3.101997
C	-3.830296	1.374379	4.689187

N	2.057531	-1.990062	-0.682854
C	2.758591	-4.095856	-1.606491
C	-0.832390	0.193161	2.737589
C	-2.539150	0.931724	4.416165
N	3.464365	-0.788848	1.740302
C	1.235070	-0.556015	2.672100
C	4.799108	-1.046316	1.789961
C	-3.892425	-2.683769	0.519292
N	-2.763449	-1.971752	0.841735
C	0.217084	-0.290818	3.564436
C	2.660261	-0.920930	2.834427
C	0.786925	-2.474167	-0.579389
C	1.477700	-4.608366	-1.431446
C	5.370469	-1.494082	2.984346
C	0.475602	-3.784410	-0.938490
C	-1.838602	-2.616271	1.602100
C	-4.040146	-4.031980	0.938937
C	3.198868	-1.356476	4.049437
C	4.563808	-1.650876	4.116427
C	-3.075197	-4.660773	1.694269
C	-1.937921	-3.922389	2.042683
H	-4.990530	1.218890	1.501358
H	-5.749567	1.839324	3.794306
H	-4.121680	1.627147	5.703649
H	-1.803148	0.845050	5.207960
H	0.210435	-0.428589	4.634417
H	2.575901	-1.466260	4.927912
H	4.998525	-1.991322	5.047256
H	6.430346	-1.707020	3.035769
H	5.424586	-0.896407	0.925662
H	-0.962559	-2.048350	1.865553
H	-1.137214	-4.345728	2.639414
H	-3.197237	-5.692374	2.010255
H	-4.953026	-4.530655	0.636471
H	-3.692780	4.581738	-2.237997
H	-1.594026	5.806783	-1.599995
H	0.092396	4.567327	-0.163419
H	-0.420198	2.236797	0.480266
H	1.175000	2.020689	2.119396
H	1.432328	4.311363	2.827531
H	3.280829	5.685083	1.919148
H	4.875752	4.677863	0.332758
H	3.526572	-4.718676	-2.048598
H	1.254822	-5.629351	-1.713108
H	-0.537244	-4.153293	-0.838722
H	-0.001743	-1.837009	-0.237504
N	-4.357707	2.271822	-1.638966
N	-4.956930	-2.221180	-0.202230
C	-7.094151	1.299336	-2.668404

C	-7.456340	-1.391572	-1.801981
H	-6.945013	2.323281	-2.995522
H	-7.583141	-2.416577	-1.468814
C	-8.247195	0.579911	-3.004775
C	-8.425549	-0.744693	-2.578181
H	-9.017567	1.053334	-3.606624
H	-9.331269	-1.275786	-2.856496
N	4.323362	-2.263588	-1.647601
N	4.935661	2.237289	-0.529227
C	7.153110	-1.438687	-2.619059
C	7.494542	1.308733	-2.004223
C	8.381558	-0.800792	-2.867416
C	8.551727	0.566802	-2.560796
H	7.018499	-2.490399	-2.835835
H	9.204260	-1.364219	-3.287970
H	9.504544	1.045164	-2.746437
H	7.621956	2.352526	-1.748328
C	-1.600807	-1.119804	-2.644974
C	0.680111	1.248344	-2.349592
C	-1.281989	-1.728955	-3.930866
H	-1.543080	-1.047193	-4.746542
H	-0.211360	-1.952131	-3.985771
H	-1.843445	-2.660253	-4.056024
C	-0.059073	1.851162	-3.459105
H	0.237288	2.914910	-3.564541
H	0.172471	1.305754	-4.396834
H	-1.147846	1.792562	-3.257657

Transition State

1 1

C	2.219355	0.963142	4.839461
C	1.096615	0.972485	4.001065
C	3.447082	0.671269	4.284018
C	-2.886273	2.104531	4.546789
C	-3.707341	1.053004	4.170384
C	1.276151	0.727422	2.652172
C	-5.848872	-2.161039	1.357268
C	-2.033949	2.663939	3.611147
C	3.569982	0.374421	2.904225
C	-3.684540	0.573393	2.853314
C	6.534486	-0.942617	1.056553
N	2.476583	0.449165	2.083744
C	-5.007587	-0.976634	1.446640
N	-1.746456	-1.288546	0.409807
C	5.161050	-0.491854	1.357985
C	-1.997967	2.144908	2.317802
N	-2.806571	1.104938	1.930938

C	-5.812529	-2.587392	0.057137
C	6.536074	-1.386241	-0.270927
N	-4.528539	-0.596495	0.161180
N	2.099699	-1.985171	0.620802
C	-4.952143	-1.669116	-0.673870
N	4.393095	-0.668390	0.224359
Ru	-2.739094	0.448247	-0.139142
Ru	2.495766	-0.072348	0.023770
C	4.486878	2.130753	-0.708619
C	4.986337	3.361969	-1.107156
N	3.168558	1.851767	-0.592848
C	5.164510	-1.204166	-0.786921
N	0.338128	1.376135	-0.426107
C	-3.582545	-1.190678	-2.679192
N	-1.001242	1.606008	-0.481669
C	2.289944	2.842817	-0.891726
C	4.088024	4.381455	-1.410850
N	-2.764215	-0.180766	-2.217139
C	-3.558969	-1.560286	-4.031179
C	0.850730	2.584741	-0.792846
C	2.732215	4.110501	-1.300516
N	-3.667210	2.253588	-0.703512
C	-1.327087	2.867774	-0.859991
C	-5.007809	2.457759	-0.783483
C	3.588024	-1.398573	-2.563505
N	2.497963	-0.826796	-1.963590
C	-0.158170	3.548688	-1.074265
C	-2.759264	3.228609	-0.983882
C	-1.984903	0.498995	-3.119662
C	-2.760483	-0.871050	-4.930993
C	-5.486776	3.713086	-1.169142
C	-1.979695	0.177420	-4.476054
C	1.310610	-0.885460	-2.617859
C	3.473420	-1.966807	-3.856228
C	-3.200321	4.497360	-1.373590
C	-4.576245	4.734962	-1.464728
C	2.257864	-2.012965	-4.505163
C	1.139526	-1.468456	-3.859940
H	5.162876	1.326338	-0.469041
H	6.059330	3.504461	-1.173911
H	4.431309	5.361360	-1.726978
H	2.010984	4.882533	-1.533876
H	-0.040472	4.573382	-1.384330
H	-2.496222	5.286876	-1.602693
H	-4.937333	5.710201	-1.764439
H	-6.551643	3.893341	-1.238422
H	-5.698946	1.659985	-0.551858
H	0.479636	-0.441515	-2.085998
H	0.157744	-1.504690	-4.314238

H	2.168801	-2.467875	-5.487010
H	4.376411	-2.381281	-4.288316
H	4.353510	0.623637	4.875623
H	2.124122	1.167021	5.901657
H	0.104951	1.159456	4.393091
H	0.441116	0.734894	1.964492
H	-1.302420	2.603271	1.649800
H	-1.385621	3.485486	3.888322
H	-2.913474	2.485755	5.559423
H	-4.382644	0.619945	4.898410
H	-4.186649	-2.367713	-4.388436
H	-2.754151	-1.143656	-5.978434
H	-1.354399	0.729610	-5.166081
H	-1.347768	1.303909	-2.826056
N	4.827547	-0.008131	2.515738
N	4.836423	-1.502906	-2.007032
C	7.685056	-0.981347	1.835901
C	7.688776	-1.884150	-0.867682
H	7.672735	-0.636092	2.864685
H	7.679838	-2.226286	-1.897549
C	8.850292	-1.479386	1.240992
C	8.851986	-1.923796	-0.089809
H	9.769580	-1.523338	1.817788
H	9.772614	-2.304866	-0.522227
N	-4.498769	-1.915121	-1.856021
N	-4.599558	-0.485701	2.566877
C	-6.456707	-3.756320	-0.348498
C	-6.530123	-2.875278	2.343049
C	-7.170279	-4.486106	0.618951
C	-7.206769	-4.047162	1.960128
H	-6.405189	-4.095631	-1.374877
H	-7.684922	-5.394977	0.335669
H	-7.749050	-4.621324	2.700005
H	-6.534156	-2.542043	3.372696
C	2.277288	-3.080455	0.956548
C	-1.334398	-2.317613	0.736398
C	2.519085	-4.456247	1.378497
H	3.596997	-4.638980	1.437010
H	2.077805	-4.636233	2.363868
H	2.081702	-5.157569	0.660925
C	-0.888652	-3.642983	1.157640
H	-0.295616	-4.109868	0.345572
H	-0.283225	-3.553779	2.082119
H	-1.775567	-4.275714	1.366551

APENDIX B

EXPERIMENTAL SUPPORTING INFORMATION FOR:

Substitution Reactions in Dinuclear Ru-Hbpp Complexes: An evaluation of intrasupramolecular effects

Nora Planas,[a] Gemma Christian,[a] Elena Mas-Marza,[a] Mohan Rao,[b] Jordi Benet-Buchholz,[a] Feliu Maserasa,[b,*] and Antoni Llobet [a,b,*]

[a]Institute of Chemical Research of Catalonia (ICIQ), Av. Països Catalans 16, E-43007 Tarragona, Spain and
[b]Departament de Química, Universitat Autònoma de Barcelona, Cerdanyola del Vallès, E-08193 Barcelona, Spain.

email: fmaseras@iciq.es and allobet@iciq.es.

The supporting information section also includes "cif" magnetic files of the crystal structures of complexes $3b^{3+}$, 4^{3+}, **3a'**$^{+}$, and $3c^{3+}$.

1-HNMR characterization:

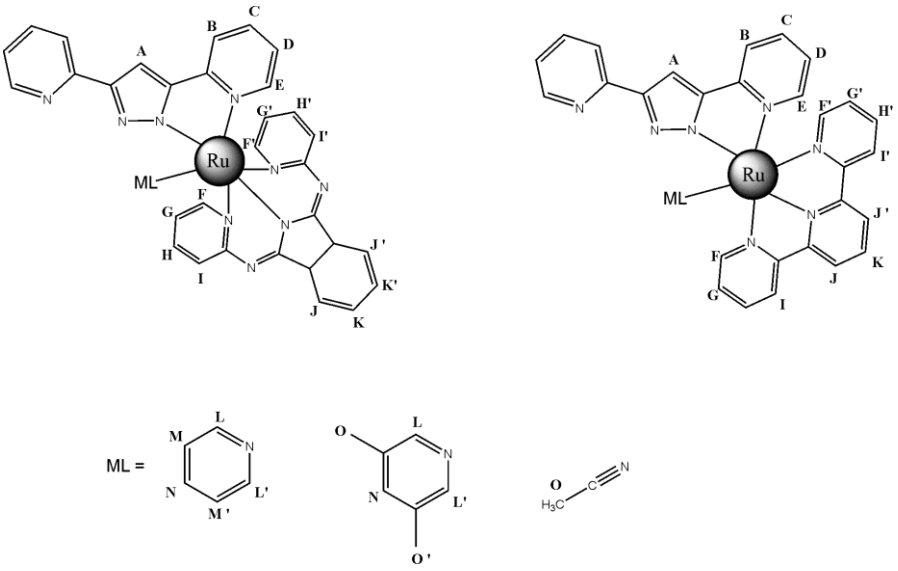

Figure S1.1. HNMR nomenclature for symmetric compunds

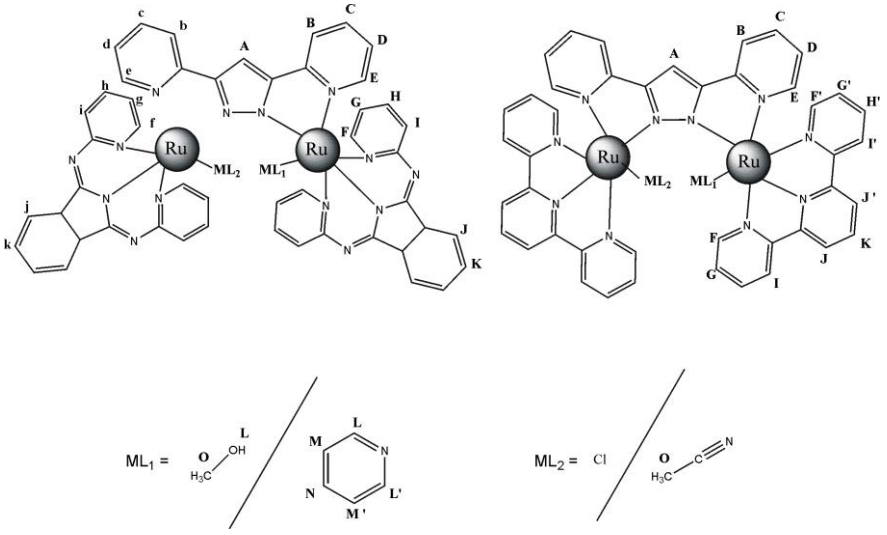

Figure S1.2. HNMR nomenclature for asymmetric compounds

Figure S1-0. 1D and 2D NMR spectra (500 MHz, 298K, CD_2Cl_2) for complex **1'** (a) ^{1}H-NMR, (b) COSY and (c) NOESY .

(a)

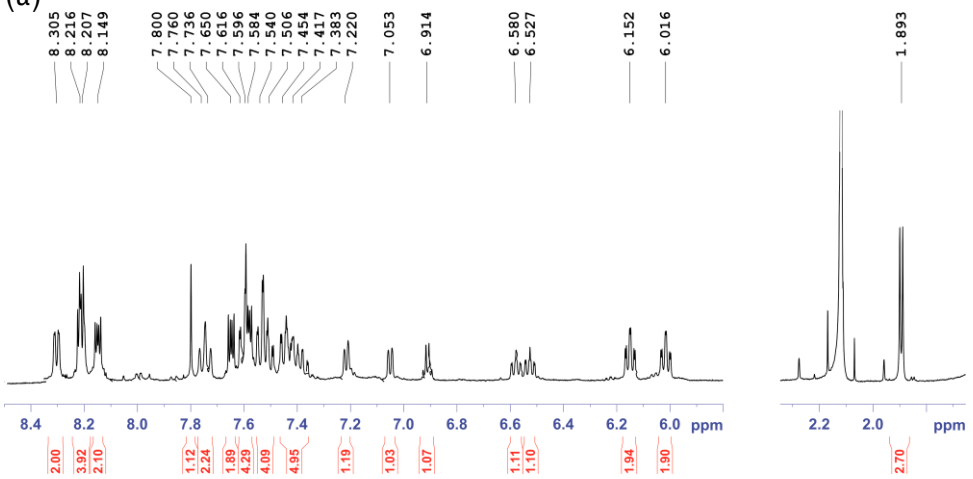

(b)

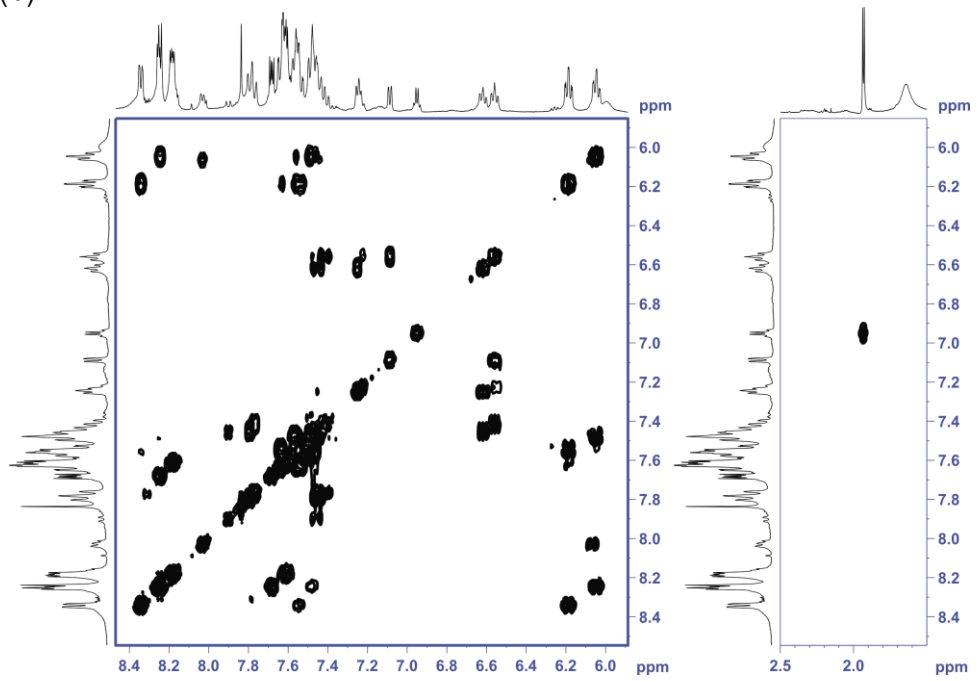

(c)

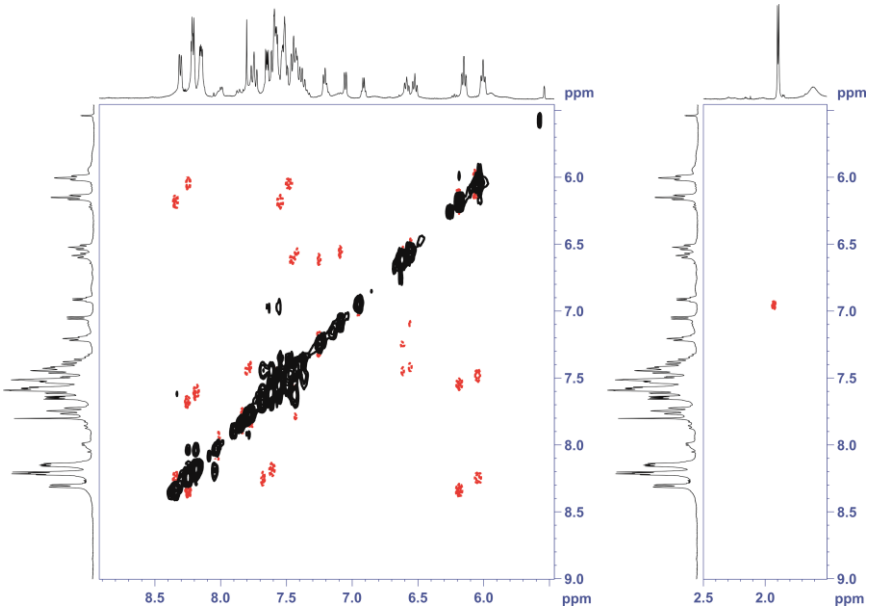

Figure S1-1. 1D and 2D NMR spectra (400 MHz) for complex 3b (a) ^{1}H-NMR at 298K in CD_3CN, (b) COSY at 298K in CD_3CN. HNMR in Acetone-d_6 allready reported previously [S1]

a)

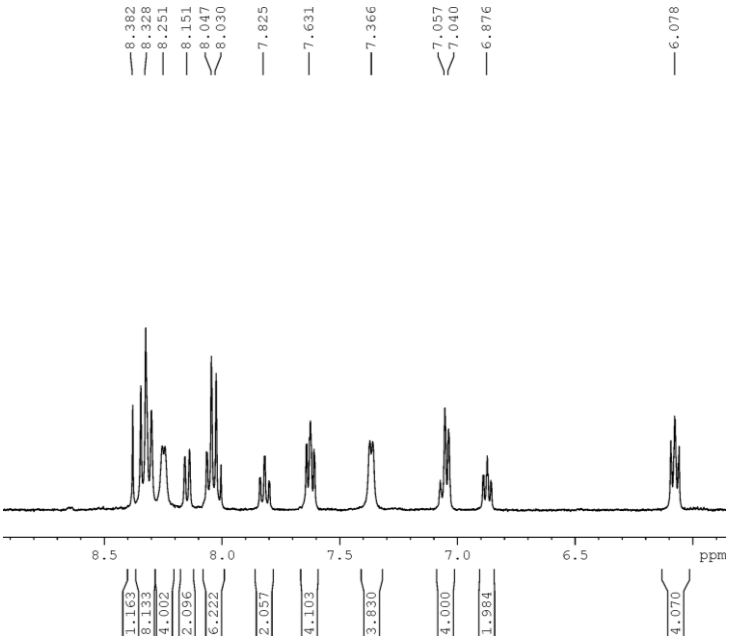

b)

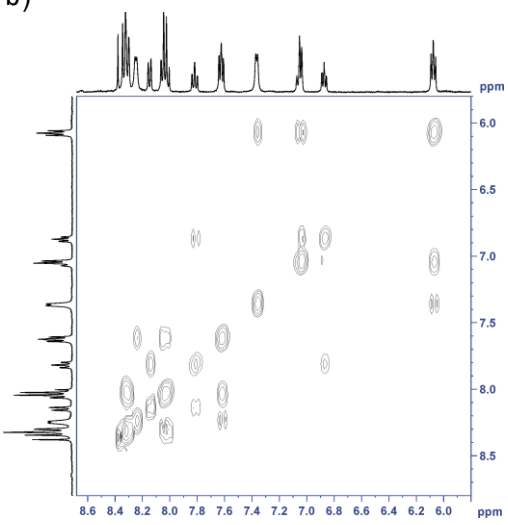

Figure S1-2. 1D and 2D NMR spectra (400 MHz, CD_3CN) for complex 3a. (a) ^{1}H-NMR at 298K, (b) COSY at 298K, (c) ^{1}H-NMR at 240K, (d) COSY at 240K, (e) NOESY at 240K,

a)

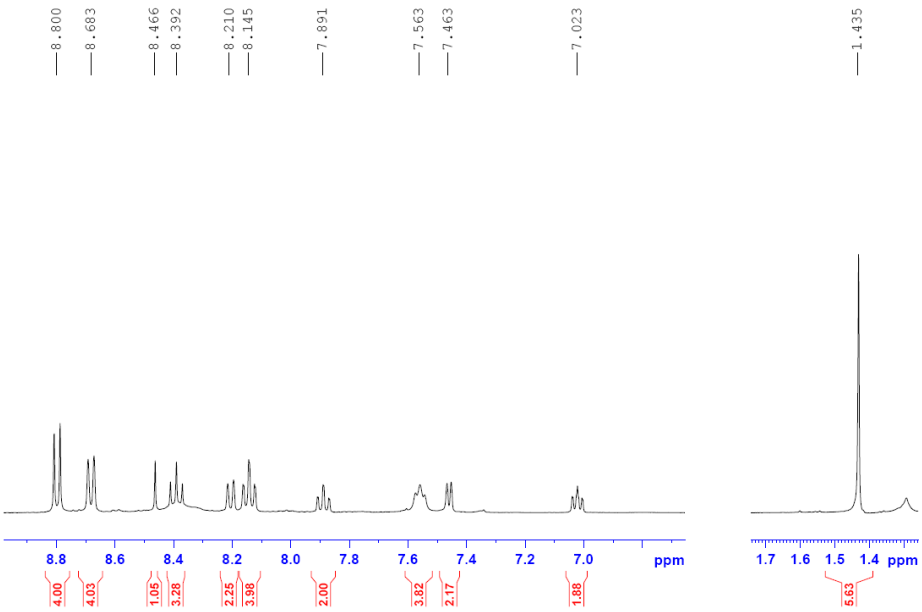

b)

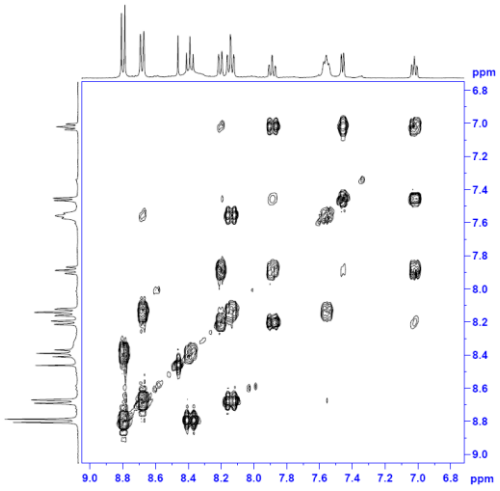

c)

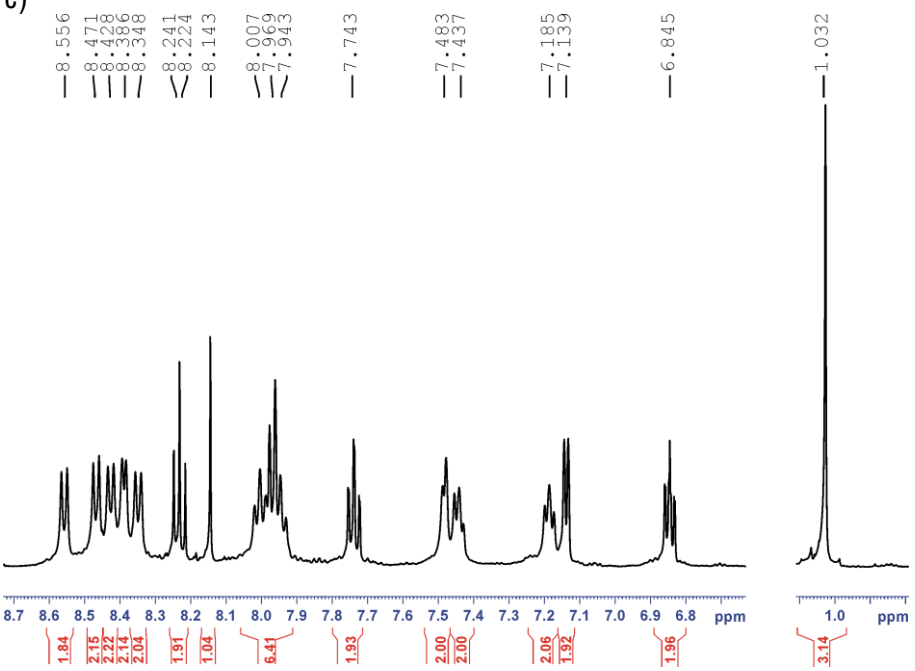
8.556
8.471
8.428
8.386
8.348
8.241
8.224
8.143
8.007
7.969
7.943
7.743
7.483
7.437
7.185
7.139
6.845
1.032
8.7 8.6 8.5 8.4 8.3 8.2 8.1 8.0 7.9 7.8 7.7 7.6 7.5 7.4 7.3 7.2 7.1 7.0 6.9 6.8 ppm
1.0 ppm
1.84
2.15
2.22
2.14
2.04
1.91
1.04
6.41
1.93
2.00
2.00
2.06
1.92
1.96
3.14

d)

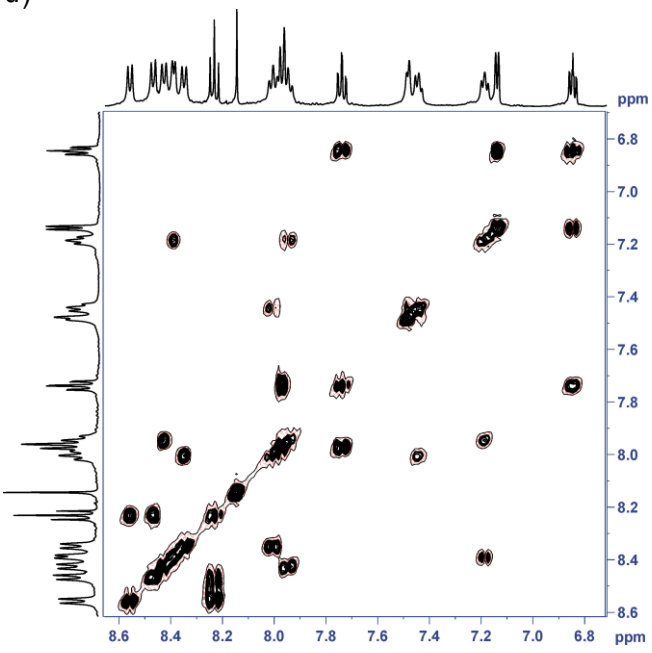
ppm
6.8
7.0
7.2
7.4
7.6
7.8
8.0
8.2
8.4
8.6
8.6 8.4 8.2 8.0 7.8 7.6 7.4 7.2 7.0 6.8 ppm

e)

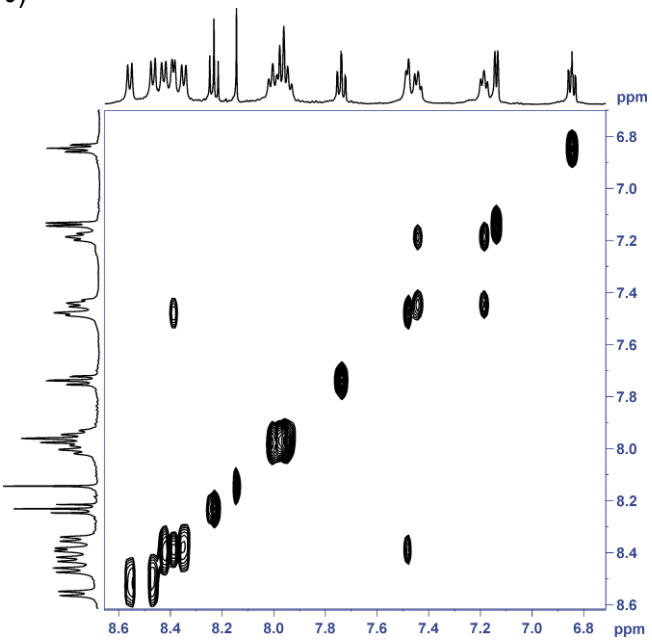

Figure S1-3. 1D and 2D NMR spectra (400 MHz) for complex 4. (a) ^{1}H-NMR at 298K in Acetone-d_6, (b) COSY at 298K in Acetone-d_6, (c) NOESY at 298K in Acetone-d_6, (d) ^{1}H-NMR at 298K in CD_3CN from an authentic sample (A) and from kinetics in the NMR tube (B). Resonances labeled with a star indicate free pyridine. The resonance labeled with X corresponds to the coordinated MeCN. In B is not observed since it it contains CD_3CN from the solvent.

a)

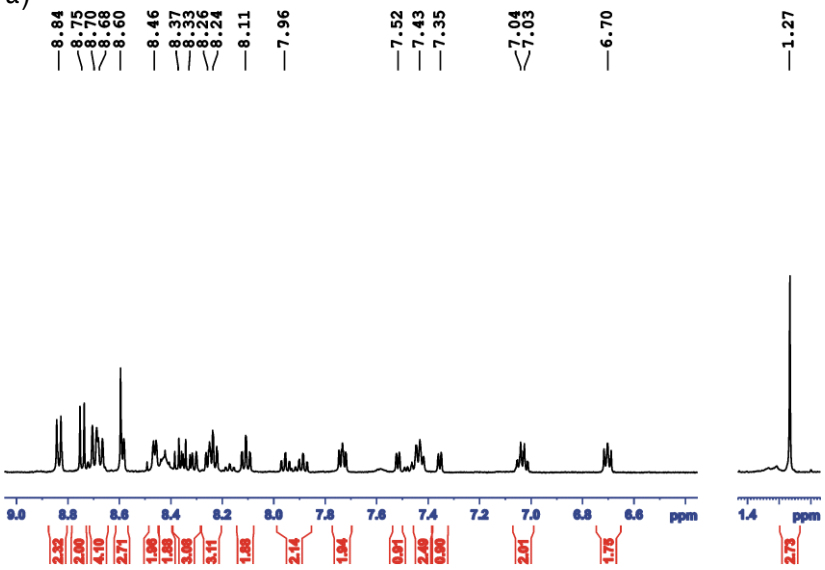

b)

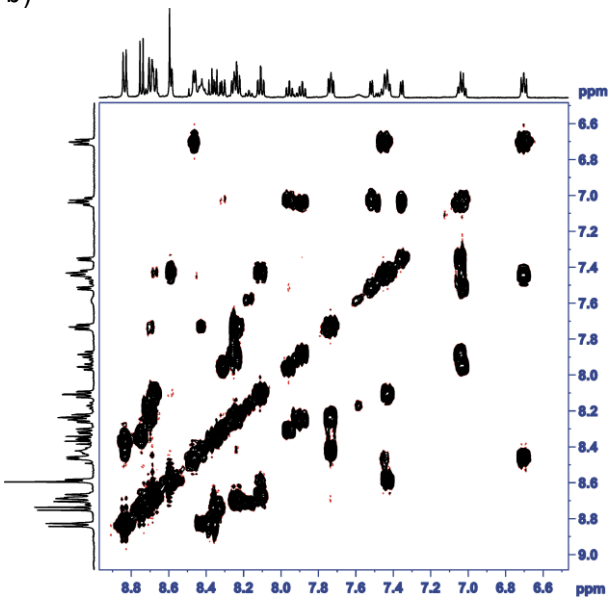

c)

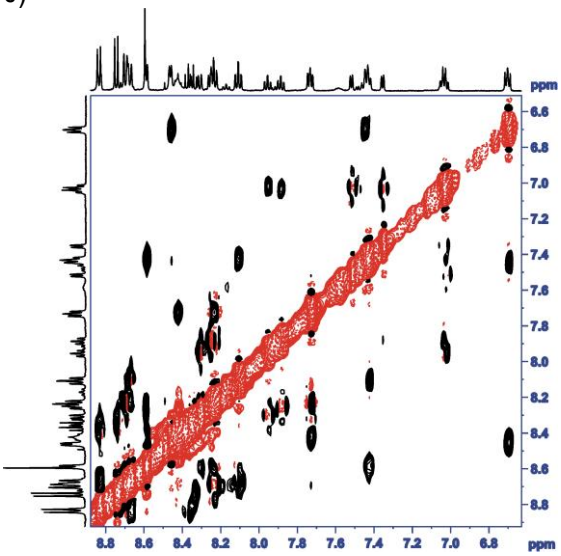
ppm
6.6
6.8
7.0
7.2
7.4
7.6
7.8
8.0
8.2
8.4
8.6
8.8
8.8 8.6 8.4 8.2 8.0 7.8 7.6 7.4 7.2 7.0 6.8
ppm

d)

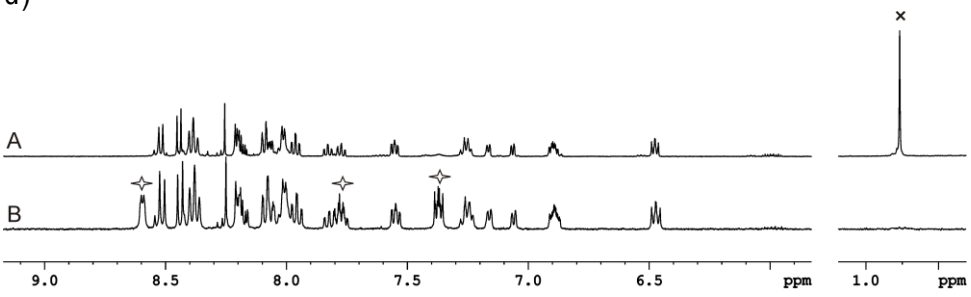
×
A
B
9.0
8.5
8.0
7.5
7.0
6.5
ppm
1.0
ppm

Figure S1-4. 1D and 2D NMR spectra (400 MHz) for complex 3c. (a) ^{1}H-NMR at 298K in Acetone-d_6, (b) ^{1}H-NMR at 188K in Acetone-d_6, (c) COSY at 188K in Acetone-d_6, (d) NOESY at 188K in Acetone-d_6, (e) ^{1}H-NMR at 298K in CD_3CN, (f) COSY at 298K in CD_3CN, (g) NOESY at 298K in CD_3CN,

a)

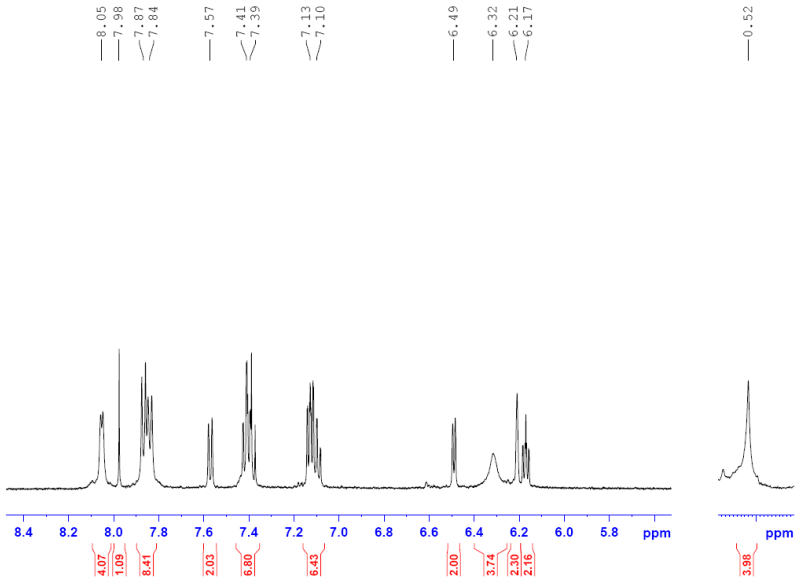

b)

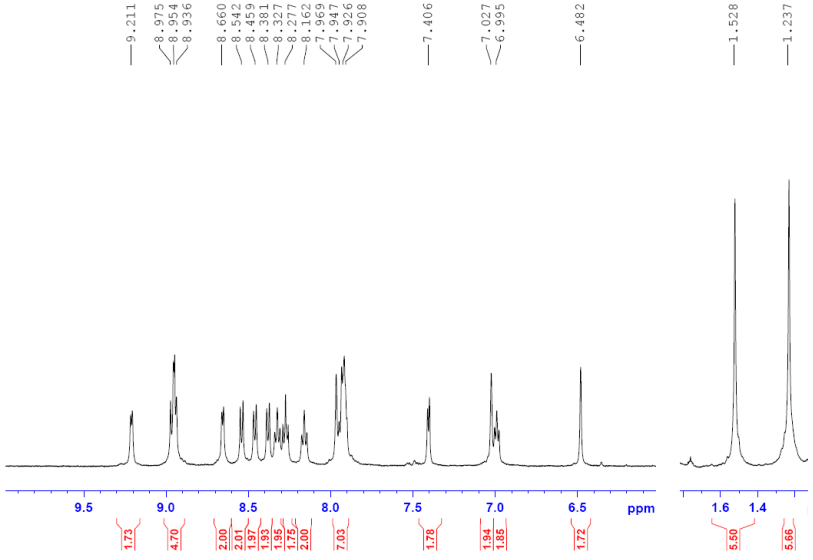

c)

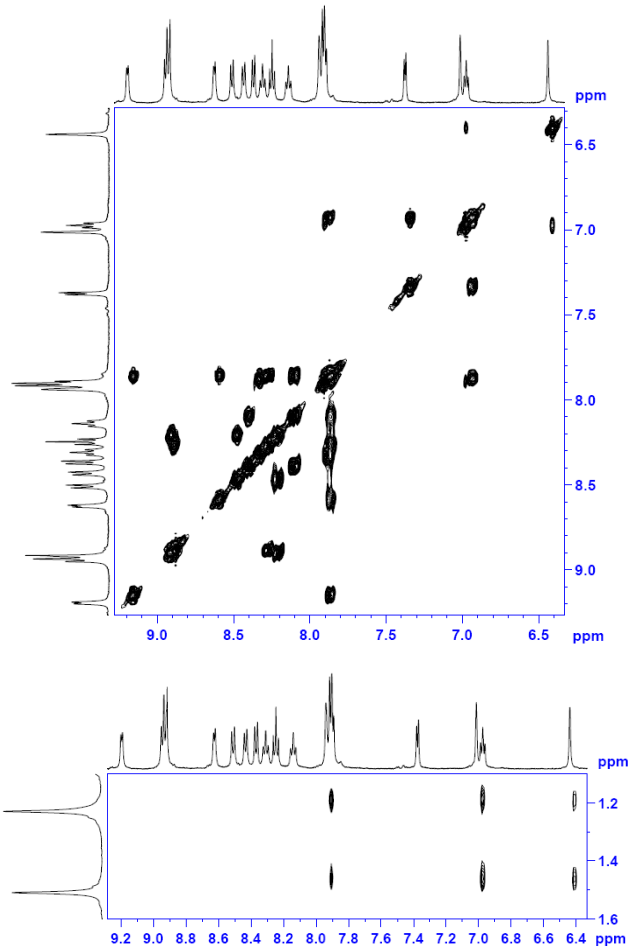
ppm
6.5
7.0
7.5
8.0
8.5
9.0
9.0 8.5 8.0 7.5 7.0 6.5 ppm
ppm
1.2
1.4
1.6
9.2 9.0 8.8 8.6 8.4 8.2 8.0 7.8 7.6 7.4 7.2 7.0 6.8 6.6 6.4 ppm

d)

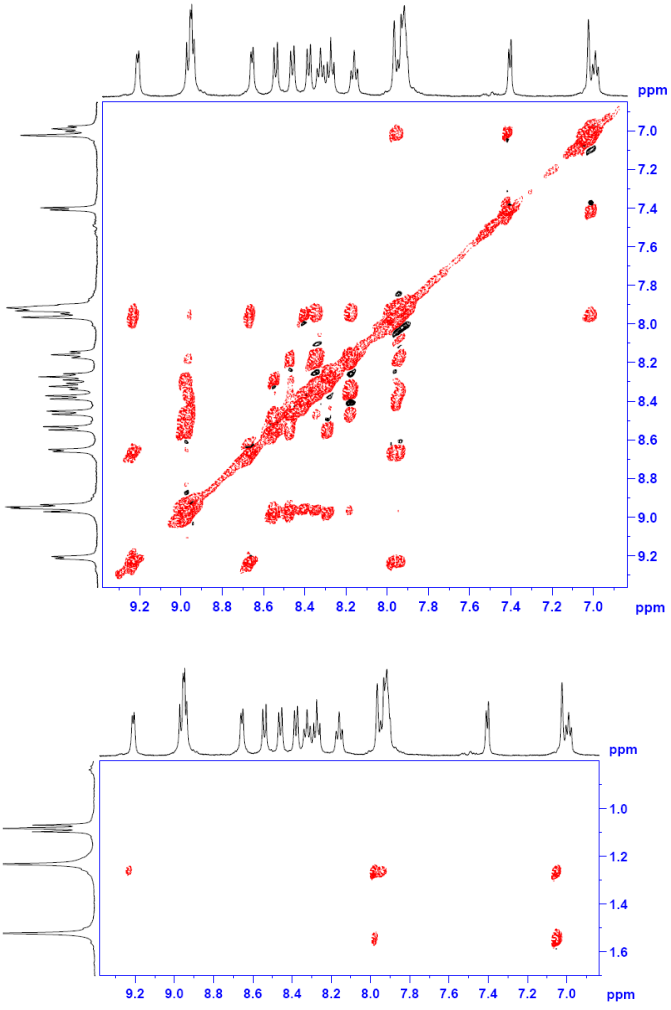
ppm
7.0
7.2
7.4
7.6
7.8
8.0
8.2
8.4
8.6
8.8
9.0
9.2
9.2 9.0 8.8 8.6 8.4 8.2 8.0 7.8 7.6 7.4 7.2 7.0
ppm
ppm
1.0
1.2
1.4
1.6
9.2 9.0 8.8 8.6 8.4 8.2 8.0 7.8 7.6 7.4 7.2 7.0
ppm

e)

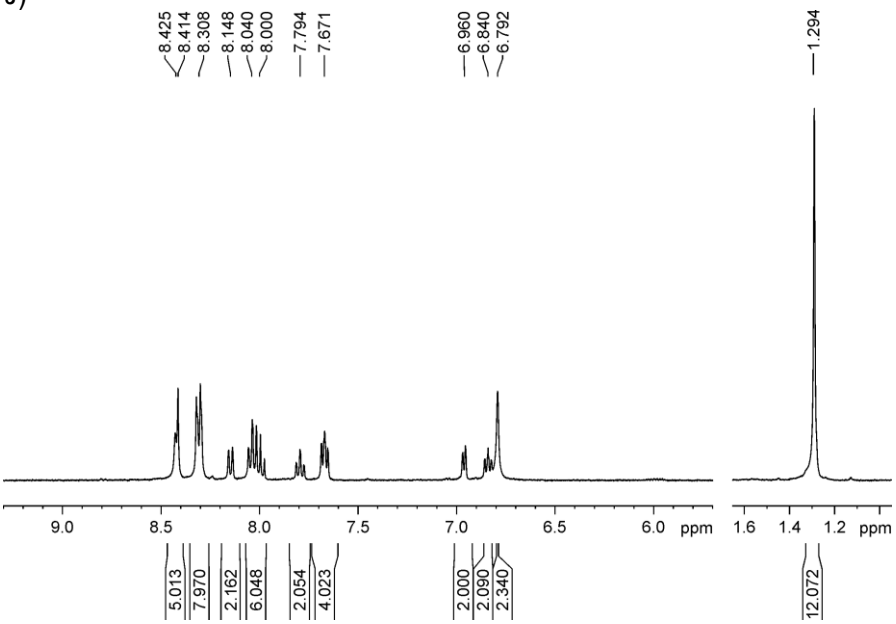
8.425
8.414
8.308
8.148
8.040
8.000
7.794
7.671
6.960
6.840
6.792
1.294
9.0
8.5
8.0
7.5
7.0
6.5
6.0 ppm
1.6
1.4
1.2 ppm
5.013
7.970
2.162
6.048
2.054
4.023
2.000
2.090
2.340
12.072

f)

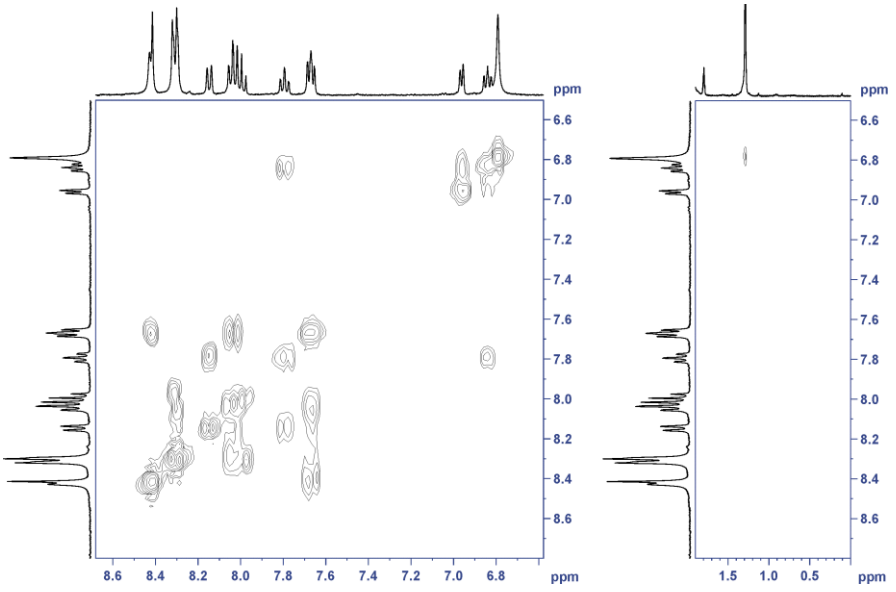
ppm
6.6
6.8
7.0
7.2
7.4
7.6
7.8
8.0
8.2
8.4
8.6
8.6
8.4
8.2
8.0
7.8
7.6
7.4
7.2
7.0
6.8
ppm
1.5
1.0
0.5
ppm

g)

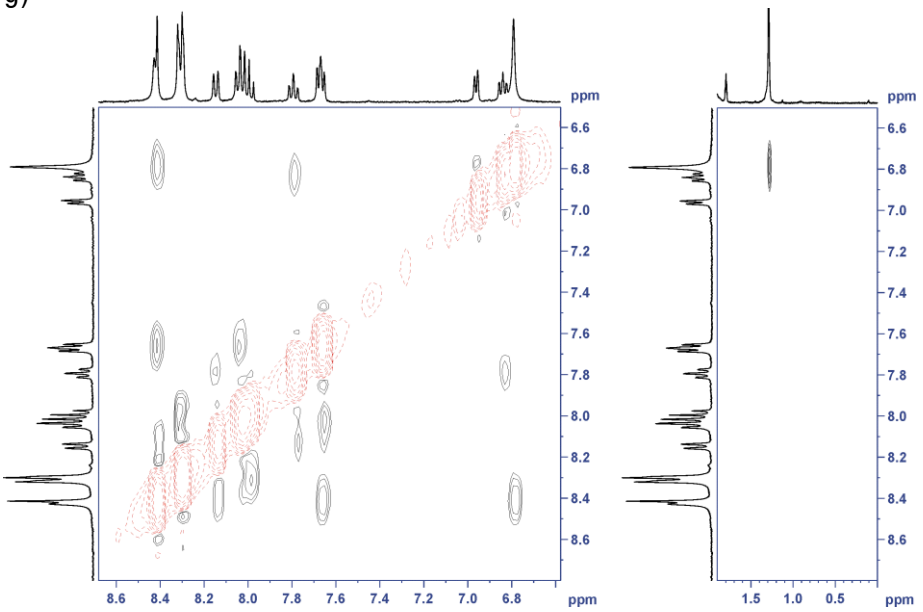

Figure S1-5. 1D and 2D NMR spectra (400 MHz in $CNCD_3$) for complex **3b'**. (a) ^{1}H-NMR at 298K, (b) COSY at 298K, (c) HNMR in CD_2Cl_2 already reported previously [S1] (d) COSY in CD_2Cl_2 (e) NOESY in CD_2Cl_2.

a)

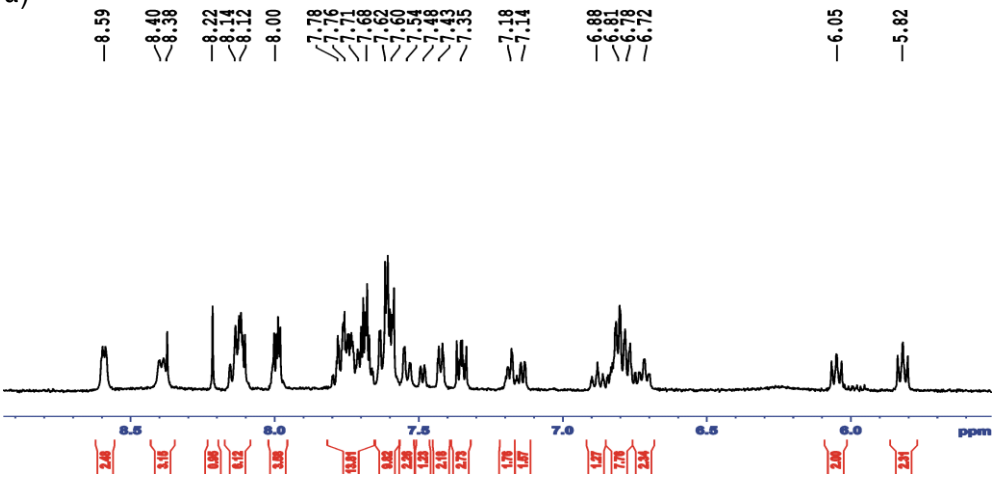

b)

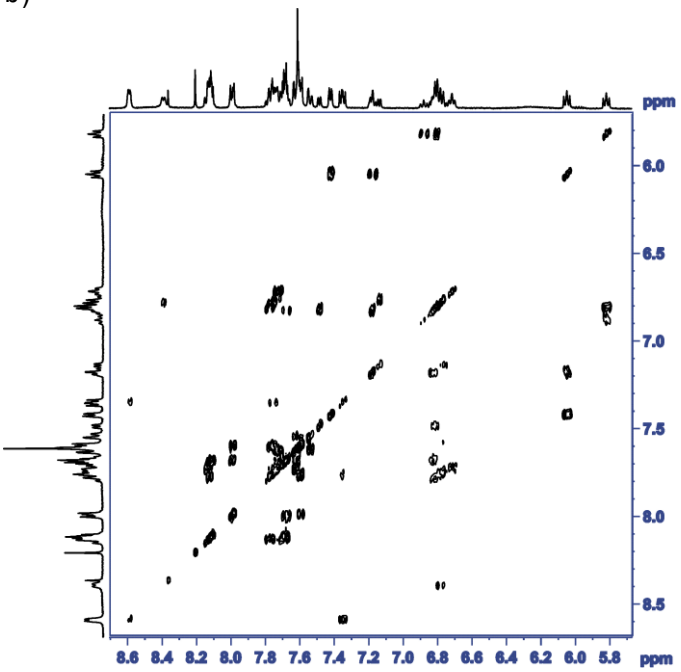
ppm
6.0
6.5
7.0
7.5
8.0
8.5
8.6 8.4 8.2 8.0 7.8 7.6 7.4 7.2 7.0 6.8 6.6 6.4 6.2 6.0 5.8 ppm

c)

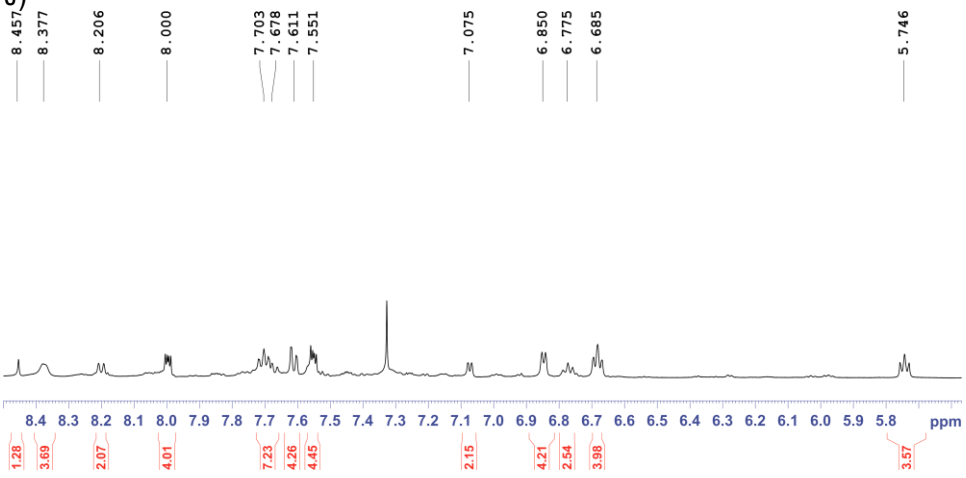
8.457
8.377
8.206
8.000
7.703
7.678
7.611
7.551
7.075
6.850
6.775
6.685
5.746
8.4 8.3 8.2 8.1 8.0 7.9 7.8 7.7 7.6 7.5 7.4 7.3 7.2 7.1 7.0 6.9 6.8 6.7 6.6 6.5 6.4 6.3 6.2 6.1 6.0 5.9 5.8 ppm
1.28
3.69
2.07
4.01
7.23
4.26
4.45
2.15
4.21
2.54
3.98
3.57

d)

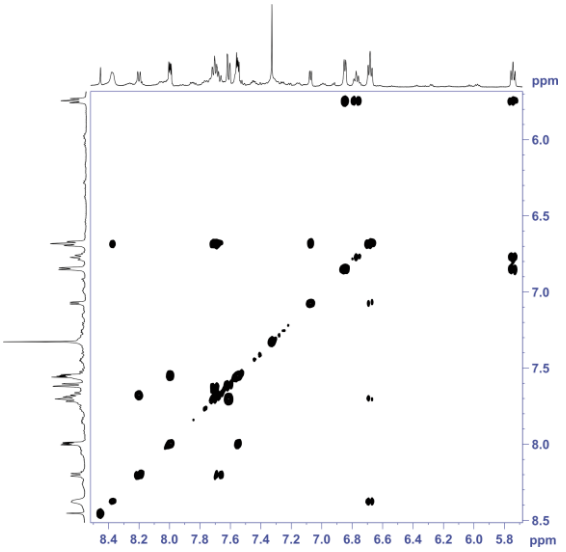
ppm
6.0
6.5
7.0
7.5
8.0
8.5
8.4 8.2 8.0 7.8 7.6 7.4 7.2 7.0 6.8 6.6 6.4 6.2 6.0 5.8
ppm

e)

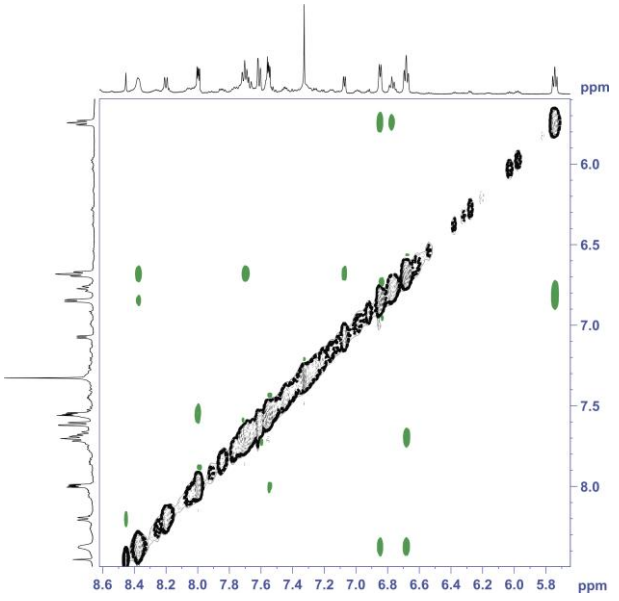
ppm
6.0
6.5
7.0
7.5
8.0
8.6 8.4 8.2 8.0 7.8 7.6 7.4 7.2 7.0 6.8 6.6 6.4 6.2 6.0 5.8
ppm

Figure S1-6. 1D and 2D NMR spectra (400 MHz in $CNCD_3$) for complex **4'**. (a) ^{1}H-NMR at 298K, (b) COSY at 298K.

a)

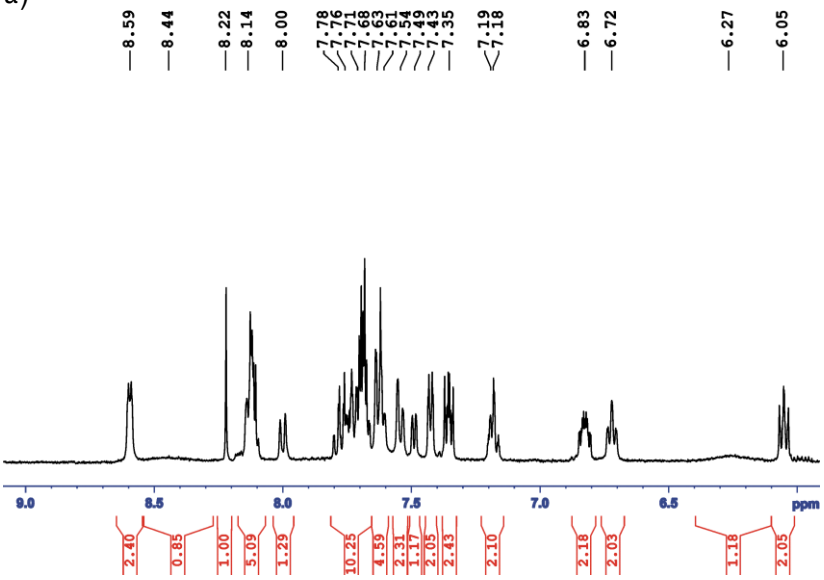

b)

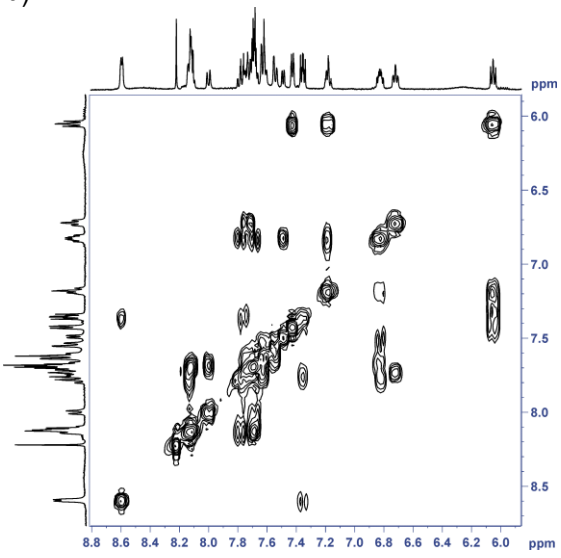

Figure S1-7. 1D and 2D NMR spectra (400 MHz in $CNCD_3$) for complex **3a'**. (a) ^{1}H-NMR at 298K, (b) ^{1}H-NMR at 240K, (c) COSY at 240K, (d) NOESY at 240K. HNMR in CD_2Cl_2 already reported previously [S1]

a)

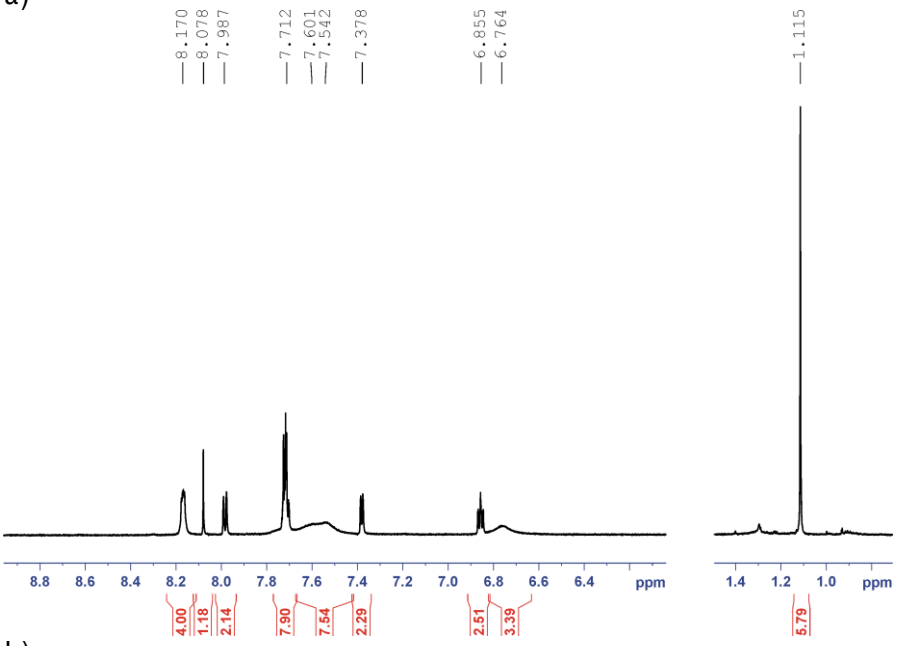

b)

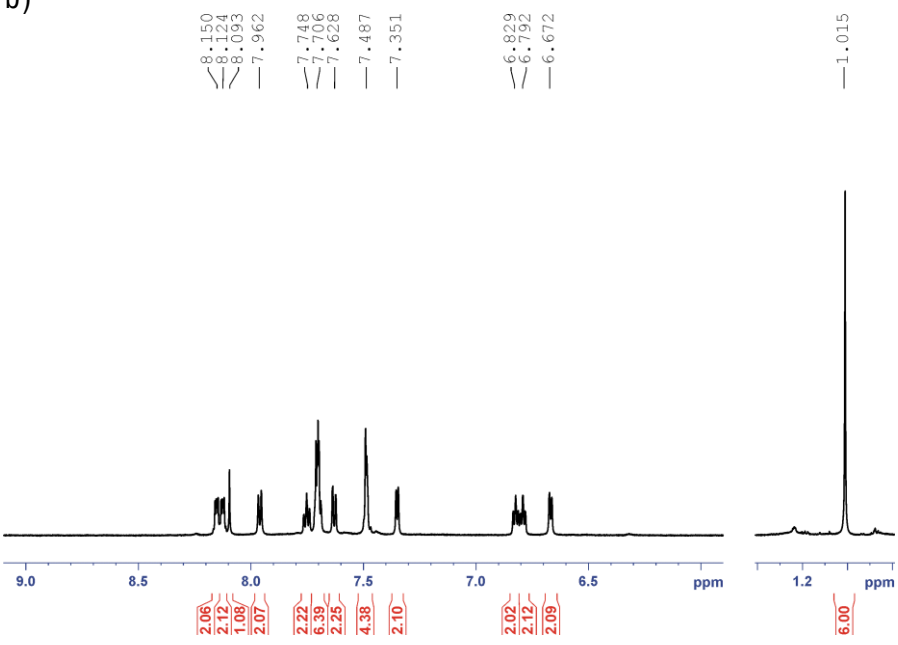

c)

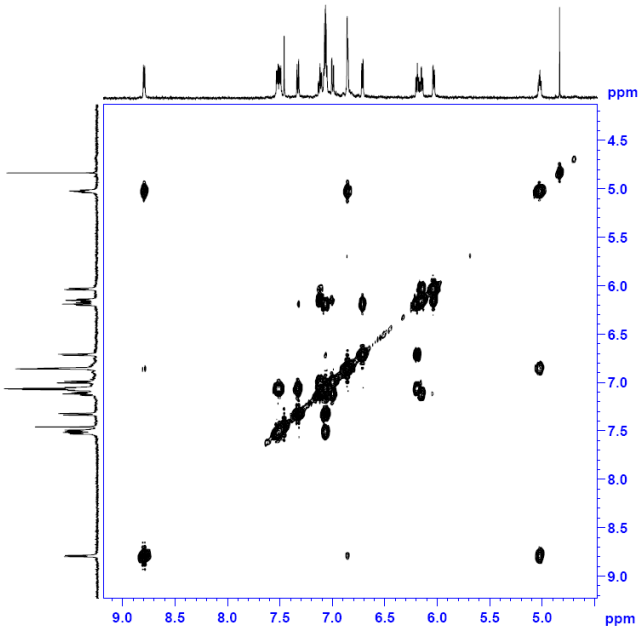
ppm
4.5
5.0
5.5
6.0
6.5
7.0
7.5
8.0
8.5
9.0
9.0 8.5 8.0 7.5 7.0 6.5 6.0 5.5 5.0
ppm

d)

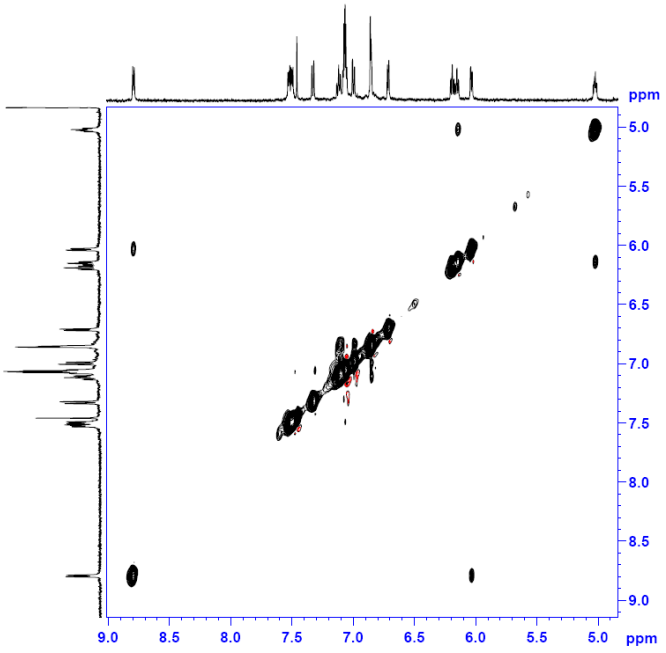
ppm
5.0
5.5
6.0
6.5
7.0
7.5
8.0
8.5
9.0
9.0 8.5 8.0 7.5 7.0 6.5 6.0 5.5 5.0
ppm

2-UV-Vis kinetic data.

2.1 Kinetic data for **3b'**: a) summary table, b) Eyring plot for k1, c) Eyring plot for k2

a)

T(°C)	k1	k 2	Ln(k1/T)	Ln(k2/T)	1/T
10	0,0023	0,000003	-11,72	-18,362	3,53E-3
20	0,0097	0,00004	-10,316	-15,807	3,41E-3
30	0,028	0,000153	-9,2893	-14,499	3,30E-3
35	0,0691	0,0004	-8,4023	-13,554	3,25E-3
40	0,12	0,0009	-7,8665	-12,759	3,19E-3

b)

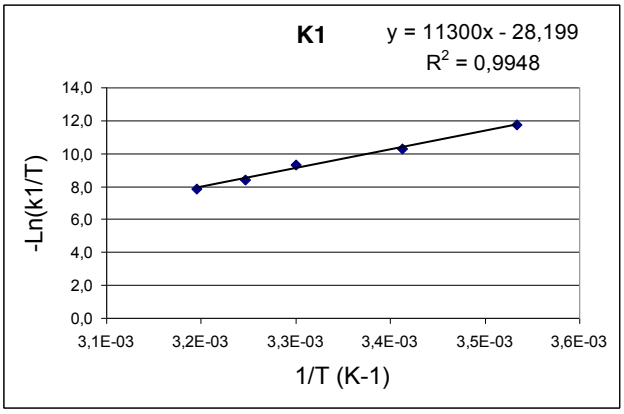

c)

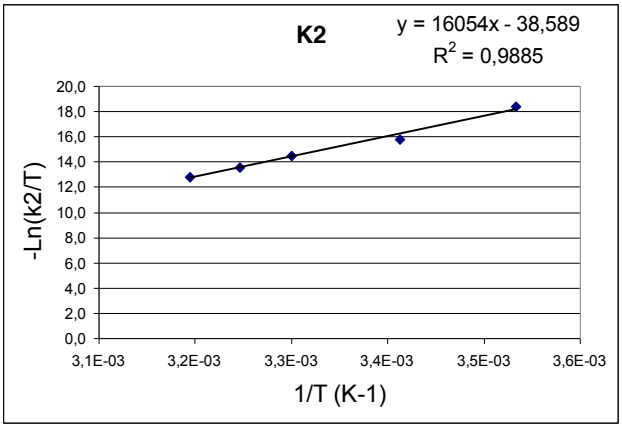

2.2. Kinetic data for 3c: a) summary table, b) Eyring plot for k1, c) Eyring plot for k2

a)

T(°C)	k1	k 2	Ln(k1/T)	Ln(k2/T)	1/T
40,0	0,00018	0,00009	-14,4	-15,0	3,25E-03
52,5	0,002	0,0006	-12,0	-13,2	3,08E-03
58,3	0,0042	0,00158	-11,3	-12,2	3,03E-03
66,3	0,009	0,0045	-10,5	-11,2	2,95E-03

b)

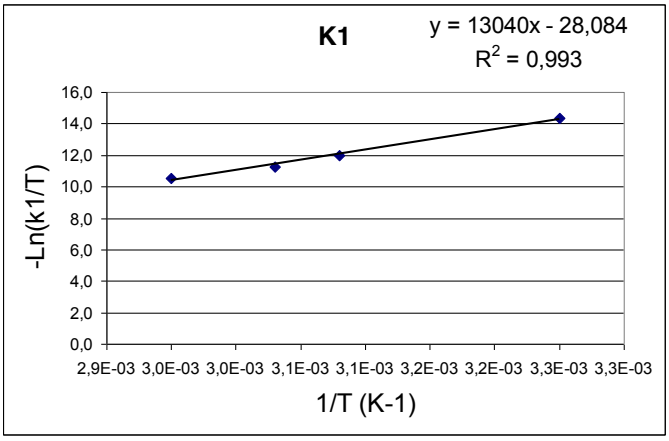

c)

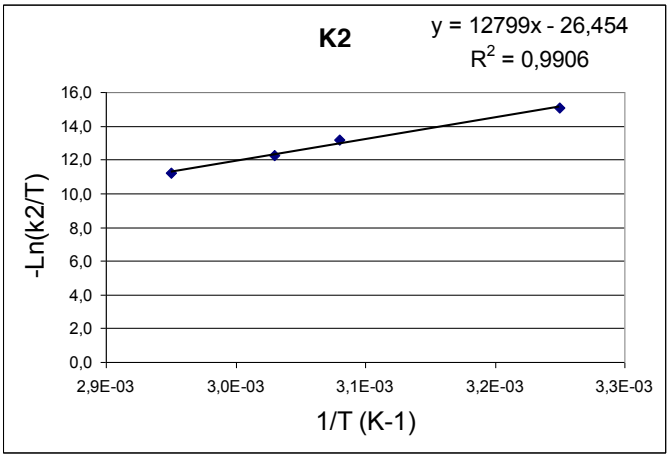

2.3. Kinetic data for 3b: a) summary table, b) Eyring plot for k1, c) Eyring plot for k2

a)

T	k1	k 2	Ln(k1/T)	Ln(k2/T)	1/T
35,0	0,00081	----------	-12,849	----------	3,25E-03
40,0	0,0017	0,0001	-12,123	-14,957	3,19E-03
52,5	0,0084	0,00054	-10,563	-13,308	3,08E-03
58,3	0,0192	0,0014	-9,755	-12,373	3,02E-03
66,3	0,04488	0,005	-8,9298	-11,124	2,95E-03

b)

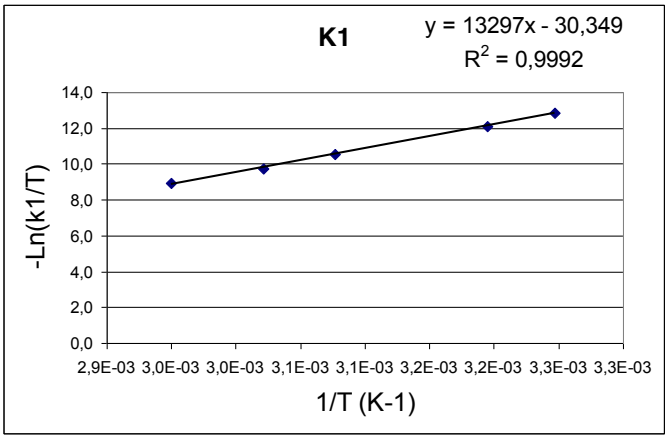

c)

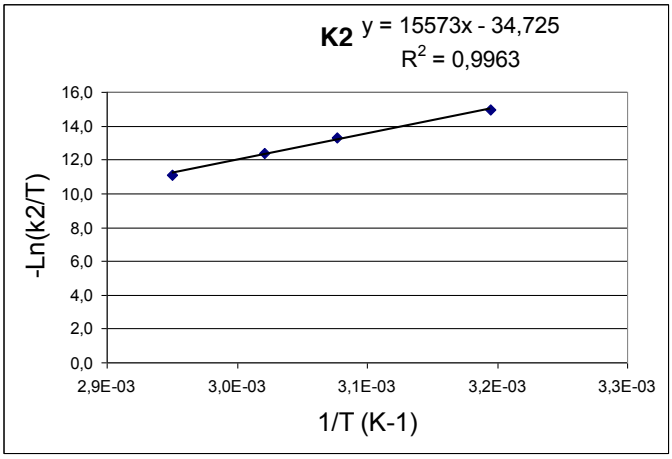

2.4. Tables of the individual spec fit results of the treated data for **3b'**:

T(°C)	rate1	rate2	error rate1	error rate2	real conc (μM)
10	0,0023	0,000003	0,0002	0,000003	314,10
20	0,0095	0,00004	0,0004	0,00003	54,00
20	0,0096	0,00005	0,0003	0,00003	27,00
20	0,0098	0,00003	0,0003	0,00002	5,40
30	0,0283	0,0002	0,0003	0,0001	60,60
30	0,0281	0,0001	0,0004	0,0002	30,30
35	0,069	0,0004	0,001	0,0001	27,00
40	0,122	0,0009	0,002	0,0003	65,00
40	0,119	0,0009	0,004	0,0001	32,50
40	0,119	0,0007	0,002	0,0002	6,50

2.5. Tables of the individual spec fit results of the treated data for 3c:

T(°C)	rate1	rate2	error rate1	error rate2	real conc (μM)
40	0,00018	0,00009	0,00002	0,00003	151,0
52.5	0,0018	0,0006	0,0004	0,0002	70,5
52.5	0,002	0,00056	0,001	0,00006	141
52.5	0,0016	0,0006	0,0002	0,0001	352,4
58.3	0,00414	0,00159	0,0003	0,00004	98,8
58.3	0,0042	0,00156	0,0002	0,00004	347
66.3	0,009	0,0043	0,002	0,0004	65,1
66.3	0,009	0,0046	0,001	0,0003	325,3

2.6. Tables of the individual spec fit results of the treated data for 3b:

T(°C)	rate1	rate2	error rate1	error rate2	real conc (μM)
35	0,00081	----------	0,00003	----------	106
40	0,00172	0,0001	4,00E-05	0,0001	57,2
40	0,00165	0,00009	5,00E-05	0,00003	114,5
40	0,0017	0,00012	4,00E-05	0,00005	286,2
52.5	0,00843	0,00054	5,00E-04	0,00004	17,9
52.5	0,00845	0,00053	2,00E-04	0,00002	35,8
58.3	0,0193	0,00133	0,0002	0,000006	62,1
58.3	0,0192	0,00142	0,0003	0,000006	124,2
58.3	0,0189	0,0014	0,0002	0,00002	310,4
66.3	0,04488	0,0054	0,00002	0,0003	61,4
66.3	0,044	0,005	0,002	0,002	122,8
66.3	0,0456	0,00546	0,0002	0,00001	307,1

Figure S2.7. Left, UV-**vis spectral changes obtained for 3b'.** Right, absorption vs. time plot (red line) and mathematical simulation (green line).

a) 10°C, 314.1 μM

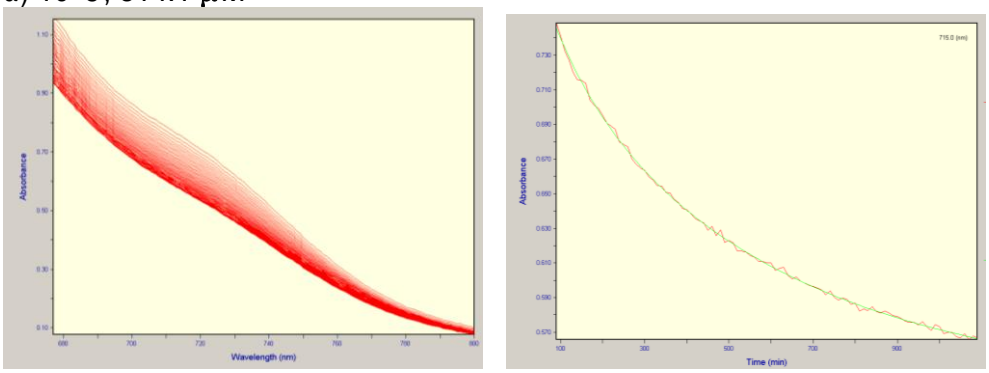

b) 20°C, 54.0 μM

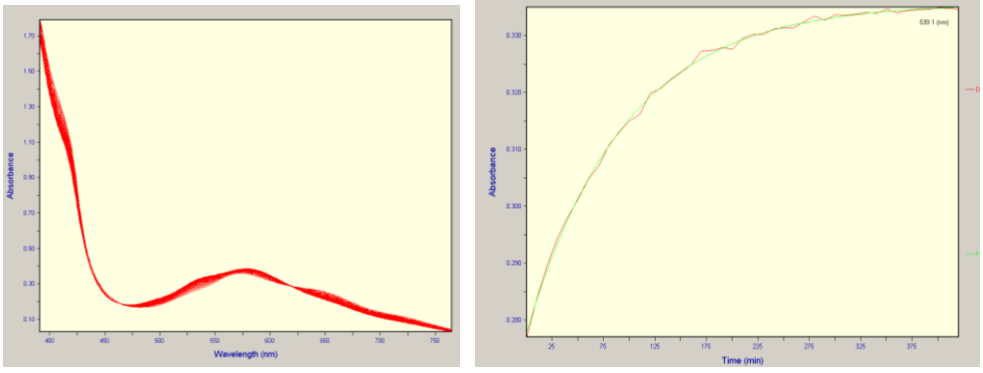

c) 20°C, 27.0 μM

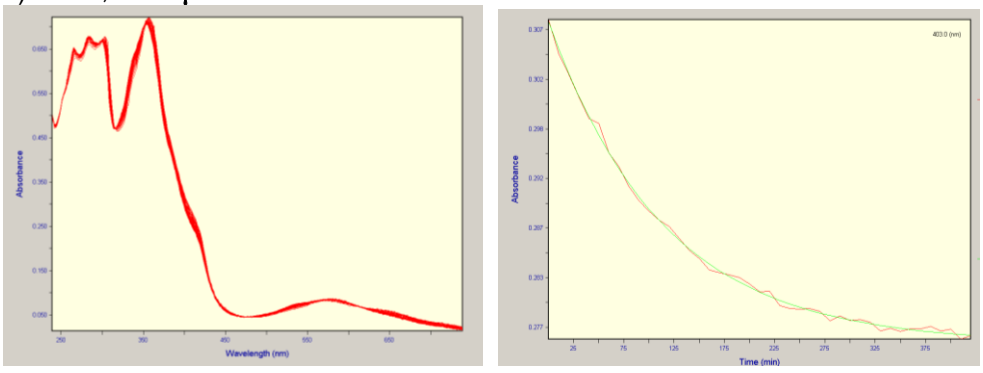

d) 20°C, 5.4 μM

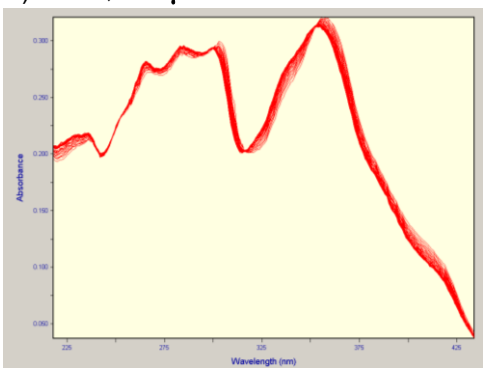

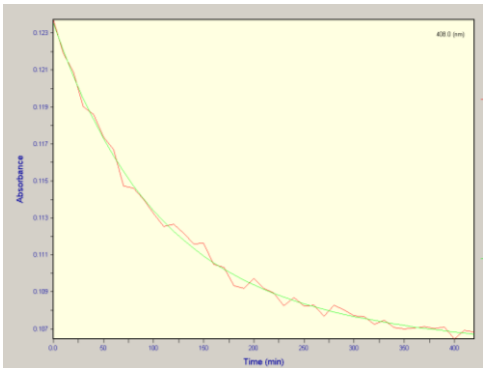

e) 30°C, 60.6 μM

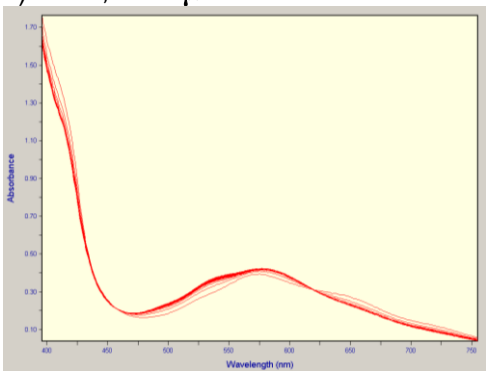

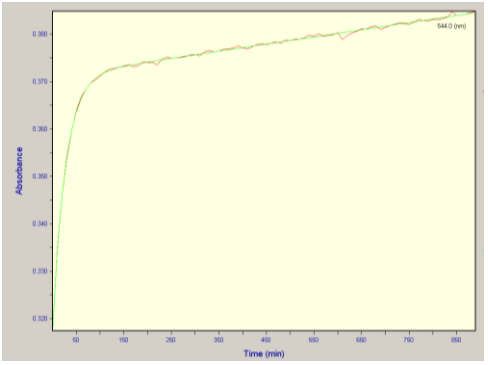

f) 30°C, 30.3 μM

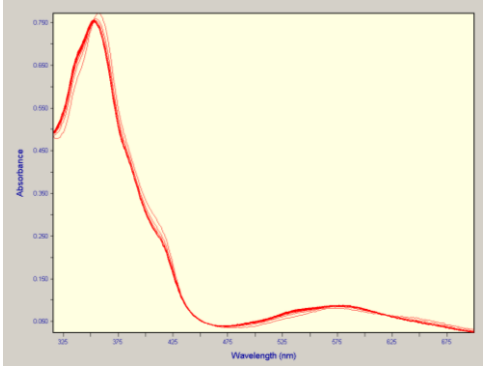

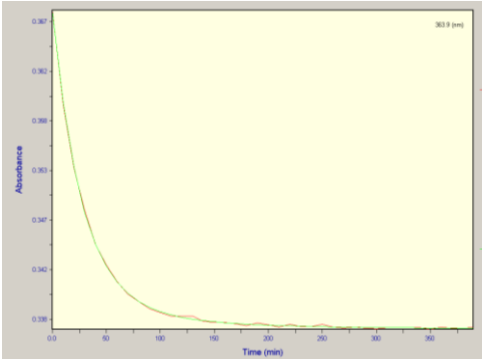

g) 35°C, 27.0 μM

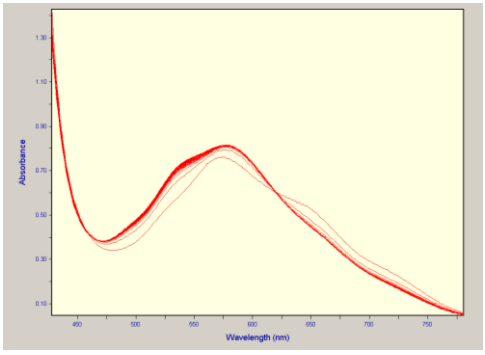

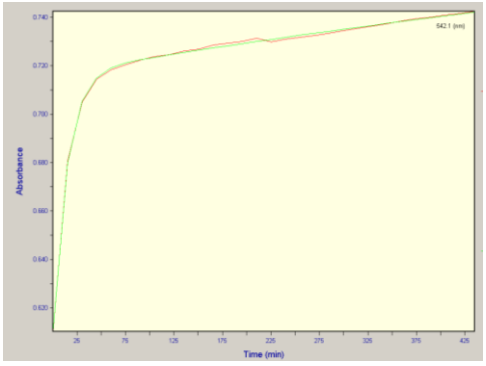

h) 40°C, 65.0 μM

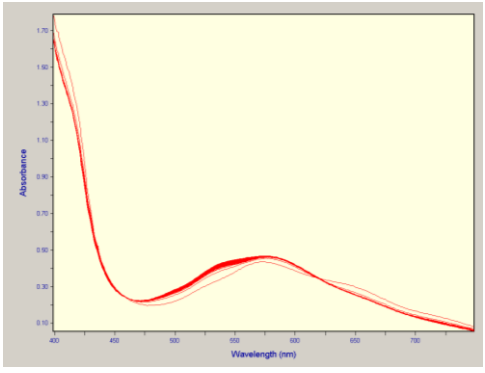

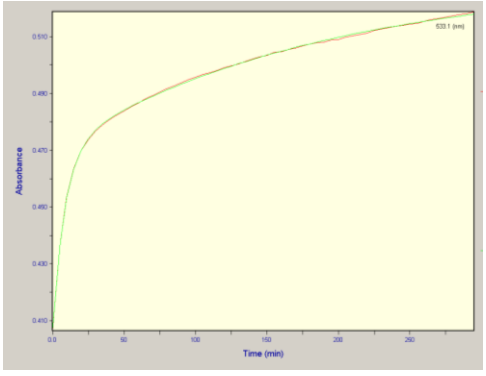

i) 40°C, 32.5 μM

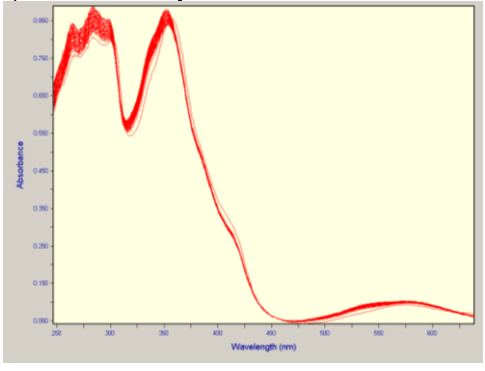

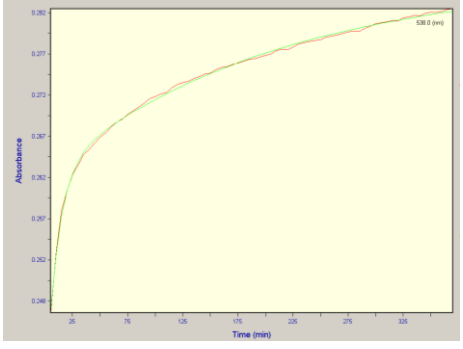

j) 40°C, 6.5 μM

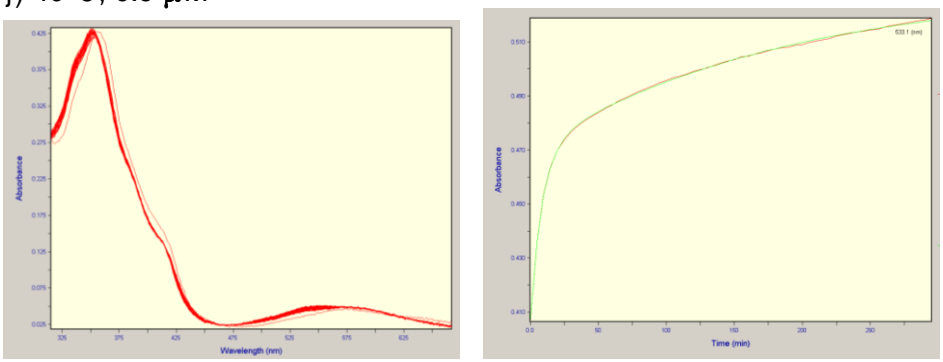

Figure S2.8. Left, UV-vis spectral changes obtained for 3c. Right, absorption vs. time plot (red line) and mathematical simulation (green line).

a) 40°C, 151.0 μM

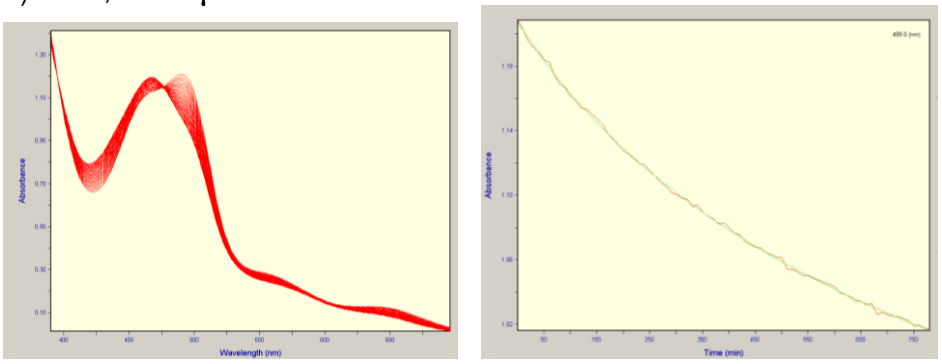

b) 52.5°C, 352.4 μM

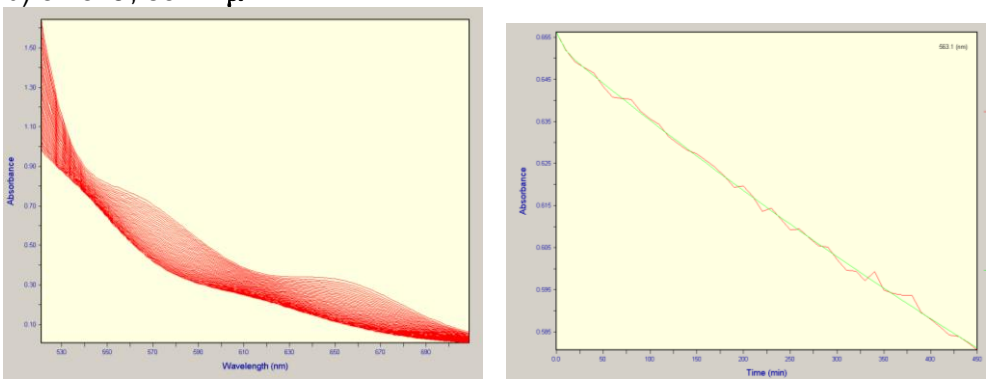

c) 52.5°C, 141.0 μM

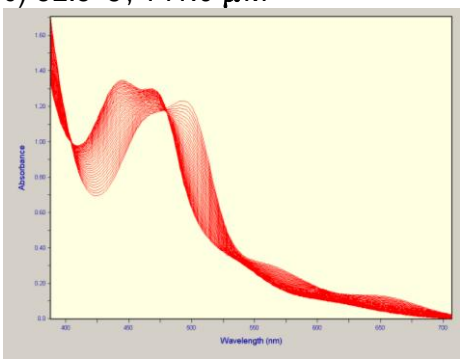

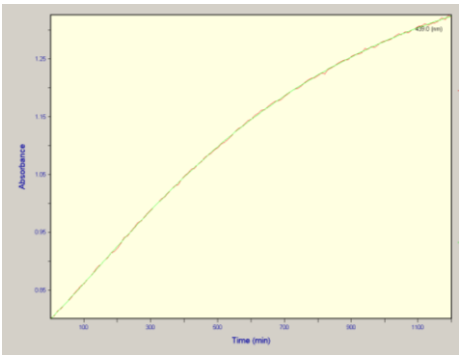

d) 52.5°C, 70.5 μM

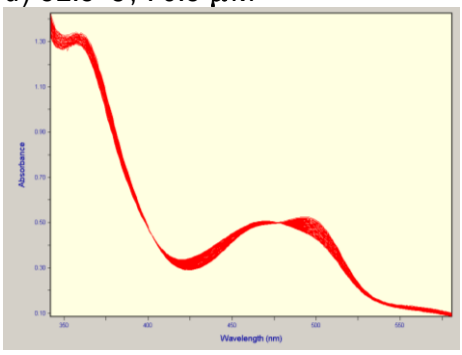

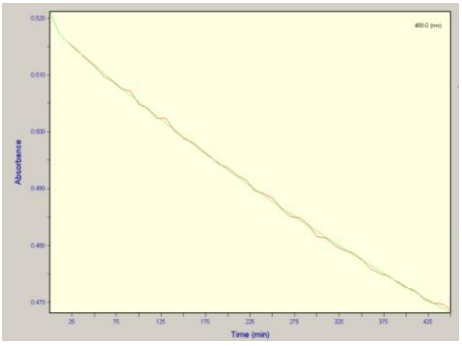

e) 58.3°C, 347.0 μM

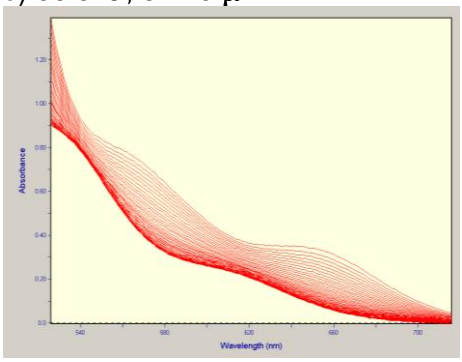

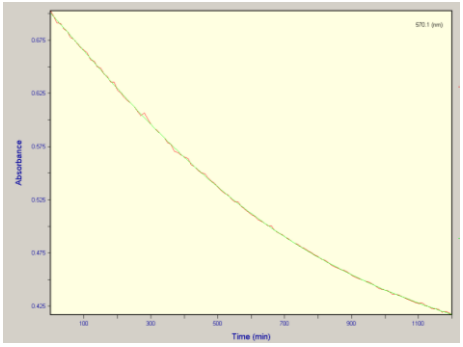

f) 58.3°C, 98.8 μM

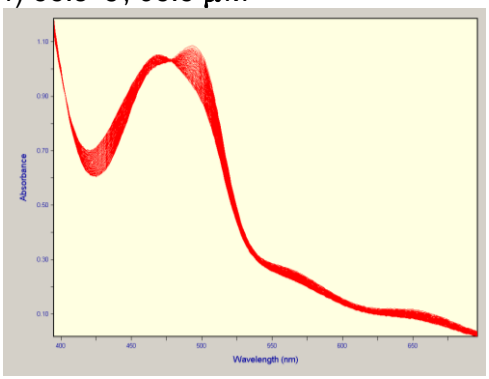

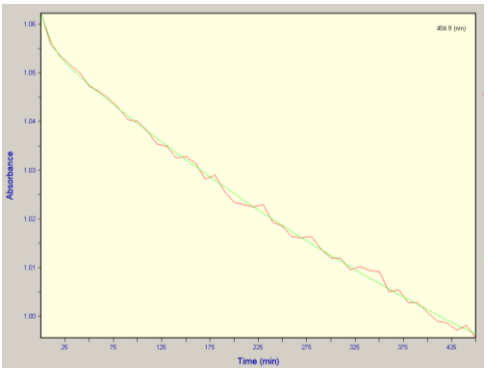

g) 66.3°C, 325.3 μM

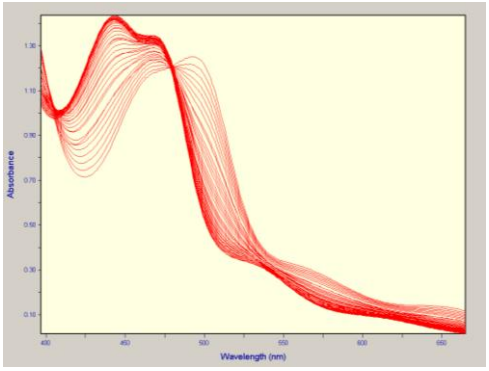

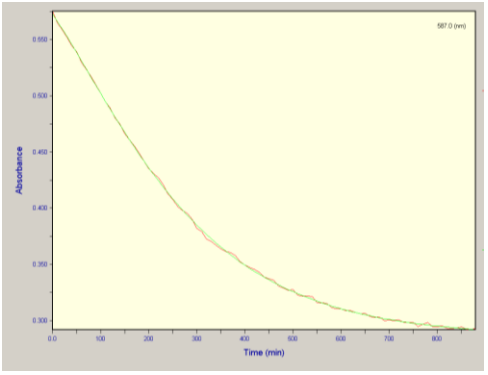

h) 66.3°C, 65.1 μM

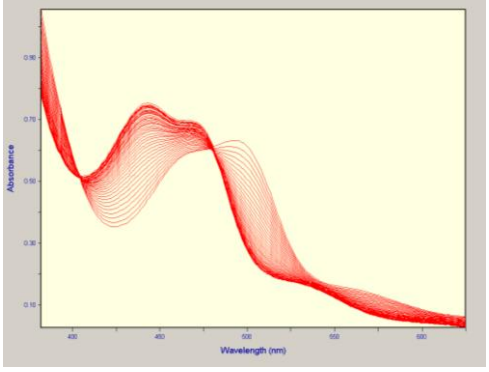

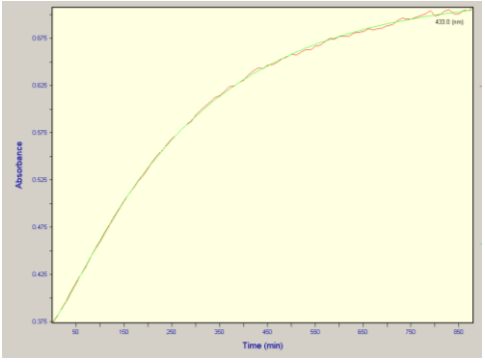

Figure S2.9. Left, UV-vis spectral changes obtained for 3b. Right, absorption vs. time plot (red line) and mathematical simulation (green line).

a) 35°C, 106.0 μM

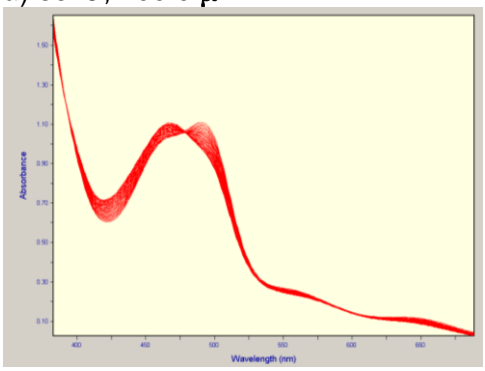

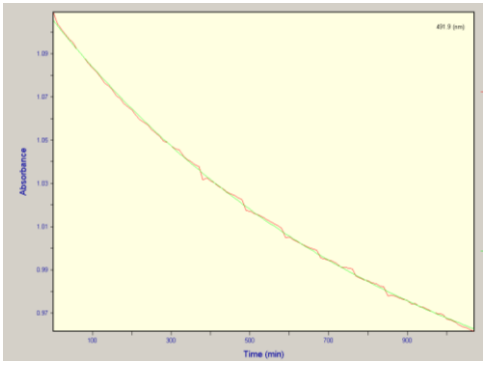

b) 40°C, 286.2 μM

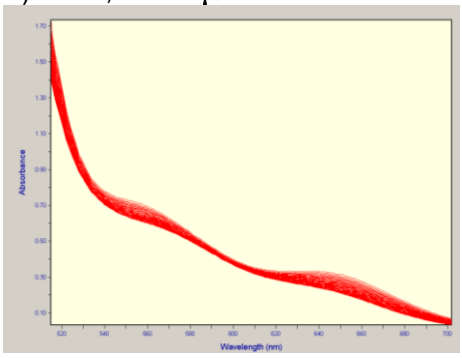

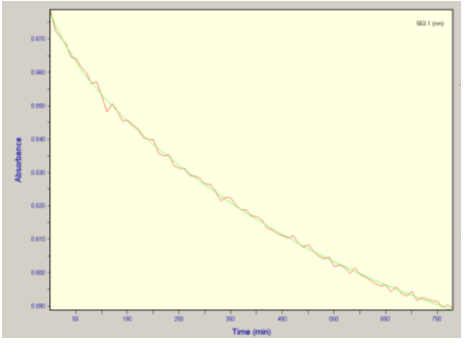

c) 40°C, 114.5 μM

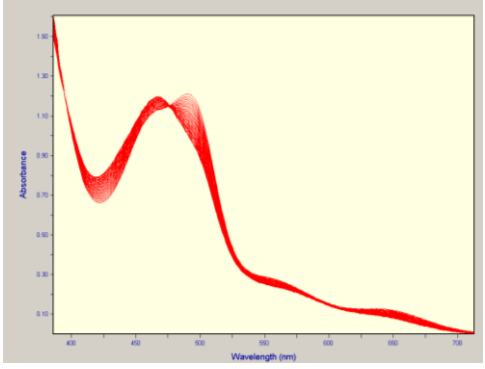

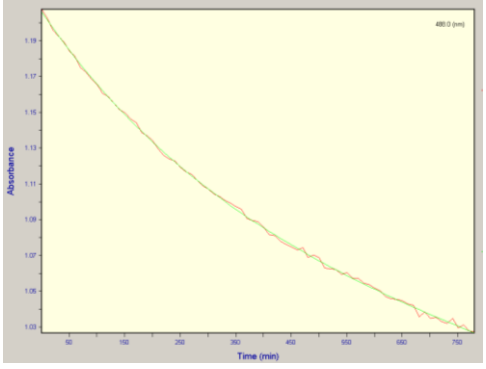

d) 40°C, 57.2 μM

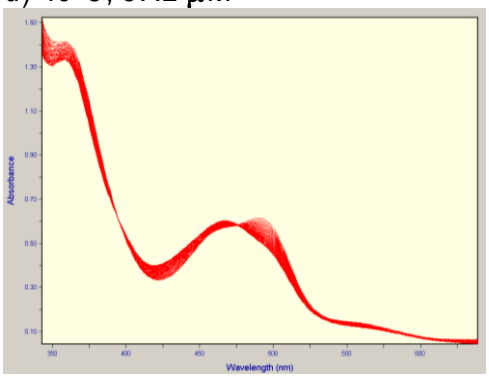

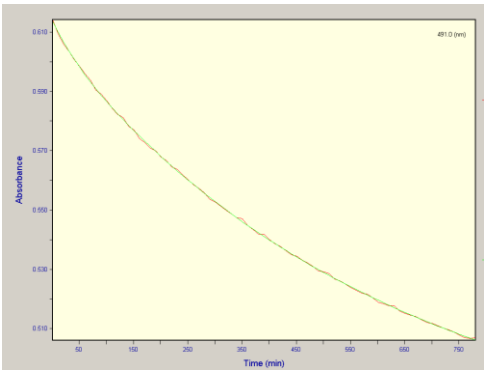

e) 52.5°C, 17.9 μM

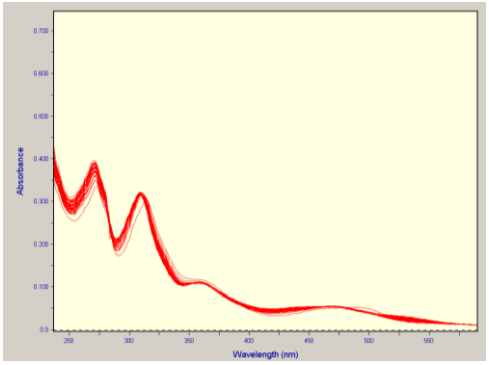

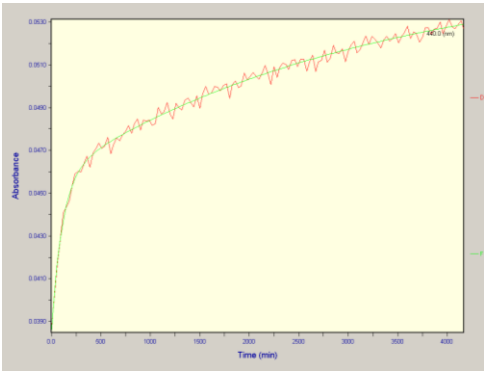

f) 52.5°C, 35.8 μM

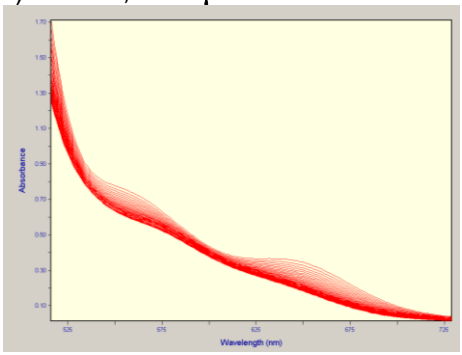

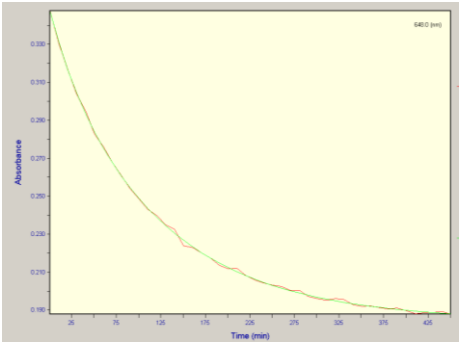

g) 58.3°C, 62.1 μM

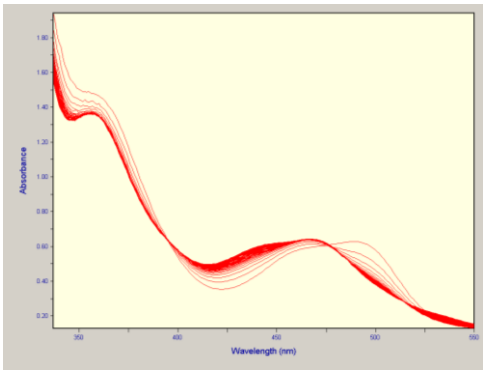

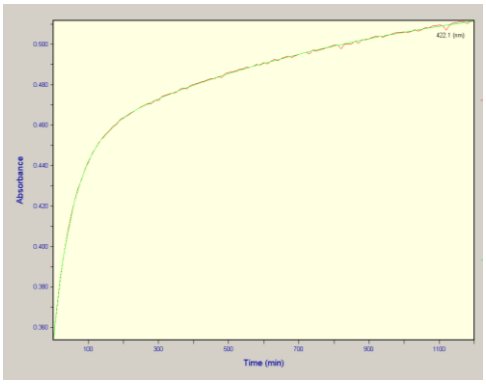

h) 58.3°C, 124.2 μM

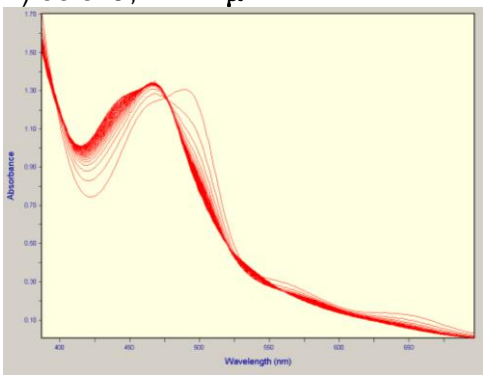

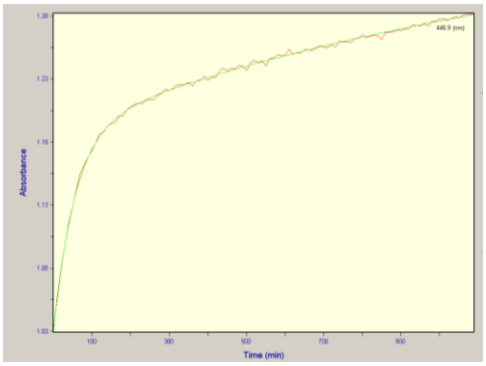

i) 58.3°C, 310.4 μM

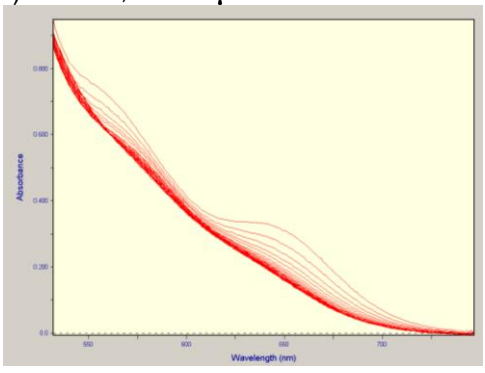

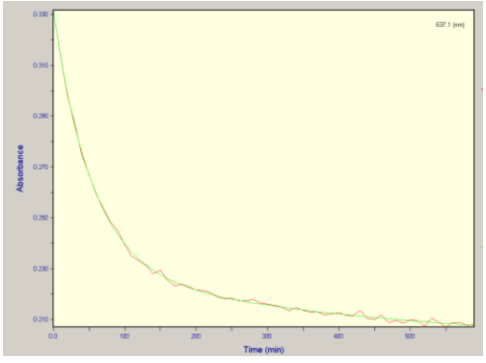

j) 66.3°C, 61.4 μM

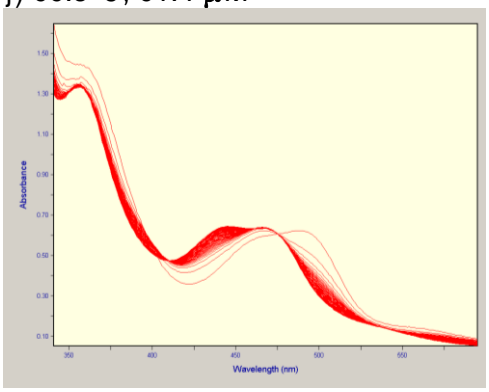

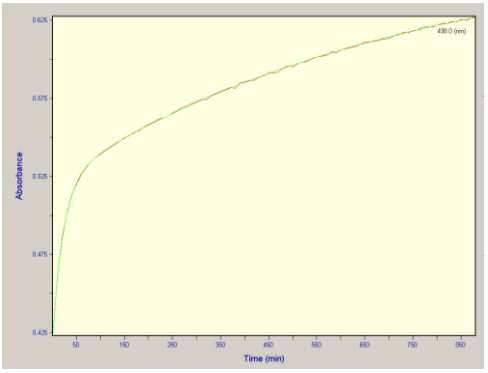

k) 66.3°C, 122.8 μM

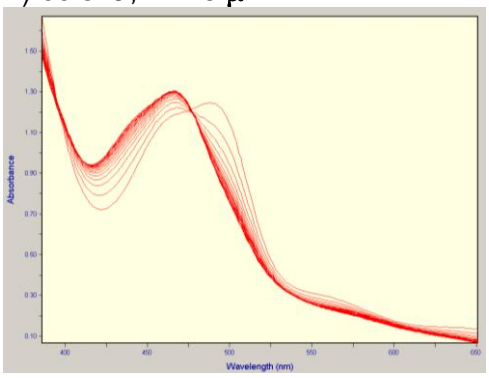

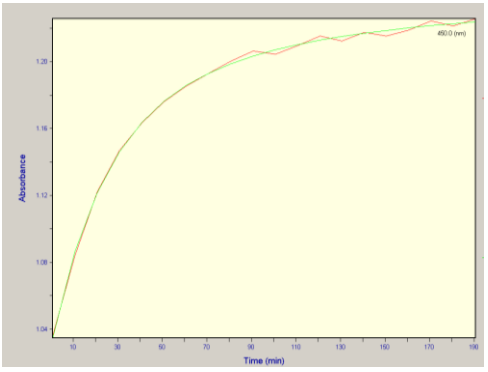

l) 66.3°C, 307.1 μM

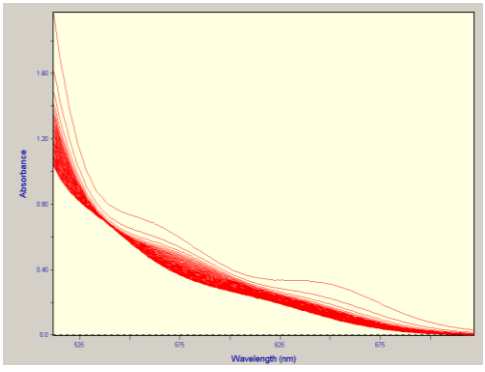

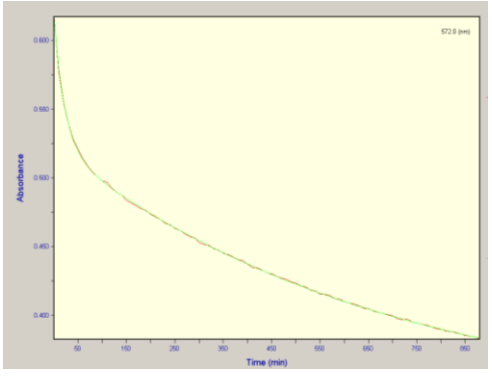

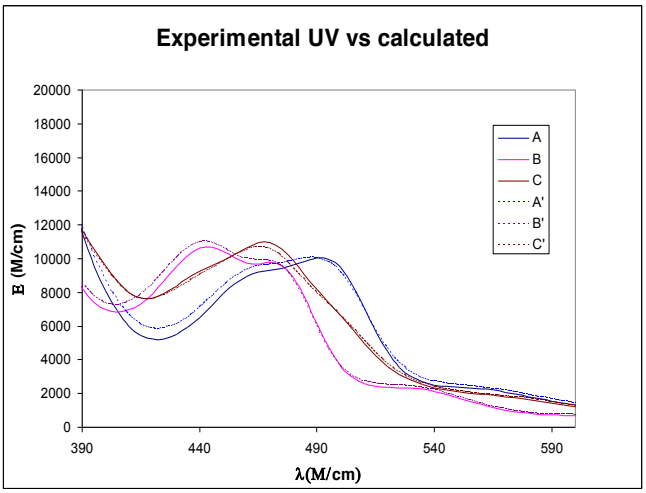

Figure S2-10. UV-vis in Acetonitrile of .A= complex $3b^{3+}$, B=complex 4^{3+} and C=complex $3a^{3+}$ A', B', C' are their calculated spectra from the Specfit programme.

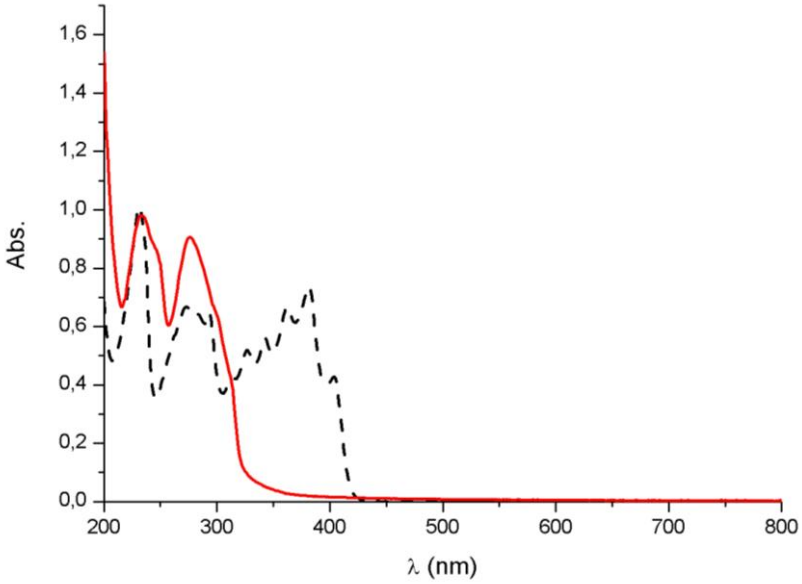

Figure S2-11. UV-vis spectra of a 0.04 mM solutuion in MeCN of the free ligands trpy (red solid line) and Hbid (black dashed line).

3- DFT Calculated structures:

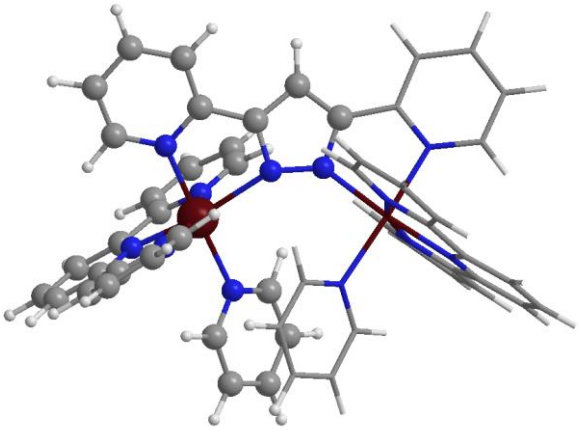

Figure S3.1 ONIOM partitioning for $[Ru_2(bpp)(trpy)_2(py)_2]^{+3}$. The DFT region is represented with the ball and stick model and low level with wire frame.

3b (*in,in*-$[Ru_2(py)_2]^{3+}$

```
3 1 2 1
 C        -3.532971    2.440304    4.135948
 C         0.301248    1.298730   -4.090283
 C        -2.321137    1.751977    4.135600
 C        -4.354949    2.354497    3.013272
 C         1.057482    2.223953   -3.374088
 C         0.081292    0.031421   -3.556407
 C         3.252079    4.327329    1.908099
 C         4.085862    3.763014    0.935182
 C        -1.971111    1.012301    3.008723
 C         5.839158    2.162408   -1.139013
 C         2.150699    3.613185    2.396370
 C        -3.950586    1.594345    1.914099
 C         1.588442    1.862293   -2.133742
 C         6.512313    1.269363   -2.004956
 C         3.783046    2.488427    0.441079
 C         0.636484   -0.294276   -2.316410
```

C	-6.004868	2.023219	0.437011
N	-2.749855	0.933303	1.913994
C	-0.698711	3.856159	-0.486943
C	4.634554	1.745712	-0.556769
C	-1.020673	2.578003	-0.046065
N	1.380555	0.611968	-1.625237
C	-4.773111	1.418527	0.698341
C	1.875242	2.342340	1.886969
N	2.654574	1.842875	0.896138
C	5.996784	-0.021521	-2.267128
C	-6.662316	1.737052	-0.760428
C	-1.143639	4.269739	-1.742264
N	4.186990	0.518616	-0.878703
N	-1.728787	1.692491	-0.780881
C	4.788375	-0.393364	-1.661857
N	-4.235906	0.565013	-0.211275
Ru	2.506104	-0.087613	0.059722
Ru	-2.426750	-0.153335	0.126312
C	-1.878206	3.367015	-2.510485
C	-6.094342	0.851352	-1.676465
C	-4.336067	-2.396133	1.047688
C	-2.136231	2.096994	-2.004484
C	-4.708478	-3.578835	1.675930
N	-3.072680	-1.923903	1.066206
C	-4.861339	0.264420	-1.378758
N	-0.433808	-1.134522	0.799852
C	4.094819	-1.729205	-1.726565
N	0.833348	-0.774039	1.179573
C	-2.126093	-2.638582	1.725810
C	-3.737472	-4.316419	2.354462
N	2.950401	-1.873439	-0.975272
C	4.565359	-2.819400	-2.468910
C	-0.774510	-2.082422	1.715879
C	-2.431165	-3.837583	2.377269
N	3.542198	-0.838259	1.737683
C	1.275898	-1.519804	2.233039
C	4.882859	-0.753113	1.951058
C	-4.136250	-0.727646	-2.201692
N	-2.921198	-1.126483	-1.703008
C	0.268165	-2.362488	2.630326
C	2.707617	-1.474528	2.599862
C	2.272086	-3.046132	-0.886132
C	3.864349	-4.029916	-2.414058
C	5.433963	-1.334990	3.096085
C	2.717894	-4.148461	-1.618687
C	-2.284087	-2.140590	-2.314213
C	-4.656638	-1.283447	-3.371638
C	3.223007	-2.080580	3.750957
C	4.597343	-2.002197	3.997732
C	-3.952457	-2.290439	-4.030970

C	-2.756674	-2.743140	-3.478423
H	-5.063857	-1.797675	0.513940
H	-5.740307	-3.909759	1.629100
H	-3.991463	-5.246881	2.851918
H	-1.647675	-4.392297	2.881174
H	0.267494	-3.069554	3.445396
H	2.575576	-2.599401	4.446180
H	5.014524	-2.460541	4.884970
H	6.498715	-1.275191	3.280442
H	5.523979	-0.247582	1.244967
H	-1.372690	-2.481073	-1.840182
H	-2.189841	-3.548073	-3.933509
H	-4.345268	-2.726038	-4.944013
H	-5.612333	-0.948591	-3.758802
H	-6.605325	0.628298	-2.605862
H	-7.617169	2.203791	-0.978793
H	-6.447620	2.711195	1.147621
H	-5.307282	2.872011	2.999345
H	-3.838899	3.029137	4.994652
H	-1.651763	1.782925	4.988573
H	-1.037486	0.463049	2.967380
H	1.063280	1.755916	2.290226
H	1.526815	4.035456	3.173314
H	3.473549	5.310553	2.302471
H	4.951846	4.310386	0.589726
H	6.261262	3.135439	-0.930117
H	7.446394	1.571902	-2.460034
H	6.540063	-0.700487	-2.909324
H	5.457930	-2.745867	-3.074541
H	4.215568	-4.881665	-2.981992
H	2.182737	-5.087812	-1.569324
H	1.391873	-3.124438	-0.264546
H	-2.673798	1.370005	-2.598961
H	-0.730343	2.240727	0.936756
H	-2.234406	3.628040	-3.501303
H	-0.115649	4.510594	0.152389
H	-0.917558	5.263685	-2.115022
H	2.186366	2.581758	-1.604279
H	0.515786	-1.288266	-1.926476
H	1.232887	3.213458	-3.775833
H	-0.495214	-0.698877	-4.108217
H	-0.117110	1.564890	-5.052153

in-$[Ru_2(py)]^{3+}$

```
3 1 2 1
 C         3.573095   -4.609695   -0.929130
 C         1.155621    1.471061   -3.325989
 C         2.484163   -4.446006   -0.076883
 C         4.232999   -3.476533   -1.408053
 C         1.173846    0.155121   -2.868687
 C         0.193500    2.355125   -2.841199
 C        -2.929335   -4.093733   -2.686986
 C        -3.637103   -2.901880   -2.885491
 C         2.092341   -3.154033    0.267459
 C        -5.158279   -0.143398   -2.970144
 C        -1.952070   -4.178763   -1.687127
 C         3.790692   -2.208704   -1.034127
 C         0.230096   -0.254189   -1.924565
 C        -5.749128    1.132344   -2.813883
 C        -3.340134   -1.795386   -2.080159
 C        -0.744603    1.904111   -1.909069
 C         5.435919   -0.841252   -2.458895
 N         2.713935   -2.055969   -0.196526
 C        -4.070947   -0.479803   -2.152136
 N        -0.716384    0.613245   -1.465740
 C         4.405428   -0.952003   -1.522857
 C        -1.679239   -3.060554   -0.896126
 N        -2.351427   -1.905329   -1.129251
 C        -5.270162    2.045244   -1.845299
 C         5.846517    0.430641   -2.862868
 N        -3.650478    0.448836   -1.275707
 C        -4.181587    1.663199   -1.049534
 N         3.841284    0.171534   -1.013577
 Ru       -2.151517   -0.107248   -0.046168
 Ru        2.247466   -0.028742    0.189196
 C         5.217880    1.570585   -2.358179
 C         4.409236    0.137104    2.265073
 C         4.961822    0.072442    3.538694
 N         3.098317   -0.088455    2.033784
 C         4.192169    1.416087   -1.423313
 N         0.577889   -0.343158    1.447366
 C        -3.539435    2.436087    0.073714
 N        -0.701303   -0.734009    1.321097
 C         2.280609   -0.390031    3.093286
 C         4.138824   -0.240033    4.622000
 N        -2.492604    1.825771    0.728832
 C        -3.946766    3.712848    0.479131
 C         0.881241   -0.597880    2.745257
```

C	2.785807	-0.472822	4.391497
N	-3.421428	-0.877912	1.456884
C	-1.246664	-1.114226	2.504777
C	-4.776524	-0.957251	1.390031
C	3.370084	2.495259	-0.828167
N	2.369353	2.080622	0.015547
C	-0.252546	-1.073049	3.462788
C	-2.719592	-1.269359	2.559535
C	-1.878111	2.378557	1.804190
C	-3.293242	4.321425	1.557252
C	-5.488205	-1.454314	2.485759
C	-2.261574	3.652914	2.228074
C	1.579410	3.007735	0.583204
C	3.552646	3.846931	-1.114810
C	-3.398205	-1.759913	3.678941
C	-4.793395	-1.854356	3.633799
C	2.710184	4.798141	-0.536278
C	1.708659	4.371771	0.331779
H	5.014133	0.371795	1.398526
H	6.021065	0.265008	3.669456
H	4.542671	-0.298783	5.627475
H	2.114864	-0.712761	5.209323
H	-0.321555	-1.330516	4.508694
H	-2.859808	-2.067150	4.566416
H	-5.336798	-2.235812	4.488495
H	-6.567561	-1.524076	2.448876
H	-5.303762	-0.636411	0.503622
H	0.827824	2.628690	1.260717
H	1.034299	5.072966	0.811250
H	2.841426	5.851824	-0.760402
H	4.341939	4.161971	-1.787598
H	5.518112	2.553348	-2.701830
H	6.645514	0.533176	-3.590001
H	5.904321	-1.722126	-2.881633
H	5.084786	-3.586248	-2.069340
H	3.908759	-5.600150	-1.219064
H	1.941375	-5.296809	0.320337
H	1.257772	-2.979076	0.935781
H	-0.941071	-3.112692	-0.109712
H	-1.416336	-5.104936	-1.524324
H	-3.147505	-4.958018	-3.300815
H	-4.403187	-2.855355	-3.646999
H	-5.555326	-0.838185	-3.696960
H	-6.592023	1.408014	-3.434106
H	-5.748663	3.007077	-1.724833
H	-4.754539	4.231297	-0.018469
H	-3.596656	5.307740	1.883537
H	-1.771877	4.115359	3.075130
H	-1.108519	1.836662	2.333412
H	0.261959	-1.266059	-1.552405

H	-1.486045	2.595542	-1.549234
H	1.919908	-0.539376	-3.232238
H	0.173174	3.381373	-3.184219
H	1.889887	1.806614	-4.046763

4 *in,in*-$[Ru_2(py)(MeCN)]^{3+}$

3 1 2 1

C	-3.442256	4.572318	1.437752
C	0.182315	-1.999009	-3.885981
C	-2.301254	3.992804	1.987590
C	-4.216440	3.823129	0.552732
C	0.901542	-0.815277	-4.025037
C	0.050678	-2.578018	-2.626700
C	2.473663	4.472612	-1.789505
C	3.496408	3.541602	-2.011081
C	-1.972211	2.687731	1.627647
C	5.613183	1.221030	-2.324789
C	1.356044	4.127737	-1.018098
C	-3.834132	2.520144	0.229325
C	1.472979	-0.224568	-2.895642
C	6.436891	0.071173	-2.332799
C	3.382358	2.264632	-1.448628
C	0.620630	-1.946878	-1.517088
C	-5.734929	2.022005	-1.424945
N	-2.703474	1.960633	0.765907
C	4.388054	1.158371	-1.647772
N	1.310161	-0.781608	-1.659286
C	-4.606489	1.652685	-0.687787
C	1.269666	2.846911	-0.468214
N	2.269776	1.961368	-0.696764
C	6.048161	-1.110474	-1.659118
C	-6.328283	1.083416	-2.270446
N	4.062063	-0.013161	-1.070701
N	-1.540577	0.775696	-1.578606
C	4.812285	-1.126271	-0.997804
N	-4.121179	0.391849	-0.793453
Ru	2.373534	-0.011554	0.034391
Ru	-2.399371	-0.040620	0.103577
C	-5.800104	-0.204167	-2.371896
C	-4.468688	-1.110706	2.131210
C	-4.915369	-1.592771	3.356738
N	-3.181304	-0.782451	1.903726
C	-4.676637	-0.537406	-1.610360
N	-0.545785	-0.449471	1.286052
C	4.239001	-2.222302	-0.136769
N	0.706828	0.075187	1.344825
C	-2.282779	-0.933978	2.914137

C	-3.997339	-1.746539	4.396595
N	3.047371	-1.955888	0.498815
C	4.860108	-3.460131	0.070352
C	-0.907660	-0.550924	2.596794
C	-2.664666	-1.412713	4.169377
N	3.349250	0.693213	1.772815
C	1.129601	0.250476	2.623648
C	4.656958	1.057598	1.861518
C	-4.018309	-1.859773	-1.541580
N	-2.902852	-1.919817	-0.746945
C	0.118019	-0.129433	3.476405
C	2.526073	0.675404	2.855279
C	2.455880	-2.830679	1.351627
C	4.254922	-4.387041	0.927514
C	5.181356	1.440077	3.099431
C	3.052634	-4.073738	1.573916
C	-2.368840	-3.124014	-0.481820
C	-4.529751	-3.003941	-2.155387
C	3.016657	1.041380	4.113123
C	4.355058	1.429601	4.228627
C	-3.929223	-4.240466	-1.920859
C	-2.847411	-4.305041	-1.046112
H	-5.151042	-0.974624	1.300600
H	-5.963106	-1.841279	3.486255
H	-4.312091	-2.123236	5.364498
H	-1.920792	-1.532911	4.949446
H	0.100664	-0.097949	4.554967
H	2.376518	1.032404	4.985972
H	4.752699	1.719889	5.192437
H	6.219321	1.734308	3.185055
H	5.294529	1.047348	0.990933
H	-1.529783	-3.129747	0.203307
H	-2.368247	-5.247526	-0.804497
H	-4.317250	-5.136439	-2.394482
H	-5.403765	-2.938309	-2.793363
H	-6.256089	-0.928532	-3.036598
H	-7.200564	1.357556	-2.854813
H	-6.142347	3.023732	-1.355555
H	-5.115704	4.251259	0.124851
H	-3.731274	5.586357	1.694609
H	-1.670464	4.533857	2.684550
H	-1.095379	2.200975	2.037667
H	0.415432	2.560424	0.124574
H	0.564305	4.846430	-0.851030
H	2.544814	5.462893	-2.220258
H	4.349116	3.816378	-2.616349
H	5.939994	2.125131	-2.819240
H	7.390111	0.103081	-2.844152
H	6.707501	-1.967030	-1.645796
H	5.794594	-3.709683	-0.412743

H	4.722700	-5.348061	1.097825
H	2.590658	-4.787918	2.243041
H	1.530747	-2.572267	1.847134
H	2.046151	0.675598	-3.024386
H	0.541984	-2.405815	-0.545736
H	1.025768	-0.362882	-5.000357
H	-0.472126	-3.517704	-2.515912
H	-0.256641	-2.475072	-4.753116
C	-1.221665	1.413940	-2.492483
C	-0.796370	2.217485	-3.634257
H	-0.883887	1.637973	-4.558820
H	-1.420437	3.112940	-3.716278
H	0.246359	2.527217	-3.509823

in,out-[Ru_2(py)(MeCN)]$^{3+}$

3 1 2 1

N	-4.631405	-0.463649	0.308788
Ru	-2.749355	0.159518	-0.004309
N	-3.396200	2.032808	-0.789194
C	-2.474258	3.028323	-0.744399
C	-2.757413	4.323360	-1.185328
C	-4.021039	4.604074	-1.698886
C	-4.964606	3.576589	-1.758115
C	-4.614713	2.312306	-1.295639
C	-1.167017	2.636678	-0.221545
N	-0.803822	1.324778	-0.268515
N	0.403705	1.304918	0.377392
C	0.786722	2.557199	0.760097
C	-0.199765	3.449230	0.413167
N	-2.588397	0.598907	2.074907
C	-2.866812	1.749714	2.709030
C	-2.745079	1.902067	4.088700
C	-2.325772	0.811510	4.847082
C	-2.048111	-0.392102	4.200493
C	-2.182626	-0.481922	2.814185
C	-1.933524	-1.728406	2.052620
N	-2.155004	-1.609944	0.723835
C	-2.146400	-2.672543	-0.114013
C	-1.779757	-3.930486	0.372320
C	-1.457200	-4.062920	1.723577
C	-1.553904	-2.965569	2.580705
C	-2.566826	-2.349236	-1.496146
C	-2.783227	-3.315645	-2.479317
C	-3.156243	-2.923326	-3.764920
C	-3.302504	-1.565192	-4.038469
C	-3.104059	-0.648669	-3.007533
N	-2.763120	-1.018254	-1.762004
H	-3.200932	2.567573	2.080686

H	-2.981013	2.855498	4.548843
H	-2.220912	0.890065	5.924429
H	-1.730312	-1.254319	4.775138
H	-1.342891	-3.081712	3.637241
H	-1.152277	-5.028194	2.114166
H	-1.735873	-4.791047	-0.285021
H	-2.649294	-4.366701	-2.250179
H	-3.319073	-3.667472	-4.537770
H	-3.573071	-1.212292	-5.027677
H	-3.225186	0.416529	-3.168741
H	-0.229962	4.515503	0.577665
H	-1.990104	5.088816	-1.144272
H	-4.261819	5.601047	-2.053643
H	-5.958700	3.746394	-2.157513
H	-5.319285	1.489321	-1.319767
Ru	2.146781	0.166848	-0.039406
N	1.138902	-1.378774	-1.131001
N	2.193403	-0.966999	1.736827
N	3.885510	-0.813291	-0.348436
N	2.712966	1.086544	-1.857388
N	3.056048	1.761615	0.997743
C	1.296915	-2.689489	-0.781471
C	0.561040	-1.049968	-2.321695
C	3.337984	-1.729189	1.805855
C	1.321335	-0.859712	2.767299
C	4.278220	-1.646500	0.632125
C	4.566910	-0.476172	-1.456751
C	3.911618	0.579815	-2.306919
C	2.059134	2.094057	-2.491383
C	4.365467	1.842700	1.355181
C	2.175700	2.771329	1.221153
C	0.921047	-3.710022	-1.657759
H	1.747240	-2.961379	0.156205
C	0.198505	-2.041205	-3.235411
H	0.417819	-0.015443	-2.588459
C	3.572153	-2.506598	2.946573
C	1.529061	-1.622213	3.919094
H	0.492228	-0.173936	2.702306
C	5.513851	-2.288171	0.473742
C	5.809114	-1.093643	-1.659167
C	4.467755	1.086599	-3.488151
C	2.590556	2.616077	-3.672677
H	1.131650	2.480304	-2.096938
C	4.833948	3.001011	1.981883
H	5.044522	1.028025	1.153182
C	2.609225	3.952919	1.831442
C	0.390160	-3.380436	-2.902277
H	1.060084	-4.746921	-1.380763
H	-0.229226	-1.771961	-4.192221
C	2.651315	-2.456084	4.000069

H	4.450249	-3.131441	3.032584
H	0.836601	-1.558390	4.747834
C	6.272457	-2.010094	-0.686778
H	5.895513	-2.972000	1.218942
H	6.415750	-0.873565	-2.526371
C	3.794983	2.105919	-4.171494
H	5.405078	0.712658	-3.875943
H	2.075904	3.410717	-4.196997
C	3.949421	4.060033	2.217794
H	5.872857	3.081484	2.274176
H	1.924188	4.771608	2.011125
H	0.107631	-4.160028	-3.597678
H	2.819184	-3.047259	4.890922
H	7.231207	-2.492818	-0.824332
H	4.212464	2.508266	-5.085395
H	4.303430	4.963654	2.696792
C	-5.706599	-0.834867	0.535020
C	-7.063497	-1.291303	0.816831
H	-7.580210	-0.566159	1.454319
H	-7.625266	-1.407611	-0.115883
H	-7.034897	-2.256523	1.333027

4 *in,in*-$[Ru_2(MeCN)(Pyr)]^{3+}$

3 1 2 1

C	3.279501	-4.643280	-1.033543
C	-0.988247	3.992244	-2.462009
C	2.201968	-4.376349	-0.180250
C	4.073503	-3.597445	-1.518287
C	-1.828576	3.051009	-3.053719
C	-0.507216	3.732490	-1.178985
C	-2.518637	-3.187500	-3.700756
C	-3.566134	-2.337646	-3.346426
C	1.921982	-3.057030	0.182673
C	-5.747857	-0.386119	-2.352529
C	-1.344211	-3.157618	-2.951085
C	3.769336	-2.283914	-1.139998
C	-2.146617	1.891833	-2.353930
C	-6.629409	0.528047	-1.772965
C	-3.417575	-1.471736	-2.261615
C	-0.876059	2.551574	-0.545389
C	5.655779	-1.037418	-2.451304
N	2.697262	-2.056176	-0.306387
C	-4.477996	-0.551614	-1.793126
N	-1.677323	1.625140	-1.115060
C	4.552457	-1.077533	-1.587602

C	-1.254535	-2.270140	-1.881591
N	-2.249966	-1.433274	-1.541836
C	-6.244579	1.259341	-0.647959
C	6.226377	0.220677	-2.756464
N	-4.125979	0.175359	-0.699735
N	1.335582	0.185954	-1.652181
C	-4.967241	1.064981	-0.115243
N	4.114831	0.093524	-1.095117
Ru	-2.317797	-0.068318	0.058701
Ru	2.476962	0.007609	0.076004
C	5.697884	1.414016	-2.210569
C	4.914040	-0.139289	1.993479
C	5.493912	-0.320912	3.252304
N	3.561626	-0.195232	1.869644
C	4.591974	1.322861	-1.354337
N	0.834001	-0.092366	1.409480
C	-4.399745	1.730374	1.079092
N	-0.424411	-0.577460	1.171395
C	2.738954	-0.414138	2.928220
C	4.671163	-0.562920	4.358947
N	-3.123062	1.358582	1.413520
C	-5.099695	2.666433	1.841788
C	1.287934	-0.481730	2.642991
C	3.281974	-0.616891	4.201437
N	-2.920829	-1.591849	1.392002
C	-0.759401	-1.204340	2.328340
C	-4.106258	-2.232937	1.371787
C	3.869305	2.441769	-0.651225
N	2.796518	2.089968	0.136752
C	0.285658	-1.165601	3.285202
C	-2.065953	-1.850244	2.417763
C	-2.556258	1.905753	2.502349
C	-4.498505	3.232156	2.965941
C	-4.496477	-3.130513	2.359903
C	-3.204523	2.842978	3.304555
C	2.179648	2.967639	0.966993
C	4.273901	3.781696	-0.694723
C	-2.400048	-2.729691	3.450853
C	-3.631665	-3.377882	3.426269
C	3.602399	4.717768	0.100565
C	2.564052	4.310510	0.947195
H	5.539021	0.039182	1.130660
H	6.569032	-0.280048	3.369244
H	5.110370	-0.710676	5.336990
H	2.644752	-0.806990	5.055620
H	0.304940	-1.604363	4.270967
H	-1.694835	-2.915057	4.253231
H	-3.906183	-4.067936	4.217548
H	-5.461332	-3.620775	2.288818
H	-4.757525	-2.009705	0.536006

H	1.412462	2.629324	1.648236
H	2.069866	5.028095	1.589058
H	3.906964	5.756173	0.083564
H	5.105317	4.099883	-1.308296
H	6.143786	2.367007	-2.458877
H	7.078319	0.271417	-3.421877
H	6.067241	-1.937859	-2.885493
H	4.905979	-3.817309	-2.172174
H	3.501241	-5.663914	-1.317285
H	1.590340	-5.186081	0.195892
H	1.094750	-2.840522	0.840163
H	-0.363373	-2.207300	-1.270705
H	-0.505681	-3.805135	-3.183596
H	-2.623745	-3.862659	-4.543795
H	-4.492119	-2.354961	-3.910065
H	-6.049942	-0.954723	-3.224528
H	-7.617979	0.669312	-2.197362
H	-6.933064	1.965601	-0.199068
H	-6.107780	2.953829	1.565746
H	-5.035129	3.961250	3.564437
H	-2.697855	3.253293	4.171418
H	-1.548588	1.574938	2.729617
H	-2.784202	1.141933	-2.803719
H	-0.542455	2.320134	0.456433
H	-2.231909	3.199987	-4.049670
H	0.138832	4.438102	-0.668939
H	-0.717536	4.904572	-2.983930
C	0.797982	0.235977	-2.675333
C	0.159999	0.272265	-3.991788
H	0.121307	1.318468	-4.357122
H	0.752199	-0.340539	-4.701705
H	-0.866082	-0.141683	-3.925200

in-$[Ru_2(MeCN)]^{3+}$

3 1 2 1

C	3.018463	-4.708001	-0.096613
C	2.072279	-4.243680	0.826117
C	3.677567	-3.811186	-0.946523
C	-3.004632	-4.623325	-1.349674
C	-3.716320	-3.528738	-1.844278
C	1.778459	-2.879279	0.881596
C	-5.062861	-0.957563	-2.882793
C	-2.031476	-4.409625	-0.377328
C	3.360067	-2.449330	-0.871164
C	-5.565047	0.292221	-3.250644

C	-3.432921	-2.248593	-1.371515
C	5.038417	-1.534098	-2.655682
N	2.396901	-2.034243	0.020388
C	-4.122375	-1.029368	-1.853162
C	4.037558	-1.378534	-1.686812
C	-1.796854	-3.107281	0.058472
N	-2.458697	-2.043033	-0.426217
C	-5.115680	1.450606	-2.613684
C	5.534074	-0.377503	-3.303145
N	-3.731412	0.105994	-1.221939
N	0.747696	-0.155124	-1.591273
C	-4.175604	1.334881	-1.587514
N	3.621002	-0.127034	-1.430235
Ru	-2.214699	0.001129	0.089664
Ru	2.147732	0.055576	-0.068625
C	5.034493	0.908024	-2.986660
C	4.788926	0.312135	1.549203
C	5.509650	0.431413	2.741158
N	3.431518	0.278308	1.593760
C	4.034280	1.012567	-2.010504
N	0.715231	0.261900	1.429684
C	-3.551497	2.448156	-0.834868
N	-0.590868	-0.029415	1.432250
C	2.734234	0.356185	2.765305
C	4.820299	0.507183	3.958018
N	-2.571842	2.085509	0.055918
C	-3.907408	3.785263	-1.003796
C	1.255351	0.290191	2.670498
C	3.421640	0.466589	3.977401
N	-3.132411	-0.245134	1.890219
C	-0.914686	-0.090345	2.750449
C	-4.466564	-0.394214	2.034356
C	3.347332	2.258917	-1.514960
N	2.380381	2.092161	-0.549776
C	0.230665	0.089355	3.577369
C	-2.338176	-0.259595	3.009666
C	-1.979254	3.042275	0.791202
C	-3.265880	4.772956	-0.254161
C	-5.066631	-0.561776	3.276594
C	-2.289534	4.394592	0.663780
C	1.710663	3.129339	0.010084
C	3.643989	3.551031	-1.965878
C	-2.890895	-0.422466	4.280856
C	-4.267237	-0.576204	4.420944
C	2.951371	4.636310	-1.414445
C	1.984449	4.429185	-0.421955
H	5.309409	0.244006	0.604788
H	6.591359	0.460229	2.723856
H	5.370749	0.595743	4.885645
H	2.887794	0.522544	4.917497

H	0.286088	0.069908	4.655056
H	-2.238513	-0.430307	5.147432
H	-4.707892	-0.705288	5.404190
H	-6.143221	-0.677994	3.336385
H	-5.049938	-0.374772	1.122585
H	0.983066	2.951492	0.786240
H	1.456359	5.269316	0.010155
H	3.169184	5.641422	-1.751659
H	4.395017	3.724660	-2.724076
H	5.421432	1.780149	-3.495076
H	6.306272	-0.478034	-4.054692
H	5.429461	-2.508466	-2.913085
H	4.423887	-4.178624	-1.637357
H	3.253107	-5.763468	-0.141408
H	1.579159	-4.934787	1.497294
H	1.078320	-2.499202	1.610355
H	-1.066973	-2.894527	0.826998
H	-1.459220	-5.228718	0.044242
H	-3.215066	-5.622834	-1.716380
H	-4.486063	-3.677558	-2.592867
H	-5.390145	-1.849061	-3.404430
H	-6.294491	0.365564	-4.050755
H	-5.484718	2.420011	-2.926937
H	-4.681086	4.060668	-1.711251
H	-3.533582	5.816668	-0.383424
H	-1.772075	5.125297	1.275839
H	-1.240669	2.699582	1.505784
C	-0.031041	-0.275631	-2.437922
C	-1.010344	-0.425884	-3.513489
H	-1.800787	0.344557	-3.404961
H	-0.505018	-0.299221	-4.492729
H	-1.464989	-1.436140	-3.461826

3a *in,in*-$[Ru_2(MeCN)_2]^{3+}$

3 1 2 1

C	4.190579	-4.295585	1.299127
C	2.957774	-3.951368	1.848802
C	4.811823	-3.403863	0.424837
C	-2.680700	-4.427148	-2.042405
C	-3.588154	-3.392740	-2.304210
C	2.392471	-2.723647	1.508993
C	-5.464938	-0.876665	-2.656229
C	-1.620546	-4.230912	-1.147432
C	4.194230	-2.190081	0.119623
C	-6.177343	0.346282	-2.671230

C	-3.415033	-2.161608	-1.660506
C	5.965662	-1.316821	-1.529346
N	2.985027	-1.856062	0.672188
C	-4.323102	-0.972619	-1.849378
N	-1.217183	0.620506	-1.605808
C	4.772910	-1.193191	-0.811373
C	-1.471150	-2.992115	-0.519477
N	-2.357892	-2.003333	-0.793631
C	-5.753183	1.449566	-1.892556
C	6.348366	-0.283245	-2.386271
N	-3.982529	0.115174	-1.137134
N	1.448455	-0.973460	-1.556340
C	-4.605620	1.304777	-1.100932
N	4.022667	-0.074557	-0.952425
Ru	-2.337134	-0.058923	0.008630
Ru	2.289606	0.045663	0.015357
C	5.549703	0.853785	-2.520980
C	4.283858	1.440030	1.934567
C	4.748565	1.917008	3.155997
N	3.050825	0.921172	1.775342
C	4.367010	0.941671	-1.781545
N	0.526985	0.239045	1.279851
C	-3.964070	2.326662	-0.197100
N	-0.709638	-0.307051	1.322993
C	2.220810	0.878915	2.856976
C	3.909252	1.854761	4.268721
N	-2.831228	1.934193	0.480248
C	-4.445125	3.629930	-0.022721
C	0.877567	0.373132	2.586289
C	2.628380	1.330462	4.113387
N	-3.391466	-0.718690	1.713877
C	-1.157061	-0.452081	2.601114
C	-4.722265	-0.989174	1.772443
C	3.409285	2.071013	-1.774445
N	2.312924	1.909078	-0.967058
C	-0.158428	-0.048362	3.460159
C	-2.584249	-0.784308	2.807493
C	-2.144270	2.760086	1.308874
C	-3.755374	4.497645	0.832834
C	-5.293777	-1.353031	2.995282
C	-2.601789	4.065972	1.500053
C	1.432396	2.918416	-0.855710
C	3.594018	3.245563	-2.505092
C	-3.121560	-1.130649	4.051140
C	-4.487495	-1.420762	4.138046
C	2.661957	4.277996	-2.401217
C	1.567847	4.116222	-1.553874
H	4.909864	1.465775	1.050675
H	5.750299	2.326809	3.225768
H	4.241937	2.214924	5.236883

H	1.941668	1.285009	4.951640
H	-0.165945	-0.043237	4.539416
H	-2.496712	-1.181827	4.933636
H	-4.921897	-1.696019	5.090322
H	-6.351557	-1.572638	3.059432
H	-5.338165	-0.918419	0.887935
H	0.594450	2.741777	-0.191194
H	0.823946	4.896185	-1.432935
H	2.795872	5.193875	-2.967664
H	4.460308	3.360566	-3.146575
H	5.847762	1.650583	-3.192408
H	7.269798	-0.365664	-2.953402
H	6.586055	-2.200038	-1.432959
H	5.770542	-3.655758	-0.013872
H	4.663514	-5.241641	1.542314
H	2.435565	-4.615167	2.529327
H	1.434624	-2.416203	1.912925
H	-0.655880	-2.820150	0.169651
H	-0.919838	-5.030948	-0.947226
H	-2.799568	-5.384260	-2.533402
H	-4.403790	-3.557463	-2.994614
H	-5.804700	-1.709566	-3.255906
H	-7.061630	0.439213	-3.288106
H	-6.309971	2.375920	-1.916734
H	-5.331388	3.976681	-0.535906
H	-4.113598	5.508710	0.977076
H	-2.067492	4.739466	2.157443
H	-1.253047	2.415179	1.812164
C	1.054530	-1.644179	-2.416087
C	0.504463	-2.451739	-3.499537
H	1.015340	-2.219889	-4.439419
H	0.627343	-3.517246	-3.281084
H	-0.562887	-2.235640	-3.616910
C	-0.655219	1.022359	-2.533990
C	0.047890	1.525995	-3.714044
H	-0.397237	1.079367	-4.626566
H	-0.046501	2.630315	-3.757811
H	1.120128	1.248606	-3.654449

Table S3.1. Bond distances and angles of the first coordination sphere for the X-ray and calculated structures of complex 3b.

Bond distance (A)/ angle (º)	3b X-ray	Calculated 3b
Ru-N1	2.071	2.10913
Ru-N2	1.953	2.01830
Ru-N3	2.060	2.11135
Ru-N4	2.111	2.14368
Ru-N5	2.056	2.11010
Ru-N6	2.128	2.12680
N1-Ru-N3	158.30	162.51
N5-Ru-N4	174.49	177.37
N2-Ru-N6	174.48	175.40
N1-Ru-N4	87.03	92.86
N1-Ru-N6	97.53	98.16
N1-Ru-N5	88.46	88.61
N1-Ru-N2	79.66	81.42
N3-Ru-N2	79.44	81.42
N3-Ru-N4	97.37	90.07
N3-Ru-N6	102.79	98.66
N3-Ru-N5	87.98	89.17

4.-References :

[S1] Planas, N; Christian, G.J; Mas-Marzá, E.; Sala, X.; Fontrodona, X.; Maseras, F.; Llobet, A. *Chem. Eur.J.* 2010, 16, 7965-7968.

APENDIX C

EXPERIMENTAL SUPPORTING INFORMATION

FOR:

The Bpp Catalyst Anchored on TiO_2 by Sulfonate Groups

Nora Planas, Stephan Roeser, Jordi Benet-Bucholz and Antoni Llobet

[a] Institute of Chemical Research of Catalonia (ICIQ), Av. Països Catalans 16, E-43007 Tarragona, Spain.

The supporting information section also includes "cif" magnetic files of the crystal structures of complex 2* and trpy*.

I. NMR spectra:

Figure S1. 1D and 2D NMR spectra (400 MHz, 298K, MeOH-d_4) for ligand *trpy** (a) ^{1}H-NMR, (b) COSY, (c) NOESY (d) ^{13}C-NMR (e) NMR nomenclature

(a)

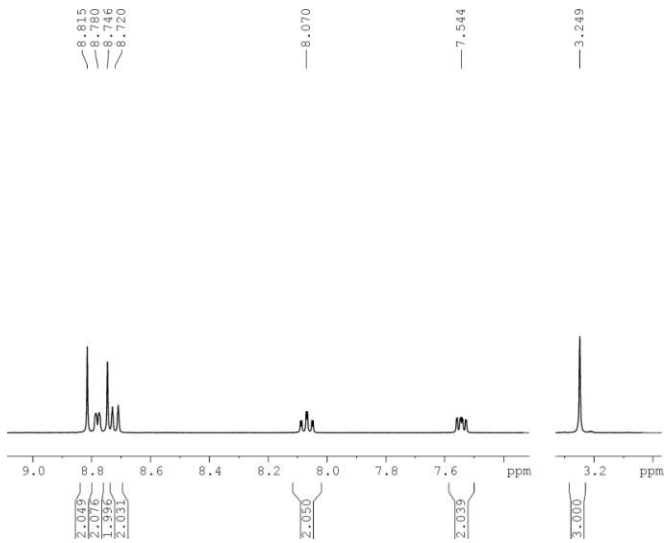

(b)

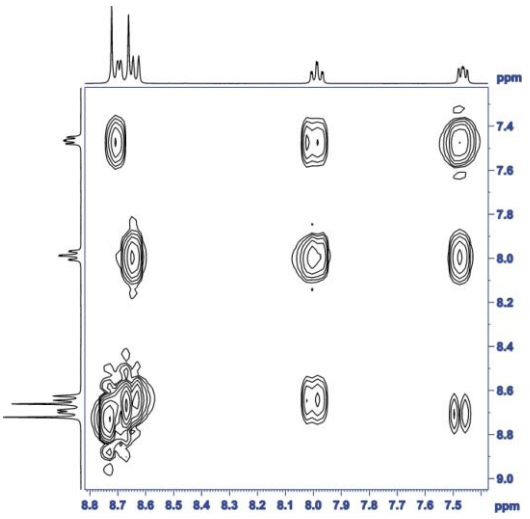

(c)

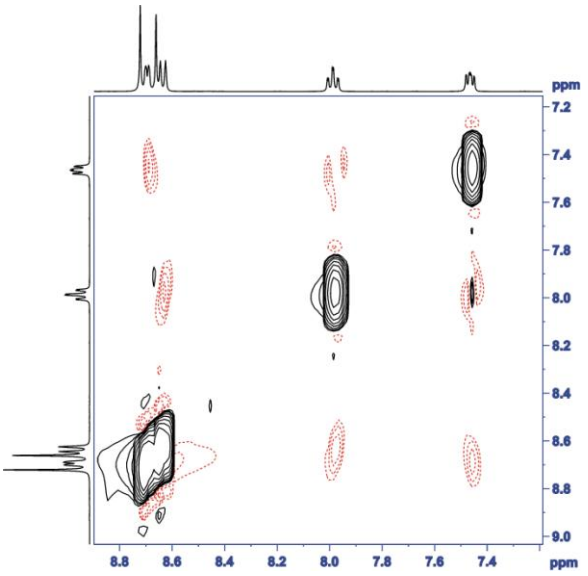
ppm
7.2
7.4
7.6
7.8
8.0
8.2
8.4
8.6
8.8
9.0
8.8
8.6
8.4
8.2
8.0
7.8
7.6
7.4
ppm

(d)

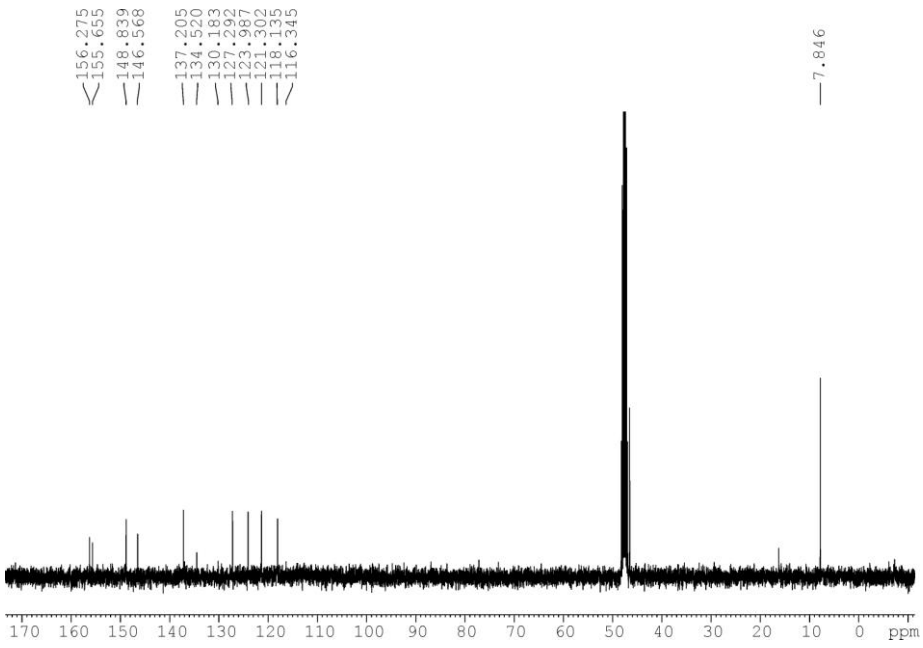
156.275
155.655
148.839
146.568
137.205
134.520
130.183
127.292
123.987
121.302
118.135
116.345
7.846
170 160 150 140 130 120 110 100 90 80 70 60 50 40 30 20 10 0 ppm

(e)

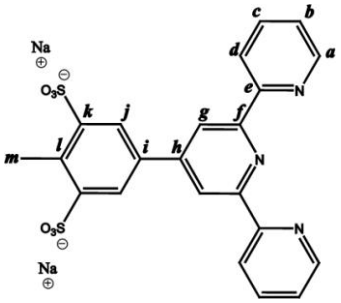

Figure S2. 1D and 2D NMR spectra (400 MHz, 298K, D_2O) for complex 2*. (a) ^{1}H-NMR, (b) COSY, (c) NOESY (d) NMR nomenclature

(a)

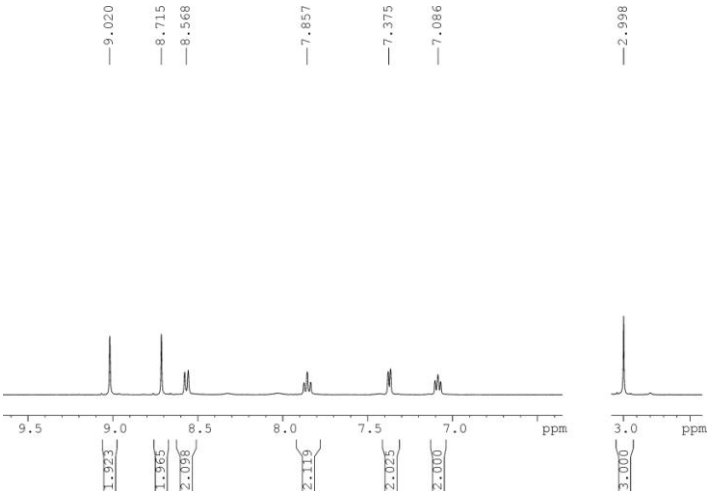

(b)

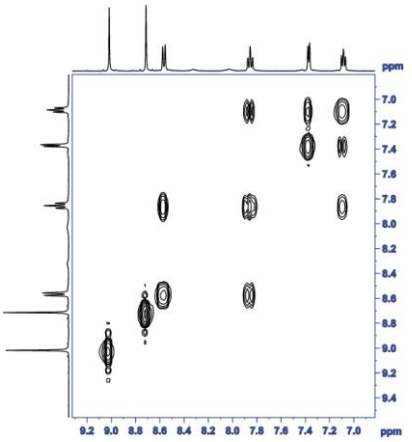

(c)

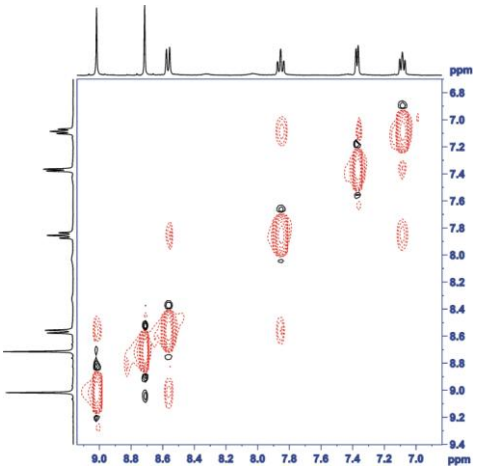
ppm
6.8
7.0
7.2
7.4
7.6
7.8
8.0
8.2
8.4
8.6
8.8
9.0
9.2
9.4
9.0 8.8 8.6 8.4 8.2 8.0 7.8 7.6 7.4 7.2 7.0
ppm

(d)

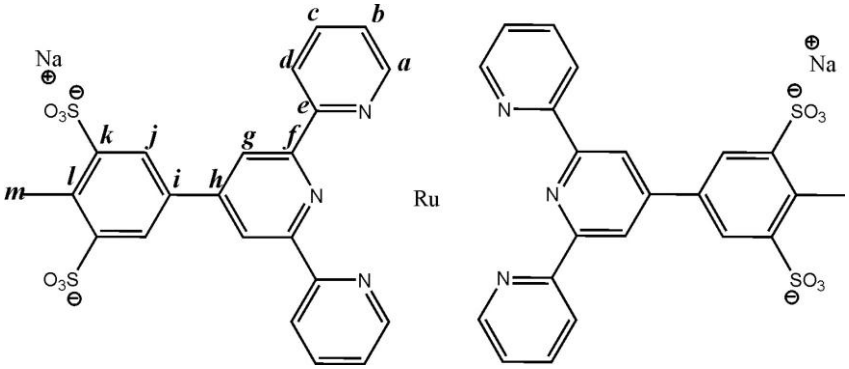
Na
O3S
k
j
l
m
i
h
g
f
c
b
d
a
e
N
N
N
O3S
Ru
N
N
N
Na
SO3
SO3

Figure S3. 1D and 2D NMR spectra (400 MHz, 298K, MeOH-d_4) for complex **3***. (a) ^{1}H-NMR, (b) COSY, (c) NOESY, (d) NMR nomenclature

(a)

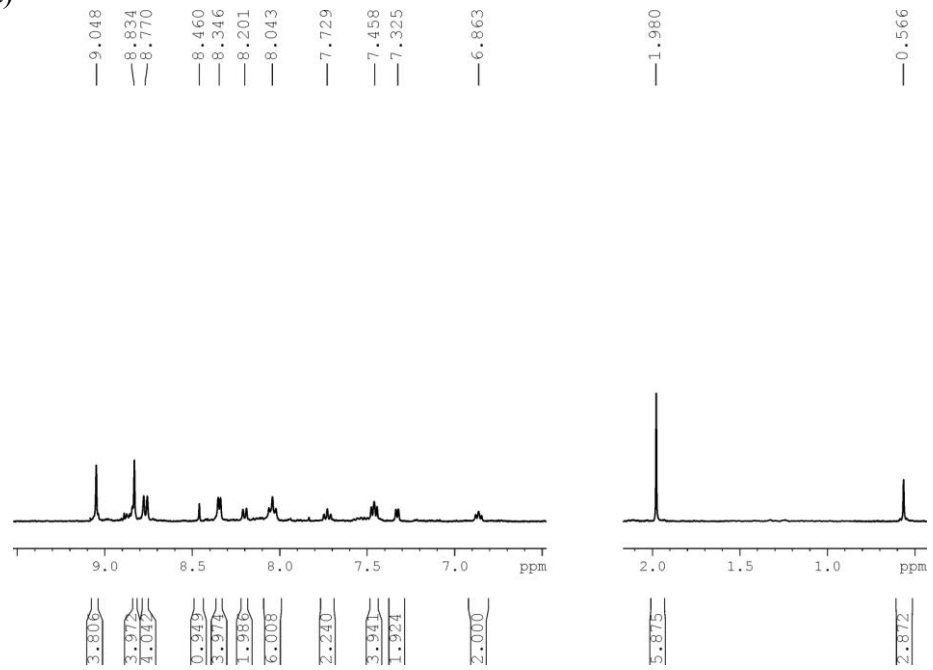

(b)

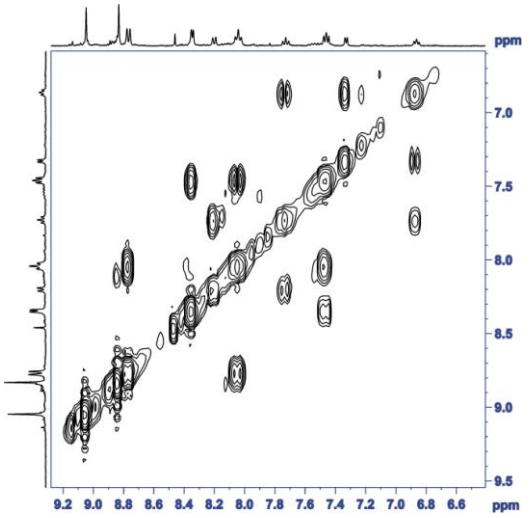

(c)

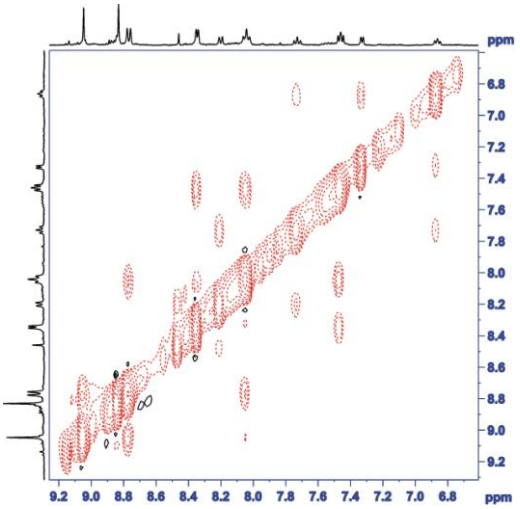
ppm
6.8
7.0
7.2
7.4
7.6
7.8
8.0
8.2
8.4
8.6
8.8
9.0
9.2
9.2 9.0 8.8 8.6 8.4 8.2 8.0 7.8 7.6 7.4 7.2 7.0 6.8
ppm

(d)

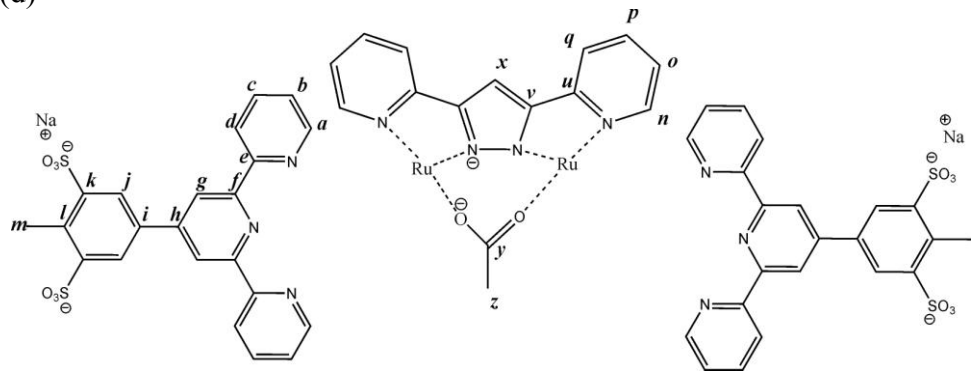
Na
O3S
a
b
c
d
e
f
g
h
i
j
k
l
m
N
Ru
Ru
O
x
y
z
p
q
o
u
v
n
Na
SO3
SO3

II. UV-vis spectra:

Figure S4. UV-vis, 0.03 mM in MeOD, of (a) trpy*, (b) 2*, (c) 3*.

(a)

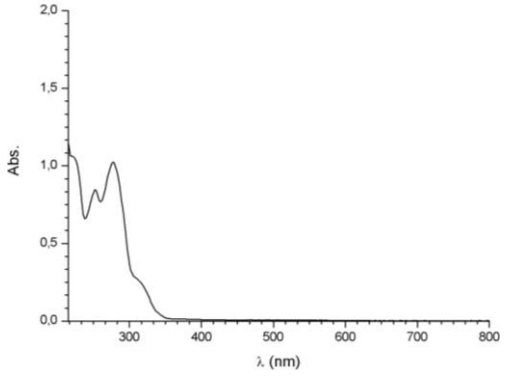

(b)

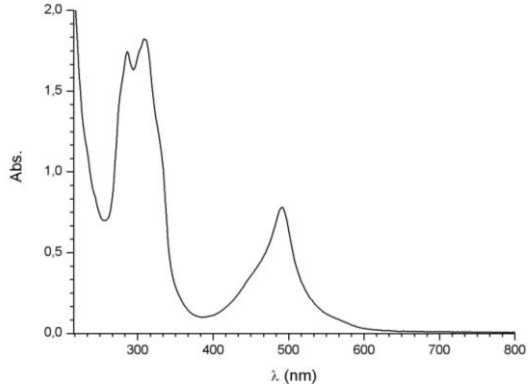

(c)

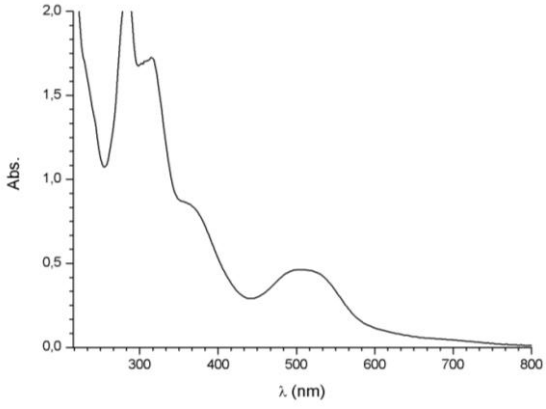

III. Electrochemistry:

Figure S5. CV for 0.3 mM of complexes (a)3* in pH7, (b) 2* in pH7.

(a)

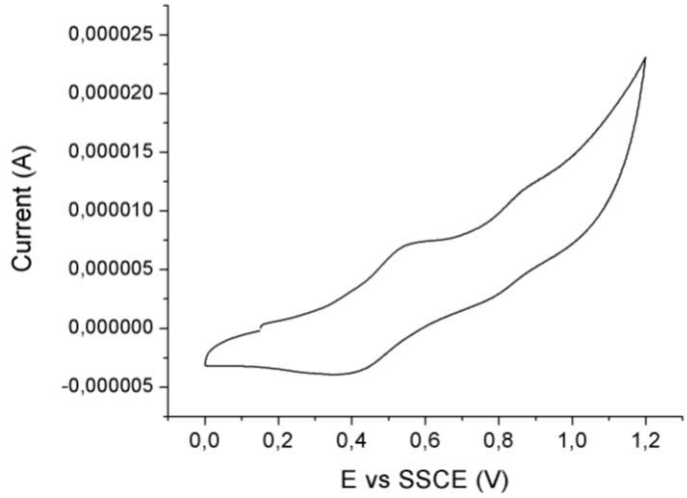

(b)

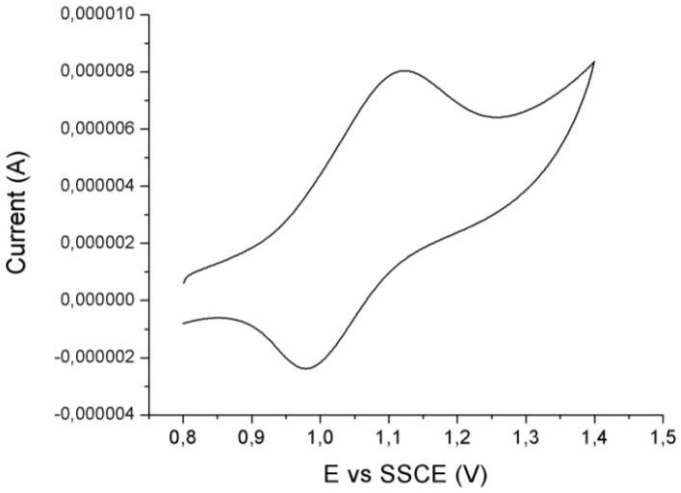

IV. Catalysis with Cerium:

Figure S6. Catalytic experiment with 2 mg of 3* anchored in 250mg anatase after the addition of 100 eq of Ce^{IV}. (a) Online manometric: measurements. (b) Online mass spectroscopy anaklysis.

(a)

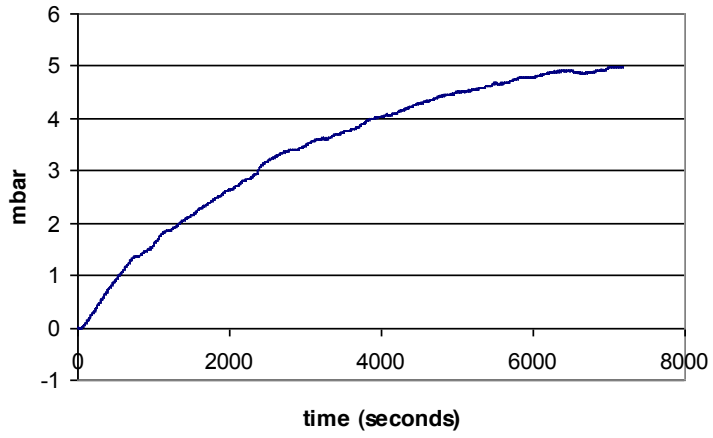

(b)

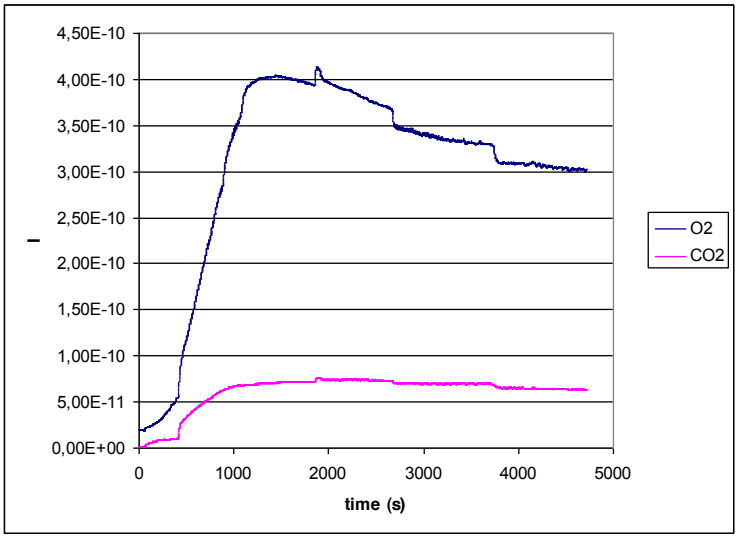

Figure S7. Catalytic experiment with 0.5 mg of 3* anchored in 250mg anatase after the addition of 100 eq of Ce^{IV}. (a) Online manometric: measurements. (b) Online mass spectroscopy anaklysis.

(a)

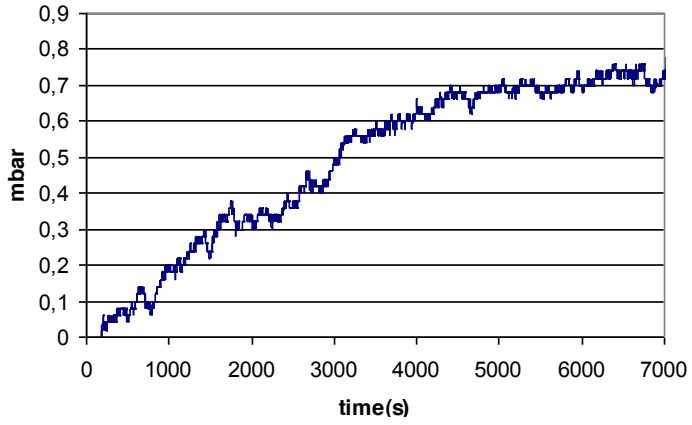

(b)

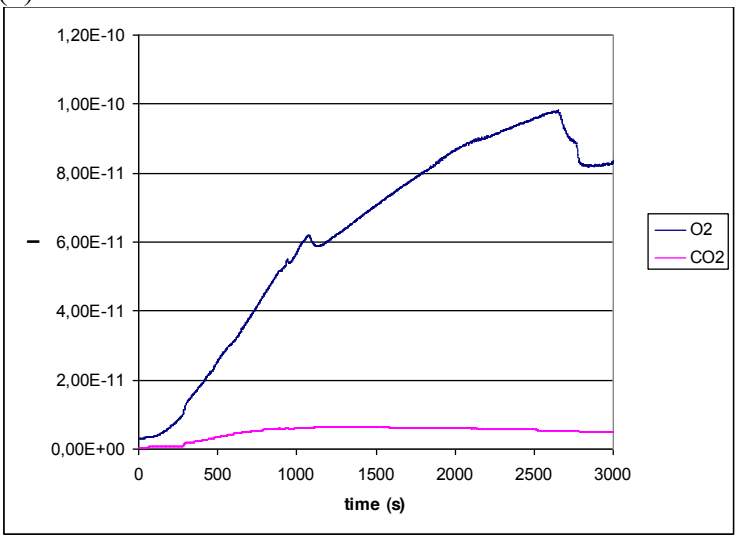

Figure S8. Catalytic experiment with 1 mg of 3* anchored in 250mg anatase after the addition of 100 eq of Ce^{IV}. (a) Online manometric: measurements. (b) Online mass spectroscopy anaklysis.

(a)

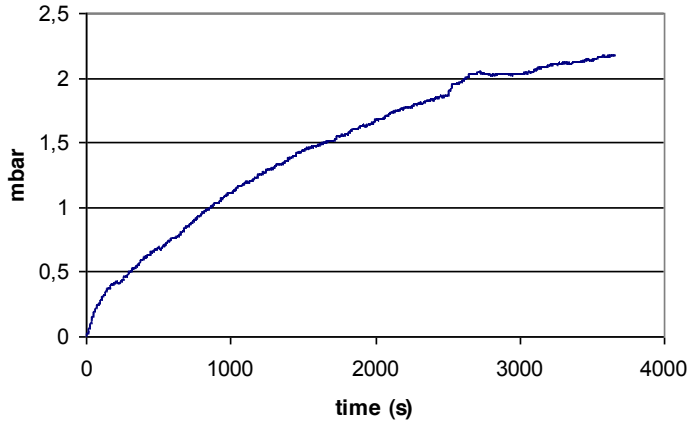

(b)

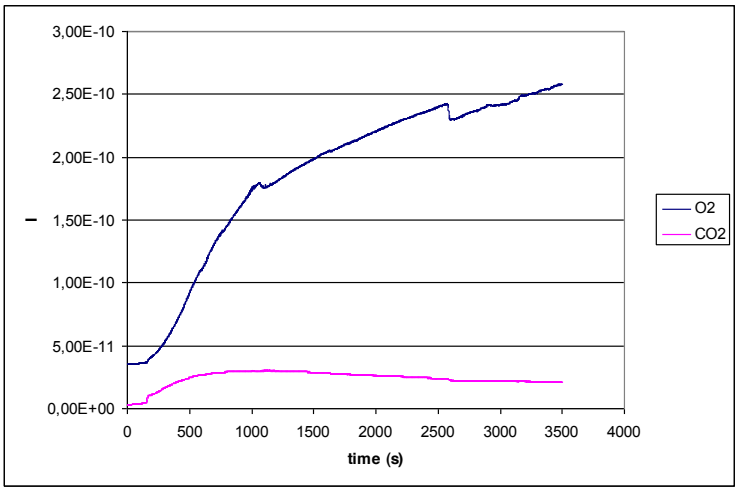

V. Electrocatalytic experiments:

Figure S9. Representative example of the Electrocatalytic experiments performed with 4*-TiO2-FTO. (a) Graph of the bulk electrolysis experiment carried out at 1.6 V vs SSCE. (b) Accumulated charge over time. The little oxigen measured with the clarck electrode probe coincided with the blank experiments, oxygen leaking from the air to the cell

(a)

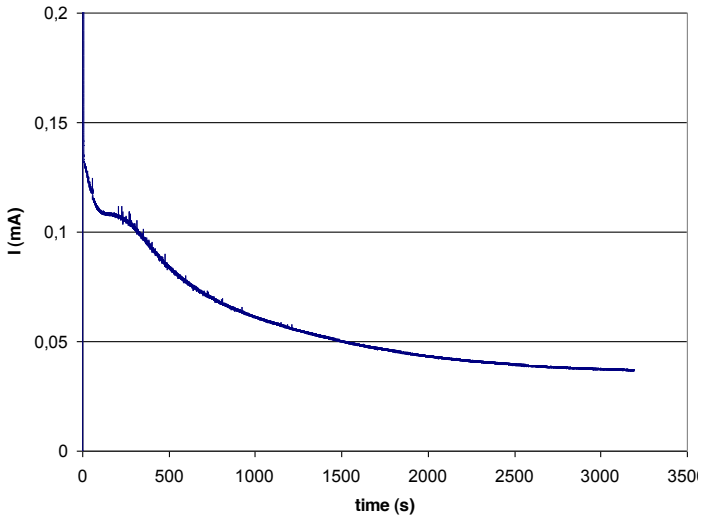

(b)

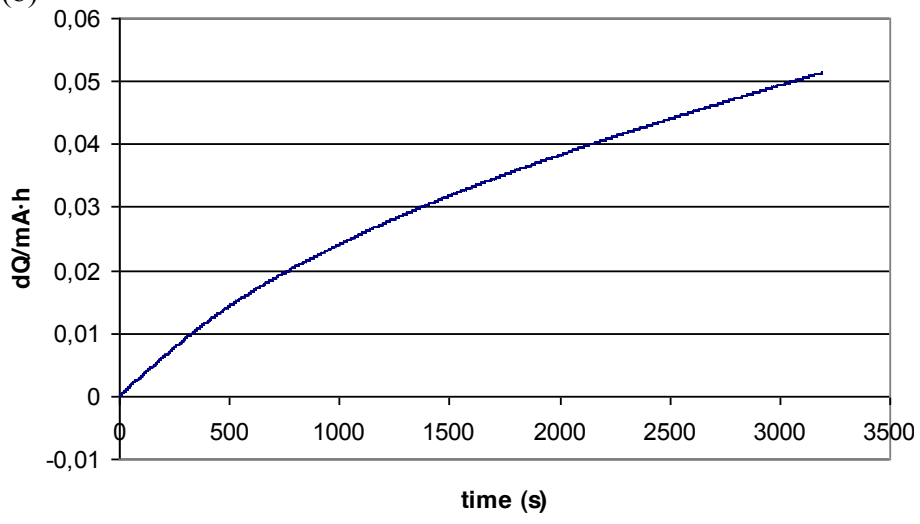

VI. Coordinates of 4* optimized geometry:

Ru	2.28251000	-0.08704500	-0.13943800
Ru	-2.26628200	0.08325700	-0.15141000
N	3.20177800	-0.83768200	1.52825300
C	4.50420300	-1.22905000	1.60122500
H	5.06176000	-1.21540900	0.66522500
N	0.65980600	-0.25841700	1.19061700
C	5.10217100	-1.62330600	2.79091100
H	6.14740600	-1.93117100	2.79462200
N	-0.63780500	0.07691700	1.20014500
C	4.34834400	-1.61394600	3.96840300
H	4.79677800	-1.91194200	4.91683700
N	-3.16964700	0.67695000	1.57648700
C	3.01525200	-1.22422600	3.91133900
H	2.39937000	-1.21699500	4.81100800
N	2.30314100	-1.90766100	-1.11521300
C	2.44968100	-0.84471900	2.68860200
N	3.88167400	0.12312400	-1.25137400
C	1.07140300	-0.45673800	2.50134400
N	2.91449800	1.81094600	0.46084800
C	-0.00109500	-0.21103900	3.36640200
H	-0.00656400	-0.26667600	4.44980100
N	-2.24770100	2.00424600	-0.94897500
C	-1.06290600	0.13040100	2.52042800
N	-3.89800600	0.03620300	-1.24048200
C	-2.43252300	0.52516000	2.73681400
N	-2.92949600	-1.85419700	0.24698400
C	-3.00382400	0.78063900	3.98935400
H	-2.40019400	0.64859000	4.88758800
C	-4.32211800	1.21030500	4.07773700
H	-4.77326000	1.41414300	5.04954900
C	-5.05779800	1.38472800	2.90121000
H	-6.09035700	1.73166200	2.92918400
C	-4.45875000	1.10626900	1.68031300
H	-5.00464800	1.22221700	0.74492900
C	1.49363100	-2.98437100	-0.91437400
H	0.73423000	-2.84777200	-0.14091200
C	1.64016300	-4.18399000	-1.60262200
H	0.97570000	-5.02222200	-1.39016900
C	2.66268700	-4.30488000	-2.54806000
H	2.80516400	-5.23440600	-3.10042800
C	3.51586400	-3.22436200	-2.75697900
H	4.33471800	-3.30723000	-3.47189700
C	3.33819200	-2.04045000	-2.03488100
C	4.22353900	-0.87354900	-2.13261000
C	5.33501200	-0.71710700	-2.96631200

H	5.61827000	-1.50000000	-3.66932000
C	6.08716300	0.45720600	-2.88902700
C	5.72508400	1.46437700	-1.99066400
H	6.31192500	2.38065200	-1.93657100
C	4.60707700	1.28501900	-1.17178200
C	4.07445300	2.22597700	-0.17617600
C	4.67302200	3.44829300	0.13785200
H	5.58584100	3.75643400	-0.37187200
C	4.11052300	4.26762000	1.11416600
H	4.57785400	5.21922800	1.37059700
C	2.94983600	3.84466000	1.76319400
H	2.48957700	4.45377100	2.54131300
C	2.38597800	2.62040300	1.41411300
H	1.48632400	2.24410300	1.90465500
C	-1.36412100	3.00824000	-0.71239500
H	-0.53787800	2.75010800	-0.04970300
C	-1.49178500	4.27449100	-1.27607200
H	-0.75837600	5.04804100	-1.04835700
C	-2.56909600	4.53722300	-2.12390200
H	-2.69618200	5.52171300	-2.57578400
C	-3.48863100	3.52206700	-2.37992100
H	-4.34054300	3.71037700	-3.03350400
C	-3.32403800	2.26804500	-1.78762100
C	-4.25321800	1.14390000	-1.97058800
C	-5.40768300	1.11799100	-2.75840400
H	-5.70257900	1.98940000	-3.34227800
C	-6.18953800	-0.03945100	-2.78932600
C	-5.81730200	-1.15825200	-2.03971600
H	-6.43147800	-2.05780900	-2.06455500
C	-4.65732800	-1.10711300	-1.26160200
C	-4.12115500	-2.16781100	-0.39566500
C	-4.74817200	-3.39945400	-0.19186700
H	-5.68408600	-3.62623300	-0.70246600
C	-4.18703700	-4.33194100	0.67867200
H	-4.67791200	-5.29092800	0.84919100
C	-2.99818200	-4.01143300	1.33650900
H	-2.54012100	-4.71000500	2.03712400
C	-2.40470600	-2.77490800	1.09976000
H	-1.48552300	-2.47392500	1.60635600
O	1.12447000	0.87184600	-1.74153300
H	1.66147300	0.94781600	-2.56630800
O	-1.15681900	-0.68637400	-1.97362000
H	-1.04980600	-1.66629400	-1.88060900
H	0.35410200	0.27938100	-1.97718200
H	-1.74182300	-0.57411300	-2.76585000
C	7.31753015	0.64298521	-3.79637631
C	8.06971953	1.81502293	-3.72047863
C	7.67964822	-0.36135211	-4.69492713
C	9.18481777	1.98290247	-4.54196740

H	7.78481282	2.60650299	-3.01222072
C	8.79421396	-0.19324290	-5.51652285
H	7.08638704	-1.28535032	-4.75463320
C	9.54710368	0.97879705	-5.43978106
C	-7.46682876	-0.08096249	-3.64863102
C	-8.24872554	-1.23544042	-3.68087801
C	-7.84176317	1.03658194	-4.39544771
C	-9.40629587	-1.27267971	-4.45876978
H	-7.95371114	-2.11614204	-3.09217354
C	-8.99881371	0.99911595	-5.17350128
H	-7.22507581	1.94671428	-4.36991026
C	-9.78136943	-0.15545412	-5.20487631
C	10.77777972	1.16397938	-6.34683342
H	11.64442894	0.77235004	-5.85648090
H	10.62329491	0.64270144	-7.26841020
H	10.92069506	2.20555229	-6.54583360
C	-11.05893681	-0.19640381	-6.06379698
H	-10.81675780	-0.54212884	-7.04701798
H	-11.76820568	-0.86113437	-5.61661586
H	-11.47950703	0.78559978	-6.12453938
S	10.14500373	3.47853341	-4.44434058
S	9.25653904	-1.47406630	-6.66288533
S	-9.47750396	2.42437986	-6.12632783
S	-10.40435375	-2.74599264	-4.49913640
O	-10.92871996	3.01711889	-5.55053918
O	-9.65050347	1.98974850	-7.72947060
O	-8.30239646	3.60345747	-5.99291732
O	-10.59510404	-3.24597359	-6.08107615
O	-9.65303389	-3.95155678	-3.62105123
O	-11.90130304	-2.42271251	-3.83315382
O	8.27252670	-2.80444181	-6.43767270
O	9.08307349	-0.91154816	-8.22569787
O	10.84777114	-1.90787987	-6.40080478
O	9.57689908	4.42390896	-3.19037798
O	10.01191163	4.32023340	-5.88056049
O	11.74704870	3.09466163	-4.17048954

APPENDIX D

SUPPORTING INFORMATION FOR:

The Electronic Structure of Higher Oxidation States Derived from *cis*--$[Ru^{II}(bpy)_2(H_2O)_2]^{2+}$ and its Photoisomerization Mechanism

To be Submitted

Nora Planas,[a] Laura Vigara,[a] Clyde Cady,[b] Ping Huang,[b] Leif Hammarstrom,[b] Stenbjorn Styring,[b] Nils Leidel,[c] Holger Dau,[c] Michael Haumann,[c] Pere Miró,[d] Laura Gagliardi,[d] Christopher Cramer[d] and Antoni Llobet[a,e,]

[a] *Institute of Chemical Research of Catalonia (ICIQ), Av. Països Catalans 16, E-43007 Tarragona, Spain.*
[b] *Department of Photochemistry and Molecular Science, Ångström Laboratory, Box 523, Uppsala University, SE-751 20 Uppsala, Sweden.*
[c] *Department of Physics, Free University Berlin, D-14195 Berlin, Germany.*
[d] *Department of Chemistry and Supercomputing Institute University of Minnesota, 207 Pleasant St. SE, Minneapolis, MN 55455-0431 (USA)*
[e] *Departament de Química, Universitat Autònoma de Barcelona, Cerdanyola del Vallès, E-08193 Barcelona, Spain.*
†*Electronic Supplementary Information (ESI) available: Experimental section,characterizations and coordinates of computed structures.*

A) Orbitals and Selected geometrical parameters:

B) Energies:

C) Coordinates:

A) Orbitals and Selected geometrical parameters:

Table 1. CASSCF orbitals of the active spaces in the two spin states for the cis isomer.

Cis/triplet (C_1)		Cis/singlet (C_2)	
Active space orbital	Occupation coefficient	Active space orbital	Occupation coefficient
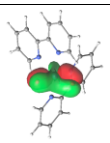	1,93	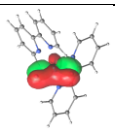	1,94
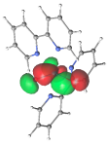	1,93	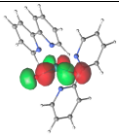	1,94
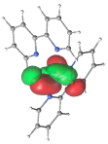	1,94	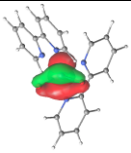	1,99
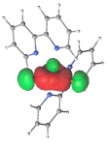	1,93	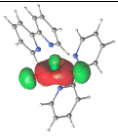	1,93
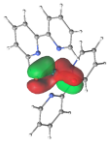	1,94	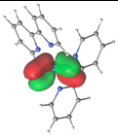	1,93
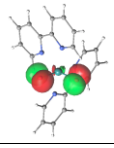	1,87	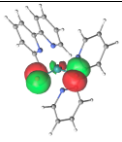	1,88
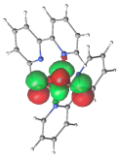	1,06	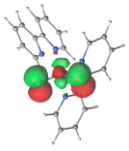	1,78

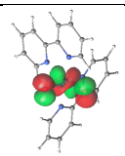	1,06	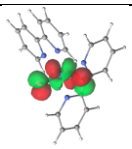	0,30
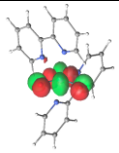	0,20	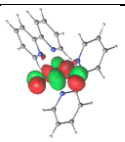	0,18
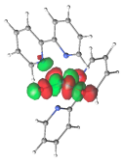	0,09	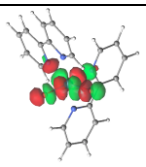	0,09
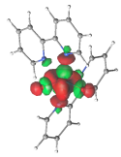	0,05	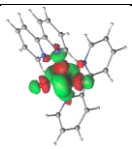	0,05

Table 2. CASSCF orbitals of the active spaces in the two spin states for the trans isomer

Trans/triplet (C_1)		Trans/singlet (d_2)	
Active space orbital	Occupation coefficient	Active space orbital	Occupation coefficient
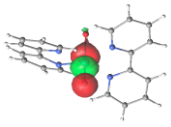	2,00	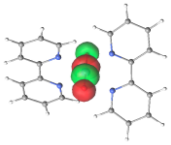	2,00
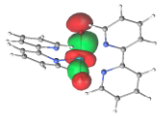	1,96	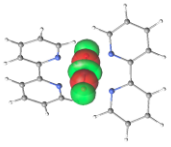	1,97
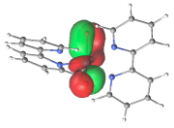	1,95	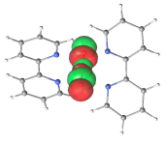	1,94

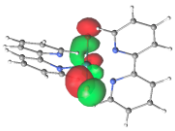	1,94	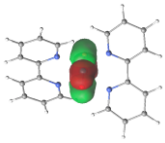	1,94
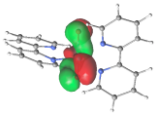	1,93	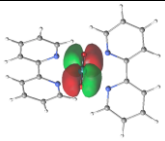	1,94
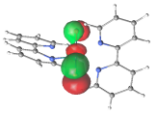	1,87	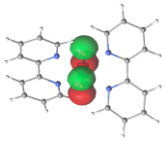	1,85
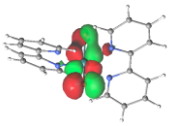	1,06	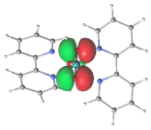	1,82
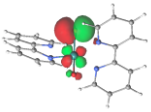	1,00	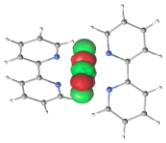	0,21
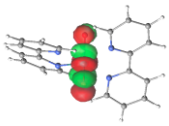	0,18	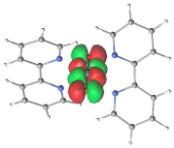	0,22
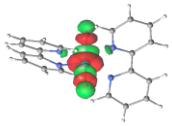	0,09	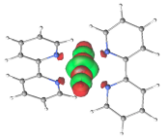	0,08
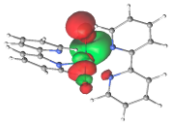	0,02	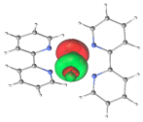	0,01

Table 3. DFT, CASSCF, CASPT2 energies ox state VI

	DFT			CASSCF		CASPT2	
	$\otimes G_{DFT\ (HS-LS)}$ (kcal·mol^{-1})	$\otimes E_{DFT\ (HS-LS)}$ (kcal·mol^{-1})	stable spin	$\otimes E_{CASSCF\ (HS-LS)}$ (kcal·mol^{-1})	stable spin	$\otimes E_{CASPT2\ (HS-LS)}$ (kcal·mol^{-1})	stable spin
cis	1,26	1,88	S	7,78	S	2,95	S
trans	31,68	33,6	S	43,49	S	39,60	S

DFT $\otimes G_{cis-trans}$ (kcal·mol^{-1})	DFT $\otimes E_{cis-trans}$ (kcal·mol^{-1})	CASSCF $\otimes E_{cis-trans}$ (kcal·mol^{-1})	CASPT2 $\otimes E_{cis-trans}$ (kcal·mol^{-1})
6,26	5,67	6,71	4,77

Table 4. Selected bond distances and angles of the optimized geometries in the isomerization process in oxidation state II:

isomer	spin	Ru-O1	Ru-O2	O-Ru-O	N1-N2-N3-N4	Ru-N1	Ru-N2	Ru-N3	Ru-N4
cis	S0	2,226	2,226	82,866	91,464	2,024	2,075	2,075	2,024
	S1	2,213	2,182	83,720	89,089	2,048	2,084	2,084	2,010
mono cis	S0	2,225	---	---	91,434	2,028	2,083	2,071	1,987
	T1	2,207	---	---	84,570	2,052	2,064	2,131	2,307
mono-TS	T1	2,222	---	---	107,210	2,245	2,106	2,068	2,073
mono trans	T1	2,454	---	---	147,584	2,114	2,098	2,098	2,114

	S0	2,111	---	---	151,624	2,097	2,109	2,098	2,111
trans	S0	2,166	2,165	176,346	154,860	2,082	2,131	2,083	2,129
	S1	2,079	2,079	178,074	155,903	2,120	2,100	2,120	2,100

B) Energies:

I) DFT-G03-Optimized geometries

		spin state	E (a.u.)	H (a.u)	G(a.u.)	S2	ΔE HS-LS (kcal)	stable spin	ΔE trans-cis (kcal)
II (d6, +2)	trans	t	-1238,05117	-1237,65345	-1237,73969	2,00	10,63	s	15,73
		u	-1238,06811	-1237,66861	-1237,74905	0,00			
		$u_{spin\ corr}$	-1238,06811						
	cis	t	-1238,05191	-1237,65333	-1237,73873	2,02	25,89	s	
		r	-1238,09317	-1237,69417	-1237,77389	0,00			
III (H_2O/H_2O) (d5, +3)	trans	d	-1237,60845	-1237,20922	-1237,28870	0,76	16,17	d	13,22
		q	-1237,58268	-1237,18507	-1237,27060	3,78			
	cis	d	-1237,62952	-1237,23040	-1237,30983	0,76	31,13	d	
		q	-1237,57991	-1237,18225	-1237,26647	3,77			
III (H_2O/OH) (d5, +2)	trans	d	-1237,46033	-1237,07339	-1237,15160	0,76	30,54	d	12,68
		q	-1237,41166	-1237,02677	-1237,11175	3,77			
	cis	d	-1237,48054	-1237,09349	-1237,17074	0,76	56,38	d	
		q	-1237,39068						
IV (H_2O/O) (d4, +2)	trans	t	-1236,83406	-1236,45877	-1236,53777	2,01	-13,93	t	9,42
		u	-1236,82198	-1236,44682	-1236,52508	0,94			
		$u_{spin\ corr}$	-1236,81187						
	cis	t	-1236,84907	-1236,47373	-1236,55154	2,01	-2,16	t	
		u	-1236,83078	-1236,45542	-1236,53190	0,96			
		$u_{spin\ corr}$	-1236,84562						
IV (OH/OH) (d4, +2)	trans	t	-1236,83370	-1236,45961	-1236,53541	2,01	-2,50	t	12,34
		u	-1236,82900	-1236,45438	-1236,52927	0,29			
		$u_{spin\ corr}$	-1236,82971						
	cis	t	-1236,84548	-1236,47131	-1236,54798	2,01	4,95	s	

		r	-1236,85337	-1236,47817	-1236,55249	0,00			
V (d4, +2)	trans	d	-1236,20207	-1235,83915	-1235,91496	0,76	26,06	d	14,65
		q	-1236,16053	-1235,79875	-1235,87613	3,77			
	cis	d	-1236,22542	-1235,86206	-1235,93699	0,76	14,13	d	
		q	-1236,20290	-1235,84032	-1235,91668	3,77			
VI (d3, +2)	trans	t	-1235,52377	-1235,17300	-1235,24875	2,03	33,6	s	8,22
		r	-1235,57731	-1235,22555	-1235,29924	0,00			
	cis	t	-1235,58334	-1235,23196	-1235,30720	2,01	4,4	s	
		u	-1235,58634	-1235,23506	-1235,30921	0,78			
		$u_{spin\ corr}$	-1235,59040						

II) DFT-G09-Optimized geometries

Optimized structure	spin	E-sol (Kcal)	E-gas (Kcal)	E-sol (a.u.)	E-gas (a.u.)	H –gas (a.u.)	G-gas (a.u.)
cis-S0	S0	0,00	-0,02	-1238,3	-1238,0932	-123,7694	-1237,7740
	S1	44,58	50,35	-1238,3	-1238,0130		
	T1	40,84	45,95	-1238,3	-1238,0200		
cis-S1	S1	40,18	45,04	-1238,3	-1238,0214		
	S0	5,16	5,31	-1238,3	-1238,0847		
mono-cis-S0	S0	25,53	34,94	-1161,9	-1161,6375	-1161,2666	-1161,3411
	S1	69,70	82,93	-1161,8	-1161,5610		
mono-cis-T1	T1	42,88	47,34	-1161,9	-1161,6178	-1161,2473	-1161,3253
mono-TS	T1	729133,18	49,63		-1161,6141	-1161,2449	-1161,3211

mono-trans-T1	T1	40,82	43,47	-1161,9	-1161,6239	-1161,2534	-1161,3319
mono-trans-S0	S0	43,38	52,80	-1161,9	-1161,6091	-1161,2368	-1161,3113
	S1	50,85	74,42	-1161,8	-1161,5746		
trans-S0	S0	12,70	15,40	-1238,3	-1238,0687	-1237,6692	-1237,7501
	S1	51,08	61,32	-1238,2	-1237,9955		
	T1	----	50,13	----	-1238,0133		
trans-S1	S1	46,75	53,92	-1238,3	-1238,0073		
	S0	19,13	20,33	-1238,3	-1238,0608		

III) CASPT2-single points

Geometry from DFT	Sym-metry	basis set	spin	E_{CASSCF} (a.u)	E_{CASPT2} (a.u)	Reference weight	ΔE_{CASSCF} spin state (kcal)	ΔE_{CASPT2} spin state (kcal)	stable spin
Cis/triplet	C1	mb	t	-5.659,5744	-5.661,0199	0,6312			
			s	-5.659,5791	-5.661,0250	0,6311	2,96	3,24	s
		dz	t	-5.661,5863	-5.665,5191	0,4520			
			s	-5.661,5937	-5.665,5174	0,4529	4,62	-1,12	t
		tz	t	-5.661,6149	-5.665,7435	0,4478			
			s	-5.661,6229	-5.665,7419	0,4486	5,03	-1,01	t
Trans/triplet	C1	mb	t	-5.659,5445	-5.660,9865	0,63199			
			s	-5.659,5727	-5.661,0202	0,63126	17,69	21,10	s
		dz	t	-5.661,5219	-5.665,4562	0,45144			
			s	-5.661,5591	-5.665,4964	0,45091	23,34	25,22	s
		tz	t	-5.661,5473	-5.665,6775	0,44713			
			s	-5.661,5855	-5.665,7194	0,44644	23,98	26,33	s
Cis/singlet	C2 (S2) C2 (S1)	mb	t	-5.659,5670	-5.661,0130	0,63107			
			s	-5.659,5788	-5.661,0263	0,63082	7,45	8,38	s
		dz	t	-5.661,5803	-5.665,5154	0,45185			
			s	-5661,5975	-5665,5229	0,45279	10,80	4,69	s
		tz	t	-5661,6090	-5665,7401	0,44762			
			s	-5661,6273	-5665,7482	0,44762	11,51	5,08	s

Trans/singlet	D2 (S3) D2 (S1)	mb	t	-5.659,5104	-5660,9517	0,63276			
			s	-5.659,5680	-5661,0170	0,63148	36,13	40,98	s
		dz	t	-5.661,5078	-5665,4330	0,45264			
			s	-5.661,5869	-5665,5144	0,45234	49,64	51,08	s
		tz	t	-5.661,5348	-5665,6562	0,44841			
			s	-5.661,6166	-5665,7406	0,44795	51,29	52,97	s

C) Coordinates:

I) G03-optimized geometries

cis-II-singlet-0

Ru	-0.00002400	-0.00003500	-0.77428800
N	2.01529900	0.48830000	-0.71949700
C	2.62886000	1.41370000	-1.48446700
C	3.99070700	1.66550100	-1.40925300
C	4.76122000	0.93095400	-0.51049800
C	4.14018300	-0.03064800	0.27651900
C	2.76634600	-0.24096800	0.15877100
N	0.66935000	-1.27528600	0.64575500
C	-0.10633600	-2.14285800	1.33073100
C	0.39752200	-2.99016400	2.30452600
C	1.75826700	-2.94817200	2.59784300
C	2.56286900	-2.05387400	1.90496200
C	2.00795500	-1.22037800	0.93442800
N	-0.66920800	1.27537700	0.64568800

C	0.10652500	2.14283800	1.33073700
C	-0.39737500	2.99050600	2.30420300
C	-1.75823400	2.94902400	2.59705700
C	-2.56288500	2.05479300	1.90413900
C	-2.00791400	1.22087900	0.93400000
N	-2.01517300	-0.48852700	-0.71917200
C	-2.62847100	-1.41462900	-1.48352500
C	-3.99031600	-1.66647500	-1.40820800
C	-4.76098400	-0.93130900	-0.51008900
C	-4.14012700	0.03087600	0.27637400
C	-2.76629700	0.24122000	0.15863200
H	1.98453700	1.95621500	-2.17341500
H	4.43417100	2.42452000	-2.04766900
H	5.83109800	1.10243400	-0.42523000
H	4.72575500	-0.61728200	0.97928800
H	-1.16146600	-2.13907900	1.06964800
H	-0.27368000	-3.66967400	2.82218100
H	2.18566200	-3.59917700	3.35585000
H	3.62646700	-2.00007600	2.12092700
H	1.16174400	2.13866000	1.06999400
H	0.27387200	3.66990000	2.82195100
H	-2.18567800	3.60034800	3.35476200
H	-3.62656400	2.00135200	2.11979800
H	-1.98384000	-1.95757500	-2.17184100

H	-4.43366300	-2.42603400	-2.04606400
H	-5.83085900	-1.10281400	-0.42481900
H	-4.72582400	0.61788000	0.97873100
H	1.17203900	-1.08413600	-3.04486200
O	0.47461600	-1.39614000	-2.44290600
H	0.74768000	-2.29278100	-2.18615900
H	-0.73901600	2.29501300	-2.18718400
O	-0.47601200	1.39518300	-2.44328400
H	-1.18121300	1.08755500	-3.03839900

trans-II-singlet-0

C	-2.84876700	0.74040500	0.19452100
C	-3.97522500	1.51619900	0.46952300
C	-3.82570800	2.82591500	0.90511500
C	-2.53893900	3.32396800	1.09188100
C	-1.45810100	2.50975000	0.79104200
N	-1.59051700	1.25375700	0.31341900
H	-4.69790700	3.43698000	1.12234700
H	-4.96911400	1.08904700	0.36956700
H	-2.36729000	4.32797600	1.46968700
H	-0.43729300	2.85298600	0.94381400
C	-2.90194900	-0.67409000	-0.16703900
C	-4.08227500	-1.33075900	-0.51485900
N	-1.69912100	-1.32526000	-0.14238700
C	-4.05657200	-2.67596200	-0.85498100

H	-5.02035200	-0.78328800	-0.53923400
C	-1.69248800	-2.62423000	-0.50450300
C	-2.83058100	-3.33376500	-0.85686300
H	-4.97154600	-3.19470500	-1.12879200
H	-0.72002700	-3.10686300	-0.52848500
H	-2.74662600	-4.38118600	-1.13270000
Ru	0.00006500	-0.05440400	0.00189500
N	1.58885400	1.25567800	-0.31108200
C	1.45409200	2.51271900	-0.78530900
C	2.84791500	0.74268500	-0.19877600
C	2.53327900	3.32777900	-1.08984300
H	0.43256900	2.85655600	-0.93185300
C	3.97285400	1.51913400	-0.47809600
C	3.82105400	2.82955500	-0.91074800
H	2.35953100	4.33262300	-1.46446400
H	4.96729500	1.09203100	-0.38351300
H	4.69206400	3.44113500	-1.13125900
N	1.70056100	-1.32301200	0.14522400
C	1.69563900	-2.62120100	0.51056100
C	2.90347800	-0.67171500	0.16269300
C	2.83551500	-3.33003600	0.85851500
H	0.72313700	-3.10343100	0.54090000
C	4.08561100	-1.32791700	0.50531900
C	4.06162200	-2.67247600	0.84815500

H	2.75291400	-4.37676700	1.13737200
H	5.02386600	-0.78051400	0.52370900
H	4.97804300	-3.19081200	1.11786400
O	-0.25759000	0.00894500	-2.14724700
O	0.25556300	0.01269400	2.15109600
H	0.46285900	0.44766100	-2.63023600
H	-0.36895000	-0.85653300	-2.57521800
H	-0.48052000	0.42298300	2.63545000
H	0.39953100	-0.84908700	2.57682700

cis-III-doublet

Ru	-0.00074100	-0.03480400	-0.76008200
N	2.03245200	0.47116700	-0.77284000
C	2.62504200	1.33953000	-1.61669400
C	3.98600700	1.60431200	-1.58401300
C	4.77469100	0.94032600	-0.64539000
C	4.17489900	0.03347200	0.22224100
C	2.80123900	-0.19277300	0.14448500
N	0.71751800	-1.19434100	0.73944000
C	-0.06022200	-2.02036100	1.47370900
C	0.46448800	-2.83196300	2.46662600
C	1.83383500	-2.78419200	2.72403400
C	2.63380200	-1.92481900	1.97851700
C	2.06494600	-1.12978700	0.98566400
N	-0.68647700	1.26084900	0.64596700

C	0.10738100	2.12666800	1.31481000
C	-0.40472500	3.04699200	2.21482100
C	-1.77917100	3.06874600	2.44790400
C	-2.59569500	2.16427900	1.77656300
C	-2.03891800	1.25847300	0.87680500
N	-2.03181100	-0.53815200	-0.68139100
C	-2.61870400	-1.52245200	-1.39269800
C	-3.98277600	-1.77142500	-1.32028900
C	-4.76925200	-0.97504800	-0.48961300
C	-4.16641300	0.03913600	0.24894000
C	-2.79160300	0.24414100	0.14375600
H	1.97963800	1.83643200	-2.33702200
H	4.41375600	2.31720800	-2.28392900
H	5.84555000	1.12323000	-0.59255400
H	4.77857800	-0.49657700	0.95415500
H	-1.12079700	-2.02159300	1.23803400
H	-0.19643300	-3.48846400	3.02624200
H	2.27439700	-3.40782900	3.49859700
H	3.70245900	-1.87535100	2.16962600
H	1.17122800	2.07010500	1.10033400
H	0.26873000	3.73192000	2.72300900
H	-2.21074900	3.77815700	3.15042600
H	-3.66746600	2.16344600	1.95644900
H	-1.96029300	-2.12508400	-2.01462000

H	-4.41327200	-2.57955500	-1.90586500
H	-5.84107600	-1.14355600	-0.41341000
H	-4.76780400	0.66282500	0.90506900
H	0.27298700	-1.32923400	-3.20231800
O	0.48316600	-1.52413300	-2.27062000
H	1.32614800	-2.01269900	-2.27844000
H	-0.26399200	1.91805500	-2.87163300
O	-0.69362400	1.13161500	-2.49286300
H	-1.65020500	1.27390100	-2.60995300

trans-III-doublet

C	-2.88884800	0.72258100	0.16422900
C	-4.03110100	1.48123400	0.41823300
C	-3.90825500	2.81228100	0.80017600
C	-2.63311700	3.35089400	0.95898800
C	-1.53234800	2.55424700	0.68341000
N	-1.64296100	1.27978300	0.25199600
H	-4.79442200	3.41053000	0.99966700
H	-5.01640700	1.02989800	0.34202900
H	-2.48516600	4.37222800	1.29953500
H	-0.52428000	2.92791000	0.83777100
C	-2.90741300	-0.69795600	-0.16707800
C	-4.07057700	-1.41807200	-0.43944500
N	-1.67856000	-1.30172400	-0.20978500

C	-3.99146200	-2.76204000	-0.78413900
H	-5.03851500	-0.92610800	-0.40187300
C	-1.61258100	-2.59463500	-0.59614900
C	-2.73483900	-3.35632800	-0.88181900
H	-4.89468600	-3.32954400	-0.99670400
H	-0.61857000	-3.01808700	-0.70333000
H	-2.61756400	-4.39421600	-1.18194300
Ru	-0.00008900	-0.01982600	0.00044500
N	1.64272400	1.28018400	-0.25149500
C	1.53165900	2.55482700	-0.68227300
C	2.88873300	0.72305400	-0.16502000
C	2.63212100	3.35165200	-0.95858000
H	0.52344700	2.92854500	-0.83551000
C	4.03068700	1.48182300	-0.41994000
C	3.90742700	2.81300400	-0.80128900
H	2.48379200	4.37314300	-1.29848600
H	5.01608800	1.03050700	-0.34483900
H	4.79339100	3.41133200	-1.00143700
N	1.67893700	-1.30129900	0.21031600
C	1.61337600	-2.59406800	0.59717300
C	2.90763800	-0.69750500	0.16622900
C	2.73593800	-3.35566700	0.88193300
H	0.61949500	-3.01754600	0.70555100
C	4.07115100	-1.41753200	0.43746000

C	3.99245000	-2.76139700	0.78261800
H	2.61898400	-4.39343100	1.18260300
H	5.03903200	-0.92555400	0.39868900
H	4.89592800	-3.32882500	0.99431400
O	-0.03849800	0.03204200	-2.07995500
O	0.03836900	0.03151700	2.08090700
H	0.75894100	-0.06285300	-2.63205700
H	-0.80755000	-0.24967000	-2.60755300
H	-0.75910300	-0.06414600	2.63277600
H	0.80732200	-0.25125800	2.60807400

cis-III-quadruplet

Ru	0.00108700	-0.00106600	0.36655100
N	-1.80454400	1.03447200	0.33691100
C	-1.96193500	2.26884600	0.86443300
C	-3.19489700	2.89739000	0.92216400
C	-4.30843400	2.23096800	0.41075700
C	-4.15257500	0.95577100	-0.12739600
C	-2.89307500	0.36322800	-0.15351100
N	-1.33330400	-1.41322800	-0.51964900
C	-0.97644500	-2.61888700	-1.00807600
C	-1.87291200	-3.44711500	-1.66760900
C	-3.18630200	-3.01355300	-1.83238800

C	-3.55644100	-1.76335000	-1.34146100
C	-2.61655900	-0.97042300	-0.68857500
N	1.34186500	1.41671500	-0.51083000
C	0.98924400	2.62447700	-0.99646900
C	1.88809600	3.45011400	-1.65645800
C	3.19939700	3.01146200	-1.82390500
C	3.56586200	1.75950200	-1.33420600
C	2.62347400	0.96981000	-0.68097900
N	1.80466100	-1.03693800	0.33828100
C	1.96138300	-2.27141100	0.86615000
C	3.19379400	-2.89915300	0.93227900
C	4.30996600	-2.23082900	0.42851100
C	4.15590700	-0.95612700	-0.11112400
C	2.89602900	-0.36474800	-0.14563300
H	-1.06489200	2.73660600	1.26440900
H	-3.27697700	3.88759900	1.36225800
H	-5.29134200	2.69662200	0.43464700
H	-5.01687500	0.42529500	-0.51765700
H	0.06312600	-2.90870700	-0.87246600
H	-1.53894200	-4.40857000	-2.04850900
H	-3.91532200	-3.63604400	-2.34651500
H	-4.57368400	-1.40793000	-1.48211600
H	-0.04861100	2.91879300	-0.85708500
H	1.55768000	4.41368000	-2.03513200

H	3.93001400	3.63165900	-2.33854800
H	4.58171600	1.40073100	-1.47642600
H	1.06164800	-2.74401200	1.25454600
H	3.27415800	-3.88964600	1.37198900
H	5.29337200	-2.69506200	0.45936600
H	5.02226200	-0.42445500	-0.49512800
H	-1.26546600	-0.56492000	3.07409000
O	-0.77395100	-1.09431700	2.42233200
H	-1.19729100	-1.96920800	2.44789900
H	1.30589300	1.89136100	2.40362800
O	**0.72348600**	**1.11273800**	**2.38771200**
H	**1.01322500**	**0.56276200**	**3.13612900**

trans-III-quadruplet

C	-2.87254300	-0.69979300	-0.21492000
C	-4.02286300	-1.43378000	-0.49182900
C	-3.91613500	-2.75280800	-0.92680200
C	-2.65128900	-3.31385000	-1.09703000
C	-1.53874600	-2.54242600	-0.80059000
N	-1.63655300	-1.27475100	-0.34585300
H	-4.81225800	-3.32952700	-1.14565100
H	-5.00439700	-0.98082300	-0.38266700
H	-2.52389100	-4.33103600	-1.45762900
H	-0.53052800	-2.92578100	-0.94339800

C	-2.87258800	0.69983100	0.21480000
C	-4.02295700	1.43374300	0.49169700
N	-1.63663200	1.27486700	0.34575200
C	-3.91632400	2.75278500	0.92664800
H	-5.00446000	0.98071300	0.38255300
C	-1.53892300	2.54254600	0.80050400
C	-2.65151800	3.31390800	1.09689500
H	-4.81248900	3.32944600	1.14548200
H	-0.53073500	2.92594700	0.94338600
H	-2.52419300	4.33110600	1.45748700
Ru	-0.00043000	0.00009700	-0.00000400
N	1.63584500	-1.27465800	0.34648000
C	1.53809000	-2.54200600	0.80208100
C	2.87179100	-0.69967300	0.21535500
C	2.65065200	-3.31314500	1.09922800
H	0.52990400	-2.92537700	0.94505300
C	4.02213800	-1.43337900	0.49293100
C	3.91546800	-2.75211700	0.92879600
H	2.52327700	-4.33007300	1.46056100
H	5.00365200	-0.98040700	0.38364500
H	4.81161000	-3.32859400	1.14820300
N	1.63593400	1.27477400	-0.34637200
C	1.53828900	2.54212900	-0.80197600
C	2.87183900	0.69969700	-0.21524100

C	2.65091000	3.31319700	-1.09907900
H	0.53013800	2.92556400	-0.94500900
C	4.02224500	1.43331500	-0.49281100
C	3.91568200	2.75207100	-0.92864600
H	2.52361500	4.33014100	-1.46039400
H	5.00372100	0.98025500	-0.38355600
H	4.81187000	3.32848100	-1.14804300
O	0.00324700	0.00455000	2.44717800
O	0.00401700	-0.00526800	-2.44717300
H	0.66084800	-0.39934800	3.03763800
H	-0.65317400	0.40882900	3.03869700
H	-0.65256200	-0.40970000	-3.03840800
H	0.66140100	0.39857100	-3.03792000

cis-IV-singlet- cis(OH)2

Ru	0.00044200	-0.88207900	-0.00101400
N	2.04243800	-0.87860700	-0.46123300
C	2.61299200	-1.77083300	-1.29004400
C	3.98087900	-1.77990500	-1.52873300
C	4.78357400	-0.83931000	-0.88991100
C	4.19457300	0.08181100	-0.03101900
C	2.81660900	0.04582700	0.17596300
N	0.74681700	0.73889700	1.14507200

C	-0.01019600	1.50747700	1.94675500
C	0.52827600	2.53102400	2.71031700
C	1.89923400	2.76946600	2.63411100
C	2.68241200	1.97555000	1.80656800
C	2.08910900	0.95317100	1.06448600
N	-0.74799200	0.73890400	-1.14559000
C	0.00785400	1.50821200	-1.94769300
C	-0.53197600	2.53155500	-2.71057200
C	-1.90304500	2.76897800	-2.63319700
C	-2.68499100	1.97433600	-1.80517900
C	-2.09036500	0.95222500	-1.06379800
N	-2.04112900	-0.88019600	0.46113700
C	-2.61037000	-1.77298200	1.29025000
C	-3.97796900	-1.78263600	1.53056400
C	-4.78179700	-0.84210600	0.89307500
C	-4.19416500	0.07956900	0.03384400
C	-2.81644200	0.04417600	-0.17479400
H	1.93279600	-2.47370000	-1.76400600
H	4.40122300	-2.51935900	-2.20443000
H	5.85808400	-0.82317200	-1.05430300
H	4.80753400	0.81992900	0.47884700
H	-1.07121000	1.26877100	1.97427900
H	-0.11654300	3.12142200	3.35488600
H	2.35544900	3.56517500	3.21792600

H	3.75318800	2.14745900	1.74160300
H	1.06901100	1.27024700	-1.97609300
H	0.11187800	3.12256900	-3.35554200
H	-2.36031500	3.56447000	-3.21648100
H	-3.75584800	2.14542600	-1.73935300
H	-1.92936700	-2.47579500	1.76310800
H	-4.39723100	-2.52251900	2.20646600
H	-5.85611500	-0.82645300	1.05876100
H	-4.80799200	0.81767900	-0.47499300
H	1.15943300	-1.97270800	1.87132700
O	0.24845100	-1.94388000	1.51701600
O	-0.24625900	-1.94271300	-1.52005000
H	-1.15707100	-1.97184100	-1.87477500

trans-IV-singlet- cis(OH)2

C	0.38863100	0.61632800	2.88577800
C	0.90803100	1.20512500	4.03842600
C	1.69423100	2.34411500	3.93800700
C	1.97551400	2.85497200	2.67442600
C	1.42807300	2.22711500	1.56689500
N	0.61590300	1.16143400	1.66055200
H	2.10692900	2.80744100	4.83056300
H	0.72202200	0.75652700	5.00987600
H	2.62100300	3.71792600	2.53942600

H	1.67022800	2.56377600	0.56333700
C	-0.38863100	-0.61632800	2.88577800
C	-0.90803100	-1.20512500	4.03842600
N	-0.61590300	-1.16143400	1.66055200
C	-1.69423100	-2.34411500	3.93800700
H	-0.72202200	-0.75652700	5.00987600
C	-1.42807300	-2.22711500	1.56689500
C	-1.97551400	-2.85497200	2.67442600
H	-2.10692900	-2.80744100	4.83056300
H	-1.67022800	-2.56377600	0.56333700
H	-2.62100300	-3.71792600	2.53942600
Ru	0.00000000	0.00000000	0.00183400
N	0.17269500	1.29944400	-1.66030900
C	0.15613300	2.64290300	-1.56736000
C	0.05086500	0.72762300	-2.89298600
C	0.10330600	3.47258800	-2.67633900
H	0.15435100	3.05478400	-0.56251300
C	0.00000000	1.51199500	-4.04557700
C	0.04357400	2.89576100	-3.94213500
H	0.09758900	4.55030200	-2.54090300
H	-0.09916200	1.04284000	-5.02027400
H	0.00217000	3.51470300	-4.83489900
N	-0.17269500	-1.29944400	-1.66030900
C	-0.15613300	-2.64290300	-1.56736000

C	-0.05086500	-0.72762300	-2.89298600
C	-0.10330600	-3.47258800	-2.67633900
H	-0.15435100	-3.05478400	-0.56251300
C	0.00000000	-1.51199500	-4.04557700
C	-0.04357400	-2.89576100	-3.94213500
H	-0.09758900	-4.55030200	-2.54090300
H	0.09916200	-1.04284000	-5.02027400
H	-0.00217000	-3.51470300	-4.83489900
O	-1.79808800	0.57584300	0.10518100
O	1.79808800	-0.57584300	0.10518100
H	-2.23865600	0.77547500	-0.74290600
H	2.23865600	-0.77547500	-0.74290600

cis-IV-triplet- cis(OH)2

Ru	-0.00664200	0.01634900	-0.83846300
N	-1.99514700	-0.56312000	-0.72962700
C	-2.52371000	-1.54583500	-1.48098900
C	-3.87700400	-1.84802300	-1.43168800
C	-4.69761200	-1.10665900	-0.58582200
C	-4.14555100	-0.08899800	0.18706500
C	-2.78097900	0.17690200	0.10449700
N	-0.74724200	1.31936700	0.66630900
C	-0.03941500	2.25231900	1.32243800
C	-0.62557900	3.14020200	2.21303100

C	-1.99770700	3.05495800	2.42952300
C	-2.73486700	2.08885700	1.75292000
C	-2.09192600	1.22528400	0.86857000
N	0.74185600	-1.29228300	0.67373200
C	-0.00249400	-2.19230900	1.33970800
C	0.54203300	-3.05814900	2.27581400
C	1.90931800	-2.99225600	2.52960900
C	2.68230300	-2.06538800	1.84106300
C	2.08077900	-1.21854000	0.91113200
N	2.03314500	0.50751800	-0.73946300
C	2.59858600	1.46897300	-1.49468700
C	3.95447700	1.75447000	-1.42700900
C	4.75314400	1.02383500	-0.55184600
C	4.16877100	0.03648100	0.23273700
C	2.80087700	-0.21180000	0.12789700
H	-1.81932600	-2.07061700	-2.12379100
H	-4.27350300	-2.64638500	-2.05235300
H	-5.76317300	-1.31526400	-0.52711000
H	-4.78105100	0.49514700	0.84645800
H	1.02690500	2.27988000	1.10797200
H	-0.01582300	3.88355300	2.71838000
H	-2.49334400	3.73599700	3.11693400
H	-3.80719300	2.01774700	1.91121700
H	-1.06273800	-2.21100400	1.09829200

H	-0.09741700	-3.77121800	2.78809300
H	2.37152400	-3.65831700	3.25391600
H	3.75120400	-2.00699500	2.02544100
H	1.92013400	2.00944500	-2.15052300
H	4.36851100	2.53754200	-2.05589400
H	5.81977800	1.22041900	-0.47784100
H	4.77809000	-0.53856100	0.92422200
H	-0.43784200	1.05282400	-2.99830200
O	-0.37235700	1.39088200	-2.08418400
O	0.30901500	-1.31599500	-2.19135900
H	1.24528500	-1.49898200	-2.38883000

trans-IV-triplet- cis(OH)2

C	0.40649200	0.60716300	2.88155400
C	0.94780300	1.17951000	4.03049500
C	1.76518200	2.29816800	3.92408900
C	2.05336700	2.80493900	2.66093700
C	1.48300300	2.19426300	1.55448900
N	0.64426600	1.15132100	1.65727500
H	2.19564800	2.74854900	4.81499500
H	0.75565500	0.73635100	5.00340000
H	2.72202800	3.64987000	2.52512600
H	1.72596000	2.51878300	0.54690300

C	-0.40649200	-0.60716300	2.88155400
C	-0.94780300	-1.17951000	4.03049500
N	-0.64426600	-1.15132100	1.65727500
C	-1.76518200	-2.29816800	3.92408900
H	-0.75565500	-0.73635100	5.00340000
C	-1.48300300	-2.19426300	1.55448900
C	-2.05336700	-2.80493900	2.66093700
H	-2.19564800	-2.74854900	4.81499500
H	-1.72596000	-2.51878300	0.54690300
H	-2.72202800	-3.64987000	2.52512600
Ru	0.00000000	0.00000000	0.01274800
N	0.13337400	1.31584900	-1.64485800
C	0.12229800	2.65715000	-1.55505500
C	0.03945300	0.73114800	-2.87156100
C	0.08062700	3.48187400	-2.66956000
H	0.12389800	3.07064400	-0.54976300
C	0.00000000	1.50923500	-4.02789200
C	0.03363000	2.89507900	-3.93039100
H	0.07701300	4.56056300	-2.54230400
H	-0.07630500	1.03720000	-5.00311700
H	0.00154500	3.50778400	-4.82791800
N	-0.13337400	-1.31584900	-1.64485800
C	-0.12229800	-2.65715000	-1.55505500
C	-0.03945300	-0.73114800	-2.87156100

C	-0.08062700	-3.48187400	-2.66956000
H	-0.12389800	-3.07064400	-0.54976300
C	0.00000000	-1.50923500	-4.02789200
C	-0.03363000	-2.89507900	-3.93039100
H	-0.07701300	-4.56056300	-2.54230400
H	0.07630500	-1.03720000	-5.00311700
H	-0.00154500	-3.50778400	-4.82791800
O	-1.86121600	0.46190500	0.03447300
O	1.86121600	-0.46190500	0.03447300
H	-2.18433600	1.13024000	-0.59311000
H	2.18433600	-1.13024000	-0.59311000

cis-IV-singlet- cis(O)(H2O)

Ru	-0.05986100	0.08473300	-0.90953500
N	-2.02470400	-0.46646700	-0.75469000
C	-2.61466000	-1.46516900	-1.44284500
C	-3.95982400	-1.75404800	-1.29811100
C	-4.72043400	-0.97861200	-0.42056200
C	-4.11163700	0.04884000	0.29124800
C	-2.75130800	0.29572200	0.12071700
N	-0.65895700	1.36587100	0.52984900
C	0.11886900	2.29235400	1.11561700
C	-0.38271400	3.19967900	2.03828700

C	-1.73555700	3.15975300	2.36145400
C	-2.54479900	2.21080700	1.74902900
C	-1.99341800	1.32222000	0.82863800
N	0.60011000	-1.30784500	0.65768600
C	-0.21369300	-2.17505300	1.29387900
C	0.23987700	-3.06423600	2.25549800
C	1.59154400	-3.06202100	2.59096200
C	2.43619400	-2.16597000	1.95048100
C	1.91849800	-1.29809100	0.98856700
N	2.02723100	0.42554900	-0.65191000
C	2.67764400	1.35788400	-1.38292000
C	4.03652800	1.58807600	-1.24166100
C	4.75692400	0.83031600	-0.32074800
C	4.09030100	-0.12869400	0.42921800
C	2.71879000	-0.31996700	0.25286500
H	-1.96889500	-2.01506900	-2.12512900
H	-4.40127000	-2.56286400	-1.87295200
H	-5.78242800	-1.17327400	-0.29214200
H	-4.69589500	0.65641900	0.97662500
H	1.16485600	2.29717900	0.82444200
H	0.28553300	3.93109000	2.48369600
H	-2.15866200	3.86304300	3.07369900
H	-3.60569500	2.17176300	1.98049700
H	-1.26340300	-2.14784700	1.01123700

H	-0.46103800	-3.74364300	2.73233000
H	1.98083100	-3.74566200	3.34088500
H	3.49377800	-2.14315700	2.19770800
H	2.06135800	1.91809800	-2.08362400
H	4.51452000	2.35154200	-1.84902200
H	5.82504200	0.98397800	-0.18806400
H	4.63490200	-0.72874600	1.15253100
O	-0.07045500	1.28121800	-2.16774800
O	0.56807900	-1.35418000	-2.47495900
H	1.44999700	-1.73976100	-2.34772300
H	0.63086500	-0.80014900	-3.27802700

trans-IV-singlet- cis(O)(H2O)

C	0.00000000	2.95092000	0.19403700
C	0.39804400	4.25258200	0.49304500
C	1.68052900	4.48481400	0.97535100
C	2.52895000	3.40060500	1.17560500
C	2.07674100	2.12913100	0.85114400
N	0.86046600	1.90293800	0.32777100
H	1.99949500	5.49427800	1.22164800
H	-0.29913700	5.07861300	0.38307300
H	3.52238700	3.52727700	1.59624500
H	2.68842800	1.25011800	1.03909800

C	-1.34693700	2.58788600	-0.23556400
C	-2.33194100	3.50644200	-0.59665500
N	-1.60611000	1.24735200	-0.28538300
C	-3.57285200	3.05796800	-1.02971300
H	-2.12277300	4.57155400	-0.55325300
C	-2.79895300	0.81668200	-0.73988600
C	-3.80699300	1.68675500	-1.11789800
H	-4.34417400	3.77086200	-1.31068600
H	-2.92446700	-0.26081900	-0.80529300
H	-4.75568600	1.29286600	-1.47065600
Ru	0.00000000	0.00000000	0.16682700
N	1.60611000	-1.24735200	-0.28538300
C	2.79895300	-0.81668200	-0.73988600
C	1.34693700	-2.58788600	-0.23556400
C	3.80699300	-1.68675500	-1.11789800
H	2.92446700	0.26081900	-0.80529300
C	2.33194100	-3.50644200	-0.59665500
C	3.57285200	-3.05796800	-1.02971300
H	4.75568600	-1.29286600	-1.47065600
H	2.12277300	-4.57155400	-0.55325300
H	4.34417400	-3.77086200	-1.31068600
N	-0.86046600	-1.90293800	0.32777100
C	-2.07674100	-2.12913100	0.85114400
C	0.00000000	-2.95092000	0.19403700

C	-2.52895000	-3.40060500	1.17560500
H	-2.68842800	-1.25011800	1.03909800
C	-0.39804400	-4.25258200	0.49304500
C	-1.68052900	-4.48481400	0.97535100
H	-3.52238700	-3.52727700	1.59624500
H	0.29913700	-5.07861300	0.38307300
H	-1.99949500	-5.49427800	1.22164800
O	0.00000000	0.00000000	-2.17612100
O	0.00000000	0.00000000	1.89432300
H	-0.07327900	-0.77265500	-2.75669100
H	0.07327900	0.77265500	-2.75669100

cis-IV-triplet- cis(O)(H2O)

Ru	-0.05722700	-0.00128500	-0.84348900
N	-2.06055200	-0.54034400	-0.67837700
C	-2.65272400	-1.54184000	-1.35038900
C	-4.01142100	-1.80092800	-1.23692100
C	-4.77918100	-0.99382800	-0.40207400
C	-4.16612700	0.04136500	0.29555900
C	-2.79830800	0.25730700	0.14359300
N	-0.70955400	1.36292600	0.53348300
C	0.06113900	2.30848800	1.10083500
C	-0.45061600	3.24631700	1.98395900

C	-1.80786000	3.20796200	2.28973100
C	-2.60624300	2.23400500	1.70257500
C	-2.04478800	1.31445200	0.81946100
N	0.73142500	-1.30914100	0.73384300
C	0.02075100	-2.19918700	1.44853000
C	0.58590900	-2.99112700	2.43745600
C	1.94636900	-2.85479800	2.69948800
C	2.68935600	-1.93758700	1.96538300
C	2.06328500	-1.17085100	0.98255200
N	1.99575700	0.47304300	-0.76477100
C	2.55674800	1.38814600	-1.57882300
C	3.90800200	1.69677100	-1.52092600
C	4.70662400	1.03852300	-0.58979700
C	4.12866100	0.09246200	0.24868500
C	2.76475300	-0.18405900	0.14887600
H	-2.00134200	-2.13396500	-1.98874800
H	-4.45326400	-2.61723600	-1.80105600
H	-5.84734500	-1.16550200	-0.29508700
H	-4.75532600	0.67951500	0.94804900
H	1.11032100	2.30176100	0.81896100
H	0.20864700	3.99435900	2.41460900
H	-2.24281900	3.93135800	2.97471600
H	-3.66840700	2.19456600	1.92672800
H	-1.03820600	-2.26769000	1.20506400

H	-0.03014000	-3.69744700	2.98662800
H	2.42664000	-3.45702000	3.46678600
H	3.75197600	-1.82452400	2.16056300
H	1.87490500	1.86740100	-2.27907300
H	4.31849000	2.44111700	-2.19743400
H	5.76907600	1.25691700	-0.51597100
H	4.74147100	-0.42984700	0.97783200
O	-0.32582700	1.03124200	-2.23549600
O	0.37566400	-1.60174200	-2.32585100
H	1.22652200	-2.07028100	-2.28126800
H	0.34260400	-1.19787700	-3.21276300

trans-IV-triplet- cis(O)(H2O)

C	2.89811600	0.65944100	-0.13680800
C	4.08215700	1.36030600	-0.36149400
C	4.03018000	2.66821400	-0.82759100
C	2.78962100	3.23731600	-1.09510500
C	1.64757800	2.49151100	-0.84106800
N	1.68959000	1.25131800	-0.32887400
H	4.94781500	3.22089800	-1.01270600
H	5.04300600	0.87765100	-0.20793700
H	2.69940200	4.23661900	-1.51096700
H	0.66073500	2.87435200	-1.08721600
C	2.85172000	-0.75446900	0.23736800

C	3.97309200	-1.48613300	0.62720400
N	1.62144900	-1.34247400	0.17372100
C	3.84525500	-2.82815000	0.96100400
H	4.94513700	-1.00444900	0.68147700
C	1.50384700	-2.63497400	0.53101600
C	2.58296000	-3.41299600	0.92077100
H	4.71679100	-3.40441100	1.26148300
H	0.49903100	-3.04725900	0.51342600
H	2.42818900	-4.45430700	1.18835700
Ru	-0.00225000	-0.01610100	-0.16769000
N	-1.59683800	1.32481900	0.20453300
C	-1.44244700	2.60657000	0.58702200
C	-2.84375300	0.77224900	0.24199800
C	-2.50458600	3.41184300	0.96807400
H	-0.42321400	2.98272800	0.59965800
C	-3.94959500	1.53434400	0.61772200
C	-3.78578700	2.86791500	0.97036900
H	-2.32237400	4.44238900	1.25899500
H	-4.93698800	1.08268100	0.64896800
H	-4.64478500	3.46805900	1.26007400
N	-1.72276000	-1.27169200	-0.27771900
C	-1.70961500	-2.52389600	-0.76132000
C	-2.91939400	-0.64215600	-0.12634500
C	-2.86689000	-3.24118600	-1.02864400

H	-0.73125400	-2.94335200	-0.97808700
C	-4.11830200	-1.31061300	-0.36970700
C	-4.09580900	-2.62866900	-0.80874300
H	-2.79616100	-4.25208700	-1.41946200
H	-5.06695200	-0.79499500	-0.25128000
H	-5.02505800	-3.15625400	-1.00860100
O	0.08875200	0.04622700	2.13478200
O	-0.03374900	-0.02689500	-1.90533900
H	-0.59287600	0.45182100	2.69275000
H	0.50834700	-0.63892200	2.67792700

cis-V-doublet

Ru	-0.02735800	-0.91405700	-0.17511600
N	-2.04285800	-0.92223300	0.36301400
C	-2.60042200	-1.88776300	1.11258300
C	-3.96640400	-1.91807300	1.35876000
C	-4.76930500	-0.92343800	0.80917300
C	-4.18610700	0.07568000	0.03552300
C	-2.81109500	0.06312900	-0.18371200
N	-0.74570000	0.88426000	-1.08077100
C	0.00019400	1.74452800	-1.79009700
C	-0.55409700	2.83896800	-2.43692200

C	-1.92824000	3.04238600	-2.34054500
C	-2.69946700	2.15034400	-1.60520500
C	-2.09079700	1.06341500	-0.97803800
N	0.74258100	0.57091900	1.26037400
C	-0.00999000	1.20404200	2.17358200
C	0.53090900	2.09160900	3.09229200
C	1.90233100	2.33050500	3.05696300
C	2.68303300	1.67393300	2.11338700
C	2.08210100	0.78835900	1.21794700
N	2.05176300	-0.78681400	-0.58653500
C	2.63170800	-1.52288900	-1.55266200
C	3.99832800	-1.47992500	-1.78894500
C	4.78994300	-0.65146400	-0.99931500
C	4.18997100	0.10996300	-0.00263300
C	2.81193700	0.03074700	0.19445900
H	-1.91371700	-2.63189100	1.50843200
H	-4.38438500	-2.71613100	1.96549300
H	-5.84344400	-0.92310800	0.97765700
H	-4.80485000	0.85545000	-0.39928500
H	1.06466100	1.52643900	-1.84221600
H	0.08148800	3.50786400	-3.00996400
H	-2.39828000	3.88737400	-2.83766500
H	-3.77287700	2.29769500	-1.52743600
H	-1.07354000	0.97268300	2.16441400

H	-0.11204600	2.57655600	3.82125000
H	2.36243600	3.01923500	3.76126300
H	3.75471800	1.84836600	2.08086700
H	1.96060800	-2.14810900	-2.13716900
H	4.42492100	-2.09165600	-2.57877500
H	5.86455600	-0.59731900	-1.15513600
H	4.79598700	0.76095200	0.62095600
O	-0.27160200	-1.68059500	-1.66785100
O	0.26330800	-2.16947300	1.19578200
H	1.19616600	-2.29258300	1.45682700

trans-V-doublet

C	2.89931200	0.67718800	-0.16325200
C	4.06465500	1.40381100	-0.40524500
C	3.97908700	2.72578800	-0.82201600
C	2.72297500	3.28924200	-1.02488100
C	1.60012700	2.51960600	-0.76119900
N	1.68118000	1.26256200	-0.29802900
H	4.88269400	3.29770400	-1.01763000
H	5.03605400	0.93004200	-0.29810100
H	2.60601300	4.30280000	-1.39713900
H	0.60089200	2.89978900	-0.95568100
C	2.88079700	-0.73971200	0.18810200

C	4.01887000	-1.45912100	0.54787500
N	1.65971300	-1.34236900	0.15867400
C	3.90932900	-2.79693300	0.90348300
H	4.98718600	-0.96798500	0.57327900
C	1.55342200	-2.61955000	0.55680700
C	2.64929500	-3.38576200	0.92160200
H	4.79268200	-3.36320400	1.18781400
H	0.54961800	-3.02764900	0.61312700
H	2.50579200	-4.41815700	1.22661000
Ru	0.00529000	-0.02843000	-0.08682000
N	-1.61243000	1.30644400	0.25788000
C	-1.45886200	2.57197500	0.68434200
C	-2.85936900	0.76339400	0.20695100
C	-2.53465800	3.38472100	1.00629600
H	-0.43635200	2.92247100	0.79339200
C	-3.97866200	1.53608600	0.51662900
C	-3.82014200	2.86080100	0.90256200
H	-2.35887200	4.40298000	1.34089000
H	-4.97154900	1.09758800	0.47829100
H	-4.68877200	3.46792000	1.14526100
N	-1.72301900	-1.29627900	-0.22148200
C	-1.69437800	-2.56811100	-0.64854600
C	-2.92040700	-0.65314600	-0.14849500
C	-2.84268900	-3.28921800	-0.94157800

H	-0.71262000	-3.00853200	-0.79319900
C	-4.10950800	-1.32504400	-0.42758900
C	-4.07566500	-2.65912800	-0.81300600
H	-2.75991800	-4.31796100	-1.27983800
H	-5.05906500	-0.80086900	-0.37126100
H	-4.99808400	-3.18889600	-1.03736400
O	0.14441900	-0.02869100	1.82996000
O	-0.08500600	0.02676300	-1.79904000
H	-0.62304300	0.10448500	2.41190400

cis-V-quadruplet

Ru	-0.03394500	-0.02676500	-0.91624000
N	-2.07532900	-0.49473600	-0.72880300
C	-2.69471700	-1.38072800	-1.52979900
C	-4.05937200	-1.61369000	-1.43954700
C	-4.80041900	-0.90292200	-0.50026600
C	-4.15890500	0.02724600	0.31063700
C	-2.78712400	0.23009500	0.17807700
N	-0.70077400	1.31621100	0.61411300
C	0.07146300	2.22753000	1.22814700
C	-0.42317500	3.08302100	2.20169800
C	-1.76655100	2.98917300	2.55191200
C	-2.56878000	2.05085600	1.91366700
C	-2.01962000	1.22117300	0.93760500

N	0.75750900	-1.34744800	0.66458100
C	0.05863800	-2.24881600	1.37482100
C	0.63517200	-3.02864400	2.36800700
C	1.99055100	-2.86267400	2.63771400
C	2.71957500	-1.92924800	1.90850000
C	2.08357200	-1.17886900	0.92025400
N	1.98843700	0.49566100	-0.80368900
C	2.52726900	1.41191600	-1.63169600
C	3.88048100	1.71320100	-1.60117600
C	4.69400500	1.04391600	-0.69131000
C	4.13354400	0.09296600	0.15666800
C	2.76912600	-0.17884300	0.08843600
H	-2.06182400	-1.88182000	-2.25846500
H	-4.52493500	-2.33389900	-2.10622100
H	-5.87230400	-1.05918500	-0.40699600
H	-4.73088100	0.60402800	1.03172700
H	1.11108300	2.26916600	0.91191700
H	0.23647400	3.80993200	2.66670500
H	-2.18934800	3.64415300	3.30961800
H	-3.62127000	1.97259500	2.17056700
H	-0.99688600	-2.34084400	1.12273900
H	0.03162800	-3.74916100	2.91262700
H	2.47889100	-3.45472100	3.40787600
H	3.77779300	-1.79254000	2.11225500

H	1.83392900	1.88796800	-2.32217300
H	4.28102100	2.45446600	-2.28672700
H	5.75993100	1.25344300	-0.64357000
H	4.76430000	-0.44188200	0.86083400
O	-0.38477600	1.17583000	-2.15750600
O	0.27718500	-1.40220400	-2.20270100
H	0.57941700	-2.24083100	-1.80397800

trans-V-quadruplet

C	-2.92441200	-0.64703700	-0.26252600
C	-4.09141100	-1.32940700	-0.59837300
C	-4.01892300	-2.66106800	-0.98905200
C	-2.77514200	-3.28367800	-1.05585600
C	-1.64570500	-2.55303700	-0.72072100
N	-1.72222400	-1.27922800	-0.30042400
H	-4.92300800	-3.20099700	-1.25935200
H	-5.04951700	-0.81787400	-0.57249900
H	-2.67117000	-4.31562500	-1.37819000
H	-0.64757200	-2.97556000	-0.80151800
C	-2.86311300	0.74892900	0.15030100
C	-3.97597200	1.52084500	0.47494500
N	-1.60401900	1.25599300	0.27110400

C	-3.80101200	2.80407000	0.97747000
H	-4.97486200	1.10810500	0.36435500
C	-1.43784800	2.46979400	0.82625300
C	-2.50780200	3.27689200	1.18105200
H	-4.66288200	3.41255900	1.23957100
H	-0.41350300	2.78139000	1.01001900
H	-2.32099900	4.25249300	1.62025200
Ru	-0.00703100	-0.08534400	0.01747300
N	1.73763100	-1.25648500	0.33521700
C	1.73100400	-2.53692000	0.73757400
C	2.91415200	-0.58817300	0.20869000
C	2.90020600	-3.23200000	1.01073400
H	0.75260400	-2.99901500	0.85522700
C	4.12006600	-1.23474300	0.47824100
C	4.11533000	-2.56669800	0.87511300
H	2.85013100	-4.26886700	1.33038300
H	5.06095500	-0.69945700	0.38913600
H	5.05213500	-3.07629700	1.08648500
N	1.54327400	1.31128500	-0.31973000
C	1.35736400	2.52988300	-0.85633400
C	2.80752300	0.80567200	-0.22848100
C	2.41275200	3.34133200	-1.24463700
H	0.32693200	2.84391000	-0.99727700
C	3.90425300	1.58602600	-0.58768100

C	3.71110000	2.86855200	-1.08720000
H	2.20907100	4.31870600	-1.67218000
H	4.90942100	1.18323400	-0.50316600
H	4.56393600	3.47756300	-1.37632100
O	-0.15709900	-0.14760500	1.98601300
O	0.20966500	-0.45440900	-1.76458100
H	0.55004900	-0.58937000	2.48455800

cis-VI-singlet

Ru	0.00005500	-0.96142800	-0.00007100
N	-2.05008400	-0.91099300	0.51549700
C	-2.59851500	-1.78698500	1.37334300
C	-3.96485200	-1.81490300	1.60981600
C	-4.77629300	-0.90911000	0.93266800
C	-4.20041000	-0.00073100	0.05058600
C	-2.82181400	-0.01119000	-0.15547900
N	-0.77143400	0.77678100	-1.14138500
C	-0.05455100	1.58050100	-1.93623800
C	-0.64342700	2.57961000	-2.69923600
C	-2.02421200	2.73818700	-2.63026500
C	-2.76604400	1.90173400	-1.80426000
C	-2.12064900	0.91330500	-1.06007000
N	0.77127400	0.77704700	1.14087800

C	0.05430200	1.58067300	1.93574500
C	0.64318100	2.57924400	2.69944300
C	2.02406500	2.73729200	2.63125200
C	2.76598800	1.90097300	1.80519000
C	2.12057600	0.91317500	1.06018100
N	2.05022900	-0.91122900	-0.51532600
C	2.59879100	-1.78710000	-1.37319900
C	3.96509200	-1.81455600	-1.60999000
C	4.77634900	-0.90834000	-0.93320400
C	4.20033700	-0.00010500	-0.05104700
C	2.82181100	-0.01110000	0.15543100
H	-1.90663800	-2.46395400	1.86991700
H	-4.37541100	-2.53771400	2.30891000
H	-5.85223900	-0.90660500	1.08924100
H	-4.82829000	0.70998200	-0.47869300
H	1.01833800	1.39948300	-1.96224500
H	-0.02905300	3.20694000	-3.33865000
H	-2.52324000	3.50465400	-3.21810100
H	-3.84460400	2.01684100	-1.74777100
H	-1.01866600	1.40005000	1.96112600
H	0.02873300	3.20653200	3.33882700
H	2.52310800	3.50324000	3.21975400
H	3.84463200	2.01562100	1.74940000
H	1.90706300	-2.46438300	-1.86955200

H	4.37573000	-2.53729800	-2.30910900
H	5.85224600	-0.90536800	-1.09011400
H	4.82807400	0.71099900	0.47787700
O	-0.40736800	-1.74771800	-1.43705300
O	0.40731100	-1.74739100	1.43713600

trans-VI-singlet (u)

C	-2.90659600	0.71080400	0.17041800
C	-4.06220400	1.43277500	0.46572900
C	-3.96876000	2.76691800	0.84104400
C	-2.71086400	3.35057200	0.94806400
C	-1.59635300	2.58409700	0.64146900
N	-1.68890800	1.31418200	0.22131000
H	-4.86635500	3.33362000	1.07577700
H	-5.03273700	0.94682400	0.42879100
H	-2.58324900	4.37702400	1.27913800
H	-0.59410000	2.98249100	0.76739700
C	-2.90659600	-0.71080400	-0.17041800
C	-4.06220400	-1.43277500	-0.46572900
N	-1.68890800	-1.31418200	-0.22131000
C	-3.96876000	-2.76691800	-0.84104400
H	-5.03273700	-0.94682400	-0.42879100
C	-1.59635300	-2.58409700	-0.64146900
C	-2.71086400	-3.35057200	-0.94806400

H	-4.86635500	-3.33362000	-1.07577700
H	-0.59410000	-2.98249100	-0.76739700
H	-2.58324900	-4.37702400	-1.27913800
Ru	0.00000000	0.00000000	0.00000000
N	1.68890800	1.31418200	-0.22131000
C	1.59635300	2.58409700	-0.64146900
C	2.90659600	0.71080400	-0.17041800
C	2.71086400	3.35057200	-0.94806400
H	0.59410000	2.98249100	-0.76739700
C	4.06220400	1.43277500	-0.46572900
C	3.96876000	2.76691800	-0.84104400
H	2.58324900	4.37702400	-1.27913800
H	5.03273700	0.94682400	-0.42879100
H	4.86635500	3.33362000	-1.07577700
N	1.68890800	-1.31418200	0.22131000
C	1.59635300	-2.58409700	0.64146900
C	2.90659600	-0.71080400	0.17041800
C	2.71086400	-3.35057200	0.94806400
H	0.59410000	-2.98249100	0.76739700
C	4.06220400	-1.43277500	0.46572900
C	3.96876000	-2.76691800	0.84104400
H	2.58324900	-4.37702400	1.27913800
H	5.03273700	-0.94682400	0.42879100
H	4.86635500	-3.33362000	1.07577700

O	0.00000000	0.00000000	-1.71302900
O	0.00000000	0.00000000	1.71302900

cis-VI-triplet

Ru	0.00024000	-0.09294800	-0.94353700
N	2.05238600	0.42942100	-0.88188600
C	2.60445500	1.23665900	-1.80597700
C	3.96889100	1.48499600	-1.83478100
C	4.78105100	0.87665000	-0.88263000
C	4.20489300	0.04488000	0.07183700
C	2.82988000	-0.17533900	0.05897100
N	0.77808200	-1.10450600	0.85252200
C	0.03918700	-1.85878100	1.67971800
C	0.60349100	-2.57809200	2.72350900
C	1.98150500	-2.50943400	2.90925400
C	2.74627000	-1.72682900	2.05208600
C	2.12257600	-1.02731400	1.01930500
N	-0.77997700	1.25396200	0.61671100
C	-0.04294100	2.15854400	1.27788300
C	-0.60864300	3.06890400	2.15919500
C	-1.98633900	3.03455300	2.35645200
C	-2.74915100	2.09671000	1.67036400
C	-2.12442700	1.20931300	0.79439500
N	-2.04917800	-0.59837100	-0.77722400

C	-2.59736500	-1.57757400	-1.51932300
C	-3.96156800	-1.82767300	-1.50253300
C	-4.77773300	-1.03656100	-0.69991400
C	-4.20558400	-0.02840500	0.06920500
C	-2.82981000	0.18356800	0.01991000
H	1.91645600	1.67568400	-2.52496900
H	4.37757700	2.13998500	-2.59888000
H	5.85522800	1.04481800	-0.88133500
H	4.82793300	-0.43516600	0.82110900
H	-1.03073300	-1.88653600	1.48251700
H	-0.02802700	-3.18300500	3.36781300
H	2.45941800	-3.06374700	3.71337300
H	3.82305900	-1.66881600	2.18403200
H	1.02698700	2.14833900	1.07880200
H	0.02187600	3.79023800	2.67126900
H	-2.46542400	3.73398700	3.03708200
H	-3.82550700	2.06294200	1.81339100
H	-1.90630600	-2.15202000	-2.13238500
H	-4.36741300	-2.62456700	-2.11901300
H	-5.85227600	-1.19997200	-0.67095300
H	-4.83268100	0.59360700	0.70138400
O	0.26166400	-1.56607200	-1.78888000
O	-0.26313200	1.18579000	-2.06112500

trans-VI-triplet

C	-2.89038600	0.70398200	0.19343500
C	-4.04246600	1.42431900	0.50657100
C	-3.93923800	2.74607500	0.91972900
C	-2.67672200	3.31961700	1.04085600
C	-1.56617900	2.55661100	0.71455000
N	-1.66675500	1.29650700	0.26213800
H	-4.83258100	3.31213300	1.17160700
H	-5.01596800	0.94555100	0.45496200
H	-2.54438100	4.33784200	1.39483900
H	-0.55986500	2.94607400	0.84129000
C	-2.89038600	-0.70398200	-0.19343500
C	-4.04246600	-1.42431900	-0.50657100
N	-1.66675500	-1.29650700	-0.26213800
C	-3.93923800	-2.74607500	-0.91972900
H	-5.01596800	-0.94555100	-0.45496200
C	-1.56617900	-2.55661100	-0.71455000
C	-2.67672200	-3.31961700	-1.04085600
H	-4.83258100	-3.31213300	-1.17160700
H	-0.55986500	-2.94607400	-0.84129000
H	-2.54438100	-4.33784200	-1.39483900
Ru	0.00000000	0.00000000	0.00000000
N	1.66675500	1.29650700	-0.26213800
C	1.56617900	2.55661100	-0.71455000

C	2.89038600	0.70398200	-0.19343500
C	2.67672200	3.31961700	-1.04085600
H	0.55986500	2.94607400	-0.84129000
C	4.04246600	1.42431900	-0.50657100
C	3.93923800	2.74607500	-0.91972900
H	2.54438100	4.33784200	-1.39483900
H	5.01596800	0.94555100	-0.45496200
H	4.83258100	3.31213300	-1.17160700
N	1.66675500	-1.29650700	0.26213800
C	1.56617900	-2.55661100	0.71455000
C	2.89038600	-0.70398200	0.19343500
C	2.67672200	-3.31961700	1.04085600
H	0.55986500	-2.94607400	0.84129000
C	4.04246600	-1.42431900	0.50657100
C	3.93923800	-2.74607500	0.91972900
H	2.54438100	-4.33784200	1.39483900
H	5.01596800	-0.94555100	0.45496200
H	4.83258100	-3.31213300	1.17160700
O	0.00000000	0.00000000	-1.81353600
O	0.00000000	0.00000000	1.81353600

II) G09-optimized geometries

cis-II-singlet-0

Ru	-0.00001800	-0.00008500	-0.77702000

N	2.01673300	0.48455500	-0.72017600
C	2.63326500	1.40982100	-1.48292100
C	3.99490700	1.66156900	-1.40285100
C	4.76192500	0.92703700	-0.50106900
C	4.13781200	-0.03427100	0.28390900
C	2.76435700	-0.24445300	0.16127900
N	0.66556100	-1.27857900	0.64340600
C	-0.11164400	-2.14691600	1.32571800
C	0.39004500	-2.99576200	2.29941600
C	1.75023300	-2.95392600	2.59558700
C	2.55636800	-2.05864800	1.90561800
C	2.00359200	-1.22389000	0.93482900
N	-0.66536600	1.27860300	0.64334600
C	0.11193100	2.14680700	1.32571300
C	-0.38973400	2.99596600	2.29915500
C	-1.75001300	2.95462100	2.59496800
C	-2.55624300	2.05944000	1.90498000
C	-2.00347400	1.22431300	0.93450600
N	-2.01669600	-0.48473400	-0.71988100
C	-2.63313200	-1.41045900	-1.48216300
C	-3.99480000	-1.66209200	-1.40203600
C	-4.76186300	-0.92700300	-0.50074500
C	-4.13778800	0.03468700	0.28380600
C	-2.76431200	0.24473400	0.16119400

H	1.99182900	1.95224100	-2.17466000
H	4.44079300	2.42039200	-2.03985400
H	5.83159700	1.09827100	-0.41186300
H	4.72079100	-0.62065600	0.98903700
H	-1.16639900	-2.14326700	1.06270100
H	-0.28219900	-3.67608500	2.81462900
H	2.17628600	-3.60590500	3.35362500
H	3.61952400	-2.00544600	2.12398400
H	1.16675400	2.14279000	1.06295900
H	0.28259300	3.67615600	2.81443700
H	-2.17606100	3.60688400	3.35276500
H	-3.61946500	2.00658200	2.12311000
H	-1.99153000	-1.95327600	-2.17343300
H	-4.44067300	-2.42127600	-2.03861900
H	-5.83155300	-1.09813600	-0.41154700
H	-4.72080900	0.62143100	0.98860200
H	1.17281500	-1.08887600	-3.04464900
O	0.47052800	-1.39645500	-2.44607100
H	0.73505000	-2.29597100	-2.19052000
H	-0.73006100	2.29693500	-2.19139900
O	-0.47175900	1.39546500	-2.44643100
H	-1.17887600	1.09051100	-3.04065400

trans-II-singlet-0

C	2.84387900	0.75323200	-0.20207400
C	3.96250200	1.53958100	-0.47937900
C	3.80016500	2.85158800	-0.90355900
C	2.50839100	3.34149200	-1.07693600
C	1.43585000	2.51675000	-0.77463400
N	1.58095800	1.25825800	-0.30731200
H	4.66633200	3.47073500	-1.12220400
H	4.96040800	1.11943600	-0.38979200
H	2.32639900	4.34711800	-1.44555400
H	0.41160400	2.85423800	-0.91687400
C	2.91034500	-0.66324200	0.15020200
C	4.09970600	-1.31539400	0.47560800
N	1.71053300	-1.32149500	0.14069000
C	4.08732500	-2.66273900	0.80831300
H	5.03517400	-0.76299900	0.48778600
C	1.71780200	-2.62285700	0.49530300
C	2.86531100	-3.32775400	0.82607400
H	5.00972800	-3.17759100	1.06419900
H	0.74890000	-3.11155300	0.53106900
H	2.79161500	-4.37724400	1.09701800
Ru	0.00040100	-0.06011500	0.01089500
N	-1.58974600	1.24773900	0.32056600
C	-1.45781100	2.50040200	0.80676300
C	-2.84798800	0.74101400	0.17821300

C	-2.53928700	3.32067200	1.08835400
H	-0.43784500	2.83469600	0.98323500
C	-3.97476700	1.52393200	0.43112600
C	-3.82510300	2.83198800	0.87197600
H	-2.36908100	4.32170000	1.47463600
H	-4.96944300	1.10376800	0.31109300
H	-4.69762500	3.44849300	1.07212200
N	-1.70259600	-1.33362100	-0.12507100
C	-1.70087200	-2.63924400	-0.46171200
C	-2.90164900	-0.67597600	-0.17474600
C	-2.83864200	-3.34783700	-0.81742100
H	-0.73249100	-3.13011300	-0.46135000
C	-4.08102500	-1.33071200	-0.52945400
C	-4.05957700	-2.68149000	-0.84719500
H	-2.75793700	-4.40103700	-1.07141200
H	-5.01524800	-0.77799000	-0.57513800
H	-4.97401000	-3.19852600	-1.12621600
O	0.25644200	0.01808900	2.15975500
O	-0.26906900	-0.00089900	-2.13728500
H	-0.52782200	0.31356400	2.65184100
H	0.52170400	-0.82097900	2.57244400
H	0.44394000	0.44427000	-2.62529400
H	-0.37234800	-0.86903800	-2.56180100

cis-II-singlet-1

Ru	0.00463700	-0.85027900	-0.16142700
N	2.06617900	-0.73430300	-0.43996700
C	2.78223900	-1.39926000	-1.36829400
C	4.13331300	-1.17589400	-1.57026600
C	4.77752400	-0.22061300	-0.77935600
C	4.05780500	0.44994500	0.19810100
C	2.69848200	0.17298000	0.36842500
N	0.55477300	0.30238300	1.39011600
C	-0.29747100	0.71611100	2.35242300
C	0.09801600	1.57036100	3.36666800
C	1.41272500	2.04137200	3.38286200
C	2.29085700	1.62373500	2.39560200
C	1.85474400	0.74138200	1.40407700
N	-0.50225900	0.86112200	-1.16486000
C	0.34910600	1.62128300	-1.88041300
C	-0.03132200	2.80387500	-2.48204900
C	-1.35637800	3.24474100	-2.29697200
C	-2.23466300	2.48428100	-1.55974500
C	-1.82371800	1.25596000	-0.99569400
N	-2.05944200	-0.82957500	0.12750800
C	-2.79087800	-1.77504600	0.75488200
C	-4.13585300	-1.62707600	1.01993300
C	-4.76650700	-0.42626000	0.62520200
C	-4.03821300	0.54771400	-0.01844700

C	-2.66566600	0.35210000	-0.28612800
H	2.23161100	-2.12686200	-1.96237300
H	4.66683100	-1.73322100	-2.33467300
H	5.83477100	-0.00991600	-0.92037500
H	4.55018900	1.18312900	0.83124400
H	-1.31441000	0.33908700	2.28222500
H	-0.62061200	1.86791100	4.12462900
H	1.74673000	2.72409600	4.15992500
H	3.32019900	1.97200000	2.39638700
H	1.36855400	1.24856100	-1.96230700
H	0.68644800	3.37264300	-3.06334700
H	-1.68698300	4.18333500	-2.73490300
H	-3.25895800	2.81784500	-1.41748700
H	-2.24567900	-2.66465600	1.06715600
H	-4.67908200	-2.41585300	1.52966500
H	-5.82279100	-0.27046800	0.82871900
H	-4.51870400	1.47281500	-0.32619900
H	0.16707700	-3.55551600	0.37297300
O	0.32217900	-2.74082000	0.88169100
H	1.12603000	-2.89180000	1.40673700
H	-0.24361000	-2.01491300	-2.73358800
O	-0.60219700	-2.15774400	-1.84079400
H	-1.57108500	-2.10497200	-1.94325000

trans-II-singlet-1

C	-2.89060900	0.72471300	0.13899900
C	-4.02908800	1.52052100	0.35197700
C	-3.89311400	2.84189300	0.72407100
C	-2.60540800	3.36438200	0.92096300
C	-1.51804600	2.55083800	0.67724700
N	-1.63138900	1.27520400	0.24407600
H	-4.77261000	3.45812100	0.89190300
H	-5.01861500	1.08437400	0.24641200
H	-2.45042300	4.38217800	1.26554200
H	-0.50649900	2.90627100	0.85431300
C	-2.91918000	-0.68068900	-0.14617600
C	-4.09074200	-1.41979200	-0.38457000
N	-1.68340100	-1.29928400	-0.18913600
C	-4.01895500	-2.75956300	-0.70195700
H	-5.05651600	-0.92431600	-0.33528900
C	-1.63546400	-2.60204900	-0.55426200
C	-2.75538900	-3.36427600	-0.81070000
H	-4.92505600	-3.33033500	-0.88761500
H	-0.64270800	-3.02956300	-0.66435300
H	-2.64494000	-4.40600300	-1.09593700
Ru	0.00002500	-0.02402800	0.00002900
N	1.63144000	1.27518400	-0.24396000
C	1.51803800	2.55088900	-0.67695900
C	2.89066300	0.72478100	-0.13910500

C	2.60539600	3.36443800	-0.92074300
H	0.50646700	2.90635000	-0.85380400
C	4.02910700	1.52048800	-0.35227300
C	3.89310900	2.84194100	-0.72419800
H	2.45035400	4.38229500	-1.26513100
H	5.01864100	1.08428900	-0.24697600
H	4.77258600	3.45816000	-0.89215100
N	1.68352400	-1.29922200	0.18909500
C	1.63558500	-2.60201700	0.55407600
C	2.91924400	-0.68069600	0.14616900
C	2.75555100	-3.36423600	0.81049900
H	0.64283700	-3.02956500	0.66407100
C	4.09081200	-1.41967200	0.38465000
C	4.01906200	-2.75950200	0.70195900
H	2.64510200	-4.40601200	1.09556800
H	5.05655800	-0.92413100	0.33551800
H	4.92517100	-3.33023800	0.88769400
O	-0.04647500	0.01122400	-2.07789800
O	0.04592400	0.01059600	2.07798000
H	0.76279000	-0.19004100	-2.57972400
H	-0.79888400	-0.39742700	-2.54035400
H	-0.76367500	-0.19111400	2.57910200
H	0.79806500	-0.39817100	2.54076400

mono-cis-II-singlet-0

Ru	-0.01985800	-0.19924400	-0.80309400
N	1.97077500	0.35745400	-0.92960400
C	2.52470100	1.10625900	-1.90310800
C	3.88097500	1.39663000	-1.94270500
C	4.70567800	0.89412000	-0.93810000
C	4.14282300	0.12525400	0.07354600
C	2.77238300	-0.13046200	0.06205000
N	0.70552900	-1.01677300	0.85620200
C	-0.05609500	-1.67029900	1.76149000
C	0.48145700	-2.24185400	2.90326200
C	1.85210700	-2.14047100	3.13176400
C	2.63613800	-1.45988900	2.20997500
C	2.05426500	-0.89425700	1.07650700
N	-0.73054400	1.42009700	0.18983000
C	0.02585700	2.44619600	0.63185400
C	-0.51010200	3.53859600	1.29543200
C	-1.88278800	3.58084400	1.52187500
C	-2.66792100	2.52376100	1.07916800
C	-2.08097700	1.44681000	0.41814700
N	-2.04394700	-0.67184100	-0.66899800
C	-2.63512000	-1.77198600	-1.17438100
C	-4.00621400	-1.97562400	-1.11742700
C	-4.80373600	-1.00487000	-0.51748500
C	-4.20258500	0.13629300	0.00136500

C	-2.82011900	0.28756200	-0.08338600
H	1.83989000	1.48090300	-2.66296500
H	4.27744300	2.00605600	-2.74996000
H	5.77285800	1.10044300	-0.94092200
H	4.76879700	-0.27263100	0.86806300
H	-1.11755100	-1.72321800	1.53616900
H	-0.17388600	-2.75839800	3.59887100
H	2.30267700	-2.58082500	4.01732300
H	3.70633900	-1.36002300	2.37106400
H	1.09105600	2.37021400	0.42994400
H	0.14515800	4.33972400	1.62529300
H	-2.33675500	4.42320000	2.03737700
H	-3.74087600	2.53596000	1.24972100
H	-1.96800800	-2.49090700	-1.64422300
H	-4.43489800	-2.87893800	-1.54204500
H	-5.88189200	-1.13041500	-0.45799400
H	-4.81205500	0.90792700	0.46364000
H	1.07627100	-1.95089800	-2.72629800
O	0.47260500	-2.02989500	-1.96842600
H	0.80127000	-2.79053400	-1.46062000

mono-trans-II-singlet-0

C	2.90993900	-0.59467300	0.00980800
C	4.10718700	-1.28478100	0.19539800
C	4.08428800	-2.59262600	0.66312900

C	2.85681200	-3.17187400	0.97207400
C	1.69978300	-2.43830100	0.75675000
N	1.70648300	-1.19089600	0.24684000
H	5.01192700	-3.13953500	0.81157400
H	5.05634500	-0.79281600	0.00119800
H	2.78897000	-4.17579500	1.38143900
H	0.72325700	-2.83913100	1.01706700
C	2.82735600	0.81089200	-0.38394600
C	3.90762000	1.53908000	-0.87814300
N	1.58881000	1.37822400	-0.24224000
C	3.74013000	2.86917100	-1.24179800
H	4.87499400	1.05945100	-1.00008500
C	1.43919800	2.66361300	-0.62584300
C	2.47673100	3.43900300	-1.11946600
H	4.57705700	3.44349500	-1.63072700
H	0.43451900	3.06905700	-0.55404200
H	2.28615700	4.46811400	-1.41033900
Ru	0.00279900	0.01876200	0.05898000
N	-1.54769500	-1.34624900	-0.30166000
C	-1.36127200	-2.61667500	-0.71377300
C	-2.80610600	-0.81991400	-0.39343400
C	-2.38777800	-3.42077300	-1.18567200
H	-0.33984300	-2.98412200	-0.68125100
C	-3.87725500	-1.57925900	-0.85993900

C	-3.67468900	-2.89677400	-1.25091800
H	-2.17053500	-4.43678000	-1.50275600
H	-4.86571700	-1.13530700	-0.93962900
H	-4.50406100	-3.49569200	-1.61819200
N	-1.72727800	1.21319500	0.22765100
C	-1.75762100	2.47400400	0.70675100
C	-2.91812000	0.58187000	0.00693000
C	-2.93192700	3.17886900	0.92234600
H	-0.79136400	2.91924100	0.93304700
C	-4.13248800	1.24180300	0.19513000
C	-4.14530900	2.55652800	0.64203200
H	-2.88826700	4.19456900	1.30521300
H	-5.06877700	0.72106900	0.01448500
H	-5.08739600	3.07797100	0.79108800
O	-0.06165500	-0.16044300	2.16173300
H	0.70197200	0.24123100	2.61280900
H	-0.85028200	0.24800000	2.56149000

mono-cis-II-triplet-1

Ru	-0.16418000	-0.39409900	-0.72233900
N	1.85577600	0.16168700	-1.11018500
C	2.19951800	0.68667900	-2.30434800
C	3.49495600	1.07130400	-2.61295400
C	4.48495200	0.90037700	-1.64826200
C	4.14082100	0.35668600	-0.41736900

C	2.81807900	-0.00761300	-0.15818500
N	1.04115400	-0.85772800	1.18876400
C	0.53562400	-1.36380000	2.32135900
C	1.31762800	-1.63392200	3.43777300
C	2.68024300	-1.35701600	3.37302400
C	3.20944300	-0.82143000	2.20434200
C	2.36497900	-0.57917000	1.11893200
N	-0.84503700	1.34888500	0.11971500
C	-0.06198400	2.39899300	0.44144800
C	-0.57387700	3.57769400	0.95754800
C	-1.94881700	3.68119100	1.15958300
C	-2.76033500	2.59970100	0.84444200
C	-2.19524800	1.43610700	0.32453900
N	-2.17744100	-0.79276300	-0.49914700
C	-2.77264600	-1.96378400	-0.80765400
C	-4.13714400	-2.16336600	-0.67641300
C	-4.92756200	-1.11558400	-0.20797900
C	-4.32207400	0.08858100	0.12659600
C	-2.94352600	0.23388900	-0.01893300
H	1.38901000	0.79967500	-3.02346600
H	3.71663900	1.49296300	-3.58915700
H	5.51400000	1.18635900	-1.85171400
H	4.90374700	0.21657300	0.34312100
H	-0.53711600	-1.55622600	2.32090600

H	0.86521700	-2.04933000	4.33397000
H	3.32680000	-1.55284900	4.22495400
H	4.27117900	-0.59763200	2.14604700
H	1.00287200	2.26798800	0.26560000
H	0.09766200	4.39790500	1.19441900
H	-2.38350900	4.59299700	1.56128900
H	-3.83362500	2.65996400	1.00232600
H	-2.11250200	-2.75397300	-1.15755300
H	-4.56769200	-3.12553900	-0.93867300
H	-6.00230300	-1.23700900	-0.09932700
H	-4.92191300	0.91296000	0.50226100
H	0.01658000	-2.45498700	-2.63355900
O	0.31251600	-2.30458400	-1.72025700
H	1.23940400	-2.59649800	-1.69544200

mono-trans-II-triplet-1

C	-2.91974600	0.54808000	-0.01562300
C	-4.13469300	1.21384200	0.14483900
C	-4.14964000	2.52004700	0.61562300
C	-2.94162100	3.13103500	0.94344400
C	-1.76528400	2.42361500	0.75303400
N	-1.73587100	1.17016900	0.25789800
H	-5.09214000	3.04597900	0.74529700
H	-5.06904500	0.70511200	-0.07560900
H	-2.90535700	4.13967700	1.34504600

H	-0.80144700	2.85150800	1.02113200
C	-2.79782300	-0.84347600	-0.43891300
C	-3.85588000	-1.60020200	-0.93844400
N	-1.54272300	-1.37437600	-0.32423400
C	-3.63834300	-2.91080300	-1.34397500
H	-4.84469500	-1.15972600	-1.03166900
C	-1.34075300	-2.63893500	-0.74511100
C	-2.35306400	-3.43726500	-1.25398400
H	-4.45744700	-3.50595100	-1.73971600
H	-0.32033800	-3.00729600	-0.68199700
H	-2.12937700	-4.44984300	-1.57716800
Ru	-0.00008900	-0.00003300	0.12135500
N	1.54282800	1.37463500	-0.32390900
C	1.34107000	2.63923700	-0.74464200
C	2.79777800	0.84346700	-0.43894000
C	2.35341600	3.43736400	-1.25380800
H	0.32078600	3.00789900	-0.68116300
C	3.85586500	1.59991700	-0.93882600
C	3.63851500	2.91058200	-1.34428100
H	2.12986800	4.45001800	-1.57684800
H	4.84453600	1.15919800	-1.03241700
H	4.45762800	3.50551800	-1.74032400
N	1.73575200	-1.17012400	0.25789900
C	1.76509500	-2.42358000	0.75311300

C	2.91962300	-0.54810200	-0.01561500
C	2.94140200	-3.13100300	0.94358800
H	0.80122500	-2.85138800	1.02121500
C	4.13456700	-1.21388500	0.14492500
C	4.14945600	-2.52005600	0.61576700
H	2.90514200	-4.13961600	1.34526300
H	5.06893500	-0.70516700	-0.07547300
H	5.09193000	-3.04601500	0.74552700
O	0.00030700	-0.00012000	2.57485800
H	-0.76999300	0.01813600	3.16262300
H	0.77171700	-0.01706300	3.16120400

mono-TS-triplet-1

C	2.82196600	0.16491900	-0.04011500
C	4.11733900	0.68351500	-0.09254900
C	4.39547600	1.78241800	-0.89444100
C	3.36597200	2.35104600	-1.64114800
C	2.09827100	1.79818600	-1.54951400
N	1.81719800	0.73269600	-0.77024500
H	5.40314500	2.18823500	-0.93739100
H	4.91129900	0.22610400	0.49099500
H	3.53601300	3.20934300	-2.28495400
H	1.25670000	2.20937600	-2.10549000
C	2.44377300	-1.00096100	0.76800700

C	3.32975700	-1.69344300	1.59480300
N	1.14517200	-1.38432500	0.66154000
C	2.87635900	-2.79307300	2.31397200
H	4.36696200	-1.38193300	1.68227100
C	0.71449700	-2.44574400	1.36008900
C	1.54456000	-3.18106400	2.19547800
H	3.55756600	-3.34025100	2.96112000
H	-0.33663200	-2.70229200	1.23708300
H	1.15163400	-4.03483200	2.74035400
Ru	-0.11641300	-0.09615200	-0.67626100
N	-0.99773900	1.40210900	0.45416100
C	-0.36280200	2.46004600	0.99987200
C	-2.34639600	1.25713900	0.64790600
C	-1.02331300	3.42446200	1.74232500
H	0.70791200	2.51331900	0.81985800
C	-3.05617400	2.19852000	1.38984100
C	-2.39607800	3.29198300	1.93790400
H	-0.46795500	4.25995200	2.15860200
H	-4.12478900	2.07937100	1.54419200
H	-2.94794600	4.02935300	2.51559600
N	-2.07101100	-0.76520000	-0.59372500
C	-2.53320600	-1.90644600	-1.14171100
C	-2.94699900	0.06315100	0.05021200
C	-3.87049500	-2.26938700	-1.09845900

H	-1.78552400	-2.53966300	-1.61676200
C	-4.30286200	-0.25161200	0.12139600
C	-4.77318800	-1.42295400	-0.45988600
H	-4.19161700	-3.20034600	-1.55699300
H	-4.99404400	0.41490200	0.62958400
H	-5.82970600	-1.67326800	-0.40947300
O	0.46809100	-1.29959000	-2.44973400
H	1.39553800	-1.30168600	-2.73992000
H	-0.06520100	-1.28943600	-3.26131600

APPENDIX E

SUPPORTING INFORMATION FOR:

CO_2 Reduction by Mononuclear Ruthenium Polypyridyl Complexes†

To be Submitted

Nora Planas,[a] Takashi Ono,[a] Lydia Vaquer,[a] Laura Gagliardi,[b] Christopher Cramer,[b] and Antoni Llobet*[a, c]

[a] *Institute of Chemical Research of Catalonia (ICIQ), Av. Països Catalans 16, E-43007 Tarragona, Spain. Fax: 34 977 902 228; Tel: 34 977 902 200; E-mail: fmaseras@iciq.es, allobet@iciq.es*

[b] *Department of Chemistry and Supercomputing Institute University of Minnesota, 207 Pleasant St. SE, Minneapolis, MN 55455-0431 (USA)*

[c] *Departament de Química, Universitat Autònoma de Barcelona, Cerdanyola del Vallès, E-08193 Barcelona, Spain.*

I. NMR:

Figure S1. 1D and 2D NMR spectra (500 MHz, 298K, CD_2Cl_2) for complex $[Ru^{II}(bid)(bpy)Cl]$ (1): (a) ^{1}H-NMR, (b) COSY, (c) NOESY (d) DEPTQ135 (e) HSQC and (f) HMBC

(a)

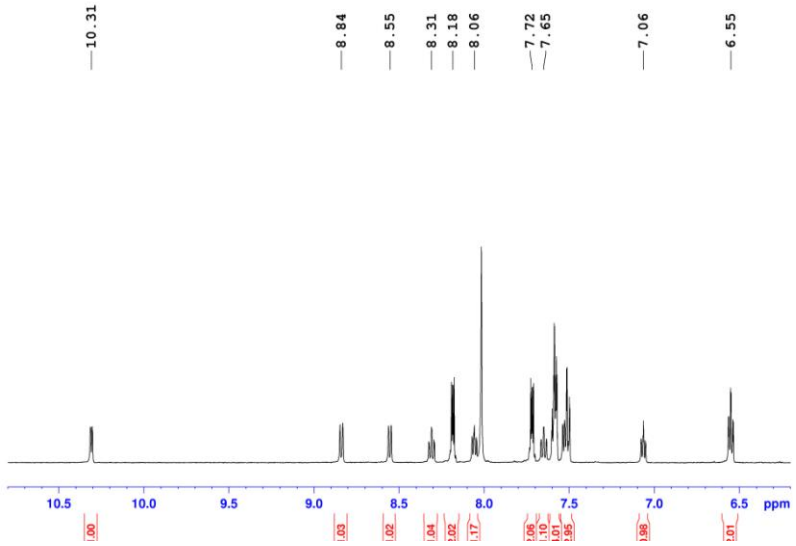

(b)

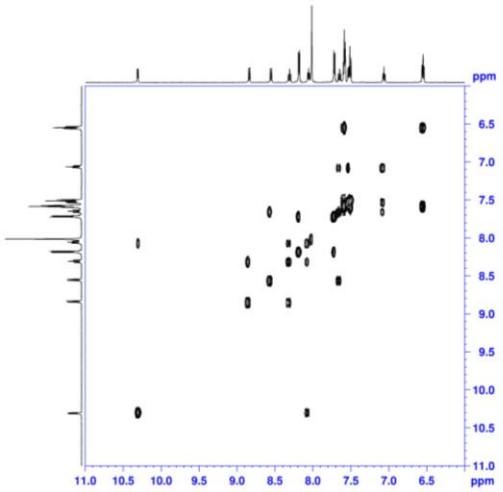

(c)

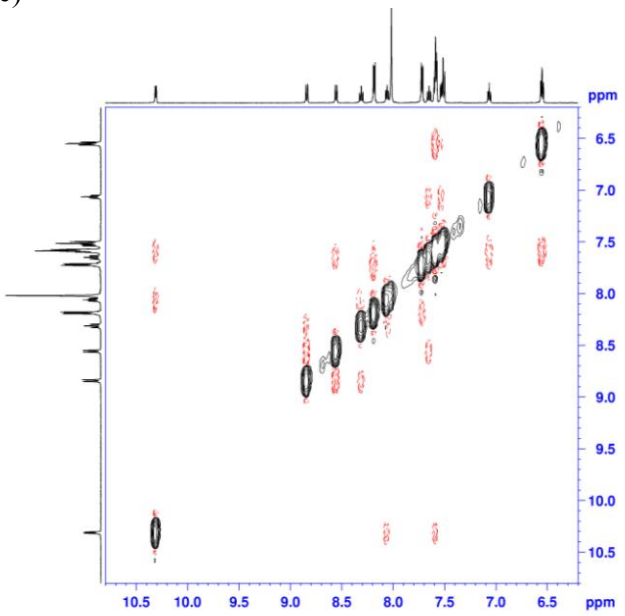
ppm
6.5
7.0
7.5
8.0
8.5
9.0
9.5
10.0
10.5
10.5 10.0 9.5 9.0 8.5 8.0 7.5 7.0 6.5 ppm

(d)

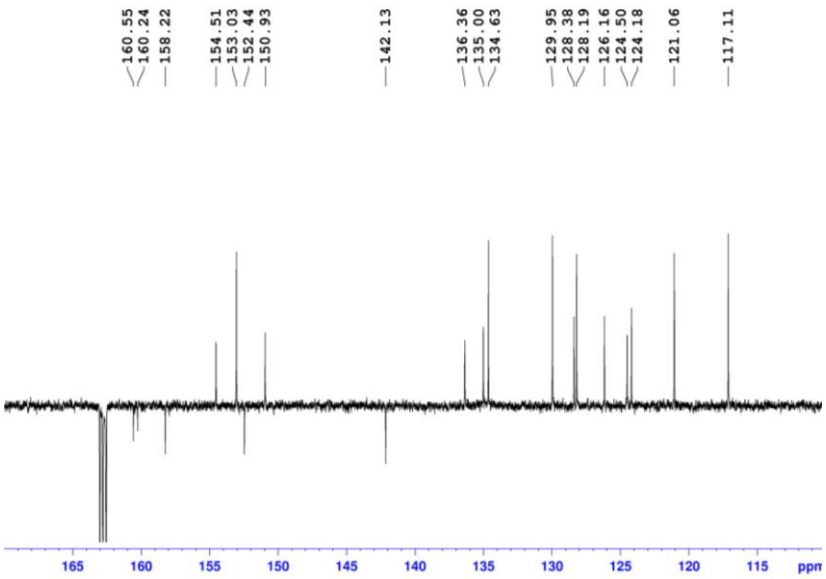
160.55
160.24
158.22
154.51
153.03
152.44
150.93
142.13
136.36
135.00
134.63
129.95
128.38
128.19
126.16
124.50
124.18
121.06
117.11
165 160 155 150 145 140 135 130 125 120 115 ppm

(e)

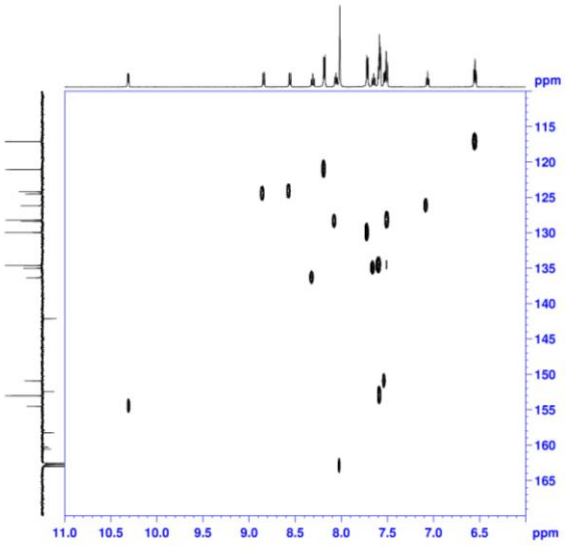
ppm
115
120
125
130
135
140
145
150
155
160
165
11.0
10.5
10.0
9.5
9.0
8.5
8.0
7.5
7.0
6.5
ppm

(f)

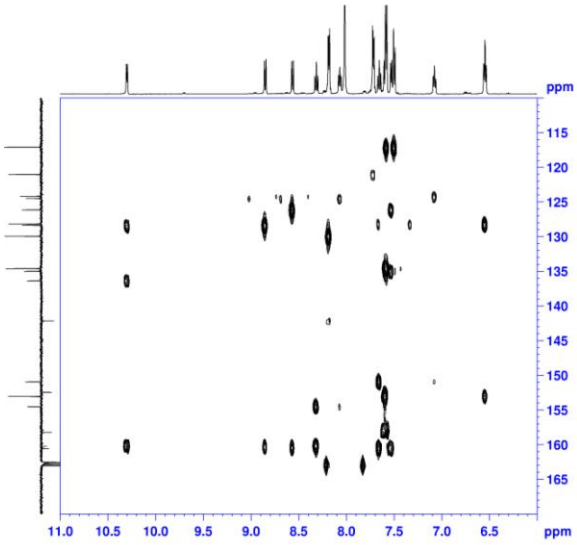
ppm
115
120
125
130
135
140
145
150
155
160
165
11.0
10.5
10.0
9.5
9.0
8.5
8.0
7.5
7.0
6.5
ppm

Figure S2. 1D and 2D NMR spectra (500 MHz, 298K, DMF-d_7) for complex [Ru^{II}**(bid)(4,4'-**$(MeO)_2$bpy)Cl] (1d): (a) ^{1}H-NMR, (b) COSY, (c) NOESY (d) DEPTQ135 (e) HSQC and (f) HMBC.

(a)

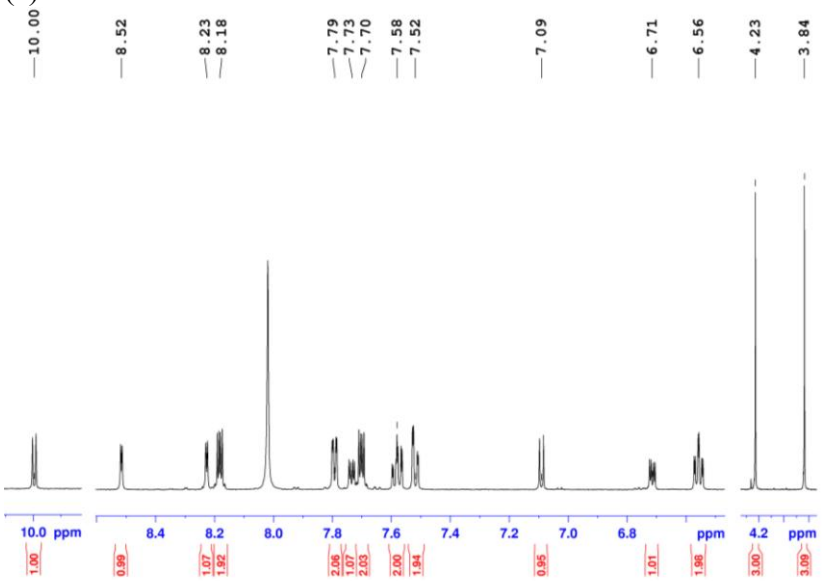

(b)

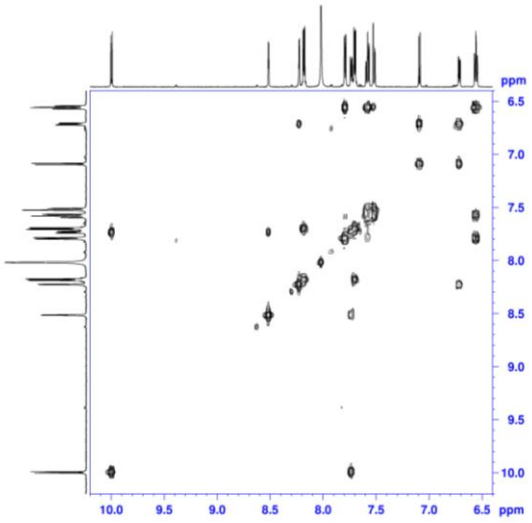

(c)

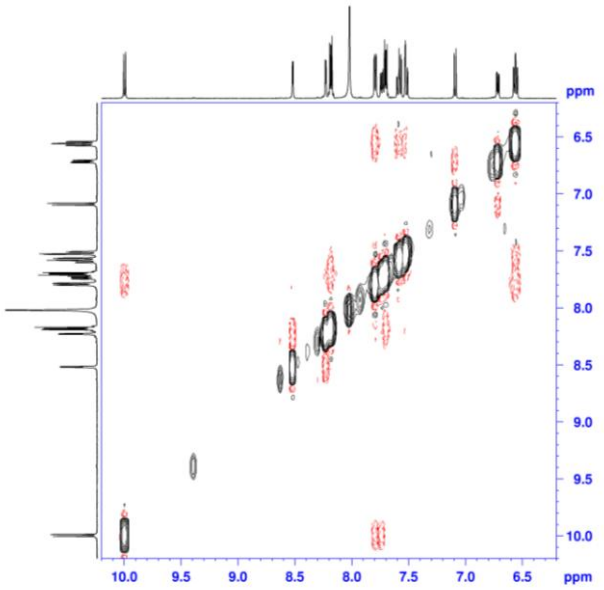
ppm
6.5
7.0
7.5
8.0
8.5
9.0
9.5
10.0
10.0
9.5
9.0
8.5
8.0
7.5
7.0
6.5
ppm

(d)

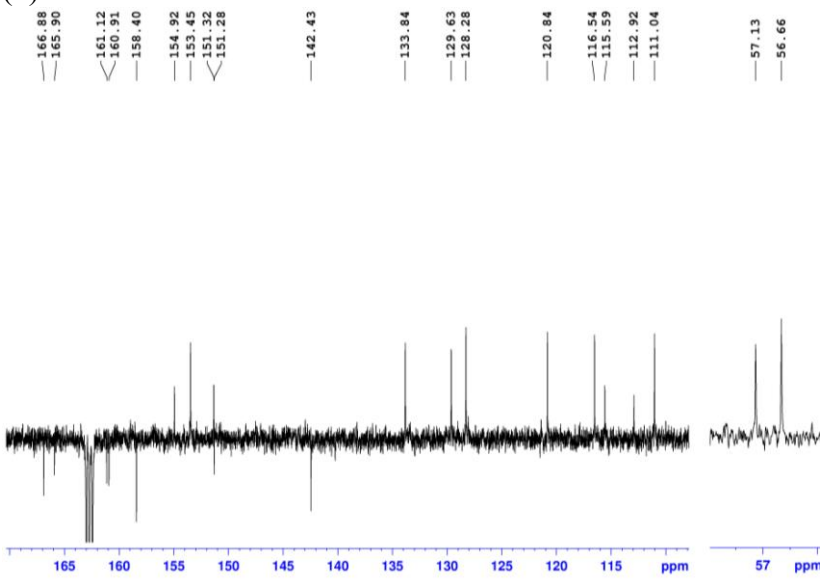
166.88
165.90
161.12
160.91
158.40
154.92
153.45
151.32
151.28
142.43
133.84
129.63
128.28
120.84
116.54
115.59
112.92
111.04
57.13
56.66
165
160
155
150
145
140
135
130
125
120
115
ppm
57
ppm

(e)

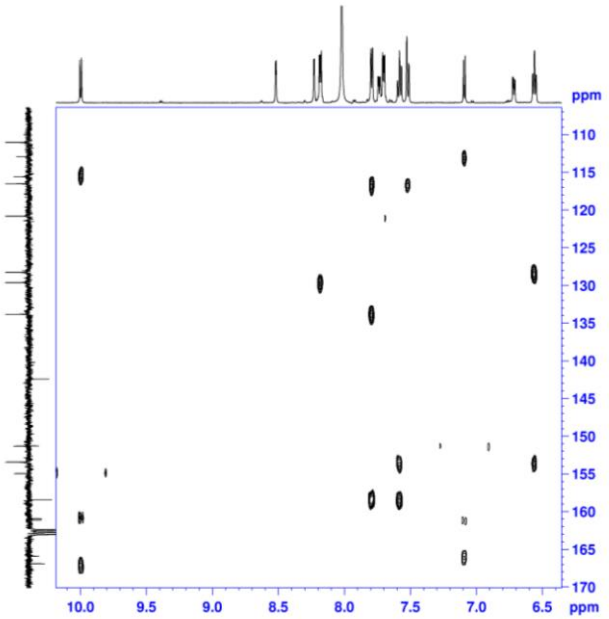
ppm
110
115
120
125
130
135
140
145
150
155
160
165
170
10.0
9.5
9.0
8.5
8.0
7.5
7.0
6.5
ppm

(f)

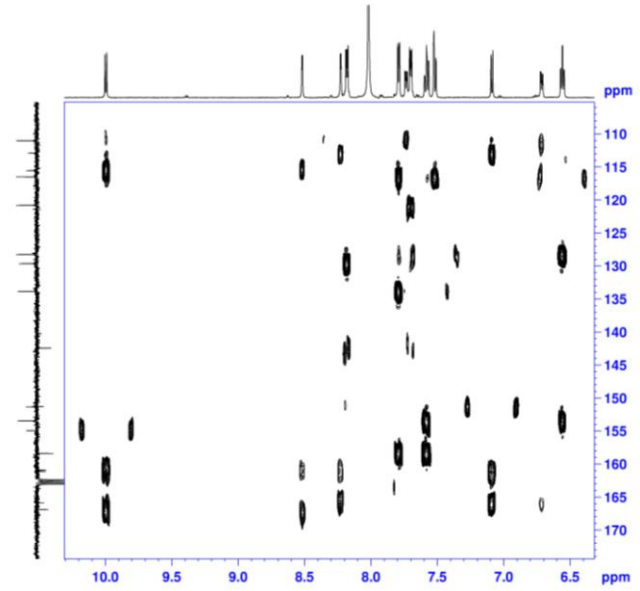
ppm
110
115
120
125
130
135
140
145
150
155
160
165
170
10.0
9.5
9.0
8.5
8.0
7.5
7.0
6.5
ppm

Figure S3. 1D and 2D NMR spectra (400 MHz, 298K, DMF-d_7) for complex [Ru^{II}**(bid)(4,4'-**$(EtOCO)_2$bpy)Cl] (1w) (a) ^{1}H-NMR, (b) COSY, (c) NOESY (d) DEPTQ135 (e) HSQC and (f) HMBC.

(a)

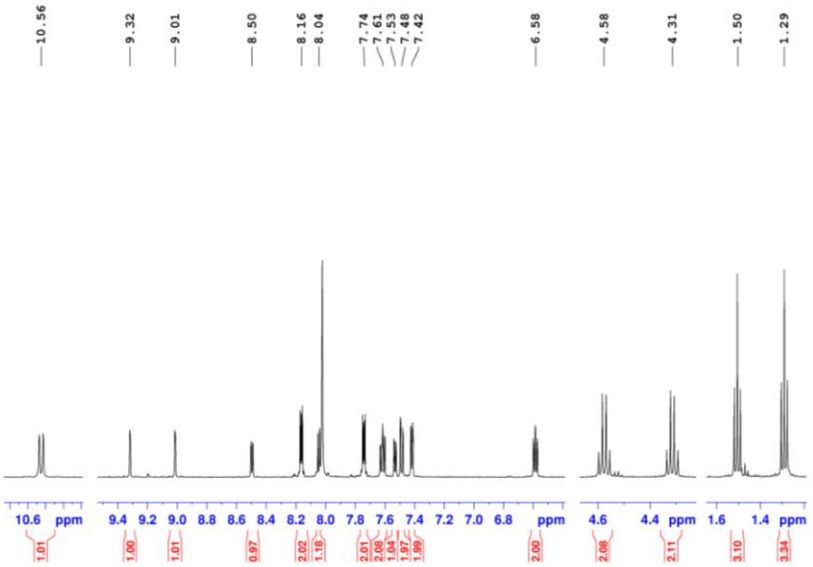

(b)

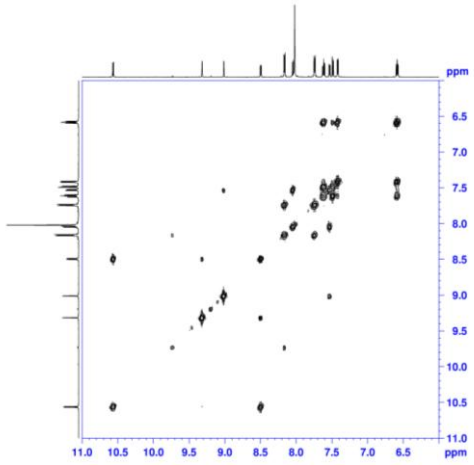

(c)

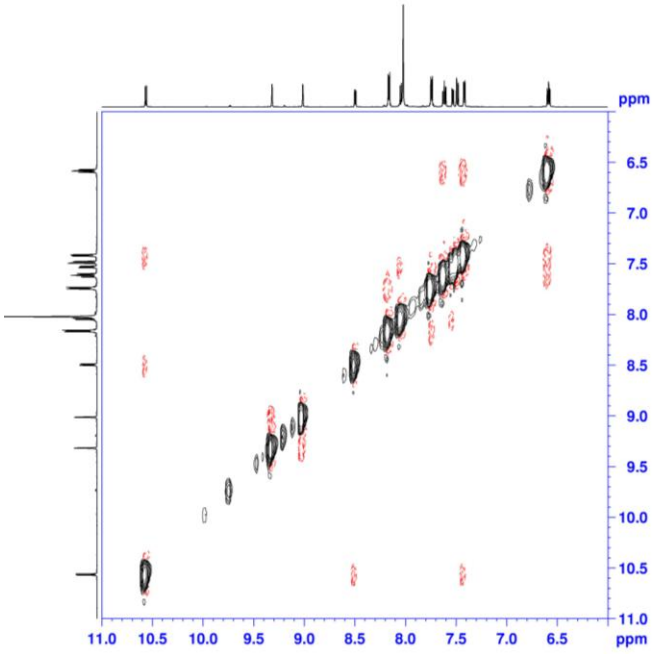
ppm
6.5
7.0
7.5
8.0
8.5
9.0
9.5
10.0
10.5
11.0
11.0 10.5 10.0 9.5 9.0 8.5 8.0 7.5 7.0 6.5 ppm

(d)

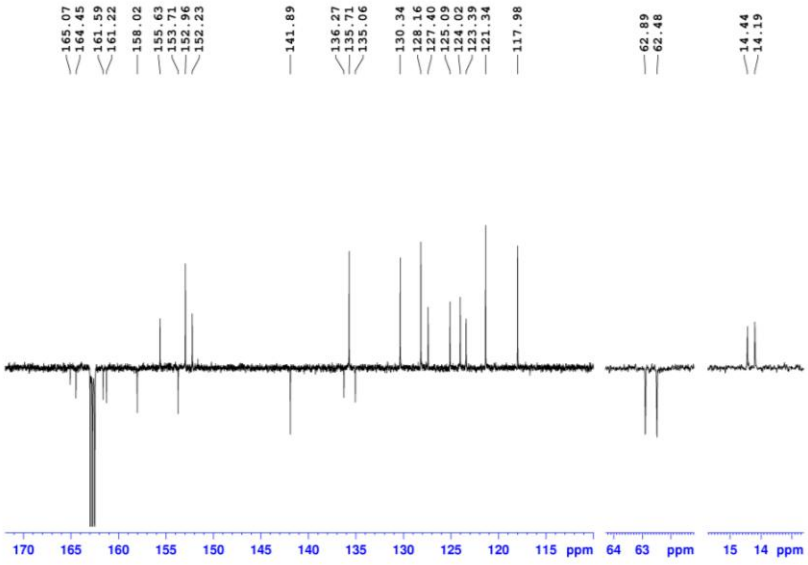
165.07
164.45
161.59
161.22
158.02
155.63
153.71
152.96
152.23
141.89
136.27
135.71
135.06
130.34
128.16
127.40
125.09
124.02
123.39
121.34
117.98
62.89
62.48
14.44
14.19
170 165 160 155 150 145 140 135 130 125 120 115 ppm
64 63 ppm
15 14 ppm

(e)

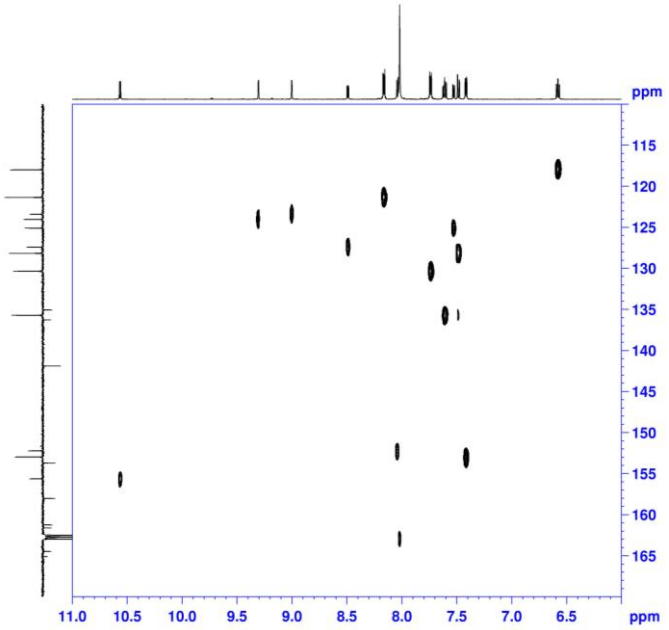
ppm
115
120
125
130
135
140
145
150
155
160
165
11.0
10.5
10.0
9.5
9.0
8.5
8.0
7.5
7.0
6.5
ppm

(f)

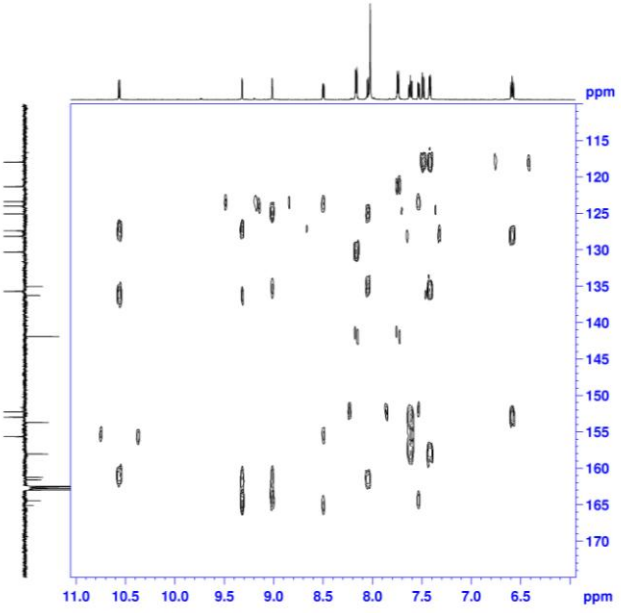
ppm
115
120
125
130
135
140
145
150
155
160
165
170
11.0
10.5
10.0
9.5
9.0
8.5
8.0
7.5
7.0
6.5
ppm

II. UV-vis:

Figure S4. UV-vis, 0.036 mM in DCM, of (a) [Ru^{II}**(bid)(4,4'-**$(MeO)_2$bpy)Cl] (1d), (b) [Ru^{II}**(bid)(4,4'-**$(EtOCO)_2$bpy)Cl] (1w), (c) [Ru^{II}(bid)(bpy)Cl] (1), (e) [Ru^{II}(trpy)(bpy)Cl] (2)

(a)

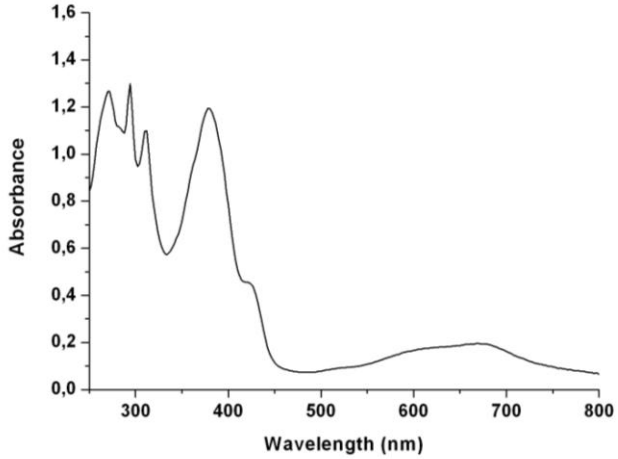

(b)

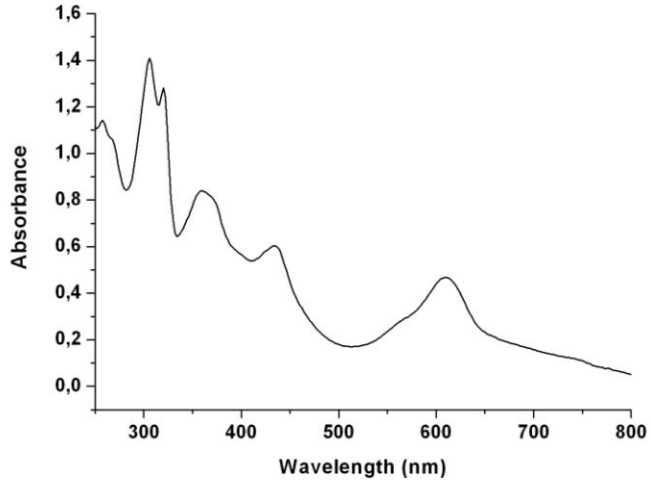

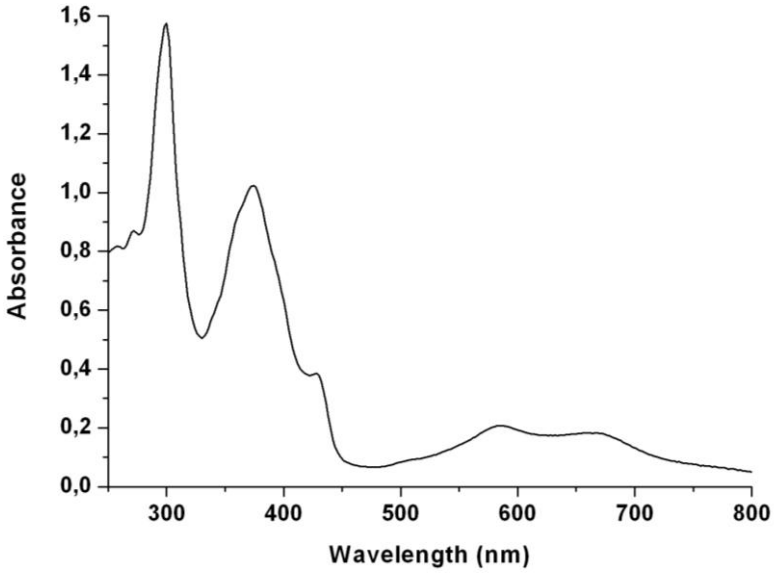
Absorbance
1,6
1,4
1,2
1,0
0,8
0,6
0,4
0,2
0,0
300
400
500
600
700
800
Wavelength (nm)

(c)

(e)

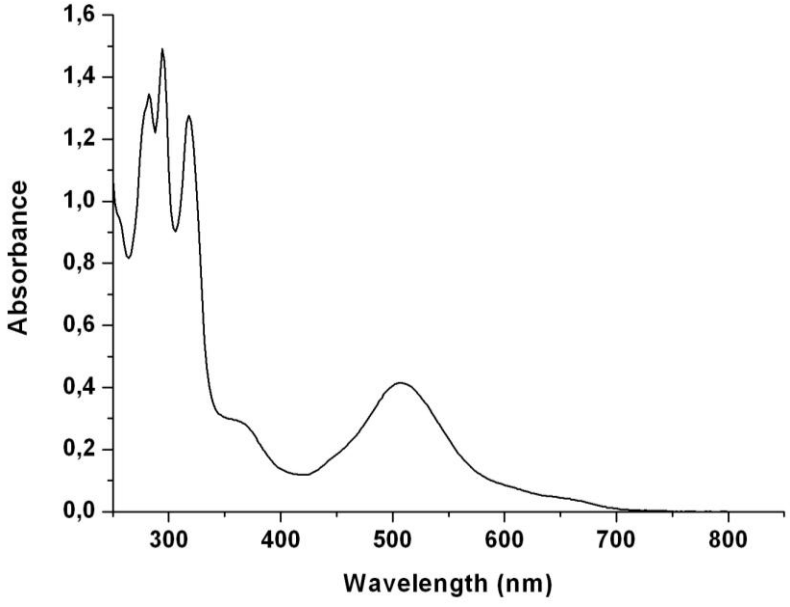
Absorbance
1,6
1,4
1,2
1,0
0,8
0,6
0,4
0,2
0,0
300
400
500
600
700
800
Wavelength (nm)

III. Electrochemistry:

Figure S5. Cyclic voltammograms in DCM, of (a) Ru^{II}**(bid)(4,4'-**$(MeO)_2$bpy)Cl (0.51 mM), (b) Ru^{II}**(bid)(4,4'-**$(EtOCO)_2$bpy)Cl (0.26 mM), (c) Ru^{III}(bid)(acac)Cl (1.9 mM), (d) Ru^{II}(bid)(bpy)Cl (0.66 mM), (e) Ru^{II}(trpy)(bpy)Cl (0.65 mM)

(a)

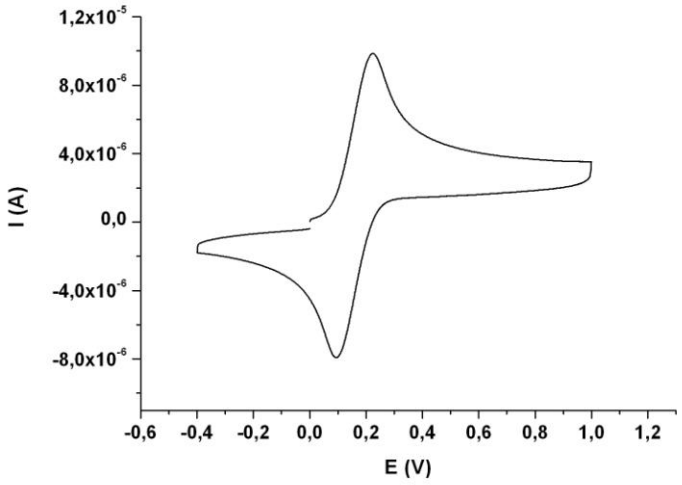

(b)

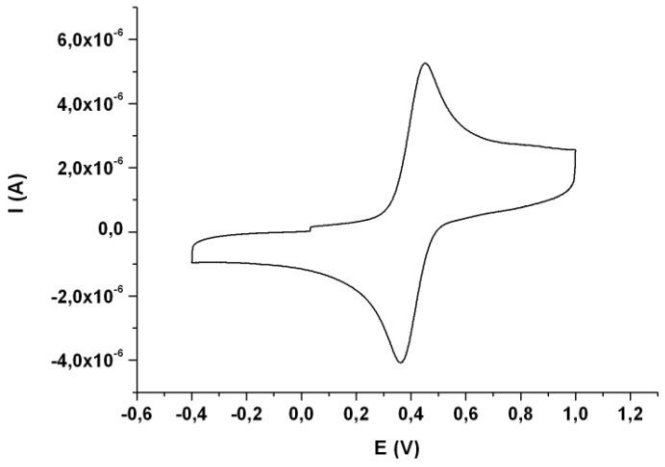

(c)

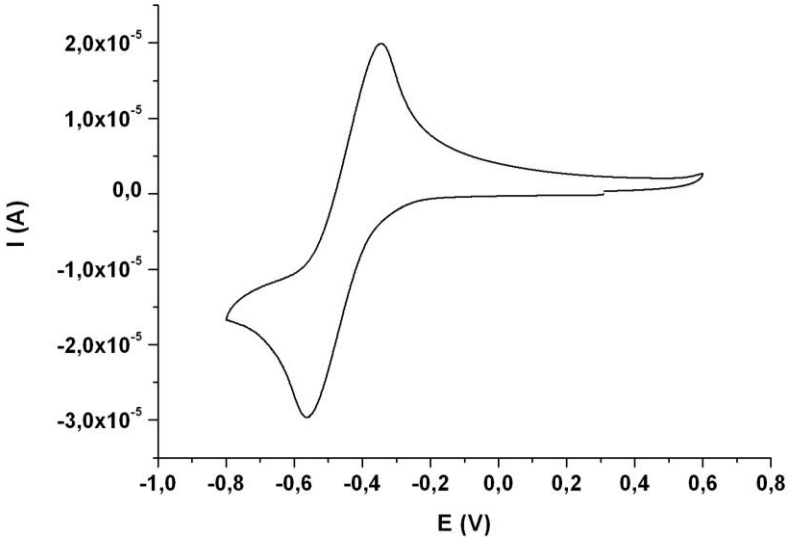
2,0x10-5
1,0x10-5
0,0
-1,0x10-5
-2,0x10-5
-3,0x10-5
I (A)
-1,0
-0,8
-0,6
-0,4
-0,2
0,0
0,2
0,4
0,6
0,8
E (V)

(d)

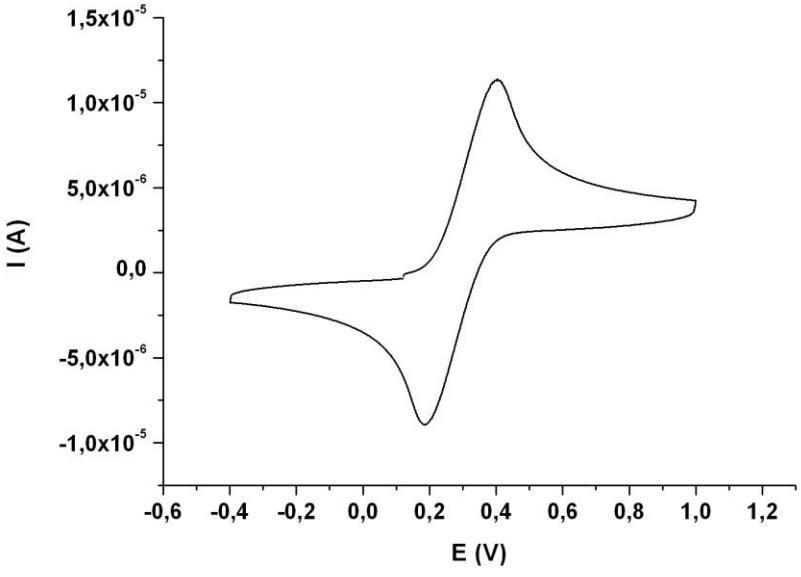
1,5x10-5
1,0x10-5
5,0x10-6
0,0
-5,0x10-6
-1,0x10-5
I (A)
-0,6
-0,4
-0,2
0,0
0,2
0,4
0,6
0,8
1,0
1,2
E (V)

(e)

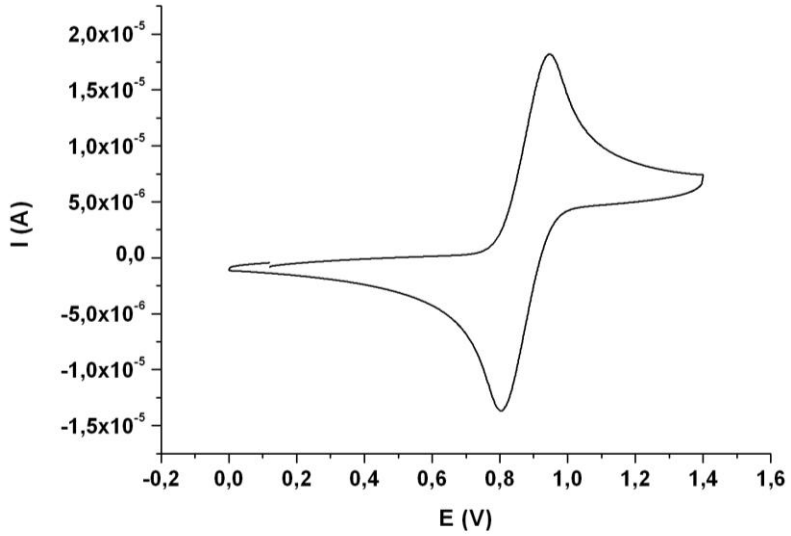

III. X-Ray:

- The cif file for complex 1 is adjointed with the following code:
  LV009Rub_0m

IV. Catalytic experiments

Table S1. Formic acid produced (TON) by the different catalysts over time.

Time (min)	1 (TON)	1w (TON)	1d (TON)	2 (TON)
15	16	18	11	0
30	52	61	47	0
105	256	300	202	<1
115	273	341	222	<1
130	310	388	246	1
2700	793	988	615	44
5520	1074	1309	856	44
10080	1090	1354	880	----

V. Optimized structures

All molecular geometries were fully optimized in 2,2,2-Trifluoroethanol as solvent at the M06-L level of density functional theory (DFT) using the Stuttgart [8s7p6d2f | 6s5p3d2f] ECP28MWB[i] contracted pseudopotential basis set on Ru, the 6-31G(d, p) basis set was employed for the relevant atoms involved in the reaction and MIDI! [ii]minimal basis set on all other atoms in Gaussian 09 program[iii] to account for solvation SMD[iv] at the M06-L[v] level was used. The basis sets employed for each molecule is described in detail in the Supporting Information. The starting structures were taken from experiment, when available. Integral evaluation made use of the grid defined as "ultrafine" in the Gaussian 09 program. In addition, an automatically generated density-fitting basis set was used within the resolution-of-the-identity approximation for the evaluation of Coulomb integrals. The nature of all stationary points was verified by analytic computation of vibrational frequencies, which were also used for the computation of molecular partition functions and 298 K thermal contributions to free energies at the respective temperatures, invoking the usual rigid-rotator, harmonic-oscillator, ideal-gas approximation. Additional single point calculations were run for all structures in Trifluoroethanol as solvent at the M06-L level using the Stuttgart [8s7p6d2f | 6s5p3d2f] ECP28MWB contracted pseudopotential basis set on Ru and the 6-311+G (2df, p) basis set on all other atoms.

Frequencies computed with the smaller basis set were used to compute thermal contributions to ΔG. Those thermal contributions were added to single-point energies obtained with the larger basis set to compute what might be called "composite" free energies. Thus, composite free energy was computed as follows:

$\Delta G(\text{composite}) = \Delta G(\text{small basis}) + [\Delta E(\text{large basis}) - \Delta E(\text{small basis})]$

Tables with selected bond distances and angles:

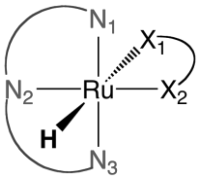

Table S2. Significant structural parameters for the corresponding Ru-H species

	Ru-**H**	Ru-N1	Ru-N2	Ru-N3	Ru-X1	Ru-X2	N1-Ru-N3	N1-Ru-**H**	X1-Ru-**H**	N1-Ru-X2
2	1.638	2.068	1.949	2.068	2.149	2.077	158.4	90.4	168.1	100.8
1w	1.643	2.100	2.019	2.110	2.156	2.037	176.3	87.1	173.9	93.2
1w'	1.643	2.079	2.014	2.096	2.175	2.068	177.7	88.0	174.6	92.2
1	1.647	2.095	2.017	2.106	2.167	2.060	177.2	87.9	174.0	92.5
1d	1.653	2.109	2.021	2.114	2.155	2.058	176.7	87.9	174.1	92.8
1d'	1.651	2.097	2.013	2.101	2.176	2.090	177.7	88.6	174.3	92.0
3	1.650	2.065	1.985	2.065	2.178	2.119	179.0	89.5	178.1	89.9

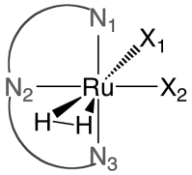

Table S3. Significant structural parameters for the corresponding Ru-H2 Species

	Ru-H1	Ru-H2	H1-H2	alpha	Ru-N1	Ru-N2	Ru-N3	Ru-X1	Ru-X2	N1-Ru-N3	N1-Ru-H1
2	1.755	1.756	0.835	86.1	2.097	1.980	2.099	2.070	2.070	157.4	78.8
1w	1.745	1.747	0.837	2.1	2.124	2.036	2.124	2.063	2.078	176.6	88.9
1w'	1.744	1.742	0.840	7.6	2.110	2.033	2.113	2.076	2.093	177.4	90.1
1	1.741	1.739	0.841	4.4	2.119	2.034	2.121	2.074	2.087	177.1	89.7
1d	1.739	1.737	0.842	7.2	2.127	2.035	2.122	2.069	2.086	176.7	87.9
1d'	1.734	1.737	0.845	4.4	2.116	2.031	2.117	2.083	2.103	177.5	89.8
3	1.714	1.725	0.853	0.3	2.088	2.011	2.088	2.062	2.110	179.3	89.7

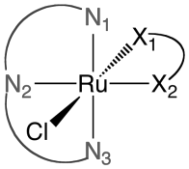

Table S4. Significant structural parameters for the corresponding Ru-Cl species

	Ru-Cl	Ru-N1	Ru-N2	Ru-N3	Ru-X1	Ru-X2	N1-Ru-N3	N1-Ru-Cl	X1-Ru-Cl	N1-Ru-X2
2	2.456	2.071	1.955	2.071	2.041	2.081	159.0	89.6	172.9	100.5
1w	2.478	2.106	2.017	2.113	2.016	2.048	177.0	88.2	175.1	92.7
1w'	2.478	2.106	2.017	2.113	2.016	2.048	177.0	88.2	175.1	92.7
1	2.488	2.098	2.014	2.108	2.029	2.064	177.3	88.6	174.7	92.5
1d	2.494	2.109	2.016	2.115	2.021	2.062	177.0	88.3	174.9	92.6
1d'	2.493	2.099	2.011	2.102	2.045	2.086	177.8	88.6	174.5	91.6
3	2.490	2.069	1.990	2.069	2.059	2.098	178.7	89.3	178.5	90.0

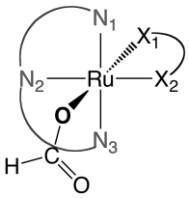

Table S5. Significant structural parameters for the corresponding Ru-H-CO_2 species

	Ru-H	Ru-H-C	O1-C-O2	Ru-N1	Ru-N2	Ru-N3	Ru-X1	Ru-X2	N1-Ru-N3	N1-Ru-H	X2-Ru-H
2	1.828	125.9	134.7	2.080	1.969	2.074	2.044	2.066	158.4	97.3	97.3
1w	1.846	129.4	33.5	2.110	2.021	2.113	2.029	2.057	176.9	95.4	90.4
1w'	1.872	132.2	133.8	2.098	2.017	2.110	2.034	2.073	177.3	95.04	95.8
1	1.846	129.4	133.5	2.110	2.021	2.113	2.029	2.057	176.9	95.43	90.3
1d	1.864	167.7	133.2	2.113	2.021	2.120	2.020	2.059	176.2	94.6	91.3
1d'	1.841	129.1	133.2	2.109	2.017	2.108	2.041	2.076	177.4	95.9	90.9
3	1.829	123.0	132.5	2.081	1.997	2.079	2.050	2.098	179.0	86.8	98.1

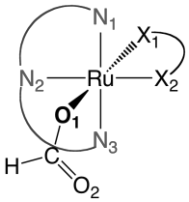

Table S6. Significant structural parameters for the corresponding Ru-O1-CHO2 species

	Ru-O1	Ru-O1-C	O1-C-O2	X1-Ru-O1-O2	Ru-N1	Ru-N2	Ru-N3	Ru-X1	Ru-X2	N1-Ru-N3	N1-Ru-O
2	2.103	126.8	128.4	-165.0	2.071	1.955	2.071	2.044	2.074	158.8	86.5
1w	2.119	125.8	128.8	-139.5	2.104	2.012	2.101	2.019	2.038	176.5	84.4
1w'	2.125	126.6	128.8	-142.9	2.091	2.011	2.091	2.041	2.066	177.7	84.5
1	2.130	126.8	128.9	-139.7	2.100	2.012	2.099	2.032	2.054	177.3	84.1
1d	2.137	127.6	129.1	-145.8	2.111	2.014	2.106	2.023	2.054	176.6	84.0
1d'	2.131	127.3	129.0	-143.5	2.097	2.008	2.094	2.048	2.076	177.7	84.6
3	2.133	125.5	128.7	-166.4	2.071	1.993	2.063	2.060	2.094	176.9	86.6

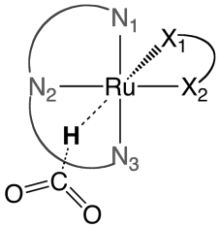

Table S7. Significant structural parameters for the corresponding transition state: Ru-H---CO2

	Ru-H	H-C	Ru-H-C	O1-C-O2	O1-C	C-O2	Ru-N1	Ru-N2	Ru-N3	Ru-X1	Ru-X2
2	1.685	1.617	129.1	151.8	1.196	1.196	2.072	1.957	2.075	2.113	2.069
1w	1.685	1.679	126.2	153.4	1.192	1.194	2.098	2.017	2.116	2.112	2.036
1w'	1.681	1.673	127.9	153.4	1.192	1.193	2.087	2.014	2.101	2.133	2.067
1	1.687	1.700	125.3	153.7	1.192	1.193	2.099	2.015	2.112	2.125	2.061
1d	1.688	1.718	125.7	154.0	1.191	1.192	2.108	2.017	2.120	2.115	2.057
1d'	1.687	1.714	124.7	153.7	1.192	1.193	2.098	2.013	2.110	2.137	2.085
3	1.672	1.732	125.3	154.8	1.191	119.092	2.073	1.989	2.082	2.145	2.106

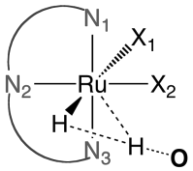

Table S7. Significant structural parameters for the corresponding transition state: Ru-H--H-OCHO

	Ru-H1	Ru-H2	H1-H2	Ru-H1-H2	H2-**O**	H1-H2_**O**	Ru-N1	Ru-N2	Ru-N3	Ru-X1	Ru-X2
2	1.720	2.083	0.913	100.1	1.395	162.9	2.084	1.967	2.080	2.084	2.073
1w	1.730	2.205	0.940	107.6	1.324	166.8	2.130	2.029	2.122	2.094	2.082
1w'	1.733	2.189	0.924	107.0	1.344	168.2	2.099	2.021	2.106	2.086	2.070
1	1.731	2.197	0.938	107.0	1.325	167.6	2.118	2.023	2.112	2.085	2.070
1d	1.733	2.225	0.940	109.0	1.315	168.7	2.116	2.023	2.121	2.076	2.060
1d'	1.723	2.205	0.945	108.0	1.311	167.7	2.113	2.019	2.107	2.099	2.093
3	1.717	2.155	0.966	103.3	1.303	166.7	2.074	1.995	2.078	2.102	2.115

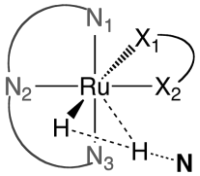

Table S8. Significant structural parameters for the corresponding transition state: Ru-H--H-Nme

	Ru-H1	Ru-H2	H1-H2	Ru-H1-H2	H2-**N**	H1-H2_**N**	Ru-N1	Ru-N2	Ru-N3	Ru-X1	Ru-X2
2	1.724	2.026	0.877	96.9	1.624	144.0	2.088	1.970	2.079	2.075	2.071
1w	1.722	2.063	0.893	99.2	1.535	148.0	2.111	2.024	2.109	2.069	2.047
1w'	1.718	2.070	0.900	99.7	1.516	147.0	2.096	2.070	2.102	2.088	2.070
1	1.720	2.100	0.907	101.7	1.494	149.4	2.109	2.022	2.106	2.084	2.064
1d	1.719	2.128	0.918	103.4	1.463	150.5	2.114	2.023	2.114	2.078	2.059
1d'	1.715	2.123	0.920	103.2	1.464	150.0	2.105	2.018	2.103	2.098	2.086
3	1.695	2.094	0.953	100.8	1.430	149.2	2.072	2.000	2.074	2.102	2.107

-------Optimized geometries for catalytic system of 2-----

[Ru(Trpy)(bpy)Cl]$^{1+}$

Ru	0.03543800	0.00051600	-0.43157800
Cl	-0.54405700	0.00225100	-2.81773900
N	-0.33526200	2.03621500	-0.35541300
N	-0.33427000	-2.03552000	-0.35845100
N	2.09163400	0.00143000	-0.75392700
N	0.75783000	-0.00123600	1.47700400
C	-2.53209100	-1.19532100	0.12371900
C	-2.53270000	1.19421800	0.12532600
C	-3.89745700	1.20926400	0.42270100
H	-4.42762400	2.15495300	0.53514700
C	-4.57648400	-0.00137000	0.57351000
H	-5.64186000	-0.00179400	0.80700300
C	-3.89683200	-1.21145600	0.42111400
H	-4.42651000	-2.15757100	0.53230000
C	-1.65485300	-2.35137300	-0.07899800
C	-2.07739700	-3.68126100	-0.00852300
H	-3.12286600	-3.90638800	0.20298600
C	-1.16363200	-4.71060700	-0.21450500
H	-1.48716100	-5.75109200	-0.16235300
C	0.16712400	-4.39019500	-0.49028400
H	0.91261900	-5.16772600	-0.65835900
C	0.54223000	-3.05302200	-0.55591200
H	1.56883100	-2.75869200	-0.77846900
C	-1.65606400	2.35099200	-0.07576800
C	-2.07935800	3.68055700	-0.00370500
H	-3.12498400	3.90484900	0.20793600
C	-1.16614100	4.71066200	-0.20831700
H	-1.49025700	5.75090300	-0.15495900
C	0.16483100	4.39132600	-0.48430800
H	0.90991200	5.16948000	-0.65134700
C	0.54070100	3.05444600	-0.55151000
H	1.56750900	2.76096600	-0.77424100
C	2.71787400	0.00344400	-1.96318200
H	2.05526100	0.00441700	-2.83050500
C	4.10023100	0.00420900	-2.09402200
H	4.54510300	0.00585800	-3.08953200
C	4.89685200	0.00290900	-0.94589500

H	5.98529700	0.00352800	-1.01949200
C	4.27667200	0.00086300	0.29823300
H	4.87477100	0.00002500	1.20912600
C	2.87985400	0.00015500	0.37763200
C	2.12951900	-0.00171100	1.62882300
C	2.71397700	-0.00383200	2.90007000
H	3.79910400	-0.00444500	2.99566300
C	1.91241800	-0.00532700	4.03539700
H	2.36311700	-0.00704000	5.02861400
C	0.52409800	-0.00460900	3.87886800
H	-0.14347700	-0.00565700	4.74081100
C	-0.01474500	-0.00257500	2.60000100
H	-1.09281200	-0.00201300	2.44248200
N	-1.87222600	-0.00029600	-0.00272800

[Ru(Trpy)(bpy)$^{2+}$

Ru	0.04515700	-0.00012100	-0.63895400
N	-0.33379000	2.04682100	-0.55646500
N	-0.33560900	-2.04676400	-0.55643000
N	2.08973100	-0.00091500	-0.88739800
N	0.64094500	-0.00026400	1.25152800
C	-2.55993300	-1.19304600	-0.21478400
C	-2.55888300	1.19504900	-0.21487000
C	-3.94130300	1.21255900	-0.02169400
H	-4.47703300	2.15870900	0.04768600
C	-4.63018100	0.00192600	0.07386300
H	-5.71071700	0.00240400	0.22187000
C	-3.94237800	-1.20931900	-0.02165300
H	-4.47895700	-2.15498300	0.04776400
C	-1.66850600	-2.35338000	-0.32546900
C	-2.09158100	-3.67772900	-0.20317700
H	-3.14446500	-3.89597900	-0.02294200
C	-1.16447200	-4.71236900	-0.30463500
H	-1.48756900	-5.74976600	-0.20809100
C	0.17720800	-4.40192000	-0.52723200
H	0.93283300	-5.18369400	-0.60778200
C	0.55370200	-3.06821200	-0.64622000
H	1.59071900	-2.78175300	-0.82517000
C	-1.66644900	2.35459900	-0.32566600

C	-2.08842000	3.67932500	-0.20363100
H	-3.14114300	3.89850000	-0.02357500
C	-1.16041800	4.71316400	-0.30511800
H	-1.48264800	5.75084800	-0.20877200
C	0.18102600	4.40154500	-0.52749400
H	0.93732700	5.18266300	-0.60804900
C	0.55639900	3.06750100	-0.64628000
H	1.59318900	2.78013600	-0.82508200
C	2.75208200	-0.00144100	-2.07409900
H	2.12294300	-0.00150300	-2.96633500
C	4.13887500	-0.00185700	-2.15107600
H	4.62517900	-0.00228800	-3.12673000
C	4.88788800	-0.00169300	-0.97062200
H	5.97824200	-0.00197000	-1.00333500
C	4.22409800	-0.00117500	0.25184000
H	4.78965900	-0.00104700	1.18323000
C	2.82644200	-0.00083800	0.27539000
C	2.00723600	-0.00048000	1.48080400
C	2.51046800	-0.00045400	2.78446700
H	3.58805300	-0.00063100	2.94340400
C	1.64271900	-0.00022000	3.87024800
H	2.03326900	-0.00019400	4.88840200
C	0.26706500	-0.00003800	3.63187000
H	-0.45107400	0.00012400	4.45201000
C	-0.20046800	-0.00006400	2.32554300
H	-1.26714400	0.00006400	2.10865900
N	-1.89711700	0.00070600	-0.31051900

$[Ru(Trpy)(bpy)(H_2)]^{2+}$

Ru	0.04116200	-0.00315400	-0.68583100
N	-0.33586400	2.05682200	-0.54893000
N	-0.35488200	-2.05732500	-0.54582800
N	2.10277000	-0.01209900	-0.87579300
N	0.65227800	-0.00255300	1.29181400
C	-2.56978900	-1.18295900	-0.20606900
C	-2.55876400	1.20162500	-0.20796100
C	-3.93485800	1.22585500	0.02739100
H	-4.46165900	2.17442900	0.12517100
C	-4.62755400	0.01917900	0.13608400

H	-5.70331000	0.02433800	0.31532100
C	-3.94631600	-1.19390800	0.02911600
H	-4.48192800	-2.13733000	0.12868000
C	-1.68521300	-2.34951000	-0.30290500
C	-2.11266800	-3.66935300	-0.14486600
H	-3.16473200	-3.87930400	0.04846100
C	-1.18975300	-4.70884200	-0.22652000
H	-1.51588400	-5.74238800	-0.10239400
C	0.15127300	-4.40932900	-0.46538300
H	0.90373000	-5.19526500	-0.53206700
C	0.53128800	-3.07969000	-0.61849900
H	1.56765100	-2.80003400	-0.81168300
C	-1.66384500	2.36048300	-0.30807500
C	-2.08096600	3.68433800	-0.15668700
H	-3.13150000	3.90369400	0.03445200
C	-1.14970600	4.71613400	-0.24292000
H	-1.46787600	5.75281800	-0.12446000
C	0.18895100	4.40498600	-0.47937500
H	0.94763300	5.18460200	-0.54950900
C	0.55841000	3.07146900	-0.62576500
H	1.59254300	2.78253100	-0.81716400
C	2.78348200	-0.02064500	-2.05432500
H	2.17037200	-0.02431900	-2.95613600
C	4.17063000	-0.02484000	-2.11620500
H	4.66596800	-0.03214400	-3.08727300
C	4.90649700	-0.01939100	-0.92881900
H	5.99717400	-0.02196000	-0.94803900
C	4.22659100	-0.01097000	0.28412400
H	4.78201600	-0.00706600	1.22138100
C	2.82811500	-0.00810900	0.29430500
C	2.01186100	-0.00172000	1.50668000
C	2.53053700	0.00427000	2.80531200
H	3.60808600	0.00477400	2.96102800
C	1.66841400	0.00999900	3.89610600
H	2.06790500	0.01510900	4.91108300
C	0.29112700	0.00906700	3.67195000
H	-0.41875500	0.01311600	4.49895200
C	-0.18001000	0.00248900	2.36518500
H	-1.24879000	0.00105900	2.15225300
N	-1.90935600	0.00614500	-0.34259400

H	-0.27267900	0.41749100	-2.36099700
H	-0.21809700	-0.41605200	-2.37248700

[Ru(Trpy)(bpy)(H)]$^{1+}$

Ru	-0.00871400	0.00049600	-0.65216100
N	-0.38840300	2.03154600	-0.57710000
N	-0.38792000	-2.03073200	-0.57904100
N	2.05295000	0.00106500	-0.90569700
N	0.75145500	-0.00092200	1.35767600
C	-2.59320200	-1.19582300	-0.15575100
C	-2.59349400	1.19569800	-0.15469600
C	-3.96433000	1.20838900	0.10938000
H	-4.49332000	2.15576900	0.21347100
C	-4.65195900	-0.00048700	0.23455300
H	-5.72392700	-0.00070200	0.43550600
C	-3.96402900	-1.20908900	0.10836500
H	-4.49279500	-2.15668500	0.21165200
C	-1.71089500	-2.34981500	-0.29788400
C	-2.12051200	-3.67945800	-0.15630000
H	-3.16476400	-3.90019800	0.06731200
C	-1.19647100	-4.70959700	-0.29287900
H	-1.50918800	-5.74890500	-0.18279700
C	0.13580200	-4.38914800	-0.57057800
H	0.89168100	-5.16700500	-0.68347800
C	0.49963100	-3.05587500	-0.70436200
H	1.52691900	-2.76447000	-0.92720600
C	-1.71148600	2.35004500	-0.29575800
C	-2.12146200	3.67945800	-0.15303500
H	-3.16578600	3.89973000	0.07072000
C	-1.19768000	4.70995500	-0.28867200
H	-1.51066800	5.74908600	-0.17770000
C	0.13469400	4.39009100	-0.56657000
H	0.89037700	5.16824600	-0.67874100
C	0.49888600	3.05703600	-0.70148400
H	1.52627400	2.76610000	-0.92448300
C	2.68514800	0.00254600	-2.11708600
H	2.02758400	0.00329400	-2.98619900
C	4.06547100	0.00309300	-2.25309000
H	4.50622600	0.00429900	-3.25049200

C	4.86650200	0.00212500	-1.10699700
H	5.95474400	0.00255700	-1.18314200
C	4.24681200	0.00063900	0.13645700
H	4.84595300	0.00000400	1.04670700
C	2.84959900	0.00013000	0.22374500
C	2.11755700	-0.00129400	1.48972000
C	2.72434200	-0.00296600	2.75249400
H	3.81046800	-0.00338600	2.83829800
C	1.93375000	-0.00421000	3.89616400
H	2.39693600	-0.00555800	4.88401600
C	0.54238200	-0.00373300	3.76006400
H	-0.11108600	-0.00465500	4.63290800
C	-0.00701300	-0.00208800	2.48400300
H	-1.08797100	-0.00171200	2.32950100
N	-1.92550000	0.00008600	-0.30279900
H	-0.26055000	0.00130500	-2.27085600

TS = [Ru(Trpy)(bpy)(H—H—NMe_3]$^{2+}$

Ru	0.17760600	0.01735100	-0.27117900
N	0.59044200	1.96601800	-0.86821100
N	-0.80358800	-1.54287600	0.70990000
N	1.83695400	-0.99576900	-0.98501300
N	1.50834700	0.19118200	1.31173700
C	-2.24915100	0.29348900	1.28571700
C	-1.44959200	2.33647200	0.34486500
C	-2.52828100	3.03218200	0.89461400
H	-2.62963200	4.10563900	0.73712800
C	-3.47445900	2.33552000	1.64849700
H	-4.32222600	2.86716400	2.08201200
C	-3.33509700	0.96211000	1.85522700
H	-4.06772600	0.41865200	2.45122100
C	-1.94261900	-1.13770400	1.38701600
C	-2.72047400	-2.05411400	2.09906400
H	-3.61831700	-1.71694500	2.61762700
C	-2.34182500	-3.39328300	2.14722300
H	-2.94404500	-4.11418000	2.70188800
C	-1.18297800	-3.79484200	1.48099400
H	-0.85119800	-4.83305600	1.49958800
C	-0.44523600	-2.84963500	0.77609900

H	0.45928800	-3.12252200	0.23034400
C	-0.34469200	2.89456100	-0.43996800
C	-0.20174400	4.25116300	-0.73952900
H	-0.95022500	4.96366200	-0.39164100
C	0.89827200	4.68568500	-1.47381700
H	1.01699300	5.74373500	-1.71129200
C	1.84372500	3.74977800	-1.89626600
H	2.72023300	4.05082400	-2.47048000
C	1.65913600	2.40878200	-1.57817300
H	2.36958700	1.64319300	-1.89266200
C	1.92619700	-1.60692500	-2.19953000
H	1.04415300	-1.52398400	-2.83587100
C	3.06025100	-2.29131700	-2.61431800
H	3.07527400	-2.76101400	-3.59808100
C	4.16371500	-2.36556700	-1.75969500
H	5.06776200	-2.89723200	-2.05970600
C	4.09046600	-1.75078100	-0.51497700
H	4.93727200	-1.79761100	0.16943300
C	2.92448500	-1.07346400	-0.14187200
C	2.74045200	-0.39865600	1.14146100
C	3.71359200	-0.33289800	2.14437400
H	4.68269100	-0.80660100	1.99318000
C	3.44069000	0.33776300	3.33115200
H	4.19528800	0.39194000	4.11716700
C	2.19133600	0.93831300	3.49776900
H	1.93905500	1.47603900	4.41176900
C	1.25594800	0.84757700	2.47492100
H	0.27095900	1.30552900	2.56849100
N	-1.33785100	0.98499700	0.53417000
H	-0.55036300	-0.07054800	-1.83177900
H	-1.27603800	-0.49640900	-1.58603900
N	-2.66384500	-1.14448900	-2.12445200
C	-2.69574000	-2.59758600	-1.90035100
H	-1.72438300	-3.03225000	-2.19219600
H	-2.87707900	-2.80435300	-0.83351700
H	-3.49486000	-3.08655400	-2.49474300
C	-3.88675500	-0.50059400	-1.62039400
H	-4.05976700	-0.80069200	-0.57491500
H	-3.77132000	0.59591800	-1.66660000
H	-4.77591900	-0.78749700	-2.21897100

C	-2.48993100	-0.85343000	-3.55687600
H	-2.43216800	0.23797500	-3.70370900
H	-1.55019100	-1.30937200	-3.91146600
H	-3.32913100	-1.25191200	-4.16053200

TS = [Ru(Trpy)(bpy)(H—CO_2]$^{1+}$

Ru	-0.04455300	0.02905600	-0.36221100
H	0.39185700	-0.11817000	-1.98323900
N	0.60968200	-1.88626000	0.09673000
N	0.03671600	2.08272800	-0.60996900
N	-2.03700500	-0.31666300	-0.79994100
N	-0.98202300	0.21510400	1.52175400
C	2.29255100	1.67132200	0.09605500
C	2.62470700	-0.65655600	0.52283100
C	3.95694700	-0.41875700	0.86611600
H	4.60471200	-1.24299700	1.16363000
C	4.45395100	0.88480900	0.81800900
H	5.49428900	1.08126200	1.07991000
C	3.62093100	1.93734400	0.43488900
H	4.00588500	2.95615800	0.39733100
C	1.27433900	2.63818600	-0.31577300
C	1.48591100	4.01644700	-0.41073400
H	2.46758600	4.43041500	-0.17950600
C	0.44422600	4.85450700	-0.79550700
H	0.60405900	5.93099000	-0.87027600
C	-0.80355100	4.29550300	-1.08136900
H	-1.64594600	4.91824400	-1.38356300
C	-0.96904100	2.91975500	-0.98009100
H	-1.92409200	2.44175800	-1.20203500
C	1.93164700	-1.94553800	0.51491600
C	2.51466500	-3.15938400	0.88864900
H	3.55493200	-3.18359500	1.21323300
C	1.76483100	-4.33076500	0.84667300
H	2.21407700	-5.28150900	1.13703300
C	0.43302600	-4.26885700	0.42921900
H	-0.18633400	-5.16490700	0.38283300
C	-0.10632400	-3.04163200	0.06448200
H	-1.13883400	-2.94846200	-0.27614900
C	-2.52441800	-0.57482200	-2.04783200

H	-1.78006600	-0.61184700	-2.84400300
C	-3.87240700	-0.78456400	-2.30155200
H	-4.20138300	-0.98676100	-3.32130000
C	-4.78457100	-0.73287700	-1.24321400
H	-5.84967400	-0.89554000	-1.41392500
C	-4.30910000	-0.46784200	0.03577200
H	-4.99940100	-0.42107000	0.87792200
C	-2.94049800	-0.26080500	0.24223800
C	-2.34429500	0.03195800	1.54441400
C	-3.06535200	0.12788800	2.74073800
H	-4.14487400	-0.01911700	2.74067300
C	-2.39906800	0.41082900	3.92756900
H	-2.95367700	0.48747100	4.86394700
C	-1.01398900	0.59437700	3.90159000
H	-0.45563300	0.81683300	4.81116600
C	-0.34374600	0.48931700	2.68929800
H	0.73679100	0.62628900	2.62243500
N	1.81416800	0.38397600	0.13736400
C	1.13831600	-1.34198700	-2.73115800
O	0.24229400	-2.04407400	-3.09709800
O	2.29735000	-1.05258000	-2.68262200

[Ru(Trpy)(bpy)(H-CO_2]$^{1+}$

Ru	0.06952400	-0.00648200	-0.35316900
N	-0.06444500	2.05641600	-0.52560100
N	-0.53916300	-1.95880400	0.02886900
N	2.06780800	-0.29226200	-0.79357500
N	0.93234200	0.15601200	1.49322600
C	-2.58284100	-0.79152100	0.51232700
C	-2.31308300	1.55391000	0.16182300
C	-3.65155300	1.77443700	0.49380500
H	-4.06698000	2.78146000	0.47841600
C	-4.45480000	0.68720100	0.84005200
H	-5.50243600	0.84643600	1.09814100
C	-3.92409400	-0.60381000	0.85214000
H	-4.55306800	-1.45378400	1.11484200
C	-1.85660800	-2.06499700	0.44418800
C	-2.41309000	-3.30771100	0.75312800
H	-3.45178400	-3.37328600	1.07646800

C	-1.63795300	-4.45961600	0.64398900
H	-2.06698300	-5.43354000	0.88362000
C	-0.31153400	-4.34884300	0.22482600
H	0.32545900	-5.22783300	0.12548800
C	0.20125100	-3.09097400	-0.07329700
H	1.23076100	-2.95684900	-0.40851900
C	-1.31902300	2.56248900	-0.22216500
C	-1.57405400	3.93404900	-0.28443600
H	-2.56873200	4.31290900	-0.04934200
C	-0.55613500	4.81288700	-0.64533000
H	-0.74986900	5.88522300	-0.69515700
C	0.70860400	4.30182200	-0.93928700
H	1.53176000	4.95764900	-1.22326600
C	0.91688500	2.92868300	-0.87077200
H	1.88700300	2.48573800	-1.10043900
C	2.57205500	-0.54615200	-2.03211000
H	1.83335500	-0.63197200	-2.83197600
C	3.93162700	-0.70305100	-2.26642300
H	4.28278000	-0.90384400	-3.27889900
C	4.82614200	-0.60272900	-1.19667600
H	5.89907200	-0.72164500	-1.35374600
C	4.32610500	-0.35264600	0.07676700
H	5.00220200	-0.27682900	0.92819800
C	2.94823800	-0.20080500	0.26118600
C	2.30671200	0.05576800	1.54605400
C	2.98941000	0.18988900	2.75926000
H	4.07595900	0.11146200	2.77862300
C	2.28114400	0.42254200	3.93239900
H	2.80843400	0.52912700	4.88131500
C	0.88885200	0.51728600	3.87433800
H	0.29572500	0.69753400	4.77095900
C	0.25026600	0.38164000	2.64887400
H	-0.83381800	0.45165600	2.56264100
N	-1.80407900	0.28398600	0.17878900
C	-1.06420700	-0.77950200	-2.69876500
H	-0.39231400	0.03961200	-2.12135200
O	-2.25677600	-0.46115200	-2.74928800
O	-0.38356600	-1.68546400	-3.19370200

[Ru(Trpy)(bpy)(O-COH)]$^{1+}$

Ru	-0.08682500	0.04572400	-0.38754200
N	0.38218700	-1.97180700	-0.36937800
N	0.18379000	2.09259900	-0.22148100
N	-2.11129700	-0.02772100	-0.83357300
N	-0.90973800	-0.11204000	1.47668700
C	2.37378500	1.33163900	0.40243800
C	2.46862700	-1.05456000	0.38467600
C	3.79726000	-1.02174500	0.80799000
H	4.34892700	-1.94898900	0.96220400
C	4.41650200	0.21247900	1.01996700
H	5.45715600	0.25049200	1.34408000
C	3.70650200	1.39657700	0.81671100
H	4.18667400	2.36136800	0.98008600
C	1.46838600	2.45562000	0.15377800
C	1.82860300	3.80046100	0.27396200
H	2.84579400	4.06444600	0.56363200
C	0.88952500	4.79482000	0.01681000
H	1.16488500	5.84659000	0.10666800
C	-0.40418400	4.42633100	-0.35868300
H	-1.16699500	5.17616400	-0.56919800
C	-0.71821000	3.07670500	-0.46881900
H	-1.71391700	2.74407500	-0.76543000
C	1.66856300	-2.24044400	0.07440700
C	2.13100700	-3.55298300	0.18669800
H	3.14754500	-3.73954000	0.53338500
C	1.29388500	-4.61436400	-0.14664300
H	1.64955100	-5.64215800	-0.06184300
C	-0.00133600	-4.34220400	-0.59078800
H	-0.68632300	-5.14597200	-0.86150100
C	-0.42024400	-3.01980500	-0.68799500
H	-1.42290800	-2.76119200	-1.03147300
C	-2.65887800	0.03289700	-2.07842300
H	-1.94390400	0.10825000	-2.89890100
C	-4.02980600	0.00442100	-2.29561000
H	-4.41411400	0.05609200	-3.31469900
C	-4.89362600	-0.08641200	-1.20053200
H	-5.97509900	-0.10496000	-1.34230700
C	-4.35172000	-0.15263100	0.07816300
H	-5.00636800	-0.21935200	0.94662500

C	-2.96283000	-0.12678700	0.24564300
C	-2.28695400	-0.19442500	1.53874500
C	-2.94620000	-0.33510700	2.76470800
H	-4.03293700	-0.40839300	2.79051600
C	-2.21614800	-0.38671500	3.94625000
H	-2.72574700	-0.49840000	4.90418200
C	-0.82390200	-0.29284800	3.88231900
H	-0.21225400	-0.32469300	4.78427900
C	-0.20965000	-0.15853900	2.64515200
H	0.87407100	-0.08242200	2.55820200
N	1.77853200	0.11507700	0.19262700
C	1.39409900	-0.02936500	-3.05509100
H	1.34595900	0.23169500	-4.13527800
O	0.31122100	0.28866900	-2.43767300
O	2.40848700	-0.56189400	-2.59864900

TS = [Ru(Trpy)(bpy)(H--H-OCHO)]$^{1+}$

Ru	0.09778200	0.05137400	-0.38321000
N	0.63036400	2.02017300	-0.78925000
N	-1.08756800	-1.53835800	0.25793600
N	1.91793100	-0.87459500	-0.74255600
N	0.99848800	0.09969800	1.49548600
C	-2.63627700	0.26918800	0.55646300
C	-1.63228300	2.34911300	-0.04782300
C	-2.80479400	3.02987500	0.28655300
H	-2.86482500	4.11246000	0.17868800
C	-3.90256500	2.30801000	0.75855000
H	-4.82413100	2.82961900	1.01980500
C	-3.82166400	0.92221900	0.90047600
H	-4.67353600	0.35587900	1.27600400
C	-2.36005500	-1.16572000	0.65299500
C	-3.28797700	-2.11507100	1.08800300
H	-4.28711700	-1.79865800	1.38808900
C	-2.93472600	-3.46028600	1.12266700
H	-3.65611600	-4.20924500	1.45245600
C	-1.64782100	-3.83427500	0.72997300
H	-1.33284500	-4.87779000	0.74515400
C	-0.75625200	-2.85316800	0.31117500
H	0.25671000	-3.09954600	-0.01008700

C	-0.38079700	2.93454300	-0.53782300
C	-0.18145100	4.30184100	-0.74361200
H	-0.99097600	5.00392900	-0.54417900
C	1.05061800	4.76205300	-1.19966700
H	1.21237600	5.82849700	-1.36261200
C	2.07019200	3.84070900	-1.44297700
H	3.04968100	4.16158000	-1.79832600
C	1.82633900	2.48868400	-1.22857100
H	2.59263000	1.73466000	-1.41257400
C	2.35373400	-1.31877800	-1.95525800
H	1.65843400	-1.18933200	-2.78454200
C	3.60212300	-1.89650800	-2.14069800
H	3.89548200	-2.23274400	-3.13558300
C	4.46148600	-2.03343300	-1.04744500
H	5.44933700	-2.48092200	-1.16495300
C	4.03778600	-1.58183000	0.19714100
H	4.69534600	-1.66614100	1.06191100
C	2.76900000	-1.00901500	0.33509900
C	2.23691500	-0.49174000	1.59472800
C	2.89969600	-0.57110300	2.82493300
H	3.87254800	-1.05700200	2.89039200
C	2.30972200	-0.03645800	3.96470000
H	2.81992100	-0.09712900	4.92700600
C	1.05911700	0.57564000	3.85696500
H	0.56431600	1.00997100	4.72574200
C	0.43631300	0.62315700	2.61663900
H	-0.54236500	1.08803900	2.49268000
N	-1.56925200	0.98591700	0.08205600
H	-0.44072300	0.08046600	-2.01612600
H	-0.57431600	-0.81160700	-2.15604600
C	-2.06563200	-2.31279900	-2.68086900
H	-2.31495200	-3.35990500	-2.97390900
O	-0.81148400	-2.04525200	-2.76256800
O	-2.97620200	-1.55280600	-2.32460300

-------Optimized geometries for catalytic system of 1-----

[Ru(Bid)(bpy)(Cl)]

Ru	-0.40593600	0.15874700	-0.41870300
Cl	-0.06020000	0.60043600	-2.84299000
N	1.58879200	-0.02435500	-0.20820800
N	1.83146500	-2.45591100	-0.18673000
N	-0.50270400	-1.91716600	-0.77415100
N	2.25432300	2.32470600	-0.09973400
N	-0.21064500	2.21816300	-0.06874900
N	-2.46607200	0.27164300	-0.47073900
N	-0.86759400	-0.24000600	1.51657500
C	2.27903200	-1.21963200	-0.13223300
C	3.71207300	-0.91845000	0.04082500
C	3.83864900	0.47752200	0.03872700
C	2.47988600	1.03080400	-0.10720500
C	4.82271700	-1.74210600	0.17345000
H	4.71953100	-2.82950800	0.17304000
C	6.07862100	-1.13214300	0.30711800
H	6.97183500	-1.75148000	0.41476200
C	6.20532500	0.26497800	0.30355800
H	7.19525300	0.71470700	0.40662900
C	5.07863600	1.08938100	0.16908000
H	5.17111700	2.17767400	0.16499900
C	1.00233300	2.89953800	-0.08292700
C	1.02618400	4.31766500	-0.01784200
H	2.00677700	4.79043600	-0.05738300
C	-0.13106400	5.05560900	0.11481000
H	-0.09845600	6.14551200	0.16741300
C	-1.34666800	4.36238900	0.20041700
H	-2.29484200	4.88435700	0.33159900
C	-1.33743400	2.98240400	0.10542000
H	-2.27422800	2.43407300	0.15961400
C	0.53390000	-2.80093300	-0.49125800
C	0.31514800	-4.20294300	-0.56105500
H	1.16006100	-4.84096300	-0.30496300
C	-0.89543900	-4.72673500	-0.96132100
H	-1.04904700	-5.80621700	-1.01516200
C	-1.91297700	-3.83209600	-1.32305900
H	-2.87972200	-4.18154000	-1.68620200

C	-1.67639600	-2.47353800	-1.21640900
H	-2.45152800	-1.76877200	-1.50680000
C	-3.23600100	0.63744400	-1.53465100
H	-2.67827300	0.93820600	-2.42423500
C	-4.62344500	0.61238100	-1.50358500
H	-5.18780500	0.91105100	-2.38769500
C	-5.27323600	0.19425500	-0.33745400
H	-6.36233200	0.15442800	-0.28791400
C	-4.50623700	-0.16485800	0.76527400
H	-4.99155200	-0.48320900	1.68751200
C	-3.10965100	-0.11184100	0.68915600
C	-2.21062000	-0.40162700	1.80411200
C	-2.63483700	-0.77442000	3.08484400
H	-3.69755200	-0.90519100	3.28840700
C	-1.70210200	-0.97498200	4.09576900
H	-2.02622400	-1.26978300	5.09476200
C	-0.34688800	-0.78544800	3.80918500
H	0.41753100	-0.92253800	4.57450700
C	0.03121700	-0.42221900	2.52454400
H	1.07672900	-0.26545400	2.25927500

$[Ru(Bid)(bpy)(H_2)]^{1+}$

Ru	-0.45782700	0.03713400	-0.67020100
N	1.56588700	0.00463400	-0.46658700
N	1.97964800	-2.40375600	-0.34583800
N	-0.43558400	-2.08282300	-0.74676400
N	2.05884500	2.39585600	-0.32356600
N	-0.37991100	2.15388400	-0.62877100
N	-2.53989200	0.04532100	-0.53248800
N	-0.74917700	-0.04022100	1.38202200
C	2.33293400	-1.14147300	-0.32870300
C	3.73193700	-0.73322800	-0.10548800
C	3.75564000	0.66636300	-0.10122800
C	2.37064300	1.12287100	-0.31779700
C	4.89093200	-1.47563900	0.08092800
H	4.86650800	-2.56748700	0.07802900
C	6.09064800	-0.77572900	0.27068700
H	7.02116500	-1.32800100	0.41836500
C	6.11438800	0.62722300	0.27457400

H	7.06298400	1.14709500	0.42469800
C	4.93893800	1.36819900	0.08934900
H	4.95105300	2.46024300	0.09254200
C	0.78461800	2.89741900	-0.48400400
C	0.73265400	4.31514000	-0.48897700
H	1.68127400	4.83650700	-0.37004000
C	-0.45738900	4.99524400	-0.63857900
H	-0.48240100	6.08651800	-0.64179400
C	-1.62953400	4.24385400	-0.78856100
H	-2.60226200	4.71907500	-0.91554300
C	-1.54440100	2.86318700	-0.77877400
H	-2.44616800	2.27144000	-0.90771300
C	0.69629800	-2.86394600	-0.55104700
C	0.59912900	-4.27929800	-0.56450900
H	1.52260400	-4.83141800	-0.39674900
C	-0.60120300	-4.91998000	-0.78705700
H	-0.66143100	-6.00979400	-0.79540700
C	-1.73592000	-4.13054400	-1.01148000
H	-2.71225300	-4.57352900	-1.20837400
C	-1.60828900	-2.75350600	-0.98374600
H	-2.47944600	-2.13205900	-1.17096100
C	-3.41860400	0.10096500	-1.57387900
H	-2.97225400	0.14879200	-2.56797200
C	-4.79566600	0.09927700	-1.40070200
H	-5.44732000	0.14556900	-2.27335000
C	-5.31779800	0.03960700	-0.10649800
H	-6.39520300	0.03811800	0.06340200
C	-4.43800900	-0.01600900	0.96812200
H	-4.82233500	-0.05991900	1.98609600
C	-3.05743900	-0.01391400	0.74114400
C	-2.05746600	-0.06704300	1.80816600
C	-2.37261100	-0.13521200	3.16934000
H	-3.41399500	-0.15916900	3.48763300
C	-1.35411000	-0.17172500	4.11494600
H	-1.59217900	-0.22335800	5.17821200
C	-0.02905000	-0.13986400	3.67931200
H	0.80042800	-0.16436300	4.38609400
C	0.23571900	-0.07613300	2.31700700
H	1.25777900	-0.04881900	1.94208400
H	0.09973200	0.05891200	-2.31901200

H	-0.73253800	0.16484200	-2.38268200

[Ru(Bid)(bpy)(H)]

Ru	-0.39860400	0.20758900	-0.62877300
H	-0.19338100	0.49137900	-2.23839600
N	1.59807800	0.01354200	-0.42371600
N	1.82269500	-2.42221600	-0.37039900
N	-0.50936900	-1.86972800	-0.95467300
N	2.27784600	2.35902200	-0.29622000
N	-0.18738000	2.26863900	-0.31739500
N	-2.45599200	0.32412200	-0.60853200
N	-0.88208100	-0.22834300	1.43776900
C	2.27749000	-1.18690400	-0.31211300
C	3.70505100	-0.89617700	-0.09254500
C	3.84202400	0.49954500	-0.09298200
C	2.49408800	1.06095400	-0.28889800
C	4.80455400	-1.72742200	0.08293200
H	4.69273800	-2.81404500	0.08226400
C	6.05986300	-1.12692500	0.26028300
H	6.94382900	-1.75284800	0.40164900
C	6.19702600	0.26925900	0.25836600
H	7.18598600	0.71213000	0.39594300
C	5.08174800	1.10170000	0.08177600
H	5.18271700	2.18934200	0.07993500
C	1.03408300	2.94389200	-0.31610400
C	1.06888100	4.36437100	-0.27333400
H	2.05500300	4.82648000	-0.30545200
C	-0.08151500	5.11528100	-0.16870100
H	-0.04016200	6.20556800	-0.13175500
C	-1.30521900	4.43204400	-0.08904300
H	-2.25042900	4.96386300	0.02415600
C	-1.30833400	3.05234400	-0.16592000
H	-2.25104000	2.51395500	-0.12044400
C	0.52716000	-2.76110700	-0.67838900
C	0.30143500	-4.16375400	-0.74270600
H	1.14874900	-4.80293200	-0.49707100
C	-0.91702000	-4.68573800	-1.11712900
H	-1.07538200	-5.76485500	-1.16493400
C	-1.94044000	-3.78690700	-1.45693500
H	-2.91768200	-4.13399200	-1.79374200

C	-1.69613700	-2.42983700	-1.36491000
H	-2.47373600	-1.72326400	-1.64393900
C	-3.24101300	0.69234600	-1.66760000
H	-2.69677700	0.98565400	-2.56559600
C	-4.62687400	0.69057500	-1.62793400
H	-5.19063300	0.99100300	-2.51192300
C	-5.27570700	0.29550900	-0.45296000
H	-6.36472200	0.27528900	-0.39251100
C	-4.50175800	-0.06507700	0.64319600
H	-4.98418200	-0.36399900	1.57334000
C	-3.10376500	-0.04084800	0.56011100
C	-2.22560300	-0.36631400	1.68941300
C	-2.69075500	-0.77090600	2.94869200
H	-3.75891100	-0.88149800	3.13325600
C	-1.78091800	-1.03575500	3.96653000
H	-2.13357500	-1.35515300	4.94861100
C	-0.41470000	-0.88596600	3.71224900
H	0.32898900	-1.08158200	4.48527100
C	-0.01045000	-0.48450300	2.44475300
H	1.04544900	-0.35176200	2.19889300

Ts3N-Bid-Ru-H2-NMe3

TS = [Ru(Bid)(bpy)(H--CO2)]

Ru	-0.39165800	0.18761400	-0.35592500
H	-0.04068000	0.34579800	-1.99814900
N	1.59674400	0.07556900	-0.04651700
N	1.89546900	-2.33424400	0.24138800
N	-0.44755800	-1.92324400	-0.41222000
N	2.22211300	2.43127200	-0.24826400
N	-0.24005800	2.27914700	-0.26200200
N	-2.44334500	0.27698200	-0.52438200
N	-1.02458100	0.01358400	1.66516400
C	2.31274200	-1.08787000	0.16942900
C	3.73785800	-0.73945200	0.31068800
C	3.83685100	0.64806300	0.13879700
C	2.46892400	1.15042700	-0.08050700
C	4.86390000	-1.51794800	0.54761100

H	4.78233000	-2.59915600	0.67960900
C	6.10652200	-0.87046500	0.61208800
H	7.01114600	-1.45344400	0.79883700
C	6.20538600	0.51810600	0.43880600
H	7.18545400	0.99734900	0.49182200
C	5.06357900	1.29686100	0.19943400
H	5.13415300	2.37828600	0.06315900
C	0.96274800	2.98111700	-0.31596400
C	0.96187100	4.39920600	-0.39794400
H	1.93605200	4.88201300	-0.46607600
C	-0.20836600	5.12629800	-0.36290900
H	-0.19432500	6.21643700	-0.41879000
C	-1.41454100	4.42234900	-0.23106800
H	-2.37342000	4.93772000	-0.16983200
C	-1.38238800	3.04082000	-0.18708500
H	-2.31189600	2.48543300	-0.09695300
C	0.60910100	-2.74277400	-0.02120400
C	0.42229100	-4.14794300	0.08677500
H	1.28542400	-4.72896800	0.40919800
C	-0.78007600	-4.74491600	-0.22255700
H	-0.90801700	-5.82589800	-0.13934100
C	-1.82697100	-3.92357200	-0.66814700
H	-2.79389800	-4.33549900	-0.95770400
C	-1.61954400	-2.55922500	-0.74542700
H	-2.41748400	-1.91505000	-1.10591200
C	-3.13165000	0.48821200	-1.68509100
H	-2.51427600	0.64604100	-2.57028800
C	-4.51742200	0.49325900	-1.75389100
H	-5.00836600	0.66330800	-2.71271500
C	-5.25985300	0.27530700	-0.58878100
H	-6.35049300	0.26781400	-0.61246900
C	-4.58044200	0.07445200	0.60762200
H	-5.13775800	-0.08490800	1.53034000
C	-3.18126100	0.08317900	0.62928200
C	-2.38409500	-0.08328500	1.84784700
C	-2.92936400	-0.31115100	3.11821600
H	-4.00841900	-0.39364800	3.24650100
C	-2.08659500	-0.43993500	4.21696800
H	-2.50225000	-0.62092200	5.20950000
C	-0.70558100	-0.33567300	4.02951700

H	-0.01282800	-0.43162400	4.86592500
C	-0.21651700	-0.11215000	2.74801200
H	0.85346400	-0.02557000	2.54962000
C	0.26912200	-0.94152300	-3.06393600
O	1.44673200	-1.10171000	-2.97433000
O	-0.80546000	-1.15236900	-3.53657400

[Ru(Bid)(bpy)(H-CO_2)]

Ru	-0.44716500	0.08920700	-0.32607200
N	1.54498300	-0.05663100	-0.02075400
N	1.86491400	-2.47481400	-0.17800700
N	-0.48443800	-1.98075100	-0.74857400
N	2.15829600	2.29958100	0.20567400
N	-0.30045400	2.15822700	0.06025800
N	-2.49389600	0.19813900	-0.49894900
N	-1.02328200	-0.32071800	1.57570000
C	2.26855700	-1.23586000	-0.01309000
C	3.68779400	-0.91011600	0.21726800
C	3.77607900	0.48433300	0.30926900
C	2.40863400	1.01243900	0.15781400
C	4.81631400	-1.71265200	0.32468300
H	4.74311100	-2.79975900	0.24925200
C	6.05083300	-1.08054800	0.53190300
H	6.95797100	-1.68207700	0.62225800
C	6.13905400	0.31671300	0.62276800
H	7.11352800	0.78397400	0.78054900
C	4.99465700	1.11910300	0.51089100
H	5.05715200	2.20739700	0.57720700
C	0.89862100	2.85548300	0.16144700
C	0.89885000	4.27064100	0.26565000
H	1.87340700	4.75360200	0.32199400
C	-0.27430400	4.99282400	0.30952400
H	-0.26056500	6.08136400	0.38965900
C	-1.48282800	4.28501200	0.26340300
H	-2.44587100	4.79333200	0.31395200
C	-1.44772400	2.90789100	0.14283600
H	-2.38012100	2.35284000	0.10204200
C	0.58494600	-2.84178600	-0.52636600
C	0.42286400	-4.24193700	-0.70062200
H	1.29602000	-4.86034700	-0.49738100

C	-0.77075500	-4.78563200	-1.12297900
H	-0.88015300	-5.86359500	-1.25562000
C	-1.83201900	-3.91128000	-1.39554300
H	-2.79362300	-4.27379800	-1.75910500
C	-1.64763800	-2.55506400	-1.19937900
H	-2.45922500	-1.86728500	-1.42056000
C	-3.18560400	0.55643300	-1.61724900
H	-2.57329800	0.84067100	-2.47546700
C	-4.57283000	0.56022600	-1.67055400
H	-5.07630000	0.85289200	-2.59235800
C	-5.29983300	0.18216600	-0.53735600
H	-6.39050300	0.16782800	-0.55347900
C	-4.61073300	-0.16876000	0.61899400
H	-5.15810600	-0.45406900	1.51714600
C	-3.21227500	-0.14801300	0.62579700
C	-2.38142300	-0.44538300	1.79125700
C	-2.87814200	-0.80239000	3.04929800
H	-3.95296300	-0.90079000	3.19958800
C	-2.00051500	-1.02909000	4.10374900
H	-2.38179100	-1.31055800	5.08615500
C	-0.62821600	-0.88683000	3.88344000
H	0.09325700	-1.04937200	4.68428000
C	-0.17608800	-0.53549800	2.61862700
H	0.88509200	-0.41401600	2.40192600
C	0.53115700	0.84142200	-2.79031100
H	-0.27290500	0.24081300	-2.15807100
O	0.15269700	1.98495000	-3.08942200
O	1.51651500	0.15899200	-3.10623700

[Ru(Bid)(bpy)(O-COH)]

Ru	-0.42608800	0.07089000	-0.28802600
N	1.55704700	0.03214200	0.09315400
N	1.99038000	-2.37641700	0.11400600
N	-0.40799500	-2.05477200	-0.37227500
N	2.07073900	2.42335800	0.11774900
N	-0.37230800	2.17217000	-0.13921600
N	-2.43418400	0.10841300	-0.67706600
N	-1.16563300	-0.10951800	1.54105100
C	2.33696700	-1.11243300	0.16964700

C	3.74444400	-0.70558800	0.33241000
C	3.76900300	0.69417200	0.32226800
C	2.37620500	1.14788300	0.16387000
C	4.91240000	-1.44642900	0.46255100
H	4.88826600	-2.53835500	0.46488300
C	6.12048500	-0.74575300	0.58824800
H	7.05724100	-1.29748500	0.69344300
C	6.14472900	0.65716100	0.57879500
H	7.09976400	1.17797700	0.67686100
C	4.96129500	1.39671300	0.44356400
H	4.97363500	2.48878800	0.43208300
C	0.79259400	2.92069900	0.00827900
C	0.73205200	4.33797400	0.07239200
H	1.68304800	4.85882700	0.17528300
C	-0.46645600	5.01575400	0.02319400
H	-0.49834600	6.10542000	0.07869800
C	-1.64148100	4.26073800	-0.09246900
H	-2.62360500	4.73242800	-0.13004800
C	-1.54862100	2.88351900	-0.16749600
H	-2.45694400	2.29711100	-0.26730900
C	0.71319500	-2.83625000	-0.11485900
C	0.61322600	-4.25258700	-0.10523800
H	1.53042600	-4.80234800	0.10118000
C	-0.57949700	-4.89621800	-0.35457200
H	-0.64126600	-5.98604600	-0.34794300
C	-1.70541100	-4.10803400	-0.62753800
H	-2.67562600	-4.55292100	-0.84957600
C	-1.57544000	-2.73114900	-0.62484500
H	-2.44054000	-2.11666300	-0.85628800
C	-2.99620500	0.25091500	-1.90749200
H	-2.28969200	0.34507000	-2.73487300
C	-4.37210400	0.27069900	-2.09836900
H	-4.77509900	0.38677200	-3.10473000
C	-5.21759400	0.13917000	-0.99172600
H	-6.30125800	0.15087000	-1.11552500
C	-4.65762400	-0.00699700	0.27420900
H	-5.29613000	-0.10878100	1.15169200
C	-3.26746700	-0.01929300	0.41378600
C	-2.54399800	-0.15802000	1.67196600
C	-3.14077300	-0.33071500	2.92424800

H	-4.22757500	-0.36946600	2.99995300
C	-2.35002900	-0.45801500	4.06045200
H	-2.80962900	-0.59615300	5.03985600
C	-0.95962000	-0.40918800	3.92277000
H	-0.30249700	-0.50782500	4.78689500
C	-0.40198900	-0.23702300	2.66410900
H	0.67584600	-0.19603700	2.51110300
C	1.04755300	-0.00151400	-3.50834800
H	1.52529100	0.17584800	-4.50749900
O	0.45101000	0.99413000	-3.01060200
O	1.16739400	-1.15099800	-3.02560500

TS = [Ru(Bid)(bpy)(O--COH)]

Ru	-0.42608800	0.07089000	-0.28802600
N	1.55704700	0.03214200	0.09315400
N	1.99038000	-2.37641700	0.11400600
N	-0.40799500	-2.05477200	-0.37227500
N	2.07073900	2.42335800	0.11774900
N	-0.37230800	2.17217000	-0.13921600
N	-2.43418400	0.10841300	-0.67706600
N	-1.16563300	-0.10951800	1.54105100
C	2.33696700	-1.11243300	0.16964700
C	3.74444400	-0.70558800	0.33241000
C	3.76900300	0.69417200	0.32226800
C	2.37620500	1.14788300	0.16387000
C	4.91240000	-1.44642900	0.46255100
H	4.88826600	-2.53835500	0.46488300
C	6.12048500	-0.74575300	0.58824800
H	7.05724100	-1.29748500	0.69344300
C	6.14472900	0.65716100	0.57879500
H	7.09976400	1.17797700	0.67686100
C	4.96129500	1.39671300	0.44356400
H	4.97363500	2.48878800	0.43208300
C	0.79259400	2.92069900	0.00827900
C	0.73205200	4.33797400	0.07239200
H	1.68304800	4.85882700	0.17528300
C	-0.46645600	5.01575400	0.02319400
H	-0.49834600	6.10542000	0.07869800
C	-1.64148100	4.26073800	-0.09246900
H	-2.62360500	4.73242800	-0.13004800

C	-1.54862100	2.88351900	-0.16749600
H	-2.45694400	2.29711100	-0.26730900
C	0.71319500	-2.83625000	-0.11485900
C	0.61322600	-4.25258700	-0.10523800
H	1.53042600	-4.80234800	0.10118000
C	-0.57949700	-4.89621800	-0.35457200
H	-0.64126600	-5.98604600	-0.34794300
C	-1.70541100	-4.10803400	-0.62753800
H	-2.67562600	-4.55292100	-0.84957600
C	-1.57544000	-2.73114900	-0.62484500
H	-2.44054000	-2.11666300	-0.85628800
C	-2.99620500	0.25091500	-1.90749200
H	-2.28969200	0.34507000	-2.73487300
C	-4.37210400	0.27069900	-2.09836900
H	-4.77509900	0.38677200	-3.10473000
C	-5.21759400	0.13917000	-0.99172600
H	-6.30125800	0.15087000	-1.11552500
C	-4.65762400	-0.00699700	0.27420900
H	-5.29613000	-0.10878100	1.15169200
C	-3.26746700	-0.01929300	0.41378600
C	-2.54399800	-0.15802000	1.67196600
C	-3.14077300	-0.33071500	2.92424800
H	-4.22757500	-0.36946600	2.99995300
C	-2.35002900	-0.45801500	4.06045200
H	-2.80962900	-0.59615300	5.03985600
C	-0.95962000	-0.40918800	3.92277000
H	-0.30249700	-0.50782500	4.78689500
C	-0.40198900	-0.23702300	2.66410900
H	0.67584600	-0.19603700	2.51110300
C	1.04755300	-0.00151400	-3.50834800
H	1.52529100	0.17584800	-4.50749900
O	0.45101000	0.99413000	-3.01060200
O	1.16739400	-1.15099800	-3.02560500

TS = [Ru(Bid)(bpy)(H--H--OCOH)]

Ru	0.42327000	0.14980400	-0.38167200
N	-1.59014800	0.09249900	-0.19180400
N	-2.16952000	2.41747400	-0.68747400

N	0.28993500	2.22695900	-0.73751500
N	-1.93705000	-2.22945000	0.49725900
N	0.45636700	-1.93786900	-0.02566100
N	2.49217300	0.21833100	-0.34944700
N	0.81476200	0.43883200	1.64560700
C	-2.43714400	1.17632000	-0.34905100
C	-3.81091500	0.74562600	-0.03231700
C	-3.74066100	-0.60445400	0.33309900
C	-2.32635000	-1.00622400	0.22086900
C	-5.01942300	1.43023700	-0.03603900
H	-5.06759700	2.48329500	-0.32182400
C	-6.17230100	0.72507000	0.33873400
H	-7.13867500	1.23395900	0.34662500
C	-6.10217100	-0.62761300	0.70426500
H	-7.01492200	-1.15387000	0.99234800
C	-4.87749200	-1.31124100	0.70405800
H	-4.81732300	-2.36466900	0.98616400
C	-0.64928300	-2.69235800	0.35045200
C	-0.52049500	-4.08633800	0.58909900
H	-1.42708100	-4.61473900	0.88075700
C	0.68398000	-4.73822500	0.43713000
H	0.76676400	-5.81253900	0.61264500
C	1.79492200	-3.98029300	0.04285200
H	2.77499700	-4.43434400	-0.10446600
C	1.63741600	-2.62212200	-0.16682000
H	2.48946100	-2.03145900	-0.48956200
C	-0.90590900	2.92511800	-0.88192300
C	-0.89480800	4.30547000	-1.21840700
H	-1.86629700	4.78449400	-1.33339000
C	0.28265900	5.00445400	-1.37198700
H	0.27657400	6.06591500	-1.62684900
C	1.48633300	4.31207100	-1.17781600
H	2.45297700	4.80804900	-1.26824400
C	1.44124700	2.96436200	-0.87163500
H	2.36935300	2.41775900	-0.73255100
C	3.31393400	0.16046300	-1.43763100
H	2.80815900	0.11547600	-2.40237000
C	4.69828100	0.15651200	-1.34064000
H	5.30085200	0.10452000	-2.24797000
C	5.29317800	0.21782100	-0.07672700

H	6.37855800	0.21077000	0.03184000
C	4.47487900	0.29715900	1.04455800
H	4.91651900	0.36099800	2.03874400
C	3.08334700	0.30169800	0.89521900
C	2.14239600	0.42185700	2.01008600
C	2.52522000	0.53566200	3.35186200
H	3.58011800	0.51081800	3.62294600
C	1.55529200	0.67969200	4.33771600
H	1.84525200	0.76562200	5.38590700
C	0.20997800	0.71604000	3.96305200
H	-0.58082700	0.83360600	4.70429500
C	-0.11975100	0.59330800	2.61920600
H	-1.15691900	0.61374500	2.28262200
H	0.55236400	-0.73737600	-2.38774400
H	0.11196700	0.03130900	-2.08024400
C	0.23001000	-2.71053400	-3.12527500
H	0.66215000	-3.64596800	-3.54994800
O	1.07710200	-1.73994500	-3.07782700
O	-0.95137400	-2.69273000	-2.76452800

-------Optimized geometries for catalytic system of 1d-----

[Ru(Bid)(4,4'-OMe_2Bpy)(Cl)]

Ru	-0.02289800	-0.50503000	-0.50550900
N	-2.01832600	-0.29373800	-0.37272600
N	-2.35413400	1.76272900	-1.65274200
N	0.01510700	1.10488400	-1.85705200
N	-2.59637200	-2.22233300	1.01484400
N	-0.13808500	-2.12577100	0.82338200
N	2.06146200	-0.57452500	-0.50309100
N	0.42786700	0.81540800	0.98963600
C	-2.75124900	0.74289200	-0.92184900
C	-4.16505000	0.56478000	-0.54552700
C	-4.23858400	-0.60844700	0.21822400
C	-2.86615900	-1.13515900	0.32658200
C	-5.30088800	1.31408800	-0.82594300
H	-5.23868200	2.22706100	-1.42238600
C	-6.52743500	0.86044300	-0.31900300
H	-7.43891900	1.42754800	-0.52068300
C	-6.60130300	-0.31477200	0.44381500

H	-7.56944600	-0.64760200	0.82459600
C	-5.44987300	-1.06579700	0.72206600
H	-5.50177300	-1.98189900	1.31473900
C	-1.33052200	-2.70897800	1.24569100
C	-1.31247100	-3.89521600	2.02828400
H	-2.28163400	-4.30483500	2.31049500
C	-0.13163600	-4.48537500	2.42289400
C	1.06896600	-3.87061900	2.03768400
H	2.03823300	-4.27501000	2.33059700
C	1.01668600	-2.72735800	1.26185200
H	1.94133600	-2.25062700	0.95007200
C	-1.06974100	1.93989800	-2.11200600
C	-0.91563700	3.08143400	-2.94522700
H	-1.80107600	3.69924900	-3.09034500
C	0.28456800	3.37702400	-3.55386000
C	1.36196500	2.50427500	-3.33964600
H	2.33011000	2.66344500	-3.81523700
C	1.18368700	1.41314900	-2.50929500
H	2.00680900	0.72211200	-2.34883900
C	2.85706600	-1.35582100	-1.28145200
H	2.32181300	-2.02873100	-1.95559100
C	4.24258900	-1.31920000	-1.25187100
H	4.80845900	-1.97612000	-1.90859800
C	4.87505400	-0.42453400	-0.36911900
C	4.07214500	0.38383200	0.44932100
H	4.56054900	1.07193900	1.13799500
C	2.68783300	0.29079600	0.37103000
C	1.76970000	1.07281700	1.20608000
C	2.19085700	1.99687800	2.15388600
H	3.24875300	2.19429200	2.31756600
C	1.25017600	2.69998900	2.92006600
C	-0.11450800	2.43605600	2.70529300
H	-0.89536500	2.94288800	3.26742300
C	-0.47049300	1.50098700	1.74631700
H	-1.51984900	1.27192600	1.55914000
H	0.38813600	4.25437200	-4.19513500
H	-0.13212600	-5.39621500	3.02473000
O	6.21828300	-0.26579200	-0.22618500
O	1.75501200	3.58776500	3.81732600
C	7.04231500	-1.11019800	-1.08048600
H	8.07461900	-0.84052300	-0.82279900

H	6.86709700	-2.17781800	-0.86539600
H	6.85160400	-0.89706200	-2.14584200
C	0.76424500	4.33008700	4.58502100
H	0.14945800	3.64993000	5.19818100
H	1.35527400	4.98840200	5.23454800
H	0.12335100	4.93317300	3.91992000
Cl	-0.34011700	-2.10697700	-2.38909300

$[Ru(Bid)(4,4'\text{-}OMe_2Bpy)]^+$

Ru	0.04510600	0.35636100	-0.73709400
N	2.05194600	0.25310400	-0.60537800
N	2.45285300	-2.07299000	-1.25258300
N	0.04074700	-1.61580000	-1.50680100
N	2.58498300	2.50594800	0.18701000
N	0.13079400	2.33180100	-0.02370100
N	-2.03793200	0.43672200	-0.82796800
N	-0.46140300	-0.39240200	1.03567200
C	2.81952000	-0.87825600	-0.85252700
C	4.22910300	-0.55358300	-0.57502100
C	4.26816600	0.78450500	-0.16289300
C	2.88208700	1.28081200	-0.17661900
C	5.38805600	-1.31526000	-0.66250400
H	5.35267300	-2.35797000	-0.98543400
C	6.60116200	-0.70144500	-0.32110600
H	7.53054500	-1.27249700	-0.37578400
C	6.64004400	0.63948400	0.09155200
H	7.59889700	1.09284200	0.35218200
C	5.46648600	1.40136100	0.17491700
H	5.48990800	2.44493500	0.49604000
C	1.31120700	3.01836700	0.26037900
C	1.27144700	4.36922100	0.69859400
H	2.23262300	4.84630100	0.88544100
C	0.08072300	5.03203800	0.89676900
C	-1.10831300	4.32782300	0.65752300
H	-2.08512100	4.78749200	0.81019800
C	-1.03763100	3.02162000	0.21410200
H	-1.95515900	2.47537700	0.02019500
C	1.16527600	-2.43466600	-1.57454100
C	1.05232000	-3.77466300	-2.03215700
H	1.97199300	-4.35745100	-2.05792100

C	-0.15542200	-4.30477200	-2.42910400
C	-1.28605500	-3.47708000	-2.37213400
H	-2.26963900	-3.83033200	-2.68259500
C	-1.14534800	-2.18086400	-1.91496900
H	-2.01349600	-1.52972900	-1.87973300
C	-2.78750000	0.92246100	-1.85067100
H	-2.22526800	1.31685200	-2.69939300
C	-4.17388000	0.93080100	-1.84906700
H	-4.70676500	1.33570100	-2.70607500
C	-4.85101800	0.40918900	-0.73047000
C	-4.09040500	-0.09224100	0.33850700
H	-4.60985000	-0.49353300	1.20727700
C	-2.70533900	-0.06680700	0.26708100
C	-1.80942200	-0.55843600	1.31377900
C	-2.23773100	-1.15598200	2.48973100
H	-3.29821300	-1.28943700	2.69925300
C	-1.30286400	-1.61537500	3.42928900
C	0.06457900	-1.43731400	3.15073100
H	0.83936000	-1.76461800	3.83960000
C	0.43561000	-0.83171000	1.96235200
H	1.48658600	-0.68112700	1.71899900
H	-0.22747900	-5.33504800	-2.78223600
H	0.06429600	6.06783900	1.24047900
O	-6.19829800	0.34304500	-0.58137400
O	-1.81482100	-2.20490000	4.53821200
C	-6.98083900	0.84317600	-1.70525500
H	-8.02486600	0.70075700	-1.39886200
H	-6.78107500	1.91387700	-1.87830200
H	-6.77175900	0.25974600	-2.61742500
C	-0.83222600	-2.71718500	5.48636300
H	-0.21230000	-1.89935900	5.88940600
H	-1.43204900	-3.16548400	6.28835500
H	-0.19820900	-3.48618700	5.01422500

$[Ru(Bid)(4,4'\text{-}OMe_2Bpy)(H_2)]^+$

Ru	-0.02019200	0.07708000	-0.96118000
N	1.99783300	0.05687700	-0.73526200
N	2.44306200	-2.34815300	-0.76306700

N	0.02106900	-2.03338000	-1.12799200
N	2.45496100	2.44231200	-0.44727200
N	0.02758500	2.18768800	-0.82384800
N	-2.11901100	0.06944800	-0.82692000
N	-0.32985200	-0.08284000	1.09229400
C	2.77919300	-1.08457300	-0.66048000
C	4.16997100	-0.67254600	-0.39708700
C	4.17331100	0.72459700	-0.30309300
C	2.78452800	1.17455700	-0.50940900
C	5.33794100	-1.40915100	-0.24566300
H	5.32931000	-2.49874700	-0.31919000
C	6.52535100	-0.70676200	0.00258500
H	7.46223100	-1.25455800	0.12482800
C	6.52873000	0.69333500	0.09688800
H	7.46808100	1.21564400	0.29053000
C	5.34469000	1.42842900	-0.05443700
H	5.34145400	2.51812300	0.01816900
C	1.17853200	2.93683000	-0.61056300
C	1.10926500	4.35290300	-0.54494200
H	2.04786800	4.87817800	-0.37438700
C	-0.08420000	5.02681200	-0.69425300
C	-1.24216200	4.27059700	-0.91623900
H	-2.21653700	4.74121200	-1.04829300
C	-1.14043400	2.89234300	-0.97244500
H	-2.02953400	2.29664500	-1.15799100
C	1.16518500	-2.81080700	-0.99416300
C	1.08673900	-4.22412700	-1.09893700
H	2.01990200	-4.77284900	-0.97990600
C	-0.10843300	-4.86623600	-1.34280700
C	-1.25830400	-4.08018100	-1.49220400
H	-2.23295900	-4.52423000	-1.69535300
C	-1.14792600	-2.70594200	-1.38063200
H	-2.03041500	-2.08532100	-1.50709500
C	-3.00460100	0.14513000	-1.85803100
H	-2.56481300	0.21672400	-2.85387800
C	-4.38045300	0.13597200	-1.69959000
H	-5.01728500	0.19907100	-2.57858900
C	-4.90852600	0.04441500	-0.39889500
C	-4.01102500	-0.03231600	0.67706900
H	-4.41632000	-0.10355400	1.68454300

C	-2.64233800	-0.02048700	0.44482100
C	-1.64154500	-0.10644100	1.51655300
C	-1.96933800	-0.20923500	2.86090100
H	-3.00523900	-0.22693300	3.19413300
C	-0.95564000	-0.29880400	3.82743500
C	0.38140900	-0.28125100	3.39425200
H	1.21326900	-0.34885300	4.09115500
C	0.64031400	-0.17199600	2.03734000
H	1.66762200	-0.15102800	1.67435800
H	0.55931500	0.17605400	-2.59279900
H	-0.27836100	0.25122800	-2.67011000
H	-0.12273500	6.11652000	-0.64410800
H	-0.15451800	-5.95395400	-1.42145400
O	-6.22593100	0.02227100	-0.07818900
O	-1.37044400	-0.39832300	5.11401200
C	-0.31011700	-0.52953200	6.10702700
H	0.32882800	0.36929400	6.11851800
H	-0.83968100	-0.62675900	7.06321200
H	0.29510800	-1.43100500	5.91565000
C	-7.14551700	0.09268700	-1.20859500
H	-8.14382100	0.04582100	-0.75570500
H	-7.02117100	1.04212500	-1.75535000
H	-6.99725700	-0.76492700	-1.88553300

[Ru(Bid)(4,4'-OMe_2Bpy)(H)]

Ru	0.04412800	0.50226800	-0.80631500
H	0.21795700	1.23853500	-2.27408200
N	2.04167100	0.30950600	-0.65166100
N	2.34298100	-1.99509600	-1.42292400
N	-0.02353600	-1.37671500	-1.74442100
N	2.64421800	2.47105300	0.32484600
N	0.18874000	2.38771000	0.09899400
N	-2.04329500	0.53847700	-0.71754500
N	-0.39267500	-0.50387600	1.07277200
C	2.75574800	-0.84273800	-0.93410600
C	4.16610700	-0.61897100	-0.57435600
C	4.25714600	0.68887800	-0.07586800
C	2.89906500	1.25706200	-0.11766600
C	5.28650900	-1.43676700	-0.65941200

H	5.21018100	-2.45469900	-1.04847400
C	6.51581000	-0.91342500	-0.23163600
H	7.41536900	-1.53071800	-0.28678300
C	6.60697100	0.39487400	0.26686400
H	7.57625400	0.77880100	0.59301400
C	5.47084700	1.21345500	0.35186200
H	5.53600500	2.23245700	0.74006300
C	1.39092900	3.02291400	0.41965800
C	1.39001500	4.34999400	0.93279700
H	2.36546200	4.78765500	1.14313600
C	0.22052400	5.03789800	1.16576400
C	-0.99046200	4.38312400	0.88739900
H	-1.95334600	4.86426500	1.06241400
C	-0.95652200	3.10162900	0.37250600
H	-1.88765500	2.59311600	0.13941000
C	1.05673000	-2.25746700	-1.82419700
C	0.88593600	-3.55580900	-2.38123200
H	1.76900700	-4.19364800	-2.40087700
C	-0.32479700	-3.97710800	-2.88335700
C	-1.40088100	-3.07554900	-2.84240900
H	-2.38031300	-3.33608100	-3.24472500
C	-1.20734800	-1.82731600	-2.28302200
H	-2.02690900	-1.11383200	-2.26576100
C	-2.87373400	1.12364500	-1.62794300
H	-2.37151700	1.64896500	-2.44109700
C	-4.25729400	1.07691600	-1.57009000
H	-4.84081300	1.57103000	-2.34356600
C	-4.86292200	0.38362600	-0.50697200
C	-4.03188200	-0.21514400	0.44928300
H	-4.50008000	-0.74235800	1.27843600
C	-2.64838000	-0.12708700	0.33411600
C	-1.72855000	-0.71890200	1.32132600
C	-2.16051600	-1.43466100	2.43362300
H	-3.21601600	-1.61172800	2.63250700
C	-1.22201800	-1.95487300	3.33724100
C	0.14377800	-1.73056200	3.09035700
H	0.91775200	-2.10625300	3.75550900
C	0.49823100	-1.01045100	1.95854400
H	1.54964000	-0.81591200	1.73504600
H	-0.43998200	-4.97470400	-3.31166500

H	0.23490900	6.05519700	1.56172700
O	-6.20278600	0.23856000	-0.31157300
O	-1.73348900	-2.64321300	4.39371700
C	-7.04848300	0.87578300	-1.31099000
H	-8.07392300	0.65073500	-0.99081400
H	-6.88853800	1.96717400	-1.32385700
H	-6.86568300	0.45043400	-2.31230700
C	-0.74994900	-3.16704600	5.33166900
H	-0.16035400	-2.35043200	5.78122700
H	-1.34572900	-3.66890600	6.10488600
H	-0.08347100	-3.89461200	4.83839600

TS = [Ru(Bid)(4,4'-OMe_2Bpy)(H—H—NMe_3)]$^+$

N	1.86522300	-0.01762000	0.11519300
N	2.43937900	0.12527500	2.48678700
N	0.01991100	-0.32829300	2.31459200
N	2.13251600	0.23235700	-2.30386800
N	-0.09767700	-0.73160400	-1.87092700
N	-2.16205400	-0.73699200	0.25111400
N	-0.75253100	1.46757600	-0.01212500
C	2.68971600	0.22609200	1.20097100
C	3.99993500	0.67656000	0.69683800
C	3.90289600	0.72744000	-0.70093700
C	2.54092000	0.28555600	-1.05322100
C	5.17331100	1.02972500	1.35163000
H	5.24300200	0.99009000	2.44088100
C	6.26290300	1.43782800	0.56868700
H	7.20042200	1.72074100	1.05238900
C	6.16604300	1.48860600	-0.82997400
H	7.02943100	1.81088700	-1.41621600
C	4.97761800	1.13141300	-1.48337900
H	4.89764800	1.16963100	-2.57203000
C	0.91674400	-0.27532500	-2.70675900
C	0.77665500	-0.36625300	-4.11737400
H	1.59913600	0.02489300	-4.71487500
C	-0.33029600	-0.94682800	-4.69829900
H	-0.42115800	-1.01884400	-5.78373500
C	-1.32470400	-1.46045900	-3.85267700
H	-2.21144800	-1.95643500	-4.24788700
C	-1.17003800	-1.33115000	-2.48463200

H	-1.92781000	-1.73384300	-1.81697500
C	1.20282000	-0.15129200	3.02727300
C	1.19807500	-0.19621900	4.44692900
H	2.16008300	-0.06786700	4.94157900
C	0.03210600	-0.36945700	5.16135900
H	0.04152200	-0.39655200	6.25264600
C	-1.16653700	-0.49178000	4.44362900
H	-2.12561900	-0.60939200	4.94859900
C	-1.12460700	-0.46772300	3.06157300
H	-2.04478800	-0.57276900	2.49305400
C	-2.85026400	-1.89662100	0.43882500
H	-2.23680200	-2.77522200	0.64730500
C	-4.23021200	-2.00002600	0.37183100
H	-4.70177800	-2.96657600	0.53249900
C	-4.97944500	-0.84305400	0.08975600
C	-4.29115300	0.36623400	-0.08877400
H	-4.87007000	1.26532200	-0.29314500
C	-2.90479800	0.39923500	-0.00107900
C	-2.11590400	1.63272000	-0.13951700
C	-2.68133800	2.88297900	-0.35497600
H	-3.75703600	3.01242900	-0.46049000
C	-1.86207100	4.01976400	-0.43513800
C	-0.47405400	3.85529100	-0.28398100
H	0.21421400	4.69613800	-0.32494400
C	0.02444400	2.57757300	-0.08130300
H	1.09684800	2.41729200	0.03833600
H	0.89793500	-2.37801200	0.02949800
H	0.14355000	-2.18169700	0.51819000
N	1.88352400	-3.35110900	-0.44471300
Ru	-0.08889100	-0.50872400	0.22209200
C	1.21318600	-4.60956500	-0.07346300
H	0.98893100	-4.59467200	1.00601600
H	0.26613400	-4.69197200	-0.63290400
H	1.84522600	-5.48890700	-0.29848500
C	3.12399000	-3.17511300	0.32962700
H	3.63714000	-2.26156200	-0.00730600
H	2.87370100	-3.07632900	1.39933700
H	3.80601000	-4.03764300	0.19899500
C	2.14858500	-3.30943900	-1.89303300
H	1.19502900	-3.36826600	-2.44249300

H	2.65861000	-2.36733900	-2.14503300
H	2.79207000	-4.15585100	-2.20458000
O	-2.50127600	5.19831400	-0.65050100
O	-6.33203800	-0.78310300	-0.02694800
C	-7.03066300	-2.04915200	0.15706000
H	-6.87312900	-2.44046800	1.17620800
H	-8.09010800	-1.80445800	0.00850700
H	-6.70535300	-2.78900200	-0.59341800
C	-1.64302700	6.37595200	-0.68890900
H	-2.33028600	7.21280200	-0.86709400
H	-1.12323400	6.51195800	0.27411100
H	-0.91336600	6.30544300	-1.51276900

TS = [Ru(Bid)(4,4'-OMe_2Bpy)(H—CO_2)]

Ru	0.06194200	-0.62268600	0.19134800
H	0.39963400	-2.05480400	1.01558900
N	2.04648200	-0.30197900	0.08870100
N	2.36500100	1.28087500	1.92728300
N	0.00759800	0.55246200	1.94269600
N	2.64729900	-1.72485900	-1.80888300
N	0.19150500	-1.75262700	-1.57175500
N	-2.01608300	-0.78815400	0.21771300
N	-0.56876500	1.12586800	-0.86270200
C	2.77036500	0.53124600	0.92341900
C	4.18608500	0.48415000	0.51837200
C	4.27132700	-0.40667600	-0.56071300
C	2.90467900	-0.88921600	-0.82531700
C	5.31484600	1.12457800	1.01445100
H	5.24265700	1.81726200	1.85594700
C	6.54643600	0.85328900	0.40028100
H	7.45258400	1.34105700	0.76650200
C	6.63168500	-0.03838000	-0.67954200
H	7.60301800	-0.23335200	-1.13963500
C	5.48719400	-0.68109200	-1.17436600
H	5.54816600	-1.37676900	-2.01431900
C	1.38806800	-2.13027600	-2.18128700
C	1.37769600	-2.98033100	-3.32078000
H	2.34971300	-3.25229900	-3.73064400
C	0.20188600	-3.41734400	-3.88977500
C	-1.00346100	-2.99215700	-3.31005500

H	-1.97004400	-3.28667800	-3.71981400
C	-0.95978700	-2.18784900	-2.18694700
H	-1.88709800	-1.86507700	-1.72303600
C	1.08078900	1.30851600	2.41412400
C	0.91112000	2.18326000	3.52289000
H	1.78901800	2.75003300	3.83088600
C	-0.29314800	2.29445800	4.18172700
C	-1.36118900	1.50090700	3.73421000
H	-2.33357200	1.52070200	4.22690200
C	-1.16808200	0.67028700	2.64682500
H	-1.98266500	0.03718200	2.30625500
C	-2.72653300	-1.82401700	0.74409600
H	-2.12769300	-2.64721600	1.13619900
C	-4.11048900	-1.86421100	0.80694800
H	-4.59959800	-2.72910000	1.24896900
C	-4.84030500	-0.77559900	0.29685100
C	-4.13025900	0.29121200	-0.27294900
H	-4.69457600	1.12828800	-0.68090500
C	-2.74093100	0.26586000	-0.30774600
C	-1.92871700	1.33746000	-0.90625200
C	-2.47136800	2.47978500	-1.48376500
H	-3.54621900	2.64911900	-1.51709700
C	-1.62569100	3.45343700	-2.03701300
C	-0.23634200	3.23924000	-1.99299800
H	0.47009900	3.95651300	-2.40399200
C	0.23342500	2.07515400	-1.40240700
H	1.30488400	1.87098700	-1.35109700
C	0.66796400	-2.16794400	2.70431200
O	1.84347900	-2.00482000	2.81053900
O	-0.41765300	-2.42871600	3.12317200
H	-0.40824500	2.96779900	5.03323500
H	0.20876400	-4.06428300	-4.76922400
O	-6.19598900	-0.65708300	0.30085200
O	-2.24300200	4.53845500	-2.57641200
C	-6.91437800	-1.76242000	0.91993600
H	-7.97208900	-1.47639900	0.85449800
H	-6.74377500	-2.70193100	0.36774300
H	-6.62056000	-1.88029200	1.97670000
C	-1.35307000	5.55204100	-3.12694600
H	-0.75343900	5.14061300	-3.95607700

H	-2.02474400	6.33457300	-3.50293200
H	-0.69450100	5.96427700	-2.34406800

[Ru(Bid)(4,4'-OMe_2Bpy)(H-OCO)]

Ru	-0.01202500	-0.44316000	-0.36954700
N	-1.99632400	-0.14196100	-0.17059500
N	-2.35446600	1.66928400	-1.77326700
N	0.00213700	0.95642400	-1.94631700
N	-2.56867900	-1.85839300	1.47402700
N	-0.11725200	-1.86091600	1.18830700
N	2.05123400	-0.64540100	-0.47984100
N	0.61172200	1.03189700	0.89497500
C	-2.73711700	0.79142800	-0.87340300
C	-4.14698500	0.67490200	-0.45941400
C	-4.21286200	-0.36699100	0.47431000
C	-2.84018900	-0.87444300	0.64839200
C	-5.28491300	1.37392900	-0.84183600
H	-5.22826100	2.18351200	-1.57279500
C	-6.50622900	1.00400100	-0.26042000
H	-7.41998300	1.53405600	-0.53816100
C	-6.57227600	-0.04014600	0.67431700
H	-7.53665500	-0.30974000	1.11039500
C	-5.41852700	-0.74107800	1.05380600
H	-5.46449900	-1.55563700	1.78001200
C	-1.30402600	-2.33187100	1.74234700
C	-1.28463500	-3.38063100	2.69935500
H	-2.25138500	-3.71024000	3.07752300
C	-0.10381200	-3.94125400	3.13508700
H	-0.10245200	-4.74603600	3.87268900
C	1.09391200	-3.43576700	2.61102900
H	2.06373100	-3.82288400	2.92439300
C	1.03934800	-2.42579800	1.66825700
H	1.96287200	-2.03482200	1.25262300
C	-1.08205600	1.75894200	-2.28916800
C	-0.94357000	2.76178400	-3.28599000
H	-1.82857600	3.36002500	-3.49864200
C	0.24266600	2.95512900	-3.95931000
H	0.33327800	3.72752600	-4.72546900
C	1.32242900	2.11880900	-3.64177900

H	2.28170600	2.20355500	-4.15276800
C	1.16031000	1.16286900	-2.65632800
H	1.98686700	0.50254800	-2.40943600
C	2.73514000	-1.59179300	-1.17680500
H	2.11751600	-2.31763700	-1.71040200
C	4.11876600	-1.66112800	-1.22435700
H	4.59498700	-2.44898800	-1.80317300
C	4.86695700	-0.70246200	-0.51626900
C	4.17755700	0.27564800	0.21759200
H	4.75525500	1.01013400	0.77679900
C	2.78951800	0.28230700	0.22528500
C	1.97562100	1.23754400	0.98513300
C	2.50310600	2.26704700	1.75204600
H	3.57751300	2.43149100	1.81600900
C	1.64896300	3.12386600	2.46317800
C	0.26190000	2.90770100	2.37755800
H	-0.45212600	3.53474500	2.90570200
C	-0.20375100	1.86682900	1.59023200
H	-1.27238000	1.67174500	1.49743600
C	-1.00830500	-2.54104400	-1.83545600
H	-0.23266300	-1.65088600	-1.74138000
O	-0.57578700	-3.61529700	-1.38723700
O	-2.03062200	-2.23525500	-2.46728400
O	6.22278500	-0.63420800	-0.46802300
O	2.25438600	4.10266600	3.18241300
C	6.92740600	-1.66545600	-1.21877100
H	6.69248500	-1.59836200	-2.29425800
H	7.99060000	-1.45028900	-1.05200900
H	6.68003000	-2.66895800	-0.83397900
C	1.35775700	4.97783200	3.92769600
H	2.02379500	5.68976800	4.43137800
H	0.67791900	5.51509100	3.24557500
H	0.78220100	4.40532300	4.67412500

[Ru(Bid)(4,4'-OMe_2Bpy)(O-COH)]

Ru	-0.00745500	-0.55284500	-0.32797300
N	-1.99001500	-0.26679700	-0.18384100
N	-2.26549800	1.69727100	-1.61197200

N	0.05050500	0.87827100	-1.85575100
N	-2.60926100	-2.07520600	1.33823400
N	-0.14741300	-1.99527400	1.18812000
N	2.06244100	-0.69980600	-0.38081800
N	0.54032100	0.94074500	0.96122000
C	-2.69319800	0.75283100	-0.80186600
C	-4.10945900	0.64121900	-0.41097500
C	-4.21447200	-0.47877900	0.42697400
C	-2.85688500	-1.03411900	0.57176000
C	-5.22481300	1.40154300	-0.73980300
H	-5.13779400	2.27140600	-1.39452700
C	-6.46272400	1.01597300	-0.20491800
H	-7.35849100	1.59401900	-0.44275800
C	-6.56799400	-0.10517600	0.63175000
H	-7.54444200	-0.38633600	1.03237700
C	-5.43738900	-0.86847500	0.95836900
H	-5.51458800	-1.74294800	1.60834600
C	-1.34913500	-2.54133000	1.63535900
C	-1.34336600	-3.64588400	2.52939300
H	-2.31606400	-4.03886700	2.82303600
C	-0.16908700	-4.17321500	3.02123600
C	1.03748800	-3.57728200	2.62380100
H	1.99934900	-3.92980800	2.99713800
C	0.99964900	-2.52310200	1.73007000
H	1.92678100	-2.05681200	1.40817900
C	-0.99198500	1.76174900	-2.12965400
C	-0.80720800	2.81484900	-3.06482400
H	-1.65380900	3.48296300	-3.21832400
C	0.37012200	2.96255200	-3.76655700
C	1.39146500	2.02772700	-3.54226200
H	2.33295200	2.06621400	-4.09070400
C	1.19187200	1.03203300	-2.60337500
H	1.97168300	0.29482500	-2.42790800
C	2.79593200	-1.63115400	-1.04594100
H	2.21533000	-2.39495300	-1.56724300
C	4.18133400	-1.63372900	-1.08992400
H	4.69677400	-2.41189000	-1.64778900
C	4.87968500	-0.61902700	-0.40952100
C	4.14044100	0.34372600	0.29418600
H	4.67981300	1.12149200	0.83272200

C	2.75226600	0.28344700	0.29956900
C	1.89425800	1.21454800	1.04179400
C	2.37985500	2.27677100	1.79360300
H	3.44558200	2.49420700	1.84488200
C	1.49360700	3.09751300	2.50649200
C	0.11899200	2.80668500	2.44502100
H	-0.61873300	3.39848500	2.98155000
C	-0.30208400	1.73785400	1.66999200
H	-1.36094500	1.48587200	1.60035000
C	-1.01304300	-2.24472300	-2.70106200
H	-0.95255100	-3.23175400	-3.21532600
O	-0.28159000	-2.20401200	-1.64734600
O	-1.73135800	-1.36071400	-3.18657100
H	-0.17968900	-5.01784900	3.71298800
H	0.49441400	3.77128800	-4.48922100
O	6.23227200	-0.48243100	-0.36309000
O	2.05797700	4.11645800	3.20764000
C	1.12427400	4.95715000	3.94533100
H	1.75533500	5.71559800	4.42593200
H	0.40730300	5.44150600	3.26127300
H	0.58913100	4.37085500	4.71111700
C	6.98622300	-1.49840200	-1.08513800
H	6.74798700	-1.47505400	-2.16183400
H	8.03785500	-1.22674300	-0.92734000
H	6.79112800	-2.50200100	-0.67082800

Ts4-BidBpyOMe-O-CHO

TS = [Ru(Bid)(4,4'-OMe_2Bpy)(---OCOH)]

Ru	0.03898200	-0.46158400	0.26642200
N	2.02995300	-0.17968600	0.13768800
N	2.39534700	1.42475600	1.94641000
N	0.00193500	0.81492900	1.94867000
N	2.59798600	-1.68230400	-1.70949500
N	0.14567100	-1.68624200	-1.44513100
N	-2.01268900	-0.71234000	0.38299200
N	-0.60133600	1.07337500	-0.83115300

C	2.77894300	0.64428500	0.96248900
C	4.19452900	0.53541200	0.56744600
C	4.25384700	-0.38031000	-0.49114000
C	2.87396200	-0.82376600	-0.75458500
C	5.34276000	1.14305100	1.06015800
H	5.29092800	1.85446100	1.88734400
C	6.56675500	0.81298500	0.46116900
H	7.48819600	1.27375800	0.82391200
C	6.62609700	-0.10468600	-0.59882900
H	7.59280700	-0.34605500	-1.04628200
C	5.46283500	-0.71517100	-1.08832900
H	5.50339000	-1.43247600	-1.91104300
C	1.33014100	-2.09181500	-2.05256100
C	1.30257200	-2.99208400	-3.15083400
H	2.26733000	-3.27880800	-3.56732900
C	0.11731100	-3.46718900	-3.66868900
H	0.11013900	-4.15864000	-4.51347400
C	-1.07752000	-3.02734500	-3.08121900
H	-2.05025700	-3.35587600	-3.44814100
C	-1.01550500	-2.16293700	-2.00405700
H	-1.93580400	-1.82675200	-1.53624700
C	1.10594400	1.52124500	2.41770300
C	0.97133800	2.42705500	3.50440600
H	1.87537300	2.94988500	3.81391000
C	-0.23486700	2.62239200	4.14061800
H	-0.32315000	3.31876600	4.97660100
C	-1.33990000	1.88861500	3.68713200
H	-2.31915200	1.97856500	4.15792600
C	-1.17762000	1.02394900	2.62020200
H	-2.02707100	0.44071000	2.27759100
C	-2.66928100	-1.71230500	1.02567200
H	-2.03153700	-2.46545000	1.49389700
C	-4.05145800	-1.79069900	1.10684000
H	-4.50875200	-2.61880800	1.64305000
C	-4.82313300	-0.78650700	0.49255500
C	-4.16004500	0.24734900	-0.18827600
H	-4.75479900	1.02207900	-0.67032200
C	-2.77319900	0.26183000	-0.23063700
C	-1.97034000	1.27550000	-0.91681600
C	-2.50035100	2.35341400	-1.61151900

H	-3.57660300	2.50903900	-1.66877300
C	-1.65012400	3.26744300	-2.25135700
C	-0.26144200	3.05615800	-2.17072800
H	0.45056400	3.72554400	-2.64743500
C	0.21204500	1.96497100	-1.46155400
H	1.28137800	1.77189500	-1.37838600
C	0.90905200	-3.03865000	2.32706200
H	1.19537400	-3.88531700	3.00405100
O	0.55471200	-3.34228300	1.15881900
O	0.97109200	-1.89092000	2.83450400
O	-2.25726500	4.29261400	-2.90373700
O	-6.18022500	-0.71922800	0.49470300
C	-1.35780200	5.23998100	-3.54998400
H	-2.02221100	5.98595900	-4.00443200
H	-0.69841200	5.72280000	-2.80941500
H	-0.75894100	4.74245400	-4.33113600
C	-6.85768700	-1.79020000	1.21402200
H	-7.92575700	-1.55947900	1.11133900
H	-6.63800000	-2.77032000	0.75858600
H	-6.57196300	-1.78892600	2.27932800

TS = [Ru(Bid)(4,4'-OMe_2Bpy)(H--H--OCOH)]

Ru	-0.00533100	0.38019600	-0.55581600
N	1.99849800	0.19775500	-0.39261100
N	2.45058100	-1.48258600	-2.11387600
N	0.02610500	-1.02270600	-2.12695800
N	2.45559800	1.66872300	1.51006300
N	0.04345400	1.79984200	1.00888600
N	-2.09845100	0.37506100	-0.53220400
N	-0.43631500	-1.13209000	0.83491200
C	2.78143800	-0.67066600	-1.13348400
C	4.16524100	-0.59767300	-0.63114900
C	4.16551800	0.31626500	0.43037700
C	2.78300200	0.80738700	0.57373300
C	5.32891000	-1.24780600	-1.02324400
H	5.32289600	-1.96106800	-1.85054900
C	6.50912000	-0.95723600	-0.32354400

H	7.44158700	-1.45029300	-0.60745100
C	6.50981500	-0.04006800	0.73815600
H	7.44269100	0.16863000	1.26655400
C	5.32984900	0.60973700	1.12906700
H	5.32477300	1.32499200	1.95458800
C	1.19065000	2.17385100	1.70254600
C	1.12988600	3.17380500	2.71030000
H	2.06788800	3.42086700	3.20591100
C	-0.05138100	3.80367500	3.03478500
H	-0.08289500	4.57676600	3.80498700
C	-1.20969900	3.42008400	2.34354400
H	-2.17741400	3.87766300	2.55050600
C	-1.11554300	2.44233500	1.37027700
H	-2.00414200	2.15364500	0.81700700
C	1.17694300	-1.64579700	-2.60470100
C	1.10087000	-2.55983000	-3.69120300
H	2.04034200	-3.00512400	-4.01607400
C	-0.09646100	-2.86647200	-4.29893000
H	-0.13980600	-3.57020200	-5.13247200
C	-1.25633500	-2.24556400	-3.81200900
H	-2.23640200	-2.44190200	-4.24753600
C	-1.14808200	-1.35834800	-2.75756700
H	-2.03820600	-0.86160600	-2.38370000
C	-2.92058800	1.17816200	-1.26257200
H	-2.41684500	1.86840200	-1.94060400
C	-4.30391100	1.15485200	-1.18002300
H	-4.88666300	1.83392500	-1.79821500
C	-4.91025800	0.24865900	-0.29132700
C	-4.08246800	-0.59596200	0.46271300
H	-4.55027500	-1.29995400	1.14917000
C	-2.70146600	-0.52042200	0.32862600
C	-1.77074100	-1.37553300	1.07906400
C	-2.18173700	-2.36087600	1.96813500
H	-3.23617200	-2.55427300	2.15666100
C	-1.22877300	-3.13406900	2.64844000
C	0.13299700	-2.88584900	2.40148200
H	0.92084100	-3.44923000	2.89570300
C	0.47236600	-1.89018600	1.49796500
H	1.51968500	-1.67387300	1.28163900
H	-0.04750300	2.33946700	-1.56592700

H	0.32564500	1.50808200	-1.81539100
C	0.44467100	4.30730100	-0.96675900
H	0.09059700	5.32642700	-0.68815900
O	-0.48419200	3.57216200	-1.47611000
O	1.62419800	3.99492400	-0.77585600
O	-1.72185800	-4.07104700	3.50016000
O	-6.24737400	0.10866600	-0.08840000
C	-0.72151400	-4.84542800	4.22328500
H	-1.30446400	-5.52538800	4.85749800
H	-0.09342100	-5.42571900	3.52673800
H	-0.09491000	-4.18873900	4.84998000
C	-7.09423200	0.99650500	-0.87397400
H	-6.96065800	0.81371900	-1.95353700
H	-8.11823200	0.73877200	-0.57468000
H	-6.88536400	2.05278800	-0.63464400

-------Optimized geometries for catalytic system of 1w-----

[Ru(Bid)(4,4'-$(COOMe)_2$Bpy)(Cl)]

Ru	0.56208600	-0.85838400	0.19545600
N	2.52233800	-0.38141700	0.19008700
N	2.70493900	0.85667500	2.28915500
N	0.46056600	-0.16140400	2.18791600
N	3.23049500	-1.36526600	-1.93227400
N	0.77673000	-1.56721000	-1.77656100
N	-1.46213800	-1.16859800	0.18797900
N	-0.08626300	0.95506300	-0.40201800
C	3.16951600	0.35095200	1.16824700
C	4.57890000	0.51766900	0.76719000
C	4.73924100	-0.15547500	-0.45094900
C	3.42139900	-0.71063300	-0.81137800
C	5.64415500	1.16605600	1.37851000
H	5.51381700	1.68805200	2.32897300
C	6.88970200	1.12818200	0.73489600
H	7.74774100	1.62964900	1.18787000
C	7.05034100	0.45362800	-0.48453000
H	8.03150600	0.43744600	-0.96394600
C	5.96919200	-0.19911300	-1.09432800
H	6.08910600	-0.72650300	-2.04322400
C	2.00116400	-1.78042900	-2.39775800

C	2.05858600	-2.42910400	-3.65844300
H	3.05006500	-2.58342000	-4.08215000
C	-0.32112900	-2.54467700	-3.72384400
H	-1.26260200	-2.80588300	-4.20748500
C	-0.34065700	-1.93365400	-2.48248500
H	-1.29331400	-1.72307700	-2.00359300
C	1.44426100	0.61471300	2.78908300
C	1.21356200	1.19510900	4.06405200
H	2.01487500	1.81004000	4.47170400
C	-0.91210600	0.12272400	4.18401200
H	-1.83977800	-0.12687500	4.69929900
C	-0.66738900	-0.40498000	2.92874100
H	-1.39635300	-1.07181700	2.47496600
C	-2.11456500	-2.34586800	0.41964200
H	-1.46511100	-3.20726700	0.58715300
C	-3.49491000	-2.44510300	0.46002000
H	-3.96562500	-3.40784800	0.65474800
C	-4.27023500	-1.29480800	0.25591100
C	-3.62256200	-0.08836700	0.00232900
H	-4.22143800	0.80583600	-0.17074700
C	-2.23038800	-0.04145500	-0.03941500
C	-1.45666700	1.15157400	-0.36732700
C	-2.02103400	2.39127500	-0.66855300
H	-3.10067700	2.52638300	-0.62473100
C	-1.20144000	3.45737700	-1.02982900
C	0.18248400	3.24889500	-1.09235800
H	0.84264000	4.06654300	-1.38174800
C	0.70091500	2.00623500	-0.77802900
H	1.77180000	1.80915000	-0.81476000
C	0.04627500	0.96694400	4.76121400
H	-0.11603700	1.41573400	5.74303600
C	0.91500300	-2.82057700	-4.32269700
H	0.97313500	-3.31644500	-5.29342200
C	-5.75357300	-1.30137100	0.28357800
C	-1.73447800	4.80225200	-1.35771100
O	-6.45195200	-0.30332400	0.11100600
O	-1.03738000	5.75729900	-1.69486800
O	-6.24383100	-2.54937500	0.51736900
O	-3.09060700	4.84807900	-1.23815900
C	-7.70654400	-2.58959100	0.53197600

H	-8.10542300	-2.26111300	-0.44019700
H	-7.95326000	-3.64127000	0.72163800
H	-8.10003700	-1.94468200	1.33272100
C	-3.64090400	6.16499500	-1.56105500
H	-3.41246800	6.42718100	-2.60572300
H	-4.72211600	6.05972700	-1.41106600
H	-3.22384000	6.92871200	-0.88665700
Cl	1.16226000	-3.12564300	0.99424800

$[Ru(Bid)(4,4'\text{-}(COOMe)_2Bpy)]^+$

Ru	0.58271500	-0.93345500	0.32851400
N	2.56684700	-0.57069500	0.30540300
N	2.79955500	0.85861400	2.27315800
N	0.51503900	-0.07458500	2.25717400
N	3.24226600	-1.79924600	-1.69815900
N	0.78103200	-1.88553100	-1.53674700
N	-1.44335200	-1.23199000	0.36164900
N	-0.03619100	0.76464200	-0.43057400
C	3.24738800	0.22735500	1.21401000
C	4.66412900	0.27862400	0.81469400
C	4.79786400	-0.51752800	-0.32993700
C	3.45835100	-1.03862900	-0.65320400
C	5.75836600	0.92181000	1.37878000
H	5.64831500	1.53804000	2.27360200
C	7.00514600	0.75217900	0.76086300
H	7.88602600	1.24570100	1.17683500
C	7.13929000	-0.04496700	-0.38600400
H	8.12287500	-0.16154700	-0.84592600
C	6.02988900	-0.69317800	-0.94685200
H	6.12913300	-1.31681000	-1.83779800
C	1.99913100	-2.21365600	-2.12425600
C	2.03275900	-2.99965800	-3.30446900
H	3.01798300	-3.24441600	-3.69878800
C	-0.34969600	-2.99886100	-3.38999900
H	-1.29861000	-3.25585500	-3.86100400
C	-0.35015400	-2.25838000	-2.22315000
H	-1.29415900	-1.93991400	-1.79003800
C	1.52830200	0.71964000	2.78500800
C	1.32007600	1.43093600	3.99491000
H	2.14583900	2.04868100	4.34487400

C	-0.85401200	0.47426700	4.20047000
H	-1.79534800	0.32245700	4.72861400
C	-0.63215000	-0.18409100	3.00587200
H	-1.39230200	-0.85490500	2.61391400
C	-2.09612500	-2.37540400	0.71210100
H	-1.45682500	-3.22370800	0.96232500
C	-3.47872800	-2.46254700	0.75724700
H	-3.95622400	-3.39900800	1.04210700
C	-4.24473400	-1.33247000	0.44039600
C	-3.59209300	-0.15887600	0.06959000
H	-4.18425100	0.72006100	-0.18670700
C	-2.20105300	-0.13009700	0.02298700
C	-1.40291500	1.00299100	-0.42180100
C	-1.92560200	2.22028000	-0.85461700
H	-3.00115900	2.38932200	-0.82704600
C	-1.07183000	3.21433200	-1.32423800
C	0.30382000	2.95778500	-1.36064400
H	0.98832500	3.71817700	-1.73673500
C	0.78913600	1.74299400	-0.91410300
H	1.85245500	1.51182600	-0.92655500
C	0.14115700	1.32457000	4.70136600
H	-0.00502600	1.87437600	5.63283700
C	0.87573000	-3.40347400	-3.93649000
H	0.91532000	-4.00225500	-4.84812900
C	-5.73058700	-1.32321800	0.46750600
C	-1.55887100	4.53452600	-1.79706900
O	-6.41423300	-0.33689400	0.19996400
O	-0.82461000	5.42340800	-2.22244800
O	-6.23426400	-2.53627900	0.81626900
O	-2.91202800	4.63357100	-1.70089900
C	-7.69874300	-2.55368900	0.83617800
H	-8.09438200	-2.28640100	-0.15572300
H	-7.96056300	-3.58557400	1.09914100
H	-8.07781600	-1.84689800	1.59047600
C	-3.41569600	5.92622300	-2.16892400
H	-3.17537500	6.06497600	-3.23427300
H	-4.50026400	5.87442500	-2.01562000
H	-2.97397500	6.74362600	-1.57875800

$[Ru(Bid)(4,4'\text{-}(COOMe)_2Bpy)(H_2)]^+$

Ru	0.53925700	-1.16324900	0.16199100
N	2.53268100	-0.75554900	0.09330600
N	2.97338300	-0.19696800	2.43488800
N	0.60296600	-0.86420000	2.26411900
N	2.96725800	-0.94798900	-2.30670500
N	0.59166700	-1.50655400	-1.93329100
N	-1.53709700	-1.24516400	0.18011700
N	0.04557600	0.82096900	-0.11670800
C	3.29985300	-0.35115000	1.17544700
C	4.65769400	-0.04883200	0.68746100
C	4.65575000	-0.26621600	-0.69502200
C	3.29677200	-0.70347200	-1.06261900
C	5.80052300	0.38024800	1.34997100
H	5.79539400	0.55041600	2.42861200
C	6.95759200	0.58711300	0.58624400
H	7.87446800	0.92388200	1.07457700
C	6.95572300	0.36886800	-0.79996000
H	7.87134500	0.53855900	-1.37038500
C	5.79668800	-0.06192800	-1.46017600
H	5.78934000	-0.23251700	-2.53876500
C	1.71652800	-1.34393700	-2.73072700
C	1.64636200	-1.59618400	-4.12474900
H	2.56264000	-1.44385800	-4.69294500
C	-0.64920900	-2.19766700	-3.91652600
H	-1.60020700	-2.53812600	-4.32591800
C	-0.54875900	-1.93637300	-2.56192100
H	-1.41586400	-2.08457400	-1.92512300
C	1.72508100	-0.44443700	2.96544700
C	1.65428300	-0.23644300	4.36655700
H	2.56756700	0.09969500	4.85512000
C	-0.63404800	-0.90012500	4.36573000
H	-1.58135000	-1.10289300	4.86528500
C	-0.53327700	-1.08678700	2.99874000
H	-1.39606000	-1.44313100	2.44307200
C	-2.30602400	-2.36352800	0.33013600
H	-1.76134100	-3.29829000	0.46505900
C	-3.69079300	-2.33522900	0.31341800
H	-4.25455300	-3.25879600	0.43606500
C	-4.34332300	-1.11030300	0.13764500

C	-3.57632800	0.04071900	-0.01283400
H	-4.08368100	0.99471100	-0.15460500
C	-2.18444700	-0.04108600	0.01094600
C	-1.30002500	1.11270600	-0.13961800
C	-1.75607900	2.42271200	-0.29424700
H	-2.82281400	2.63779000	-0.30356400
C	-0.83913100	3.45980000	-0.43516500
C	0.52474300	3.16005500	-0.41753300
H	1.26070600	3.95655200	-0.52616700
C	0.93003400	1.84525300	-0.25701300
H	1.98600700	1.58275100	-0.23655000
H	1.27517400	-2.72723000	0.40153900
H	0.45413500	-2.89180500	0.39701000
C	0.47930500	-2.01842000	-4.72552400
H	0.44018300	-2.21166100	-5.79902900
C	0.48993000	-0.45498900	5.07202900
H	0.44973100	-0.29045000	6.15026700
C	-5.82417500	-0.97607300	0.10199700
C	-1.25468200	4.87879800	-0.60357000
O	-0.46620500	5.80967800	-0.74344800
O	-6.41156700	0.09736800	-0.01231100
O	-6.43525500	-2.18458900	0.20455900
O	-2.60667800	5.00669700	-0.58107800
C	-7.89636700	-2.08669900	0.15881000
H	-8.24538900	-3.12485300	0.21027700
H	-8.26393500	-1.50528300	1.01825100
H	-8.21542000	-1.60812600	-0.77966900
C	-3.04813400	6.39442800	-0.74019800
H	-4.14248300	6.34420200	-0.69284800
H	-2.64556300	7.01622500	0.07400100
H	-2.71507100	6.78979600	-1.71205900

[Ru(Bid)(4,4'-$(COOMe)_2$Bpy)(H)]

Ru	0.62149900	-1.02228200	0.41718000
H	0.95332000	-2.39159500	1.26197900
N	2.58554700	-0.55562600	0.40102400
N	2.66837100	1.13988700	2.16273200
N	0.44446300	0.07515500	2.21042300
N	3.37721600	-1.95215600	-1.44251900
N	0.92223800	-2.15267500	-1.32675400

N	-1.40140000	-1.25638900	0.35774900
N	-0.01438200	0.78026800	-0.58072800
C	3.18044900	0.41057700	1.19356700
C	4.59096300	0.54174900	0.78751700
C	4.80556100	-0.37761500	-0.24867700
C	3.51957800	-1.05493300	-0.49300100
C	5.61644400	1.35520400	1.25305500
H	5.44397300	2.06924600	2.06139000
C	6.87722900	1.22896300	0.65167400
H	7.70448700	1.85491200	0.99353600
C	7.09208000	0.30887800	-0.38519900
H	8.08404300	0.22929500	-0.83529000
C	6.05092800	-0.50821500	-0.85001100
H	6.21244700	-1.22577100	-1.65752100
C	2.17446600	-2.49465500	-1.83356000
C	2.28574400	-3.43131200	-2.89523400
H	3.29524700	-3.67497300	-3.22422500
C	-0.08874100	-3.57393600	-3.03753400
H	-1.00853100	-3.94688000	-3.48881300
C	-0.16290100	-2.68371200	-1.98255500
H	-1.13485300	-2.36871300	-1.61154500
C	1.39945300	0.97925100	2.66892500
C	1.11751200	1.81041800	3.78604200
H	1.89959400	2.50838700	4.08218100
C	-1.00574800	0.75939500	4.05190800
H	-1.95157800	0.61321900	4.57406000
C	-0.71087900	-0.01924600	2.94831400
H	-1.41528900	-0.78137500	2.62231800
C	-2.09531700	-2.37148100	0.75601100
H	-1.47706200	-3.21447600	1.06390900
C	-3.47547000	-2.44032200	0.78706200
H	-3.96588800	-3.35349400	1.12177400
C	-4.22694600	-1.32247400	0.39287800
C	-3.54520600	-0.18840900	-0.04080000
H	-4.12330200	0.67793200	-0.36218700
C	-2.15183600	-0.16721900	-0.06612000
C	-1.37594900	0.97165000	-0.56391600
C	-1.95171700	2.16244800	-1.01785300
H	-3.03052600	2.30683900	-0.98991400
C	-1.13277800	3.17639800	-1.50859300

C	0.25243000	2.97428200	-1.54113500
H	0.90679600	3.75668800	-1.92607400
C	0.76734400	1.77668200	-1.07233800
H	1.84059500	1.57676200	-1.07793700
C	-0.07295200	1.71849600	4.47414400
H	-0.27487100	2.36010200	5.33402300
C	1.17319700	-3.98113600	-3.49519400
H	1.27250800	-4.69717600	-4.31316900
C	-5.70687400	-1.29106100	0.40732600
C	-1.67094400	4.46903600	-2.00408700
O	-6.38381000	-0.32637700	0.05066200
O	-0.97516600	5.37552500	-2.45714600
O	-6.22923800	-2.46328700	0.86682600
O	-3.02701500	4.52591900	-1.89499700
C	-7.69166100	-2.46022900	0.89355800
H	-8.09334000	-2.31473700	-0.12124700
H	-7.96481800	-3.44874800	1.28234600
H	-8.06058200	-1.66300400	1.55728200
C	-3.57767200	5.79048300	-2.38432800
H	-3.35803100	5.91230500	-3.45628300
H	-4.65790000	5.70911500	-2.21359000
H	-3.15365300	6.63537200	-1.82024000

TS = [Ru(Bid)(4,4'-$(COOMe)_2$Bpy)(H—H—NMe_2)]

N	2.33949600	0.07985500	0.11030300
N	3.00977100	-0.09554900	2.45329700
N	0.61753800	-0.67520700	2.29685600
N	2.47776500	0.70160500	-2.25078600
N	0.43110000	-0.63333400	-1.91665100
N	-1.53317000	-1.14713700	0.22036800
N	-0.43632800	1.22838300	0.17702700
C	3.19180700	0.22338800	1.19399300
C	4.43324600	0.86431500	0.72198400
C	4.26287100	1.12842400	-0.64377400
C	2.93123600	0.61778400	-1.01873200
C	5.60386300	1.21238600	1.38367800
H	5.73233300	1.00374000	2.44792600
C	6.61465900	1.83697700	0.63888900
H	7.54847200	2.12207000	1.12818300

C	6.44371600	2.10235700	-0.72790600
H	7.24621600	2.59207200	-1.28360800
C	5.25867700	1.74731600	-1.38837700
H	5.12112700	1.95117000	-2.45241500
C	1.32669100	0.08640600	-2.69691100
C	1.13774800	0.16962500	-4.10068300
H	1.85731600	0.76913900	-4.65638900
C	-0.73661600	-1.29918600	-3.94977800
H	-1.54095700	-1.88559400	-4.39389800
C	-0.54686900	-1.32905700	-2.57989000
H	-1.19377100	-1.94426200	-1.95800700
C	1.81442600	-0.53031100	2.98777300
C	1.86459800	-0.77225500	4.38463200
H	2.83619700	-0.66380300	4.86479600
C	-0.48624500	-1.17028900	4.41433700
H	-1.42122600	-1.39322600	4.92854600
C	-0.49550100	-0.95764100	3.04733100
H	-1.43206700	-1.01804800	2.49867800
C	-2.04999800	-2.40957200	0.31369000
H	-1.31671300	-3.20799000	0.43703200
C	-3.40644200	-2.67684800	0.24732600
H	-3.76454700	-3.70246100	0.32721600
C	-4.30344600	-1.61528100	0.06873700
C	-3.79776500	-0.32086000	-0.01596400
H	-4.49439000	0.50719500	-0.14665100
C	-2.42484100	-0.10061600	0.07437400
C	-1.81000800	1.22623700	0.06685100
C	-2.53455200	2.41740400	-0.00389400
H	-3.61968100	2.39867000	-0.09039200
C	-1.86278000	3.63604900	0.04291600
C	-0.46995200	3.63556400	0.16811100
H	0.07325800	4.57957300	0.21055500
C	0.20439600	2.42738600	0.23521900
H	1.28841300	2.38667300	0.34292300
H	1.57589700	-2.31951900	-0.21799600
H	0.87523700	-2.30434600	0.33588500
N	2.68067600	-3.14074000	-0.89691300
Ru	0.44986200	-0.64128600	0.19437100
C	2.09610200	-4.48711900	-0.78577300
H	1.84666100	-4.68826700	0.26964100

H	1.16950300	-4.53030800	-1.38347600
H	2.79313300	-5.26887900	-1.14445500
C	3.87425000	-3.02175100	-0.04448500
H	4.32445200	-2.02612400	-0.18176700
H	3.58044400	-3.14156800	1.01240500
H	4.63121200	-3.79191600	-0.29330300
C	2.99912100	-2.82756800	-2.29895400
H	2.08182400	-2.88459100	-2.90711500
H	3.41498200	-1.81026900	-2.36453900
H	3.74142300	-3.54073500	-2.71147100
C	0.11501700	-0.50686700	-4.73213000
H	-0.01347000	-0.44274400	-5.81419500
C	0.73241800	-1.09870000	5.10191200
H	0.78328200	-1.27793400	6.17739600
C	-5.77241900	-1.80334800	-0.02630800
C	-2.57213900	4.94142500	-0.02208200
O	-6.57542000	-0.88698900	-0.19362800
O	-2.00974700	6.03279700	0.02268500
O	-6.11627800	-3.11349200	0.09880100
O	-3.91668900	4.76990500	-0.12993900
C	-7.56131600	-3.32888300	0.01058900
H	-7.69045700	-4.40900300	0.14932100
H	-8.07926600	-2.76624000	0.80252300
H	-7.93421600	-3.01235200	-0.97571400
C	-4.65072600	6.03540600	-0.17892100
H	-4.35048600	6.61548500	-1.06507900
H	-5.70554600	5.74257000	-0.24254500
H	-4.46072300	6.62172200	0.73313200

TS = [Ru(Bid)(4,4'-$(COOMe)_2$Bpy)(H—CO_2)]

Ru	0.61324800	-0.72398400	-0.00801000
H	1.18875000	-2.25211200	0.40748200
N	2.54068400	-0.12915700	-0.03025100
N	2.69150600	1.06945300	2.09365400
N	0.49526400	-0.04326900	1.99183500
N	3.30068100	-1.16542500	-2.11012100
N	0.84365100	-1.34940400	-1.99741400
N	-1.36339700	-1.21259700	0.00746000

N	-0.29077700	1.11611300	-0.51380800
C	3.17527000	0.58061100	0.97219200
C	4.59985000	0.71394800	0.61799800
C	4.78615900	0.02538000	-0.58827400
C	3.46857800	-0.49792500	-0.99094200
C	5.65988200	1.33950400	1.26169500
H	5.50994300	1.87362000	2.20248100
C	6.92639400	1.26260400	0.66400100
H	7.78074100	1.74507900	1.14390500
C	7.11284700	0.57253000	-0.54307100
H	8.11023200	0.52471400	-0.98554800
C	6.03695500	-0.05616700	-1.18653600
H	6.17651500	-0.59540600	-2.12605300
C	2.07522500	-1.53912200	-2.61716800
C	2.14181600	-2.11822100	-3.91072500
H	3.13746100	-2.26497600	-4.32753400
C	-0.23844300	-2.18087100	-4.02144000
H	-1.17587300	-2.39056500	-4.53704400
C	-0.26931600	-1.64747600	-2.74554900
H	-1.22541000	-1.44495400	-2.26943900
C	1.43173800	0.80256600	2.57825700
C	1.15158600	1.42061200	3.82637500
H	1.91639800	2.08786800	4.22195700
C	-0.92257000	0.25194400	3.95615800
H	-1.84533100	-0.02231200	4.46775400
C	-0.63150700	-0.31395000	2.72874800
H	-1.31837100	-1.03557200	2.29291000
C	-1.87326700	-2.47075100	0.18384700
H	-1.13184400	-3.26587600	0.26733200
C	-3.22914100	-2.73143300	0.27243900
H	-3.57802900	-3.75251200	0.42132600
C	-4.13918400	-1.66786300	0.18114600
C	-3.64244600	-0.38323700	-0.02881400
H	-4.34691500	0.44427700	-0.11638500
C	-2.26947900	-0.17079900	-0.12794100
C	-1.66286200	1.13211500	-0.40549400
C	-2.39168400	2.31215400	-0.57490700
H	-3.47665500	2.31067400	-0.48394600
C	-1.72028300	3.49868000	-0.85905100
C	-0.32557800	3.47803700	-0.97841500

H	0.21454200	4.39790000	-1.20325100
C	0.34819700	2.28034200	-0.80202100
H	1.43421300	2.21503200	-0.88471400
C	1.68666700	-2.74233700	1.93384500
O	2.83708400	-2.43225700	1.97408500
O	0.70516100	-3.26055800	2.37302400
C	1.00291000	-2.44696600	-4.61561300
H	1.06811800	-2.88435100	-5.61355400
C	-0.01580500	1.16596100	4.51299200
H	-0.21746700	1.64601700	5.47251500
C	-2.42794300	4.79277400	-1.04046400
C	-5.60565100	-1.84373800	0.29377500
O	-6.41990100	-0.92206800	0.24357500
O	-1.86352000	5.85783400	-1.28065400
O	-5.94143200	-3.15349800	0.46026200
O	-3.77495400	4.65095900	-0.90850800
C	-4.49542500	5.91126000	-1.09609700
H	-4.32175900	6.30038900	-2.11133400
H	-5.55131800	5.65309600	-0.95123900
H	-4.16667700	6.65285100	-0.35203400
C	-7.38520200	-3.35557600	0.58172000
H	-7.90083700	-2.98041600	-0.31575200
H	-7.50764400	-4.44107300	0.67858200
H	-7.76819900	-2.83693800	1.47427100

[Ru(Bid)(4,4'-(COOMe)$_2$Bpy)(H-CO$_2$)]

Ru	0.41885900	-0.79737900	0.09297600
N	2.39803600	-0.37250300	0.10427800
N	2.72771900	0.24886400	2.44605800
N	0.40437100	-0.54506900	2.19407000
N	2.99462000	-0.82323400	-2.22360900
N	0.55803400	-1.13437300	-1.99201500
N	-1.60850100	-1.07188700	0.07158700
N	-0.21642700	1.10368200	-0.16359500
C	3.11567200	0.05868900	1.20698800
C	4.50995400	0.29505500	0.79071900
C	4.59172700	-0.03293500	-0.56748400
C	3.24429200	-0.45525700	-0.99013500
C	5.62304400	0.73462700	1.49534500
H	5.55486100	0.98511300	2.55613600

C	6.83513800	0.84491700	0.79879500
H	7.72957800	1.18994300	1.32195900
C	6.91703000	0.51597800	-0.56255000
H	7.87416800	0.60875800	-1.08030100
C	5.78861400	0.06890400	-1.26460900
H	5.84671900	-0.19217600	-2.32342500
C	1.74990900	-1.16228300	-2.70645600
C	1.75677500	-1.53813700	-4.07450100
H	2.72679700	-1.55365400	-4.56919300
C	0.59423800	-1.85686900	-4.74289400
H	0.61333600	-2.14555600	-5.79534300
C	-0.61135400	-1.78653500	-4.03322400
H	-1.56786300	-2.01098700	-4.50552700
C	-0.58158900	-1.43129800	-2.69710500
H	-1.51212900	-1.38539400	-2.13970800
C	1.47396200	-0.04926300	2.93030900
C	1.33894500	0.17057900	4.32631300
H	2.21169800	0.56928300	4.84130500
C	0.16934300	-0.11919300	4.99490400
H	0.08046900	0.05293100	6.06912600
C	-0.89573900	-0.65219900	4.25676800
H	-1.84131400	-0.92128000	4.72757600
C	-0.73686800	-0.84272500	2.89664500
H	-1.55242400	-1.26821400	2.31891300
C	-2.26069900	-2.26851900	0.15211300
H	-1.61871500	-3.14994200	0.20130800
C	-3.64183700	-2.36863600	0.17278800
H	-4.11578900	-3.34643300	0.24429400
C	-4.41206100	-1.19984000	0.10557000
C	-3.76218800	0.02802800	0.00404100
H	-4.35888400	0.93833000	-0.05739500
C	-2.37025900	0.07543400	-0.01742000
C	-1.58489300	1.29797000	-0.15581900
C	-2.13017300	2.57263600	-0.29687100
H	-3.21004300	2.72320700	-0.29469400
C	-1.29333200	3.67443000	-0.45066700
C	0.09190100	3.47393500	-0.45863400
H	0.77751000	4.31163200	-0.57560400
C	0.59207200	2.19012100	-0.31422200
H	1.66326300	1.99209600	-0.31792300

C	1.56136500	-3.31170400	0.24313200
H	0.67143600	-2.57190000	0.51411700
O	1.33715000	-3.97202300	-0.78110000
O	2.45519200	-3.32748000	1.10005300
C	-5.89674900	-1.20646800	0.13526500
C	-1.91701900	5.01465400	-0.60709100
O	-6.59056500	-0.19366800	0.06514000
O	-3.12959200	5.21557700	-0.59023400
O	-6.38640500	-2.46968700	0.25304500
O	-0.97673200	5.98154900	-0.77620000
C	-7.84888600	-2.50953500	0.30333400
H	-8.27394000	-2.10697900	-0.62883600
H	-8.09361100	-3.57255300	0.41663500
H	-8.21628000	-1.92843600	1.16305800
C	-1.55505500	7.31558100	-0.94602800
H	-2.12349500	7.60229700	-0.04802500
H	-0.69066000	7.97511200	-1.08834300
H	-2.21348500	7.33612100	-1.82802500

[Ru(Bid)(4,4'-$(COOMe)_2$Bpy)(O-COH)]

Ru	0.52780900	-0.84152900	0.06118300
N	2.44509900	-0.23074200	0.07667500
N	2.50581700	1.00826100	2.17964800
N	0.38472900	-0.24496500	2.07101400
N	3.25289400	-1.21035100	-2.00957700
N	0.79859000	-1.44634400	-1.93524800
N	-1.45228900	-1.32508300	0.04742000
N	-0.28353300	0.94245900	-0.42325600
C	3.02671200	0.54029500	1.06716100
C	4.43532300	0.77443800	0.70090000
C	4.66523500	0.08717600	-0.49940500
C	3.38619100	-0.53299800	-0.89159800
C	5.45105800	1.48130900	1.33161300
H	5.26850700	2.01334600	2.26776700
C	6.71665900	1.48921700	0.72714500
H	7.53638400	2.03707200	1.19693700
C	6.94649200	0.80082100	-0.47317300
H	7.94250400	0.82026500	-0.92079900
C	5.91576100	0.08847100	-1.10336000

H	6.08934200	-0.45076800	-2.03709000
C	2.04520400	-1.64063100	-2.51870100
C	2.14533900	-2.26823400	-3.78698600
H	3.15000300	-2.41634100	-4.18105700
C	-0.23357400	-2.36466600	-3.94333600
H	-1.15684200	-2.60455900	-4.47099700
C	-0.29617900	-1.78244400	-2.68979500
H	-1.26326600	-1.56689500	-2.24105700
C	1.27468000	0.63532800	2.67502200
C	0.98219700	1.17004800	3.95612400
H	1.70239500	1.87648800	4.36672000
C	-0.98015900	-0.18074900	4.08805400
H	-1.85587800	-0.56164700	4.61365100
C	-0.68726900	-0.65278200	2.82066200
H	-1.32616600	-1.40517200	2.36279500
C	-1.98667800	-2.57456200	0.18484000
H	-1.25953900	-3.38538600	0.25613500
C	-3.35009600	-2.79688400	0.25383900
H	-3.74423500	-3.80669300	0.37079200
C	-4.23063500	-1.70732700	0.18605800
C	-3.70373200	-0.42810200	0.01980700
H	-4.37020700	0.43004200	-0.05387200
C	-2.32233100	-0.25645200	-0.06212200
C	-1.66303800	1.01988900	-0.32227600
C	-2.33430500	2.22621900	-0.51070700
H	-3.41898500	2.28450400	-0.41719700
C	-1.62099800	3.37914100	-0.82839200
C	-0.22888000	3.29366300	-0.96486200
H	0.36187600	4.17149900	-1.22311600
C	0.39752900	2.07681000	-0.75683000
H	1.47815100	1.96852600	-0.84793900
C	1.91378200	-3.16496800	1.48039800
H	2.07183000	-4.26715100	1.51298100
O	1.12760500	-2.82090300	0.52303900
O	2.47393700	-2.44938500	2.31874700
C	1.02349900	-2.64042800	-4.49840800
H	1.11446000	-3.11779200	-5.47587400
C	-0.13749500	0.78106300	4.66201500
H	-0.34651000	1.19325000	5.65096700
O	-6.19081400	-3.08007400	0.37818600

O	-3.59682100	4.74108100	-0.88560100
O	-6.40138300	-0.80104800	0.25059800
O	-1.55246400	5.67517800	-1.33578300
C	-2.37711200	4.64268400	-1.01134600
C	-5.68843200	-1.96184600	0.28180700
C	-2.27032600	6.93452700	-1.53484500
H	-1.49205700	7.65874300	-1.80378600
H	-3.00716600	6.83015600	-2.34627400
H	-2.77966000	7.23442900	-0.60587600
C	-7.84530800	-1.02023200	0.33373400
H	-8.28056200	-0.01396900	0.31049500
H	-8.19044400	-1.61532100	-0.52586800
H	-8.10183900	-1.53755400	1.27107700

TS = [Ru(Bid)(4,4'-(COOMe)$_2$Bpy)(--O-COH)]

Ru	0.46670900	-0.70721400	0.07217400
N	2.44033500	-0.27010700	0.06798700
N	2.67578800	0.83072400	2.23684800
N	0.38435400	-0.07057500	2.09451900
N	3.11698800	-1.20741200	-2.08557600
N	0.65350800	-1.28033300	-1.94525000
N	-1.52171100	-1.13392700	0.08988700
N	-0.27748800	1.06058200	-0.37220000
C	3.12343400	0.35462800	1.09896100
C	4.54923000	0.42588200	0.73187900
C	4.68276000	-0.19626600	-0.51599900
C	3.33473600	-0.62378200	-0.93158600
C	5.64860500	0.95394900	1.39629700
H	5.53840300	1.43672100	2.36968700
C	6.90118500	0.84573400	0.77586800
H	7.78626800	1.25169700	1.27037500
C	7.03542900	0.22077000	-0.47302100
H	8.02337800	0.14707600	-0.93260000
C	5.92005300	-0.30950900	-1.13689100
H	6.01905600	-0.79794300	-2.10866100
C	1.86703300	-1.50517000	-2.58532900
C	1.89110100	-2.04362800	-3.89685300
H	2.87364400	-2.21894500	-4.33293600
C	0.72955500	-2.30388800	-4.59329900
H	0.76288800	-2.71346100	-5.60446400

C	-0.49087800	-2.00592000	-3.97370300
H	-1.44354200	-2.16332100	-4.47968700
C	-0.48114100	-1.50894500	-2.68282400
H	-1.42248100	-1.28132700	-2.18966900
C	1.39434600	0.65590600	2.71254500
C	1.17321000	1.24014300	3.98680500
H	1.99649200	1.81422000	4.40969000
C	-0.01401100	1.06443700	4.66574500
H	-0.16948900	1.51646700	5.64711600
C	-1.00119900	0.26664900	4.07218300
H	-1.94485500	0.05472100	4.57505600
C	-0.76378700	-0.26708900	2.81807700
H	-1.51327500	-0.90385300	2.35503200
C	-2.07626200	-2.36755700	0.25772500
H	-1.36535700	-3.19009600	0.35906900
C	-3.44697900	-2.56366800	0.31408000
H	-3.84884800	-3.56600900	0.45571000
C	-4.30237500	-1.45861200	0.19786400
C	-3.74898500	-0.19352300	0.00856500
H	-4.40917100	0.66819100	-0.09298800
C	-2.36594900	-0.05102700	-0.05187200
C	-1.65740500	1.19624600	-0.30063800
C	-2.26754900	2.43229600	-0.49121100
H	-3.35111900	2.53213200	-0.42034100
C	-1.49672800	3.55616400	-0.77538300
C	-0.10671700	3.41112500	-0.87511300
H	0.52882400	4.26565600	-1.10315300
C	0.46637700	2.16783600	-0.66984800
H	1.54270700	2.01482400	-0.73233400
C	1.90610400	-3.70065400	1.20868100
H	2.44503900	-4.66893400	1.37889400
O	1.37778600	-3.56955600	0.06996800
O	1.89733400	-2.88750800	2.16216600
C	-5.78119900	-1.57059900	0.26641200
C	-2.19362100	4.85438800	-0.95540100
O	-3.40999800	5.00116700	-0.84966800
O	-6.54883200	-0.61363100	0.18120600
O	-6.17815600	-2.86036300	0.43662300
O	-1.32059800	5.85445300	-1.24979400
C	-1.98248800	7.14784700	-1.43028300

H	-1.17250700	7.84143700	-1.68568000
H	-2.72227100	7.08756700	-2.24334500
H	-2.48088600	7.45315700	-0.49716900
C	-7.63310800	-2.99588700	0.52393000
H	-7.80458500	-4.07123400	0.65357400
H	-8.01614500	-2.43042900	1.38736300
H	-8.10673300	-2.62969600	-0.39989600

TS = [Ru(Bid)(4,4'-(COOMe)$_2$Bpy)(H--H--O-COH)]

Ru	-0.08913100	-0.35257000	-0.27492800
N	-0.21585800	1.64771500	-0.07574100
N	2.14718500	2.23003600	0.16823600
N	1.99942500	-0.15487600	-0.46139400
N	-2.63458000	1.98619500	-0.20645800
N	-2.19439100	-0.44168700	-0.14851800
N	0.08715500	-2.39829500	-0.31261700
N	0.19486200	-0.75044200	1.68850500
C	0.86112200	2.49332200	0.12902000
C	0.34543500	3.86437300	0.30254500
C	-1.04710200	3.79872300	0.16009200
C	-1.38940500	2.38113700	-0.06815200
C	0.98927000	5.07148500	0.54111800
H	2.07526700	5.11671800	0.64836000
C	0.20042200	6.22711700	0.63970500
H	0.67623700	7.19190400	0.82919200
C	-1.19319200	6.16193300	0.49529600
H	-1.78425000	7.07719600	0.57292800
C	-1.83527700	4.93849600	0.25206400
H	-2.92004000	4.88250800	0.13683700
C	-3.03326600	0.66535500	-0.26967200
C	-4.42561600	0.49695800	-0.40475200
H	-5.04258900	1.38673500	-0.50942900
C	-5.01644600	-0.76236500	-0.37688600
C	-4.17603100	-1.87509800	-0.17747800
H	-4.56071800	-2.88975300	-0.10795800
C	-2.81408500	-1.65900100	-0.07578900
H	-2.15753400	-2.51347000	0.07127700
C	2.70444200	1.00442000	-0.13958800
C	4.11310900	1.01275500	-0.15964100
H	4.62520900	1.93510700	0.10556400

C	4.84708100	-0.10594600	-0.54059700
C	4.13288500	-1.25563800	-0.92807900
H	4.62738900	-2.16051200	-1.27249900
C	2.75143900	-1.22130000	-0.86881500
H	2.19455200	-2.10364500	-1.17691900
C	-0.06403200	-3.20207900	-1.40350900
H	-0.35560800	-2.68658500	-2.32061100
C	0.15282000	-4.57195900	-1.36324400
H	0.02309900	-5.16556900	-2.26884200
C	0.54414400	-5.16603800	-0.15767700
H	0.73310900	-6.23894100	-0.09972500
C	0.68437900	-4.36589100	0.97094800
H	0.97845500	-4.80796900	1.92280500
C	0.44418600	-2.98954600	0.88284000
C	0.50390200	-2.06177000	2.00895900
C	0.80686400	-2.43515900	3.32348500
H	1.05313800	-3.47299900	3.54814900
C	0.79165400	-1.48500400	4.33789500
H	1.03067100	-1.76817400	5.36381400
C	0.45959200	-0.16460700	4.01725800
H	0.42891000	0.61155700	4.78257600
C	0.17007500	0.16344300	2.70087300
H	-0.09371300	1.18064400	2.41067900
C	0.01997428	0.60058101	-3.84395873
H	-0.37036772	0.45664101	-4.87836873
O	-0.54973572	-0.18127599	-3.00098773
O	0.90512028	1.44511401	-3.65109273
O	-6.37176600	-0.80891400	-0.52456600
O	6.20575600	0.01584500	-0.52234200
C	-6.95619600	-2.13980100	-0.46525900
H	-6.78093700	-2.60624100	0.51920000
H	-8.03160600	-1.97717700	-0.61495600
H	-6.55929000	-2.78383900	-1.26833800
C	6.94078400	-1.16961600	-0.93579000
H	7.99789600	-0.88684000	-0.84615600
H	6.72289200	-2.02361000	-0.27185800
H	6.71083700	-1.43237000	-1.98242200

-------Optimized geometries for catalytic system of 1d'-----

[Ru(4,4'-(OMe)$_2$ Bid)(Bpy)(Cl)]

Ru	-0.04718000	-0.31400300	-0.37389300
N	-0.22164100	1.68705100	-0.19857900
N	2.12789500	2.34861100	-0.01451800
N	2.04478500	-0.05857200	-0.55300500
N	-2.65434100	1.95382600	-0.23444000
N	-2.14506600	-0.46253600	-0.22063400
N	0.19204300	-2.36169000	-0.37512500
N	0.23085400	-0.66928900	1.59575500
C	0.83305800	2.57080800	-0.05202900
C	0.28212300	3.93302100	0.08466900
C	-1.11129800	3.82090600	-0.00332200
C	-1.41729500	2.38657000	-0.16874900
C	0.89652000	5.16685300	0.25513700
H	1.98366100	5.24854000	0.32127200
C	0.07619900	6.30168500	0.33778700
H	0.52820400	7.28694700	0.47209300
C	-1.31916400	6.18955300	0.24836800
H	-1.93516600	7.08920900	0.31327900
C	-1.93116900	4.93904900	0.07663800
H	-3.01717700	4.84562600	0.00605100
C	-3.01896900	0.62197500	-0.26714500
C	-4.41307500	0.41946100	-0.30294600
H	-5.05675100	1.29529800	-0.34492700
C	-4.96950100	-0.85491900	-0.26260000
C	-4.08827700	-1.94899300	-0.16980600
H	-4.43971500	-2.97646500	-0.11528800
C	-2.72836200	-1.69759700	-0.15373400
H	-2.04313300	-2.53874200	-0.08700500
C	2.71868100	1.12438200	-0.25490600
C	4.12785400	1.16021800	-0.23039700
H	4.61318400	2.10224800	0.01555500
C	4.89378500	0.04160300	-0.54133800
C	4.21262900	-1.13418000	-0.91131900
H	4.73376300	-2.04120200	-1.20730900
C	2.82992100	-1.12345100	-0.89853600
H	2.29874200	-2.02477200	-1.19560500
C	0.08449400	-3.19703200	-1.44809400
H	-0.20406000	-2.70890100	-2.38154100
C	0.33931100	-4.55898500	-1.37144400

H	0.24240800	-5.17616100	-2.26534800
C	0.72425100	-5.11455000	-0.14612200
H	0.94023700	-6.18036900	-0.05849100
C	0.82249400	-4.28363700	0.96420500
H	1.11111600	-4.69418100	1.93149200
C	0.54646600	-2.91696000	0.83892400
C	0.56700100	-1.96602600	1.94621900
C	0.86227200	-2.30501500	3.27201900
H	1.13195800	-3.33153300	3.52075700
C	0.81007500	-1.33605900	4.26702000
H	1.04278400	-1.59281800	5.30129300
C	0.44838100	-0.03132700	3.91546600
H	0.38730700	0.75881100	4.66454400
C	0.16824400	0.26398800	2.58947300
H	-0.11586000	1.26854900	2.27627800
O	-6.33103800	-0.93399200	-0.30109200
O	6.24913800	0.18656700	-0.47944300
C	-6.87484700	-2.28161500	-0.23238100
H	-7.96357400	-2.14366100	-0.26463400
H	-6.54790500	-2.88614800	-1.09552800
H	-6.58772200	-2.77724500	0.71065300
C	7.01526000	-0.99737500	-0.83742600
H	8.06447300	-0.69531800	-0.72155000
H	6.78963000	-1.83754500	-0.15870300
H	6.82336200	-1.29085100	-1.88350000
Cl	-0.31721900	-0.08351100	-2.84213200

$[Ru(4,4'\text{-}(OMe)_2\,Bid)(\,Bpy)]^+$

Ru	-0.05500900	-0.31837300	-0.49734000
N	-0.19089700	1.69490100	-0.38464200
N	2.16943600	2.31898300	-0.18031500
N	2.05446800	-0.09778500	-0.67250700
N	-2.61873400	2.00257200	-0.37939100
N	-2.15275300	-0.42569400	-0.41170000
N	0.13259700	-2.37301700	-0.53581500
N	0.16718600	-0.71150700	1.42014900
C	0.88230600	2.56300500	-0.22451100
C	0.35207200	3.93078100	-0.07710700
C	-1.04317500	3.84219900	-0.15178600
C	-1.37691500	2.41635000	-0.32520000

C	0.98955900	5.15209800	0.09954800
H	2.07839400	5.21417600	0.15660000
C	0.18924500	6.29838400	0.20311700
H	0.65842600	7.27443000	0.34461400
C	-1.20907100	6.21003400	0.12717300
H	-1.80891400	7.11894700	0.21014100
C	-1.84398400	4.97286400	-0.05201200
H	-2.93201400	4.89830300	-0.11055000
C	-3.00743800	0.67881400	-0.43718800
C	-4.40362300	0.50547400	-0.48644400
H	-5.02839400	1.39527400	-0.51490700
C	-4.98735500	-0.75729700	-0.47197500
C	-4.12881000	-1.87093400	-0.38697600
H	-4.50289300	-2.89090400	-0.34464600
C	-2.76577200	-1.65161700	-0.35801800
H	-2.10126700	-2.50883000	-0.29455800
C	2.74446600	1.08256000	-0.39813600
C	4.15196800	1.10201700	-0.36874100
H	4.64756800	2.04437700	-0.14653000
C	4.90575900	-0.03650200	-0.63683600
C	4.21031200	-1.21794400	-0.96108400
H	4.72138500	-2.14412500	-1.21163500
C	2.82942600	-1.19061800	-0.95865400
H	2.29091400	-2.09875000	-1.21714700
C	0.04386200	-3.17015500	-1.63558400
H	-0.19363200	-2.65567800	-2.56875300
C	0.24824900	-4.54246900	-1.58390500
H	0.16805300	-5.13482400	-2.49574100
C	0.56016600	-5.13903700	-0.35744200
H	0.73370500	-6.21383100	-0.28939400
C	0.64399900	-4.34109800	0.77884200
H	0.87954900	-4.78317100	1.74668100
C	0.42215600	-2.96450500	0.67326900
C	0.44175100	-2.02185800	1.78285000
C	0.68341900	-2.36537000	3.11627800
H	0.90459500	-3.40228400	3.37077000
C	0.63904500	-1.39159700	4.10661300
H	0.82967700	-1.65290300	5.14810100
C	0.33952100	-0.07583300	3.74083600
H	0.28591000	0.71904700	4.48512900

C	0.11090900	0.23144900	2.40803100
H	-0.12257000	1.24552300	2.08802100
O	-6.34676800	-0.80699400	-0.52450400
O	6.25959800	0.09370700	-0.57652800
C	-6.92294300	-2.14346300	-0.48391600
H	-8.00728500	-1.97788400	-0.52655200
H	-6.59941200	-2.74004100	-1.35358600
H	-6.65928000	-2.65993200	0.45439900
C	7.01449900	-1.10926900	-0.89885900
H	8.06636600	-0.81287600	-0.79509700
H	6.78235600	-1.92459400	-0.19314000
H	6.81581300	-1.43270500	-1.93458100

$[Ru(4,4'\text{-}(OMe)_2\,Bid)(\,Bpy)(H_2)]^+$

Ru	0.00222500	-0.35494900	-0.57446800
N	0.01568500	1.67505800	-0.43113900
N	2.42047100	2.12010200	-0.29538900
N	2.12393700	-0.31522700	-0.59155300
N	-2.38361700	2.15289700	-0.30067900
N	-2.12332900	-0.28469900	-0.61347500
N	-0.02302000	-2.43020500	-0.36440900
N	-0.00894600	-0.56993800	1.48359600
C	1.15445500	2.45496700	-0.29342800
C	0.72938500	3.85371900	-0.09229100
C	-0.66977100	3.86286100	-0.09434100
C	-1.11296100	2.47009600	-0.29702800
C	1.45891000	5.02268400	0.08237100
H	2.55097700	5.00913400	0.08395800
C	0.74609400	6.21757400	0.25426500
H	1.28818900	7.15553800	0.39254700
C	-0.65701000	6.22665500	0.25234600
H	-1.18740700	7.17149500	0.38919900
C	-1.38466600	5.04112800	0.07836700
H	-2.47681700	5.04141500	0.07695800
C	-2.88182300	0.87393900	-0.46678100
C	-4.28779200	0.81820400	-0.48290700
H	-4.83837000	1.74817800	-0.36155900
C	-4.97208300	-0.38199900	-0.65497300
C	-4.20523600	-1.55047400	-0.82188200

H	-4.65775600	-2.52708200	-0.97341900
C	-2.82775600	-1.44274300	-0.79365800
H	-2.23325200	-2.34154800	-0.93415000
C	2.89964000	0.83342300	-0.45895100
C	4.30432100	0.75748900	-0.48729900
H	4.86936300	1.68035800	-0.37868000
C	4.96970300	-0.45362200	-0.65737600
C	4.18518500	-1.61299300	-0.80467100
H	4.62305600	-2.59720400	-0.95006600
C	2.80961300	-1.48550000	-0.76547300
H	2.20012600	-2.37640500	-0.89196600
C	-0.03668200	-3.35002000	-1.37227000
H	-0.02767700	-2.94350000	-2.38449500
C	-0.06332500	-4.71901900	-1.14621800
H	-0.07207500	-5.40384500	-1.99448800
C	-0.08143400	-5.19172200	0.16840700
H	-0.10620400	-6.26173300	0.37879900
C	-0.06832000	-4.27106500	1.20943900
H	-0.08632300	-4.61570500	2.24256700
C	-0.03507900	-2.90021700	0.92960600
C	-0.01347400	-1.86191800	1.95933800
C	0.00352300	-2.12730500	3.33278500
H	0.00915700	-3.15695200	3.68749100
C	0.01692600	-1.07601200	4.24213300
H	0.03014000	-1.27560800	5.31440400
C	0.01421200	0.23253700	3.75684200
H	0.02352100	1.08736900	4.43318200
C	0.00335900	0.44768100	2.38472300
H	0.00547500	1.45564200	1.97276600
H	-0.01304100	0.14403400	-2.24078600
H	0.07879600	-0.69254500	-2.27654000
O	-6.33152500	-0.32058100	-0.65269800
O	6.32960600	-0.41050400	-0.67211600
C	6.98978600	-1.69421300	-0.86810500
H	8.06171800	-1.45762100	-0.86073800
H	6.75259300	-2.38840600	-0.04447800
H	6.70938000	-2.13764400	-1.83815600
C	-7.01038900	-1.59531400	-0.84432600
H	-8.07919900	-1.34604800	-0.82077900
H	-6.74944900	-2.03807600	-1.82004900

H	-6.76961600	-2.29565700	-0.02694300

[Ru(4,4'-(OMe)$_2$ Bid)(Bpy)(H)]

Ru	-0.07002200	-0.32618600	-0.56202600
H	-0.23546300	-0.23864900	-2.20412200
N	-0.25270700	1.68078100	-0.41651400
N	2.09747700	2.35052100	-0.22816100
N	2.02080600	-0.06345900	-0.73603500
N	-2.68892600	1.93475900	-0.38389400
N	-2.16929300	-0.47725000	-0.43460800
N	0.18606300	-2.36493100	-0.44701100
N	0.23161300	-0.64295100	1.54788800
C	0.79925500	2.56603300	-0.24692800
C	0.24442800	3.91876100	-0.05434800
C	-1.15054100	3.80058100	-0.11595300
C	-1.45061500	2.37243300	-0.32806700
C	0.85437400	5.15021700	0.14878600
H	1.94223700	5.23667600	0.19524500
C	0.02933400	6.27616400	0.29090900
H	0.47849900	7.25888900	0.45143400
C	-1.36699300	6.15776700	0.22854000
H	-1.98715100	7.04992900	0.34097700
C	-1.97486100	4.90975500	0.02431900
H	-3.06172000	4.81122400	-0.02416100
C	-3.05012600	0.60679800	-0.45387200
C	-4.44569500	0.40063200	-0.50036300
H	-5.09048900	1.27649500	-0.52406200
C	-4.99926200	-0.87378400	-0.49427700
C	-4.11456800	-1.96804300	-0.42361900
H	-4.46367500	-2.99746600	-0.39415400
C	-2.75590300	-1.71491300	-0.39672900
H	-2.06879200	-2.55588700	-0.35306400
C	2.69253900	1.13203500	-0.47157000
C	4.10359400	1.17861600	-0.46862000
H	4.58349700	2.13063400	-0.25196500
C	4.87455900	0.05877500	-0.75485500
C	4.19756400	-1.13522900	-1.07365500
H	4.72253700	-2.04910300	-1.34067000
C	2.81556900	-1.13398900	-1.04935100
H	2.28825200	-2.04785700	-1.31296700

C	0.09759500	-3.24182800	-1.49602400
H	-0.19018200	-2.79417000	-2.44751500
C	0.35979300	-4.59812800	-1.38367500
H	0.27531500	-5.23662100	-2.26380900
C	0.73510900	-5.12070500	-0.14077500
H	0.95677300	-6.18211200	-0.02112300
C	0.81454100	-4.25673100	0.94434700
H	1.09511600	-4.64186400	1.92417600
C	0.53398500	-2.89318900	0.78624800
C	0.56371700	-1.93226400	1.89273900
C	0.88105000	-2.27310400	3.21569000
H	1.14592800	-3.29842500	3.47269500
C	0.85813500	-1.29565500	4.20423200
H	1.10613200	-1.55103400	5.23574000
C	0.51092500	0.01316200	3.85522300
H	0.47854300	0.80708900	4.60217700
C	0.20775600	0.29523900	2.52915600
H	-0.07140500	1.30230100	2.21192200
O	-6.36244400	-0.95678400	-0.54284100
O	6.23151500	0.21572400	-0.71831900
C	-6.89987700	-2.30737500	-0.51808400
H	-7.98905100	-2.17442700	-0.55909900
H	-6.56010800	-2.88635500	-1.39390200
H	-6.62205200	-2.82959600	0.41352100
C	6.99927300	-0.97188700	-1.05624300
H	8.04833600	-0.65759500	-0.97618100
H	6.79867700	-1.79247700	-0.34623200
H	6.78549700	-1.30205700	-2.08721200

TS = [Ru(4,4'-$(OMe)_2$ Bid)(Bpy)(H—H—NMe_3)]$^+$

N	0.16135800	1.54280900	0.18261700
N	2.56019700	2.00721400	0.05260300
N	2.24400900	-0.43165600	-0.16040100
N	-2.20943100	1.96405500	0.62769600
N	-1.97871800	-0.32849400	-0.26083900
N	0.04280300	-2.50011600	-0.31427700
N	-0.00473100	-0.98391800	1.81891400
C	1.30406700	2.32379500	0.25895900
C	0.90584800	3.68693200	0.66194800

C	-0.48133500	3.66591700	0.85809000
C	-0.94034100	2.29850900	0.54560400
C	1.64505900	4.84549400	0.86296300
H	2.72621600	4.85670500	0.70877800
C	0.95751200	5.99912200	1.26753800
H	1.50889400	6.92728000	1.43288500
C	-0.43121200	5.97808600	1.46398800
H	-0.94226000	6.88971400	1.78142600
C	-1.17013900	4.80359700	1.25936400
H	-2.25141000	4.78211000	1.41171900
C	-2.72344900	0.74959200	0.21267600
C	-4.13032100	0.69001900	0.24047700
H	-4.67402100	1.55091900	0.62323800
C	-4.82549700	-0.41776800	-0.23543000
C	-4.07367500	-1.48278000	-0.76942100
H	-4.53941200	-2.37100300	-1.18921500
C	-2.69465800	-1.38449600	-0.75362400
H	-2.10615600	-2.19906700	-1.17111500
C	3.02338600	0.72389100	-0.16997900
C	4.41773000	0.64835000	-0.35454200
H	4.98572100	1.57597600	-0.36634300
C	5.07279600	-0.57240900	-0.48708900
C	4.29411700	-1.74297100	-0.40688400
H	4.73013900	-2.73687100	-0.46791700
C	2.92662000	-1.61400900	-0.24918600
H	2.31947500	-2.51456500	-0.19601600
C	0.11860200	-3.23965100	-1.46023400
H	0.27885200	-2.66693000	-2.37528800
C	-0.00425500	-4.62130800	-1.47941900
H	0.06447200	-5.15519600	-2.42778100
C	-0.21856100	-5.30353700	-0.27745500
H	-0.32579800	-6.38895200	-0.26125400
C	-0.29060300	-4.57200000	0.90246000
H	-0.45058600	-5.08359000	1.85147400
C	-0.15305400	-3.17918600	0.87241200
C	-0.17229300	-2.33005200	2.06418100
C	-0.32324800	-2.81494100	3.36859700
H	-0.45674300	-3.88205800	3.54195600
C	-0.30119300	-1.93227800	4.44267300
H	-0.42029900	-2.30241400	5.46195700

C	-0.11857500	-0.56993900	4.19301500
H	-0.08929200	0.15555000	5.00641200
C	0.02562200	-0.13631500	2.88152000
H	0.17610700	0.91779100	2.64609000
H	-0.15357400	0.43051700	-2.10221200
H	0.33274700	-0.31809700	-1.88638900
N	-0.65793000	1.37864100	-3.09519800
Ru	0.13014300	-0.44660400	-0.18393800
C	-0.53445600	0.57292300	-4.32229800
H	0.50484600	0.21826700	-4.42103900
H	-1.20254200	-0.30165800	-4.24638200
H	-0.80363400	1.15763600	-5.22187600
C	0.27847900	2.51555100	-3.12102700
H	0.12441200	3.13395800	-2.22356300
H	1.31355700	2.13377000	-3.12206200
H	0.12619900	3.14322000	-4.02017800
C	-2.04627900	1.83515900	-2.91252000
H	-2.71483100	0.96193200	-2.84550400
H	-2.12159200	2.42402100	-1.98579600
H	-2.37122000	2.46669100	-3.76293600
O	6.42360800	-0.52994900	-0.66337400
O	-6.18521500	-0.36679900	-0.16081700
C	7.07188000	-1.82683000	-0.79518100
H	6.68810900	-2.37203300	-1.67415300
H	8.13525400	-1.59274200	-0.93528100
H	6.93663700	-2.43014100	0.11833100
C	-6.88149100	-1.54170000	-0.66411200
H	-7.94560200	-1.31876000	-0.51159200
H	-6.67990100	-1.69333500	-1.73806500
H	-6.60158400	-2.44242900	-0.09168100

TS = [Ru(4,4'-$(OMe)_2$ Bid)(Bpy)(H—CO_2)]

Ru	-0.12686800	-0.31496600	-0.32042900
H	-0.31328600	-0.06359300	-1.97922200
N	-0.30359600	1.67929200	-0.07251700
N	2.03943700	2.33401100	0.20991200
N	1.97682400	-0.06158200	-0.38209700
N	-2.73138400	1.95875400	-0.22757700
N	-2.22871500	-0.45790100	-0.24829600
N	0.09988300	-2.35753200	-0.39902300

N	0.09904100	-0.82036700	1.72100900
C	0.74572500	2.55806900	0.13552700
C	0.19342900	3.91875200	0.27371100
C	-1.19490800	3.81374900	0.11876100
C	-1.49622400	2.38452400	-0.08858200
C	0.80254200	5.14692700	0.49709600
H	1.88559200	5.22314800	0.61604900
C	-0.01741700	6.28320500	0.56407400
H	0.43084700	7.26387800	0.73883200
C	-1.40732600	6.17832200	0.40727100
H	-2.02308400	7.07893300	0.46099400
C	-2.01422000	4.93358400	0.18236000
H	-3.09603200	4.84592200	0.05895200
C	-3.10019500	0.63107200	-0.29472400
C	-4.49431400	0.43358500	-0.37022300
H	-5.13343900	1.31254700	-0.41690000
C	-5.05614600	-0.83818000	-0.35679400
C	-4.18103000	-1.93658900	-0.24896400
H	-4.53790600	-2.96286900	-0.20787900
C	-2.82104000	-1.69179400	-0.20047400
H	-2.14004600	-2.53564200	-0.12551100
C	2.63880900	1.11576600	-0.02960700
C	4.04657400	1.14945700	0.05986000
H	4.51878500	2.08787700	0.34220000
C	4.82595400	0.03507900	-0.22797100
C	4.16131100	-1.13798000	-0.63700800
H	4.69535900	-2.04406400	-0.91193400
C	2.78049900	-1.12578400	-0.69387900
H	2.26588300	-2.02405800	-1.02678400
C	0.01334300	-3.12683900	-1.52559600
H	-0.25678000	-2.58917000	-2.43495000
C	0.26114600	-4.49160100	-1.53392300
H	0.18161200	-5.04711900	-2.46908200
C	0.61589500	-5.12937500	-0.34006400
H	0.82731600	-6.19933100	-0.31778700
C	0.68564000	-4.37294700	0.82418400
H	0.94494100	-4.85076700	1.76904700
C	0.41818000	-2.99913700	0.78607900
C	0.42274200	-2.13501800	1.96861700
C	0.70487100	-2.57939600	3.26727300

H	0.96551500	-3.62226200	3.44514100
C	0.65347300	-1.68383800	4.32988900
H	0.87619000	-2.02006700	5.34371500
C	0.31114900	-0.35185000	4.07812300
H	0.25694700	0.38017400	4.88452800
C	0.04259700	0.03764000	2.77213600
H	-0.22904000	1.06589400	2.52660900
C	0.93485500	0.38320800	-3.07138500
O	0.94758100	1.57269900	-3.01261900
O	1.27321600	-0.67163000	-3.51178900
O	-6.41743200	-0.91242300	-0.43254800
O	6.17825900	0.17824400	-0.10520000
C	-6.96635100	-2.25845600	-0.38996400
H	-6.71068900	-2.76223700	0.55784200
H	-8.05328700	-2.11763000	-0.45493300
H	-6.61417700	-2.85813700	-1.24663300
C	6.95848200	-0.99971500	-0.45130200
H	8.00241400	-0.69863700	-0.29274900
H	6.71063900	-1.84954100	0.20741300
H	6.80621400	-1.27924400	-1.50773100

[Ru(4,4'-(OMe)$_2$ Bid)(Bpy)(H-CO$_2$)]

Ru	-0.00716600	-0.34429400	-0.25369300
N	-0.12337700	1.65834900	-0.00801200
N	2.24707900	2.26911200	0.04105900
N	2.08815600	-0.13473300	-0.49882000
N	-2.54763500	1.99531400	0.01982700
N	-2.11150600	-0.43265200	-0.07866300
N	0.14575400	-2.39487700	-0.35816700
N	0.28989900	-0.81145800	1.68902500
C	0.95933800	2.51636700	0.08923100
C	0.44937200	3.88853100	0.27113800
C	-0.94791800	3.81234300	0.24924100
C	-1.29881900	2.39011900	0.07352200
C	1.10406000	5.10347400	0.42577400
H	2.19487300	5.15612100	0.43793100
C	0.31830400	6.25672600	0.56350800
H	0.80113800	7.22845000	0.68828500
C	-1.08236100	6.18069000	0.54067700

H	-1.67083200	7.09464900	0.64729700
C	-1.73448400	4.94932600	0.38154900
H	-2.82455200	4.88467700	0.36015200
C	-2.95326100	0.67779700	-0.06972600
C	-4.35130000	0.52103400	-0.12306300
H	-4.96741800	1.41729700	-0.12415800
C	-4.94607800	-0.73600400	-0.16506900
C	-4.09846300	-1.85937400	-0.12457000
H	-4.48069100	-2.87710300	-0.13105700
C	-2.73286000	-1.65185100	-0.08155400
H	-2.07674900	-2.51736600	-0.05473100
C	2.79906000	1.03639300	-0.24373200
C	4.20636500	1.04882500	-0.30495500
H	4.72023800	1.98437700	-0.09600300
C	4.93517500	-0.08584600	-0.64588700
C	4.21500800	-1.25787400	-0.94754200
H	4.70404700	-2.18023400	-1.25065000
C	2.83645500	-1.22276900	-0.85912400
H	2.27679400	-2.12198200	-1.10361000
C	-0.00239400	-3.15630900	-1.47941600
H	-0.26925400	-2.60760000	-2.38504200
C	0.17415200	-4.53315000	-1.47900400
H	0.04672100	-5.09301200	-2.40594500
C	0.65636700	-4.41838700	0.87240100
H	0.91498100	-4.90007800	1.81543900
C	0.46047000	-3.03408700	0.82239300
C	0.54312200	-2.14000800	1.97412700
C	0.83200600	-2.55297400	3.27922800
H	1.03076500	-3.60509500	3.48178500
C	0.59695400	-0.28227800	4.02079300
H	0.60744400	0.47939100	4.80077700
C	0.31650100	0.08696300	2.71264900
H	0.10283200	1.12080600	2.44261500
C	-0.69553500	0.44180500	-2.83016800
H	-0.01676000	-0.20688400	-2.11298400
O	-1.71938300	-0.15457800	-3.20166300
O	-0.18704400	1.53015400	-3.13884600
C	0.51834600	-5.17672300	-0.28547000
H	0.67260400	-6.25626600	-0.25829200
C	0.86340600	-1.62286800	4.31213100

H	1.09078500	-1.93823300	5.33120700
O	-6.30689600	-0.77113500	-0.22638700
O	6.29155700	0.03959800	-0.67189300
C	7.02040900	-1.16382400	-1.04546600
H	8.07780700	-0.87154000	-1.00563900
H	6.82925600	-1.98201700	-0.33060200
H	6.75764100	-1.48231000	-2.06843300
C	-6.89073600	-2.10270100	-0.29104800
H	-6.65270100	-2.68598900	0.61456900
H	-7.97309900	-1.92781400	-0.34688200
H	-6.54897200	-2.63919100	-1.19236900

[Ru(4,4'-(OMe)$_2$ Bid)(Bpy)(O-COH)]

Ru	-0.08913100	-0.35257000	-0.27492800
N	-0.21585800	1.64771500	-0.07574100
N	2.14718500	2.23003600	0.16823600
N	1.99942500	-0.15487600	-0.46139400
N	-2.63458000	1.98619500	-0.20645800
N	-2.19439100	-0.44168700	-0.14851800
N	0.08715500	-2.39829500	-0.31261700
N	0.19486200	-0.75044200	1.68850500
C	0.86112200	2.49332200	0.12902000
C	0.34543500	3.86437300	0.30254500
C	-1.04710200	3.79872300	0.16009200
C	-1.38940500	2.38113700	-0.06815200
C	0.98927000	5.07148500	0.54111800
H	2.07526700	5.11671800	0.64836000
C	0.20042200	6.22711700	0.63970500
H	0.67623700	7.19190400	0.82919200
C	-1.19319200	6.16193300	0.49529600
H	-1.78425000	7.07719600	0.57292800
C	-1.83527700	4.93849600	0.25206400
H	-2.92004000	4.88250800	0.13683700
C	-3.03326600	0.66535500	-0.26967200
C	-4.42561600	0.49695800	-0.40475200
H	-5.04258900	1.38673500	-0.50942900
C	-5.01644600	-0.76236500	-0.37688600
C	-4.17603100	-1.87509800	-0.17747800
H	-4.56071800	-2.88975300	-0.10795800
C	-2.81408500	-1.65900100	-0.07578900

H	-2.15753400	-2.51347000	0.07127700
C	2.70444200	1.00442000	-0.13958800
C	4.11310900	1.01275500	-0.15964100
H	4.62520900	1.93510700	0.10556400
C	4.84708100	-0.10594600	-0.54059700
C	4.13288500	-1.25563800	-0.92807900
H	4.62738900	-2.16051200	-1.27249900
C	2.75143900	-1.22130000	-0.86881500
H	2.19455200	-2.10364500	-1.17691900
C	-0.06403200	-3.20207900	-1.40350900
H	-0.35560800	-2.68658500	-2.32061100
C	0.15282000	-4.57195900	-1.36324400
H	0.02309900	-5.16556900	-2.26884200
C	0.54414400	-5.16603800	-0.15767700
H	0.73310900	-6.23894100	-0.09972500
C	0.68437900	-4.36589100	0.97094800
H	0.97845500	-4.80796900	1.92280500
C	0.44418600	-2.98954600	0.88284000
C	0.50390200	-2.06177000	2.00895900
C	0.80686400	-2.43515900	3.32348500
H	1.05313800	-3.47299900	3.54814900
C	0.79165400	-1.48500400	4.33789500
H	1.03067100	-1.76817400	5.36381400
C	0.45959200	-0.16460700	4.01725800
H	0.42891000	0.61155700	4.78257600
C	0.17007500	0.16344300	2.70087300
H	-0.09371300	1.18064400	2.41067900
C	0.12526100	0.56142600	-3.22082600
H	-0.26508100	0.41748600	-4.25523600
O	-0.44444900	-0.22043100	-2.37785500
O	1.01040700	1.40595900	-3.02796000
O	-6.37176600	-0.80891400	-0.52456600
O	6.20575600	0.01584500	-0.52234200
C	-6.95619600	-2.13980100	-0.46525900
H	-6.78093700	-2.60624100	0.51920000
H	-8.03160600	-1.97717700	-0.61495600
H	-6.55929000	-2.78383900	-1.26833800
C	6.94078400	-1.16961600	-0.93579000
H	7.99789600	-0.88684000	-0.84615600
H	6.72289200	-2.02361000	-0.27185800

H	6.71083700	-1.43237000	-1.98242200

TS = [Ru(4,4'-(OMe)$_2$ Bid)(Bpy)(--OCO$_3$)]

Ru	-0.03399100	-0.31886600	-0.28837100
N	-0.14340900	1.69389900	-0.13259900
N	2.22425100	2.29322900	0.05394800
N	2.09241900	-0.13651400	-0.36494800
N	-2.56965700	2.02679200	-0.11030700
N	-2.13548200	-0.40376900	-0.13479000
N	0.11819200	-2.36314400	-0.37952700
N	0.15775900	-0.76135600	1.62726300
C	0.93793600	2.54773100	0.01986000
C	0.42295400	3.92143200	0.17620000
C	-0.97355700	3.84712500	0.11148200
C	-1.32167400	2.42458900	-0.06627100
C	1.07318400	5.13505100	0.35968400
H	2.16302600	5.18596500	0.40938400
C	0.28495500	6.28832000	0.48031400
H	0.76473000	7.25840400	0.62796200
C	-1.11464600	6.21417800	0.41433200
H	-1.70530500	7.12784600	0.51118200
C	-1.76248500	4.98453500	0.22817400
H	-2.85166600	4.92066400	0.17771500
C	-2.97562500	0.70746100	-0.15524700
C	-4.37470000	0.55019400	-0.18272700
H	-4.99074200	1.44628400	-0.20526300
C	-4.97092500	-0.70686100	-0.16491800
C	-4.12376500	-1.82873200	-0.09656600
H	-4.50647600	-2.84568200	-0.05995400
C	-2.75652600	-1.62068600	-0.08348100
H	-2.09994700	-2.48554400	-0.03944700
C	2.78831200	1.04768000	-0.13957100
C	4.19742700	1.06322700	-0.12513700
H	4.69761800	2.01134000	0.05906500
C	4.94442400	-0.08433300	-0.36886500
C	4.24134300	-1.27388700	-0.63743500
H	4.74520800	-2.21012400	-0.86399100
C	2.85899800	-1.23875100	-0.62127900
H	2.31780100	-2.15365300	-0.84817100
C	0.02661400	-3.12196100	-1.50685400

H	-0.19293100	-2.57276600	-2.42512600
C	0.21200700	-4.49800000	-1.49598900
H	0.13355700	-5.06025400	-2.42691700
C	0.50346500	-5.13832000	-0.28607500
H	0.66232100	-6.21706100	-0.25194600
C	0.58575400	-4.37964300	0.87736800
H	0.80453100	-4.85787000	1.83217500
C	0.38474300	-2.99691500	0.81539300
C	0.40613400	-2.08765100	1.95375600
C	0.62544900	-2.47481000	3.27949500
H	0.82639100	-3.52230700	3.50573900
C	0.58547400	-1.53036400	4.29826300
H	0.75928600	-1.82585600	5.33356300
C	0.31237800	-0.19856100	3.96850400
H	0.26361800	0.57430800	4.73607400
C	0.10469800	0.15131400	2.64287400
H	-0.10742200	1.17818300	2.34769000
C	-0.28794300	0.23217200	-3.54337200
H	-0.37515200	0.42227700	-4.64430500
O	-1.37391100	0.10462300	-2.92349300
O	0.87209200	0.16065600	-3.06302600
C	-6.91899100	-2.07414500	-0.17494300
H	-6.60731600	-2.66005400	-1.05634600
H	-6.65207800	-2.60880700	0.75254400
H	-8.00267800	-1.90080000	-0.20603800
C	7.04488000	-1.16468100	-0.65721500
H	6.84364300	-1.96032900	0.08003800
H	6.80613900	-1.51909400	-1.67430000
H	8.09976200	-0.86502900	-0.60462400
O	-6.33362700	-0.74254300	-0.19938000
O	6.30161800	0.04549700	-0.34037300

TS = [Ru(4,4'-$(OMe)_2$ Bid)(Bpy)(H—H—OCHO)]

Ru	-0.15431900	-0.34544000	-0.28696100
N	-0.22105200	1.67261800	-0.15496300
N	2.13474900	2.19884500	0.25977600
N	1.96157900	-0.22052700	-0.20408800
N	-2.62860700	2.07832500	-0.35395500

N	-2.26693800	-0.36313000	-0.40019700
N	-0.05738800	-2.40019700	-0.18074100
N	-0.16969500	-0.66291800	1.76482600
C	0.86266400	2.49040400	0.12469400
C	0.37368400	3.87457000	0.27419900
C	-1.01146800	3.84284800	0.07309800
C	-1.37726000	2.43567000	-0.17929500
C	1.03582000	5.06444100	0.54700600
H	2.11687000	5.08265100	0.70154300
C	0.27138000	6.23834500	0.61670700
H	0.76152000	7.19099200	0.82958600
C	-1.11645000	6.20678800	0.41440000
H	-1.68829800	7.13565700	0.47159600
C	-1.77656700	5.00019500	0.13901000
H	-2.85662100	4.96979100	-0.02093300
C	-3.06695300	0.77615900	-0.48065300
C	-4.46007600	0.66401200	-0.66526600
H	-5.04325000	1.57982200	-0.73291300
C	-5.09141800	-0.57222800	-0.74662400
C	-4.28987700	-1.72334600	-0.62151500
H	-4.70423900	-2.72783000	-0.65583400
C	-2.92716700	-1.56045500	-0.45546900
H	-2.30325900	-2.44630200	-0.37109400
C	2.67758700	0.94529400	0.05974200
C	4.08600000	0.93107900	0.10570700
H	4.60105800	1.86690600	0.31029100
C	4.81437200	-0.22860800	-0.13484600
C	4.09344800	-1.40405200	-0.41862400
H	4.58258300	-2.35210200	-0.62749300
C	2.71226300	-1.34030300	-0.43390900
H	2.15519300	-2.24284800	-0.66917300
C	-0.05347400	-3.26147300	-1.24109800
H	-0.16986200	-2.79515600	-2.22006700
C	0.09258800	-4.63398400	-1.10122200
H	0.09321600	-5.26818800	-1.98837600
C	0.24173400	-5.17752400	0.17917300
H	0.36781500	-6.25181400	0.32040300
C	0.21944900	-4.32173600	1.27459100
H	0.32131500	-4.72273000	2.28280700
C	0.06295700	-2.94389100	1.08349600

C	-0.01322200	-1.97033200	2.17234600
C	0.03583800	-2.30536500	3.53093600
H	0.16431000	-3.34457200	3.83242700
C	-0.08197700	-1.30960700	4.49405100
H	-0.04316000	-1.56180600	5.55472700
C	-0.25547300	0.01366300	4.07914000
H	-0.35686400	0.82395200	4.80161600
C	-0.29444100	0.29670700	2.72010800
H	-0.42783300	1.31566500	2.35472200
C	2.33392200	0.08865700	-3.34578700
H	3.27708700	-0.25216200	-3.83177500
O	1.47139200	-0.85876700	-3.19998400
O	2.20655300	1.27247900	-3.01727100
O	-6.44328600	-0.56360100	-0.92837700
O	6.17385300	-0.12536300	-0.08265700
C	-7.06270400	-1.87689000	-1.02344500
H	-6.92313100	-2.44957000	-0.09085600
H	-8.12969300	-1.67005000	-1.17894600
H	-6.66095600	-2.44130800	-1.88203900
C	6.89817800	-1.35012900	-0.38546800
H	7.95790100	-1.07433900	-0.30527600
H	6.66117900	-2.14381300	0.34330500
H	6.67736800	-1.69645800	-1.40948300
H	0.50398800	-0.44765700	-2.40956200
H	-0.28099400	-0.12991400	-2.00231800

-------Optimized geometries for catalytic system of 1w'-----

[Ru(4,4'-$(COOMe)_2$ Bid)(Bpy)(Cl)]

Ru	0.56208600	-0.85838400	0.19545600
N	2.52233800	-0.38141700	0.19008700
N	2.70493900	0.85667500	2.28915500
N	0.46056600	-0.16140400	2.18791600
N	3.23049500	-1.36526600	-1.93227400
N	0.77673000	-1.56721000	-1.77656100
N	-1.46213800	-1.16859800	0.18797900
N	-0.08626300	0.95506300	-0.40201800

C	3.16951600	0.35095200	1.16824700
C	4.57890000	0.51766900	0.76719000
C	4.73924100	-0.15547500	-0.45094900
C	3.42139900	-0.71063300	-0.81137800
C	5.64415500	1.16605600	1.37851000
H	5.51381700	1.68805200	2.32897300
C	6.88970200	1.12818200	0.73489600
H	7.74774100	1.62964900	1.18787000
C	7.05034100	0.45362800	-0.48453000
H	8.03150600	0.43744600	-0.96394600
C	5.96919200	-0.19911300	-1.09432800
H	6.08910600	-0.72650300	-2.04322400
C	2.00116400	-1.78042900	-2.39775800
C	2.05858600	-2.42910400	-3.65844300
H	3.05006500	-2.58342000	-4.08215000
C	-0.32112900	-2.54467700	-3.72384400
H	-1.26260200	-2.80588300	-4.20748500
C	-0.34065700	-1.93365400	-2.48248500
H	-1.29331400	-1.72307700	-2.00359300
C	1.44426100	0.61471300	2.78908300
C	1.21356200	1.19510900	4.06405200
H	2.01487500	1.81004000	4.47170400
C	-0.91210600	0.12272400	4.18401200
H	-1.83977800	-0.12687500	4.69929900
C	-0.66738900	-0.40498000	2.92874100
H	-1.39635300	-1.07181700	2.47496600
C	-2.11456500	-2.34586800	0.41964200
H	-1.46511100	-3.20726700	0.58715300
C	-3.49491000	-2.44510300	0.46002000
H	-3.96562500	-3.40784800	0.65474800
C	-4.27023500	-1.29480800	0.25591100
C	-3.62256200	-0.08836700	0.00232900
H	-4.22143800	0.80583600	-0.17074700
C	-2.23038800	-0.04145500	-0.03941500
C	-1.45666700	1.15157400	-0.36732700
C	-2.02103400	2.39127500	-0.66855300
H	-3.10067700	2.52638300	-0.62473100
C	-1.20144000	3.45737700	-1.02982900
C	0.18248400	3.24889500	-1.09235800
H	0.84264000	4.06654300	-1.38174800

C	0.70091500	2.00623500	-0.77802900
H	1.77180000	1.80915000	-0.81476000
C	0.04627500	0.96694400	4.76121400
H	-0.11603700	1.41573400	5.74303600
C	0.91500300	-2.82057700	-4.32269700
H	0.97313500	-3.31644500	-5.29342200
C	-5.75357300	-1.30137100	0.28357800
C	-1.73447800	4.80225200	-1.35771100
O	-6.45195200	-0.30332400	0.11100600
O	-1.03738000	5.75729900	-1.69486800
O	-6.24383100	-2.54937500	0.51736900
O	-3.09060700	4.84807900	-1.23815900
C	-7.70654400	-2.58959100	0.53197600
H	-8.10542300	-2.26111300	-0.44019700
H	-7.95326000	-3.64127000	0.72163800
H	-8.10003700	-1.94468200	1.33272100
C	-3.64090400	6.16499500	-1.56105500
H	-3.41246800	6.42718100	-2.60572300
H	-4.72211600	6.05972700	-1.41106600
H	-3.22384000	6.92871200	-0.88665700
Cl	1.16226000	-3.12564300	0.99424800

[Ru(4,4'-(COOMe)$_2$ Bid)(Bpy)]$^+$

Ru	-0.02572400	-0.25714600	-0.47376000
N	-0.03483100	1.75730400	-0.34517300
N	2.35763500	2.23278700	-0.15948200
N	2.09040400	-0.19513700	-0.52866500
N	-2.43667500	2.21843700	-0.35619500
N	-2.12583200	-0.23026800	-0.46239800
N	0.00260800	-2.33028200	-0.54739100
N	0.04273400	-0.71387500	1.45335100
C	1.08830300	2.56081300	-0.19598200
C	0.64730400	3.95877300	-0.05650600
C	-0.75091900	3.95598400	-0.12511100
C	-1.17092700	2.55519100	-0.29440200
C	1.35973700	5.13912500	0.11321400
H	2.45052500	5.13551800	0.16574300
C	0.63054600	6.33200900	0.21673200
H	1.15864900	7.27798500	0.35413000

C	-0.77096000	6.32921700	0.14746700
H	-1.31379800	7.27309400	0.23162400
C	-1.48160300	5.13321600	-0.02562300
H	-2.57234300	5.12485300	-0.07878800
C	-2.90165500	0.92824100	-0.43635700
C	-4.31479200	0.84274600	-0.46210800
H	-4.87805700	1.77438600	-0.45285900
C	-4.96950000	-0.37029600	-0.47087900
C	-4.19054300	-1.53830900	-0.45781400
H	-4.65022600	-2.52495000	-0.45377000
C	-2.81687000	-1.42221300	-0.45389700
H	-2.21044000	-2.32198900	-0.45216100
C	2.84459100	0.95870300	-0.32540600
C	4.25888500	0.89190500	-0.29692400
H	4.80556200	1.81800300	-0.12765600
C	4.93354900	-0.29536400	-0.48461400
C	4.17512900	-1.45610500	-0.70531000
H	4.65147000	-2.42057500	-0.87161300
C	2.79955200	-1.36023000	-0.71433900
H	2.20901900	-2.25216000	-0.89847300
C	-0.05168300	-3.08921600	-1.67377300
H	-0.13702100	-2.53507600	-2.61040000
C	0.00140700	-4.47685200	-1.64158700
H	-0.04493800	-5.04057900	-2.57351900
C	0.11814700	-5.12483900	-0.40809300
H	0.16730000	-6.21313900	-0.35397200
C	0.16892400	-4.36207000	0.75469600
H	0.25704500	-4.84526100	1.72742800
C	0.10543600	-2.96859000	0.66636700
C	0.12437100	-2.05164400	1.79928600
C	0.20243000	-2.44307700	3.13867600
H	0.26686500	-3.50270800	3.38558200
C	0.19604800	-1.48466900	4.14526000
H	0.25721100	-1.78406700	5.19212500
C	0.10814500	-0.13626500	3.79097800
H	0.09773600	0.64813200	4.54780400
C	0.03377900	0.21643500	2.45105400
H	-0.03728000	1.25675000	2.13780900
C	-6.45480700	-0.38065300	-0.46960200
C	6.41928200	-0.28597700	-0.45192300

O	-7.15433400	0.62946200	-0.50052500
O	7.10152100	0.71669300	-0.25249200
O	6.92814700	-1.52907800	-0.67286600
O	-6.94268800	-1.65062200	-0.41773600
C	-8.40530400	-1.69273200	-0.37814000
H	-8.65145300	-2.75894400	-0.30370400
H	-8.77748500	-1.14054700	0.49849800
H	-8.82553300	-1.25805400	-1.29811900
C	8.39105200	-1.55686100	-0.63756300
H	8.75385400	-1.24493900	0.35399800
H	8.65390900	-2.60231600	-0.83961900
H	8.80550100	-0.89177500	-1.41069400

$[Ru(4,4'\text{-}(COOMe)_2\ Bid)(\ Bpy)(H_2)]^+$

Ru	-0.01077500	-0.29615600	-0.53915700
N	-0.01216300	1.73129700	-0.38802100
N	2.38762700	2.18603000	-0.27481300
N	2.10204900	-0.24916300	-0.58242200
N	-2.40961100	2.18350800	-0.23786900
N	-2.12122800	-0.25351900	-0.52901700
N	0.00028800	-2.38000100	-0.33917200
N	0.03518200	-0.52551900	1.52327900
C	1.12007500	2.52185000	-0.27489400
C	0.68933300	3.91987900	-0.09555600
C	-0.71045300	3.91924100	-0.08260700
C	-1.14277800	2.52080500	-0.25435200
C	1.41270800	5.09652000	0.04964900
H	2.50471900	5.09106400	0.04030300
C	0.69251600	6.28909800	0.20642900
H	1.22921200	7.23324800	0.32104300
C	-0.71044000	6.28847100	0.21919400
H	-1.24584300	7.23212600	0.34340200
C	-1.43219200	5.09516700	0.07557200
H	-2.52419200	5.08869900	0.08570200
C	-2.88454600	0.89905900	-0.37894500
C	-4.29762600	0.81917900	-0.37036000
H	-4.85676300	1.74403600	-0.23954700
C	-4.95736400	-0.38166100	-0.53039800
C	-4.18657900	-1.54005200	-0.70527300
H	-4.65053900	-2.51407200	-0.84906200

C	-2.81070700	-1.42874300	-0.69675700
H	-2.20441700	-2.31723900	-0.84434500
C	2.86406100	0.90290100	-0.42155800
C	4.27716200	0.82347200	-0.40761800
H	4.83567900	1.74709900	-0.26573800
C	4.93802100	-0.37597800	-0.57338700
C	4.16850000	-1.53251100	-0.76603300
H	4.63346100	-2.50488300	-0.91762600
C	2.79257500	-1.42177400	-0.76255900
H	2.18712000	-2.30874100	-0.92260300
C	-0.01677900	-3.29237300	-1.35195600
H	-0.02184900	-2.88052300	-2.36201800
C	-0.02760100	-4.66302700	-1.13230100
H	-0.04140100	-5.34403700	-1.98344300
C	-0.02412200	-5.14107200	0.17993000
H	-0.03741600	-6.21215100	0.38576100
C	-0.00353200	-4.22579600	1.22588400
H	-0.00275100	-4.57606800	2.25710300
C	0.01309400	-2.85377200	0.95207100
C	0.04561100	-1.82003400	1.98823700
C	0.08852400	-2.09327300	3.35918400
H	0.10284700	-3.12440200	3.70903000
C	0.11617300	-1.04627000	4.27369100
H	0.14874300	-1.25230300	5.34434600
C	0.10253500	0.26488700	3.79759100
H	0.12295900	1.11551300	4.47880300
C	0.06389400	0.48780600	2.42679900
H	0.05369900	1.49796600	2.02025100
H	-0.00486200	0.21568900	-2.20587800
H	-0.12248200	-0.61514100	-2.24802000
C	6.42474000	-0.38145500	-0.54472000
C	-6.44434000	-0.38664300	-0.51673400
O	-7.13777100	0.61453800	-0.35363600
O	7.11638600	0.61831600	-0.36592500
O	6.91985900	-1.63369300	-0.74067100
O	-6.93725300	-1.64030600	-0.70882600
C	8.38273300	-1.67640800	-0.70749100
H	8.63401400	-2.72819100	-0.89035900
H	8.80210600	-1.03038700	-1.49393900
H	8.75064800	-1.35022300	0.27754700

C	-8.40044400	-1.68234400	-0.69508400
H	-8.64961900	-2.73544300	-0.87318200
H	-8.78123000	-1.34845700	0.28241300
H	-8.80903500	-1.04250000	-1.49220600

[Ru(4,4'-$(COOMe)_2$ Bid)(Bpy)(H)]

Ru	-0.09512100	-0.24226500	-0.50747700
H	-0.27621800	-0.06361800	-2.13057500
N	-0.13801300	1.76347700	-0.33528600
N	2.24536900	2.26473000	-0.13526800
N	1.99140800	-0.13224200	-0.67923400
N	-2.54506600	2.17173800	-0.40827100
N	-2.16849400	-0.26910500	-0.35156700
N	0.01354000	-2.30686600	-0.45700800
N	0.22574800	-0.66395500	1.60185200
C	0.96635400	2.57822600	-0.16400300
C	0.50244500	3.96660000	0.00017700
C	-0.89597700	3.94361500	-0.10201900
C	-1.28569400	2.53756700	-0.30316700
C	1.19017200	5.15558800	0.20720300
H	2.27954900	5.16810600	0.28566300
C	0.44080000	6.33684100	0.31182400
H	0.95172000	7.28825000	0.47569800
C	-0.95785200	6.31426800	0.20727300
H	-1.51742300	7.24869300	0.28982200
C	-1.64514000	5.10905900	-0.00071800
H	-2.73417800	5.08588000	-0.08182000
C	-2.97720100	0.86896200	-0.43717600
C	-4.38595600	0.73955200	-0.49989700
H	-4.97387500	1.65068800	-0.60181800
C	-4.20144500	-1.62398600	-0.22712400
H	-4.63663600	-2.61546800	-0.11321100
C	-2.83208900	-1.46967100	-0.20936900
H	-2.19736800	-2.34276000	-0.08854600
C	2.74149700	1.00965200	-0.38531000
C	4.15699000	0.94542100	-0.35960800
H	4.69860900	1.85613400	-0.10867200
C	4.08652200	-1.35063100	-1.00546900
H	4.56891900	-2.28750500	-1.27876100

C	2.71116300	-1.26028900	-1.00671400
H	2.12019700	-2.12379300	-1.29989300
C	-0.16912500	-3.13004900	-1.53308300
H	-0.44645500	-2.62621200	-2.45927800
C	-0.00739500	-4.50625800	-1.47546200
H	-0.16372200	-5.10436400	-2.37385800
C	0.36238000	-5.09853900	-0.26390300
C	0.53438500	-4.28493300	0.84980200
H	0.81298300	-4.72761300	1.80570700
C	0.34941500	-2.90031900	0.74696400
C	0.47352900	-1.98346400	1.88749000
C	0.80053100	-2.39432900	3.18724700
H	0.99571000	-3.44408600	3.40278500
C	0.87726700	-1.45236800	4.20775200
C	0.62205500	-0.11030100	3.91556400
H	0.67131400	0.65660100	4.68911000
C	0.30254100	0.23975700	2.60873800
H	0.09152800	1.27500100	2.33172200
C	4.84011400	-0.21541100	-0.65529700
H	5.90917585	-0.23446892	-0.61475614
C	-5.01086400	-0.48672700	-0.40308500
H	-6.07719309	-0.55290760	-0.46192715
C	0.57015062	-6.62073330	-0.15733898
C	1.23916013	-1.89026896	5.63914157
O	0.90290927	-7.13942586	0.93983934
O	1.30896219	-1.03917693	6.56344703
O	0.38430778	-7.44761413	-1.30913347
O	1.49676741	-3.26877269	5.91890212
C	0.65966900	-8.80897408	-0.96887581
H	-0.01119861	-9.12670663	-0.19823798
H	0.52823890	-9.42618227	-1.83298240
H	1.66800617	-8.89267287	-0.62080878
C	1.82110007	-3.42241557	7.30313555
H	0.99929309	-3.08807567	7.90125770
H	2.01741086	-4.45347813	7.51115499
H	2.68927869	-2.84065641	7.53274861

TS = $[Ru(4,4'\text{-}(COOMe)_2\,Bid)(Bpy)(H—H—NMe_3)]^+$

N	0.13650000	1.61009900	0.21468600

N	2.52288600	2.10490600	0.07649500
N	2.23788700	-0.34391300	-0.07573600
N	-2.24137100	1.98956600	0.62906400
N	-1.95591500	-0.30898900	-0.22870600
N	0.08869600	-2.44511000	-0.25492300
N	-0.01658400	-0.92007900	1.87905800
C	1.26202200	2.41457300	0.27137900
C	0.83866000	3.77989600	0.63167800
C	-0.54953000	3.73876000	0.82219800
C	-0.97969500	2.35555000	0.54743000
C	1.55598900	4.95692000	0.80156700
H	2.63742900	4.98375400	0.65183500
C	0.84497300	6.10852100	1.16916100
H	1.37831700	7.05112200	1.30957100
C	-0.54399600	6.06753500	1.36009400
H	-1.07318900	6.97851700	1.64804000
C	-1.26105300	4.87455300	1.18704200
H	-2.34241700	4.83860800	1.33537900
C	-2.71819300	0.76031500	0.23300100
C	-4.13056300	0.66444500	0.25759300
H	-4.68988300	1.51346900	0.64707700
C	-4.79079800	-0.44470000	-0.23025100
C	-4.02093700	-1.49425800	-0.75849900
H	-4.48782900	-2.38117400	-1.18289200
C	-2.64545800	-1.38493400	-0.73220400
H	-2.03609000	-2.18561300	-1.14423300
C	2.99663500	0.82422600	-0.09860400
C	4.40158800	0.75626300	-0.25550500
H	4.95370100	1.69390700	-0.29216400
C	5.06550400	-0.45101500	-0.33397000
C	4.30678800	-1.62840300	-0.23713300
H	4.77783200	-2.60932900	-0.26459900
C	2.93616300	-1.52738000	-0.11222500
H	2.33721300	-2.43154300	-0.04744600
C	0.19202600	-3.18169500	-1.39801400
H	0.35605900	-2.60766000	-2.31174200
C	0.09067300	-4.56578300	-1.41536200
H	0.18211200	-5.10139200	-2.36068300
C	-0.13217800	-5.24631100	-0.21503400
H	-0.22360300	-6.33312700	-0.19717500

C	-0.23374600	-4.51389600	0.96268700
H	-0.40161000	-5.02609900	1.90986100
C	-0.11493600	-3.11990200	0.93014700
C	-0.16286500	-2.26717600	2.12103500
C	-0.32041900	-2.75262600	3.42382100
H	-0.43548900	-3.82135200	3.59931700
C	-0.32779000	-1.86627000	4.49565900
H	-0.45188000	-2.23711200	5.51409600
C	-0.16907000	-0.50180400	4.24714600
H	-0.16407100	0.22529500	5.05939700
C	-0.01663600	-0.06812500	2.93588700
H	0.11608600	0.98800400	2.69877100
H	-0.15316400	0.42792600	-2.01432900
H	0.41169300	-0.24584600	-1.82347300
N	-0.74695000	1.32557400	-3.08127700
Ru	0.14302600	-0.37941400	-0.13178500
C	-0.63796200	0.43148900	-4.24587900
H	0.40069900	0.07016600	-4.33093300
H	-1.30373000	-0.43560300	-4.09566100
H	-0.91844200	0.94465800	-5.18552700
C	0.18569200	2.45772300	-3.20195800
H	0.05049800	3.13355200	-2.34318800
H	1.22152600	2.07693900	-3.20084600
H	0.01702700	3.02805700	-4.13651600
C	-2.13224000	1.79481800	-2.91631100
H	-2.79992700	0.92853100	-2.78375200
H	-2.19867900	2.44622000	-2.03123700
H	-2.46815200	2.36774300	-3.80408200
C	6.54180100	-0.44575300	-0.49880900
C	-6.27627200	-0.46322300	-0.19713500
O	7.22939600	0.57063900	-0.57201700
O	-6.97159500	0.43076300	0.28076500
O	7.03873000	-1.71232900	-0.56041200
O	-6.77186800	-1.59499700	-0.77027200
C	8.49239600	-1.74283600	-0.72268000
H	8.74538500	-2.80909000	-0.76864000
H	8.78408900	-1.22912400	-1.65186100
H	8.98367000	-1.26139700	0.13701100
C	-8.23458600	-1.64059800	-0.75890000
H	-8.48870000	-2.58060200	-1.26363500

H	-8.60732000	-1.63882900	0.27697700
H	-8.64758500	-0.77773600	-1.30365200

TS = [Ru(4,4'-(COOMe)$_2$ Bid)(Bpy)(H—CO$_2$)]

Ru	-0.12766300	-0.35341300	-0.29403600
H	-0.35906200	0.01396300	-1.91830000
N	-0.15600200	1.63546900	0.02161800
N	2.23254200	2.11901200	0.19034300
N	1.96650800	-0.25702400	-0.42905600
N	-2.55636700	2.07717500	-0.09863700
N	-2.20939600	-0.36696800	-0.14728400
N	-0.07349000	-2.41039000	-0.48644300
N	0.14132800	-1.00258500	1.71976200
C	0.95657500	2.44088200	0.17780200
C	0.50768300	3.83638500	0.32513100
C	-0.88932000	3.82785300	0.21357000
C	-1.29382500	2.42393500	0.02421900
C	1.20817400	5.02031000	0.51701200
H	2.29716300	5.02207800	0.60075800
C	0.47145000	6.21121600	0.59837600
H	0.99199400	7.15941100	0.74984100
C	-0.92666600	6.20282500	0.48506100
H	-1.47596500	7.14472000	0.54851300
C	-1.62631400	5.00260900	0.29089300
H	-2.71473400	4.99043800	0.20052200
C	-3.00487500	0.77989900	-0.16091100
C	-4.41820000	0.67347600	-0.19952200
H	-4.98259700	1.60297900	-0.23517900
C	-5.05170200	-0.55214000	-0.16885600
C	-4.25137100	-1.70373700	-0.08470000
H	-4.71106000	-2.69021200	-0.03247800
C	-2.88071400	-1.56816800	-0.07362800
H	-2.25636300	-2.45452200	-0.01432100
C	2.72082700	0.86558700	-0.08544600
C	4.13714900	0.79130800	-0.03911200
H	4.66907300	1.69576500	0.24823800
C	4.81103000	-0.36840900	-0.35988700
C	4.05189600	-1.48284500	-0.75607800
H	4.54482900	-2.41069000	-1.04442500
C	2.67855100	-1.38298200	-0.77898000

H	2.08680300	-2.23498000	-1.10167500
C	-0.25993000	-3.09286800	-1.65304600
H	-0.46369700	-2.47418800	-2.52770200
C	-0.19052200	-4.47632600	-1.73906900
H	-0.34645400	-4.96479800	-2.70143800
C	0.08197000	-5.21834200	-0.58592600
H	0.14715900	-6.30662000	-0.62269900
C	0.26237500	-4.54345400	0.61661900
H	0.46354700	-5.10256600	1.52996400
C	0.17707300	-3.14737400	0.65514600
C	0.31494200	-2.35588700	1.88223200
C	0.58833300	-2.90369000	3.14221200
H	0.73013600	-3.97804200	3.25613800
C	0.68607900	-2.06818300	4.24988700
H	0.90199400	-2.48567800	5.23460300
C	0.50554900	-0.69301400	4.08202000
H	0.57439900	-0.00626200	4.92592000
C	0.23811300	-0.20143100	2.80962600
H	0.08819300	0.86427000	2.62791000
C	0.79238600	0.47222200	-3.04239800
O	0.85369700	1.65698500	-2.92512400
O	1.07261900	-0.56502300	-3.56202500
C	-6.52516900	-0.70861400	-0.20562100
C	6.28848400	-0.48686900	-0.32094800
O	-7.10291200	-1.79503000	-0.20885600
O	6.90714200	-1.51254200	-0.60197000
O	6.88097600	0.67770200	0.06619700
O	-7.16375800	0.49489400	-0.23301300
C	8.33897600	0.57847800	0.11756500
H	8.74059100	0.32275800	-0.87514700
H	8.67503200	1.57431100	0.43141200
H	8.64454300	-0.18665900	0.84810200
C	-8.61980000	0.36072300	-0.27081600
H	-8.97646700	-0.18191400	0.61848100
H	-8.99340700	1.39185200	-0.27638900
H	-8.93171200	-0.17421700	-1.18142900

[Ru(4,4'-$(COOMe)_2$ Bid)(Bpy)(H-CO_2)]

Ru	-0.00473300	-0.27781600	-0.23524500
N	-0.03157700	1.72758100	-0.01995500

N	2.36076000	2.22232400	0.04805900
N	2.09493900	-0.18867400	-0.41789400
N	-2.43613900	2.16579300	0.01088500
N	-2.09832300	-0.27734000	-0.09950500
N	0.06182200	-2.34792900	-0.31523400
N	0.21636900	-0.75435700	1.73001000
C	1.08602300	2.53814300	0.07503600
C	0.63991300	3.93340300	0.23366900
C	-0.75982200	3.91879600	0.21264800
C	-1.17177000	2.51301100	0.05567100
C	1.34794600	5.12018100	0.37167400
H	2.43999600	5.12575100	0.38392500
C	0.61309800	6.30842700	0.49263800
H	1.13811800	7.25963100	0.60387500
C	-0.78947900	6.29399000	0.47074300
H	-1.33703300	7.23430300	0.56443800
C	-1.49586900	5.09078400	0.32909800
H	-2.58767000	5.07399300	0.30901000
C	-2.88793100	0.86969100	-0.07175900
C	-4.29928900	0.76537200	-0.10282300
H	-4.87589100	1.68888600	-0.09623900
C	-4.93651700	-0.45742000	-0.13383900
C	-4.14151100	-1.61433800	-0.11659600
H	-4.58624000	-2.60781700	-0.12336400
C	-2.76910700	-1.47759200	-0.09667200
H	-2.14812000	-2.36790200	-0.08977000
C	2.84867300	0.95939400	-0.18666600
C	4.26377500	0.89997400	-0.21345600
H	4.81113200	1.81945100	-0.01352200
C	4.93700400	-0.26970900	-0.49507700
C	4.17615900	-1.41710900	-0.77118500
H	4.64939500	-2.36382600	-1.02519100
C	2.80040800	-1.32909400	-0.72297100
H	2.20565100	-2.20735800	-0.95440700
C	-0.07451500	-3.10577800	-1.43769400
H	-0.29628200	-2.55096900	-2.35245900
C	0.05234600	-4.48883400	-1.42500800
H	-0.06332500	-5.04930600	-2.35301500
C	0.45793600	-4.37737200	0.94157700
H	0.66779900	-4.86307100	1.89445000

C	0.31479900	-2.98778900	0.87724700
C	0.39886300	-2.08886100	2.02716900
C	0.62601000	-2.50598200	3.34270400
H	0.76937500	-3.56420000	3.55890500
C	0.47126000	-0.22082600	4.06409100
H	0.49089100	0.54461800	4.83996300
C	0.25092600	0.15097000	2.74448600
H	0.09420100	1.19163300	2.46122700
C	-0.77295200	0.38136400	-2.85816600
H	0.03984700	-0.01648400	-2.08859600
O	-1.53751400	-0.50654300	-3.26450600
O	-0.62175400	1.57680300	-3.13952000
C	0.33081100	-5.13631500	-0.21764600
H	0.44397700	-6.22061800	-0.17975100
C	0.66605700	-1.56952600	4.36998200
H	0.84494100	-1.88785100	5.39781400
C	6.42254900	-0.25566200	-0.50403000
C	-6.42047700	-0.48783400	-0.17960200
O	7.10963200	0.73648300	-0.27016300
O	-7.13569100	0.51174100	-0.15864700
O	-6.89017400	-1.76416000	-0.25563700
O	6.92980300	-1.48422900	-0.80068800
C	-8.35029600	-1.82601200	-0.32879700
H	-8.57907500	-2.89438500	-0.42504800
H	-8.79723600	-1.41169300	0.58812700
H	-8.71200800	-1.26606600	-1.20485100
C	8.39287400	-1.50431000	-0.80566000
H	8.78043700	-1.21149300	0.18239100
H	8.65595700	-2.54332500	-1.03855900
H	8.78267800	-0.81937500	-1.57457800

[Ru(4,4'-$(COOMe)_2$ Bid)(Bpy)(O-COH)]

Ru	-0.10184200	-0.38757900	-0.30767500
N	-0.14315500	1.60655600	-0.05408800
N	2.23993500	2.08013900	0.18308500
N	1.97753400	-0.28027200	-0.49472700
N	-2.54558400	2.03066100	-0.14628100
N	-2.18449300	-0.41224200	-0.12782400
N	-0.01023400	-2.44896000	-0.41013800
N	0.19439100	-0.87178500	1.65256600

C	0.96768700	2.40865200	0.13835400
C	0.51176900	3.79999200	0.30360300
C	-0.88442000	3.78941500	0.17603900
C	-1.28465400	2.38675400	-0.03499900
C	1.20604700	4.98243600	0.52442500
H	2.29392600	4.98593000	0.62120600
C	0.46475200	6.16944100	0.61787800
H	0.98066300	7.11628500	0.79164100
C	-0.93190700	6.15896800	0.48859800
H	-1.48472100	7.09804600	0.56208400
C	-1.62570100	4.96042400	0.26595400
H	-2.71302400	4.94680400	0.16376200
C	-2.98434400	0.72758500	-0.18442300
C	-4.39653400	0.60817300	-0.22647600
H	-4.96988100	1.53079300	-0.28784300
C	-5.01836700	-0.62237400	-0.16526500
C	-4.21087100	-1.76538100	-0.04653100
H	-4.66347800	-2.75367600	0.02822200
C	-2.84094400	-1.61687300	-0.02805300
H	-2.20673500	-2.49384900	0.06495200
C	2.73016700	0.83204500	-0.12331700
C	4.14518300	0.75893800	-0.09632500
H	4.68054600	1.64941600	0.22599100
C	4.81668500	-0.37884900	-0.49679800
C	4.05596300	-1.46860300	-0.94988200
H	4.54705200	-2.37131800	-1.31163100
C	2.68048800	-1.37777000	-0.93023600
H	2.08298100	-2.21197500	-1.28899800
C	-0.20447400	-3.20627900	-1.52492900
H	-0.47920900	-2.64997800	-2.42299900
C	-0.04958200	-4.58590900	-1.53011500
H	-0.21292900	-5.14415000	-2.45239100
C	0.32423800	-5.23370900	-0.34817600
H	0.46608300	-6.31510000	-0.32552700
C	0.50861400	-4.47784100	0.80479900
H	0.79105300	-4.96440600	1.73835100
C	0.32849700	-3.09090500	0.76198100
C	0.44171000	-2.20403100	1.91994300
C	0.74350700	-2.63606200	3.21611700
H	0.93833600	-3.69124900	3.40529500

C	0.79256500	-1.71843500	4.25968900
H	1.03110800	-2.04776500	5.27188200
C	0.52822000	-0.37340600	3.98900900
H	0.55078300	0.37803900	4.77862300
C	0.23552500	0.01073500	2.68755100
H	0.02164200	1.04909000	2.43302500
C	0.18379600	0.57563500	-3.20789700
H	-0.22654100	0.51727300	-4.24180200
O	-0.48748300	-0.14609900	-2.38304800
O	1.17972800	1.27689600	-2.99268900
C	6.29597900	-0.49035900	-0.49635500
C	-6.49198500	-0.79081800	-0.19851000
O	-7.06057600	-1.88150600	-0.17973300
O	6.91356400	-1.47557200	-0.89782700
O	6.88689900	0.62948900	0.00680900
O	-7.13855600	0.40707200	-0.24527300
C	-8.59416300	0.26310900	-0.27029500
H	-8.93995600	-0.27205700	0.62775500
H	-8.97437100	1.29169800	-0.28451900
H	-8.90922500	-0.28364800	-1.17266100
C	8.34711600	0.54692700	0.01463500
H	8.67569300	1.48392400	0.48046400
H	8.67948900	-0.32197200	0.60316000
H	8.73103900	0.46664300	-1.01436400

TS = [Ru(4,4'-(COOMe)$_2$ Bid)(Bpy)(--OCOH)]

Ru	-0.03837700	-0.25831100	-0.25876100
N	-0.03684100	1.72860000	0.09933600
N	2.36233000	2.19641100	0.16271300
N	2.07540100	-0.21818900	-0.26997600
N	-2.43426500	2.20646600	0.07046600
N	-2.13590900	-0.23483400	-0.17026100
N	-0.03960300	-2.27387100	-0.62701800
N	0.06855500	-0.98199600	1.58734500
C	1.09318400	2.52773000	0.18368700
C	0.66414000	3.93124600	0.31330600
C	-0.73533700	3.93479100	0.28000900
C	-1.16487100	2.53312800	0.13738000
C	1.38638600	5.11164200	0.43379500

H	2.47829300	5.10349000	0.45415500
C	0.66623100	6.31126800	0.52528100
H	1.20265500	7.25774700	0.62158700
C	-0.73645200	6.31470300	0.49179800
H	-1.27240500	7.26370100	0.56225400
C	-1.45705900	5.11843700	0.36674500
H	-2.54877000	5.11517200	0.33646000
C	-2.90548200	0.92101800	-0.04457800
C	-4.31897200	0.83889800	-0.02031200
H	-4.87781300	1.76914200	0.06844500
C	-4.97945800	-0.36912300	-0.09822900
C	-4.20512400	-1.53563100	-0.19778600
H	-4.66759700	-2.51901100	-0.25971600
C	-2.83097000	-1.42149800	-0.22549600
H	-2.23150600	-2.32180800	-0.31106200
C	2.83758600	0.92010000	-0.01951800
C	4.25020900	0.83675900	0.03441800
H	4.80350000	1.75315100	0.23276300
C	4.91663200	-0.35394400	-0.16438000
C	4.14970400	-1.49946700	-0.42818000
H	4.61721900	-2.46594500	-0.60765800
C	2.77529500	-1.38452100	-0.46848200
H	2.18116200	-2.26438800	-0.69369400
C	-0.12278200	-2.84493100	-1.85799500
H	-0.18906300	-2.14515900	-2.69402500
C	-0.12132200	-4.22252600	-2.03841100
H	-0.18979600	-4.63461100	-3.04532900
C	-0.03104300	-5.05697600	-0.91993300
H	-0.02719900	-6.14166400	-1.03476400
C	0.05341100	-4.48673100	0.34734000
H	0.12122700	-5.12042800	1.23149400
C	0.04624400	-3.09542100	0.47655000
C	0.11692600	-2.35798300	1.73370100
C	0.22413600	-2.93856300	3.00089500
H	0.26453000	-4.02355800	3.09498100
C	0.28342900	-2.13326000	4.13264800
H	0.36949400	-2.58101800	5.12335000
C	0.23342900	-0.74533100	3.97761600
H	0.27836200	-0.07790200	4.83826500
C	0.12744000	-0.20367800	2.70458200

H	0.08764600	0.87203700	2.53681300
C	0.09553500	1.10315500	-3.47776500
H	-0.02050600	1.56861600	-4.49123700
O	-0.95214300	0.59195800	-2.99390600
O	1.23771700	1.15127800	-2.96533200
C	-6.46370300	-0.37686600	-0.07040900
C	6.40031900	-0.36123100	-0.10206100
O	-7.16139600	0.62820000	0.04924400
O	7.09015300	0.63009700	0.12767900
O	-6.95573300	-1.64099800	-0.19757700
O	6.90270500	-1.60603200	-0.33376000
C	-8.41805900	-1.68449700	-0.18026600
H	-8.66653700	-2.74305100	-0.32457900
H	-8.79950500	-1.32152800	0.78671400
H	-8.82880300	-1.07074000	-0.99664700
C	8.36420800	-1.64540900	-0.27643500
H	8.71586200	-1.34231100	0.72191400
H	8.62240100	-2.69145900	-0.48173900
H	8.79478300	-0.97866100	-1.03936400

TS = [Ru(4,4'-$(COOMe)_2$ Bid)(Bpy)(H—H—OCOH)]

Ru	-0.15901700	-0.38193100	-0.27530400
N	-0.17098000	1.62514400	-0.03980500
N	2.21142000	2.08046800	0.25318300
N	1.94645300	-0.32155100	-0.26205100
N	-2.56537700	2.09022100	-0.19502500
N	-2.25760400	-0.35939400	-0.26765400
N	-0.12451000	-2.45124900	-0.32701400
N	-0.07795900	-0.86377100	1.75234500
C	0.94387500	2.41603400	0.17827100
C	0.50185500	3.81448600	0.32703000
C	-0.89033700	3.81969700	0.17263700
C	-1.30223200	2.42195400	-0.04755000
C	1.20646000	4.98911100	0.55564700
H	2.29229500	4.98004100	0.67251800
C	0.47767700	6.18530700	0.62860800
H	1.00138000	7.12707500	0.80642900
C	-0.91640800	6.19048800	0.47294900
H	-1.45933600	7.13638700	0.53092000
C	-1.61999400	4.99931300	0.24260400

H	-2.70506100	4.99763500	0.11825400
C	-3.03059900	0.80069700	-0.29081100
C	-4.44407400	0.71976100	-0.37854000
H	-4.99114800	1.65952600	-0.41285000
C	-5.09797000	-0.49467600	-0.39853800
C	-4.32073600	-1.66145100	-0.32341500
H	-4.79721200	-2.64111000	-0.31928900
C	-2.94913900	-1.54927600	-0.25962200
H	-2.34255100	-2.44813600	-0.20952900
C	2.69797000	0.81555900	0.02139900
C	4.11437400	0.75213000	0.04990600
H	4.64485800	1.67366300	0.27872300
C	4.78999000	-0.41867800	-0.22279100
C	4.03207000	-1.55935800	-0.52971000
H	4.52491100	-2.50229800	-0.76395400
C	2.65676500	-1.46742000	-0.53303800
H	2.06703600	-2.34326200	-0.78522800
C	-0.20829300	-3.22218300	-1.44850300
H	-0.34149500	-2.67642300	-2.38311300
C	-0.12907300	-4.60776200	-1.41818900
H	-0.19976600	-5.17132000	-2.34892300
C	0.04416800	-5.25392500	-0.19086600
H	0.11756000	-6.34091800	-0.13666700
C	0.11547200	-4.48646800	0.96683500
H	0.24015200	-4.96994000	1.93557900
C	0.02280400	-3.09290000	0.88600100
C	0.04490800	-2.20166900	2.04847900
C	0.15738900	-2.63958200	3.37329700
H	0.25575400	-3.70235200	3.59162500
C	0.14182600	-1.71281000	4.41029400
H	0.23087100	-2.04541800	5.44549100
C	0.00764900	-0.35639700	4.10570100
H	-0.01172400	0.40072500	4.88982800
C	-0.09890600	0.02851500	2.77501900
H	-0.20691100	1.07582000	2.48994900
C	2.19647000	0.11117400	-3.41788700
H	3.09097900	-0.25165800	-3.97564600
O	1.28832600	-0.79110500	-3.27554000
O	2.16263200	1.27917800	-3.01483400
C	6.27029500	-0.52238600	-0.21828300
C	-6.57353000	-0.62469000	-0.48069500

O	-7.16793600	-1.70071000	-0.52530900
O	6.89039300	-1.55311700	-0.47497800
O	6.85961300	0.66221000	0.10424100
O	-7.19016000	0.58942900	-0.49582900
C	-8.64721700	0.48147100	-0.57335700
H	-9.03522400	-0.07160800	0.29610000
H	-9.00273300	1.51890500	-0.56809700
H	-8.94473400	-0.03081600	-1.50159400
C	8.31992300	0.58368800	0.10703100
H	8.65192400	1.59471100	0.37251000
H	8.66252900	-0.15032000	0.85303100
H	8.68831000	0.29785700	-0.89036200
H	0.36867700	-0.35159000	-2.39948500
H	-0.35624000	0.00712000	-1.95217500

[i] M. Dolg, U. Wedig, H. Stoll, .H. Preuss, J. Chem. Phys. **1987**, 86, 866.

[ii] Easton, R. E.; Giesen, D. J.; Welch, A.; Cramer, C. J.; Truhlar, D. G. *Theor. Chim. Acta* **1996**, *93*, 281.

[iii] [Frisch, M. J.; Trucks, G. W.; Schlegel, H. B.; Scuseria, G. E.; Robb, M. A.; Cheeseman, J. R.; Scalmani, G.; Barone, V.; Mennucci, B.; Petersson, G. A.; Nakatsuji, H.; Caricato, M.; Li, X.; Hratchian, H. P.; Izmaylov, A. F.; Bloino, J.; Zheng, G.; Sonnenberg, J. L.; Hada, M.; Ehara, M.; Toyota, K.; Fukuda, R.; Hasegawa, J.; Ishida, M.; Nakajima, T.; Honda, Y.; Kitao, O.; Nakai, H.; Vreven, T.; Montgomery, J. A.; Peralta, J. E.; Ogliaro, F.; Bearpark, M.; Heyd, J. J.; Brothers, E.; Kudin, K. N.; Staroverov, V. N.; Kobayashi, R.; Normand, J.; Raghavachari, K.; Rendell, A.; Burant, J. C.; Iyengar, S. S.; Tomasi, J.; Cossi, M.; Rega, N.; Millam, J. M.; Klene, M.; Knox, J. E.; Cross, J. B.; Bakken, V.; Adamo, C.; Jaramillo, J.; Gomperts, R.; Stratmann, R. E.; Yazyev, O.; Austin, A. J.; Cammi, R.; Pomelli, C.; Ochterski, J. W.; Martin, R. L.; Morokuma, K.; Zakrzewski, V. G.; Voth, G. A.; Salvador, P.; Dannenberg, J. J.; Dapprich, S.; Daniels, A. D.; Farkas, Ö.; Foresman, J. B.; Ortiz, J. V.; Cioslowski, J.; Fox, D. J. *Gaussian 09, Revision A.02*; Gaussian, Inc.: Wallingford, CT, 2010.

[iv] Marenich, A. V.; Cramer, C. J.; Truhlar, D. G. *J. Phys. Chem. B*, **2009**, *113*, 6378.

[v] Y. Zhao, D. G. Truhlar, J. Chem. Phys. **2006**, 125, 194101.